Abstract Volume
6th Swiss Geoscience Meeting

Lugano, 21st – 23rd November 2008

Apply! Geosciences
6th Swiss Geoscience Meeting 2008 - Lugano

sc | nat
Geosciences
Platform of the Swiss Academy of Sciences

SUPSI
University of Applied Sciences
of Southern Switzerland
Institute of Earth Sciences

6th Swiss Geoscience Meeting, Lugano 2008

Table of contents

http://geoscience-meeting.scnatweb.ch

Organisation

Host Institution

Institute of Earth Sciences, University of Applied Sciences of Southern Switzerland (SUPSI)

Patronnage

Platform Geosciences, Swiss Academy of Sciences

Program Committee

Daniel Ariztegui
Peter Baumgartner
Damien Becker
Gilles Borel
Reynald Delaloye
Pierre Dèzes
Hans-Rudolf Egli
Karl Föllmi
Alain Geiger
Bernard Grobéty
Martin Hölzle
Adrian Jakob
Angelika Kalt
Eduard Kissling
Rainer Kündig
Neil Mancktelow
Nils Oesterling
Rolf Philipona
Christian Preiswerk
Frank Preusser
Bruno Schädler
Urs Schaltegger
Guido Schreurs
Manfred Thüring
Hugo Van den Bergh
Doris Wastl-Walter
Helmut Weissert
Rolf Weingartner
Adrian Wiget

Local Organizing Committee

Manfred Thüring
Silvio Seno
Manuel Lüscher
Marina Dalle Fusine

Participating Societies and Organisations

International Geographical Union, Commission Geography and Public Policy (IGU)
International Lithosphere Program (ILP)
International Union of Geological Sciences, Swiss Committee (IUGS)
Kommission der Schweizerischen Paläontologischen Abhandlungen (KSPA)
Open Source Geospatial Foundation (OSGeo)
Schweizerische Geotechnische Kommission (SGTK)
Swiss Association of Geologists (CHGEOL)
Swiss Geodetic Commission (SGC)
Swiss Geography Association (SGV)
Swiss Geological Society (SGG/SGS)
Swiss Geological Survey (swisstopo)
Swiss Geomorphological Society (SGGm/SSGm)
Swiss Geophysical Commission (SGPK)
Swiss Hydrological Commission (CHy)
Swiss Society for Hydrology and Limnology (SGHL / SSHL)
Swiss Meteorological Society (SGM)
Swiss Paleontological Society (SPG/SPS)
Swiss Commission for Quaternary Research (SKQ/CSQ)
Swiss Snow, Ice and Permafrost Society (SIP)
Swiss Society of Mineralogy Petrography (SMPG / SSMP)

0. Plenary Session

1

The art of using weather radars for hydrology in the Alps

Urs Germann

MeteoSwiss, Locarno-Monti

To use weather radars in mountainous regions is like pitching tents during snowstorm: The practical use is obvious and large – but so are the problems.

The most obvious strength of weather radars is their ability to make four-dimensional "radiography" of precipitation with time and space resolution of a few minutes and a few km over a large area of more than 100 thousand km^2. The applications of the Swiss weather radar network range from providing four-dimensional monitoring of precipitation systems and wind information in the forecast office, to quantitative precipitation measurement for hydrogeological risk management, hail mapping for insurance business, as well as identification, tracking, and extrapolation of thunderstorms for public warnings.

Successfull operation of weather radars in mountainous regions, however, requires appropriate system design and sophisticated data processing. Of particular difficulty are the elimination of ground echoes and the correction of errors caused by shielding of the radar beam by mountain ranges. The paper presents the Swiss solution with focus on 10 years of progress in operational applications. This includes thunderstorm ranking, wind profiling, as well as nowcasting heavy orographic precipitation. A novel promising solution is to generate an ensemble of radar precipitation fields. Each member of the ensemble is a possible realization of the unknown true precipitation field given the observed radar field and knowledge of the space-time error structure of radar precipitation estimates. The real-time implementation of the radar ensemble generator coupled with a rainfall runoff model in the framework of the hydrometeorological forecast demonstration project MAP D-PHASE is one of the first experiments of this type worldwide.

2

Simple models for complex hydrologic behavior: a challenge for basic research and engineering

J.W. Kirchner

Swiss Federal Institute for Forest, Snow, and Landscape Research (WSL), Birmensdorf, Switzerland
(james.kirchner@wsl.ch / Phone: +41 44 7392 655)
Department of Environmental Sciences, Swiss Federal Institute of Technology (ETH), Zürich, Switzerland
Department of Earth and Planetary Science, University of California, Berkeley, U.S.A.

An old joke defines a 'scientist' as someone who wants to understand a problem without solving it, and an 'engineer' as someone who wants to solve a problem without understanding it. Hydrologists need to defy these stereotypes, both to advance the science of hydrology and to solve practical water resource problems. Effectively solving water resource problems will require better scientific understanding of hydrologic processes. Conversely, and perhaps less obviously, a deeper respect for the practical realities of real-world problems will help to advance the science of hydrology.

Recent progress in hydrologic science is challenging the intuitively appealing and computationally convenient models that have been the foundation for engineering approaches to streamflow forecasting and contaminant transport problems. For example, although catchments have often been conceptualized as linear reservoirs, it has become clear that the intrinsic nonlinearity of many hydrological processes is essential to understanding catchments' rainfall-runoff behavior. Similarly, although subsurface transport and mixing in catchments has often been modeled by tank reactors with exponential residence time distributions, there is now clear evidence that typical residence time distributions in real-world catchments are markedly non-exponential. At smaller scales, contaminant transport has often been modeled by Gaussian plumes although field data clearly show that many contaminant plumes are dramatically non-Gaussian. The immediate challenge is to capture these kinds of real-world complexities in prediction and analysis tools that are still useful in an operational context.

For scientific reasons as well as practical ones, hydrology needs new conceptual models that make the complex realities of hydrological systems understandable and analytically tractable. In attempting to embrace the full complexity of hydrological systems, many hydrological models have not only become too complex for operational use; they have become too complex to be understood, too highly parameterized to be rigorously tested, and too data-hungry to be widely applied.

These considerations point to the need to develop new models which find a 'middle path' between the conceptually simple linear models often used in engineering approaches, and the complex spatially distributed models often used in research hydrology. The goal of such 'gray box' models is to capture the aggregate behavior of complex hydrologic systems directly in their governing equations, so that complex model structures and elaborate mathematical schemes are not required.

Catchment hydrology is controlled by processes and material properties that are known to be complicated, highly coupled, heterogeneous on all scales, and poorly characterized by direct measurement. This observation raises the question of how one can identify the appropriate constitutive equations that describe the large-scale behavior of these complex heterogeneous systems. Here I show that some small catchments can be usefully characterized as first-order nonlinear dynamical systems, and that one can infer their nonlinear governing equations at catchment scale, directly from field data. This approach assumes that discharge depends on the aggregate volume of water stored in the catchment, but makes no a priori assumption about the functional form of this storage-discharge relationship, instead estimating it from rainfall-runoff data.

This approach not only allows one to predict streamflow from measurements of rainfall, but also allows one to "do hydrology backwards": that is, to infer effective rainfall and evapotranspiration at whole-catchment scale, directly from fluctuations in streamflow. This approach also directly explains the relationship between the power spectra of the incident precipitation and the resulting streamflow fluctuations. Thus it allows one to understand how catchments filter rainfall fluxes that are complex in space and time, yielding streamflow fluctuations that are predictable over wide ranges of time scales.

3

Annual Opening and Closure of Alpine Valleys

Simon Löw*, Jürgen Hansmann*, Franz Ebneter**

* *Professur für Ingenieurgeologie, ETH Zürich, 8093 Zürich*
** *AlpTransit Gotthard AG, Zentralstrasse 5, 6003 Luzern*

Alpine tunnels in hard rocks induce small surface deformations as a result of groundwater drainage and associated pore pressure reduction. As shown in the example of the Zeuzier Dam, strong groundwater inflows to deep tunnels (1000 meters or more) in fractured limestones can lead to surface settlements and horizontal strains which can result in fracturing concrete arch dams within a lateral distance of a few kilometers. The Gotthard Base Tunnel (GBT), currently under construction in the central part of the Swiss Alps, runs close to 3 existing arch dams (Curnera, Nalps, Santa Maria) contributing to a hydropower system owned by Kraftwerke Vorderrhein AG (KVR). The excavation front as of fall 2008 is at the upstream end of lake Nalps (subsection Sedrun direction South) and at below Piora valley (subsection Faido direction North). In order to maintain safe operations of these hydropower dams and not unnecessarily stop tunnel excavations, a comprehensive surface deformation monitoring system has been installed in the surroundings of the Gotthard Base Tunnel, which is in operation since 2001/2002. This system includes automatic tachymeters, borehole extensometers, high-precision leveling, and differential GPS.

Shown here are some of the results of this monitoring project, which comprises the total station measurements of 6 local tachymetric networks installed in 2000 and 2001. These local networks are either located at the dam sites or 1.0-3.5 kilometers before (north or south of) the dams and focus on deformations within cross sections perpendicular to the valley axes. Some of these monitoring areas have not been affected by the Gotthard Base Tunnel or any other underground construction for a period of 6 years. These long-term “background” measurements are critical for the understanding of tunnel induced deformations and the definition of intervention thresholds. On the other hand this data set offers new insights into the natural deformations occurring in the three valleys located above or close to the Gotthard Base Tunnel route (from West to East: Val Curnera, Val Nalps and Val Medel/Termine).

The observed natural deformations are significant and include seasonal variations in horizontal and vertical distances measured at different elevation across these valleys. A rapid closure of the valley is observed in spring, followed by a slow opening in fall and winter. The observed annually reversible horizontal strains measured across Alpine valleys are in the order of 1 to 3 E-5. For example, at 250 m elevation above valley bottom, the separation of the sidewalls is 550 meters and changes annually by up to 17 mm. These strains also include minor vertical components and mainly occur mainly in planes oriented normal to valley axes. Preliminary investigations with hydromechanically coupled models (equivalent poro-elastic or discrete elastic fracture models) indicate that these strains are most probably related to annual variations in groundwater table elevation, controlled by recharge from snow melt in spring and early summer.

4

Peak oil or not peak, that is the question

Stampfli Gérard M.

Université de Lausanne, Institut de Géologie et Paléontologie, Anthropole 1015 lausanne
gerard.stampfli@unil.ch

Peak oil or not peak, that is the question

The whole world is looking at the price of the barrel of oil with a renewed interest since the beginning of 2008, and it became a common subject of discussion if not of worries. Most people and all sorts of experts are also speculating on the world oil reserves, and the most often asked question is: for how long do we have oil? Unfortunately, and despite the experts confident statements, any answer to that question is bound to be wrong, so is any speculation on the future price of the barrel. It is clear that there is still a lot of oil around and certainly some major quantities to be found in the near future, but what is certain is that, one day, we will run out of oil, and this is the only certainty regarding this global problem.

So, we certainly need to worries about the reserves, but on the short term the worries is about the capacities of production of the oil exporting countries. Any oil geologist would know that producing oil is an intricate business, blending technologies, a bit of luck and geological know-how, the latter being the most important, as structures in which the oil is trapped can be highly complicated in terms of distribution and quality of reservoirs, and often also in terms of structural trapping, to speak only of the obvious problems. To increase oil production is not a simple affair, in many instances it would take years to do so intelligently in order not to jeopardize future production. So, the hope that from the 80 M bpd production of a few years ago, a figure of 100 M bpd could be reached in the coming 10 years is a real gamble, and might prove to be impossible, despite the reserves. As the demand will certainly persist (at least from emerging countries such as China), we can be sure that the price of the barrel will go up. On the other hand, if it goes up too much, consumption will slow down, but slowing the consumption of oil means a decrease in economic profit and will inevitably run into recession. Then, can some sort of balance be found? it could be possible if speculation was not part of the game and if large parts of the world population were indeed ready to decrease their standard of living,. This sounds really unrealistic!

On the longer term, and as shortage there will be, a proper track of actions should be taken in order to avoid any sort of major worldwide crisis touching mainly the trading of merchandises, the main oil consuming factor in our modern world. Indeed, everything is transported, including billions of people on a daily basis, and mainly with oil. If we just wait for the shortage to come, we shall face major disasters such as famines and industrial and social unrests in the populated areas of the planet, so, everywhere... It has been shown that mitigation programs starting 20 year before the oil production peak are necessary in order to avoid a major crash in production, thus a major crash of the society. Some mitigation programs were started some years ago with the implementation of new and alternative sources of energy, but so far these are absolutely unable to replace oil for transportation of goods and people. Proper worldwide mitigation programs in term of reduction of oil in transportation just do not exist, and as most experts agree that we have already passed the oil peak, it seems that an oil crash is inevitable.

Thus, we shall be forced to travel less and buy locally. Most of us might be ready to do so, but can we do it? The main problem here is that politicians cannot implement and encourage such a responsible behaviour and for several reasons; the first one being that they just don't care about it, by ignorance or willingly, the other main reason is that the economy is not working in that direction whatsoever, the persistent "philosophy" being: the cheapest the better! And the politicians have no say in that process.

So, the solution is really in the hands and consciousness of the consumers, everyone of us... Besides a pro-active behaviour to buy locally, we should realised and be convinced that chasing the cheapest product is a highly egoistical behaviour, it may give us the illusion to generate jobs in some remote parts of the world, but what we give to these people is a promise for poverty and struggle for life in which millions shall perish. If we cannot change our consumer habits so easily –although we might soon be forced to do so, we could at least try to change our consciousness and open to the fact that the rich exist because the poor exist, and try to do our best for this situation not to remain for ever.

5

Hochwasserschutz in der Schweiz - eine Generationenherausforderung

Hans Peter Willi

Abteilungschef Gefahrenprävention, Bundesamt für Umwelt, Bern

Das Unwetterjahr 1987 gilt in der Schweiz als das Schlüsseljahr für den Paradigmawechsel im Hochwasserschutz. Aus der breit angelegten Ursachenanalyse wurden wichtige Schlüsse für die Zukunft gezogen. Man musste Abschied nehmen vom Glauben an die absolute Sicherheit. Die einfachen Rezepte mussten durch differenziertere Betrachtungsweisen abgelöst werden.

In den letzten 20 Jahren häuften sich die Schadenereignisse:

1987 (Uri), 1993 (Brig), 1999 (Mittelland), 2000 (Wallis), 2002 (Appenzell a. Rh., Graubünden), 2005 (17 Kantone betroffen), 2007 (Aargau, Solothurn, Bern, Waadt); Stürme in den Jahren 1990 (Vivian) und 1999 (Lothar); Lawinenwinter 1999. Seit 1987 hat sich offensichtlich die Frequenz von extremen Ereignissen erhöht. In den letzten 20 Jahren ereigneten sich 7 von 17 Hochwasser-Grossereignissen der letzten 200 Jahre.

Mit der Klimaerwärmung muss davon ausgegangen werden, dass die Anzahl Extremereignisse weiter zunehmen wird. Eine Anpassung der Schutzmassnahmen an die Auswirkungen des Klimawandels wird somit zu einer Herausforderung der ganzen Gesellschaft. Hinzu kommt, dass eine Reihe grosser wasser- und waldbaulicher Schutzmassnahmen erneuerungsbedürftig sind, weil sie die heutigen Anforderungen nicht mehr erfüllen. Erneuerungen und Sanierungen sind zwingend, wenn der entsprechende Schutz weiterhin gewährleistet bleiben soll. Eine angemessene Sicherheit des Wirtschafts- und Lebensraums ist eine wichtige Voraussetzung für eine volkswirtschaftliche Entwicklung.

Trotz den Bemühungen zeigt die Schadenstatistik der letzten 35 Jahre eine Vervierfachung der Schäden in der 2. Hälfte der Periode.

Um der ungünstigen Schadensentwicklung begegnen zu können, muss ein integrales Risikomanagement umgesetzt werden. Schäden können nur vermindert oder verhindert werden, wenn alle Beteiligten im Rahmen ihrer Handlungsmöglichkeiten ihre Verantwortung wahrnehmen. Nur wenn alle Massnahmen die zur Schadensminderung beitragen ergriffen werden, führt dies zu einer wirkungsvollen Schadensreduktion. Damit ist auch klar, dass die ganze Gesellschaft mit dieser Herausforderung konfrontiert ist.

Es stellt sich nun die Frage, wer was auf welcher Ebene dazu beitragen kann.

Aufgrund einer umfassenden Aufgabenanalyse des Bundesamtes für Umwelt im Bereich der Gefahrenprävention zum Ziel „Sicherheit für Mensch, Umwelt und Sachwerte“ (gesetzlicher Auftrag), wurden die verschiedenen prioritären Handlungsschwerpunkte ermittelt.

Wichtig ist das Bewusstsein, dass eine einzelne beteiligte Instanz allein die Sicherheitsziele nicht erreichen kann. Eine gute Zusammenarbeit, Koordination und Kommunikation ist Grundvoraussetzung. Es gilt also dafür zu sorgen, dass alle Beteiligten, auf allen Stufen, ihre Aufgabe optimal erfüllen und gut zusammenarbeiten.

Der Bundesrat hat dazu wichtige Entscheide zur Stärkung der Gefahrenprävention gefällt.

1. Structural Geology and Tectonics (Open Session)

Neil Mancktelow, Stefan Schmid

Swiss Tectonics Studies Group, Swiss Geological Society

Application to Carboniferous turbidites in South-West Portugal

1.29 Li Zhonghai & Gerya Taras: Numerical modeling of poly-phase formation and exhumation of HP-UHP rocks in continental subduction zone

1.30 Linckens J., Herwegh M., Müntener O., Mercolli I.: Evolution of a mantle shear zone and the influence of second phases, Hilti massif, Oman

1.31 Löw F.I., Gerya T.V.: Influence of rheological weakening by fluids and melts on subduction at an active margin: Numerical modelling

1.32 Martin M., Kindler P., Sartori M., Charollais J.: The Rochers de Leschaux (Bornes Massif, Subalpine domain, Haute-Savoie, France): a complex record of Cretaceous, Paleogene, and Neogene tectonics

1.33 Marzorati A., Ghiselli A., Bini A.: Structural influence on glacial cirque morphology: the case of Pizzo Arera (Orobic Alps, Southern Alps, Italy)

1.34 Matasci B., Epard J.-L., Masson H.: The Teggiolo zone: stratigraphy and tectonics in the Val Bavona (Lower Penninic, Ticino)

1.35 Matzenauer E., Ibele T., Mosar J.: Brittle tectonics in the Subalpine Molasse and in the Prealpes Klippen

1.36 Mishin Y., Gerya T., Burg J.-P., Connolly J.: Double subduction dynamics: Insight from petrological-thermomechanical numerical models

1.37 Misra S., Burlini L.: Deformation and reaction of Quartz-Muscovite aggregates: results from torsion experiments

1.38 Misra S., Tumarkina E., Burlini L.: Migration and storage of melts in rocks under dynamic conditions: insights from physical experiments

1.39 Moix P., Champod E., Stampfli G.M.: The Triassic detrital units in southern Turkey: synrift or syncollisional series?

1.40 Mosar J., Kangarli T., Bochud M., Rast A.: The Greater Caucasus - Tectonics and paleotectonics East of Eden

1.41 Nikolaeva K., Gerya T., Marques F.: Numerical modelling of subduction initiation at passive margins: Critical effects of continental mantle strength and density

1.42 Nommensen L., Stipp M., Pomella H. & Fügenschuh B.: Structural Mapping along the Meran-Mauls and the Faltleis Faults in the Sarntaler Alps (South Tyrol, Northern Italy)

1.43 Nováková L.: Comparative study of geological and GPS research of reactivated fractures in the north of Silesia (NE part of the Bohemian Massif, Czech Republic)

1.44 Pleuger J., Nagel T., Froitzheim N.: Structural evolution of the Monte Rosa and Adula nappes and the formation of the Lepontine dome

1.45 Pomella H., Fügenschuh B., Stipp M.: The Giudicarie Fault System at the transition between Southern and Eastern Alps (Northern Italy). A new structural analysis

1.46 Rahn M., Selbekk R., Spikings R., Zaugg A., Burkhalter R.: Volcanic ash layers in OSM sediments: clues to their origin and the post-sedimentary tectonic history

1.47 Ruiz G.M.H.: Direct versus indirect thermochronology – what do we trully trace? Examples and implications for the Central Andes

1.48 Ruiz G.M.H., Negro F., Foeken J., Stuart Babault J.F., Ivy-Ochs S., Kober F., Saddiqi O., Stockli D., Champagnac J-D., Frizon de Lamotte D.: The Atlas Mountains: why there? Why now?

1.49 Schefer S., Egli D., Frank W., Fügenschuh B., Ovtcharova M., Schaltegger U., Schoene B., Schmid S.M.: Metamorphic and igneous evolution of the innermost Dinarides in Serbia

1.50 Schlatter A.: Recent vertical movements from precise levelling in Switzerland

1.51 Sizova E., Gerya T.: Initiation of plate tectonics in the early Earth

1.52 Smit J., Burg J.-P., Dolati A., Sokoutis D.: The effects of large sub-marine landslides on the mechanics of thrust wedges

1.53 Sue C., Champagnac J.-D., Tricart P.: Neotectonics of the Western and Central Alps : geodynamic implications

1.54 Sue C., Daoud A.M., Le Gall B., Rolet J.: How rose up the Ali Sabieh bloc (Afar triple junction)? New insights from faulting analysis

1.55 Tackley P., Nakagawa T., Deschamps F., Connolly J.: Coupled models of mantle geochemical evolution, plate tectonics, magmatism and core evolution incorporating self-consistently calculated mineralogy

1.56 Thust A., Tarantola A., Heilbronner R., Stünitz H.: The Availability of H_2O for Deformation in Natural Quartz Single Crystal Experiments

1.57 van Heck H. & Tackley P.: Transitions in tectonic mode based on calculations of self-consistent plate tectonics in a 3D spherical shell

1.58 Yuan D.-Y., Champagnac J.-D., Ge W.-P., Molnar P.,Zhang P.-Z., Zheng W.-J., Zhang H.-P., Liang M.-J.: Late Quaternary slip rates of active faults adjacent lake Qinghai, northeastern margin of the Tibetan Plateau

1.1

Neogene transtensional brittle tectonics in the Lepontine Dôme (Central Swiss Alps)

Allanic Cecile*, Sue Christian**, Champagnac Jean-Daniel***

*Geological Institute, Neuchâtel University
**IUEM/UMR6538/UEB/UBO, Brest University, France
***Insitute of Mineralogy, Hannover University, Germany

The Lepontine Dome is investigated in term of faulting and paleostress, which allows to constrain the late brittle deformation of this gneissic core. Its tectonic evolution under brittle conditions was determined using fault mapping and paleostress inversions. Three brittle phases were reconstructed. The older phase is a NW-SE extension restricted to the eastern parts of the Dome. The second phase (major signal) is an upper Miocene transtension with stable orogen-parallel σ3 axes (NE-SW), which is found from the Mont-Blanc to the Bergell massifs. The late phase is a N-S extension, expressed north of the Dome, and probably linked to the current collapse of the belt.

The stress fields we determine for the Lepontine Dome are very similar to the stress fields determined by Champagnac et al (2006) westward in the South-Valais area, with a major signal in orogen-parallel extension and a minor signal in orogen-perpendicular extension. In the close vicinity of the Simplon fault, Grosjean et al (2004) only reported the orogen-parallel extensional stress field. Eastward, in the Bergell area, Ciancaleoni and Marquer (2008) also found a very regular NE-SW extensional paleostress field, using similar methods. Indeed, the main paleostress field determined in the Lepontine Dome is very homogeneous from a regional viewpoint. It is largely dominated by the NE-SW brittle extension, described in the whole northwestern Alps. The Lepontine Dome also bears witness of two minor extensional signals (N-S and WNW-ESE directions of extension).

The absolute dating of this orogen-parallel extensional phase is based on the occurrence of pseudotachylytes locally injected in the related fault system. Pseudotachylyte development is directly linked to frictional heating due to earthquake and faulting. The Ar/Ar dating of three pseudotachylytes samples of the Lepontine Dome provided ages in the range of 9-11 Ma ±1 (Allanic, et al., 2006). Thus, one can attribute a global 10 Ma age for the orogen-parallel extensional phase, at least in the Lepontine Dome.

We propose a kinematic model for the Central Alps in which the emplacement of the Lepontine Dome is driven by a pull-apart-like process controlled by the counterclockwise rotation of the Apulian indenter. This model refers to the paleostress field we documented and to kinetics of the main faults bounding the dome. Associated to these processes, lateral escape linked to the Apulia indentation/rotation would have enhanced the global extensional scheme of the Lepontine Dome.

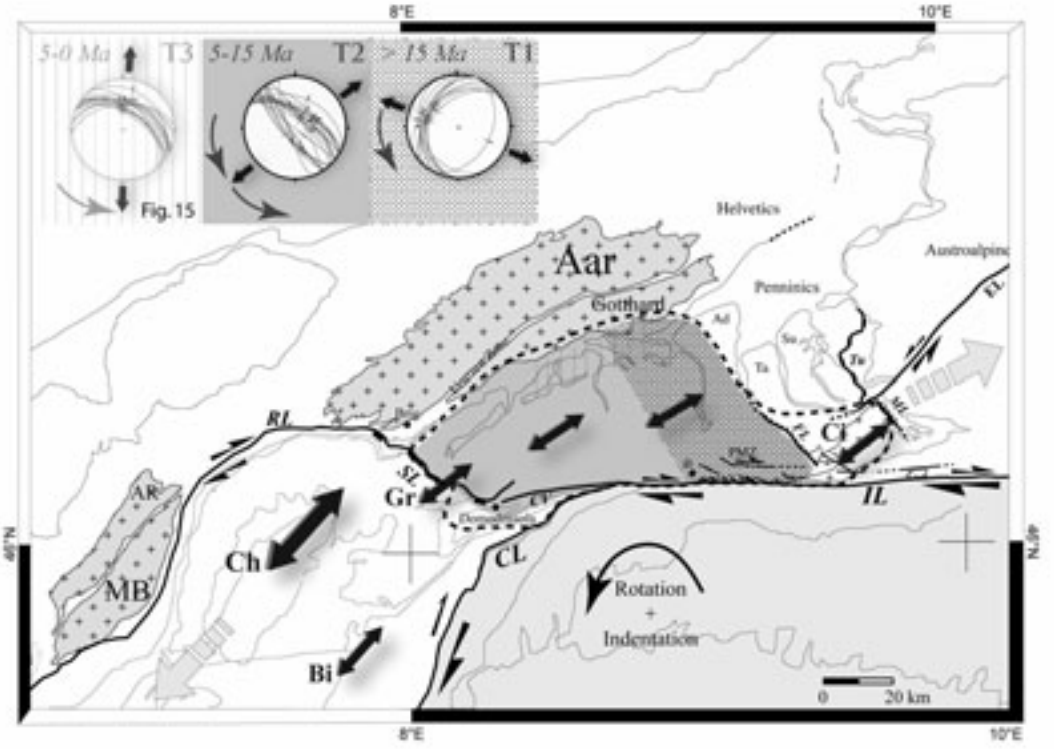

Figure 1. Transtensional to extensional brittle evolution of the Lepontine dome with relative chronology between the different states of stress recorded, showing a rotation of around 90° of the extensional axes. Mean direction of σ3 axes calculated from previous studies on brittle deformation in the extended Central Alps are reported as follow: Bi: Bistacchi and Massironi (2000); Ch: Champagnac et al (2006); Ci: Ciancaleoni and Marquer (2008); Gr: Grosjean et al (2004).

REFERENCES

Allanic, C., et al. (2006), A paleo-seismogenic Lepontine dome? New insights from pseudotachylytes-generating faults, Geochimica et Cosmochimica Acta, Vol. 70 (18), Suppl. 1, p9 Goldschmidt conf. Melbourne.

Bistacchi, A., and Massironi M. (2000), Post-nappe brittle tectonics and kinematic evolution of the north-western Alps: an integrated approach, Tectonophysics, 327, 267-292.

Champagnac, J. D., Sue, C., Delacou, B., Burkhard, M. (2006), Miocene orogen-parallel extension in the inner Western Alps revealed by dynamical fault analyses, Tectonics, 25, 1-26.

Ciancaleoni, L., and Marquer D. (2008), Late Oligocene to early Miocene lateral extrusion at the eastern borders of the Lepontine dome of the Central Alps (Bergell and Insubric areas, Eastern Central Alps), Tectonics, 27, TC4008, doi:10.1029/2007TC002196, 2008.

Grosjean, G., Sue, C., Burkhard, M. (2004), Late Neogene brittle extension in the vicinity of the Simplon fault zone, central Alps, Switzerland., Eclogae Geologicae Helvetiae, 97, 33-46.

1.2

Origin of the magnetic anisotropy in a two marble lithologies from the Morcles Nappe shear zone

Almqvist Bjarne*, Hirt Ann*, Herwegh Marco**

*Institut für Geophysik, ETH Zurich, Schaffmattstrasse 30, CH-8093 Zurich (bjarne.almqvist@mag.ig.erdw.ethz.ch)
**Institut für Geologie, Universität Bern, Baltzerstrasse 1-3, CH-3012 Bern

Anisotropy of magnetic susceptibility (AMS) arises from the sum of ferromagnetic (*sensu lato*), paramagnetic and diamagnetic minerals in a rock. The AMS is generally controlled by the ferromagnetic and paramagnetic phases, since these have the strongest magnetic susceptibility. However, when the ferromagnetic contribution to the AMS is negligible, it may be possible to separate the paramagnetic and diamagnetic fabrics using high-field magnetic-torque measurements at room temperature and 77K. This is illustrated in a study of two marble lithologies from the Morcles Nappe shear zone. The AMS of the marbles are compared with that of a set of quartzites from the Navia-Alto Sil slate belt in northwestern Spain, which have been studied using the same technique.

From the room temperature AMS studied in a weak magnetic field it is possible to distinguish each marble based on its bulk susceptibility and degree of anisotropy. Texture mapping using electron backscatter diffraction (EBSD) shows that the AMS is controlled by the microtexture of the marbles. High-field AMS measurements, performed at 77K, produce an anisotropy that is in some cases more than 100 times stronger than that measured at room temperature, indicating that paramagnetic phases contribute to the total AMS. Separation of the paramagnetic and diamagnetic fabrics shows an inversion of the AMS ellipsoid, from oblate and triaxial shapes at room temperature to strongly prolate shape at 77K. This is commonly seen in marbles from the shear and root zones of the Morcles Nappe, and can be attributed to the presence paramagnetic cations (e.g. Fe^{2+} and Mn^{2+}) in the calcite crystal lattice (Figure 1). Further texture mapping together with determination of the chemical composition of the calcites and secondary phases in the marbles should help identify the origin of their magnetic anisotropy.

In contrast, the diamagnetic quartzites have similar bulk susceptibility as the marbles, but are only a few times more anisotropic at low temperature as compared to the room temperature measurements. This suggests that the quartzites have an AMS with a significantly lower paramagnetic contribution, and that the inherent AMS of the quartzite is less than that of the marble.

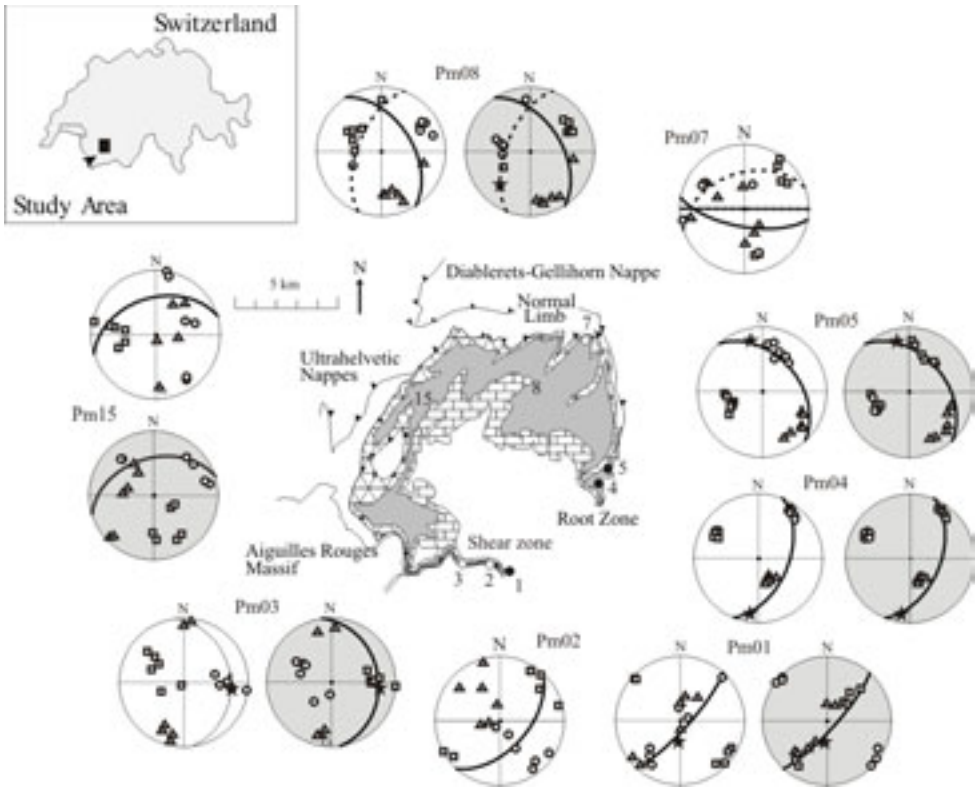

Figure 1. Paramagnetic (white background stereonets) and diamagnetic (gray background stereonets) anisotropies are illustrated for different locations around the Morcles Nappe, on equal-area stereonets. Stereonet symbols refer to the maximum (squares), intermediate (triangles) and minimum (circles) susceptibilities; solid-line great circles refer to the orientation of the cleavage plane; dashed great circles indicate the bedding plane; stars indicate the mineral stretching lineation.

1.3

Structural and kinematic analysis in the Dourbie river valley, Cévennes, SE French Massif central

Augenstein Clemens* & Burg Jean-Pierre*

* *Geological Institute, ETH Zurich, Leonhardstrasse 19, 8092 Zurich (aclemens@ethz.ch)*

In Summer 2007 and 2008 two field seasons have been carried out in the SW Cévennes (SE French Massif Central) in order to gain data for structural and kinematic analysis. During structural mapping rocks were sampled for microstructural, crystallographic preferred orientation (CPO) and petrological investigations. Main lithologies in the mapping area are two micaschists divided by a quartzite and the St-Guiral granitic intrusion. The structures suggest a continuous deformation history: 1. SSW-SW directed shearing, 2. drag folds, 3. evolution of non-cylindrical folds due to heterogeneous shear, 4. buckling of open folds 5. intrusion of the granite in a depth of 3kbar with 650°C generated small-scale kinks and flexures. Recorded CPO patterns of the dynamically recrystallised quartzite can be classified into two types, one with a monoclinc symmetry (type I) and one with an orthorhombic symmetry (type II). Type I is related to a simple shear deformation and type II to an apparent constrictive coaxial deformation. These two types are consistent with the results of structural observations, where a constrictive coaxial deformation regime could have been active during formation of non-cylindrical folds. In the contact metamorphic aureole CPO patterns intensify towards the granite during static recrystallisation, until grain growth and mica band spacing lead to preferred grain orientations parallel to the mica bands.

1.4

Structural geology, stress and strain across the Eastern Greater Caucasus

Bochud Martin*, Mosar Jon*, Kangarli Talat**

*Science de la Terre, Département des Géosciences, Université de Fribourg, Chemin du Musée 6, CH-1700 Fribourg (martin.bochud@unifr.ch)
**Geology Institute of Azerbaijan (GIA), National Academy of Sciences, H.Javid Av., 29A, Baku AZ1143, Azerbaijan

The Eastern Greater Caucasus is located in the northern part of Azerbaijan to the West of the Caspian Sea. The Greater Caucasus undergoes a rapid uplift since the Miocene and is submitted to a regional compressional tectonic regime related to the Alpine closure of Neo-Tethys during the Arabia – Eurasia collision. The near South Caspian Basin is one of the deepest basins in the world with more than 20 km of sediment and with important oil deposits. This research is part of different international research projects in the Caucasus-Caspian Sea area including MEBE, INTAS, SCOPES, UNIFR. The focus of the research is on the Mesozoic to Present evolution of the region and the link between the processes leading to the present geomorphology and the deeper seated tectonic processes.

Fieldwork since 2003 has made it possible to gather data and present regional tectonic profiles across the easternmost Greater Caucasus of Azerbaijan. In addition we carried out a thorough stress analyses combined with a fracture and lineament analyses (remote sensing). Our investigation allowed us to distinguish and document different tectonic phases since the Middle Jurassic and to highlight some local tectonic stresses associated with the different discrete events.

Overall the geometry of the orogen is one of a doubly vergent fold-and-thrust belt. The present orogeny is associated with south-directed thrusting and folding in its central and southern parts. The northern regions, to the N of the topographic crest, around the area of the Shadag, also show important N-directed folding and thrusting. Near the Shadag summit, at an altitude of 3500m, marine deposits of Sarmatian (Pliocene) age are evidence of the rapid uplift of the area. Both S-directed and N-directed thrusting appear to be linked to rapid uplift. On top and to some extent contemporaneously, we can observe vertical to subvertical faults that dissect the whole mountain range with a trend more or less perpendicular to the NW-SE strike of the major fold and thrusts.
Analysis of paleo-stress data show a combination of thrust-related compressive stresses, but most prominently strike-slip faults linked with recent anticaucasian faults. We will discuss the different stress/fault families and their relationship with the recent tectonic evolution.

1.5

Mechanical and microstructural changes during torsion testing on Carrara marble with pre-existing deformation history

Bruijn Rolf* & Burlini Luigi*

* Geological Institute, Leonhardstrasse 19, CH-8092 Zürich (rolf.bruijn@erdw.ethz.ch)

We are conducting extended research on Carrara marbles samples in order to broaden earlier investigations on superimposed deformation events. Initially three types of experiments were designed to ascertain the mechanical and microstructural behaviour of double-deformed Carrara marble. These types include: 1. samples deformed to a specific strain followed by reversed deformation with equal strain, 2. deformation of a composite comprising a deformed (γ=5) part and an undeformed part, 3. sample deformed until γ=9 with a static annealing pause at γ=5. The results are summarized in Delle Piane and Burlini 2008.
More recently, a fourth type of deformation experiment was conducted, involving stack of samples previously deformed anticlockwise (top) and clockwise (bottom part), see figure 1. The first deformation phase reached strains of $\gamma = 1$, $\gamma = 2.6$ and $\gamma = 5$. The second phase of deformation (i.e. the deformation of the sandwich of samples) is currently under execution and is going to reach $\gamma = 1$, 2.5 and 5 in anticlockwise direction.
This fourth type of Carrara marble sample will allow us to examine the interaction between the different sections of the sample and the effect that this interaction might have on rock strength and microstructure.
Deformation experiments, using a Paterson type internally heated gas-medium deformation apparatus, were conducted at 300 MPa confining pressure, 1000° K and with a shear strain rate of $3 \cdot 10^{-4}$ s^{-1}.
Produced microstructures were examined using light and scanning electron microscopy. In addition, EBSD (Electron backscatter diffraction) was used to analyse fabrics. The rest of the planned experiments will be at the same strain rate, pressure

and temperature conditions.
The first three deformation types of tests already indicated that the mechanical behaviour of Carrara marble is dependent on pre-existing deformation history. In comparison with undeformed marble, deformed Carrara marble undergoes plastic strain at relatively lower shear stresses. Microstructures of deformed Carrara marble up to γ=2 are restored during strain reversal. More strained marble demonstrates an evident foliation with shear sense indicators displaying a shear sense that is in agreement with the reversed sense of shearing. Reversed strain of at least $\gamma = 3$ is required to overprint any pre-existing foliation. Although developed fabric is very similar to that of single phase and equivalently deformed Carrara marble, CPO development is less prominent, indicating a more complex microstructural interaction during plastic reactivation.
In addition, the first three types of deformation tests indicate that the prime cause of strain weakening in Carrara marble is grain size refinement initiated by dynamic recrystallization. Development of CPO contributes about one third of the total observed weakening.

REFERENCES

Delle Piane, C., & Burlini, L. 2008: Influence of strain history on the mechanical and micro-fabric evolution of calcite rocks: insights from torsion experiments, Swiss J. Geosci, in press.

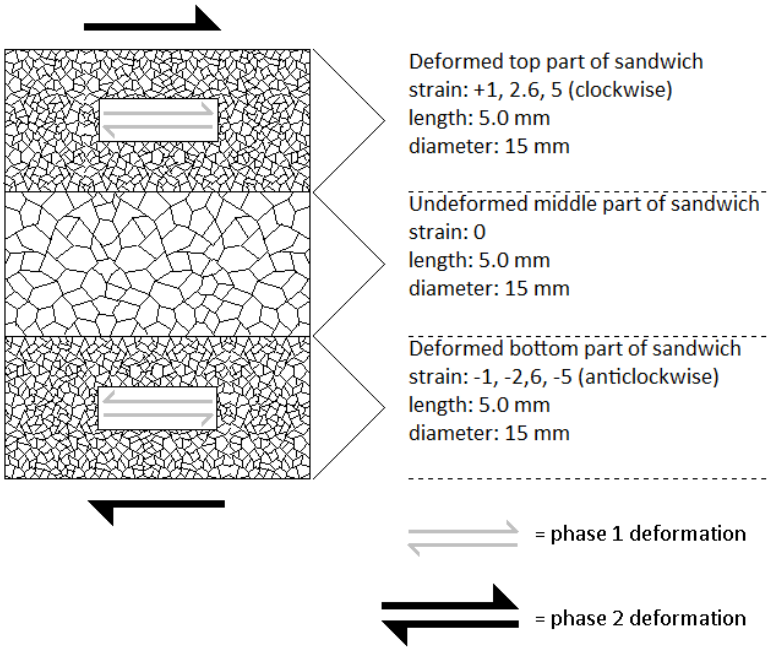

Figure 1. Sketch of type four deformation assembly, comprising a clockwise deformed top part, undeformed centre part and anticlockwise deformed bottom part.

1.6

Neotectonics slip rate at the front of the Qilian Shan, NE Tibetan plateau

Champagnac Jean-Daniel*, Molnar Peter**, Yuan Daohuang*** & Ge Weiping ***

* *Institut für Mineralogie, Universitat Hannover, Callinstrasse 1, D-30167 Hannover, champagnac@gmail.com*
** *Department of Geological Sciences and CIRES, University of Colorado, Boulder, USA,*
*** *Institute of Seismology, China Eearthquake Administration, Lanzhou, Gansu, China*

We derive a slip rate for the frontal thrust at the north Qilian Shan (NE Tibet) mountain front by combining structural investigations, satellite imagery, topographic profiling, and 10Be exposure dating.
We used two terrace levels, and from each we took 6-7 samples in profiles dug to depths of two meters. These allowed us to constrain inheritance (less than a couple of thousand years, for each) and to yield precise ages of abandonment of the terraces:

The lower terrace yields an exposure age of 19 kyr; the upper yields 30.5 kyr.

Topographic profiles 4 km in length give us offsets of the terraces with respect to the present-day footwall of 14.7 and 33.1 meters. The combination of these two offsets and the two ages allows a calculation of the burial of the footwall, around 8 meters.

These data yield a vertical displacement rate of ≈1.3 mm/yr, more than twice that of previous studies further northwest (Hetzel et al., 2004). The associated shortening rate due to thrust slip calculated with end member values of the thrust dip (30 to 60 degrees) range between 1.5 and 2.5 mm/yr. Again, this is significantly higher than the results from further northwest (Hetzel et al., 2004). This might be explained by the in-sequence propagation of an active back thrust (north of the Hexi Corridor) where Hetzel et al. (2004) obtained their results. At continental scale our results are consistent with GPS studies (Zhang et al., 2004).

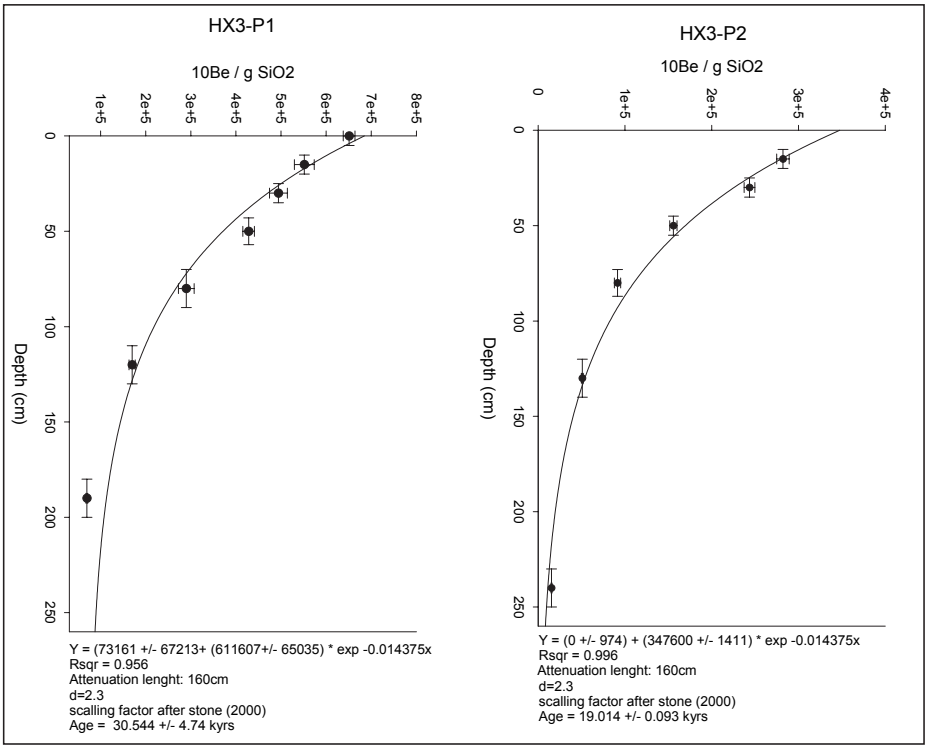

Figure 1: Concentration of cosmogenic ([10Be] / gSiO2) with respect to depth. Scaling factor for production rate (Stone [2000]) and consideration of inheritance yields the age of exposure beginning. Exposure ages are 30.5 kyrs (upper surface S1) and 19 kyrs (lower surface S2). Calculations done with Cosmocalc (Vermeesch, 2007).

REFERENCES:

Hetzel, R., Tao, M., Stokes, S., Niedermann, S., Ivy-Ochs, S., Gao, B., Strecker, M.R., Kubik, P.W. 2004: Pleistocene/Holocene slip rate of the Zhangye thrust (Qilian Shan, China) and implications for the active growth of the northeastern Tibetan Plateau. Tectonics 23 (6), 1-17.

Stone, J. 2000: Air pressure and cosmogenic isotope production, J. Geophys. Res. 105, 23,753–23,759.

Vermeesch, P. 2007: CosmoCalc: An Excel add-in for cosmogenic nuclide calculations, Geochem. Geophys. Geosyst., 8, Q08003, doi:10.1029/2006GC001530.

Zhang, P.-Z., Shen, Z., Wang, M., Gan, W., Burgmann, R., Molnar, P., Wang, Q., Niu, Z., Sun, J., Wu, J., Hanrong, S., Xinzhao, Y. 2004: Continuous deformation of the Tibetan Plateau from global positioning system data Geology, 32 (9), 809-812.

1.7

Models of thermo-chemical convection: what is needed to fit probabilistic tomography?

Deschamps Frédéric & Tackley Paul J.

Institute of Geophysics, ETH Zurich, Switzerland (deschamps@erdw.ethz.ch)

A growing amount of seismological observations indicate that strong lateral density anomalies, likely due to compositional anomalies, are present in the deep mantle. We aim to identify models of thermo-chemical convection that can generate strong thermo-chemical density anomalies in the lower mantle – particularly at its bottom –, and maintain them for a long period of time. For this, we explore the model space of thermo-chemical convection, determine the thermal and chemical density distributions predicted by these models, and compare their power spectra against those from probabilistic tomography. We run 3D-Cartesian numerical experiments using STAG3D, in which we varied compositional (buoyancy ratio, fraction of dense material), physical (Clapeyron slope of the phase change at 660 km, internal heating), and viscosity (thermal, radial, and compositional viscosity contrasts) parameters, and identified five important ingredients for a successful (in the sense that it fits seismological observations well) model of thermo-chemical convection. (1) A reasonable buoyancy ratio, between 0.15 and 0.25 (corresponding to chemical density contrasts in the range 60-100 kg/m^3). Larger density contrasts induce stable layering for long period of time, rather than the strong topography required by seismic observations. (2) A moderate (typically in the range 0.1-10), chemical viscosity contrast. Small chemical viscosity contrasts induce rapid mixing, whereas large chemical viscosity contrasts lead to stable layering. (3) A large ($\geq 10^4$), thermal viscosity contrast. Temperarure-dependent viscosity creates and maintains pools of dense material with large topography at the bottom of the mantle. (4) A 660-km viscosity contrast around 30. (5) And a Clapeyron slope of the phase transition at 660-km around 1.5-3.0 MPa/K. These two last ingredients help to maintain dense material in the lower mantle. Interestingly, they strongly inhibit thermal plumes, but still allow the penetration of downwellings in the lower mantle. Finally, we test models that include various combinations of the previous ingredients. The power spectra of these models are in excellent agreement with those from probabilistic tomography except for the spectra of chemical anomalies in the layer located right below the 660-km boundary. This discrepancy might be related to the stacking of slabs at these depths. Because our treatment of the chemical field does not specifically account for the compositional differences between the descending slabs and the regular mantle, our models cannot reproduce the chemical signal due to the slab stacking. This will be fixed in future works, which will also include calculations in spherical geometry and the effects of the post-perovskite phase transition.

1.8

Direct numerical simulation of two-phase flow: homogenization and collective behaviour in suspensions

Deubelbeiss Yolanda*,**, Kaus Boris J.P.**,***, Connolly James*

**Institute for Mineralogy and Petrology, ETH Zurich, Clausiusstr. 25, CH-8092 Zurich (yolanda.deubelbeiss@erdw.ethz.ch)*
***Institute for Geophysics, ETH Zurich, Schafmattstr. 30, CH-8093 Zurich*
****Department of Earth Sciences, University of Southern California, 3651 Trousdale Parkway, Los Angeles, CA 90089-740, USA.*

Melt transport mechanism has received much attention recently, since melting and melt migration play dominant roles in heat, composition and mass budget of the Earth. Whereas many aspects of melt migration processes are well known the physics of the processes remain a matter of discussion.

Melt migration and partial melting processes are generally solved by coupling solid and fluid flow. The theory of compaction-driven two-phase flow is based on macroscopic models considering the motion of a low-viscosity fluid moving through a high-viscosity, permeable and deformable matrix (e.g. McKenzie 1984). Previous work concerning modeling of two-phase flow has been performed by different authors. Nevertheless, models commonly are solved by neglecting and simplifying parts of the whole complex dynamical system such as the mechanical deformation of the solid, melting processes or the porosity treatment of the rock. Therefore many numerical codes use very simplified models. However, by reducing the number of unknowns and assumptions it is possible to study the dynamics of partially molten systems.

Here, we study the dynamics of two-phase flow by solving the equations directly on grain-size-scale using the Stokes equations for low-viscosity and high-viscosity regions in two dimensions. We performed systematic studies in order to characterize the mechanical behaviour of the system as a function of material parameters and melt fraction. Results indicate that for moderate to large melt fractions, particle interactions are significant, and result in macroscopic Rayleigh-Taylor like instabilities. This allows us to derive a formula for effective viscosity in a particle-suspension system. Additionally, we quantified the transition between Rayleigh-Taylor mode (strong interaction between particles) and Stokes-suspension (simple sinking of particles) mode systems.
To complete the scaling law in the full range of fluid fractions, we currently perform simulations at very low porosities.

REFERENCES

McKenzie, D.P. 1984: The generation and compaction of partially molten rock. Journal of Petrology, 25(3), 713-765.

1.9

New results of tectono-sedimentary history of the Makran accretionary prism

Dolati Asghar*, Müller Carla**, Smit Jeroen*, Bernoulli Daniel*, Spezzaferri Silvia*** & Burg jean-Pierre*

*Earth Sciences, ETH-Zurich, Leonhardstr. 19, CH-8092 Zurich (dolati@erdw.ethz.ch)
**6 bis r Haute 92500 RUEIL MALMAISON, France
*** Department of Geosciences, University of Fribourg, ch du Musee 6, 1700 Fribourg

The Makran Accretionary Prism (MAP) is one of the largest accretionary wedge in the world. It results from the active convergence between the Arabian and Eurasian plates which began in the late Cretaceous. The MAP grows seawards by frontal accretion and underplating of trench-fill sediments since the Miocene. Nowadays, the frontal 100–150 km are submarine and >350 km of the Cenozoic accretionary wedge are exposed on land, in Iran and Pakistan.

New results of stratigraphy and tectono-sedimentary history show that it was a turbidite basin on an active margin between the late Paleocene – early Eocene and the Serravallian. The oldest, well-dated turbidites are Lower Eocene with typically rhythmic alternation of brown, usually volcanogenic sandstone, and lighter-coloured shales; this upward-coarsening unit represents relatively distal slope deposits conformably covering a series of pillow basalts, basaltic flows, pelagic limestones and shales of early Palaeogene age. New fossil determinations reveal that many turbidite units that were previously mapped as Eocene are in fact late Oligocene in age. Towards the Lower Miocene the deposits become more proximal and the influx of turbidites ceased. Carbonate reefs and gypsiferous mudstones indicate a shallow marine and lagoonal environment during the Burdigalian.

The MAP includes a giant catastrophic mud-and-debris flow inserted between Lower Miocene and Upper Miocene sediments. We provide evidence for sedimentary gravitational emplacement of the resulting olistostrome between 11.8 and 5.8 Ma or shortly thereafter. The olistostrome includes blocks of ophiolites and oceanic sediments derived from the ophiolite-bearing, imbricate thrust zone to the north, and reworked chunks of the turbidites on which it rests with an erosional unconformity.

The chaotic scattering of blocks of any size and lithology and the soft-sediment deformation of the matrix argue against a tectonic emplacement of the olistostrome. Its size and internal structure make it a fossil equivalent of the large debris flows found along continental margins and unstable volcanic edifices.

REFERENCES

Burg, J.P., Bernoulli, B., Smit, J., Dolati, A. & Bahroudi, A. 2008 : A giant catastrophic mud-and-debris flow in the Miocene Makran. Terra Nova, 20, 188-193.

1.10

Structural evolution and fission track ages of the Makran accretionary wedge in SE Iran

Dolati Asghar*, Seward Diane*, Smit Jeroen*, Burg Jean-Pierre*

* *Earth Sciences, ETH-Zurich, Leonhardstr. 19, CH-8092 Zurich (dolati@erdw.ethz.ch)*

The Makran Accretionary Prism (MAP) is formed by active convergence between the Eurasian and the Arabian plates. The oceanic crust of the Arabian plate has subducted to the north under the Eurasian continent, thereby building the MAP. This wedge is characterized by a shallow subduction angle (<2°), great sediment thickness on the Oman Sea and a wedge width of >500 km, >300 km of which are exposed onshore.
New mapping results and structural sections document the structural development of the accretionary wedge. Shortening in the internal Makran is accommodated along large E-W trending thrusts, and folds, which are sealed by a giant catastrophic mud-and-debris flow (11.8 - 5.8 Ma). To the south of inner Makran, sediments younger than middle Miocene are affected by open synclines with long wavelength (>20 km) and low amplitude alternating with tighter anticlines. Normal faults in the south of MAP, are further imaged offshore by seismic data. Field observation and seismic data indicate that most of normal faults cut Plio-Pleistocene sediments.
Low temperature geochronology (apatite and zircon fission track ages) provides new time constraints. Apatite has undergone partial annealing since sedimentation. However, analysis of the radial plots suggests that cooling began in the late Miocene, after burial. Zircon fission track ages span 60-180 Ma with no evidence for annealing or resetting. We conclude that the burial thickness of the MAP as always been shallower than annealing zone (≈210°C).

1.11

Stability of thermal boundary layers for convection in spherical shell: Application to the dynamics of planetary mantles

Duchoiselle Lionel*, Deschamps Frédéric*, Tackley Paul *

**Institut für Gepophysik, ETH Hönggerberg (HPP) CH-8093 Zürich (duchoiselle@erdw.ethz.ch)*

Improving the knowledge of convection into mantle of terrestrial planets required a better understanding of its physical and chemical state. Recently, with the help of massive computational resources, significant progresses were achieved in the numerical modeling of planetary mantles convection. Models with a high degree of complexity (including realistic viscosity laws, mixed mode of heating, spherical geometry, thermo-chemical convection, ...) are now available. Among the parameters that recently became accessible, spherical geometry is a key ingredient because it affects the relative strength of the top and bottom thermal boundary layers. Despite these progresses, many details of planetary mantles convection remain unclear and so far, no model of Earth's mantle convection fits all available geophysical, geochemical, and geological constraints. Using STAGYY, which solve the usual conservative equations of mass, energy and momentum on a yin-yang grid, we explored the influence of various parameters on convection in spherical geometry. First, we have performed several numerical experiments varying important parameters including the Rayleigh number, the curvature (ratio between radius of the core and the planet one), the mode of heating (only from below or with an internal heating component), rheology (isoviscous or temperature dependence). In particular, we studied the evolution of the style of convection, average temperature, heat flux and critical Rayleigh number depending on these parameters. We have then built scaling laws between the parameters and observables, for instance between the Nusselt and Rayleigh number, and between the temperature and curvature factor. Our results suggest that extrapolations previously made from Cartesian models may not be valid in spherical geometry. In particular, the dependence of temperature on curvature differs significantly from that expected by Cartesian scaling laws. In addition, it also depends on the Rayleigh number. A possible explanation for these discrepancies is the asymmetry between the top and bottom thermal boundary layers, which may alter their relative stability. The new scaling laws we obtained enable to reconsider some aspects of thermal evolution and physical states of terrestrial planets like Earth, Mars, Mercury or some giant planets satellites.

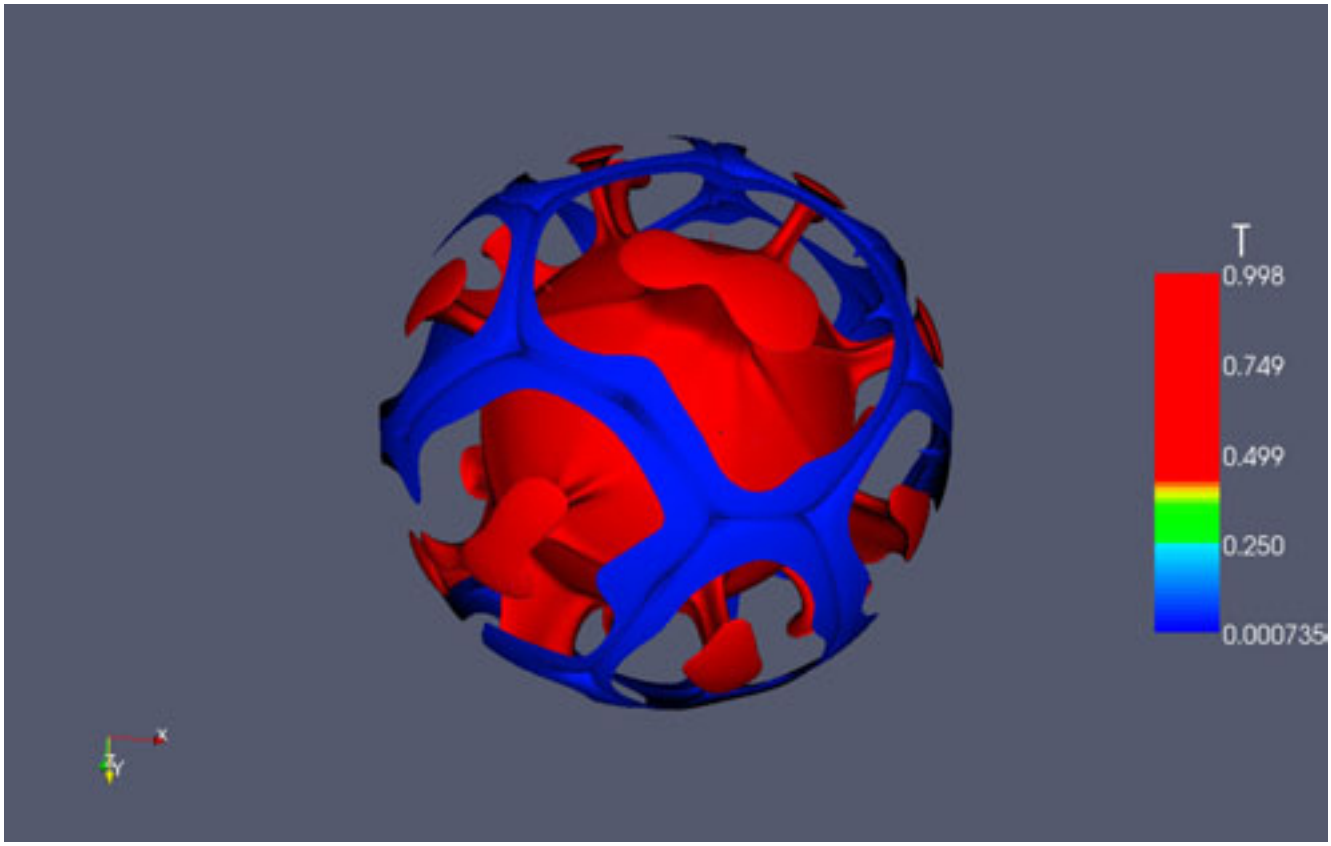

1.12

Dynamics of orogenic metamorphism: Diachronic evolution in the Central Alps

Engi Martin*, Janots Emilie**, Allaz Julien* and Berger Alfons***

*Institut für Geologie, Baltzerstrasse 3, CH-3012 Bern (engi@geo.unibe.ch)
** Institut für Mineralogie, Correnssstrasse 24, D-48149 Münster
*** Institut for Geografi og Geologi, Øster Voldgade 10, DK-1350 København K

The Central Alps arguably represent Earth's best studied collisional orogen. Despite many decades of research, fundamental aspects of the PTt-evolution across the Lepontine belt and its margin have not been satisfactorily resolved. Recent studies combining petrology and mineral chronometry have focussed on several of the critical tectonic units and have confirmed substantial differences in age across the orogen. Integrating the results within the structural framework yields a consolidated basis to interpret the geodynamic evolution of the metamorphic belt now surfacing in the Central Alps. A brief outline is presented here.

Early convergence is now known to have yielded HP metamorphic sequences typical of subduction in a few units only. In northern parts of the Lepontine, accretionary wedge units attained LT-HP conditions (e.g. carpholite in Valaisan units; Bousquet et al. 2002); further south, portions of the tectonic accretion channel (TAC; Engi et al. 2003) comprise a tectonic mélange, with eclogite facies fragments. Much of the HP-stage was reached in the Eocene, but prograde lawsonite-blueschist facies conditions in the TAC (Brouwer & Engi, 2005) were attained prior to 55 Ma ago. Eclogite facies garnet growth in some parts of the TAC initiated >70 Ma ago, in others it lasted to 36 Ma (Brouwer et al., 2005). Tectonic extrusion of portions of the TAC (from Mantle depths) and their incorporation as thrust sheets (Adula) or tectonic slivers (e.g. Mergoscia-Arbedo zone) into the stack of gneiss nappes (e.g. Simano, Maggia) must have preceded intrusion of tonalite melts of the Bergell suite, i.e. prior to ≈32 Ma ago (Oberli et al., 2004), at pressures of 5-6 kbar. This marks the important transition in the metamorphic evolution from HP-conditions (experienced by a small and well defined subset of the tectonic units) to the regional Barrovian phase, which encompassed *all* of the Lepontine units, at mid-crustal depths (15-20 km).

Tectonic units not involved in the early LT-HP cycle, notably those derived from the European margin, experienced a much less spectacular start, in that they never were subducted to depths >20-25 km. Frontal units (e.g. the cover of the Gotthard-Lucomagno nappe) show prograde LP-MT conditions of metamorphism. There is a clear age progression across the Lepontine from N to S: Near Lucomagno Pass, for instance, 450 °C were attained 30-29 Ma ago, and T_{max} (560 °C at ≈6 kbar) was reached at 20-18 Ma (Janots et al. 2008). In the central portion of the belt T_{max} was attained at subsequently earlier stages (Köppel et al., 1978, 1981), greater depth and higher temperature (Engi et al., 1995); e.g. near Biasca: ≈600 °C, 7-8 kbar, at ≈23 Ma. Further south, the Barrovian overprint reached T_{max} earlier yet, but at lower pressures; e.g. near Castione: ≈650 °C, 5-6 kbar, at ≈26 Ma (Todd & Engi, 1997). Within the SSB (Southern Steep Belt), partial melting occurred in suitable lithotypes during decompression in this period of upper amphibolite facies conditions (Burri et al., 2005; Berger et al. 2008). Heating rates for the Barrovian metamorphism are well constrained in the north (8-10 °C, Janots et al., 2008), but not in the south of the Lepontine belt. The regional distribution of robust ages across the entire belt shows that the thermal peak was diachronic from the southern to the northern part of the Central Alps, with T_{max} being reached at 30-27 Ma in the SSB, but only 20-18 Ma in the northern Lepontine.

Ages documenting the cooling path above 500 °C remain difficult to interpret with certainty, bit fission track data for zircon (reviewed by Vernon et al., 2008) yield constraints for cooling below ≈250 °C. For the interval from T_{max} to ≈250 °C the age data result in cooling rates of 31-53 °/My in the northern Lepontine, and of 44-58 °/My in the SSB. Exhumation rates are far mor difficult to obtain, notably in the south. Cooling here was associated not only with tectonic unroofing and erosion, but with lateral heat flow into the Southern Alps, owing to dextral transpression along the Insubric Line. The timing of this movement is poorly known, exhumation rates cannot be obtained from cooling rates.

REFERENCES

Berger, A., Burri, T., Alt-Epping, P. & Engi, M., 2008. Tectonically controlled fluid flow and water-assisted melting in the middle crust: An example from the Central Alps. Lithos, 102, 598-615.

Berger, A., Mercolli, I. & Engi, M., 2005. The central Lepontine Alps: Notes accompanying the tectonic and petrographic map sheet Sopra Ceneri (1:100'000). Schweiz. Mineral. Petrogr. Mitt., 85(2/3), 109-146.

Bousquet, R., Goffé, B., Vidal, O., Oberhänsli, R. & Patriat, M., 2002. The tectono-metamorphic history of the Valaisan domain from the Western to the Central Alps: New constraints on the evolution of the Alps. GSA Bulletin, 114(2).

Brouwer, F. M., Burri, T., Engi, M. & Berger, A., 2005. Eclogite relics in the Central Alps: PT-evolution, Lu-Hf ages and implications for formation of tectonic mélange zones. Schweiz. Mineral. Petrogr. Mitt., 85(2/3), 147-174.

Burri, T., Berger, A. & Engi, M., 2005. Tertiary migmatites in the Central Alps: Regional distribution, field relations, conditions of formation, and tectonic implications. Schweiz. Mineral. Petrogr. Mitt., 85(2/3), 215-232.

Engi, M., Todd, C. S. & Schmatz, D. R., 1995. Tertiary metamorphic conditions in the eastern Lepontine Alps. Schweiz. Mineral. Petrogr. Mitt., 75(3), 347-369.

Janots, E., Engi, M., Rubatto, D., Berger, A. & Gregory, C., 2008. In-situ determination of heating rates in collisional orogeny. Geology, accepted.

Köppel, V., Günthert, A. & Grünenfelder, M., 1981. Patterns of U-Pb zircon and monazite ages in polymetamorphic units of the Swiss Central Alps. Schweiz. Mineral. Petrogr. Mitt., 61, 97-120.

Oberli, F., Meier, M., Berger, A., Rosenberg, C. L. & Gieré, R., 2004. U-Th-Pb and 230Th/238U disequilibrium isotope systematics: precise accessory mineral chronology and melt evolution tracing in the Alpine Bergell intrusion. Geochim. Cosmochim. Acta, 68(11), 2543-2560.

Todd, C. S. & Engi, M., 1997. Metamorphic field gradients in the Central Alps. Jour. Metam. Geol., 15, 513-530.

Vernon, A.J., van der Beek, P.A., Sinclair, H.D., Rahn, M.K. 2008. Increase in late Neogene denudation of the European Alps confirmed by analysis of a fission-track thermochronology database, Earth Planet. Sci. Lett. 270, 316-329.

1.13

Subduction Zone anisotropic Patterns Induced by Faulting and Hydration of the Slab

Faccenda Manuele*, Burlini Luigi**, Gerya Taras V.*, Mainprice David***

* *Institute of Geophysics, ETH Zürich, Schafmattstr. 30, 8093 Zürich, Switzerland (faccenda@erdw.ethz.ch)*
** *Institute of Geology, ETH Zürich, Leonhardstr. 19, 8092 Zürich, Switzerland*
*** *Geosciences Montpellier, Université Montpellier II and CNRS, Montpellier, France*

Normal faulting and hydration of the subducting oceanic plate is widely observed at the outer rise of subduction zones.
In order to investigate these processes, we performed 2D numerical models of a spontaneously bending oceanic plate using I2ELVIS code that account for visco-elasto-plastic rheologies. At the outer rise, bending-related slab faulting occurs and provides a pathway for water percolation in the slab. Faults generally deep trenchward, but antithetic faults are also common. As the slab subducts, serpentinized faults acquire a sub-vertical position. The upper part of the slab is, hence, formed by a sub-vertical layering of rocks with different elastic properties (dry and hydrated portions) that, for long wavelength SKS waves, appears as transverse isotropic body with a horizontal axis of symmetry (SPO). Furthermore, hydration of ultramafic rocks leads to the formation of sheet silicates such as lizardite, antigorite, talc and chlorite. Such hydrous minerals are highly anisotropic (80-100%) and tend to orient parallel to the shear zone walls. Hence, along the hydrated normal faults these minerals will tend to align parallel to the faults (LPO).
Calculations of the slab anisotropy lead to ≈1 second time delay for a 30-40 km thick anisotropic layer, depending on the aspect ratio of the hydrated fractures. Indeed, in medium to very old slabs, the vertical distance between the upper and lower planes of the Double Benioff Zone is around 30-45 km.
The spatial distribution of fault sets at the outer rise is consistent with the common trench-parallel orientation of the fast SKS component measured in the forearc. We also found that in areas where the fast SKS component is normal to the trench, fault sets are oriented at high angle respect to the trench. Therefore, slab anisotropy produced by localized hydration of the slab can significantly contribute to the observed splitting patterns at subduction zones.

1.14

Finite element method versus finite difference method: Numerical accuracy study for two different applications

Frehner Marcel*, Deubelbeiss Yolanda*, Schmalholz Stefan M.*,
Kaus Boris J.P.*, Saenger Erik H.**,***, Steeb Holger***

* *Department of Earth Science, ETH Zurich, 8092 Zurich, Switzerland, marcel.frehner@erdw.ethz.ch, yolanda.deubelbeiss@erdw.ethz.ch*
** *Spectraseis AG, 8005 Zurich, Switzerland*
*** *Multi Scale Mechanics, TS, CTW, University of Twente, 7500 AE Enschede, The Netherlands*

Despite its wide-spread use in geology and geophysics, it is unclear whether there is a difference in accuracy between finite element (FEM) and finite difference methods (FDM). For this reason, we here compare the accuracy of the two methods for two different geophysical problems. In both cases an analytical solution is available that provides the exact solution to the respective problem and allows quantifying the numerical errors of the different methods.

The first study considers two-dimensional scattering of elastic waves in a medium containing a circular heterogeneity. Different combinations of the FDM and the FEM are used to approximate both time and space derivatives of the elastodynamic wave equation. The different numerical algorithms are compared for simulations of an incident plane P-wave that is scattered by a mechanically weak circular inclusion whereby the diameter of the inclusion is of the same order than the P-wave's wavelength. Staircase-like spatial discretization of the inclusion's circular shape with the FDM using a rectangular grid provides accurate velocity and displacement fields close to the inclusion boundary only for very high spatial resolutions. Implicit time integration based on either the FDM or the FEM does not provide computational advantages compared to explicit schemes. The best numerical algorithm in terms of accuracy and computation time for the investigated scattering problem consists of a FEM in space using an unstructured mesh combined with an explicit FDM in time.

The second study considers the two-dimensional pressure- and velocity field around a viscous circular inclusion embedded in a mechanically stiffer viscous matrix under pure shear boundary conditions. A number of different FDM and FEM are used to solve the Stokes equations. For the FDM, viscosity needs to be defined at different discrete points in a numerical control volume. The necessary viscosity interpolation is done in different ways, which yields differences in accuracy of up to one order of magnitude. In addition to the standard FDM, markers (i.e. marker-in-cell-technique) are used to carry the material parameters. Harmonic (in some cases geometric) averaging of the viscosity from markers to nodal points yields the most accurate results. Unstructured FEM with elements fitting exactly the material boundary are one to two orders of magnitude more accurate then Eulerian FDM or FEM. If viscosities are directly sampled at integration points of the finite elements, however, the FEM is less accurate than the FDM.

REFERENCES

Frehner, M., Schmalholz, S.M., Saenger, E.H. and Steeb, H., 2008: Comparison of finite difference and finite element methods for simulating two-dimensional scattering of elastic waves, Physics of the Earth and Planetary Interiors, doi:10.1016/j.pepi.2008.07.003

Deubelbeiss, Y. and Kaus, B.J.P., 2008: Comparison of Eulerian and Lagrangian numerical techniques for the Stokes equations in the presence of strongly varying viscosity, Physics of the Earth and Planetary Interiors, doi:10.1016/j.pepi.2008.06.023

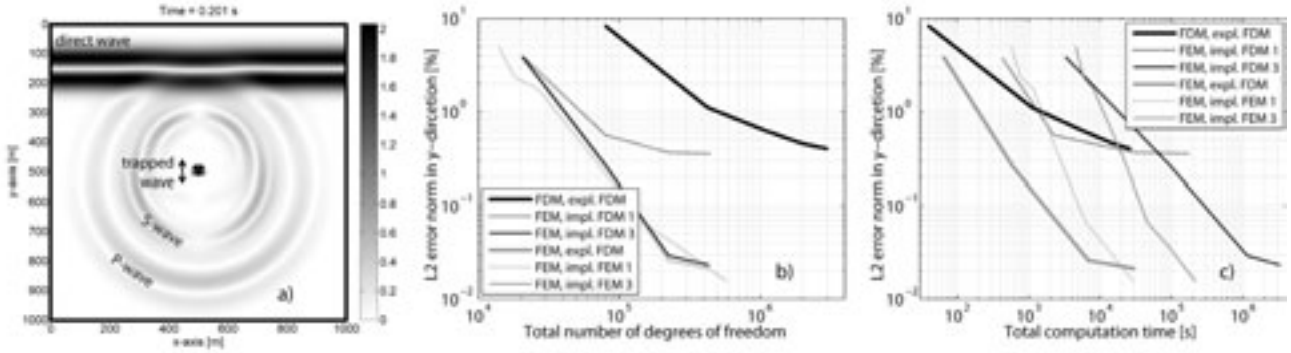

Figure 1: a) Snapshot of the simulated 2D wave field. Plotted is the normalized absolute value of the displacement field ($\sqrt{v_x^2 + v_y^2}$). A plane P-wave travels from bottom to top of the model and is scattered at the inclusion. b) and c) L2 error norm for particle displacement in y-direction versus total number of unknowns in the domain (b) and versus total computation time for the whole simulation (c). Different lines in b) and c) correspond to different numerical methods and/or different implicit time increments. Abbreviations in the legends before the comma (FDM or FEM) stands for the spatial discretization method, second abbreviation stands for the time discretization whereas expl. and impl. refers to explicit implicit time integration, respectively. Implicit time increments for both temporal FDM and temporal FEM are: 1: $\Delta t = 2.37 \bullet 10^{-4}$s, 3: $\Delta t = 2.96 \bullet 10^{-5}$

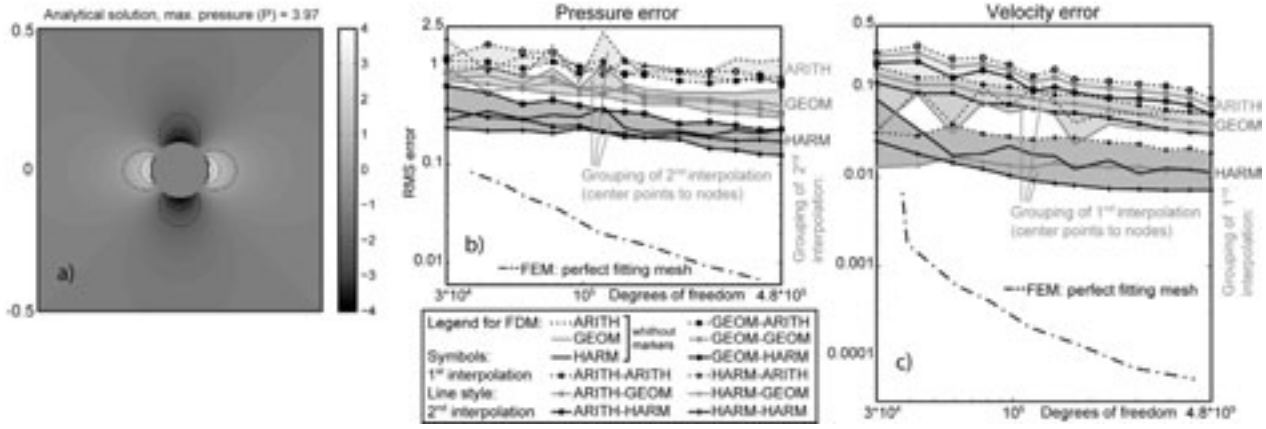

Figure 2: a) Normalized 2D pressure field around clast with pure-shear boundary conditions and viscosity contrast of μ_{clast}/μ_{matrix}=1000. b) and c) RMS error of pressure (b) and velocity (c) versus resolution for different viscosity interpolation methods. Displayed are the staggered grid FDM and the FEM with elements perfectly fitting the material boundary. Most FDM employ markers with viscosity first interpolated from markers to center points (marker2center), then interpolated from center to nodal points (center2node). In cases where no markers are employed (viscosity directly sampled at center points) only the second interpolation step is applied. Both interpolation steps can be performed with harmonic (HARM) or arithmetic (ARITH) averaging.

1.15

Evolution of the Morondava basin shoulder in western Madagascar - an apatite fission-track study

Giese Jörg*, Seward Diane** & Schreurs Guido*

*Institute of Geological Sciences, University of Bern, Baltzerstrasse 1 & 3, CH-3012 Bern, Switzerland (giese@geo.unibe.ch)
**Geological Insitute, ETH Zürich, Leonhardstrasse 19, CH-8092 Zürich, Switzerland

The Morondava basin is the largest and oldest of three Phanerozoic sedimentary basins in Madagascar and is bound to the east by the crystalline basement of Proterozoic age and stretches into the Mozambique Channel to the west (Fig. 1a). The basin is related to the break-up of Gondwana and the separation of Madagascar from eastern Africa. Extensional structures very often reactivated pre-existing ductile structures within the basement (e.g. Montenat et al. 1993; Piqué et al. 1999). The structural style changed from development of local pull apart basins during the deposition of the oldest sedimentary units of Late Carboniferous to Late Permian times, the Sakoa Group, to transtensional and later pure tensional strain during the deposition of the mainly siliciclastic sediments of the Sakamena and Isalo Groups in Middle Permian to Early Jurassic times (Schandelmeier et al. 2004). After a gap in sedimentation, final separation between Madagascar and Eastern Africa was achieved during Middle Jurassic times (Geiger et al. 2004) and Madagascar was displaced relatively southward along the Davie Ridge and parallel oriented fault systems (Coffin and Rabinowicz 1992).

Apatite fission track (AFT) analysis and thermal modelling of a series of 5 basement and 4 sediment samples (depositional age varies between Late Permian and Late Triassic) along a transect across the eastern border of the Morondava basin (Fig. 1b) was carried out in order to refine the exhumation history, topographic evolution and low temperature thermal history of the Morondava basin shoulder. Here, the boundary between the basement and the sediment is characterized by an escarpment with an altitude difference of about 1000 m within ≈10 km of horizontal east-west distance.

Four consecutive basement and all sedimentary samples show progressively younger AFT ages towards the basin. Furthermore, the apparent AFT ages of the sediments are all younger than the corresponding stratigraphic ages, indicating partial annealing of the fission tracks. This partial annealing is most likely caused by an extensive sedimentary overburden, whose thickness increases towards the basin. Modelled time – temperature paths also indicate reburial of the area after sedimentation to temperatures between ≈60 and 80°C for the eastern samples and up to 120°C for the westernmost sample.

REFERENCES

Besairie, H. 1969/70: Cartes géologique de Madagascar (1:500.000), Service Géologique de Madagascar, Antananarivo.

Coffin, M.F. & Rabinowicz, P.D. 1992: The Mesozoic East African and Madagascan conjugate continental margins; stratigraphy and tectonics. In: Watkins, J.S., Feng, Z. & Mc Millen, K.J. (Eds.), Geology and Geophysics of Continental Margins. AAPG, 207-240.

Geiger, M., Clark, D.N. & Mette, W. 2004: Reappraisal of the timing of the break-up of Gondwana based on sedimentological and seismic evidence from the Morondava Basin Madagascar. J. Afr. Earth Sci. 38, 363-381.

Montenat, C., Ramahavory, L. & Croisile, M. 1993: La séquence tectono-sédimentaire de la marge ouest-malgache au Jurassic (bassin de Morondava, Madagascar). C. R. Acad. Sci., Ser. II 317(6), 811-818.

Pique, A., Laville, E., Bignot, G., Rabarimanana, M. & Thouin, C. 1999: L´ouverture et le dévelopment du bassin de Morondava (Madagascar) du Carbonifère supérieur au Jurassic moyen. Données stratigraphiques, sédimentaires, paléontologique et structurales. J. Afr. Earth Sci. 28(4), 931-948.

Schandelmeier, H., Bremer, F. & Holl, H.G. 2004: Kinematic evolution of the Morondava rift basin of SW Madagascar – from wrench tectonics to normal extension. J. Afr. Earth Sci. 38, 321-330.

Seward, D., Grujic, D. & Schreurs, G. 2004: An insight into the breakup of Gondwana: identifying events through low-temperature thermochronology from the basement rocks of Madagascar. Tectonics 23, 1-20.

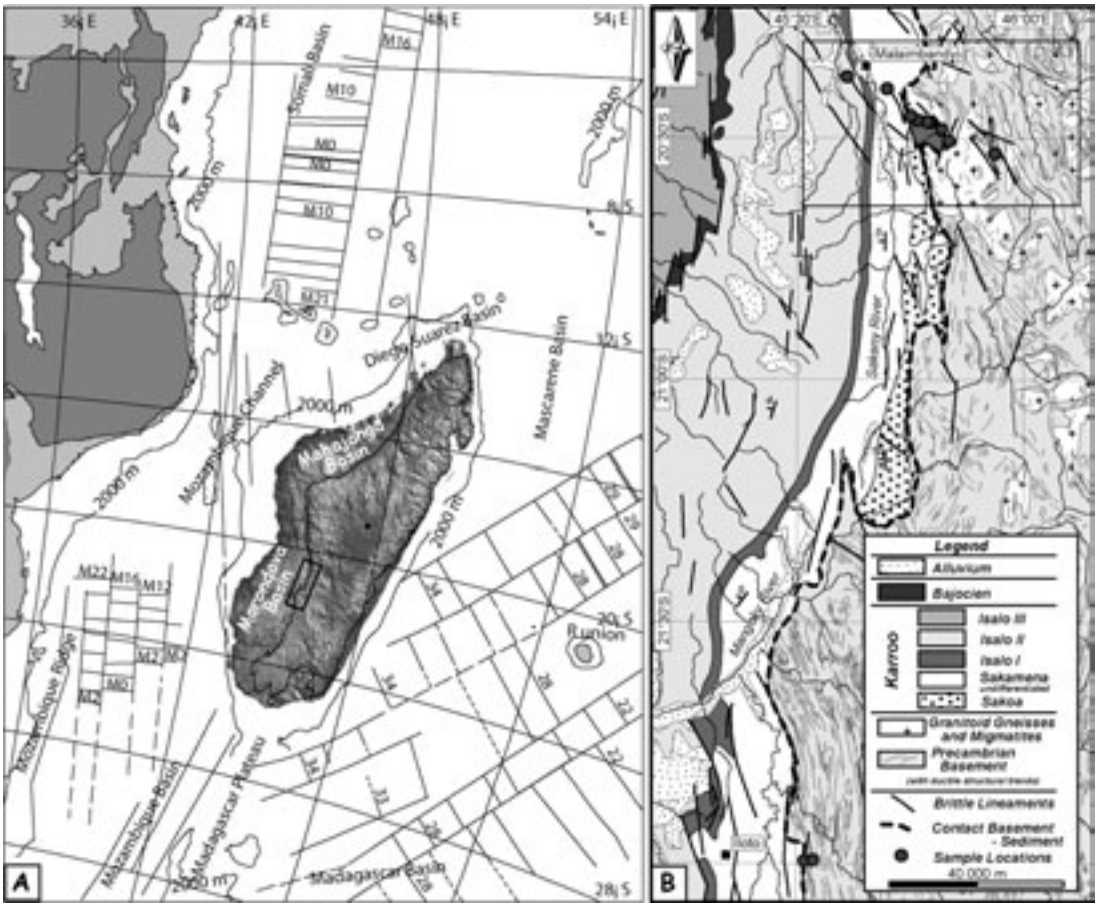

Figure 1: (A) Present day position of Madagascar (background DEM) with location of sedimentary basins, magnetic anomalies and transform faults at the ocean floor, box indicates position of (B), figure modified after Seward et al. (2004). (B) detailed geological map (modified after Besairie (1969/70)) with sample locations.

1.16

Recent Site Motions in the Lower Rhine Embayment from 15 years of GPS data

Görres Barbara

Institute of Geodesy und Geoinformation, University of Bonn, Nussallee 17, D-53115 Bonn
(goerres@uni-bonn.de)

As a part of the West European Rift System horizontal and vertical site motions occur in the Lower Rhine Embayment due to present-day seismo-tectonic activity as well as extensive brown coal mining. The intensive brown coal mining activities occurring since the mid-fifties of the last century in the Lower Rhine Embayment have caused massive landscape changes. Less obvious but equally dramatic are the effects on the earth's surface such as ground movements which are mainly due to groundwater withdrawal associated with the ongoing open pit mining activities. Larger discontinuities in the pattern of motion tend to appear at pre-existing fault lines and are causing sizable damage to buildings and roads.

Precision levellings have been supplemented by GPS observations since 1992 to measure the ground motions and monitor their behaviour with high accuracy.

Less prominent are the site motions due to recent tectonics smaller by at least an order of magnitude and only marginally detectable. Indications of a south-west to north-east extension of the Lower Rhine Embayment had been visible after 7 years (Campbell et al. 2002). Also visible was a small uplift of about 1 mm/y at two points in the Eifel near the Belgium Border

which seems to be consistent with the uplift of the Rhenish Shield as seen in earlier levelling results.

Having continued with the GPS observations and carried out an extension of the network as a coverage of the Northern Rhenish Massif up to 50 measuring points can be analysed which also include the observations in the Ardennes on Belgian territory (Demoulin et al. 2005).

As a recent example, the measurements of the local deformation GPS network 'Donatussprung', a section of the Erft Fault system where the surface trace can be identified from topography and effects on buildings and roads, have revealed displacements of up to 6 mm/y in horizontal and 22 mm/y in vertical direction with high accuracy (Görres & Kuhlmann 2008). Vertical and horizontal motions due to recent tectonics in this region are smaller by at least an order of magnitude. The observed pattern of vertical and horizontal velocity vectors shows a remarkable difference in the motion of point groups on either side of the fault. The scenario suggested by these measurements indicates that the sediment layers on the Erft Block are indeed sinking in proportion to the groundwater withdrawal, but that near the fault the pattern of motions is strongly influenced by the fault geometry. Modelling options include mining subsidence troughs as well as fault slip motion.

There is reasonable hope that after 15 years of annual GPS observations in an entire reprocessing of all points and all observation epochs (currently worked on) the indications (Extension and Uplift) can be clarified.

REFERENCES

Campbell, J., Kümpel, H.-J., Fabian, M., Fischer, D., Görres, B., Keysers, Ch., & Lehmann, K. 2002: Recent movement pattern of the Lower Rhine Basin from tilt, gravity and GPS data, Netherlands Journal of Geosciences/ Geologie en Mijnbouw, Vol. 81 (2), 223-230.

Demoulin, A., Campbell, J., De Wulf, A., Muls, A., Arnould, R., Görres, B., Fischer, D., Kötter, T., Brondeel, M., Van Damme, D., & Jacqmotte, J.M. 2005: GPS monitoring of vertical ground motion in northern Ardenne-Eifel: five campaigns (1999-2003) of the HARD project, Int. J. Earth Sci (Geolog. Rundsch) 94: 515-524.

Görres, B. & Kuhlmann, H. 1998: How groundwater withdrawal and recent tectonics cause damages of the earth's surface: Monitoring of 3D site motions by GPS and terrestrial measurements, Journal of Applied Geodesy, 1(2008), 223-232, deGruyter Berlin, DOI 10, 1515/JAG.2007.024.

1.17

Terrestrial core formation aided by flow channelling instabilities induced by iron diapirs

Golabek Gregor*, Tackley Paul* & Schmeling Harro**

*Institut für Geophysik, Geophysical Fluid Dynamics, Schafmattstrasse 30, CH-8093 Zürich (gregor.golabek@erdw.ethz.ch)
**Institut für Geowissenschaften, Facheinheit Geophysik, Altenhöferallee 1, D-60438 Frankfurt am Main

The terrestrial core formation process remains poorly known. Isotopic constraints by Hf/W systematics indicate a fast process which was largely completed within 33 Ma for the Earth. An unstable gravitational configuration of dense molten metallic ponds overlying a chondritic protocore is predicted by most studies at latest for the time a planetary embryo reaches Mars size. This leads to the formation of Rayleigh-Taylor instabilities. We propose the application of Stevenson's stress-induced melt channelling mechanism in the regions surrounding incipient iron diapirs. We therefore perform numerical experiments solving the two-phase, two compositions flow equations within a 2D rectangular box. We apply the Compaction Boussinesq Approximation (CBA) and include a depth-dependent gravity. We use a temperature and stress-dependent viscosity for the solid phase and melt fraction dependent rheology for the partially molten region around the diapir. We investigate the development of the channelling instability in cases with and without interaction with surrounding diapirs. In interactive cases we vary the distance between the diapir centres between 1 and 5 diapir radii and apply pseudoplasticity with power law exponents ranging from 1 to 6. As a result for single diapirs we observe for sufficiently small retention numbers the development of iron-rich melt channels within a region of approximately twice the diapir's radius. This could lead to effective draining of the surrounding region and might initiate cascading daughter diapirs or iron dykes. For small distances between interactive diapirs the channelling mechanism is delayed for several million years compared with models without

close-by neighbours. Channels seem also to develop preferentially in directions pointing away from the closest neighbouring diapir. The iron channels propose an effective mechanism to extract iron melt also from deeper parts of the initially chondritic protocore. This mechanism could effectively enhance melt accumulation in the Earth's protocore, accelerate the process of iron core formation and affect the metal-silicate equilibration in the deep planetary interior prior the Moon-forming giant impact. Therefore the channelling mechanism could also be interesting for planets like Mars, which probably never experienced complete melting.

REFERENCES

Melosh, H.J. 1990: Giant impacts and the thermal state of the early Earth, in: Origin of the Earth, 69-83.

Rubie, D.C., Melosh, H.J., Reid, J.E., Liebske, C. & Righter, K. 2003: Mechanisms of metal-silicate equilibration in the terrestrial magma ocean, Earth and Planetary Science Letters, 205, 239-255.

Schmeling, H. 2000: Partial Melting and Melt Segregation in a Convecting Mantle, in: Physics and Chemistry of partially molten rocks, 141–178.

Stevenson, D.J. 1989: Spontaneous small-scale melt segregation in partial melts undergoing deformation, Geophysical Research Letters, 16, 1067–1070.

Tackley, P.J. & Stevenson, D.J. 1993: A mechanism for spontaneous self-perpetuating volcanism on the terrestrial planets, in: Flow and Creep in the Solar System: Observation, Modeling and Theory, 307-321.

1.18

Rheological controls on the terrestrial core formation mechanism

Golabek Gregor*, Gerya Taras* & Tackley Paul*

Institut für Geophysik, Geophysical Fluid Dynamics, Schafmattstrasse 30, CH-8093 Zürich (gregor.golabek@erdw.ethz.ch)

Knowledge about the terrestrial core formation mechanism is still very limited. The fracturing mechanism was proposed for cold central protocores surrounded by an iron layer, which develops from the overlying magma ocean. In this case the cold protocore is displaced from the centre of the accreting planet and fractured due to the large stresses, whereas the consideration of short-lived radioactive radioactive heating may result in warmer central regions and the preference of iron diapirism as core formation mechanism. Until now most numerical models of core formation via diapirism were limited to the simulation of the sinking of a single diapir. We perform 2D spherical simulations using the code I2ELVIS applying the newly developed "spherical-Cartesian" methodology combining finite differences on a fully staggered rectangular Eulerian grid and Lagrangian marker-in-cell technique for solving momentum, continuity and temperature equations as well as the Poisson equation for gravity potential in a self-gravitating planetary body. In the model the planet is surrounded by a low viscosity ($\eta = 10^{19}$ Pa s), massless fluid ("sticky air") to simulate a free surface. We applied a temperature- and stress-dependent viscoplastic rheology inside Mars- and Earth-sized planets and included heat release due to radioactive decay. As initial condition we use randomly distributed diapirs with random sizes in the range 50 to 100 km radius inside the accreting planet, which represent the iron delivered by predifferentiated impactors. A systematic investigation of the diapir behaviour for different activation volumes and yield stresses is being performed, and results are being compared to the isotopic time scale of core formation on terrestrial planets. We show that the rheology controls which formation mechanism becomes dominant.

We observe 3 major regimes of core formation: First a weak viscous protocore for low activation volumes and low yield stress, which is very similar to the already modelled diapirism. Second a plastic protocore for high activation volumes and low yield stress, which shows a mixture of diapirism and the fracturing mechanism even in warm planetary conditions. We find that the diapir sinking in this case may differ significantly from previous assumptions as we observe large asymmetries induced by a collective Rayleigh-Taylor like behaviour of neighbouring diapirs, which leads to the formation of "convective channels". The final regime is the strong protocore, which develops an asymmetric iron layer surrounding the central part of the planet. It requires heating by radioactive decay and/or displacement of the central region towards the surface due to gravitational instability of the iron layer to allow for iron core formation.

REFERENCES

Karato, S.-i. & Murthy, V.R. 1997: Core formation and chemical equilibrium in the Earth I. Physical considerations, Physics of the Earth and Planetary Interiors, 100, 61-79.

Lin, J.-R., Gerya, T.V., Tackley, P.J. & Yuen, D.A. 2008: Primordial core destabilization during planetary accretion: Influence from deforming planetary surface, Icarus, in revision.

Gerya, T.V. and Yuen, D.A. 2007: Robust characteristics method for modelling multiphase visco-elasto-plastic thermo-mechanical problems, Physics of the Earth and Planetary Interiors, 163, 83-105, doi:10.1016/j.pepi.2007.04.015.
Sasaki, T. & Abe, Y. 2007: Rayleigh-Taylor instability after giant impacts: Imperfect equilibration of the Hf-W system and its effect on the core formation time, Earth Planets and Space, 59, 1035-1045.
Schmeling, H. et al. 2008: A benchmark comparison of spontaneous subduction models - Towards a free surface, Physics of the Earth and Planetary Interiors, doi:10.1016/j.pepi.2008.06.028, in press.
Stevenson, D.J. 1981: Models of the Earth's core, Science, 214, 611–619.
Ziethe, R. & Spohn, T. 2007: Two-dimensional stokes flow around a heated cylinder: A possible application for diapirs in the mantle, Journal of Geophysical Research, 112, B09403, doi:10.1029/2006JB004789.

1.19

Interaction between meteoric and metamorphic water along the Simplon fault zone: constraints from oxygen and carbon stable isotope geochemistry

Guerra Ivan* ***, Vennemann Torsten**, Mancktelow Neil***, Negro François* & Kalt Angelika*

*Institut de Géologie et d'Hydrogéologie, Université de Neuchâtel, Rue E. Argand 11, CH-2009 Neuchâtel (ivan.guerra@unine.ch)
**Institut de Minéralogie et Géochimie, Université de Lausanne, L'Anthropole, CH-1015 Lausanne
***Geologisches Institut, ETH Zürich, Leonhardstrasse 19, CH-8092 Zürich

The role of fluids during faulting and fracturing associated with the Miocene to present exhumation of the Lepontine dome is examined along its south-western border, the Simplon Fault Zone (SFZ). The latest generation of tension gashes, major regional fault families and fault rocks were studied to establish their geometric relationships, the time of activity and the composition of the circulating fluids.

Structural data show that the major strike orientation of late tectonic structures is NW-SE, i.e. parallel to the major crustal Simplon fault. Two other important strike directions, NE-SW and E-W, can be also highlighted. The E-W direction appears to be the latest one. Most measured fault planes are normal faults, consistent with extension and exhumation of the region since the Miocene.

Oxygen stable isotope analyses on filling material of late tectonic structures mentioned above - both in the hanging wall and footwall of the SFZ - reveal two different fluid circulation systems. In the footwall, all along the SFZ, the $\delta^{18}O$ values of quartz both for host rock and late veins range between 10 ‰ and 12 ‰ – which are values typical for metagranitic rocks. This supports complete buffering of infiltrating, circulating fluids by the host rock prior to fracturing and vein precipitation.
In the Simplon hanging wall the situation is different: similar $\delta^{18}O$ values for quartz from host rock and late veins are found at the northern and southern part of the detachment. In these two areas both hanging wall and footwall have the same metamorphic degree: greenschist facies to the north and amphibolite facies to the south. In contrast, in the central part of the SFZ the $\delta^{18}O$ values for quartz from the hanging wall late veins are approximately 3.0 ‰ lower than the values observed in the footwall (8.0 ± 0.4 ‰ and 11.1 ± 0.8 ‰ respectively; modern meteoric water has a $\delta^{18}O$ value of around -13 ‰). In this region there is an offset in metamorphic degree: greenschist facies in the hanging wall and amphibolite facies in the footwall.

Field observations indicate that the Simplon footwall has been less affected than the hanging wall by the brittle deformation occurred starting from 8-12 Ma (Campani et al., 2008); the hanging wall is also much more pervasively fractured than the footwall. These observations, together with the distribution of the Alpine metamorphism and the isotopic values obtained, may indicate that the diffusion of meteoric water along the SFZ has probably been controlled by brittle extensional deformation style, temperature (i.e. closure temperature to diffusive exchange) and perhaps deformation/recrystallization style to the oxygen isotope exchange between an infiltrating fluid and the host rock to the veins. The isotopic data collected along the SFZ also reflect a rock-buffered system in the footwall and a meteoric fluid influenced system in the hanging wall. In this context the clay-rich fault gouge marking the detachment is acting as an impermeable barrier - if such fluid-rock exchange occurred together with or after the displacement along the fault – helping the differences in meteoric water diffusion.

Oxygen stable isotope investigations in progress for mineral pairs in structural and chemical equilibrium (i.e. quartz-muscovite, quartz-hematite, calcite-muscovite, quartz-calcite) in late veins will give precise indications on their formation temperature, while oxygen and carbon stable isotope analyses on carbonates will provide additional information on the origin of circulating metamorphic fluids.

REFERENCES

Campani, M., Mancktelow, N.S., Seward, D. & Rolland, Y.: Thermochronological evidence for a continuous transition from ductile to brittle deformation in the Simplon low-angle normal fault, Central Alps. 2008 EGU General Assembly, abstract EGU2008-A-02179

1.20

Brittle tectonics in the Swiss Molasse Basin

Ibele Tobias*, Matzenauer Eva*, Mosar Jon*

**Département de Géosciences Université de Fribourg, Chemin du Musée 6, CH-1700 Fribourg (tobias.ibele@unifr.ch)*

In an ongoing study we examine the tectonic and neotectonic structures of the Molasse Basin of the Canton Fribourg and adjacent areas in western Switzerland. Extensive field work allows us to determine the type and spread of structures, as well as the style and grade of deformation observed in the outcrops. The preliminary results of this work and the scope of our future research are presented in the poster.

Due to late Tertiary alpine tectonics the region investigated is structurally subdivided into several zones: 1) The subalpine Molasse, resembling a narrow bend of inclined and imbricated rocks at the former front of the alpine fold and thrust belt, 2) the Plateau Molasse being affected only by very flat ample folds and extending throughout most of the study area.

Within the Sandstones, mudstones and scarce conglomerates of the Lower Freshwater and Upper Marine Molasse (USM and OMM) of the study area we observed the following brittle structures: Joints and fractures, slickensides, deformation bands in sandstones and pitted/fractured pebbles in conglomerates. The brittle deformation is regional extended but the structures are not uniformly distributed. Areas of undisturbed rock are present, separated by as strongly fractured areas with well developed fault zones containing cataclasites and fault gauges.

The brittle structures observed in the field are steeply inclined and show a Riedel-type pattern. The tectonic regime is of nearly pure strike slip nature, expressed in WNW-ESE striking right lateral and NNW-SSE striking left lateral shear zones that are governed by an overall NW-SE orientated sub-horizontal maximum compressive stress. More detailed investigation of the deformation bands and deformation band shear zones in the sandstone will probably allow us to determine successive stages of deformation. Their intersection relationships seam to show cyclic stress rotations between strain increments.

The timing of deformation is not yet well determined by our field observations but since some published data of Quaternary deformation and focal mechanisms of recent earthquakes show the same kinematics as inferred from the field data it may be speculated that the deformation is recent and possibly still ongoing.

1.21

Stress and strength of the continental lithosphere.

Kaus Boris*,**

*Geophysical Fluid Dynamics, Department of Earth Sciences, Schaffmattstrasse 30, CH-8093 Zurich (boris.kaus@erdw.ethz.ch)
**University of Southern California, Los Angeles, USA.

The processes that generate stress in the lithosphere are incompletely understood. Whereas it is obvious that lithospheric deformation (and topography) is ultimately caused by cooling of the Earth from the time of formation, it is less clear how lithospheric deformation is coupled to mantle flow and how this affect stresses. Part of this is due to the somewhat complicated rheology of the lithosphere, which varies from brittle (elastoplastic) to ductile (viscous). In addition, vertical layering of the lithosphere may give rise to instabilities which affect its dynamics and stress evolution in a non-trivial manner. Obtaining a better insight in these processes thus requires numerical tools that can model the mantle-lithosphere system in a self-consistent manner (i.e. in a single computational domain) including topographic effects (i.e. free surface) and visco-elasto-plastic rheologies.

Recently, a number of modelling techniques have been developed that have the above-mentioned features and that are useful to model long-term tectonic scenarios (on a Myrs) timescale. A problem, however, with many of these long-term tectonic simulations is that they are computationally expensive and that the parameter space is too wide to sample with brute-force forward simulations. For this reason, I take a different approach and use the numerical technique to obtain insight in the most likely present-day rheological stratification of the lithosphere. The advantage of such quasi-instantaneous lithospheric models is that they require only a few timesteps per simulations and can therefore cover a wider parameter space. Moreover, they take relatively well-constraint geophysical data such as Moho depth, topography, GPS velocity and earthquake locations as input.

Model results, applied to the India-Asia collision zone and to Taiwan demonstrate that the approach gives constraints on the effective viscosity and rheological stratification of the lithosphere. They also show that the distribution of high effective viscosities, representing the strength distribution in the ductilly and plastically deforming areas of the lithosphere, does not necessaily correspond to the distribution of high differential stresses, presumably representing the areas of high earthquake activity. The reason is that strain rates are not necessarily constant with depth in continental collision zones, as assumed in constructing yield strength envelopes (‚Christmas trees') and thin-sheet models. A direct transformation from stress to strength (i.e. effective viscosity) in the lithosphere is not possible without knowledge of the strain rate distribution. Consequently, the analogy of lithospheric areas with high earthquake activity and lithospheric areas with high mechanical strength is questionable for continental collision zones.

In the case of the India/Asia collision, results show that differential stresses in the mantle lithosphere underneath the Himalaya and Tibet are small even if it is strong (i.e. has a large effective viscosity). The scarcity of large earthquakes underneath the Moho in this region can thus not be used as evidence for a weak (or water-rich) mantle lithosphere.

1.22

Implementation and geodynamical application of iterative and multigrid solvers for 2D finite-element Stokes flow

Keller Tobias*, Kaus Boris*

*Geophysikalisches Institut, Schafmattstrasse 30, CH-8093 Zürich

The standard approach to solve problems with the finite element method usually involves the use of a direct solver. To do so, the global stiffness matrix **L** is assembled to bring the problem into the well known and useful form **Lx = R**. To solve this system of equations in a direct way, a large number of methods including sophisticated elimination schemes, preconditioning or matrix decomposition methods have already been tested against each other, e.g. (May & Moresi 2008). One approach that is used less frequently, is to solve the set of equations with an iterative scheme. This scheme is relatively easy to implement, but requires many iterations per timestep. To overcome the weakness of iterative solvers, a multigrid solver can be

developed on the basis of simple iterations. By taking iteration on several levels of coarser grids, the residual of the equations is simultaneously relaxed over a wide range of wavelength. This usually speeds up iterative solvers to a large extent. Additionally, the solution speed scales only linearly with grid resolution and therefore is especially attractive to use in high resolution simulations.

Here, we compare a number of iterative and direct solver techniques (including multigrid) for solving the 2D Stokes equations with a finite-element approach. In a first step, we use an iterative Gauss-Seidel smoother on only one grid level. As a second step we employ this smoother in a multigrid solver. Performance tests are employed to evaluate the effectiveness of the various techniques for a number of geodynamics test scenarios.

REFERENCES

May, D. A. & Moresi, L. 2008: Preconditioned iterative methods for Stokes flow problems arising in computational geodynamics, PEPI (in press).

1.23

Change of deformation mechanism of quartz with increasing strain in mylonites

Kilian Rüdiger, Heilbronner Renee, Stünitz Holger*

Geological Institute, Basel University, Switzerland, Bernoullistr. 32, 4056 Basel, ruediger.kilian@unibas.ch
**Geological Institute, University Tromsø, Norway*

The microstructural and textural evolution of a small scale metagranodiorite shear zone from the Gran Paradiso nappe (Western Alps) is studied in detail.
The shear zone formed at lowermost amphibolite facies conditions. Quartz deformed as the mechanically stronger phase in a fine grained matrix of biotite and decomposed plagioclase grains with a grain size of approx. 5-15 μm. In the coarse aggregates, quartz textures are measured using the CIP method (Panozzo Heilbronner & Pauli, 1993). EBSD is used for the analysis of the fine grained phase mixtures.

In the core of the shear zones two microstructurally different parts can be defined.

In the mylonitic outer part of the shear zone, layers of recrystallized quartz and matrix are parallel to the shear zone boundary. Quartz deforms by dislocation creep. Recovery is dominated by grain boundary migration recrystallization and minor subgrain rotation recrystallization. Quartz c-axis crystallographic preferred orientations (CPO) typically show synthetically rotated peripheral maxima and - occasionally - weak single girdles coinciding with the activity of basal <a> and only minor prism <a> slip (Fig.1a).
Calculations using estimates of the shear strain accommodated in the quartz aggregates, recrystallized grain size piezometry and quartz flow laws yield strain rates 5 to 10 times higher in the matrix than in quartz aggregates.

The ultramylonitic central part of the shear zone shows compositional layering consisting of feldspar layers, relict recrystallized quartz aggregates and phase mixtures with single quartz grains dispersed in the matrix. Quartz aggregates are boudinaged at the grain scale with primarily K-feldspar precipitating between torn apart grains. No fractures penetrating quartz grains were observed. Large quartz grains still reflect the size of the quartz aggregates of the mylonitic part they originate from but do not show subgrain structures. Small quartz grains below 10 μm are evenly dispersed in the ultramylonite and spatially unrelated to the disrupted aggregates. The quartz CPO is generally weakened compared to the mylonitic part of the shear zone (Fig.1b). The larger grains reflect the geometry of the original CPO in the mylonite with peripheral, inclined c-axis orientations. The smallest grains (< 3μm) show a very different CPO with c-axes close to the centre of the polefigure (Fig.1c). Intermediate grain sizes have a close to random orientation.

The disruption process and the randomization of the CPO is interpreted to be caused by dissolution-precipitation accommodated granular flow. There is no evidence for fracturing or dynamic recrystallization driving further grain size reduction of the quartz in the ultramylonite. Dissolution-precipitation and growth of quartz can account for its spatial distribution in the ultramylonite. The peculiar CPO of the smallest grains can not be understood in terms of normal quartz growth but could be explained by a preferred orientation of nuclei or faster growth perpendicular to the c-axis in the imposed stress field.

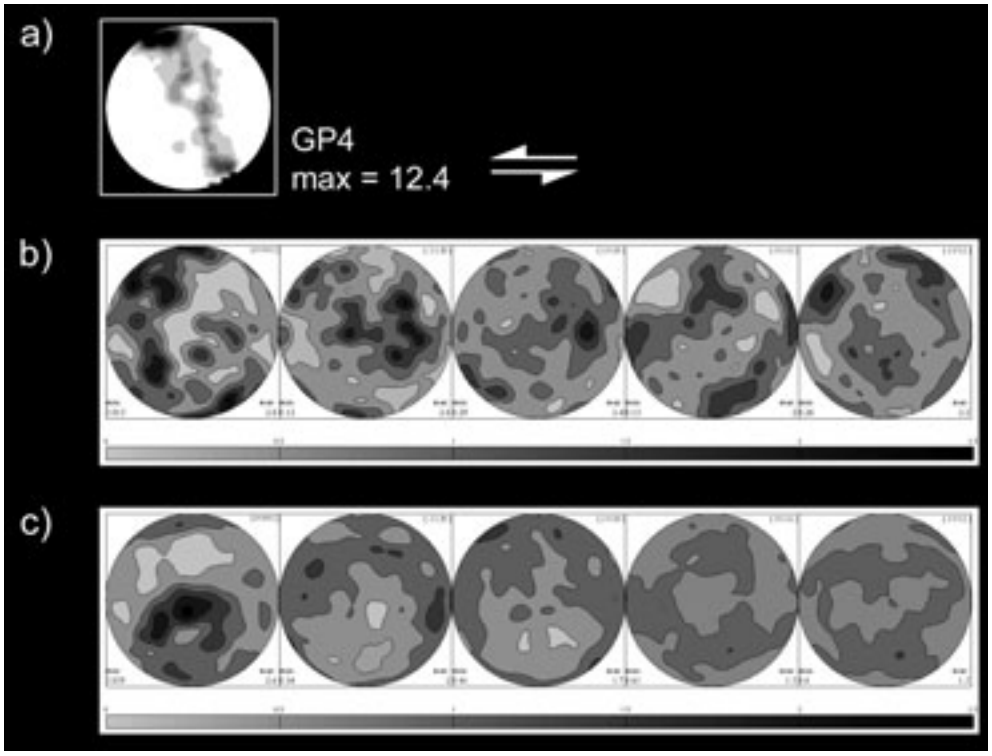

Figure 1: a) CIP derived c-axis pole figure of the mylonitic part of the shear zone. b) Polefigures of grains larger 40 μm in the ultramylonite. c) Polefigures of grains smaller 3 μm in the ultramylonite. Shear sense is sinistral .

REFERENCES
Panozzo Heilbronner, R. and Pauli, C., 1993. Integrated spatial and orientation analysis of quartz c-axes by computer-aided microscopy. J. Struct. Geol., 15 (3-5): 369-382.

1.24

Physical properties of granular materials for analogue modelling.

Klinkmüller Matthias*, Rosenau Matthias**, Kemnitz Helga** & Schreurs Guido*

*Universität Bern, Institut für Geologie, Baltzerstrasse 1-3, CH-3012 Bern, Schweiz
**Helmholtz-Zentrum Potsdam, Deutsches GeoForschungsZentrum GFZ, Telegrafenberg, D-14473 Potsdam, Deutschland
Corresponding author: matthias@geo.unibe.ch

An improved knowledge of the mechanical behaviour of granular material is essential to determine their suitability for simulating brittle deformation. Here we report mechanical tests on granular analogue materials used by different laboratories worldwide. We performed ring shear tests, uniaxial compression tests, creep tests and analysed grain characteristics by means of sieve analysis and scanning electron microscope analysis. In total, 18 dry sands have been mechanically characterized.
Parameters of frictional strength of dry sands have been determined by ring shear testing at experimental conditions (< 2150 Pa normal load, 3 mm/min shear velocity, 23-25°C, 30-40% humidity). Parameters include the friction coefficient and apparent cohesion during formation of a shear zone ("peak" strength), during sliding on an existing shear zone ("stable dynamic" strength) and during reactivation of a pre-existing shear zone ("stable static" strength). For sand, peak strength is generally highest followed by static stable and dynamic stable strength. For the sands tested, friction coefficients range between 0.65 – 0.82 for peak strength, 0.50 – 0.74 for static stable strength and 0.53 – 0.69 for dynamic stable strength. Apparent cohesion is in the order of 10 – 100 Pa. We found no significant correlation between friction parameters and grain size or grain size distribution but a correlation with grain shape. Accordingly, peak, static and dynamic friction coefficients increase linearly by a value of about 0.1 as the fraction of angular grains increases from 0 – 100 %. This is consistent with previous findings of Mair et al. (2002) who suggested that shear strain in synthetic fault gouges is accommodated by mechanisms of rolling of spherical particles versus sliding of angular particles with the latter requiring higher stresses. Grain shape in combination

with grain size and sorting seems also to control frictional stability: A single fine-grained, well-sorted sand from Taiwan dominated by rounded grains shows distinctive stick-slip behaviour. This is consistent with current ideas of stick-slip of bulk solids as a phenomenon controlled by the breakdown of force-chains that is promoted by round particle shape and a narrow particle size distribution (e.g. Mair et al., 2002).

Under laterally confined axial loading, the stress-strain relationship of dry sand reflects both elastic and inelastic deformation (i.e. compaction). We determined elasticity and compaction behaviour of dry sands by uniaxial compression tests. We performed 50 loading-unloading cycles up to 2 MPa. Induced strains decrease from about 1 % in the first cycle to 0.1 % in the last cycle. About 50 – 90 % of total strain during loading in the first cycle is inelastic (i.e. remains as compaction). Compaction decreases to less than 10% over 50 cycles. Again, we found that the compaction behaviour of sieved dry sand is controlled by grain shape: Sands composed of dominantly rounded grains compact less under a given load than sands composed dominantly of angular grains. This is probably due to the fact that rounded sand grains arrange in closer packing during sieving than angular grains. We thus expect analogue models composed of angular grains to accommodate more diffuse volumetric strain than models with spherical grains. Apparent bulk moduli have been determined by regression through the loading branch of the stress-strain curve and range from about 100 – 400 MPa (1st cycle) to 700 – 1500 MPa (50th cycle). The lower ones are representative for experimental conditions (sieved sand layers) and the higher ones reflect the properties of highly compacted sand layers not realized in analogue modelling.

By combining and weighting parameters, which may control strain localization in granular media (i.e. compaction, grain size, density, frictional and elastic strength), we can calculate a “structural attractor index” for each sand reflecting the affinity of a model composed of this material to form new structures during its evolution. The prediction may be tested in future benchmark initiatives.

REFERENCES

Mair, K., Frey, K. M., & Marone C. 2002: Influence of grain characteristics on the friction of granular shear zones, Journal of Geophysical Research, 107(B10), 2219.

1.25

Calculation of Tide Correction in Precise Levelling of IRAN

Kordi Kobra*, Arabi Siavash*, *

**National Cartographic Center in IRAN(NCC) (kobra_kordi@yahoo.com)*

One of the Geodetic measurment methods is Precise Levelling. We can calculate Height's points with Precise Levelling. We shoud Estimate all corrections for get to result with high accuracy. One of them Tide corrections. We get the appropriate correction as Vanicek Formula 1980. To calculate any of the above corrections, it is necessary to evaluate numerically either the tidal potential or some of its horizontal derivatives. Tidal potential computing of Tidal accelerations due to the Moon and the Sun. This correction Depends on Azimuth.

Here we focus on Iran Levelling Network. This network has 167 lines. We calculated Tide Correction on Levelling Measurments in per Section. Length of section is 2 Kilometers. Maximum value of tide correction for one section is 0.005 millimeters. This value is very small in compersion with others corrections. We can ignore effect of Tide on Levelling observation.

REFERENCES

Vanicek, P., & Krakiwsky, E.,1986: Geodesy the concepts.

Vanicek, P., M.R. Elliott & R.O. Castle 1980: Geodetic Levelling and its applications. Rev. Geophys. and Space Phys. 18(2), pp. 505-524.

Longman, I.M., 1959: Formulas for Computing the Tidal Accelerations Due to the Moon and the Sun. Journal of Geophysical, Volume 64, No. 12.

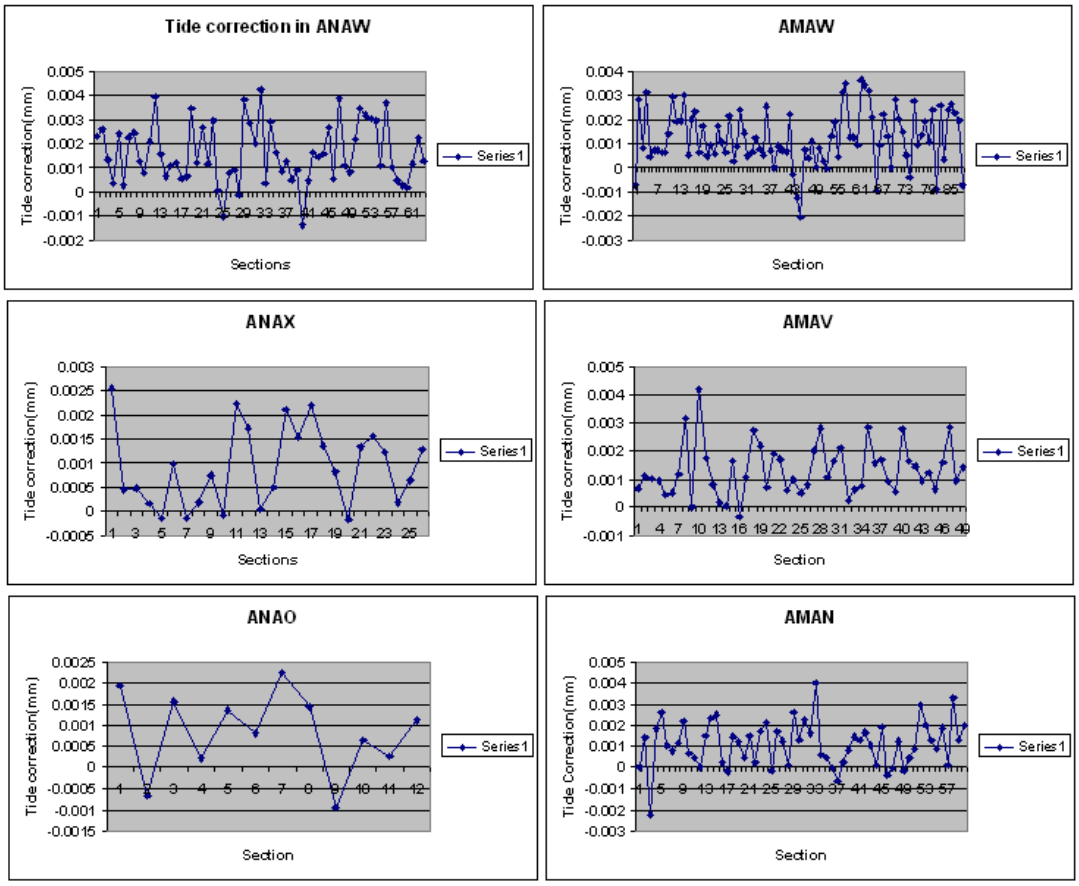

1.26

Calculation of Orthometric Correction with Geopotential Models

Kordi Kobra*, Arabi Siavash*, *

National Cartographic Center in IRAN(NCC) (kobra_kordi@yahoo.com)

In Presice Levelling for calculate height points with high accuracy, it is necessary that we estimate Orthometric Correction. We need to height and Gravitty of two point. Height of point calculate in Precise Levelling and we should compute gravity of point.

There are many way for determine Gravity acceleration. We can measure gravity of point directly. We can use Coordinate of point and Geopotential Coefficients and compute its Gravity. Usually used of Direct measurement for determine Gravity. If results of Geopotential model to be near the result of Direct measurement, we can use the Geopotential Models for our aid.

In this paper, 3 Geopotential model use in research. These models are EGM96, Grace & Eigen-2. We focus on 3 loops of Iran Precise Levelling Network. Result of four models show in fig(1), fig(2) and fig(3).

Orthomethric Correction calculated for Levelling Lines with used four model. There is difference between geopotential models and measurements, so Directly measurements is better method for determine Orthometric correction.

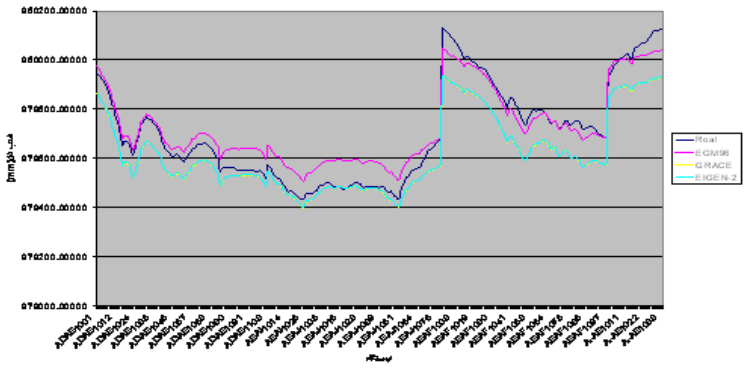

Fig. 1) Compersion of results of Geopotential models with Direct measurement for loop AE

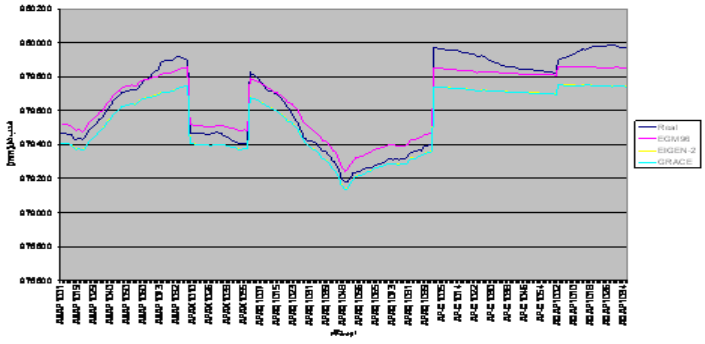

Fig. 2) Compersion of results of Geopotential models with Direct measurement for loop AP

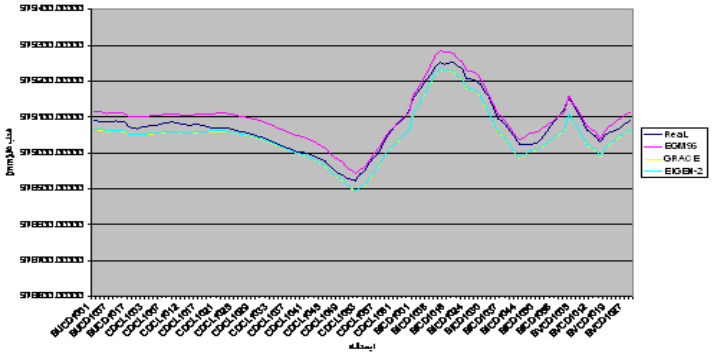

Fig.3) Compersion of results of Geopotential models with Direct measurement for loop CD

REFERENCES

Vanicek, P., & Krakiwsky, E.,1986: Geodesy the concepts.

1.27

Tectonic evolution and denudation of the Atlantic passive margin: New insights from apatite fission-track analysis on the western coast of South Africa.

Kounov Alexandre*, Viola Giulio**, de Wit Maarten***, Andreoli Marco**** & Niedermann Samuel*****

*Institute of Geology and Paleontology, Basel University, 4056 Basel, Switzerland (a.kounov@unibas.ch)
**Geological Survey of Norway, 7491 Trondheim, Norway
***AEON and Department of Geological Sciences, UCT, 7701 Rondebosch, South Africa
****South African Nuclear Energy Corporation, PO Box 582, 0001 Pretoria, South Africa
*****GeoForschungsZentrum Potsdam, Telegrafenberg, 14473 Potsdam, Germany

Continental passive margins with high elevation have been of particular interest to the geoscience community due to their impressive geomorphological features, including a low-lying coastal plain separated from an elevated inland region by seaward-facing escarpments. In the early schemes of margin evolution, the formation of the escarpment was generally attributed to the downflexing of the lithosphere and the development of a broad monocline that was subsequently eroded by backwearing during successive denudational phases (e.g. King 1953)

Over the past two decades a number of low-temperature thermochronological studies, including apatite fission-track (AFT), (U-Th)/He and cosmogenic nuclide analysis, have provided new quantitative geochronological constraints on the denudational history of passive margins, thus allowing the testing of earlier evolutionary models (e.g. Brown et al. 2000; Cockburn et al. 2000). Based on these recent geochronological advances, new conceptual models have been proposed that differ from the classical escarpment retreat (backwearing) schemes essentially in the character of the post break-up tectonics, the initial position and subsequent migration of the drainage divide, and in the spatial and temporal pattern of related denudation (e.g. Cockburn et al. 2000; Brown et al. 2002).

Our AFT work contributes further to the understanding of the evolution of Atlantic African margin by providing a new, detailed reconstruction of the spatial and temporal patterns of denudation along two transects (Fig.1, Namaqua and Karoo traverses) across the western passive margin of South Africa and its interior since the onset of continental rifting.

AFT results across the western coast of South Africa and its interior reported here are consistent with the existence of a discrete, tectonically-induced, Mid-Cretaceous (115 - 90 Ma) pulse of substantial denudation. Thermal modelling of the new fission track data indicates up to 2.5 km of denudation in the coastal zone and less than 1 km on the elevated interior plateau during this phase of accelerated denudation (Fig.1). Greater tectonic activity occurred along the passive margin and its interior during this period than in the Cenozoic. This suggests that the Mid-Cretaceous was probably the time when most of the present day Southern African high-elevation topography was formed.

The spatial patterns of denudation reported here suggest localised, post-rifting and fault-controlled uplift along the passive margin (Fig.1). It is tentatively suggested that the substantial Mid-Cretaceous pulse of denudation is a direct consequence of significant uplift associated with the African Superswell, a tomographically-imaged low-velocity zone at the lower mantle-core boundary

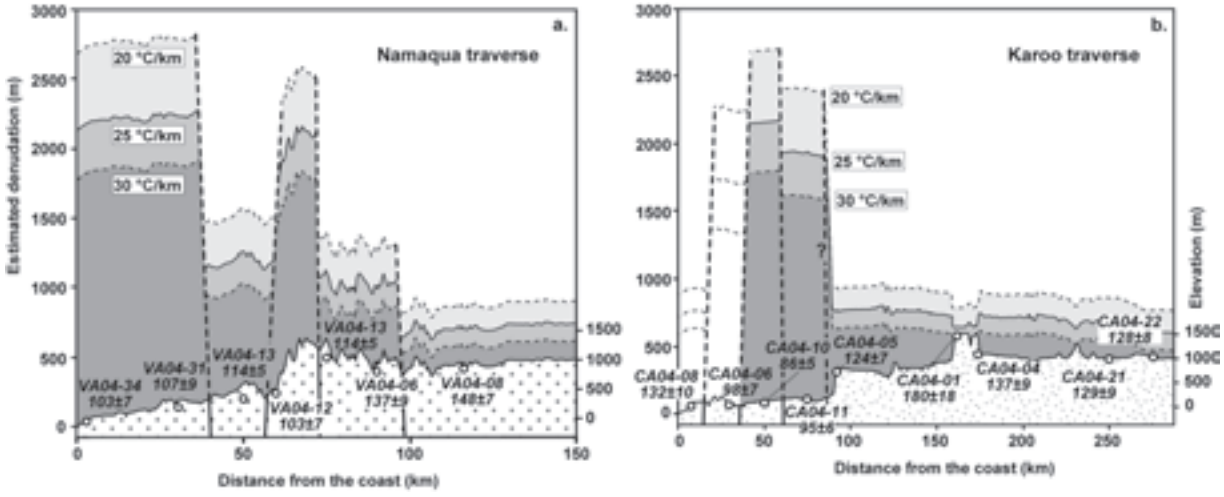

Figure 1. Estimated denudation for the time period between 115 and 90 Ma calculated from AFT data modelling and based on three possible paleo-geothermal gradients of 20, 25 and 30 °C/km for: a) Namaqualand traverse and b) Karoo traverse. For the samples CA04/06 and CA04/08 from the Karoo traverse the presented dash lines for the estimated denudation are only suggestive. The samples were not modelled because of insufficiency of the track lengths record.

REFERENCES

Brown, R.W., Gallagher, K., Gleadow, A.J.W. & Summerfield, M.A. 2000: Morphotectonic evolution of the South Atlantic margins of Africa and South America. In: Summerfield, M.A. (ed) Geomorphology and Global Tectonics. John Wiley and Sons Ltd, 255-284.

Brown, R.W., Summerfield, M.A. & Gleadow, A.J.W. 2002: Denudation history along a transect across the Drakensberg Escarpment of southern Africa derived from apatite fission track thermochronology. Journal of Geophysical Research, 107, doi:10.1029/2001JB000745.

Cockburn, H.A.P., Brown, R.W., Summerfield, M.A. & Seidl, M.A. 2000: Quantifying passive margin denudation and landscape development using a combined fission-track thermochronometry and cosmogenic isotope analysis approach. Earth and Planetary Science Letters, 179, 429-435.

King, L.C. 1953: Cannons of landscape evolution. Geological Society of America Bulletin, 64, 721-752.

1.28

2D dynamic retro-deformation of folded multilayers: Application to Carboniferous turbidites in South-West Portugal

Lechmann Sarah M.*, Schmalholz Stefan M.*, Burg Jean-Pierre* & Marques Fernando O.**

* *Geological Institute, ETH Zurich, CH-8092 Zurich (sarahl@student.ethz.ch)*
** *Universidade Lisboa, P-1749-016 Lisboa*

Two-dimensional numerical finite element models of power-law viscous flow are employed to retro-deform folded multilayers. Our aims are to demonstrate the applicability of dynamic retro-deformation as a tool to appraise an interpreted geological profile and its mechanical forming processes. The application of this approach to a fold train situated in South-West Portugal furthermore aims at determining its folding history and the material parameters of the constituting rocks. The sketched sections are digitized and meshed in MATLAB and then stretched perpendicularly to the fold axes. This produced the initial geometry for finite element simulation.

A sensitivity study is performed in order to determine model parameters, such as boundary conditions, geometry and viscosity ratio. Boundary conditions exert little influence on the final retro-deformed geometry, the initial geometry however does. A lower limit of 25 could be assigned to the viscosity ratio between layer and matrix, above which reasonable results are achieved when retro-deforming the multilayer stack.

Kinematic models, so-called balanced cross sections, and synthetic forward and reverse models of the respective structures serve as comparative value. Balanced cross sections aim at the same as dynamic retro-deformation, give however only a minimum estimate of the amount of compression contained in a structure and allow no evaluation of material parameters. Synthetic forward and reverse models serve to prove the retro-deformability of a specific structure.

The challenging retro-deformation of one of the prominent structures, a collapsed hinge, present in one of the studied profiles, led to the reevaluation of the profile, which apparently was mechanically inconsistent. A second field investigation revealed that one limb of this collapsed hinge includes rupturing and separation of 4.9 m length, which were not included in the first model. This allowed correction of retro-deformation resulting in excellent fit between modeled and geological sections. Further possibilities for a successful retro-deformation of the collapsed hinge are a 3D-model and a rheology including power-law viscous layers.

This work demonstrates that a close link of field work and numerical modeling can give new insights into mechanical processes, the material parameters of the studied rocks and also improve field based interpretations.

1.29

Numerical modeling of poly-phase formation and exhumation of HP-UHP rocks in continental subduction zone

Li Zhonghai* & Gerya Taras*

* *Geophysical Fluid Dynamics Group, Institute of Geophysics, Department of Geosciences, ETH-Zurich, CH-8093 Zurich (lzhhai@gmail.com)*

High-pressure-ultrahigh-pressure (HP-UHP) metamorphic rocks commonly form and exhume during the early continental collision, with the protoliths mainly derived from subducted upper and middle continental crust. While geodynamic significance of HP-UHP complexes is widely recognized and their appearance in the Neoproterozoic is considered as a "hallmark" for establishing modern plate tectonic styles many questions related to their origin still remain unresolved. Of particular importance is polymetamorphic origin of many HP-UHP terranes composed of tectonic units having strongly variable ages, peak metamorphic conditions and P-T paths.

In order to address this issue we conducted 2D high-resolution thermomechanical numerical modeling of the continental subduction associated with formation and exhumation of the HP-UHP rocks, with testing different geometrical configurations and varied width of subducting continental margins, convergence velocity and sedimentation and erosion rates.

Most of our experiments confirm poly-phase origin of HP-UHP terranes and predict existence of several consequent episodes of (U)HP rocks exhumation related to the inherently cyclic origin of continental crust subduction-detachment-exhumation process. Periodicity of formation of rheologically weak zones (thrusting faults) controlling HP-UHP rocks exhumation processes depends on the competing effects of downward directed subduction drag and upward directed crustal buoyancy forces. The buoyancy forces and related deviatoric stresses accumulate in the subduction channel due to subduction of low-density crustal rocks and are then reset back during rapid exhumation episodes.

Our reference model predicts three distinct phases of detachment/exhumation processes: 1) first detachment and exhumation of HP rocks; 2) second detachment and exhumation of HP rocks; 3) exhumation of the UHP-HT rocks. Residence time of UHP rocks in the overriding plate channel is on the order of several million years which allows strong rising of peak metamorphic temperatures toward 800-900°C due to conductive heat exchange with underlying asthenospheric mantle. The model results are applicable to the Sulu UHP terrane in eastern China with similar characteristics in terms of 1) spatial distribution of metamorphic units (HP-UHP-Suture zone); 2) peak P-T conditions of the HP-UHP metamorphism; 3) temporal constraints for polyphase processes (the formation and exhumation of HP-I slices are about 10 Ma earlier than the UHP slices); and 4) provenance (mixed various crustal and mantle rock types with protoliths mainly from the subducted continental margin).

The presence of the incoming continental margin with relatively thin crust is important for the onset of continental deep subduction and exhumation processes. The smaller margin width doesn't produce efficient exhumation before real collision of the thick subducting continental interior and the overriding plate. Convergence velocity is another major parameter controlling subduction/exhumation processes by affecting them into three different scenarios: (1) "first-step" exhumation processes of the subducted rocks without intruding into the sub-lithospheric channel, under low convergence velocity; (2) "polyphase" exhumation processes with three phases of the formation and exhumation of HP-UHP rocks, under intermediate convergence velocity; (3) "last-step" exhumation processes without effective exhumation until the subducting continental interior collides with overriding plate, under high convergence velocity. The surface processes (sedimentation and erosion rates) affect the size and exhumation time of HP-UHP units but don't change the polyphase characteristics of subduction-detachment-exhumation processes.

1.30

Evolution of a mantle shear zone and the influence of second phases, Hilti massif, Oman.

Linckens Jolien*, Herwegh Marco*, Müntener Othmar**, Mercolli, Ivan*

*Institute of Geological Sciences, Baltzerstrasse 1-3, CH-3012 Bern (linckens@unibe.ch)
**Institute of Geology and Paleontology, BFSH-2, CH-1015 Lausanne

Localization of deformation in shear zones is a common feature in the Earth's crust and upper mantle (e.g., thrusts, strike slip faults). The evolution of such high strain zones is often long lasting incorporating variations in physical (e.g. P, T) and chemical conditions with time. To learn more about the distribution and evolution of deformation in mantle rocks as a function of variable physico-chemical conditions, detailed mapping and microstructural investigations of a large-scale peridotite shear zone in the Hilti massif (Oman ophiolite) was performed.

Detailed mapping of the shear zone shows that the largest part of the shear zone experienced moderate deformation, whereas high deformation is localized in meso-scale shear zones. In some parts of these meso-scale shear zones the deformation is further localized in ultramylonitic bands.

In terms of tectonites, four different types can be discriminated: (i) astenospheric flow related tectonites (outside of the shear zone), (ii) weakly-moderately deformed protomylonites, (iii) mylonites and (iv) ultramylonites.

In the area investigated, both dunites and harzburgites occur. Particularly in case of the harzburgites, both mineralogy and modal compositions can vary. In these rocks, secondary minerals like (opx, cpx, spinel) can affect the grain size of the predominating olivine in the matrix, which can have an influence on the deformation mechanisms (e.g. diffusion vs. dislocation creep). In order to test the effect of such secondary phases on microstructure, deformation mechanisms and strain localization behaviour, microstructures of the different tectonites were quantitatively investigated. For this purpose, grain size (dp) and volume fractions (fp) of olivine and the second phases (opx, cpx and spinel) as well as CPOs and deformation temperatures were analyzed. In addition, geothermometry, using opx (Ca and Al-Cr in opx) has been performed to gain information on the deformation temperature.

Similar to previous studies performed on calcite mylonites, each of the different mantle tectonites can be subdivided into two different microfabric types: (a) second phase controlled microstructures, where the olivine grain size increases with increasing Zener parameter (Z = dp/fp, second phase grain size/second phase volume fraction e.g. see Herwegh and Berger, 2004). (b) Recrystallization controlled microstructures, where the olivine grain size shows no dependence on the second phase content and remains constant with increasing Z.

The ultramylonites show weak CPOs at all Zener parameters, indicating that diffusion creep was the mean mechanism for deformation. For the mylonites, the second phase controlled microstructures show weaker CPOs, indicating a decrease in intracrystalline plasticity with increasing second phase content. Furthermore, the CPOs suggests deformation of both mono- and polymineralic layers under the presence of water (Jung and Karato, 2001).

The comparison of the Zener trends for the different tectonites gives the following results:

(i) Three different meso-scale shear zone mylonites give the same Zener trend and yield the same deformation temperatures (≈800°C) indicating that these different shear zones were formed under the same deformation conditions (e.g. strain rate, stress and temperature). It can therefore be postulated, that the variations in second phase type and content was no major parameter for strain localization. In contrast, the microstructures adapt to the local Zener parameter, enabling specific combination of dislocation creep and diffusion creep to maintain an overall homogeneous deformation within the meso-scale shear zones.

(ii) The Zener trend of the ultramylonites is shifted to lower olivine grain sizes compared to the mylonites and the geothermometry results show that they were formed under lower temperatures (≈690°C). Therefore the shift in the Zener trend is most likely caused by the lower deformation temperatures and is eventually accompanied by a higher strain rate.

(iii) The Zener trend of the weakly deformed protomylonites show, compared to that of the mylonites, larger olivine grain sizes but the same deformation temperatures. Indicating that the shift in the trend is only caused by the lower strain rate of the protomylonite compared to that of the mylonite.

(iv) The asthenosphere flow fabrics show a shift to even larger olivine grain sizes. These fabrics formed at higher temperatures (≈1150°C) and the shift can be explained by a combination of higher deformation temperature probably accompanied by lower strain rates.

The Zener trend is different for each tectonite and can be explained by variations in both strain rate and deformation temperature. From a geodynamic point of view, Zener trends can therefore be applied as a tool to determine the deformation conditions and their variations in space and time in case of mantle rocks.

REFERENCES

Boudier, F., Ceuleneer, G., Nicolas, A., 1988: Shear zones, thrusts and related magmatism in the Oman ophiolite: initiation of thrusting on an oceanic ridge, Tectonophysics 151: 275-296.

Herwegh, M., Berger, A., 2004: Deformation mechanisms in second-phase affected microstructures and their energy balance. Journal of Structural Geology 26: 1483-1498

Herwegh, M., Berger, A. and Ebert, A., 2005: Grain coarsening maps: A new tool to predict microfabric evolution of polymineralic rocks, Geology 33: 801-804

Jung, H. and Karato, S.,2001, Water induced fabric transitions in olivine. Science 293, 1460-1463

Michibayashi, K. and Mainprice, D., 2004: The role of pre-existing Mechanical anisotropy on shear zone development within oceanic mantle lithosphere: and example from the Oman ophiolite. Journal of Petrology 45: 405-414

Nicolas, A., Boudier, F., Ildefons, B., Ball, E., 2000: Accretion of Oman and United Arab Emirates ophiolite-Discussion of a new structural map. Marine Geophysical Researches 21: 147-179.7

1.31

Influence of rheological weakening by fluids and melts on subduction at an active margin: Numerical modelling

Löw Felicitas Irena*, Gerya Taras V*

**Institut für Geophysik, ETH Zürich, Schafmattstrasse 30, CH-8093 Zürich (irenaloew@web.de)*

The dynamics of subduction under an active margin is analyzed by using a 2D coupled geochemical-petrological-thermomechanical numerical model of an oceanic-continental subduction process. This model includes spontaneous slab retreat and bending, dehydration of the subducted crust, aqueous fluid transport, partial melting of both crustal and mantle rocks and melt extraction processes resulting in magmatic arc crust growth. The innovation in this model is the consideration of rheological weakening effects by fluids and melts.

The numerical experiments revealed that rheological weakening by fluids and melts controls the mode of subduction. By varying the weakening effects, five different regimes can be induced showing the following characteristics: (1) formation of a backarc basin, occurance of plumes that (2) ascend and intrude into the continental crust or (3) extend horizontally beneath the continental plate (underplating) or (4) remain above the subducting plate and (5) neither formation of backarc basins nor occurance of plumes. The transition between the different tectonic regimes of subduction at an active margin is caused by the concurrence of rheological weakening by (1) aqueous fluids percolating from the subducting slab into the mantle wedge and (2) melts propagating from the mantle wedge toward the surface.

The aqueous fluids mainly affect the forearc region: strong fluid-related weakening of rocks atop the slab promotes the stacking of sediments and the development of an accretion wedge. Since the material in the subduction channel is weak the coupling of the plates in these regimes of subduction is low facilitating extension in the subduction channel. In contrast, a small weakening effect by fluids results in strong coupling of the plates inducing collision-like subduction and subduction erosion. Lithospheric thickening and large sedimentary plumes are the consequence.

Extracted melts rheologically weaken the lithosphere below the arc. Strong rheological weakening by melts in combination with low coupling of the plates allows for necking of the continental lithosphere and leads to the formation of a backarc basin. In the case of sedimentary plumes, weakening of the continental lithosphere by extracted melts generates a weak channel in which the positive-buoyant plumes may ascend. That way silicic intrusions are emplaced in the continental crust. If the continental lithosphere is not sufficiently weakened by melts, the plumes cannot ascend but may extend horizontally leading to underplating.

In general, the degree of coupling of the plates is of great importance as it influences the topographic evolution and the crust production rate of subduction zones. Strong coupling leads to an extreme topography whereas low coupling enhances the production of new crust. The fact that the coupling is strongly influenced by fluid- and melt-related weakening emphasizes the significance of fluids and melt in subduction.

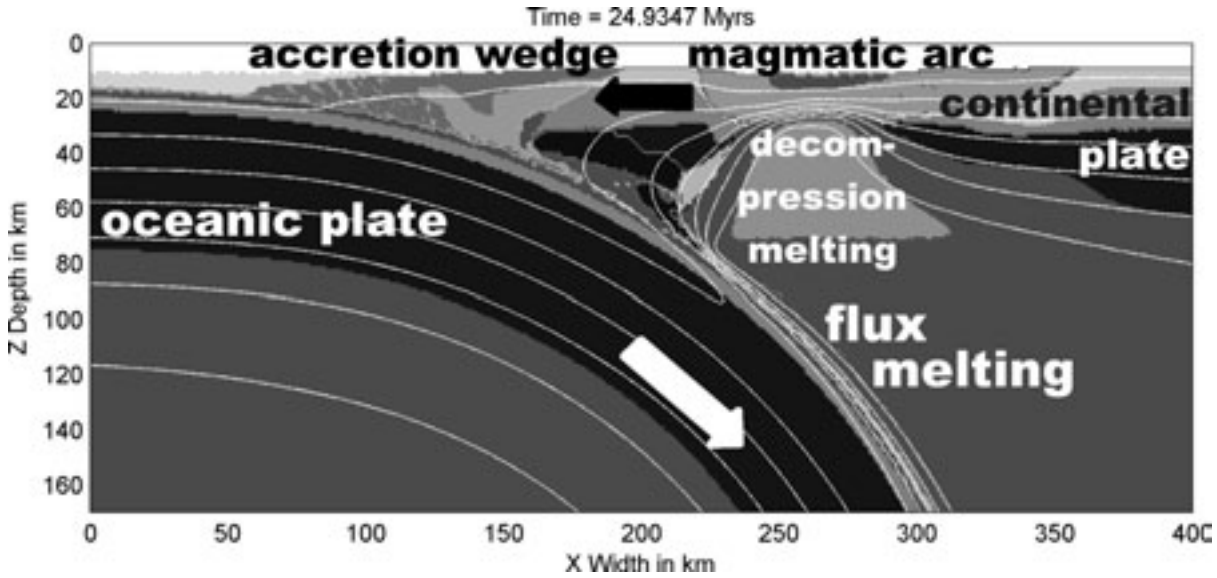

Figure 1. Subduction at an active margin - formation of a backarc basin: hydration above the descending oceanic plate promotes flux melting. The melts ascend, build a magmatic arc atop the continental plate and weaken the material below the arc so that necking of the continental lithosphere is possible and trench retreat and decompression melting take place. The result is a backarc basin including a new spreading centre.

1.32

The Rochers de Leschaux (Bornes Massif, Subalpine domain, Haute-Savoie, France): a complex record of Cretaceous, Paleogene, and Neogene tectonics

Martin Marc*1, Kindler Pascal*, Sartori Mario*, Charollais Jean*

*Section of Earth Sciences, University of Geneva, Maraîchers 13, CH-1205 Geneva, Switzerland (pascal.kindler@terre.unige.ch)
1present address: IHS Energy, chemin de la Mairie 24, CH-1258 Perly, Switzerland

Based on new stratigraphic and structural data, the complex structure of the Rochers de Leschaux has been reinterpreted, providing additional information on the type, the age, and the number of tectonic phases that have affected the Subalpine domain, as well as on the amount of shortening this domain experienced during the Alpine orogeny.

The Rochers de Leschaux (Fig. 1) is a complex faulted fold located in the Borne Valley (NE part of the Bornes Massif, Subalpine fold-and-thrust belt, Haute-Savoie, France). Particularly impressive is the tectonic superposition of two cliffs made of Urgonian Limestones (Early Cretaceous): the Bouchat-Gérats cliff, at the base, and the Leschaux cliff, at the top (Fig. 1). The presence of a thrust fault in this complex structure has long been recognized, but the overall geometry of this accident is still controversial (Maillard, 1889; Butler, 1923; Charollais et al., 1977; Huggenberger and Wildi, 1991; Gidon, 1996). Estimates of the amount of displacement along the thrust plane vary between <1 to 4 km, hampering a precise reconstruction of tectonic shortening in the Bornes massif.

New geological mapping at the 1:5'000 scale, detailed structural and stratigraphic analyses, and the elaboration of balanced structural cross-sections yielded the following new results:

- The thrust plane with a ramp geometry separating the Bouchats cliff from the Leschaux cliff can be followed in the Cirque des Boitons, towards the SSE, and in the Solaison syncline, towards the NNW.
- A sub-vertical N50 fault (the Dresse fault) separates the Kieselkalk (siliceous limestones of Hauterivian age) exposed in the Cirque des Boitons from the Urgonian limestones forming the Bouchats cliff, the latter representing the downward-thrown block. This fault is cut trough by the thrust ramp.
- At the NW end of the Leschaux cliff, another vertical fault (the Leschaux fault) offsets the Urgonian limestones in the hanging-wall of the thrust. Its orientation (N50), apparent direction of movement and throw are the same as those of the Dresse fault.

- Tectonic breccias, most likely associated with syn-sedimentary faulting, have been found in the Cretaceous limestones along the Leschaux Fault.
- A steep fault, with a fault trace trending towards N150, parallel to the plane of the picture in Fig.1, separates the Leschaux cliff from the Gérats cliff, the latter representing the downward-thrown block.

Relying on these new observations, the following interpretations can be proposed:

- The Dresse fault and the Leschaux fault represent one single ancient (probably upper Cretaceous) structure that has been cut through and offset during a post middle-Oligocene phase of thrusting.
- Using the two offset segments of the Leschaux-Dresse paleo-fault as markers, the throw along the thrust plane is estimated at about 750 m.
- The Gérats cliff has been down-faulted from the Leschaux cliff and is not directly related to the Bouchat cliff. Similar structures can be observed on both flanks of the Borne Valley, suggesting the latter is partly of tectonic origin, and emphasizing the orogen-parallel stretching in the Bornes massif.

Besides providing a new interpretation and a kinematic model for the Rochers de Leschaux, this study confirms the existence of a late Cretaceous tectonic phase in the Subalpine domain and provides a prime example of the cutting trough of a Mesozoic subvertical fault by a thrust ramp in a 150 m-thick massive limestone.

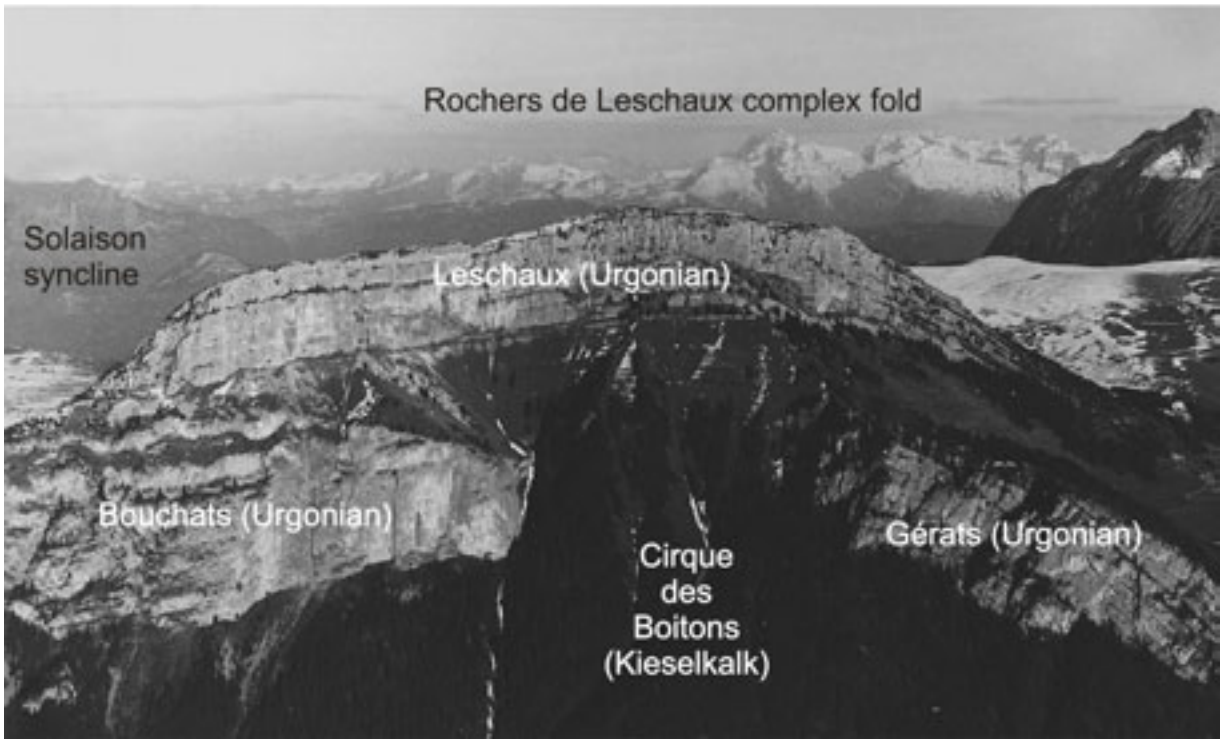

Fig. 1: Oblique aerial view of the Rochers de Leschaux showing its main structural elements.

REFERENCES

Bütler H. 1923: Le pli-faille des Rochers de Leschaux (vallée du Borne, Haute-Savoie). C. R. Séanc. Soc. Phys. Hist. Nat. Genève 40, 137-139.

Charollais, J., Pairis, J.-L. & Rosset, J. 1977: Compte rendu de l'excursion de la Société Géologique Suisse en Haute-Savoie (France) du 10 au 12 octobre 1976. Eclogae geol. Helv. 70, 253-285.

Gidon, M. 1996: Vues nouvelles sur la structure des massifs des Bornes et des Bauges orientales. Géol. Alp. 72, 35-39.

Huggenberger, P. & Wildi, W. 1991: La tectonique du massif des Bornes (Chaînes Subalpines, Haute-Savoie, France). Eclogae geol. Helv. 84, 125-149.

Maillard G. 1889: Note sur la géologie des environs d'Annecy, La Roche, Bonneville et de la région comprise entre le Buet et Sallanches (Haute-Savoie). Bull. Serv. Carte géol. France 6, 1-64.

1.33

Structural influence on glacial cirque morphology: the case of Pizzo Arera (Orobic Alps, Southern Alps, Italy)

Marzorati Andrea*, Ghiselli Alice* & Bini Alfredo*

**Dipartimento di Scienze della Terra „A. Desio", via Mangiagalli 34, I-20133 Milano (andrea.marzorati@email.it)*

Glacial cirques are typical, common morphologies in high mountain areas. They are represented by a semicircular hollow open downslope and bounded upslope by steep walls. The aim of this study is to point out the relationships between cirque morphology, bedrock structures and lithology and to suggest a genetic model of these landforms.

The study area includes six glacial cirques and is located in the Orobic Alps, between Val Brembana and Val Seriana, on the Pizzo Arera (2512 m a.s.l.) massif. The Orobic Alps belong to the Central Southern Alps domain and are characterized by a series of thrust and folds with an E-W trend, a ramp and flat geometry and a southward transport direction (Schumacher et al., 1997). In particular, in the Pizzo Arera area the variable stratigraphy controls the distribution of detachment layers and lateral ramps of three thrust sheets (Schönborn, 1992). These thrust sheets are constituted by Triassic platform/basin limestones and dolostones, and are separated by continuos and thick detachment horizons controlled by interbedded marls.

Geological, geomorphologic and structural data has been collected on the field (mapping scale 1:5.000) and then elaborated through a structural analysis (both at meso and micro-scale) and a geomorphologic analysis.

The meso-structural analysis led to the identification of three deformation phases of Alpine age. The first one (D1 phase) is the most important: during this phase the emplacement of regional thrust surfaces is accompanied by minor structures such as folds (F1), foliations (S1 and S1bis), boudins, faults and fractures. The following deformation phases (D2 and D3) are characterized only by brittle deformation, producing faults and fracture planes. The micro-structural analysis was conducted on thin sections of rocks belonging to the thrust deformation zones. The thrust sheet limestones resulted affected by brittle-ductile deformation with the formation of cataclastic and mylonitic rocks in which five deformation stages have been detected.

The geomorphological analysis permitted the recognition of macro and meso forms produced by gravitational processes, glacial action and karst dissolution. DEM (Digital Elevation Models) and aerial photos analysis allowed the identification of the distribution and morphological relief of structural elements in an area wider then the mapped one.

Afterwards, in each cirque, the results of the different analysis were integrated, in order to find out the relationships between the different factors.

In all the six cirques an important role is played by structural discontinuities, but differently in two group of cirques: the northward and westward open cirques and the southward open cirques. The first group shows a strong structural control on the different sectors that make up the cirque morphology: the bottom of three cirques follows the course of the same thrust surface and the lateral walls are always bounded by a fault, a fracture or the stratification surface; the slope processes are mainly represented by rock falls and slidings and the rupture surfaces are often controlled by faults and fractures. The second group exhibits the outcropping of more erodible rocks, therefore the structural surfaces have a less important control on slope processes (mainly debris flow and soil creep). In one of these cirque, though, a lateral wall is internally confined by an important fault and the difference in hight between the cirque floor and the ridge is compatible with the displacement and the kinematic of the fault, showing a possible active role played by tectonics.

In conclusion, the genesis and development of the studied cirques was mainly due to gravitational movements directly controlled by the distribution of structures. Faults and fractures often lead the development of weakness zones playing a passive role in the slope shaping, except for one case.

The glaciers seem to have played only a secondary role, filling the cirques already existing and removing the debris previously produced; however other studies are in progress to point out the extension of glaciers and better define their role.

REFERENCES

Schönborn G. 1992: Alpine tectonics and kinematic models of the Central Southern Alps. Memorie di Scienze Geologiche, 44, 229-393.

Schumacher M. E., Schönborn G., Bernoulli D. & Laubscher H. P. 1997: Rifting and collision in the Southern Alps. Deep Structure of the Swiss Alps, 186-204

1.34

The Teggiolo zone: stratigraphy and tectonics in the Val Bavona (Lower Penninic, Ticino)

Matasci Battista, Epard Jean-Luc & Masson Henri

Institut de Géologie et Paléontologie, Université de Lausanne, 1015 Lausanne (Battista.Matasci@unil.ch)

The Teggiolo zone is the sedimentary cover of the Antigorio nappe (Lower Penninic, Central Alps). Our study is based on detailed mapping, stratigraphy and structural analysis between Robiei and the Pizzo Castello, on the eastern side of Val Bavona. There the Antigorio nappe is overthrusted by the Sambuco nappe (formerly northern part of the Maggia nappe, cf Berger et al. 2007). The sedimentary cover of the latter thins out and disappears near Robiei, and SE of this locality the Sambuco gneissic basement directly overlies the Antigorio cover. Thus the metasediments pinched between the Antigorio and Sambuco basements entirely belong to Antigorio.

In the Teggiolo zone several sedimentary cycles are distinguished, separated by erosive surfaces that are discordant at the map scale:

1.- Where the stratigraphic column is the most complete, it starts with Triassic layers (mainly dolomite). In the survey area the Triassic is only preserved at Campo, elsewhere it has been eroded below the Jurassic transgression.

2.- The second sedimentary cycle is comprised of a detrital series passing upwards to a limestone formation. Its base is conglomeratic. This conglomerate is thin in the survey area, often reduced to dispersed pebbles in a matrix of coarse-grained sandstone, but much thicker on the opposite bank of the valley, in the Val Antabia, where it consists of several layers alternately rich in pebbles of gneiss (eroded from the basement), dolomite (from the Triassic), and other sedimentary rocks unknown in the normal stratigraphic column (presumably originating from the erosion of a post-Triassic and pre-conglomeratic, completely destroyed part of the column). The sandstone shows various depositional structures (graded-bedding, etc) and is overlaid first by a slightly micaceous and quartzic limestone (yellowish marble), then by a pure limestone (white marble). The age of all this series (traditionally attributed to the Triassic) is clearly post-Triassic, probably Middle to Late Jurassic. At its top there is a layer of banded marble whose presumed protolith has similarities with rocks of earliest Cretaceous age in the Helvetic domain.

3.- The third cycle consists of the main mass of the calcschists of the Teggiolo zone. In other parts of the nappe its base truncates the two preceding cycles and is eroding deep into the Antigorio basement. The sedimentary discontinuity with the underlying series is supposed to be a major stratigraphic gap and the age of these calcschists is presumed to be latest Cretaceous to Tertiary. In the Val Bavona this series is thick on the western side (Val Antabia) and on the eastern side around Campo, but from there it disappears towards SE because it is itself truncated by the base of the overlying wildflysch.

4.- The top part of the Teggiolo zone is a more or less chaotic formation of calcschists, often rich in blocks of various rocks, interpreted as a meta-wildflysch (Robiei Formation, Masson 2002). It seems to fill channels eroding down to various depths the older layers of the Teggiolo zone. SW of Robiei, it can be subdivided into a lower part characterized by blocks of marble (similar to the white marble of the underlying section), and an upper part characterized by blocks of gneiss (whose probable source is in the Sambuco nappe, Bussien et al. 2008). In both parts a gradual vertical evolution is observed from fine-grained detritus to small blocks (of marble or gneiss, respectively), then to large blocks of dam or even hm size. SE of Robiei the blocks of gneiss disappear and only the lower subdivision with marble blocks continues, but around the Pizzo Castello it passes laterally to an accumulation of blocks of all sizes (up to several hm) and various lithologies. The largest ones are often composite and present a stratigraphic succession gneiss-sandstone-marble similar to the lower part of the Teggiolo zone in this region, with the difference that the gneiss is not identical to the usual Antigorio orthogneiss.

Conclusion: The Teggiolo zone has a complex geological history, with several sedimentary cycles and stratigraphic gaps, presumed to cover the whole time span from Triassic to Early Tertiary. Its lower part (Triassic-Jurassic-Lower Cretaceous?) presents similarities with some Middle Jurassic thresholds of the Helvetic realm (e.g. internal Mont Blanc), while its upper part (Upper Cretaceous to Tertiary) typically belongs to the North-Penninic domain. Thus the Antigorio nappe occupies a crucial position in the restoration of the main paleogeographical domains of the Alps. The highest formation of calcschists with blocks is interpreted as a wildflysch: its sedimentation is probably contemporaneous with the beginning of the translation of the overlying Sambuco nappe. The increasing amount and size of the blocks towards the East seems to announce a tectonic connection of the Antigorio and Sambuco nappes..

REFERENCES

Berger, A., Mercolli, I. & Engi, M. 2007: Tectonic and petrographic map of the Central Lepontine Alps 1 : 100000, Explanatory notes. Carta geol. spec. 127, Swisstopo.

Bussien, D., Bussy, F., Masson, H., Magna, T. & Rodionov, N. 2008: Variscan lamprophyres in the Lower Penninic domain (Central Alps): age and tectonic significance. Bull. Soc. Géol. France 179/4, 369-381.

Masson, H. 2002: Ophiolites and other (ultra)basic rocks from the West-Central Alps: new data for a puzzle. Bull. Géol. Lausanne 356.

1.35

Brittle tectonics in the Subalpine Molasse and in the Prealpes Klippen

Matzenauer Eva*, Ibele Tobias*, Mosar Jon*

* *Département de Géosciences Université de Fribourg, Chemin du Musée 6, CH-1700 Fribourg (eva.matzenauer@unifr.ch)*

The study of the tectonic and neotectonic structures of the Subalpine Molasse and Prealpes Klippen of the Canton Fribourg is the scope of this ongoing PhD research. A more global aim of this study is to gain a better insight into the present and past stress and strain fields of the transition between the Prealpes Klippen, the Subalpine Molasse and the Molasse Basin. Observing regional structures by analysing aerial photographs and DEMs of the study area, combined with field measurements, permits the investigation of different kinds of structures as yet unknown.

The investigation area is structurally subdivided into two major zones:

(1) the Subalpine Molasse - stacked Molasse slices which are inclined due to the Alpine orogeny, and
(2) the Prealpes, mainly the Klippen and the Gurnigel Nappe which are situated at the frontal part of the Prealpes and in direct contact with the Alpine Foreland. The north-western part of the Prealpes Klippen, is mainly governed by several large-scale fault-related folds whereas the south-eastern part is dominated by imbricated thrust slices dipping to the N/NW.

Field measurements in limestone, marls and shales (Prealpes Klippen) and sandstones (Gurnigel and Subalpine Molasse) exposed a whole suite of brittle tectonic features such as joints and fractures, slickensides, and veins, but also hitherto undescribed features such as deformation bands. Combined these structures allow paleostress reconstructions. With the analysis of aerial photographs and DEMs, lineaments were detected which correspond mostly to vertical - subvertical tectonic faults.
The combination of two observation methods makes it possible to distinguish different fault hierarchies.

First kinematic analysis of the observed faults allowed us to distinguish between different fracture families and their hierarchical order. The fault distribution and their senses of movement probably governed by a Riedel shear pattern. As shown by previous investigations, the tectonic regime is dominated by two main fault directions: a right lateral WNW-ESE and a left lateral NNW-SSE striking system of shear zones. The two fault families are possibly linked to a common “conjugated” fault system with a regional extent.

1.36

Double subduction dynamics: Insight from petrological-thermomechanical numerical models

Mishin Yury, Gerya Taras, Burg Jean-Pierre & Connolly James

Department of Earth Sciences, ETH Zurich, Schafmattstr. 30 / HPP, CH-8093 Zurich (yury.mishin@erdw.ethz.ch)

Double subduction is a geodynamic process in which two plates following each other are synchronously subducted. Double subductions are known for both modern (Izu-Bonin-Marianas and Ryukyu arcs) and ancient (West Himalaya collision zone) plate tectonics. However, our knowledge about this process is limited to conceptual schemes and some restricted analogue experiments. In order to fill this gap we performed 2D numerical experiments using a coupled petrological-thermomechanical approach based on finite differences and marker-in-cell techniques combined with thermodynamic database for the mantle. We investigated the influence of convergence rate, intermediate plate length, activation volume of the mantle dislocation creep and age of the lithosphere. Based on these experiments we conclude that: (A) Subduction rates at two zones running in parallel differ and vary in time even when the total convergence rate remains constant. Supremacy of either subduction zone depends on physical parameters such as (i) relative rates of the plates, (ii) slab ages and (iii) length of the middle plate. (B) Subduction dynamics of the double subduction system involves several processes unknown in simple subduction systems, such as (i) eduction (i.e. “un-subduction”), (ii) subduction re-initiation, (iii) subduction flip triggered by shallow slab breakoff and (iv) turn-over of detached slabs to up-side-down attitudes. (C) Simulated tomographic structures related to slab propagation account for both penetration and non-penetration of the 660 km discontinuity. Non-penetration is favored by (i) low convergence rate, (ii) faster relative movement of the overriding plate, (iii) young age of the subducting slab and (iv) up-side-down turn-over of detached slab.

1.37

Migration and storage of melts in rocks under dynamic conditions: insights from physical experiments

Misra Santanu, Tumarkina Elizaveta, Burlini Luigi

Experimental Rock Deformation Laboratory, Geological Institute, ETH, Leonhardstrasse 19, Zurich, CH-8092, Switzerland (santanu.misra@erdw.ethz.ch; elizaveta.tumarkina@erdw.ethz.ch; luigi.burlini@erdw.ethz.ch)

Partial melting of crustal materials occurs in the dynamically-active upper mantle regimes, and the melts thereby produced show complex flow behaviour through the solid crystalline residue. Using physical experiments, we investigated a quartz-muscovite system giving rise to melts through disequilibrium reactions in a dynamic state. The experiments were conducted on dry, porous synthetic rock samples, containing homogeneously dispersed porous quartz lenses of varying dimensions in a matrix of quartz-muscovite (1:1 volume ratio) mixture. We ran the experiments at varying temperatures (700 - 800°C) and a constant confining pressure (300 MPa). During experiments, the samples were subjected to shear deformation (maximum shear strain (γ = 15), maintaining a constant strain rate ($3x10^{-4}$-$1x10^{-3}$/s).

Experiments at 700°C did not show any melt generation and reaction in rocks. The sheared (γ = 3) rock samples developed low angle Riedel shear fractures. At ca. 750°C a small fraction of melt was produced. The melt did not show any tendency to flow, and collected along grain boundaries and pre-existing pores when finite shear strain is low (γ = 2). At higher shear strain (γ > 5) the melt migrated and localized preferentially into the pore spaces of quartz lenses. Such melt localization occurred along the periphery of quartz lenses (60-80 % by area), forming a melt-saturated rim. With increasing shear ($\gamma \approx 15$), the melt, however, did not flow towards the core of lenses. Instead, partial melting of quartz grains resulted in the formation of rounded quartz grains in the melt-saturated rim. At 775-800°C, the reaction yielded significant amounts of melt that migrated and stored into the quartz lenses even at very low shear (γ <1). Our results suggest that the equilibrium reaction kinetics of quartz and muscovite is extremely slow, even when the system is under dynamic conditions. The kinetic becomes further sluggish due migration and segregation of the melt in relatively inert strain domains.

1.38

Deformation and reaction of Quartz-Muscovite aggregates: results from torsion experiments

Misra Santanu and Burlini Luigi

Experimental Rock Deformation Laboratory; Geological Institute, ETH; Leonhardstrasse 19, Zurich, CH-8092, Switzerland

Torsion experiments were performed on synthetic aggregates of quartz and muscovite in order to illustrate the evolution of microstructure and rheology with progressive shear strain under conditions favouring mineral reactions. The pre-deformation grain sizes of quartz and muscovite in the fabricated rock were 4-6 and 30-40 μm, respectively, with 15% porosity. The experiments were conducted at 700-800°C with a constant confining pressure of 300 MPa, constant strain rates of $3x10^{-4}$ - $3x10^{-3}$ s^{-1}, and variable strains (γ = 0.5-15).

The yield strength of the material is strongly affected by temperature. The peak shear strength drops from ≈120 MPa to ≈50 MPa when temperature was raised from 750 to 777°C, respectively, at a constant strain rate of $3x10^{-4}$ s^{-1}. The mechanical behaviour of the system is characterized by a very strong weakening, which reduces with increasing temperature, in a linear-viscous way. This is due to production of melt at the grain boundaries. The inferred deformation mechanism is granular flow at the initial stage of deformation; with progressive shearing it turns to reaction-accommodated grain boundary sliding with a governing flow law:

$$\dot{\varepsilon} = 1.8^{15}\sigma^{5.18}e^{\frac{-403.005\ KJ\ .\ mol^{-1}}{RT}}$$

The material was very hard to deform at lower temperatures (700-750°C) with a higher strain rate (≈$3x10^{-3}$ s^{-1}). At temperatures 700-777°C and strain rate $3x10^{-4}$ s^{-1}, the aggregate did not react to produce K-feldspar and aluminosilicate up to a very high shear strain ($\gamma = 15$). The deformed product is characterized by generation of significant amount of melt and solid residue of quartz and muscovite. On the other hand, at 800°C and strain rate $3x10^{-3}$ s^{-1}, the disequilibrium reaction started and produced K-feldapar and oriented fibers of Sillimanite at a finite shear strain of $\gamma = 2$.

1.39

The Triassic detrital units in southern Turkey: synrift or syncollisional series?

Moix Patrice*, Champod Eric* & Stampfli Gérard M.*

* *Institut de Géologie et de Paléontologie, Anthropole, Université de Lausanne, CH-1015 Lausanne (Patrice.Moix@unil.ch)*

Turkey is composed of several terranes separated by complex suture zones. The present day juxtaposition results of large lateral displacements and north/south shortening from the Variscan to the Alpine cycles (Moix et al., 2008). The first amalgamation was realised during the Late Carboniferous Variscan orogeny (closure of the Rheic Ocean and opening of the Paleotethys). At this time, several terranes were detached from Gondwana and collided with the southern margin of Eurasia, *e.g.* Pelagonia, Anatolian Terrane, Sakarya. Then, the second amalgamation took place during the Late Triassic with the closure of the Paleotethys and the concomitant opening of the Neotethys along the Gondwana northern margin. Meanwhile, the southward retreat of the Paleotethyan slab caused the collapse of the Variscan Cordillera and the opening of back-arc basins along the southern margin of Eurasia (e.g. Maliac, Pindos oceans). The closure of the Paleotethys (Cimmerian Event) between the Taurus and the Anatolian terranes produced at places large flysch-molasse deposits often sealed by Liassic platforms. Finally, the last amalgamation corresponds to the Alpine cycle and is marked by a *quasi*-synchronous obduction of SSZ-type ophiolites during the Late Cretaceous.

For a long time, the idea of a Dinarides-Hellenides-Taurides-Zagrides continuum has been discussed. The Southern Aegean Islands in Greece form an important landmark between the Hellenic-Dinaric system to the west, and the Anatolian-Tauric one to the east. The most external parts of the Hellenides-Taurides system present striking similarities (*e.g.* Bernoulli et al., 1974). In particular, the platform development of the Beydağları/Susuz Dağ para-autochthonous sequence in Turkey correlates well with the pre-Apulian units of the Paxos-Zanthe-Kastellórizo zone in Greece. The study of ophiolites related to these units and their associated mélanges is a key point for any correlations (e.g. Koepke et al., 2002). K-Ar dating of SSZ-ophiolitic remnants found in Rhodes and Karpathos yielded an early Late Cretaceous age around 90 Ma. These ophiolites show more similarities with the south Turkish ophiolites than with the Hellenic-Dinaric ones (Vardar-type ophiolites). On the contrary, the ophiolites of Crete were dated around 160 Ma and can be therefore correlated with the Hellenic-Dinaric system. The analysis of the Triassic detritic units in southern Turkey can provide new clues to decipher the complex geodynamic history of the East-Mediterranean realm. The sandstones, breccias and conglomerates usually range from the Anisian (Scythian?) to the Late Triassic (sometimes Liassic) and are especially well-developed during the Upper Triassic interval. They are found both in para-autochthonous, i.e. Gondwana-derived Taurus terrane and in allochthonous positions, *i.e.* Anatolian-derived nappes.

(1) The detritic units belonging to the para-autochthonous series are often interstratified in platform-type developments ranging locally from the Cambrian to the Tertiary. Elements from these flysch-molasse deposits have yielded Upper Carboniferous-Lower Permian pelagic radiolarian cherts, Upper Pennsylvanian Ural-type Fusulinids, Permian pelagic conodonts, Lower, Middle and Upper Permian Fusulinids, Permian and Triassic smaller foraminifers, Lower Triassic pelagic conodonts plus various granites, gneiss, micaschists, quartzites and sandstones. These detritic units may be correlated with the Shemshak Formation in the Alborz in Iran and with the base of the Tripolitza Unit known as the Ravdoucha-Tyros beds in Greece. The latter consist of conglomerates, sandstones and violet slates. The elements are polygenic and composed of limestones, sandstones and lydites ranging from Carboniferous to Norian. All these sequences are interpreted as the Eocimmerian flysch-molasse sediments, probably deposited in a foreland basin during a syn- to post-collisional stage between Gondwanan and Eurasian-derived terranes.

(2) The detritic units belonging to the allochthonous series are often associated with volcanism. They are generally situated at the base of sequences showing shallow-water sedimentation passing up to pelagic conditions and finishing with flysch/wildflysch deposits. The Köyceğiz series in the Lycian Nappes presents a typical succession of the Pindos Unit (Upper Triassic-Liassic Gereme platform, Liassic-Cenomanian Çal Dağ pelagic limestone, Turonian Çamova flysch and Late Cretaceous Karabörtlen wildflysch). To the west, these series have their equivalent in Rhodes, Tilos, and Karpathos. In the External

Hellenides, they can be correlated with the base of the Pindos Unit which shows Carnian calcareous and terrigenous sediments with rare intercalation of pillow lava (Fleury, 1980). More proximal sequences can be found at the base of the Tripolitza Unit (Ravdoucha-Tyros beds) where volcano-sedimentary series are interstratified or followed by calcareous debris-flow, olistoliths and quartzitic sediments. The blocks are Scythian-Anisian Hallstatt limestones, Anisian radiolarites and Verrucano-type sandstones. All these Upper Triassic detritic sequences are interpreted to be the synrift deposits of the Pindos back-arc basin.
In conclusion, the Upper Triassic detrital units in Turkey and adjacent regions record the opening of Paleotethyan back-arc basins like the Huǧlu-Pindos Ocean and the closure of the Paleotethys.

REFERENCES

Bernoulli, D., de Graciansky, P.-C. & Monod, O., 1974: The extension of the Lycian Nappes (SW Turkey) into the southeastern Aegean Islands, Eclogae Geologicae Helvetiae, 67(1), 39-90.

Koepke, J., Seidel, E. & Kreuzer, H., 2002. Ophiolites on the southern Aegean islands Crete, Karpathos and Rhodes; composition, geochronology and position within the ophiolite belts of the Eastern Mediterranean, Lithos, 65, 183-203.

Moix, P., Beccaletto, L., Kozur, H.W., Hochard, C., Rosselet, F. & Stampfli, G.M., 2008. A new classification of the Turkish terranes and sutures and its implication for the paleotectonic history of the region, Tectonophysics, 451(1-4), 7-39.

Fleury, J.-J., 1980. Les zones de Gavrovo-Tripolitza et du Pinde-Olonos (Grèce continentale et Péloponnèse du nord). Evolution d'une plate-forme et d'un bassin dans leur cadre alpin, Société Géologique du Nord, Publication, 4, 1-473.

1.40

The Greater Caucasus Tectonics and paleotectonics East of Eden

Mosar Jon*, Kangarli Talat**, Bochud Martin*, Rast Annick*

** Département de Géosciences Université de Fribourg, Chemin du Musée 6, CH-1700 Fribourg*
*** Geology Institute of Azerbaijan (GIA), National Academy of Sciences, H.Javid Av 29A, Baku AZ1143, AzerbaijanDépartement de Géosciences Université de Fribourg, Chemin du Musée 6, CH-1700 Fribourg (jon.mosar@unifr.ch)*

The Caucasus orogen lies at Europe's cross-road with Asia and Arabia, and is one of the world's outstanding Mountain belts. It consists of the northern foreland basins, the Greater Caucasus, the intramontane basins (Kura-Kartli-Rioni; ≈ 200 m elevation) and the Lesser Caucasus. North of the Greater Caucasus the deep sedimentary Terek and Kuban basin (> 6000 m; up to 1,600 m elevation) forms the transition to the Scythian platform. The Greater Caucasus is Europe's highest and youngest mountain range with Mt. Elbrus culminating at 5642m, and rock uplift of more than 8,000 m in the last 2 Myr. The intramontane basin is one of the world's earliest sites of human society with 1.8 Ma old humanoid remains of Dmanisi (Georgia). The Lesser Caucasus with lower topography (≈ 3000 m), is a zone of important volcanic and seismic activity. In the East and West, the Caucasus topography is bound by two very deep basins, the South Caspian Sea and the Black Sea, hosting one of the world's largest oil and gas provinces.

The presentation will address the tectonics of the Greater Caucasus, mainly along a traverse far east of Dmanisi, the Eden of 1.8-2.0 My old hominids. The overall tectonic setting of the Greater Caucasus corresponds to a doubly verging mountain-belt with two external fold-and-thrust belts. The main transport direction is to the S. Along the N slopes, N-directed thrusting is observed and a N-verging foreland fold-and-thrust belt develops. The southern active orogenic front is in, or to the S of, the Kura-Kartli-Rioni "Molasse" basin. This foreland basin is filled with Tertiary and Quaternary sediments.

The Greater Caucasus corresponds to the inverted Mesozoic Greater Caucasus Basin. The evolution of the margin shows a passive margin type geometry and is related to the back-arc rift processes resulting from the northward subduction of the oceanic domains beneath the Lesser Caucasus arc. The evolution of the margin - its successive extensional and inversion events - is related to the geodynamics of the subduction zone. The sedimentation is influenced by carbonate environment linked to the platform to the north and volcanic derived sediments coming from the south. Following a series of rifting events, a number of Jurassic to Cretaceous inversions are characteristic of the Greater Caucasus basin/margin. The basin forms the connection between the oceanic realms of the Black Sea and the South Caspian Sea. The basin entirely develops on continental crust.

A major debate concerns the existence of subduction slabs beneath the Caucasus. It is generally admitted that the Lesser Caucasus is situated above an old slab. An incipient subduction is believed to occur at the northern edge of the Black Sea and in the central Caspian Sea (Absheron Ridge), the western and eastern extensions of the southern front of the Greater Caucasus. The Moho plunges from about 40 km beneath the Kura basin to more than 60 km beneath the Greater Caucasus and rises to 40 km again under the northern foreland basin.

Starting in early Paleogene, and accelerating in early Miocene, deformation is a strong ongoing process throughout the whole Caucasus. Located since Paleogene in the paleogeographic realm of the Eastern Paratethys, it remains unclear at which time the Caucasus emerged above sea level. The zone of highest topography is thought to be the zone of fasted uplift. Uplift may be linked with N-verging backthrusting, possibly over a ramp system at depth as suggested by seismicity. A possible candidate obove which the major topography develops could be the Main Caucasus Thrust (MCT). The initial Kura basin is dissected by an accretion prism into the southern Kura basin and the northern Alasani basin. Deep seated southward migration of the orogenic front, causing the accretion prism, led to the inversion of the Pliocene to Late Pleistocene sediments, and the transport of the Alasani basin as a piggy back basin towards the south. The northern foreland basin (Terek) subsided since the early Pliocene more than 4,000 m, and recently exhibits pitted gravels of Early Pliocene age at 1,600m elevation. It is however, unclear how strain is partitionned between the active front (to the N and the S) and the zone of fastest uplift, or the MCT.

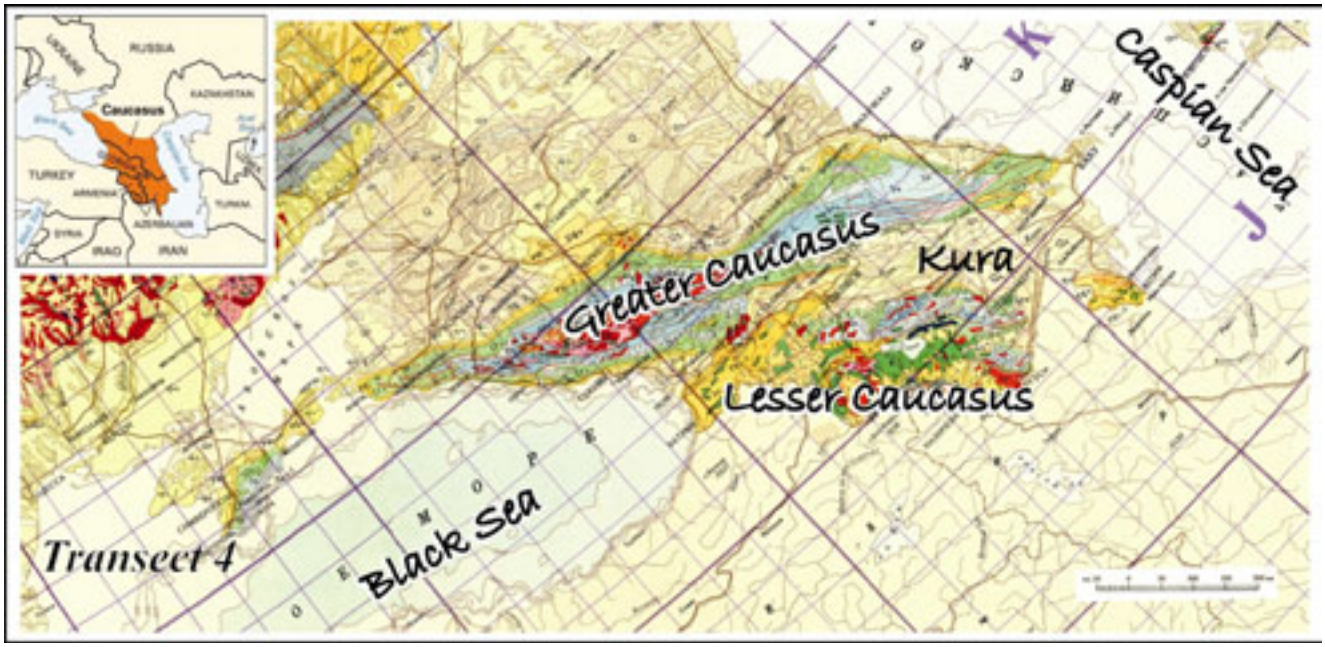

Figure: Geological map of the Caucasus area

1.41

Numerical modelling of subduction initiation at passive margins: Critical effects of continental mantle strength and density

Nikolaeva Ksenia*, Gerya Taras*, Marques Fernando**

*ETH-Zurich, Institute of Geophysics, Schafmattstrasse 30, 8093 Zurich (nikolaeva@erdw.ethz.ch)
**Univ. Lisboa, Edificio C6, Pisco 2, 1749-016 Lisboa, Portugal

Despite its crucial significance for the plate tectonics theory, subduction initiation remains a largely enigmatic open problem. It has been showed that at most passive margins elastic and frictional forces exceed gravitational instability and ridge-push forces, which preclude subduction initiation. From this point of view, the Atlantic Brazilian margin, characterized by a relatively thin lithosphere, represents a rare case where force balance is favourable for subduction initiation, which is evidenced by several tectonic/thermal features. In relation to this natural case we studied numerically physical parameters that control tectonic processes at passive margins characterized by thinned to normal continental lithosphere. The investigated parameters are thermal age of the oceanic plate, temperature structure (thickness) and density of the continental lithosphere, and the rheology of crust and mantle. Our experiments show that three different geodynamic regimes can be discriminated: (1) stable margin, (2) overthrusting and (3) subduction. Both overthrusting and subduction are driven by inherent gravitational instability of the passive margin due to the strong density contrast between the continental crust and adjacent oceanic lithosphere. This instability forces continental crust to thrust over the oceanic plate. In the case of over-

thrusting regime the thrusting of the continental crust over the oceanic plate is associated with deflection but not subduction of this plate, which remains attached to the continent. Transition from stable margin to either overthrusting or subduction is mainly dependent on the ductile strength of the lower crust with weak and hot crust favouring its oceanward movement. On the other hand, transition from overthrusting to subduction is crucially controlled by the ductile strength and density of the continental mantle lithosphere. Subduction is strongly favoured by rheologically weak (hot, hydrated) and depleted continental mantle characterized by lowered density compared to the oceanic lithosphere. Moreover, the present numerical experiments show that the age of the oceanic lithosphere at a passive margin does not play any significant role for the initiation of subduction.

REFERENCES

Feng, M., van der Lee, S., and Assumpcao, M. 2007: Upper mantle structure of South America from joint inversion of waveforms and fundamental mode group velocities of Rayleigh waves, Journal of geophysical research, 112, B04312, doi:10.1029/2006JB004449.

Gerya, T.V., and Yuen, D. 2007: Robust characteristics method for modelling multiphase visco-elasto-plastic thermo-mechanical problems, Physics of the Earth and planetary interiors, 163, 83-105.

Tassara, A., Swain, C., Hackney, R., and Kirby, J. 2007: Elastic thickness structure of South America estimated using wavelets and satellite-derived gravity data, Earth and planetary science letters, 253, 17-36.

1.42

Structural Mapping along the Meran-Mauls and the Faltleis Faults in the Sarntaler Alps (South Tyrol, Northern Italy)

Nommensen Lisa*, Stipp M.**, Pomella H. & Fügenschuh B.***

* *Geologisches Institut, Albertstr. 23B, D-79114 Freiburg (lisa.nommensen@web.de)*
** *IFM-GEOMAR, Wischhofstraße 1-3, D-24148 Kiel (mstipp@ifm-geomar.de)*
*** *Institut für Geologie und Paläontologie, Innrain 52, A-6020 Innsbruck*

The Periadriatic Fault System (PFS) separates the Southern Alps from the Western, Central and Eastern Alps to the North. The Meran Mauls fault (MF) is one segment of the PFS which connects the NNE-SSW-striking Giudicarie fault with the E-W-trending Pustertal-Gailtal fault. So far, the MF has been described as a NW-dipping thrust with SE-directed transport of the Austroalpine Meran-Mauls basement on top of the Southalpine late-Variscan Brixen granodiorite (e.g. Mancktelow et al. 2001). Located approximately 2 km NW and parallel to the MF, the Faltleis fault (FF) is a branch or parallel fault within the Austroalpine Meran-Mauls basement separating the Ky-bearing paragneisses and micaschists of the Punta Cervina unit (PCU), late Permian granitic to gabbroic intrusives (orthogneisses) with amphibolites, and Permotriassic cover sediments from the overlying San Leonardo unit (SLU) consisting mainly of banded paragneisses.

Detailed structural mapping was carried out along a part of the MF and the FF in the Sarntaler Alps of South Tyrol near the village of Weißenbach in order to analyze the kinematics of the two faults and to identify related structures in the under- and overlying rock units. The area of the two faults is characterized by a strong mylonitic foliation (S1) with an orientation of approximately 330/35 extending from the top of the Brixen granodiorite in the SE through the PCU and into the SLU in the NW except for minor portions of the granites and amphibolites as well as for the Triassic dolomites of the PCU which are not pervasively foliated. Two stretching lineations are related to S1, a steep or downdip stretching lineation indicating a top to the SE transport and an older subhorizontal stretching lineation with a transpressive right-lateral sense of shear. S1 is folded by two major folding phases. The older isoclinal to tight folds (F1) have moderately NNW plunging fold axes, while the younger tight to open folds (F2) strike NE-SW with subhorizontal axes. Locally, an F1 axial plane cleavage slightly steeper than S1 can be observed.

The MF itself is marked by a discrete cataclastic zone overprinting the Brixen granodiorite in the footwall. Hence, the MF displays the classical set-up of a major thrust fault at the frictional-viscous transition with cataclasites in the footwall and mylonites in the hanging wall. However, the thrust-related deformation overprints an earlier dextral-transpressive shearing as indicated by subhorizontal stretching lineations and related shear sense indicators within the same foliation (S1). The FF has a more complicated structural assembly with two cataclastic zones, one at the contact between the SLU in the hanging wall and the Permotriassic cover sediments of the PCU in the footwall and the other one inside the footwall at the transition

between orthogneisses and this same Permotriassic sediments. The width of the Permotriassic sediments varies significantly along strike leading eventually to their absence westwards outside the mapping area and hence to the conjunction of the two cataclastic belts. Deformation of the sediments is variable ranging from a pervasive mylonitization of the metamorphic limestones to a weak brittle overprint on the dolomites preserving their bedding plane and sedimentary structures. The calcite mylonites show a very strong mylonitic foliation (S1) with a gently SW-dipping stretching lineation. Ubiquitous kinematic indicators point to dextral transpressive shearing. The same shear sense can be derived from subhorizontal slickensides on brittle faults with similar planar orientation in the orthogneisses next to the calcite mylonites. A second set of downdip slickensides in the orthogneisses on similarly oriented fault planes indicates top to the SE thrusting.

In summary, the investigated area of the MF and FF displays a polyphase deformation history starting with dextral transpressive shearing in a wide mylonitic corridor. Brittle deformation of dolomites and plastic deformation of gneisses and limestones (i.e. marbles) indicate metamorphic temperature conditions below 450°C and clearly above 300°C. Ongoing deformation during a decrease in temperature allows for the plastic to brittle transition of the gneisses and continuous mylonitization of the limestones. Eventual changes in the indentation process or geometry may cause a rotation of the main foliation and a reactivation by thrusting under conditions of the frictional-viscous transition. Thrusting is more closely bound to the two major fault planes of the MF and the FF and becomes more and more localized during cooling temperature conditions.

REFERENCES

Mancktelow, N.S. et al. 2001: The DAV and Periadriatic fault systems in the Eastern Alps south of the Tauern window, Int. J. Earth Sciences 90, 593-622.

1.43

Comparative study of geological and GPS research of reactivated fractures in the north of Silesia (NE part of the Bohemian Massif, Czech Republic)

Nováková Lucie

Institute of Petrology and Structural Geology, Faculty of Science, Charles University, Albertov 6, Prague 2, CZ-12809, Czech Republic (lnovakova@irsm.cas.cz)

In this paper author compares two different approaches in the study of the fault reactivation – geological measurements and long time GPS monitoring. Both approaches were applied in the area of Javornický výběžek in the north of Silesia. This area is characterized by several important geological boundaries represented by faults of the Sudetic (NW-SE) and the Moravo-Silesian (NE-SW) directions, e.g. the Sudetic Marginal fault (SMF), the Ramzová overthrust, Nýznerov fault zone (Fig. 1). Almost all faults are of variscian age and were subsequently reactivated (Chlupáč et. al. 2002; Badura et. al. 2004).

The geological approach consisted of standard structural measurements of orientation of faults and joints, lineation and/or other kinematic indicator (steps etc.) have been applied on almost forty localities in the area. The data were processed using Daisy3 4.71.06 software (Salvini 2008) and results displayed into a map of the area. This map points to the system of reactivated fractures in the area.
The GPS data were collected for more than ten years in the area by the Institute of Rock Structure and Mechanics Czech Academy of Sciences. The GPS investigations confirm the recent movements along important faults in northern Silesia (Schenk et. al. 2002). The data from the nine surrounding GPS stations both permanent and epoch were averaged. The average movement of each station was corrected using an average movement in the area and displayed in another map of the area. The second map characterizes recent movements in the studied area.
The results provided by both methods were compared, discussed and displayed.

REFERENCES

Badura, J., Zuchiewicz, W. & Przybylski, B. 2004: The Sudetic Marginal fault, SW Poland: a reactivated sinistral-normal fault. Geolines, 17, 17-18.
Chlupáč, I., Brzobohatý, R., Kovanda, J. & Stráník, Z. 2002: Geological history of the Czech Republic. Academia Praha, 436.
Salvini, F. 2008: Daisy3 4.71.06 software. Available at http://host.uniroma3.it/progetti/fralab/

Schenk, V., Cacoń, S., Schenková, Z., Kontny, B., Bosy, J. & Kottnauer, P. 2002: The GPS geodynamic network East Sudeten. Five annual campaigns (1997-2001), data processing and results. Acta Montana A, 20(124), 13-23.

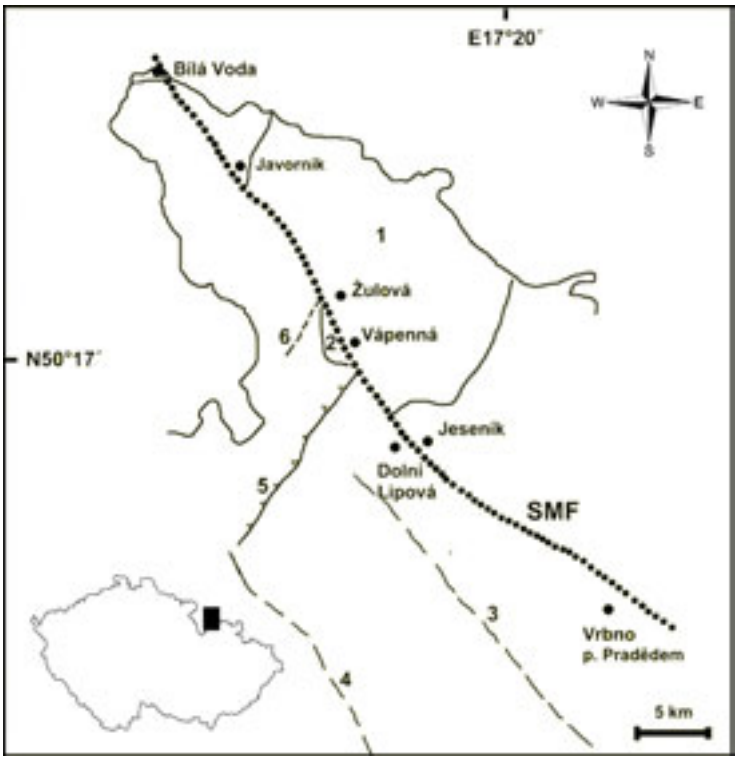

Figure 1. Tectonic situation of northern Silesia (SMF – Sudetic Marginal Fault, 1 - Žulová granite pluton, 2 - Limestones of the Branná group, 3 - Bělský fault, 4 - Klepáčovský fault, 5 – Ramzová overthrust, 6 – Nýznerov fault zone).

1.44

Structural evolution of the Monte Rosa and Adula nappes and the formation of the Lepontine dome

Pleuger Jan*, Nagel Thorsten**, Froitzheim Nikolaus**

*Geologisches Institut, ETH Zürich, Universitätsstraße 6, CH-8092 Zürich
**Steinmann-Institut, Bereich endogene Prozesse, Nußallee 8, D-53115 Bonn

The structural evolutions of the Monte Rosa and Adula nappes and their surrounding units are compared in order to develop a possible kinematic scenario for the formation of the Lepontine dome structure in the Swiss Central Alps. Towards west and east, nappe contacts and structures dip moderately away from the core of the Lepontine dome while they are bent into steeply dipping to overturned positions in the Southern Steep Belt north of the Periadriatic fault. The comparison of the Monte Rosa and Adula nappes allows to discuss the formation of the Lepontine dome structure since the Monte Rosa nappe extends into the Southern Steep Belt from the western flank of the Lepontine dome while the Adula nappe is situated in the eastern flank of that structure.

The Monte Rosa nappe was subject to five successive deformation phases postdating the eclogite-facies pressure peak at c. 42 Ma: (1) northwest-vergent shearing with only minor and small-scale folding (Mattmark phase, D_1); (2) southwest-vergent shearing with formation of large-scale tight to isoclinal folds (Malfatta phase, D_2); (3) southeast-vergent shearing with formation of large-scale open to tight southwest-vergent folds (Mischabel phase, D_3); (4) formation of the upright Vanzone fold and continuing southeast-vergent shearing (Vanzone phase, D_4); mostly dextral but also some sinistral shearing confined to the southern limb of the Vanzone antiform (Olino phase, D_5).

Similar as in the Monte Rosa nappe, the eclogite-facies pressure peak in the Adula nappe was reached c. 40 Ma ago. It was postdated by northwest-vergent shearing (Zapport phase, D_1) which in turn was followed by eastnortheast-westsouthwest-oriented shearing of the Leis phase (D_2). Though the significance of D2 Malfatta- and Leis-phase movements for the exhuma-

tion of underlying units in the core of the Lepontine dome may have been minor, they mark the onset of orogen-parallel extension of the Penninic nappe stack at c. 35 Ma. This orogen-parallel extension was replaced by orogen-perpendicular southeast-vergent extensional movements (older than c. 30 Ma) in and above the Monte Rosa (Mischabel phase, D_3) and Adula nappes (Claro phase, D_3) but continued later in deeper levels of the nappe stack at the Simplon fault in the west and at the Forcola fault in the east (from c. 19 Ma onwards and at c. 25 Ma, respectively).

Neither the ductile nor the brittle deformation at these two faults continued towards south through the meanwhile present Southern Steep Belt until the Periadriatic fault. The renewed orogen parallel-stretching in the flat-lying part of the nappe stack was probably instead accommodated by Olino-phase shearing in the Southern Steep Belt. While the Penninic nappe stack in the block north of the Periadriatic fault was stretched more or less parallel to that fault, there was no significant stretching of the south block parallel to the Periadriatic fault. This stretching-fault character of the Periadriatic fault may explain the variations in displacement (including locally sinistral shearing) that can be observed along the strike of the fault.

Although the kinematics of all deformation phases postdating D_1 (i.e. northwest-vergent nappe stacking) differed considerably, it is remarkable that all these deformation phases contributed to the formation of the Lepontine dome in that they effected thinning of the units between the European basement now exposed in the Lepontine Dome and the Periadriatic fault which developed its backthrust geometry only after D_3.

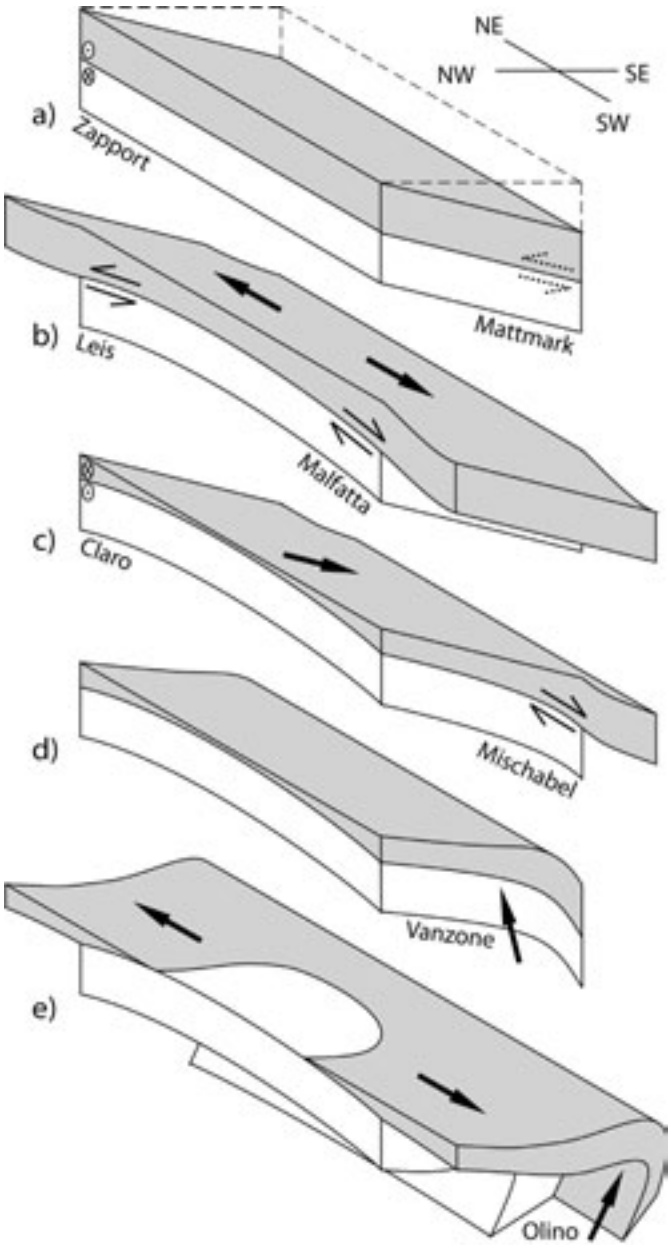

Fig1: Strongly schematized diagrams illustrating the exhumation of the Central Alps. (a) Situation after D1. (b) Orogen-parallel stretching of D2 in the western and eastern flank of the Lepontine dome accommodate a first stage of unroofing. (c) D3 SE-vergent shearing effects further exhumation by normal faulting. (d) Uplift of the nappe stack in the core of the Vanzone antiform. (e) Final orogen-parallel stretching and overturning of the Southern Steep Belt are accommodated by Olino-phase shearing in the Southern Steep Belt while extensional shearing, followed by brittle normal-faulting, in the flat-lying part of the nappe stack accommodates further unroofing.

1.45

The Giudicarie Fault System at the transition between Southern and Eastern Alps (Northern Italy) A new structural analysis

Pomella Hannah*, Fügenschuh Bernhard*, Stipp Michael**

* *Institute of Geology and Paleontology, University of Innsbruck. Innrain 52, A-6020 Innsbruck Hannah.Pomella@uibk.ac.at, Bernhard.Fuegenschuh@uibk.ac.at*
** *IFM-GEOMAR, Leibniz Institute of Marine Sciences. Wischhofstr. 1-3, D-24148 Kiel (mstipp@ifm-geomar.de)*

The NNE-SSW striking Guidicarie Fault System (composed of the Northern and Southern Giudicarie Fault and the Meran-Mauls Fault) represents a distinctive bend in the Periadriatic Fault System (PFS). It terminates the E-W striking Tonale Fault Zone to the east and the ESE-WNW striking Pustertal-Gailtal Fault to the west. The apparent sinistral offset between these two dextral strike-slip faults amounts to about 80 km realized by the 290/40-60 oriented Northern Giudicarie Fault and its northeastern prolongation the Meran-Mauls Fault (320/40-60). The NNE-SSW striking Southern Giudicarie Fault is located south of the conjunction Tonale Fault Zone – Northern Giudicarie Fault and delimits the Oligocene Adamello Pluton to the east.

Two end member models are generally discussed concerning the Cenozoic evolution of the Guidicarie Fault System as part of the Periadriatic Fault System: an originally straight Periadriatic Fault System, dissected and sinistrally offset in the Miocene (e.g. Laubscher, 1971; Frisch et al., 1998; Stipp et al., 2004) or Neogene compressional inversions of an inherited Early Permian to Lower Liassic NE-SW trending horst and graben structure (e.g. Viola et al., 2001; Castellarin et al., 2006).

At the easternmost end of the Tonale Fault Zone the mylonitic foliation of the Adamello Pluton bends from an E-W into a NE-SW trending orientation close to the intersection with the Guidicarie Fault System whereas the stretching lineation remains still nearly horizontal. Also along the NE-SW striking Meran-Mauls Fault a nearly horizontal stretching lineation with a dextral sense of shear can be observed, overprinted by a clearly younger steep dipping lineation, revealing top ESE to SE thrusting. We interpret these NE-SW oriented mylonites with horizontal stretching lineations as boudinaged elements of the Tonale mylonites which formed during dextral strike slip movements along the PFS in the Oligocene. In case of an originally curved Periadriatic Fault System transpression along the NE-SW trending sections of the Periadriatic Fault System should not allow for subhorizontal stretching lineations.

Along the Guidicarie Fault System Oligocene tonalitic bodies occur, subsumed under the term “Oligocene Tonalitic lamellae”. Along the southern part of the Northern Giudicarie Fault only a few less then 50 m thick and 200 m long lenses crop out, often strongly affected by brittle deformation. So far no tonalitic bodies have been found between the locality Rumo in the Val di Non and Pawigl south of the city of Meran, i.e. for some 20 km. From Pawigl to the NE the lenses are more continuous, up to 150 m thick and less affected by brittle deformation.

Near Pawigl on the northern end of the Northern Giudicarie Fault tonalites display a mylonitic foliation parallel to the foliation of the overlying Austroalpine Paragneisses (325/40). The ductile fault is dissected and sinistrally offset by brittle NNE-SSW striking strike-slip faults with offsets of ≈50 m. Similar faults are observed along the “Falschauer” river located a few hundred meters south of the fault (see figure 1). Towards NE a cumulative sinistral offset of about 4,5 km along one or several NNE-SSW trending sinistral strike-slip faults is necessary in order to connect the Giudicarie Fault System near Pawigl with the Meran-Mauls Fault north of Meran. The NNE-SSW trending south-western sinistral strike slip faults can be interpreted as a younger fault system related to the late Miocene Passeier Fault (Viola et al. 2001). For structural reasons the outcrops near Pawigl are interpreted to represent the southernmost part of the Meran-Mauls Fault dissected by the Miocene Passeier fault which belongs to the late sinistral offset along the Giudcarie fault.

We propose that the Meran-Mauls Fault belonged initially to the dextral transpressive segments of the PFS, ie. Tonale and Pustertal-Gailtal Fault. Afterwards it was presumably rotated and evidently reactivated as SE-directed (back)thrust. Finally, Tonale Fault (e.g. Stipp et al. 2004) and Meran-Mauls Fault were sinistrally offset by Passeier and Giudicarie strike slip faulting.

REFERENCES

Castellarin, A. et al. 2006: The Alpine evolution of the Southern Alps around the Giudicarie faults: A Late Cretaceous to Early Eocene transfer zone – Tectonophysics, 414, 203-223.

Frisch, W. et al. 1998: Palinspastic reconstruction and topographic evolution of the Eastern Alps during late Tertiary tectonic extrusion – Tectonophysics, 297, 1– 15.

Laubscher, H.P. 1971: Geologische Rundschau, 60, 710-718.

Stipp et al. 2004: Contemporaneous plutonism and strike-slip faulting - Tectonics, 23, TC3004

Viola, G. et al. 2001: Late Oligocene-Neogene evolution of Europe-Adria collision – Tectonics, 20, 999-1020.

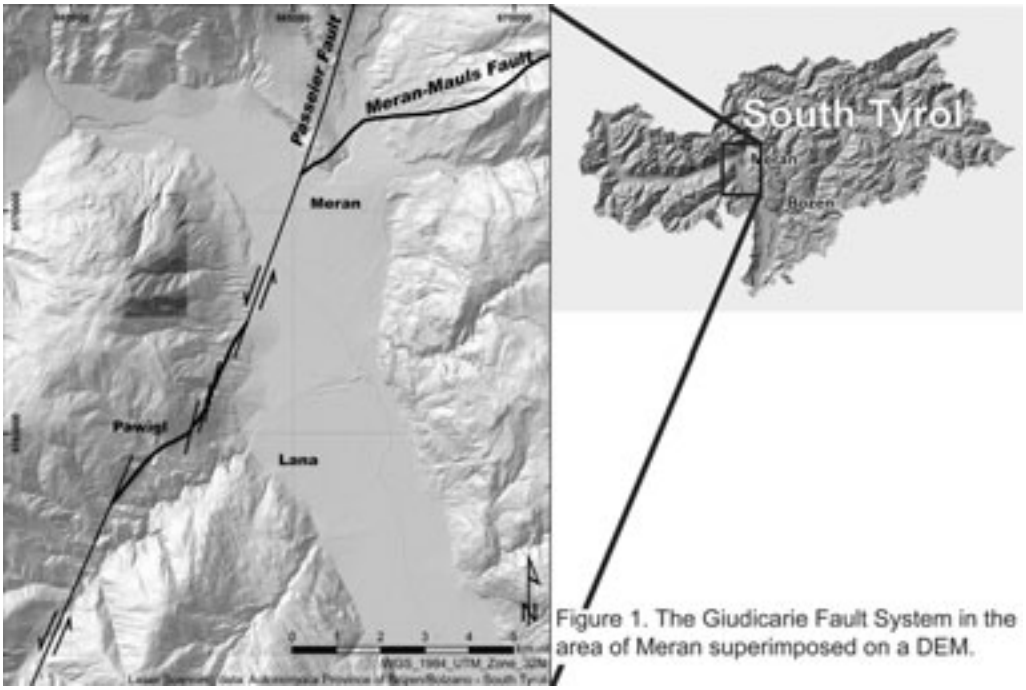

Figure 1. The Giudicarie Fault System in the area of Meran superimposed on a DEM.

1.46

Volcanic ash layers in OSM sediments: clues to their origin and the post-sedimentary tectonic history

Rahn Meinert[1], Selbekk Rune[2], Spikings Richard[3], Zaugg Alfred[4] & Burkhalter Reto[5]

[1]*Mineralogisch-Geochemisches Institut, University of Freiburg i. Brsg., Germany (meinert.rahn@hsk.ch)*
[2]*Natural History Museum, Geology, University of Oslo, Norway*
[3]*Département de Minéralogie, Rue de Maraîchaire 13, CH-1205 Genève*
[4] *CSD Ingenieure und Geologen AG, Zürcherstrasse 34, CH-8500 Frauenfeld*
[5]*Bundesamt für Landestopographie, Seftigenstrasse 264, CH-3084 Wabern*

Layers of volcanic origin have been reported from within Upper Freshwater Molasse (OSM) sediments (e.g. Pavoni 1958, Hofmann 1958, 1959, 1961, 1975, Hofmann et al. 1975, Pavoni and Schindler 1981). These layers are bentonite horizons and volcanic tuff layers of a few cm to several m thickness. While the source area of these intercalations is clear for many layers close to the Hegau Volcano area in OSM sediments of NE Switzerland and southernmost Germany, they are less obvious for e.g. the widely distributed ash layers in the Randen area (Hofmann 1958) or completely unknown for occurrences in the Tabular Jura (Hofmann 1961), with some occurrences being closer to the Kaiserstuhl volcano than to the closest volcanic cones of the Hegau.

Despite strong weathering, some layers provide fresh volcanogenic minerals that can be dated (e.g. Gubler et al. 1992, Rahn and Selbekk 2007). The radiometric ages can be compared to mammalian fossil stratigraphy (e.g. Bolliger 1998, Kälin 1993). Radiometric ages include U/Pb data from zircon (in bentonites only), Ar/Ar data from sanidine, biotite and hornblende (for a compilation, see Schreiner 1992) and apatite FT data (Rahn and Selbekk 2007).

Investigations on volcanic minerals do not only provide answers to their stratigraphic age and the bracketing of otherwise weakly constrained sedimentary events (e.g. the horizon of the “Appenzell granite”). In this contribution, we illustrate that age data of the volcanic horizons also serve to tightly estimate vertical offsets along faults that are only vaguely constrained by field mapping. In addition, the age data in combination with the composition of the dated minerals allow clarifying their origin.

We have separated apatite from ash layers from within the Heliciden marls of the Randen area, and from the Tabular Jura to determine their origin and the time period of volcanic activity. In addition, hornblende and apatites have been separated

from different localities from the Schiener Berg in the context of the launching of map sheet Steckborn-Kreuzlingen of the Geological Atlas of Switzerland 1:25'000 (Zaugg & Geyer, in prep.) in order to understand the late stage of the tectonic evolution of the area. Prior to dating, fission track lengths were measured for all apatite samples to confirm their volcanic origin. Apatites were measured on an electron microprobe to check their composition. The limited time periods of volcanic activity at the Kaiserstuhl (16-19 Ma, Keller et al. 2002) and the Hegau area (15-7 Ma, Schreiner 1992) in combination of the significant differences in apatite composition (F-OH apatites from Kaiserstuhl, Cl-OH apatites from the Hegau) provide a basis for a clear distinction of the origin of the volcanic material.

REFERENCES

Bolliger, T. (1998): Age and geographic distribution of the youngest Upper Freshwater Molasse (OSM) of eastern Switzerland. Eclogae geologicae Helvetiae 91, 321-332.

Gubler, T., Meier, M. & Oberli, F. (1992): Bentonites as time markers for sedimentation of the upper freshwater molasses: Geological observations corroborated by high-resolution single zircon U-Pb ages. SANW annual assembly, Basel, Abstract volume: 12-13.

Hofmann, F. (1958): Vulkanische Tuffhorizonte in der Oberen Süsswassermolasse des Randen und Reiat. Kanton Schaffhausen. Eclogae geologicae Helvetiae 51, 371-377.

Hofmann, F. (1959): Vulkanische Tuffhorizonte der Schienerbergeruptionen auf dem thurgauischen Seerücken. Eclogae geologicae Helvetiae 52, 462-475.

Hofmann, F. (1961): Vulkanische Aschen in den Helicitenmergeln des baslerischen, aargauischen und badischen Tafeljuras. Eclogae geologicae Helvetiae 54, 133-136.

Hofmann, F. (1975): Vulkanische Tuffe auf dem Wellenberg E von Frauenfeld und neue Funde auf dem thurgauischen Seerücken. Eclogae geologicae Helvetiae 68, 311-318.

Hofmann, F., Büchi, U.P., Iberg, R. & Peters, T. (1975): Vorkommen, petrographische, tonmineralogische und technologische Eigenschaften von Bentoniten im schweizerischen Molassebecken. Beiträge zur Geologie der Schweiz, geotechnische Serie 54, 51pp.

Kälin, D. (1993): Stratigraphie und Säugetierfaunen der Oberen Süsswassermolasse der Nordwestschweiz. Unpublished PhD thesis ETH Zürich, 238pp.

Keller, J., Kraml, M. & Henjes-Kunst, F. (2002): 40Ar/39Ar single crystal laser dating of early volcanism in the Upper Rhine Graben and tectonic implications. Schweizerische Mineralogische und Petrographische Mitteilungen 82, 121-130.

Pavoni, N. (1958): Neue Bentonitvorkommen in der Zürcher Molasse. Eclogae geologicae Helvetiae 51, 299-304.

Pavoni, N. & Schindler, K. (1981): Bentonitvorkommen in der Oberen Süsswassermolasse und damit zusammenhängende Probleme. Eclogae geologicae Helvetiae 74, 53-64.

Rahn, M. & Selbekk, R. (2007): Absolute dating of the youngest sediments of the Swiss Molasse basin by apatite fission track analysis. Swiss Journal of Geosciences 100, 371-381.

Schreiner, A. (1992): Geologische Karte 1:50 000 von Baden Württemberg - Erläuterungen zu Blatt Hegau und westl. Bodensee. Geologisches Landesamt Baden-Württemberg, Freiburg, Stuttgart: 290p.

Zaugg, A. & Geyer, M. (in prep.): Blatt 1033/1034 Steckborn-Kreuzlingen. Geologischer Atlas der Schweiz 1:25'000, Karte u. Erläuterungen.

1.47

Direct versus indirect thermochronology – what do we trully trace? Examples and implications for the Central Andes

Ruiz, G.M.H.

To quantify long-term denudation rates, research groups commonly applied low-temperature thermochronometric methods to rock now exposed at the surface. This approach on bedrocks from the hinterland is sometimes limited since erosion has often removed the record of earlier stages of orogenic growth. To overcome this shortcoming, researchers have increasingly studied since 20 years orogenic sedimentary records combining detrital thermochronological analyses with sedimentary petrography but also modelled detrital age populations from true bedrock catchments.

We propose here to study the denudation history of regions located in the Central Andes of SE Peru. Our approach consists on analysing present-day erosional products along five different river catchments for the Apatite Fission-Track (AFT) thermochronometer. Up to four age populations were extracted from the analyses of 100 grains per sample. Age populations range between 80 and 0.5 Ma with a majority of age populations and grains younger than 10 Ma. These AFT analyses from

the ‘true’ present-day erosion product of the chain are compared with ones from an 'artificial' one we generated and this to investigate the recent evolution of the eastern Andes. The artificial detrital record was engendered by the combination of 197 individual grain ages we produced from a bedrock profile in the region (Ruiz in press). Interestingly, the 'artificial' sand express a clear homogeneous AFT signal with a single and pooled AFT age of 4.1 ± 0.1 Ma. This age is identical to the youngest age population (P1) we extracted from the 'true' sand within the same catchment (4.4 ± 0.4 Ma) and suggest that the ‘true’ dated grains of the P1 population were derived from, if not this one, a region with similar thermal record. Our results are of main importance because they indicate for the first time that a detrital age population, once statistically individualized and limitations of the method perfectly excluded, most likely reflects the erosion in a single part of a catchment. In the eastern Andes of Peru, the older age populations we extracted are probably derived from upper levels within the catchment that reflect by their presence, but not directly quantify, former denudation. Reversely, the youngest age populations for all present-day river sands are younger than 6.8 Ma. These data point towards lower levels of the eastern Andes that undergo rapid denudation and this since recent time (Ruiz in press) because of the preservation of older thermal record.

The approach we developed is innovative and aims to reduce the amount of necessary analysis to constrain long-term denudation rates in different orogenic settings. It also hosts a methodological aspect by comparing results from direct (bedrock) and indirect (present-day river sands) thermochronological analyses within the same catchment.

1.48

The Atlas Mountains: why there? Why now?

Ruiz G.M.H., Negro F., Foeken J., Stuart Babault J., F., Ivy-Ochs S., Kober F., Saddiqi O., Stockli D., Champagnac J-D. & Frizon de Lamotte D.

The target area is the WSW- ENE oriented intra-continental Atlas chain in Morocco located between the West Africa Craton and the Betic-Rif system. It is a key natural laboratory encompassing the Pre-Cambrian to recent evolution of the region even though the stratigraphic record is incomplete. The presence of high surface elevations in both the High-Atlas (>4000m) and Anti-Atlas (>2500m; Figs. 1 & 2) domains to the south is subject to discussions because there is little quantitative data available at present. Phases of uplift are thus ill constrained as places where the associated erosion products were accumulated.

To better constrain the orogenic growth of the Atlas chain, we investigated the time-Temperature paths of bedrocks from two morpho-structural domains that are separated by the narrow Souss Basin, i.e. the High and Anti-Atlas (Fig. 1). Pre-Cambrian bedrocks from the Anti-Atlas domain yield old thermochronological Fission-Track ages on both zircon (390-300 Ma) and apatite (180-120 Ma) minerals that are associated with slightly younger Atlantic (U-Th)/He ages on apatite (120-110 Ma, Fig. 2). There are two possible (probably interfingering) interpretations for the preservation of such old thermal record: a) the Anti-Atlas was not affected by the 'Alpine' orogeny and (always) remain ‘stable’, or b) it is being affected since recent time but no level with such record is yet exposed.

Bedrocks from the High-Atlas yielded (U-Th)/He ages on apatite comprised between 4 and 35 Ma (Fig. 1), which is a very different signal (Alpine?) than the one of the Anti-Atlas (Fig. 2). Age-elevation relationship suggests that denudation increased towards 1.0 km/my for the Late Miocene . Continental series of Cretaceous age from both Sub-Atlas domains indicate total resetting to temperatures greater than 80°C. Using a geothermal gradient of 25°C/km, this suggests that a post Cretaceous sedimentary pile of at least 3 kilometres in thickness is missing, which would be in agreement with sourcing from the High-Atlas region. The timing of the erosion of this pile is still unknown but it is being constrained by thermal modelling through Apatite Fission-Track analysis.

Our thermochronological data provide for the first time constraints that evidence heterogeneous exhumation history between the different structural domains of the chain. Additional analyses using thermochronometers with higher temperature of closure (e.g. Fission-Track or (U-Th)/He on zircon) are being performed to investigate rates of medium to long-term processes. Our results are being compared with existing geological records from Morocco but also on the other side of the Atlantic ocean, to identify the relevant tectonic process that shaped the landscape of this mountain range in the frame of the Africa-Europe convergence but also, which is novel, opening of the Atlantic ocean.

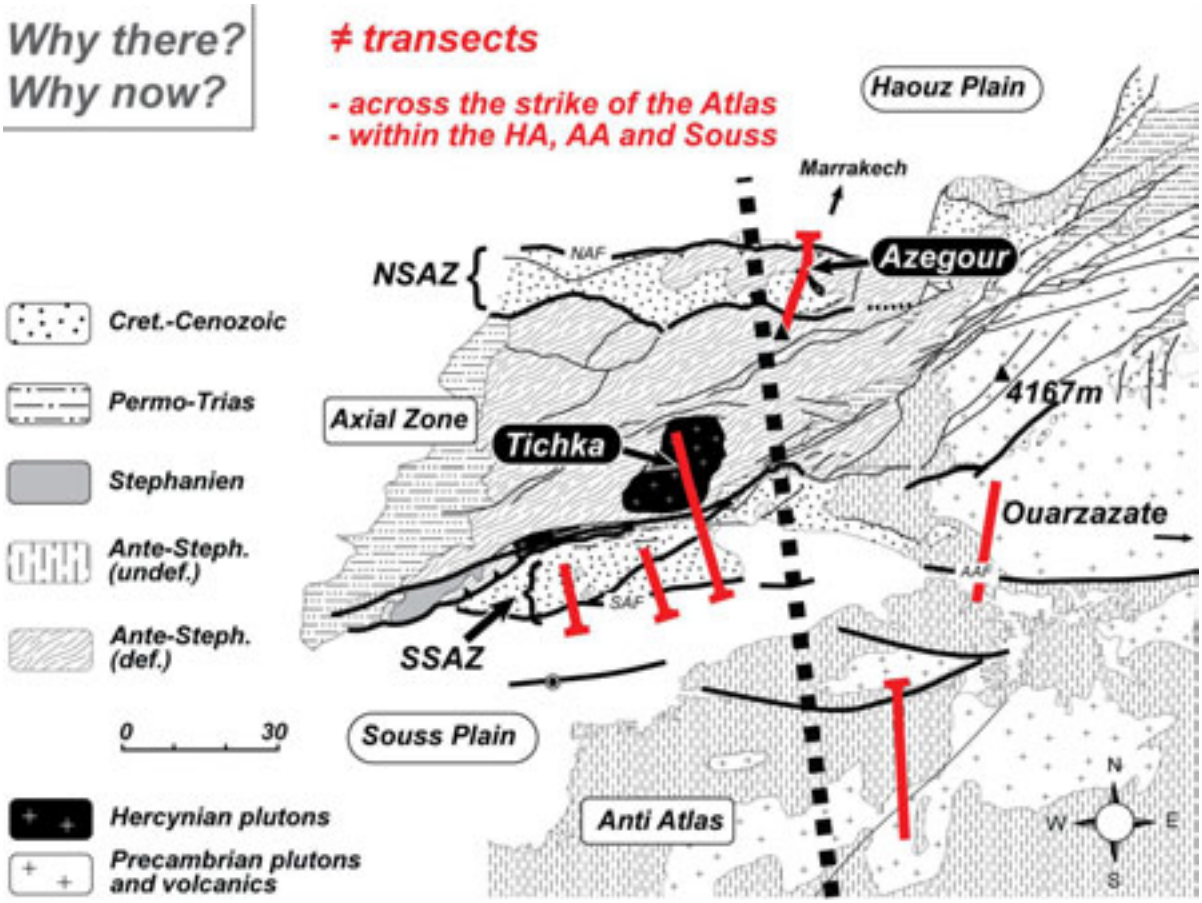

Figure 1. Morphostructural map of the Western Atlas system. In red are the different transects against the strike of the orogen along which bedrocks and present-day river sands were selected for thermochronological and cosmogenic isotopic analyses. Dashed black line: profile illustrated in Figure 2.

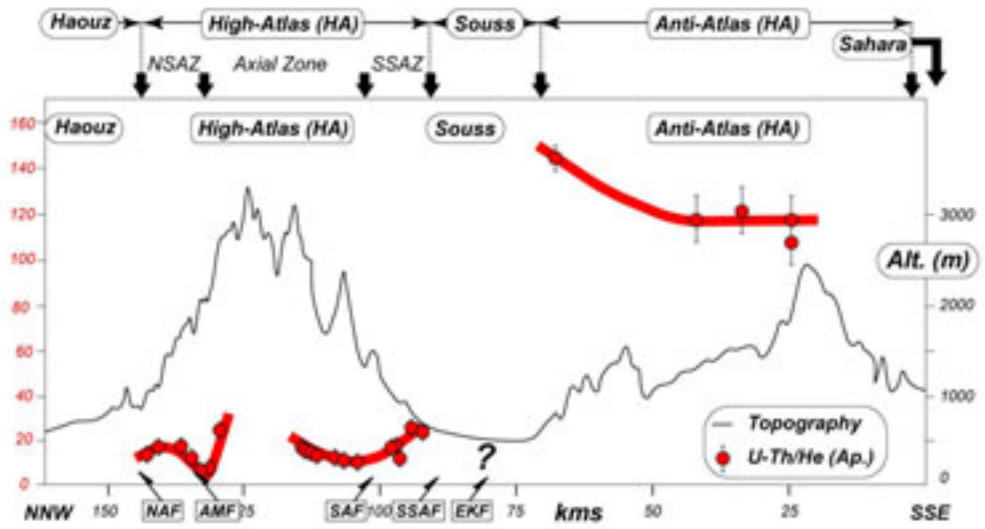

Figure 2. Topographic profile (see Fig. 1 for location) against the Atlas system in SW Morocco with associated U-Th/He ages on Apatite from the different domains. NSAZ, SSAZ, NAF, AMF, SAF, SSAF, EKF: Northern Sub-Atlas Zone, Southern Sub-Atlas Zone, North Atlas Fault, Al Medina Fault, South Atlas Fault, Southern Sub-Atlas Front, El Klea Fault.

1.49

Metamorphic and igneous evolution of the innermost Dinarides in Serbia

Schefer Senecio*, Egli Daniel*, Frank Wolfgang**, Fügenschuh Bernhard***, Ovtcharova Maria****, Schaltegger Urs****, Schoene Blair**** & Schmid Stefan*

*Geologisch-Paläontologisches Institut, Bernoullistrasse 32, CH-4056 Basel (senecio.schefer@unibas.ch)
** Geol. Insitute, Slovak Academy of Science, Dubravska Cesta 9, 84005 Bratislava
***Geologisch-Paläontologisches Institut, Innrain 52, A-6020 Innsbruck
****Département de Minéralogie, Rue des Maraîchers 13, CH-1205 Genève

During Early Paleogene collision the innermost Dinarides of Serbia, paleogeographically part of the Adriatic plate, occupy a lower plate position in respect to the Cretaceous-age Carpatho-Balkan orogen, now constituting the upper plate (Schmid et al., 2008). This study provides new timing constraints of the igneous and metamorphic events during and after collision that are crucial for a better understanding of the geodynamic evolution of the Balkan area.

The Kopaonik area in Southern Serbia, a N-S trending mountain range, exposes a part of the Jadar-Kopaonik thrust sheet in a tectonic window. There, the Kopaonik-Studenica Metamorphic Series, derived from the innermost Adriatic margin and overlying Western Vardar Ophiolitic Unit, are intruded by the Kopaonik, Drenje and Željin granodiorites, as well as by the Polumir granite. At the eastern rim of the Jadar-Kopaonik thrust sheet, a Cenozoic suture zone (Sava Zone) separates the internal Dinarides from the Carpatho-Balkan orogen consisting of Serbomacedonian "Massif" and tectonically overlying Eastern Vardar Ophiolitic Unit. The Kopaonik-Studenica Metamorphic Series (Paleozoic to Early Jurassic) are overlain by a Mid- to Late Jurassic ophiolitic mélange below the obducted Western Vardar Ophiolitic Unit. These three units are unconformably overlain by Late Cretaceous ("Senonian") flysch that contains large olistoliths, including ophiolitic blocks and reworked metamorphics. We interpret the weakly metamorphosed N-S-trending "Senonian" flysch as the southern prolongation of the Sava belt, suturing the internal Dinarides against the Carpatho-Balkan orogen. The intrusion of Oligocene granodiorite bodies led to contact metamorphism and skarn formation in the Kopaonik-Studenica Metamorphic Series.

We dated the intrusions by U-Pb (ID-TIMS) analyses of single, thermally annealed and chemically abraded zircons. All the analyses are concordant within analytical error. Two different age groups could be determined: (i) Oligocene intrusions, ranging from 31.7 to 30.6 Ma, whereby the Kopaonik intrusion yielded the youngest ages (30.94 Ma – 30.70 Ma). The Drenje and Željin intrusions cluster around 31.5 Ma. Hf isotopes for Drenje and Željin show relatively uniform εHf values ranging from 3.6 ± 0.5 to 4.3 ± 0.5. The Kopaonik sample, however, shows distinctively lower values ranging from 1.1 ± 0.5 to 1.6 ± 0.5. This indicates that the Drenje and Željin magmas had a higher juvenile component compared to the Kopaonik intrusion. (ii) A Miocene age of ca. 18.0 Ma was obtained for the westerly outcropping Polumir granite;, Hf isotopes for this intrusion are not yet available.

Fission-track analyses for these samples yielded ages of around 28 Ma for zircon and 18 – 23 Ma for apatite. This indicates rather fast post-emplacement cooling and exhumation, which is most probably tectonically assisted. An extensional tectonic setting is indicated by numerous normal faults, magmatic foliation in the Drenje locality and syn-intrusive boudinage of Polumir granitic dykes.
West of the Kopaonik area (Studenica valley) another part of the Kopaonik-Studenica Metamorphic Series crops out in the form of second tectonic window (so-called Studenica-slice, (Dimitrievič, 1997) below the obducted Western Vardar Ophiolitic Unit, again made up of Paleozoic to Early Jurassic meta-sediments. Most of these series only underwent lower greenschist facies metamorphism, but in the core of this window, along the Studenica River, amphibolite grade meta-sediments were found. Ar-Ar dating on sericite fractions (2-6 and 6-12 μ) as well as on amphibole and biotite separates evidence Cretaceous-age metamorphism, overprinted by a second Paleogene metamorphic overprint of the Studenica Metamorphic Series. While the Cretaceous event (110 – 85 Ma) reached lowest greenschist facies conditions only, Paleogene metamorphism (40.9 ± 4.9) reached amphibolite facies conditions and was probably followed by rapid exhumation assisted by normal faulting.

Our data document Cenozoic metamorphism in the innermost Dinarides of Serbia for the first time. This metamorphism is related to suturing of the Dinarides with the easterly adjacent Carpatho-Balkan orogen (including the Eastern Vardar Ophiolitic Unit) across the Sava Zone. So far Cenozoic metamorphism was only documented for the Sava Zone in northern Bosnia (Pamic, 1993; Ustaszewski et al. 2007). Moreover, our high-precision intrusion ages indicate an Oligocene-age intrusive suite, immediately followed by rapid exhumation according to the fission track data, possibly in a back-arc setting. This exhumation was then followed by a second magmatic pulse in the Miocene, again followed by rapid exhumation. This second magmatic and extensional event has to be seen in the context of the formation of the Pannonian basin.

REFERENCES
Dimitrievi ć, M.D., 1997. Geology of Yugoslavia., Geological Institute GEMINI Special Publication, Belgrade, pp. 187.
Pamic, J., 1993. Eoalpine to Neoalpine magmatic and metamorphic processes in the northwestern Vardar Zone, the easternmost Periadriatic Zone and the southwestern Pannonian basin. Tectonophysics, 226(1-4): 503-518.
Schmid, S.M. et al., 2008. The Alpine-Carpathian-Dinaridic orogenic system: correlation and evolution of tectonic units. Swiss Journal of Geosciences, 101(1): 139-183.
Ustaszewski, K. et al. 2007: The Late Cretaceous supra-subduction magmatism of North Kozara (northern Bosnia and Herzegovina): Implications for the Cretaceous to Paleogene collisional history between Tisza and the Dinarides, EGU General Assembly 2007, Volume 9: Geophysical Research Abstracts: Vienna, p. 03659.

1.50

Recent vertical movements from precise levelling in Switzerland

Schlatter Andreas

Federal Office of Topography swisstopo, Geodesy, Seftigenstrasse 264, CH-3084 Wabern (Andreas.Schlatter@swisstopo.ch)

Repeated measurements to determine national heights have shown that the Alps are still rising with respect to the Central Plateau. These so-called precise levelling lines follow major traffic arteries, pass through important tunnels and cross over main alpine passes. These networks include approx. 8,000 benchmarks whose heights serve as the vertical reference for most observations in Switzerland. The measurements used for this representation were first made between 1903 and 1945 and have since been repeated at least once.
The reference point for the investigation of vertical movements was arbitrarily chosen in Aarburg (Canton of Aargau) at the south foot of the Jura Mountains. All of the substantiated vertical changes are therefore relative uplifts or subsidences with respect to this point. Approx. 220 benchmarks were selected for the illustration in fig.1. Most of them are anchored directly in rock, some on buildings, which are known to be stable and well-founded.
The two maximum uplifts of up to 1.5 mm/year in the area between Sitten and Brig as well as in the Grisons (Chur/Engadin) are striking. Observations in the Jura Mountains are more likely to show subsidences. The Central Plateau seems to stay more or less stationary with the tendency of a tilt: subsidence in the west, uplift in the east. Even though the amounts seem small, the Alps are growing up to 15 cm in 100 years. Had a Roman citizen started out in Aarburg 2000 years ago to make his way to Rome across one of the passes in the Grisons, he would have had 3 meters less to climb. In geological terms the uplifts reach a total of several kilometers, which are of course continuously being offset by erosion. There are probably two main causes for these large-scale bulges:
1. The uplifts are a direct result of tectonic activities, in this case the penetration of the continental, European crust by the Adriatic spur.
2. The uplifts are so-called isostatic equalization movements. The earth's crust floats on the denser material of the earth's mantle. The erosion and also the melting of large ice masses at the end of the Ice Age result in delayed uplifts. This could be compared to a boat which rises in the water as it is being unloaded.

REFERENCES
Schlatter, A., D. Schneider, A. Geiger and H.-G. Kahle 2005: Recent vertical movements from precise levelling in the vicinity of the city of Basel, Switzerland. International Journal of Earth Sciences Vol. 94/2005: 507-514.
Schlatter A. 2007: Das neue Landeshöhennetz der Schweiz LHN95. Geodätisch-Geophysikalische Arbeiten in der Schweiz. Schweizerische Geodätische Kommission Band 72.

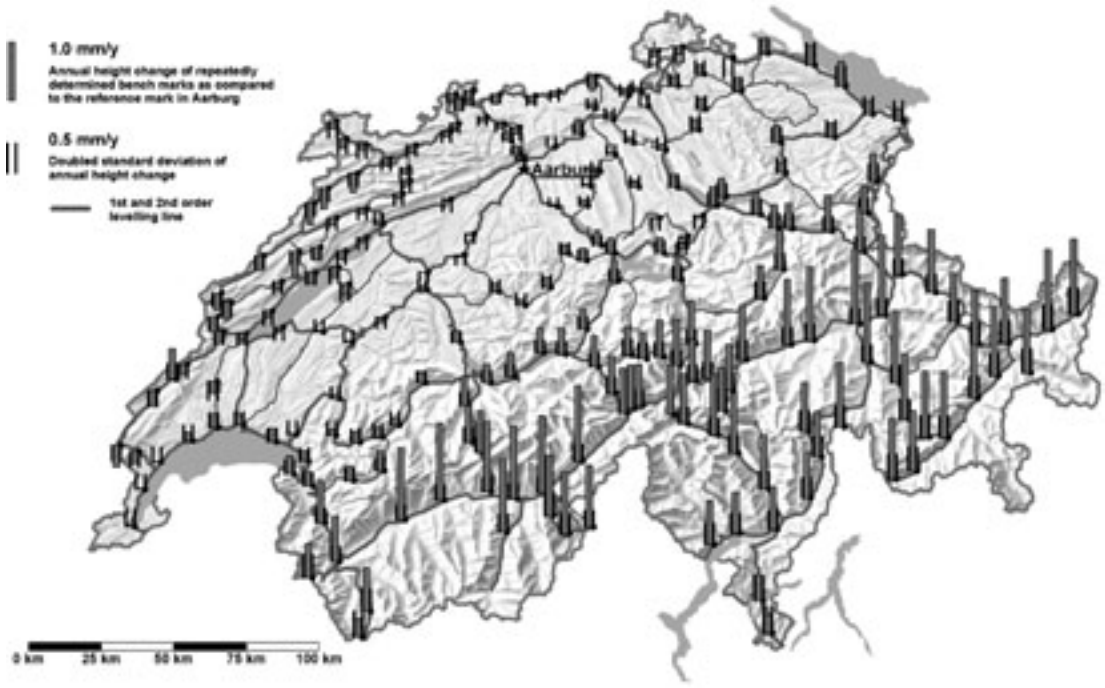

Figure 1. Swiss first and second order levelling network and annual height changes with respect to the reference bench mark in Aarburg

1.51
Initiation of plate tectonics in the early Earth

Sizova Elena*, Gerya Taras*

* *Institut of Geophysics, ETH-Zurich, Schafmattstr. 30, 8093 Zürich (sizova@erdw.ethz.ch)*

Plate tectonics is an outstanding example of a self organizing complex system, driven by the negative buoyancy of the thermal boundary layer resulting in subduction. Although the signature of plate tectonics is recognized with some confidence in the Phanerozoic geologic record of the continents, its action becomes less certain further back in time. The best way to improve our understanding of the early Earth is to combine our knowledge from petrological data and facilities of numerical modeling.

Based on 2D petrological-thermomechanical numerical model of oceanic-continental subduction (using the I2VIS code (Gerya & Yuen, 2003)) we determined sharp first order transition from modern style of subduction (fig1a) to transitional "pre-subduction" tectonic regime (fig.1b) at upper mantle temperature rising by around 160 ºC above the present one. This condition roughly corresponds to upper bound for Neoarchean (≈3Ga) mantle temperature (Davies, 1993; Komiya et al., 1999). In the "pre-subduction" tectonic regime plates are strongly internally deformable by intense percolation of melts continuously generated from underlying partially molten mantle. Their convergence results in shallow underthrusting of continental crust by oceanic plate (fig 1b). Oceanic plate goes quite far (to 200 km) under continental crust moving away and folding continental lithospheric mantle. In some experiments after the underthrusting oceanic plate starts to sink into the mantle forming at first stages two-sided subduction. In contrast to present time in the hotter "pre-subduction" regime there is no formation of backarc basin and new spreading center (the same was assumed by de Wit, 1998 for Archean time). Relatively shallow and hot tectonic style dominates. Oceanic plates weakened by sub-lithospheric melts are subjected to buckling and shallow underthrusting (rather then subduction) associated by local melting. This triggers formation of characteristic metamorphic and magmatic rocks found in Archean (such as, ultra-high-temperature and eclogite-high-pressure granulites, adakites and granitoids).

Further increase in the mantle temperature (by around 250°C above present) causes transition from "pre-subduction" regime to "horizontal-tectonics" regime (fig 1c). At this stage horizontal movements of small deformable plate fragments are predominant and even shallow underthrusts do not form under imposed convergence.

Our experiments also show that apart of mantle temperature another crucial parameter controlling the tectonic regime is degree of lithospheric weakening induced by upward movement of extracted sub-lithospheric melts. At the high Archean mantle temperatures when melts are always present in the upper mantle lithospheric weakening by melts should be low to preserve coherency of the plates and to allow stable subduction. Neither increasing radiogenic heat production nor lithospheric weakening by slab derived fluids has notable effects for the identified transitions in the early Earth.

REFERENCES

Davies G.F. 1993: Cooling the core and mantle by plume and plate flows. Geophys. J. Int. 115, 132–146.

de Wit, M. J. 1998: On Archean granites, greenstones, cratons and tectonics: does the evidence demand a verdict? Precambrian Research 91(1-2): 181-226.

Gerya, T.V. & Yuen, D.A. 2003: Characteristics-based marker-in-cell method with conservative finite-differences schemes for modeling geological flows with strongly variable transport properties. Phys. Earth Planet. Interiors 140, 295-320.

Komiya, T., S. Maruyama., T. Masuda, S. Nohda, M. Hayashi, K. Okamoto 1999: Plate tectonics at 3.8-3.7 Ga: Field evidence from the Isua Accretionary Complex, southern West Greenland. Journal of Geology 107(5): 515-554.

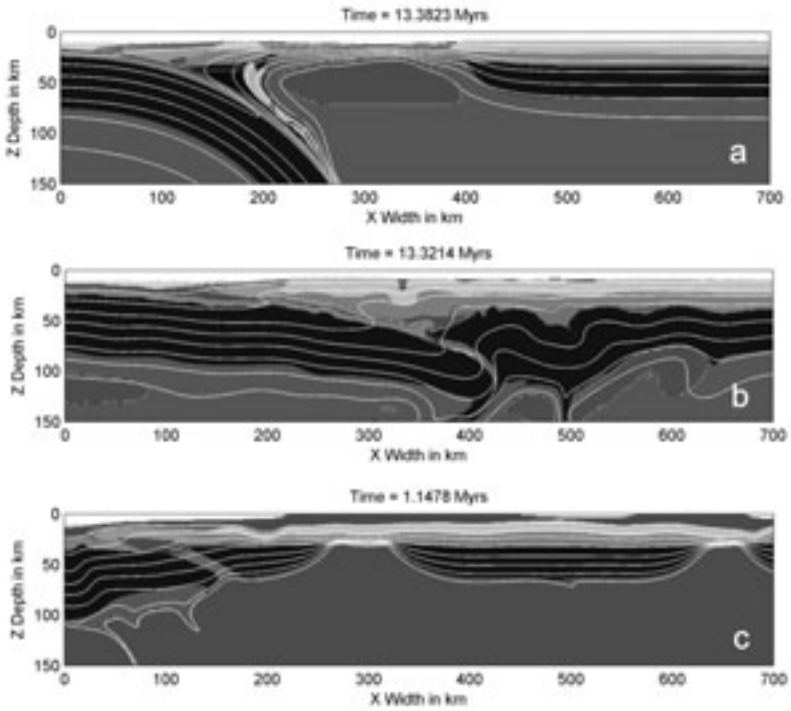

Figure 1. Illustrations of different tectonic regimes: a – "normal subduction" regime with arc and backarc basin formation – T'_m (present mantle temperature at 70 km)=1360 °C; radiogenic heating (H') – present day; b – "pre-subduction regime": underthrusting of continental crust by oceanic plate – $T_m=T'_m+175$ °C; H=H'x2.5; c – "horizontal-tectonics" regime: no subduction, no underthrusting, only horizontal movements - $T_m=T'_m+250$ °C; H=H'x3. Left parts of pictures – oceanic lithosphere, right – continental lithosphere; dark grey – lithospheric mantle; below – mantle (grey), a little darker – partial molten mantle.

1.52

The effects of large sub-marine landslides on the mechanics of thrust wedges

Smit Jeroen *, Burg Jean-Pierre *, Dolati Asghar *,** and Sokoutis Dimitrios ***

*ETH Zurich, Strukturgeologie, Leonhardstrasse, 19 /LEB, CH-8092 Zurich (smit@erdw.ethz.ch)
**Geological Survey of Iran, Meraj st. Azadi sq., P.O. Box 13185-1494, Tehran, Iran
***Faculty of Earth and Life Sciences, Vrije Universiteit Amsterdam, De Boelelaan 1085, 1081 HV Amsterdam, The Netherlands

Olistostromes cover large portions of active thrust wedges like Makran, Gulf of Cadiz and offshore Borneo. The emplacement of these olistostromes by submarine mass flows represents an instantaneous and massive mass redistribution. The effect of olistostrome emplacement on thrust wedge mechanics is discussed after the example of the Iranian Makran wedge and the results from analogue tectonic experiments.

The Makran accretionary wedge, between the Arabian and Eurasian plates, grows seawards by frontal accretion and underplating of trench fill sediments since the mid-Miocene, presently at a rate of about 2 cm/yr. The whole wedge is >500 km wide. This extreme width in combination with a low cross-sectional taper of ca. 3º and little indication for reactivation of the internal parts suggest low basal friction and, most probably, the presence of one or more weak décollements. Active mud volcanoes may indicate that such décollements take advantage of overpressured shales.

The Makran includes a giant catastrophic mud-and-debris flow inserted between Eocene to Lower Miocene turbidites and Upper Miocene deposits. The olistostrome includes blocks of ophiolites and oceanic sediments derived from the mélange to the north and reworked chunks of the underlying turbidites, on which it rests with an erosional unconformity. Its size and internal structure make it a fossil equivalent of the large debris flows found along continental margins and unstable volcanic edifices.

We performed a series of analogue tectonic experiments to test the influence of erosion and deposition on the deformation style of Makran-type wedges. Sudden erosion and resedimentation were mechanically introduced during shortening to test the effects of instantaneous mass-redistribution. After erosion/resedimenation, thrusting focused on existing faults in the emerged internal wedge. Further frontal propagation was prevented by fast redeposition of the erosional products seaward of the thrust front that locally increased wedge strength. Depending on the thickness and extent of the added load, the presence of weak décollements in the frontal wedge causes thrusting to jump to the front of the resedimented load, hence allowing the wedge to quickly grow outward by frontal accretion above the weak mid-level décollement. It seems that the striking difference in deformation style and intensity we observed in the Iranian Makran may be, at least partially, explained by the mass-redistribution caused by the Late-Miocene olistostromes.

1.53

Neotectonics of the Western and Central Alps : geodynamic implications

Sue Christian*, Champagnac Jean-Daniel**, Tricart Pierre***

* IUEM/UMR6538/UEB/UBO, Brest University, France (christian.sue@univ-brest.fr)
** Insitute of Mineralogy, Hannover University, Germany
*** LGCA/UMR5025 Grenoble University, France

The Western Alps' active tectonics are characterized by ongoing widespread extension in the highest parts of the belt and transpressive/compressive tectonics along its borders (Sue et al., 1999; Delacou et al., 2004). We examine these contrasting tectonic regimes, as well as the role of erosional processes, using a multidisciplinary approach including seismotectonics, numerical modelling, GPS, morphotectonics, fieldwork, and brittle deformation analysis. Extension appears to be the dominant process in the present-day tectonic activity in the Western Alps, affecting its internal areas all along the arc. Shortening, in contrast, is limited to small areas located along at the outer borders of the chain. Strike-slip is observed throughout the Alpine realm and in the foreland. The stress-orientation pattern is radial for $\sigma 3$ in the inner, extensional zones, and for $\sigma 1$ in the outer, transcurrent/tranpressional ones. Extensional areas can be correlated with the parts of the belt with the thickest crust. Quantification of seismic strain in tectonically homogeneous areas shows that only 10 to 20% of the geodesy-documented deformation can be explained by the Alpine seismicity. We show that Alpine active tectonics are ruled by buo-

yancy forces rather than ongoing shortening along the Alpine Europe/Adria collision zone. This interpretation is corroborated by numerical modeling.

The Neogene extensional structures in the Alps formed under increasingly brittle conditions. A synthesis of paleostress tensors for the internal parts of the West-Alpine arc documents major orogen-parallel extension with a continuous change in σ3 directions from ENE-WSW in the Simplon area, to N-S in the Vanoise area and to NNW-SSE in the Briançon area (Champagnac et al., 2006). Minor orogen-perpendicular extension increases from N to S. This second signal correlates with present-day geodynamics as revealed by focal-plane mechanisms analysis. The orogen-parallel extension could be related to the opening of the Ligurian Sea during the Early-Middle Miocene and to compression/rotation of the Adriatic indenter inducing lateral extrusion.

Interactions between the different geodynamic processes control the balance between intrinsic and extrinsic dynamics and explain the late tectonic evolution of the belt (Sue et al., 2007). Figure 1 presents a synthesis of the tectonic regimes and the links with the related geodynamic engines involved in the Neogene to present evolution of the Western and Central Alps, including boundary conditions (collision, rotation, free Ligurian boundary), deep dynamics (gravitational forces, slab dynamics, vertical indentation), and surface processes (erosion, transfer, post-glacial rebound). Three main processes seem to play a fundamental role in this tectonic evolution. First, the end of the opening of the Ligurian Sea during Late Miocene times would imply a decrease in orogen-parallel extension. Second, a progressive decrease in the rate of continental collision (Europe-Adria) appears to be critical for the change of tectonic regime. The decrease of convergence rates allows buoyancy forces to develop, and to control the actual gravitational spreading. Third, the increase of erosion rates during Pliocene times implies major geodynamic modifications, whatever is the origin of this erosion increase (Champagnac et al., 2008). We propose that the evolution from a tectonic regime characterized by extrusion and convergent plate conditions to a tectonic regime characterized by gravitational re-equilibration is controlled by a modification in the subtle balance between boundary forces and buoyancy forces. This transition probably took place during Pliocene times, contemporaneously with the increase of erosion, and in relation with the decrease of the plate convergence rate.

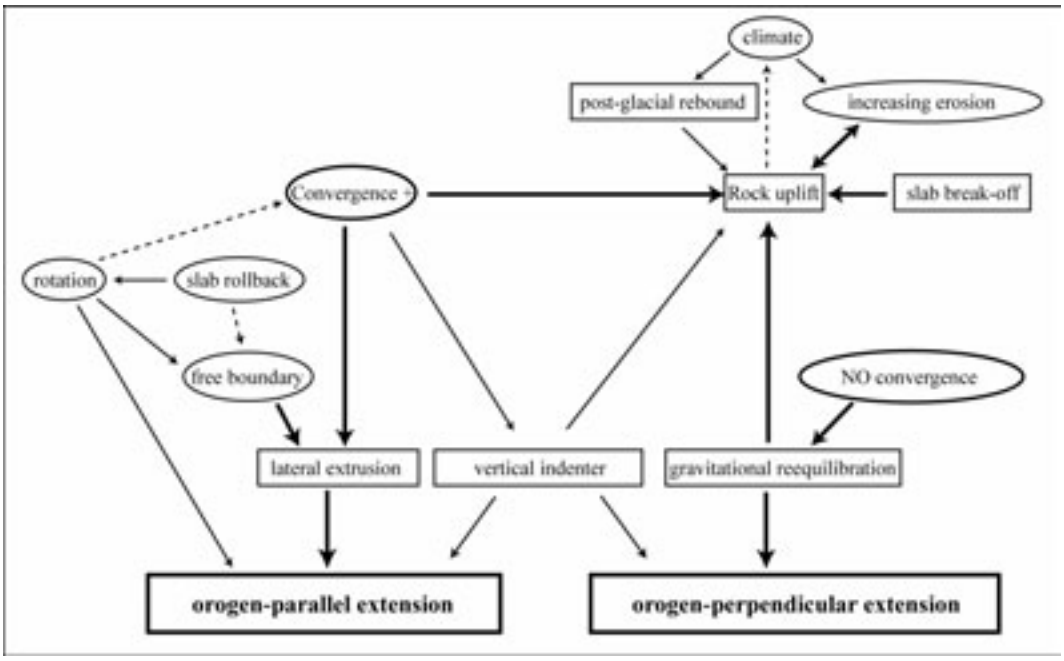

Figure 1. Conceptual diagram showing the interactions between intrinsic (rectangles) and extrinsic (ellipses) forces leading to the development of orogen-parallel versus orogen-perpendicular extension. The major roles are attributed to boundary conditions (convergence, lack of convergence, free boundary) and their equilibrium with gravitational re-equilibration (body forces).

REFERENCES

Champagnac JD, Sue C, Delacou B, Tricart P, Allanic C, Burkhard M (2006) Miocene orogen-parallel extension in the inner Western Alps revealed by dynamical fault analyses. Tectonics DOI: 10.1029/2004TC001779.

Champagnac, J.-D., van der Beek, P., Diraison, G., Dauphin, S.: Flexural isostatic response of the Alps to increased Quaternary erosion recorded by foreland basin remnants, SE France. Terra Nova 20, 213–220, doi: 10.1111/j.1365-3121.2008.00809.x.

Delacou B, Sue C, Champagnac JD, Burkhard M (2004) Present-day geodynamics in the bend of the western and central Alps as constrained by earthquake analysis. Geophys J Int 158: 753-774.

Sue C, Thouvenot F, Fréchet J, Tricart P (1999) Widespread extension in the core of the western Alps revealed by earthquake analysis. J Geophys Res B: Solid Earth 104: 25611-25622.

Sue, C., Delacou, B., Champagnac, J.D., Allanic, C., Tricart, P. & Burkhard, M. 2007a: Extensional neotectonics around the bend of the Western/Central Alps: an overview. Int. J. Earth Sci. doi:10.1007/s00531-007-0181-3.

1.54

How rose up the Ali Sabieh bloc (Afar triple junction)? New insights from faulting analysis

Sue Christian, Daoud Ahmed Mohamed, Le Gall Bernard, Rolet Joel

IUEM/UBO/UEB/UMR6538, Place Copernic, 29280 Plouzané, France (sue.christian@univ-brest.fr)

Tectonics of triple junction zones, of either continental or oceanic type, often lead to complex strain/stress patterns, generally caused by changes in the relative trajectories of the plates involved in the system. The corresponding far stress/strain fields may also interact with more local fields of either tectonic or magmatic origin. Such a geodynamic configuration occurs in the Afar Depression, Horn of Africa, where three recent (<3 Ma) rift axes converge and disrupt the eastern edge of the earlier (30 Ma-old) Afar plume-induced volcanic province. Although its recent trap-like basaltic cover (Stratoid Basalts) displayed a dominant extensional strain, complexities are documented in the overall Afar area, such as reverse faulting inferred from focal mechanism [Hofstetter and Beyth, 2003]. They are interpreted in term of local complexities or changes in the fault system due to change in the rift propagation directions [Beyth, 1991]. Compressional tectonics have also been reported, at local scale in the Arta area, involving syn- to post- 3.6 Ma-old volcanics [Arthaud et al., 1980]. Their proposed model implies stress permutation along an inferred transform fault structure. The Ali Sabieh block (ASB) is located on the southeastern edge of the Afar morphologic depression (border between the republic of Djibouti and Somalia). It exhibits a paradoxal 30 km-large anticlinorium-like structure in a regional extensional tectonic context. Indeed, Jurassic limestones and Cretaceous sandstones outcrop in the core of the structure, surrounded by Neogene volcanics (basalts and rhyolites), which get younger outward of the structure. Moreover, the ASB corresponds to a structural high, with a mean altitude in the range of 700-900m vs. 500 m for the surrounding basaltic plains. Many interpretations have been proposed for the ABS, including a dome, a horst [e.g. Gaulier and Huchon, 1991], or a large anticline formed under compressional regime.

We provide new brittle tectonic data, which allow to better constrain the tectonic evolution of the ASB, and its large-scale structure. We performed a systematic analysis of faulting in the ASB, based on microtectonic measurements and paleostress tensor inversions (600 measures, 31 tensors). This approach allowed to partly constrain the timing of the tectonic evolution, the volcanic rocks being dated. Paleostress fields inferred from brittle deformation are made of two majors signals: normal faulting and strike-slip. The relative chronology has been determined in 3 polyphased sites where extensional faulting is post-dated by strike-slip one. We also found 2 sites exhibiting reverse faulting, both of them being located at the periphery of the ASB. In term of stress fields, the first phase corresponds to ENE-WSW to WNW-ESE oriented σ3 horizontal axes and subvertical σ1 axes, and thus an E-W oriented regional extension. The second phase is associated to E-W to ENE-WSW σ3 axes and N-S to NNW-SSE σ1 axes. Both extensional and strike-slip fields are well constrained, with 15 and 14 tensors respectively, distributed all over the ASB, and a good internal homogeneity in term of stress distributions.

The stress distribution shows that these two stress fields are compatible, the σ3 axes being stable (globally E-W). Thus, the ASB may have evolved continuously from extensional to transcurrent tectonism, and/or local/regional stress permutation may have occurred between σ1 and σ2 stress axes, leading to tectonic permutation between extension and strike-slip regimes. Indeed, the very stable E-W direction of extension shows that the ASB's tectonics resulted from quite stable extensional conditions from Neogene times onwards. Neither on the field nor on structural maps of the area or satellite images, large normal faults as candidate for a 30 km-wide horst could be determined. On the contrary, we observed some folds at the periphery of the ASB, which could be associated to the 2 reverse paleostress tensors we computed. In this framework, we propose the ASB evolved as a magma-driven dome rather than a horst or an anticline.

REFERENCES

Arthaud, F., Choukroune, P., Robineau, B. (1980), Tectonique, microtectonique, et évolution structurale du golfe de Tadjoura et du sud de la dépression Afar (Rép. Djibouti). Bull. Soc. Geol. France, 6, 901-908.

Beyth M. (1991), Smooth and rough propagation of spreading Southern Red Sea - Afar depression. J. African Earth Sci., 13, 157-171.

Gaulier J.M., and Huchon, P. (1991), Tectonic evolution of the Afar triple junction. Bull. Soc. Geol. France, 3, 425-464.

Hofstetter, R., Beyth, M. (2003) The Afar Depression: interpretation of the 1960-2000 earthquakes. G. J. Int. 155 (2) , 715-732 doi:10.1046/j.1365-246X.2003.02080.x

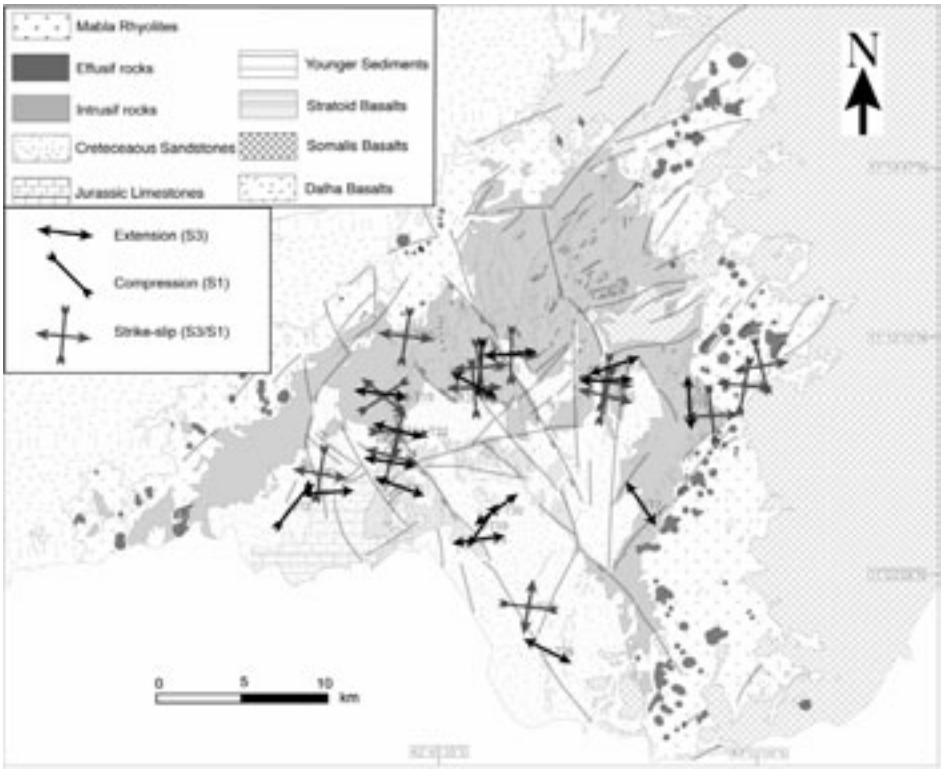

Figure 1. Paleostress maps of the ASB, calculated by Direct Inversion method (INV). Arrows show the projection on the map of the computed azimuth σ3 axis for the extensional (black) and strike-slip (grey) paleostress fields. Bars show the projection on the map of the computed azimuth σ1 axis for the reverse (black) and strike-slip (grey) paleostress fields. The shaded background represent the regional geological map, with the main faults and dyke-related lineaments.

1.55

Coupled models of mantle geochemical evolution, plate tectonics, magmatism and core evolution incorporating self-consistently calculated mineralogy

Tackley Paul*, Nakagawa Takashi**, Deschamps Frédéric*, Connolly James***

*Institute für Geophysik, ETH Zürich, Schafmattstr. 30, CH-8093, Zürich (ptackley@ethz.ch)
**Department of Earth and Planetary Sciences, Kyushu University, Fukuoka, Japan (takashi@geo.kyushu-u.ac.jp)
***Insitute für Mineralogie und Petrographie, ETH Zürich, Clausiusstrasse 25, CH-8092, Zürich

High pressure and temperature experiments and calculations of the properties of mantle minerals show that many different mineral phases exist as a function of pressure, temperature and composition [e.g. Irifune and Ringwood, 1987], and that these have a first-order influence on properties such as density, which has a large effect on the dynamics, and elastic moduli, which influence seismic velocity. Numerical models of thermo-chemical mantle convection have typically used a simple approximation to treat these complex variations in material properties, such as the extended Boussinesq approximation. Some numerical models have attempted to implement multiple, composition-dependent phases into thermo-chemical mantle convection [e.g., Tackley and Xie, 2003; Nakagawa and Tackley, 2005] and to calculate seismic anomalies from mantle convection simulations based on polynominal fitting for temperature, composition and mineral phase [Nakagawa and Tackley, 2006]. However, their linearised treatments are still approximations and may not adequately represent properties including effect of composition on phase transitions. In order to get closer to a realistic mineralogy, we here calculate composition-dependent mineral assemblages and their physical properties using the code PERPLEX, which minimizes free energy for a given combination of oxides as a function of temperature and pressure [Connolly, 2005], and use this in a numerical model of thermo-chemical mantle convection in a three-dimensional spherical shell, to calculate three-dimensionally-varying physical proporties. In this presentation we compare the results obtained with this new, self-consistently-calculated treatment, with results using the old, approximate treatment, focusing particularly on thermo-chemical-phase structures

and seismic anomalies in the CMB region and the transition zone. The numerical models treat the evolution of a planet over billions of years, including self-consistent plate tectonics arising from plastic yielding, melting-induced differentiation, and a parameterised model of core evolution based on heat extracted by mantle convection.

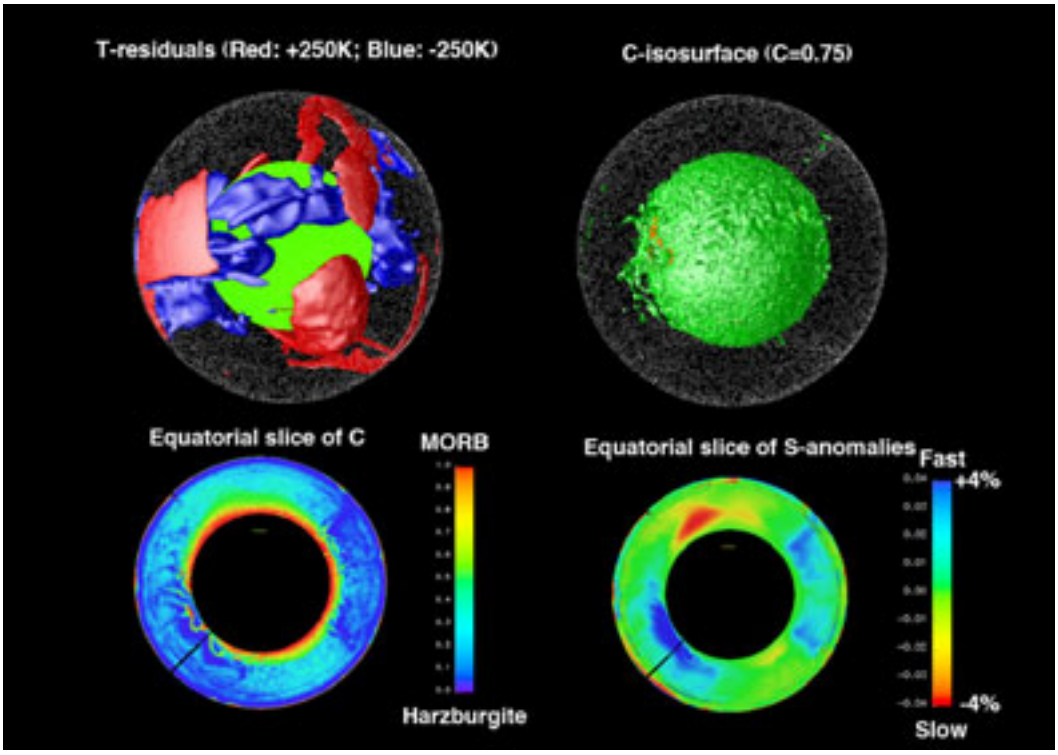

Figure 1. Example simulation with PERPLEX-calculated mineralogy and physical properties.

REFERENCES
Connolly, J. A. D., (2005), Earth Planet. Sci. Lett., 236, 524-541.
Irifune, T., and Ringwood, A. E., (1987), Earth. Planet. Sci. Lett., 86, 365-376.
Nakagawa T., and Tackley, P.J., (2006), Geophys. Res. Lett., 33, L12S11, doi:10.1029/2006GL025719.
Nakagawa, T., and Tackley, P. J., (2005), Proc. 3rd MIT conference.
Tackley, P. J., and Xie, S., (2003), Proc. 2nd MIT conference.

1.56

The Availability of H_2O for Deformation in Natural Quartz Single Crystal Experiments

Thust Anja*, Tarantola Alexandre**, Heilbronner Renée*, Stünitz Holger***

*Department of Geosciences, University Basel, Bernoullistr. 32, CH-4056 Basel, Switzerland (anja.thust@unibas.ch, renee.heilbronner@unibas.ch)
** Institute of Geological Sciences, University of Bern, Baltzerstr. 3, CH-3012 Bern, Switzerland (alexandre.tarantola@geo.unibe.ch)
*** Institutt for geologi, Universitetet i Tromsø, Dramsveien 201, 9037 Tromsø, Norway (holger.stunitz@ig.uit.no)

H_2O is very important for quartz deformation. Experimental studies on synthetic and natural quartz crystals demonstrated that H_2O dramatically reduces the strength of the material (e.g. Griggs & Blacic 1965). We have performed deformation experiments in the solid medium Griggs apparatus on natural milky quartz single crystals in order to study the effect of H_2O weakening. The compression direction has been normal to the <c>-axis and one of the prism planes.

The flow strength of the quartz crystal at 1 GPa confining pressure and 900 °C at a strain rate of 10^{-6} s^{-1} is with 150 MPa low. This strength is comparable to that of previous experiments on "wet" natural quartzites (Hirth & Tullis 1992) so that probably H_2O has been available in sufficient quantities to ensure weakening.

The milky appearance of the quartz crystal originates from a large number of fluid inclusions. Fluid inclusions on the undeformed material are arranged on planes more or less perpendicular to c <0001>. They showed a high variation in size and shape with negative-crystal to undefined morphologies.

Microthermometric measurements at low temperature revealed the presence of antarticite ($CaCl_2 \cdot 6H_2O$) and hydrohalite ($NaCl \cdot 2H_2O$). Ice melting temperature ranged between -6.9 and -7.4 °C, corresponding to an average salinity of 10.5 wt% eq. NaCl. Total homogenization temperatures were measured between 184 °C and 207 °C. Raman microspectroscopy permitted to observe the presence of small amounts of CO_2 and to identify some accidentally trapped solids in the inclusions like calcite, quartz or rutile. The molar volume of the inclusions helped us to determine the fluid pressure as a function of the temperature. At 250 °C, the fluid pressure is around 100 MPa and in the order of 850 MPa at 700 °C.

FTIR measurements on double-polished thick sections (200 to 500 μm) present an average H_2O content of 250 H/10^{-6}Si in undeformed samples (calculation after Stipp et al. 2006). The H_2O –content is heterogeneously distributed. The undeformed quartz material shows a fluid inclusions with variable size, up to 0.5 mm. FTIR measurements on inclusions often have oversaturated absorption spectrums. Next to the fluid inclusions there are can be clear regions without any inclusions and essentially no H_2O. After deformation the H_2O distribution is more homogenous throughout the sample. The majority of the big inclusions have disappeared and a lot of small inclusions are formed and are often arranged in fluid clusters. The H_2O-content of deformed regions with undulatory extinction is approximately 3000 H/10^{-6}Si. Thus, H_2O becomes dispersed during deformation. We infer that during deformation the inclusions disrupt and form micro cracks. The cracks heal rapidly at the high temperatures and confining pressures. During the healing and plastic deformation H_2O is distributed in the quartz crystals via defects and contributes to the H_2O-weakening effect.

One interesting feature in the FTIR absorption spectrum of the deformed samples is a sharp, small peak at 3595 cm^{-1}. This peak appears only in the deformed samples and there only in the visibly deformed parts (see figure1).
The sharp FTIR peak seems to be linked to the deformation. Niimi et al. 1999 consider that this peak is related to recrystallization, but in our case is no evidence for recrystallization could found.

In conclusion we can say that quartz which shows a low H_2O distribution and a lot of fluid inclusions provides enough H_2O for H_2O weakening. The inclusions changes their shape, their size, their composition and the H_2O dispersion becomes more homogeneous during deformation by microcracking and subsequent crystal plastic deformation by dislocation glide.

REFERENCES:

Griggs, D.T. & Balcic, J.D. 1965: Quartz: Anomalous Weakness of Synthetic Crystals. Science 147, 293-295.

Hirth, G. & Tullis, J. 1992: Dislocaton creep regimes in quartz aggregates. Journal of Structural Geology. 14, 145-159.

Niimi, N., Aikawa, A., Shinoda, K. 1999: The infrared absorption band at 3596 cm^{-1} of the recrystallized quartz from Mt. Takamiyama, southwest Japan. Mineralogial Magazine 63, 693-701.

Stipp, M., Tullis, J., Behrens H. 2006: Effect of water on the dislocation creep microstructure and flow stress of quartz and implications for the recrystallized grain size piezometer. Jouranl of Geophysical Research 111, B04201.

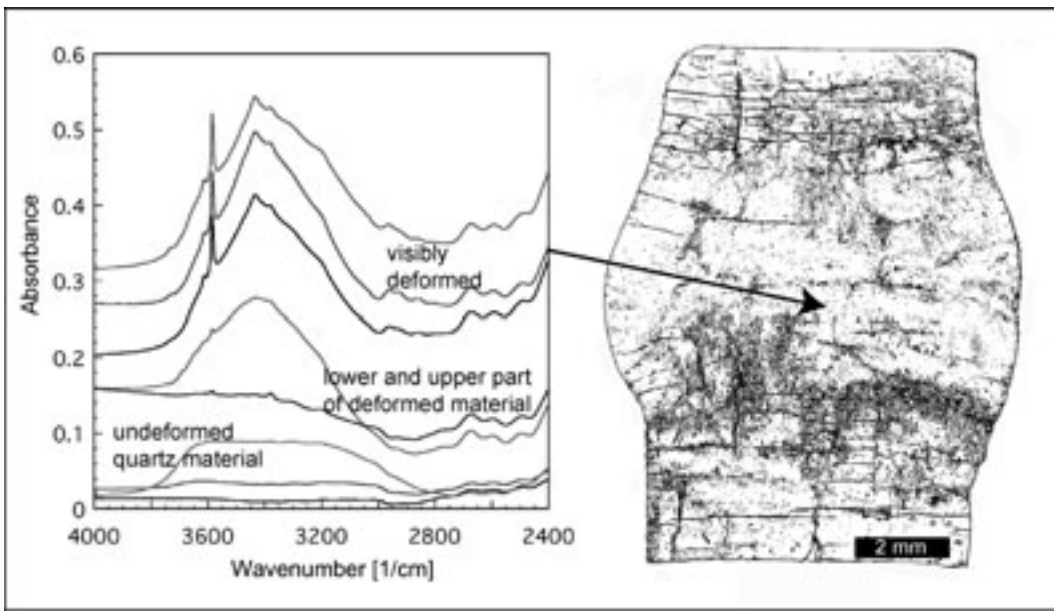

Fig.1: FTIR spectra for undeformed and deformed material. Absorbance is relative (left). Thin section of a deformed sample with the visibly deformed part in the middle (right).

1.57

Transitions in tectonic mode based on calculations of self-consistent plate tectonics in a 3D spherical shell

van Heck Hein* & Tackley Paul*

*Institute of Geophysics, Schafmattstrasse 30, CH-8093 Zuerich (hvanheck@erdw.ethz.ch)

In the past decade, several studies have documented the effectiveness of plastic yielding in causing a basic approximation of plate tectonic behavior in mantle convection models with strongly temperature dependent viscosity, strong enough to form a rigid lid in the absence of yielding. The vast majority of such research to date has been in either two-dimensional, or three-dimensional cartesian geometry. Also, scalings for mixed internally and bottom heated convection are not well established.

In the present study, mantle convection calculations are done to investigate the planforms of self consistent tectonic plates in three-dimensional spherical geometry. Several diagnostics are used to analyze how successful each model is in producing tectonic plates. We study the proposed transitions in tectonic mode (e.g. changes in plate size, rigid lid convection to tectonic plates, smoothly evolving plates to more episodic, time dependent, tectonics) as a function of yield stress envelope, Rayleigh number and heating mode.

Cases with zero bottom heat flux are compared to cases which have both internal heating and bottom heating. This enables us to investigate which tectonic mode prevails as function of lithospheric yield stress, Ra and heating mode. The results are compared to analytical scalings for boundary regimes as well as scalings for heat flux. This allows us to scale to different planets of different sizes and can be applied to the evolution of Earth, Mars and Venus as well as terrestrial extra-solar planets.

1.58

Late Quaternary slip rates of active faults adjacent lake Qinghai, northeastern margin of the Tibetan Plateau

Yuan Dao-Yang*, Champagnac Jean-Daniel**, Ge Wei-Peng*, Molnar Peter***, Zhang Pei-Zhen****, Zheng Wen-Jun****, Zhang Hui-Ping****, Liang Ming-Jian*

* *Lanzhou Institute of Seismology, China Earthquake Administration, Lanzhou 730000, China*
** *Institute of Mineralogy, University of Hannover, Callinstrasse 3, Hannover D-30167, Germany*
*** *Department of Geological Sciences, and CIRES, University of Colorado, Boulder, Colorado, 80309, USA*
**** *State Key Laboratory of Earthquake Dynamics, Institute of Geology, China Earthquake Administration, Beijing 100029, China*

Combining the terrace riser offsets with terrace ages dated by ^{14}C, OSL and ^{10}Be techniques, we determine average strike slip rates of Elashan and Riyueshan faults, two north-northwest-trending strike-slip faults along the western and eastern sides of the lake Qinghai, northeastern margin of the Tibetan plateau, to be about 1.0 ± 0.2 mm/yr and 1.2 ± 0.2 mm/yr, respectively.
Between them, the Qinghainanshan fault consists of three secondary thrust faults, whose total vertical slip rate and shortening rate are ≈0.4-1.0 mm/yr and ≈0.2-1.2 mm/yr, respectively.

The relatively low slip rates in this region reflect distributed deformation. The total right-lateral offsets of the geological contacts, which were interpreted from 1:200,000-scale Qinghai regional geological maps of the region, are about 8.8-11.9 km along the Elashan fault and 10.9-11.6 km for the northern segment of Riyueshan fault. If long−term slip rates were constant during late Cenozoic time, initiation of dextral movement would be 10.3 ± 3.6 Ma and 9.4±2.3 Ma for the two strike-slip faults, consistent with records of tectonic deformation in Cenozoic basins nearby.

Our study highlights a stage of tectonic deformation in the northeastern margin the Tibetan plateau beginning near ≈10 Ma, long after the collision between India and Eurasia began.

2. Mineralogy-Petrology-Geochemistry (Open Session)

Bernard Grobéty, Eric Reusser

Swiss Society of Mineralogy and Petrology (SSMP)

2.25 Reymond C., Leuthold-Favre L., Mucciolo A., Bonin M. : Advantages of using TEM when analysing asbestos in ambient air

2.26 Robyr M., Carlson W., Passchier C., Vonlanthen P.: Textural, chemical and microstructural records during snowball garnets growth

2.27 Schaltegger U., Antognini M., Girlanda F., Wiechert U., Müntener O. : Alkaline mantle melts in the southern Alpine lower crust mark the initiation of late Triassic rifting

2.28 Schenker F.: Shocked quartz in Ticino, and beyond

2.29 Schwarzenbach E.M., Früh-Green G.L., Bernasconi S.M.: Comparing carbon and sulfur isotopes in ophiolites and active peridotite-hosted hydrothermal systems

2.30 Shabanian N., Davoudian A.R., Khalili M. : Petrogenesis of post-collisional granitoid of Ghaleh-Dezh, NW Azna, Sanandaj-Sirjan zone, Iran: Nd–Sr isotope evidence

2.31 Studer A., Kündig R., Schenker F., Surbeck H.: Trace Elements in Miocene Subbituminous Coals from the Swiss Molasse Basin with Special Attention to Uranium and its Mode of Occurrence

2.32 Tripoli B., Mattsson H.: Physical volcanology of the Lake Natron-Engaruka monogenetic field, Tanzania

2.33 Van den Bleeken G., Müntener O., Ulmer P.: Reaction between tholeiitic melt and residual peridotite in the uppermost mantle: An experimental study at 0.8 GPa

2.34 Villagómez D., Spikings R., Magna T., Winkler W.: Late Cretaceous history of the western Colombian Andes

2.35 Zakaznova-Herzog V., Wiedenmann D., Gorbar M., Grobéty B., Vogt U., Züttel A.: Experimental geochemistry and mineralogy for industrial applications: new membranes for alkaline electrolysers

2.36 Zarasvandi. A.: Geochemistry and Source of the Recent Sediments in Southwestern of Ahvaz, Khouzestan Province, Iran

2.37 Zhou W., Stober I., Bucher K. : Surface water in the Zermatt—Matterhorn area, Switzerland, a hydrogeochemical study

2.38 Zhu C., Fu, Q., Lu P., Seyfried W.E.: New Experiments of Feldspar Hydrolysis and Implications for Interpretations of Weathering Rates

2.1

Linking thermobarometry with ^{39}Ar-^{40}Ar and U-Th-Pb ages from the northern Central Alps: implications for Rb-Sr and K-Ar data

Allaz Julien*, Engi Martin*, Berger Alfons**, Janots Emilie*** and Villa Igor*

* *Institut für Geologie, Baltzerstrasse 1+3, 3012 CH-Bern (jallaz@geo.unibe.ch)*
** *Institut for Geografi og Geologi, Øster Voldgade 10, DK-1350 København K*
*** *Institut für Mineralogie, Corrensstrasse 24, D-48149 Münster*

The Barrovian metamorphism observed in the Alps results from the collision of Europe and Africa and reaches its thermal maximum in the Central Alps (upper amphibolite facies). Age data for this orogenic cycle remain controversial, despite a multitude of studies: Based on the resetting of Rb-Sr ages in muscovite from polymetamorphic gneisses, Hunziker (1969) and Jäger (1973) had proposed an age of 38±2 Ma for this metamorphism. Also based on isotopic data in the Alps, a field-calibration for the "closure-temperature" (Dodson, 1972) was then obtained by Purdy & Jäger (1976) , based on their K-Ar data for muscovite and earlier data for biotite (Armstrong et al., 1966). However, a uniform age (near 38 Ma) for ***the*** metamorphism in the Central Alps was in conflict already with early U-Pb data of monazite and xenotime from the same area (e.g. Köppel & Grünenfelder, 1975), which indicated an age near 30 Ma in the southern Lepontine, but ≈20 Ma in the northern part of the amphibolite facies dome. A study by Janots et al. (2008) not only confirmed the young monazite age in the north (SHRIMP U-Pb of 18-19 Ma at Lucomagno, near T_{max} ≈570 °C); it furthermore demonstrated that at ≈30 Ma this part of the belt was still heating up (prograde formation of allanite near 440 °C). These recent results reopen questions about the interpretation of K-Ar and Rb-Sr data and the "closure-temperature" of each system, as well as effects of inheritance on age data in medium-pressure metamorphic rocks.

The present study makes an effort to interpret Ar-ages for mica based on thermobarometry and multi-chronometry. Based on select samples taken in the northern Central Alps, we used well equilibrated, homogeneous metasediments; exclusively Mesozoic protoliths were considered to avoid inheritance problems. ^{39}Ar-^{40}Ar ages for mica (separates) yield ages between 18.93±0.83 (Lucomagno Pass) and 15.79±0.11 Ma (Val Piora) for muscovite, and between 17.65±0.33 and 14.84±0.23 Ma for biotite (same localities). The muscovite Ar-ages pertain to conditions near the documented P-T equilibria (7-9 kbar, 550-570 °C). When compared to the monazite ages of 18-19 Ma from the same area, the Ar-loss owing to diffusion upon cooling from these conditions is minor for muscovite. Ar-loss is slightly more evident in white mica from a second area (Pizzo Molare), where slightly higher temperatures (580-600 °C) were reached.

Muscovite is chemically homogeneous in each of the samples dated; thermobarometry indicates equilibration at peak of metamorphic conditions and (stable!) preservation of muscovite along the retrogression path. This leaves diffusion as effectively the dominant resetting factor, hence the Dodson-type closure-temperatures for Ar-Ar in muscovite must be high, ≈500°C. By contrast, biotite probably was also affected chemically on retrogression, due to minor chloritization. Where such retrogression reactions occur, their effect may overwhelm (thermally activated) diffusion, and age data are more difficult or impossible to interpret. In the samples dated here, Ar-loss in biotite yields Ar-Ar ages 1-2 Ma lower than muscovite. As retrogression of biotite in these samples is very limited, an approximate closure temperature of 450 °C is inferred for such biotites (grain diameter ≈200 μm).

This study indicates that detailed micro-textural and micro-chemical investigations are a necessary (though not sufficient) prerequisite to yield meaningful geological ^{39}Ar-^{40}Ar ages. Such a characterisation is necessary to identify possible problems of inheritance or late re-equilibration, which plague many age interpretations. Moreover, the purity of mineral separates must be ascertained; at least possible impurities, even in traces, need to be accounted for. Together with diffusion, all of these factors affect isotopic systems. The art of geochronology implies identification of the dominant influences, such that an isotopic age may be correctly interpreted as (1) a crystallization age or (2) cooling stage (each corresponding to well defined tectono-metamorphic conditions), as distinguished from (3) meaningless "ages" (owing to inheritance or partial chemical retrogression).

REFERENCES

Armstrong, R.L., Jäger E. & Eberhardt, P. 1966: A comparison of K-Ar and Rb-Sr ages on Alpine biotites, Earth and Planetary Science Letters 1, 13-19.

Dodson, M.H. 1973: Closure temperature in cooling geochronological and petrological systems, Contributions to Mineralogy and Petrology 40, 259-274.

Hunziker, J.C. 1969: Rb-Sr-Alterbestimmungen aus den Walliser Alpen Hellglimmer- und Gesamtgesteinalterswerte, Eclogae geol. Helv., 62, 527-542

Jäger, E. 1973: Die alpine Orogenese im Lichte der radiometrischen Altersbestimmung, Eclogae geol. Helv. 66, 11-21.

Janots, E., Engi, M., Rubatto, D., Berger, A., Gregory, C. & Rahn, M., (2008): Metamorphic rates in collisional orogeny from in situ allanite and monazite dating, Geology (accepted).

Köppel, V. & Grünenfelder, M., 1975: Concordant U-Pb ages of monazite and xenotime from the Central Alps and the timing of the high temperature Alpine metamorphism, a preliminary report, SMPM 55, 129-132.

Purdy, J. & Jäger, E. 1976: K-Ar ages on rock-forming minerals from the central Alps, Mem. Instituti Geol. Mineral. Uni. Padova 30, 31 pp.

2.2

Discontinuous metamorphic P-T paths in the Liuling Unit (Qinling belt, central China)

Bader Thomas*, Franz Leander*, de Capitani Christian*, Ratschbacher Lothar**, Hacker Bradley R.***, Weise Carsten**, Wiesinger Maria**, Popp Michael**

**Mineralogisch-Petrographisches Institut, Universität Basel, CH-4056 Basel*
(thomas.bader@unibas.ch)
***Institut für Geologie, Technische Universität Bergakademie Freiberg, D-09599 Freiberg*
**** Geological Sciences, University of California, Santa Barbara, CA-93106*

The Liuling Unit, a probably Silurian to Permian metasedimentary sequence, is part of the Qinling orogen of central China and regarded as either the forearc basin or the subduction-accretion complex of the HP-UHP Qinling-Dabie-Sulu orogen (Ratschbacher et al. 2003). Amphibolite facies metapelites point to peak metamorphic conditions of 612-668°C at 0.68-0.79 GPa (Hu et al. 1993). The present study enhances the knowledge on tectonometamorphic history of the Liuling Unit.

P-T paths were obtained from thermodynamic modelling using the DOMINO program on two metapelites, which depict two garnet-growth stages. Microprobe profiles through large garnets reveal a discontinuous zoning between core and rim sections. The garnet core of staurolite-mica schist 75261C reveals a compositional zoning indicating a clockwise P-T loop starting at 562°C / 0.61 GPa, reaching maximum P at 573°C / 0.63 GPa (Fig. 1) and ceasing at 577°C / 0.61 GPa. The grossular-rich rim section formed at 580°C / 0.93 GPa. Large garnet porphyroblasts of garnet-mica schist 75302A reveal a similar discontinuous zoning between garnet core and rim section. The unzoned garnet core developed at 660°C / 0.51 GPa while the grossular-rich rim section formed at 590°C / 0.88 GPa. This sample also bears a second generation of numerous small garnets yielding the rim composition of the large porphyroblasts. Discontinuous garnet zoning is also present in garnet-amphibole schist 75261B, which indicates 560°C / 0.75 GPa for the grossular-rich rim section using conventionel geothermobarometry. This sample even reveals a small section at the outermost garnet rim depleted in grossular pointing to 510°C / 0.45 GPa. These investigations demonstrate two stages of metamorphic garnet growth in the Liuling Unit: the first stage is a clockwise Barrovian metamorphism, memorized by the garnet cores, which was followed by a second, pressure-dominated metamorphic event indicated by the garnet rims as well as the newly grown, second generation of garnets.

Currently, several interpretations for the garnet-growth history are possible:

1) The garnet cores are inherited and record Barrovian metamorphism in the hinterland of the Permo-Triassic (see below) orogen, i.e. in the Qinling Unit that constitutes Proterozoic-Paleozoic basement overprinted by a Devonian magmatic arc (Ratschbacher et al. 2003). LA-ICPMS and ion probe dating of detrital zircons prove Archean to Devonian provenance of the Liuling Unit rocks. Variable P-T estimates for different garnet cores may support this speculation.
2) The sampled section of the Liuling Unit is part of the forearc / accretionary wedge that was involved in the Devonian arc magmatism. Ar/Ar amphibole, U/Pb zircon, and Pb/Th monazite ages demonstrate Silurian-Middle Devonian metamorphism in the Qinling Unit and locally in the northern Liuling Unit (Ratschbacher et al. 2003 and unpublished).
3) The studied section of the Liuling Unit experienced an at least two-stage burial-exhumation history, as modeled for several subduction-accretion wedges worldwide (e.g. Gerya et al. 2002). Current Ar/Ar geochronology brackets the thermal history reflected by garnet rims between the Permian and Late Triassic (Ratschbacher et al. 2000 and unpublished) and our structural studies indicate protracted N-S shortening accommodated by vertical and horizontal, E-W stretch, typical for transpression.

Future work will trace the PT history of the Liuling Unit laterally to investigate whether the discontinuous history is a regional feature and will refine the timing of these processes.

REFERENCES

Gerya, T., Stöckhert, B. & Perchuk, A.L. 2002: Exhumation of high-pressure metamorphic rocks in a subduction channel: a numerical simulation, Tectonics 21, 1056.

Hu, N., Yang, J., An, S. & Hu, J. 1993: Metamorphism and tectonic evolution of the Shangdan fault zone, Shaanxi, China. J. metamorphic Geol. 11, 537-548.

Ratschbacher, L., Hacker, B.R., Calvert, A., Webb, L.E., Grimmer, J.C., McWilliams, M., Ireland, T., Dong, S. & Hu, J. 2003: Tectonics of the Qinling Belt (Central China): Tectonostratigraphy, geochronology, and deformation history. Tectonophysics 366, 1-53.

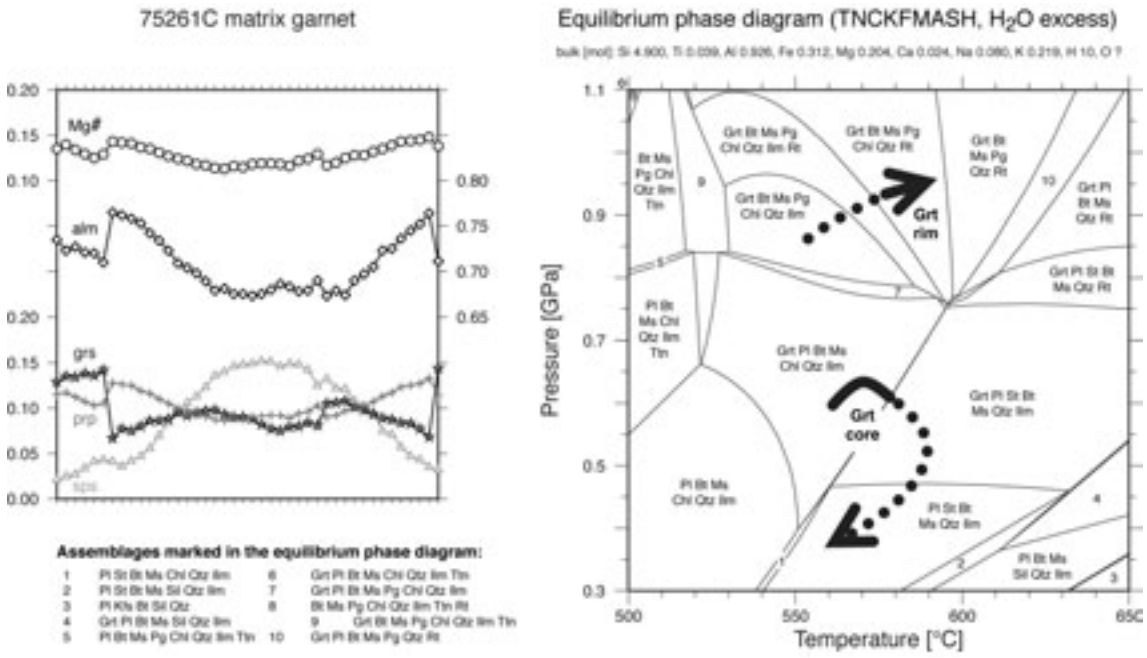

Figure 1. left: garnet profile of sample 75261C, right: equilibrium phase diagram and P-T path of sample 75261C

2.3

New hints on the tectonometamorphic history of the Douling complex (Qinling belt, central China)

Bader Thomas*, Franz Leander*, de Capitani Christian*, Ratschbacher Lothar**, Hacker Bradley R.***, Weise Carsten**, Wiesinger Maria**, Popp Michael**

**Mineralogisch-Petrographisches Institut, Universität Basel, CH-4056 Basel (thomas.bader@unibas.ch)*
***Institut für Geologie, Technische Universität Bergakademie Freiberg, D-09599 Freiberg*
**** Geological Sciences, University of California, Santa Barbara, CA-93106*

The Douling complex, probably part of the Yangtze craton, is located in the Paleozoic-Mesozoic Qinling Belt of central China. The Douling complex is composed of Proterozoic gneisses and schists with intercalated metabasites (Ratschbacher et al. 2003). Zhang et al. (1996) reported a probably Late Proterozoic metamorphism at P-T conditions of 650-700°C at 0.7-0.8 GPa for the basement rocks. Together with the cover, the Late Proterozoic Yaolinghe schists, the basement was intensively folded and underwent a low-grade metamorphism. This study presents new data on the basement and gives insight onto the late, low-grade metamorphism.

Despite of the intensive low-grade overprint, several indications for the preceding high-grade metamorphism were found. The absence of primary white mica and the presence of sillimanite and K-feldspar in most metapelitic samples point to upper

amphibolite-facies conditions. This is supported by garnet-gneiss sample 76114C, which shows the primary assemblage garnet-plagioclase-biotite ± ilmenite. Using the DOMINO program, we derived peak metamorphic conditions of 710°C at 0.80-0.85 GPa. Rutile inclusions in plagioclase point to a higher pressure stage before this upper amphibolite-facies event. Somewhat different P-T conditions are mirrored by garnet mica schist 76111A, which bears the primary assemblage garnet-biotite-muscovite-plagioclase-quartz ± rutile, ilmenite. Based on garnet zoning, we derived a P-T path starting at 485°C and 0.6 GPa and reaching peak metamorphic conditions at 575-600°C and 1.0-1.3 GPa. These data point to burial followed by high-temperature metamorphism during exhumation, i.e. a Barrovian, clockwise P-T path in the Proterozoic basement.

The low-grade metamorphic overprint led to the formation of the assemblage actinolite-albite-chlorite-epidote in metabasites. Metapelites reveal the syn-tectonic assemblage stilpnomelane-phengite-chlorite-calcite, for which PT conditions of 300-350°C at 0.6-0.7 GPa were calculated using the thermobarometer of Currie & van Staal (1999). The final metamorphic overprint occurred under lower greenschist-facies conditions as indicated by the growth of post-tectonic biotite. The timing of the low-grade metamorphic event is badly constrained. While Zhang et al. (1996) report a Paleozoic Rb-Sr whole rock isochronic age of ≈422 Ma, we rather suppose a Triassic age as the metamorphic conditions are similar to those in the Mulanshan (Zhou et al. 1993) and Zhangbaling (Ratschbacher et al. in prep.) areas in the Dabie-Sulu belt. Further geochronologic and petrologic investigations are in progress.

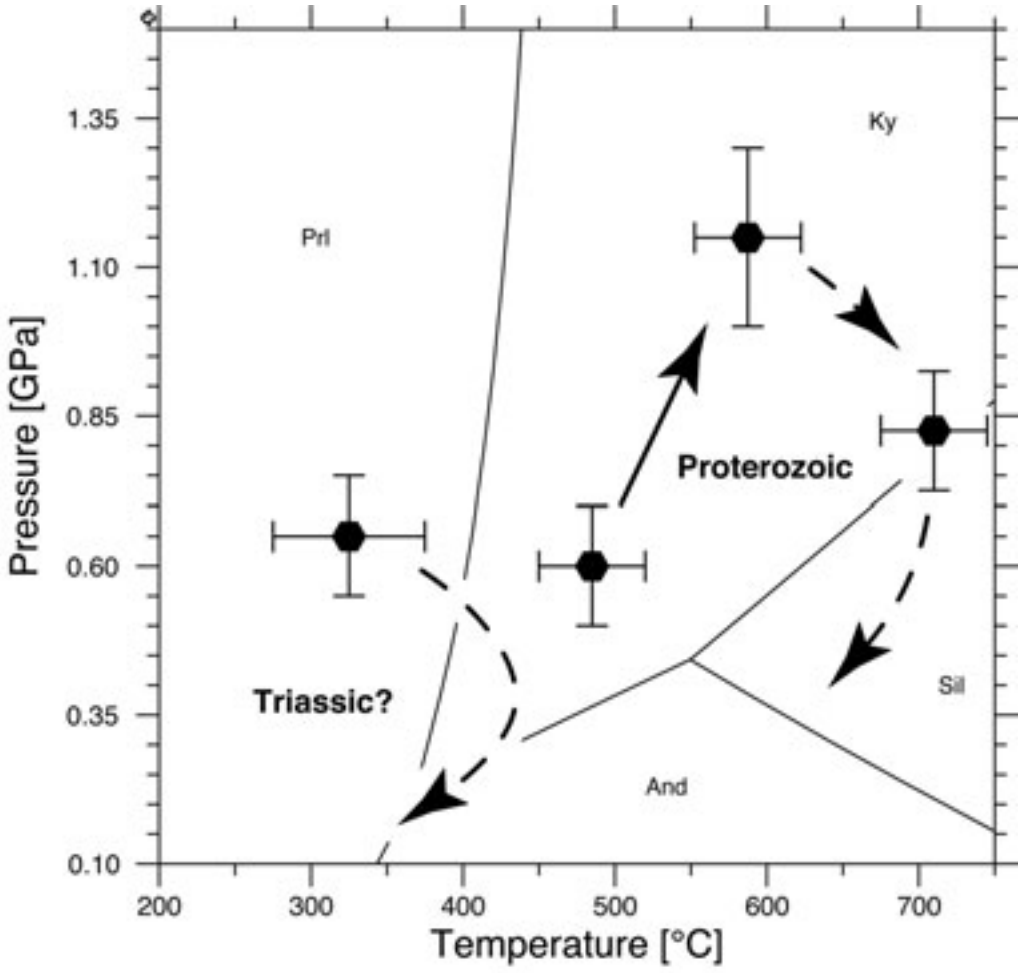

Figure 1. Metamorphic evolution of the Douling complex

REFERENCES

Currie, K.L. & van Staal, C.R. 1999: The assemblage stilpnomelane–chlorite–phengitic mica: a geothermobarometer for blueschist and associated greenschist terranes. J. metamorphic Geol. 17, 613-620

Ratschbacher, L., Hacker, B.R., Calvert, A., Webb, L.E., Grimmer, J.C., McWilliams, M., Ireland, T., Dong, S. & Hu, J. 2003: Tectonics of the Qinling Belt (Central China): Tectonostratigraphy, geochronology, and deformation history. Tectonophysics 366, 1-53.

Zhang, S., Wei, C., Zhao, Z. & Shen, J. 1996: Formation and metamorphic evolution of the Douling Complex from the East Qinling Mountains. Science in China, series D 39 supplement, 80-86.

Zhou, G., Liu, Y.J., Eide, E.A., Liou, J.G. & Ernst, W.G. 1993: High-pressure / low-temperature metamorphism in northern Hubei Province, central China. J. metamorphic Geol. 11, 561-574.

2.4

Geochemistry of the rift valley sediments at the Arctic Mid-Ocean Ridge: Preliminary results of the H2DEEP expedition to the southern Knipovich Ridge at 73°N

Baumberger Tamara*, Früh-Green Gretchen L.*, Pedersen Rolf B.**, Thorseth Ingunn H.**, Bernasconi Stefano M.*** & Plötze Michael****

*Institute for Mineralogy and Petrology, ETH Zurich, Clausiusstrasse 25, CH-8092 Zurich (tamara.baumberger@erdw.ethz.ch)
**Centre for Geobiology, University of Bergen, Allegaten 41, N-5007 Bergen
***Geological Institute, ETH Zurich, Universitätsstrasse 16, CH-8092 Zurich
****Laboratory of Clay Mineralogy, IGT, ETH Zurich, CH-8092 Zurich

The southern Knipovich Ridge (SKR, 73°N, 8°E) in the Norwegian-Greenland Sea is a permanently ice-free arctic ridge segment with an effective spreading rate of only 6 mm/year and is thus one of the most slow-spreading segments of the global ridge system. This ultra-slow spreading ridge is characterised by magmatic and amagmatic accretionary ridge segments and a partly sediment-covered rift valley, reaching water depths from 2000-2500 metres to 3500 metres in the deepest area. These sediments likely represent an important hydrological and thermal boundary to heat and fluid flow and provide a broad archive of the tectonic and alteration history. H2DEEP is an interdisciplinary, international project aimed at studying geodynamic and hydrothermal processes and their links to the deep hydrogen-based biosphere along the SKR. Our individual project of H2DEEP focuses on understanding water-rock interactions and the links between chemical and microbiological processes associated with alteration of a sediment-covered oceanic ridge and with serpentinisation in ultra-slow spreading environments.

Here we present preliminary results of mineralogical and geochemical investigations of the rift valley sediments obtained by gravity cores of the upper 4 metres of the sedimentary cover in the summer of 2007. The rift valley sediments are primarily characterised by hemipelagic sedimentation interrupted by turbiditic events. Visual observations identified glass- and iron-rich layers representing previous volcanic and probably hydrothermal activity. Radiographic analyses show a range of manganese-rich layers likely indicating hydrothermal events in the past. Powder x-ray diffraction investigations of bulk samples indicate that most of the minerals are detrital in origin. The most common mineral in the clay fraction is smectite, presumably derived from an increased volcanic activity in the investigated area. In one core, clay minerals of possible authigenic origin were identified in a layer at ≈2 metre depth. Carbon geochemistry of the sediments shows elevated total organic carbon contents, and carbon isotope compositions of total carbon reflect mixing of organic carbon with marine carbonates. Increased inorganic carbon contents in the upper sediment layers are associated with the presence of foraminifera. A significant increase in alkalinity and dissolved inorganic carbon content with sediment depth was detected in geochemical pore water profiles in the sediments from the deeper area of the rift valley. The corresponding δ^{13}CDIC values decline remarkably with increasing alkalinity and dissolved inorganic carbon contents. Our preliminary mineralogical and geochemical studies of the rift valley sediments point to an active history with various volcanic and hydrothermal events affecting the investigated area over the past twelve to twenty thousand years.

REFERENCES

Centre for Geobiology of the University of Bergen, Norway <http://www.geobio.uib.no/field-activities.aspx?pageid=1090>
Institute for Mineralogy and Petrology of the ETH Zurich, Switzerland
Marine Geology and Geochemistry Group <http://www.imp.ethz.ch/research/marine/fluidflow>

2.5

Petrographic observations in the Erstfelder Gneiss in the Gotthard Base Tunnel (NEAT) between Erstfeld and Amsteg

Bekaddour Toufik*, Schmidt Susanne*, Gnos Edwin** & Rütti Roger ***

*Département de Minéralogie, Université de Genève, bekaddo3@etu.unige.ch
**Département de Minéralogie et Petrographie, Muséum d'Histoire Naturelle de Genève
***IG GBTN, Bauleitung Amsteg-Erstfeld, 6472 Erstfeld

In the Gotthard Base Tunnel section between Erstfeld and Amsteg, various lithologies of the Erstfelder Gneiss unit have been studied macroscopically and microscopically, whole rock compositions have been determined and major mineral phases were analyzed using SEM and microprobe techniques.
The typical Erstfelder Gneiss consists of K-feldspar, plagioclase ($Ab_{81}An_{17}Or_2$), quartz and biotite. Biotite is commonly altered to chlorite and the feldspars are strongly sericitised.
Macroscopic observations within the first two kilometers of the tunnel indicate that the degree of partial fusion in the Erstfelder Gneiss unit increases from the northern tunnel entrance southward. At the entrance of the tunnel, a typical Erstfelder Gneiss with schlieren texture is found. In thin sections, areas of partial melts consisting of quartz and K-feldspar can be recognized. At approximately 800 m from the northern tunnel entrance, the neosom consisting of K-feldspar and quartz becomes visible in outcrop. In addition, lenses of grossular-rich calc-silicate rocks, as well as lenses with mafic compositions (amphibolites) are present. At tunnel kilometer 102.658 (eastern tube), the amount of partial melts has increased and garnet-bearing leucogranitic lenses reaching a size of up to 60 cm appear. Similar rocks collected at the surface yielded garnet of composition $Al_{70}Sp_{16}Py_{12}Gr_2$.
The whole rock composition of the Erstfelder Gneiss and the presence of calcsilicate rocks both point to a sedimentary origin for this part of the Erstfelder Gneiss unit.

2.6

Multi-pulse emplacement of the bimodal Matorello calc-alkaline pluton, Central Swiss Alps

Bussien Denise*, Bussy François ** & Chiaradia Massimo***

* Institut de Géologie et Paléontologie, Université de Lausanne, Anthropole, CH-1015 Lausanne (denise.bussien@unil.ch)
**Institut de Minéralogie et Géochimie, Université de Lausanne, Anthropole, CH-1015 Lausanne
*** Département de Minéralogie, Université de Genève, Rue des Maraîchers 13, CH-1205 Genève

The Matorello pluton is a Late Variscan calc-alkaline intrusion, which emplaced ca. 300 Ma ago in the basement of the present-day Sambuco nappe (lower Penninic domain, Central Lepontine Alps, Switzerland). The dominant facies are granodiorites and quartz-diorites, crosscut by acid-basic composite sills, aplitic and pegmatitic dykes and lamprophyres. Alpine orogeny induced intense polyphase folding of the pluton, as well as amphibolite-facies metamorphic recrystallisation. Despite this severe overprint, large portions of the intrusion preserve spectacular magmatic features, like composite sills, cross-bedded schlieren, hydrodynamically emplaced enclave-rich magma flows with gravitational sorting, magma mingling between adjacent layers of contrasting composition, etc. Many of these magmatic structures can be used as palaeogravity indicators. They consistently show that the northern part of the intrusion is overturned and refolded by an isoclinal upright antiform, close to the front of the Sambuco nappe, and that vertical mafic-felsic composite dykes were originally horizontal sills with internal gravitational sorting of the denser mafic enclaves in their aplogranitic matrix. Locally opposite palaeogravity indicators reveal second order isoclinal folds within the pluton.
Overall, the preserved magmatic structures point to a ca. 1-3 km (?) sill-like intrusion, emplaced by successive pulses of quartz-diorite and granodiorite, both attesting hybridization processes, like mafic microgranular enclaves and disequilibrium mineral textures. Subtle contrasts in granulometry, mineral mode or mineral sorting and/or crystal entrapment along contact surfaces are clues to distinguish injections from one another. Gravitational sorting of the enclaves in the granodiorite with load cast features at the base of the layers and sinuous biotite schlieren point to injection of low viscosity (fluid-rich?), turbulent composite magma flows in the still largely molten granodiorite host. Fluid-rich mixtures of mafic and

acidic melts were injected during the latest growth stage as metre-thick sills, attesting highly energetic hydrodynamic emplacement conditions.

The magmas involved are mantle-derived mafic liquids contaminated by crustal material as revealed by Nd epsilon values ranging between -2.1 to -4.7 and Pb isotopic ratios typical of the lower continental crust ($^{206}Pb/^{204}Pb$ = 18.7-19.0; $^{207}Pb/^{204}Pb$ = 15.66-15.69; $^{208}Pb/^{204}Pb$ = 38.6-39.0). Sr isotopic ratios are erratic, which is ascribed to Alpine metamorphic remobilization.

We propose the following scenario for the emplacement of the Matorello pluton: (1) multi-pulsed injection of an early quartz-diorite top layer, differentiated from – and hybridized with - more primitive calc-alkaline melts in a periodically replenished underlying magma chamber; (2) repeated injection of granodiorite melts, which pond below the still partially molten diorite layer; (3) evolved, water-rich melts differentiating in the lower magma chamber, are injected by hot mafic magmas, which trigger mingling processes and catastrophic emplacement of mixed materials as hydrodynamic channel deposits in the overlying Matorello laccolith; (4) late aplitic and pegmatitic dykes record the vanishing differentiation stages of the lower chamber, whereas a few calc-alkaline lamprophyres document late interaction between mantle-derived hydrous melts and crustal lithologies.

2.7

Paleozoic magmatism in the Sambuco and Maggia nappes, Lower Penninic domain

Bussien Denise*, Bussy François **, Magna Tomas** & Masson Henri*

* *Institut de Géologie et Paléontologie, Université de Lausanne, Anthropole, CH-1015 Lausanne (denise.bussien@unil.ch)*
** *Institut de Minéralogie et Géochimie, Université de Lausanne, Anthropole, CH-1015 Lausanne*

We have dated a series of magmatic rocks from the pre-Mesozoic basements of the Sambuco and Maggia nappes, Swiss Lepontine Alps, using the U-Pb zircon method coupled to the LA-ICPMS technique. Several events have been identified in the Sambuco nappe. The mafic banded calc-alkaline suite of Scheggia is dated at 540-530 Ma, an age similar to that of mafic lithologies from the Austroalpine Silvretta nappe. The Sasso Nero peraluminous augengneiss has an age of 480-470 Ma, as many other "older orthogneiss" in Alpine basement units. It hosts a large proportion of inherited zircons, which were dated at 630-610 Ma, a Panafrican age indicating a Gondwanian affiliation for the Sambuco basement. The calc-alkaline Matorello pluton, which displays spectacular features of magma mingling, including mafic enclave swarms, composite dykes and lamprophyres, yielded ages around 300 Ma, such as the lamprophyres. This age is comparable to the many Late Carboniferous intrusions from adjacent, European-derived basement units of Alpine nappes (Antigorio, Monte Leone, Verampio, Gotthard and other External Crystalline Massifs).

The Cocco granodiorite and Ruscada leucogranite, both intruded in the basement of the adjacent Maggia nappe, yielded ages of ca. 310 Ma, close to that of the Matorello pluton, but quite older than earlier age determinations by Köppel et al. (1981). This age coincidence, coupled to petrologic similarities between Cocco and Matorello granodiorites, strongly suggest a paleogeographic proximity of the Sambuco and Maggia nappes in Late Carboniferous times. However, these two nappes are currently interpreted as belonging to different Mesozoic paleogeographic domains: Helvetic for Sambuco and Briançonnais for Maggia (Berger et al., 2005), separated by an oceanic basin. In such a case, no significant transcurrent movement can be invoked along the two continental margins, as no offset is currently observed between them. Alternatively, the two nappes might belong to a single Alpine tectonic unit, as traditionally accepted.

REFERENCES

Berger, A., Mercolli, I. & Engi, M. 2005: The Central Lepontine Alps: Notes accompanying the tectonic and petrographic map sheet Sopra Ceneri (1: 100'000). Schweiz. Mineral. Petrogr. Mitt., 85, 109-146.

Köppel, V, Günthert, A. & Grünenfelder, M. 1981: Patterns of U-Pb zircon and monazite ages in polymetamorphic units of the Swiss Central Alps. Schweiz. Mineral. Petrogr. Mitt., 61, 97-119.

2.8

Mushroom garnet from the Mt. Mucrone, Sesia Zone, Italian Alps.

Darbellay Bastien *, Baumgartner Lukas **, Robyr Martin *

* *Institute of Mineralogy and Geochemistry, University of Lausanne, L'Anthropole, CH-1015 Lausanne, Switzerland.*
** *The University of Texas at Austin, Geol Science Dept., 1 University Station C1100, Austin, TX 78712-0254, USA.*

The simple dodecahedral shape and the fact that prograde zoning is typically preserved make garnets an excellent object for studying crystal growth mechanisms and to determining PT paths. Below we present some fascinating garnet textures, from the Sesia zone. They recorded a Hercynian and Alpine growth history.

Eclogites from the Mt. Mucrone area, Sesia zone, preserve relic pre-alpine structures and mineral assemblages, overprinted by the alpine high-pressure event(s). Quartz rich levels are composed of omphacite, garnet, paragonite and phengite. 3D high-resolution X-ray tomography images reveal that garnet morphology evolves from mushroom-shaped to atoll and finally to filled dodecahedral garnet forms. Mushroom garnets are composed of a roundish core (stem), which is connected to the "hat" of the mushroom by a skeletal garnet network. This poikilitic network formed along quartz grain boundaries. Progressive rim development around the core result in first an atoll, than the remaining poikilitic garnet is filled in.

These garnets are strongly zoned in five distinctive zones (garnet 1 to 5). Garnet 1 and especially 2 show poikilitic texture. Garnet 3 and 4 form the partial or complete rim and finally garnet 5 forms the outermost rim. It also replaces quartz grains in the poikilitic zone 2. Garnet 5 has sharp contacts with all other garnets. It grew after omphacite crystallization. No crystallographic missorientation between these five growth zones was detected by EBSD. Garnet 1 to 4 can be related to the prograde amphibolitic-granulitic Hercynian event by thermodynamic calculation using Theriak/Domino, assuming fractional crystallization. Textural analyses agree with P-T-calculations for garnet 5. It is of alpine age.

In spite of its important volumetric amounts, Garnet 5 shows homogeneous chemical profiles. Thus, it must have grown very fast, under near constant P/T conditions. Our Theriak/Domino model shows that fluid infiltration during alpine time or partial hydratation during the Hercynian retrograde path are needed to form large volume of unzoned garnet 5.

2.9

P-T condition of crystallization of granitoid plutons of Zayandeh -Rood river area, north of Shahrekord, Iran

Davoudian Ali Reza *, Genser Johann **, Neubauer Franz **

**Shahrekord University, Shahrekord, Iran (alireza.davoudian@gmail.com)*
** *Department of Geography and Geology, Salzburg University, Salzburg, Austria*

The granitoid plutons of Zayandeh -Rood River area occur as numerous large and small bodies in the north of Shahrekord city. The study area is located in the southwest of Iran, 330 Km southwest of Tehran and 35 km northeast of the Main Zagros Reverse fault, which is a proposed suture zone between the Arabian plate and Eurasia. The separation of Arabia from Africa and its subsequent collision with Eurasia was the last of a series of separation/collision events, all of which combined constitute the extensive Alpine-Himalayan orogenic system (Dewey et al. 1973).The studied area is a large scale ductile shear zone trending WNW-ESE nearly parallel to the Main Zagros Reverse fault (Fig. 1).
The north of Shahrekord area is characterized by the predominance of metamorphic rocks of both sedimentary and magmatic origins that are intruded by granitoid bodies. These rocks are more or less subjected to deformation. The granites show weaker metamorphic effects and they are strongly deformed during the subsequent deformation events (Davoudian et al. 2008).
The studied granitoid rocks cover a relatively large range in composition, including granite, granodiorite, trondhjomite and alkali granite. On the base of microscopic studies, the following mineral assemblages are deduced: quartz, alkali feldspars (as perthite, anti-perthite and microcline), plagioclase, biotite, amphibole, garnet, magnetite, allanite and epidote together with, sphene, zircon and apatite as accessories. Biotite and garnet are locally altered to chlorite. They are fine to medium – grained.

In order to determination of pressure (depth) and temperature condition of the plutons, some rock-forming minerals are studied by Electron Micro Probe Analysis method. All amphiboles have Ca+Na contents greater than 2.35 p.f.u., indicating that they are calcic amphiboles according to the classification of Leake et al. (1997). Amphibole compositions occupy a narrow compositional range with a Mg/(Mg +Fe^{2+}) ranging from 0.39 to 0.44 and a Si content of 6.31 to 6.51 atoms per formula unit (afu) and can be classified in the IMA nomenclature (Leak et al. 1997) as hastingsite, ferrihastingsite, ferrotschermakie and ferrohornblende. In general composition of plagioclase is $Or_{0.6\text{-}3.0}$ $Ab_{70.5\text{-}83.7}$ $An_{14.2\text{-}27.8}$.
Understanding the evolution of a granitoid pluton requires knowledge of the depth at which the various minerals crystallized and the amount of post-crystallization upward movement. The pressure of emplacement of a granite pluton can be constrained by geologic and petrologic criteria. Based either on cation exchange or solvus relations, there are several gethermobarometer applicable to granitoid rocks. Several studies revealed that Al content of hornblende in calc-alkaline granitoids varies linearly with pressure of crystallization, thereby providing means of determining the depth of pluton emplacement. Values about 5.9 – 6.5 kbar for the plutons were determined, using the calibration of Anderson and Smith (1995). These pressures are corresponding with 21 to 23 km depths. Temperatures derived from amphibole-plagioclase thermometry (Blundy and Holland, 1994) suggest crystallization at about 700- 720 °C.

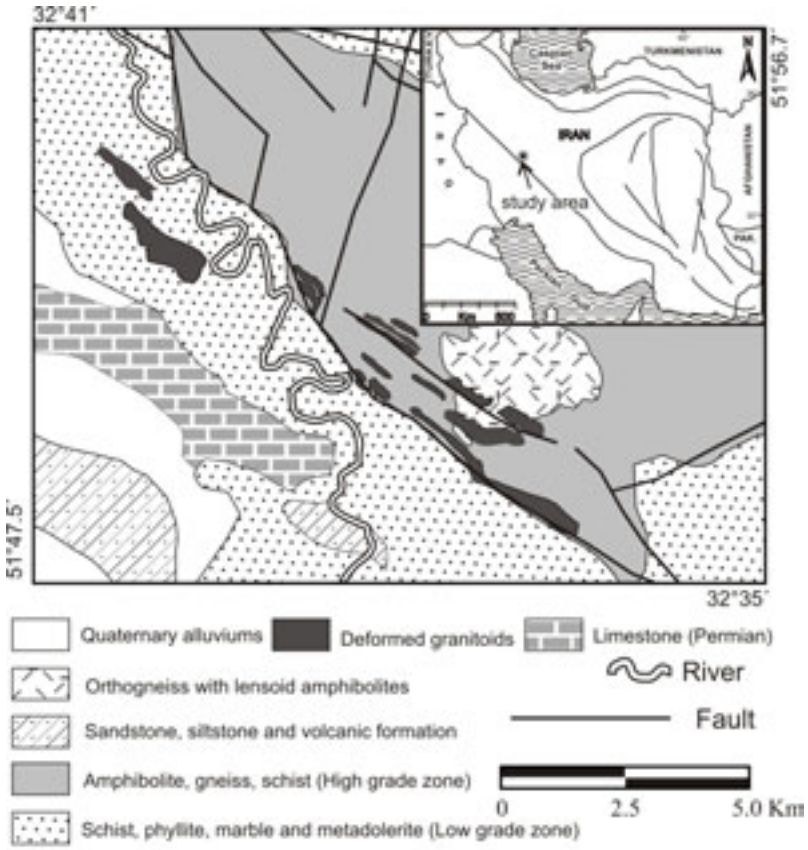

Figure 1. Geological map of the north of Shahrekord showing the distribution of granitoid plutons.

REFERENCES

Anderson, J. L. & Smith, D. R. 1995: The effect of temperature and oxygen fugacity on Al-in-hornblende Barometry. American Mineralogist, 80, 549–559.

Davoudian, A. R., Genser, J., Dachs, E. & Shabanian, N. 2008: Petrology of eclogites from north of Shahrekord, Sanandaj-Sirjan zone, Iran. Mineralogy and Petrology, 92, 393–413.

Dewey, J.F., Pitman, W.C. III, Ryan, W.B.F. & Bonnin, J. 1973: Plate tectonics and the evolution of the Alpine System. Geological Society of America Bulletin, 84, 3137–3180.

Holland T.J.B. & Blundy J.D. 1994: Non-ideal interactions in calcic amphiboles and their bearing on amphibole-plagioclase thermometry. Contributions to Mineralogy and Petrology, 116, 433–447.

Leake, B. E. & the IMA Commission 1997: Nomenclature of amphiboles. Report of the subcommittee on amphiboles of the International Mineralogical Association on new minerals and mineral names. European Journal of Mineralogy, 9, 623–651.

2.10

The Chelan complex (Washington Cascades): insights into the roots of continental arcs

Dessimoz Mathias*, Müntener Othmar*, Ulmer Peter**

*Institut de Minéralogie et Géochimie, Université de Lausanne, 1015 Lausanne (mathias.dessimoz@unil.ch)
**Department of Earth Sciences, ETH Zurich, Clausiusstrasse, 25, CH-8092 Zurich, Switzerland

The Chelan complex is a deep plutonic complex exposed in the North Cascades and crops out at the southern end of the northwest trending Chelan block. This block, bounded by the Entiat fault on the southwest and by the Ross lake fault zone on the north east, comprises much of the crystalline core of the north cascades and records Cretaceous to Palaeogene arc magmatism (from 100 Ma to 45 Ma) (Valley et al., 2003)

For a long time, Chelan migmatitic complex was interpreted as metamorphic / migmatitic unit consisting mainly of metatonalite, metabasite and widespread metaplutonic migmatite (Hopson and Mattinson, 1994) metamorphosed under upper amphibolite/lower granulite facies. The pressure of emplacement of the complex inferred from the surrounding rocks (Swakane gneiss and Napeequa complex) is thought to be around 9-12 kbar for a temperature of about 750°C (Valley et al., 2003)

Field observations in particular comb layers, pegmatitic gabbros and mafic cumulates clearly indicate that the magmatic origin is well preserved within the entire complex. While subsolidus deformations occur locally, most of the rocks are deformed in presence of melt, as indicated by a pervasive magmatic (almost no recrystallization of quartz is observed in thin section) foliation well developed in the tonalite, syn-magmatic shear zones and magmatic folding. At some places, in particular within melanocratic tonalite, numerous felsic rocks occur that are always associated with a more intense deformation. The local occurrence and discrete features of these zones are not consistent with a migmatitic origin. Thus, these "migmatite-like" rocks could rather be interpreted as plutonic feeder zones in which more evolved liquids are concentrated and migrate to high crustal levels.

Whole rock chemistry performed on hornblendite, hornblende gabbros, diorite, tonalite and mafic dykes display continuous trends for various oxides that are consistent with an evolution through magmatic processes. Comparison with experimental data (Alonso Perez, 2006; Kägi, 2000) is in good agreement with an evolution of the suite through crystal fractionation at high pressure (around 1.0 GPa, Fig. 1). This is well indicated by TiO_2, Al_2O_3, FeO and CaO, which show a good correlation with the experiments done at 1.0 GPa. The high pressure of crystallization of the Chelan complex is consistent with the widespread occurrence of primary epidote (P>0.6 GPa) in tonalite and diorite.

According to these observations, the Chelan Complex provide insights into the deep-seated processes occurring in the roots of continental arcs and could be an example of the Mixing-Assimilation-Storage-Hybridization-Zone (MASH), which form the base of the plutonic systems (Hildreth and Moorbath, 1988).

REFERENCES

Alonso Perez, R. (2006) The role of garnet in the evolution of hydrous, calc-alkaline magmas an experimental study at 0.8 - 1.5 GPa, p. 1 Band. ETH, Zürich.

Hildreth, W., and Moorbath, S. (1988) Crustal Contributions to Arc Magmatism in the Andes of Central Chile. Contributions to Mineralogy and Petrology, 98(4), 455-489.

Hopson, C.A., and Mattinson, J.M. (1994) Chelan Migmatite Complex, Washington; Cretaceous mafic magmatism, crustal anatexis, magma mixing and commingling, and protodiapiric emplacement. Geologic Field Trips in the Pacific Northwest: 1994 Geological Society of America Annual Meeting Geological Society of America, 1-21.

Kägi, R. (2000) The liquid line of descent of hydrous, primary, calc-alkaline magmas under elevated pressure an experimental approach, p. 115 S., Zürich.

Valley, P.M., Whitney, D.L., Paterson, S.R., Miller, R.B., and Alsleben, H. (2003) Metamorphism of the deepest exposed arc rocks in the Cretaceous to Paleogene Cascades belt, Washington: evidence for large-scale vertical motion in a continental arc. Journal of Metamorphic Geology, 21(2), 203-220.

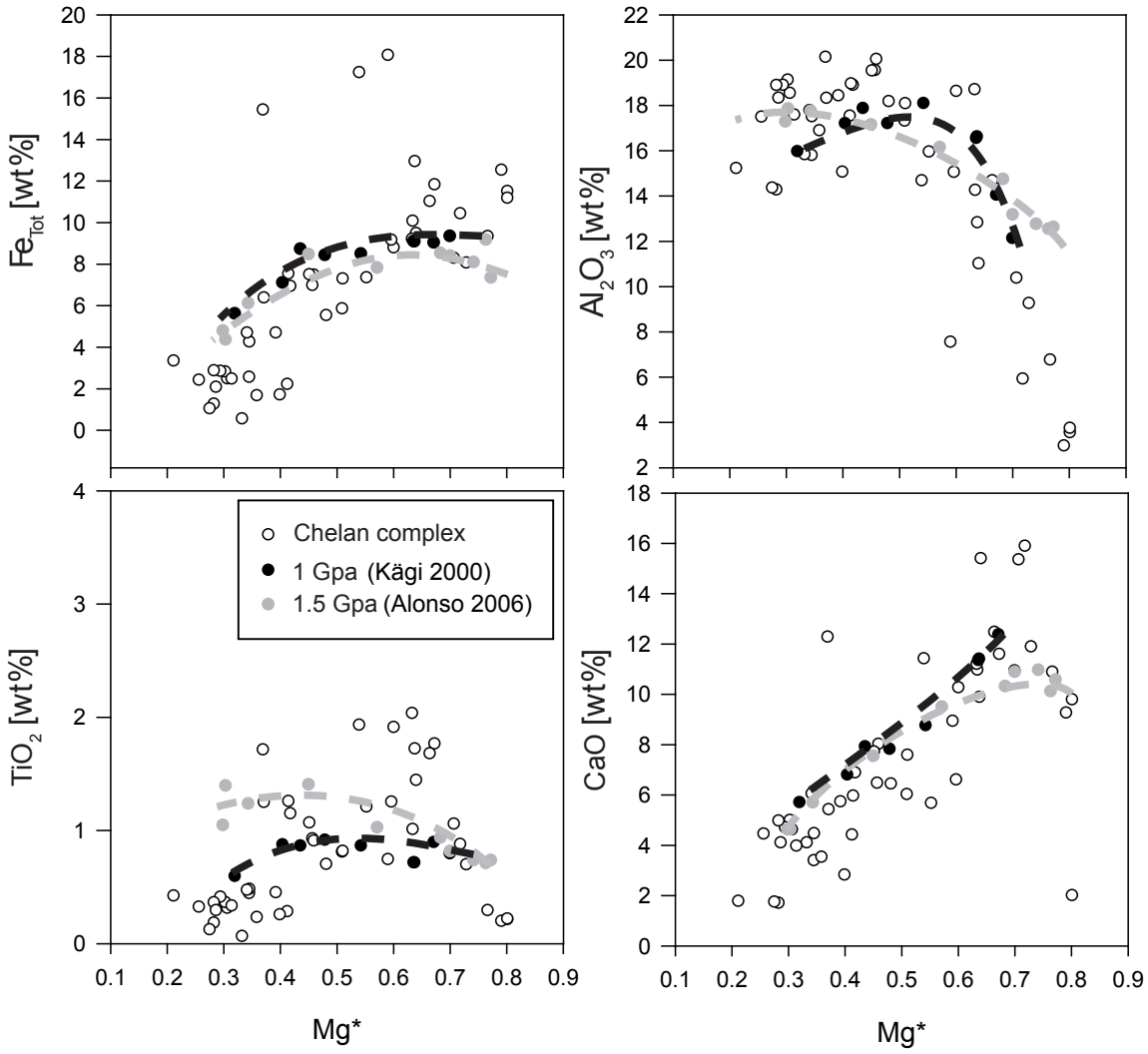

Figure 1: Comparison between whole rock analyses and experiments at 1.0 GPa (black dashed line, Kägi, 2000) and 1.5 GPa (grey dashed line, Alonso Perez, 2006).

2.11

Experimental re-determination of initial melting in the system calcite-H_2O at 100 MPa and calcite/melt element fractionation

Durand Cyril* and Baumgartner Lukas*

**Institut de Minéralogie et Géochimie, Université de Lausanne, BFSH2, CH-1015 Lausanne (cyril.durand@unil.ch)*

The study investigates the partial melting of calcite in the presence of water. We determined the temperature of initial melting in the binary calcite-H_2O system using rapid vertical quench equipment, as well as the partitioning of elements between calcite and melt for major and trace elements. The classic studies of Wyllie and Tuttle (1959; 1960) placed initial melting at ca. 740°C at 100 MPa. Hence partial melting in contact metamorphic terrains was predicted to be possible, though difficult. Field studies (Wenzel et al., 2002; Jutras et al., 2006) and discussions (Lentz, 1998, 1999) have suggested that partial melting does occur.

Vertical rapid-quench cold-seal pressure vessels were used. Temperature was measured with external NiSil-thermocouples, resulting in an estimated 5°C uncertainty. Powders were sealed into gold capsules along with variable amounts of water. Natural calcite and synthetic reaction grade calcite (>99.5%, Alfa Aesar, lot C24Q27) were used. Run times varied between 1.5h and 90h. Melting was identified by SEM and EMP. Unequivocal initial melt textures were the formation triple junction

melt pools and networks of interstitial melts. Upon quench skeletal crystals were formed in these pools surrounded by a homogeneous matrix. It was not possible to prove the presence of melts for small water/calcite ratios, which are predicted to form only small melting amounts. Small spherical blobs of quenched melt seen at 800°C are similar to smaller, more equant blobs precipitated from water vapor by quenching at sub-melting temperature.

Experiments bracket the initial melting temperature between 600°C and 650°C. This is roughly 100°C lower than those obtained by Wyllie and Tuttle (1959; 1960). These low melting temperatures suggests that partial melting of carbonates during contact metamorphism should occur often, especially in xenoliths.

The starting material consists of a mixture of synthetic carbonates ($CaCO_3$-$SrCO_3$-$MnCO_3$-$BaCO_3$) and natural ($FeCO_3$-$MgCO_3$) carbonates for partitioning experiments. The water solution was enriched in REE. Run times varied between 1h to 15 days. The Cal/H_2O ratios were fixed at 0.5. Major and trace element contents were measured by EMP and La-ICP-MS. Each measure corresponds to an average of 3 spots of 20μm for major elements and 1 spot of 100 μm for trace elements and REE to integrate the composition in the partially crystallized matrix. Calcite melts appear enriched in CaO, FeO, MnO, MgO, BaO and REE contents in comparison to the calcite. No fractionation appears between LREE and HREE. No tell a tale chemical signature was found which would permit the identification of solidified partial melts. Nevertheless, the strong partitioning of elements into the melt phase might permit identification in cases where the melt was separated from the remaining calcite, leaving depleted calcites behind.

REFERENCES

Jutras P, Macrae A, Owen JV, Dostal J, Préda M and Prichonnet G (2006) Carbonate melting and peperite formation at the intrusive contact between large mafic dykes and clastic sediments of the upper Palaeozoic Saint-Jules Formation, New-Carlisle, Quebec. Geological Journal 41: 23-48

Lentz DR (1998) Late-tectonic U-Th-Mo-REE skarn and carbonatitic vein-dyke systems in the southwesternGreenville Province: A pegmatite-related pneumatolytic model linked to marble melting. In Mineralized intrusion-related skarn systems. Mineralogical Association of Canada Short Course, 26: 519-657

Lentz DR (1999) Carbonatite genesis: a reexamination of the role of intrusion-related pneumatolytic skarn processes in limestone melting. Geology 27 (4): 335-338

Wenzel T, Baumgartner LP, Brügmann GE, Konnikov ED and Kislov E (2002) Partial melting and assimilation of dolomitic xenoliths by mafic magma: the Ioko-Dovyren intrusion (North Baikal region, Russia). Journal of Petrology 43 (11): 2049-2074

Wyllie PJ and Tuttle OF (1959) Melting of calcite in the presence of water. American Mineralogist 44: 453-459

Wyllie PJ and Tuttle OF (1960) The system CaO-CO_2-H_2O and the origin of carbonatites. Journal of Petrology 1 (1): 1-46

2.12

Experimental determination of Ra mineral/melt partitioning for leucite, feldspars, and phlogopite and ^{226}Ra-disequilibrium crystallisation ages of leucite and feldspars

Fabbrizio Alessandro*, Schmidt Max W*, Günther Detlef**, Eikenberg Jost***

*Institute for Mineralogy and Petrology, Clausiustrasse 25, ETH Zürich, CH-8092 Zürich (alessandro.fabbrizio@erdw.ethz.ch)
**Laboratory for Inorganic Chemistry, ETH Zürich, CH-8093 Zürich
***Division for Radiation and Security, Paul Scherrer Institute, CH-5232 Villigen

^{226}Ra-^{230}Th disequilibrium is frequently used to date magmatic processes such as magma residence times that occurred within the last 8000 years (e.g. Volpe & Hammond 1991; Volpe 1992; Reagan et al. 1992; Schaefer et al. 1993; Black et al. 1998; Cooper et al. 2001; Cooper & Reid 2003). With the exception of Cooper and co-authors, in all other studies the chemical behaviour of Ra was approximated by that of Ba. This experimental study detemined DRa for the most common igneous minerals that host Ra (e.g., leucite, K-feldspar, plagioclase, phlogopite), to quantify the fractionation of Ra/Ba and thus, to correctly calculate mineral ages and isochrons from Ra-Ba-Th measurements. Each mineral was crystallised from different synthetic starting materials in order to obtain crystals > 40 μm of the mineral of interest and crystal free melt pools > 200 μm of the silicate liquid. Starting materials were doped adding few μl of ^{226}Ra solution such that the lower Ra-concentration in a mineral/melt system was at least 1 ppm (detection limit of the LA-ICP-MS is ≈ 0.01 fg). The experiments were performed in an atmospheric furnace or in a piston cylinder apparatus at appropriate experimental conditions (P, T). For melt compositions in the atmospheric furnace, FeO was replaced by CoO, thus circumventing the need for fiddling with oxygen fugacity. Our re-

sults demonstrate that Ra is a compatible element in leucite, K-feldspar and phlogopite, whereas it is incompatible in plagioclase. In leucite, Onuma-type element partitioning parabola peak near Cs (and not the major cation K) for the alkalis and near Ra for the earth alkalis. In phlogopite Ra is hosted in the interlayer site and has a cation radius close to the optimum of this site, leading to high partition coefficients. In all cases DBa and DRa are significantly different, DRa/DBa ranging from 0.2-0.6 in the feldspars to 1.3 in phlogopite to 4.2 in leucite. The knowledge of DRa then allows us to recalculate correct crystal ages of various volcanic systems (e.g. Vesuvius, Mt St Helens, Mt Shasta, Nevado del Ruiz, Mt Erebus) obtaining a change from 2 to 10-fold in the ages derived from minerals (leucite, plagioclase) in which the difference between DRa and DBa is high.

REFERENCES

Black, S., Macdonald, R., DeVivo, B., Kilburn, C.R.J., Rolandi, G. 1998: U-series disequilibria in young (A.D. 1944) Vesuvius rocks: Preliminary implications for magma residence times and volatile addition. Journal of Volcanology and Geothermal Research, 82, 97-111.

Cooper, K.M. & Reid, M.R. 2003: Re-examination of crystal ages in recent Mount St. Helens lavas: implications for magma reservoir processes. Earth and Planetary Science Letters, 213, 149-167.

Cooper, K.M., Reid, M.R., Murrell, M.T., Clague, D.A. 2001: Crystal and magma residence at Kilauea Volcano, Hawaii: ^{230}Th-^{226}Ra dating of the 1955 east rift eruption. Earth and Planetary Science Letters, 184, 703-718.

Reagan, M.K., Volpe, A.M., Cashman, K.V. 1992: ^{238}U- and ^{232}Th-series chronology of phonolite fractionation at Mount Erebus, Antarctica. Geochimica et Cosmochimica Acta, 56, 1401-1407.

Schaefer, S.J., Sturchio, N.C., Murrell, M.T., Williams, S.N. 1993: Internal ^{238}U-series systematics of pumice from the November 13, 1985, eruption of Nevado del Ruiz, Colombia. Geochimica et Cosmochimica Acta, 57, 1215-1219.

Volpe, A.M., & Hammond, P.E. 1991: ^{238}U-^{230}Th-^{226}Ra disequilibria in young Mount St. Helens rocks: time constraint for magma formation and crystallization. Earth and Planetary Science Letters, 107, 475-486.

Volpe, A.M. 1992: ^{238}U-^{230}Th-^{226}Ra disequilibria in young Mt. Shasta andesites and dacites. Journal of Volcanology and Geothermal Research, 53, 227-238.

2.13

On mass fluxes and metasomatic processes above subducting slabs: An experimental solubility and melting study of Enstatite + Quartz + H_2O

Hack Alistair*, Ulmer Peter, Thompson Alan

Institute for Mineralogy and Petrology
ETH Zürich Clausiusstrasse 25, Zürich 8092, Switzerland
(Alistair.Hack@erdw.ethz.ch)

We have conducted diamond-trap type experiments to determine the solubility and melting behaviour in the poorly investigated silica-rich part of the MgO-SiO_2-H_2O (MSH) system to 700 to 1250 ˚C, 1 to 3.5 GPa. The results bear on the occurrence of complete melt-fluid miscibility (or so-called supercriticality) and other general aspects of fluid-mediated mass transport in metasomatic regions, for example: above subduction zones where slab dehydration fluids ascend and interact with overlying mantle.

Our experimental results for the solubility of enstatite + quartz in water suggest that fluids related to subsolidus metasomatic assemblages which are intermediate to model crust (quartz) and mantle (forsterite + enstatite) remain distinctly silica-rich (Si/Mg molar ratio from ≈5 to 15) with increasing *P* to > 3.5 GPa, and thus distinct from more dilute and higher Mg/Si fluids associated with forsterite + enstatite at equivalent depth (related to *P*). We find Ens + Qtz solubility in H_2O increases more rapidly with increasing *P* ($\partial X/\partial P$) compared to Qtz in H_2O; at 950 °C, ≈ 3 GPa the relative solubilities of Qtz and Qtz+Ens crossover. This solubility behaviour suggests that in MSH, fluids moving from Qtz to Ens + Qtz saturation precipitate where $P < \approx 3$ GPa, whereas dissolution is predicted along a similar path at higher *P*.

The results suggest that metasomatic assemblages may be associated with enhanced solubility at certain conditions. This is significant because lower time-integrated fluid fluxes are required where mass transport occurs at higher concentrations. In subduction zones, for example, metasomatic processes may play a significant role in maximising transfer of slab components to melting regions in overlying wedge.

Additionally, solubility data provides information on solute-solvent interactions and a means to constrain relevant thermodynamic quantities. The differences between Qtz and Qtz+Ens assemblage solubility behaviour imply Mg interactions with SiO_2-H_2O must modify solute polymerization mechanisms and are accompanied by a large volumetric effect: $\Delta rV°$ of Qtz = $SiO_{2(aq)}$ is more negative in the presence of dissolved Ens (-1.4±0.5 J bar^{-1} mol^{-1}) relative to pure H_2O (-0.28 J bar^{-1} mol^{-1}, Manning 1994). For dissolved Ens, $\Delta rV°$ (Ens = $MgSiO_{3(aq)}$) = -0.8±0.3 J bar^{-1} mol^{-1}.

Further experiments are being undertaken to constrain the conditions at which complete melt-fluid miscibility occurs in silica-rich fluids. Such knowledge is of interest because supercritical fluids may have a water/silicate ratio comparable to hydrous melts at high-temperature relative to the second critical point but have viscosity and probably density comparable to more dilute subcritical fluids. Accordingly, supercritical fluids may migrate over longer length-scales compared with melts and have a higher capacity to transfer dissolved chemical mass compared to aqueous fluids. Based on our and other published experiments in MSH together with theoretical considerations, we expect the second critical endpoint on the enstatite + quartz wet solidus to occur at lower pressure than observed in forsterite-bearing assemblages but higher pressure than for silica-water. By analogy this would imply that the temperature-depth range of melt-fluid supercriticality extends significantly shallower and to lower temperature in intermediate/metasomatic compositions relative to peridotitic mantle.

REFERENCES

Manning, C.E., 1994: The solubility of quartz in H_2O in the lower crust and upper mantle. Geochim. Cosmochim. Acta 58, 4831–4839.

2.14

The Blueschists of the Deyader Complex, Makran, SE Iran – Petrography, Geochemistry and Thermobarometry

Hunziker Daniela*

**Geological Institute, Structural Geology and Tectonics, Leonhardstrasse 19, CH-8092 Zurich (danielah@ethz.ch)*

Plate tectonic processes concerning the evolution and recycling of lithosphere are some of the most discussed subjects in earth sciences. Records of past subduction are found in blueschist and eclogites facies rocks, formed in a high pressure/low temperature environment. Studying these metamorphic rocks opens the possibility to comprehend how thermo-mechanical processes work in convergence zones at great depth. Blueschists in particular represent a record of vertical displacement at plate boundaries and are witnesses of thermal regimes in subduction zones. Understanding their evolution is crucial for understanding general global tectonic processes.

Despite of their unique setting in an active subduction, the blueschists within the metamorphic Deyader Complex in the Makran, SE Iran, are scarcely studied. They occur as blocks of various sizes being thrust over low-grade metamorphic rocks. Aim of this study is give an elaborate petrological and geochemical description of the blueschists, to identify the protolith and reconstruct their P-T-path.

During fieldwork in January 2008 a map and profile of the main blueschist outcrop at the Kuh-e Taftah has been produced. Mineralogy of the collected samples confirmed conditions typical for blueschist facies: lawsonite, sodic and sodic-calcic amphiboles, rutile, sphene, aragonite, minor albite and quartz ± pumpellyite. Different textures reveal four protoliths: basalts, gabbros, volcanoclastic sediments and sandstones. All basic blueschists have similar geochemistry, correlating well with MORB, but additionally showing arc affinity. This feature is found in many ophiolites involved in Himalayan orogeny and typical for oceanic crust evolved in a supra-subduction environment.

The metamorphic path of the Makran Blueschists reconstructed with PERPLE_X indicates burial along a cold gradient to peak metamorphic conditions at 300 – 350°C and 10 – 12kbar, what equals to about 40km of subduction. This estimation seems to be rather high regarding the mineralogy and phase relations. The geochemical results indicating formation in a supra-subduction zone also raises questions. How could such a protolith be subducted? Additionally, PERPLEX calculations suffer from weakness in the thermodynamic models for sodic amphiboles and lawsonite, which do not consider Fe^{3+} incorporation and therefore deliver unsatisfactory results for such rocks.

Whether the blueschists of the Makran were subducted during their evolution or formed in tectonic underplating processes remains to be answered.

2.15

Sr-Nd Isotopic Characteristics of Neogene volcanic rocks in Southeast of Isfahan

Khodami Mahnaz *& Davoudian Ali Reza **

* *Department of Geology, Islamic Azad, University, Mahallat Branch,Iran (mahnaz.khodami@gmail.com)*
** *Department of Natural Resources, Shahrekord University, Shahrekord, Iran*

Neogene calc-alkaline volcanic rocks are exposed in southeast of Isfahan in the Urumieh Dokhtar magmatic belt in Central Iran structural zone. These volcanic rocks have compositions ranging from basaltic andesites, andesites to dacites, which can be find as lava flow and dome. Geochemical studies show these rocks are a medium to high K calc-alkaline suite and they enriched from LILE and LREE in normalized multi-element patterns, and negative Nb, Ti, Ta and P. Condrite-normalized REE patterns display a steep decrease from LREE to HREE without any Eu anomaly. These characteristics are consistent with ratios obtained from subduction related volcanic rocks and in collision setting. Geochemical data show magma derived from a heterogeneous source. Upper mantle lithosphere and lower crust are heterogeneous source but asthenosphere normally is much more homogeneous(Seghedi, et al 2005). The mechanism of magma genesis is considered to be related to melting of a heterogeneous source, which was enriched in incompatible elements situated at the upper continental lithospheric mantle or lower crust. The geochemical characteristics of these volcanic rocks suggested that these volcanic rocks evolved by magma-mixing contamination of a parental magma derived from metasomatized upper lithospheric mantle by partial melting of the crust. These volcanic rocks carry a geochemical signature of continental crust through which they have passed. These processes complicate distinguish of the source of parental. It is thought that dacitic rocks formed from a lower crustal source and have less interaction with mantle. The mantle lithospheric derived magma evolved to basaltic andesite as result of mixing with crustal melts. The crustal melts were generated contemporaneously, with a direct influence of the mantle melts on crustal melting generation. Sr and Nd isotopic compositions (Table 1) are plotted in Fig. 2 along with regions of known calcalkaline affinity. The data suggest that rocks plot at lower $^{87}Sr/^{86}Sr$ and $^{143}Nd/^{144}Nd$ ratios, around the Bulk Silicate Earth reservoir, compared with normal calc-alkaline samples, which are much more scattered (Rosu, et al 2004). The oldest measured rock (740) has higher $^{87}Sr/^{86}Sr$ and lower $^{143}Nd/^{144}Nd$ (Fig. 2) The most important petrogenetic process involved in magma generation in this area is probably variable degrees of partial melting of a heterogeneous source, which was isotopically depleted, but enriched in incompatible elements. The initial crustal contamination and insignificant fractional crystallization processes is characteristic for an initial storage of the magmas in the crust.

REFERENCES

Rosu, E., Seghedi, I., Downes, H., Alderton, D.H.M., Szakács, A., Pécskay, Z., Panaiotu, C., Panaiotu, C. E. & Nedelcu, L., 2004: Extension-related Miocene calc-alkaline magmatism in the Apuseni Mountains, Romania: Origin of magmas. Schweizerische Mineralogische und Petrographische Mitteilungen, 84, 153–172.

Seghedi, I., Downes, H., Harangi, S., Mason P.R.D. & Pecskay, Z., 2005: Geochemical response of magmas to Neogene–Quaternary continental collision in the Carpathian–Pannonian region: A review. Tectonophysics, 410, 485–499.

Table 1. Nd–Sr isotopic data for the volcanic rocks from southeast of Isfahan, Iran

Sample	Rb	Sr	Nd	Sm	87Sr/86Sr	143Nd/144Nd
Dacite with xenocrysts	59.1	596.8	20.7	3.1	0.705991	0.512578
Andesite	68.7	1039	18.7	3.8	0.704536	0.512613
Dacite	64	551.5	19.9	3.1	0.705598	0.512601
Basaltic andesite	33.3	613.4	21.4	4.6	0.706094	0.512615

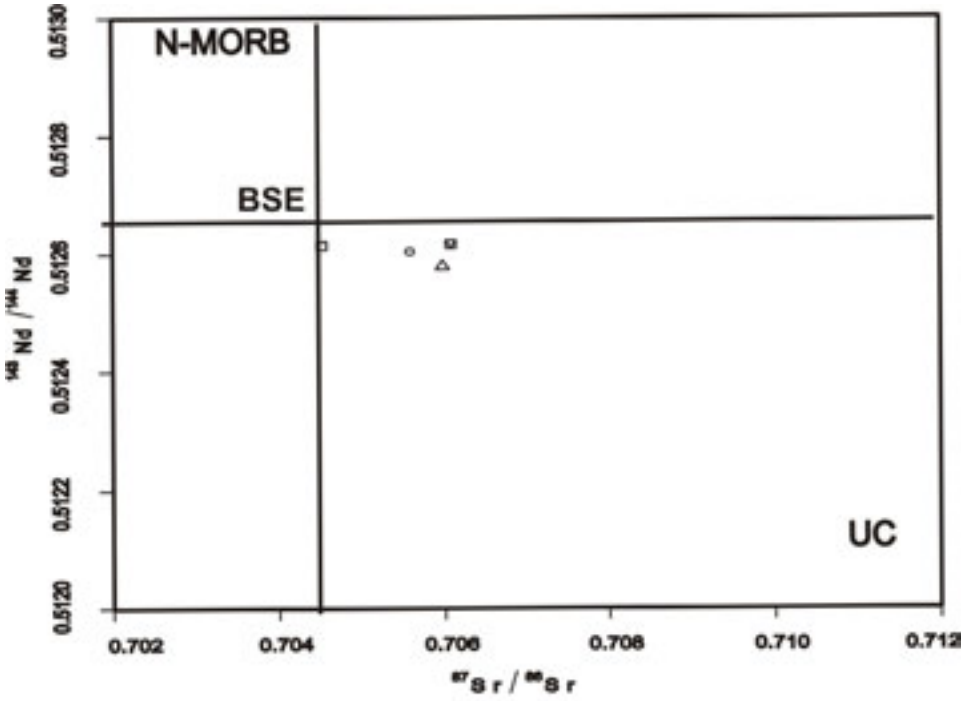

Fig. 1. $^{87}Sr/^{86}Sr$ vs. $^{143}Nd/^{144}Nd$ variation of the magmatic rocks. Fields for Upper Crust (UC); Bulk Silicate Earth (BSE), This symbole use for sample in this figure:Basaltic andesite ⊠ Andesite ■, Dacite with xenocrysts △, Dacite ○

2.16

Emplacement of the Torres del Paine mafic complex (Patagonia, Chile): A progress report

Leuthold J.*, Müntener O.*, Baumgartner L.*, Putlitz B.*, Michel J.*, Chiaradia M.**

* *Institute of Mineralogy and Geochemistry, Anthropole - UNIL, CH-1015 Lausanne, Switzerland (julien.leuthold@unil.ch)*
** *Department of Mineralogy, Rue des Maraîchers 13 – UNIGE, CH-1205 Geneva, Switzerland*

The Torres del Paine pluton (Patagonia, Southern Chile) is a composite, upper crustal mafic and granitic intrusion that was emplaced in the Miocene (Michel et al. 2008). It consists of a ≈400m thick, basal mafic complex (Paine Mafic Complex – PMC, Michael 1991) and a younger granite complex at the top (1500m thick), which have been separated into 3 units based on field data and U-Pb ages (Michel et al. 2008).

We distinguish a 'feeder zone' with subvertical contacts in the Western part of the pluton and a saucer-shaped laccolith in the central and Eastern part with predominantly subhorizontal contacts. Field observations show that three different gabbros and two different diorites can be distinguished. The relative chronology of the mafic rocks is based on intrusive relationships. The earliest intrusions are layered olivine gabbros that are exclusively exposed in the 'feeder zone', cut by biotite-hornblende (olivine-) melagabbros. The two latter ones form a large sill complex in the Central part of the PMC, where two broadly similar and generally well-exposed sections of mafic rocks have been sampled (Castillo, and Aleta de Tiburon). The lower one has brown hornblende crystallized prior to plagioclase and the upper one contains spectacular poikilitic hornblende. These mineralogical variations are reflected in the whole rock chemistry. The lower zone is generally poorer in K_2O and richer in CaO, consistent with hornblende accumulation and a higher hornblende/biotite ratio. The presence of remobilized crystals, hornblende-rich clots, and decimetre-thick boudinaged sills of hornblendite indicates remobilisation of ferro-magnesian cumulates.

There are two different types of dioritic intrusives that are injected as sills into the gabbroic crystal mush at its level of crystallization. These diorites have chemical similarities with the gabbro types. Intraplutonic contacts with gabbroic enclaves display cuspate-lobate textures and occasional chilled margins, testifying a multiple generation of mafic sills in the PMC. Interstitial liquid is pooled on top of individual sills and intrudes overlying mafic units as 'microdiapirs'. We interpret these fluid-saturated pegmatoid rocks as evolved residual melts expelled from the compacting dioritic and gabbroic rocks.
The youngest mafic rocks are included in a porphyritic granite that shows intrusive relationships to both the PMC and the granites. They propagate along cracks cutting mafic and granitic rocks, and locally accumulate in decametric (about 40 x 40 x 5m) magma bodies. They contain up to 50% of mafic enclaves, settled preferentially in stagnant areas. Some of these dioritic enclaves display chilled margins indicating mafic magma injections in a magma reservoir beneath the current emplacement level of the Paine laccolith.
Preliminary radiogenic isotopes data suggest some crustal contamination for granitic rocks ($^{87}Sr/^{86}Sr$: 0.705, $^{143}Nd/^{144}Nd$: 0.5126). Both granitic and mafic rocks ($^{87}Sr/^{86}Sr$: 0.704, $^{143}Nd/^{144}Nd$: 0.5127) overlap the Patagonian batholith isotopic composition field (Hervé et al. 2007), indicating that the isotopic signature of the Torres del Paine pluton may be acquired in reservoirs where MASH-type processes dominate. The data for the Paine mafic rocks indicate multiple pulses from a contaminated source.

REFERENCES

Hervé F, Pankhurst RJ, Fanning CM, Caldéron M, Yaxley GM; 2007; The South Patagonian batholith: 150 my of granite magmatism on a plate margin; Lithos; 97; 373-394

Michael PJ; 1991; Intrusion of basaltic magma into a crystallizing granitic magma chamber: The Cordillera del Paine pluton in southern Chile; Contrib Mineral Petrol;108; 396-418

Michel J., Baumgartner L, Putlitz B., Schaltegger U, Ovtcharova M; 2008; Incremental growth of the Patagonian Torres del Paine laccolith over 90kyrs; Geology; 36/6; 459-462

2.17

Metamorphic and deformation history of the Nufenen Pass and Lukmanier Pass area

Madonna Claudio*, Schenker Filippo*, Reusser Eric* & Burg Jean-Pierre**

*Institut für Mineralogie und Petrographie, ETH Zürich, CH-8092 Zürich (madonnac@student.ethz.ch)
**Geologisches Institut, ETH Zürich, CH-8092 Zürich

Structural and metamorphic studies have been carried out on the areas of the Nufenen Pass and the Lukmanier Pass with the aim of comparing the kinematics and metamorphic evolution of both regions. Both areas share similar lithological units of Triassic and Jurassic age. The meta-marl to meta-pelitic rocks represent para-autochthonous sediment units from the proximal European basement. Detailed mapping of both areas has led to a new interpretation of the deformation history along the Northern Penninic front.

The structures of the Nufenen Pass area generally strike NE-SW and are arranged in a subvertical position. Similar structures are observed throughout the Nufenen- and Corno-Zone. Asymmetric folds, sigma clasts and mineral stretching lineations consistently show the same top-to-north shear movement combined with a dextral strike-slip component. Therefore, the Nufenen and the Corno zone form a large imbricate shear zone due to both, the Penninic overthrust and the subsequent formation of the Lepontine dome. The estimated P-T conditions along a N-S profile are discontinuous confirming the structural interpretation. They are in agreement with metamorphic conditions previously described by Klaper and Bucher-Nurminen (1987) and Kamber (1993).

In the Lukmanier Pass area the general trend of the structures is similar to that of the Nufenen Pass area, except for the mineral elongations which plunge to the N orthogonal to the fold axes. In contrast to the Nufenen Pass, the shear indicators display a top-to-south movement – demonstrated by S-C structures in the Gotthard basement – is localised in two major backthrust systems. The southern backthrust generated large-scale drag folds: in the Mesozoic cover the antiform above Acquacalda and in the Lucomagno massif the Chiera synform. The northern backthrust developed a thick-skin tectonics in the meta-sediments. Thermodynamic modeling of the meta-pelitic rocks from Frodalera and Bronico reveal a maximum temperature of 650° C and at a pressure of 0.8 GPa.

In the two regions investigated the shortening due to Alpine N-S compression was accommodated in two different ways: In the Nufenen Pass area the shortening took place through a leading imbricate fan where the structures have been ramped up in a sub-vertical position by the development of listric thrusts in the frontal part of the imbricate zone (Burg et al., 2002). In the Lukmanier Pass area, however, the shortening was a consequence of a system of synchronous conjugate thrusts, in which the vertical position of the units is due to the frontal thrust movement and the antithetic backthrusting.

REFERENCES

Burg, J.-P., Sokoutis, D., & Bonini, M. 2002: Model-inspired interpretation of seismic structures in the Central Alps: Crustal wedging and buckling at mature stage of collision. Geological Society of America, 30 (7), 643 – 646.

Kamber, B. S., 1993: Regional metamorphism and uplift along the Southern margin of the Gotthard massif: results of the Nufenenpass area. Schweiz. Mineral. Petrogr. Mitt., 73, 241 – 257.

Klaper, E. M., Bucher-Nurminen, K., 1987: Alpine metamorphism of pelitic schists in the Nufenen Pass area, Lepontine Alps. J. Metamorphic Geol., 5, 175 – 194.

2.18

Cooling and crystallization of natrocarbonatitic lava flows: Reconciling laboratory experiments with field observations

Mattsson Hannes B.*, Caricchi, L.*

**Institute for Mineralogy and Petrology, ETH Zurich (hannes.mattsson@erdw.ethz.ch)*

Cooling and syn-emplacement crystallization of lava flows have a significant impact on the emplacement dynamics and also on the resulting surface morphologies of the lava flows. In the summer of 2007 we sampled natrocarbonatitic lavas during emplacement. Our samples comprise: (1) a lava lake feeding an aa-type lava flow, (2) the central part of the flow channel, and (3) the distal flow front.

As experimental starting material we used rock-powders from the lava lake. The powders were placed in $Ag_{70}Pd_{30}$ crucibles and heated well-above the natrocarbonatite liquidus (750°C) for 30 minutes to homogenize the starting material. The samples were subsequently cooled at different rates (ranging from instant quenching to slow cooling, e.g. 0.1°C/min). The textures in the experimental samples were compared with natural lavas collected during field-campaigns in 2006 and 2007. Our experimental data clearly show that the crystallization of natrocarbonatitic lavas is an extremely rapid process. Although gregoryite is the first mineral to start crystallizing at 1 atm, the growth of nyerereite laths is much faster. Even relatively rapidly cooled experimental samples (>3 °C/min) produces textures that overlap with natural samples from Oldoinyo Lengai in both the types of crystals formed but also in their overall size. Field observations suggests that many natrocarbonatitic lava flows remain very fluidal over steep slopes (even at high crystal contents >60 vol.%), but at lesser slopes (lower strain-rates) the crystals interact and as a result of this the viscosity increases dramatically. This may force the transition from pahoehoe to aa-type flow morphologies in crystal-rich natrocarbonatitic lavas.

2.19

Bubble- and crystal-size distributions in the emergent Capelas tuff cone, São Miguel (Azores): insights into magma-ascent and fragmentation

Mattsson Hannes B.*, Solgevik, H.**

*Institute for Mineralogy and Petrology, ETH Zurich (hannes.mattsson@erdw.ethz.ch)
**Department of Geology and Geochemistry, Stockholm University

The late Holocene Capelas eruption started in a shallow marine environment off the north coast of São Miguel (Azores). As the eruption progressed, a tuff cone grew to a subaerial setting connecting with the main island of São Miguel, and a scoria cone formed inside the main crater of the tuff cone.
In this study, we sampled different depositional facies which were subject to combined analysis of the bubble- and crystal-size distributions. With a total of 13705 bubbles and 4719 plagioclase crystals analyzed, a clear pattern emerges. During the eruption, the amount of plagioclase remain fairly constant (7±2 vol%) whereas the bubble content of the samples are much more variable (varying from 51 to 8 vol%). Inititally, in the thick fall deposits at the base of the tuff cone, bubbles are abundant (average=39.9 vol%) and individual clasts show fluidal textures consistent with jetting or fire-fountaining type of activity. The later deposits show a decrease in the total amount of bubbles (average=26.8 vol% in fall deposits and 15.7 vol% in surge-deposits) but also in the absolute size of individual bubbles.
Our textural data suggests that the Capelas magma was only briefly ponded in a crustal magma chamber, allowing bubbles to accumulate/coalesce near the top of the magmatic reservoir but not long enough to allow flotation of plagioclase laths to occur (as indicated by the constant crystal content of the deposits). The first phase of the eruption drained the upper part of this reservoir (by sustained jetting characterized by limited magma-water interaction). The decreasing amount, and size, of the bubbles with time during the eruption can be interpreted as reflecting either (i) an increase of the decompression rate, or (ii) a systematic deepening of the fragmentation level within the conduit. We favour the latter alternative as most basaltic volcanic eruptions show a clear decrease in the eruption rate over time.

2.20

Petrology of the Lake Natron – Engaruka monogenetic volcanic field, northern Tanzania

Nandedkar Rohit, Dr. Mattsson Hannes

Institute for Mineralogy and Petrology, Clausiusstrasse 25, CH-8092 Zurich (rohit@student.ethz.ch)

During fieldwork in 2006 a total of 97 monogenetic volcanic cones in the Lake Natron - Engaruka area in northern Tanzania (East African Rift) were sampled. The main goal of the project is to: (i) characterize the geochemistry of the monogenetic cones, and (ii) to see if there are any spatial and/or temporal changes in the erupted compositions. Here we present the results of 60 analyzed cones.
All investigated rocks are silica-undersaturated, ranging in composition from primitive olivine melilitites, via nephelinites to basanitic/basaltic compositions. Mg-numbers ranges from 77 to 20 (averaging 55), and roughly 10% of the 60 cones classify as being peralkaline ((Na+K)/Al). Although there is some minor scatter in Mg# vs. SiO_2, clear trends are present in major element variation diagrams going from the olivine melilitites to the basanitic compositions. The scatter, however, suggests that fractional crystallization is not the dominant process involved in the forming of the magmas. Mantle xenoliths in volcanoclastic deposits give a clear indication that most of the magmas rose directly to the surface without ponding and evolving in crustal magma chambers. Therefore these clear trends are suggested to originate out of the melting process. This is especially interesting considering that different compositions represent different degrees of melting as conclude out of REE pattern. Melilititic rock suites, which are the most common, are considered of being produced at depth by partial melting of a carbonated mantle source. Indication for such a mantle source possibly being present beneath the Lake Natron - Engaruka area is found in the metasomatic veins that crosscut lherzolitic - dunitic xenoliths (found in 13 of the investigated cones). These veins consist of amphibole, phlogopite, minor clinopyroxene and a carbonate phase. However, the exact origin of this carbonate phase is unclear and requires further work.

REFERENCES
Keller, J., Zaitsev, A.N., Wiedenmann, D. 2006: Primary magmas at Oldoinyo Lengai: The role of olivine melilitites. Lithos, 91, 150-172.
Klaudius, J., Keller, J. 2006: Peralkaline silicate lavas at Oldoinyo Lengai, Tanzania. Lithos, 91. 173-190.
Kjarsgaard, B.A., Hamilton, D.L. 1988: Liquid immiscibility and the origin of alkali-poor carbonates. Mineralogical Magazine, 52, 43-55.
LeBas, M.J. 1989: Nephelinitic and basanitic rocks. Journal of Petrology, 30, 1299-1331
Wyllie, P.J., Huang, W.L. 1976: Carbonation and melting reactions in the System CaO-MgO-SiO_2-CO_2 at mantle pressures with geophysical and petrological applications. Contrib. Mineral Petrology, 54, 79-207.

2.21

Adakite-like volcanism in Central Iranian magmatic belt,Isfahan,Iran

Noghreyan Moussa*, Khodami Mahnaz**& Davoudian Ali Reza***

* *Department of Geology, Faculty of Sciences, Isfahan University, Isfahan, Iran*
** *Department of Geology, Islamic Azad University, Mahallat Branch,Iran (mahnaz.khodami@gmail.com)*
*** *Department of Natural Resources, Shahrekord University, Shahrekord, Iran*

The Pliocene to Quaternary calc-alkaline volcanic rocks cover an area in 120 km southeast of Isfahan city. In the classification of the structural units of Iran, this area is a part of Central Iranian magmatic belt or Urumieh-Dokhtar Magmatic Belt which related to subduction between Iranian an Arabian plates. Evidences indicate that two plates contacted with each other in the Oligocene–late Miocene and ended to the active subduction between Iranian and Arabian plates, but magmatic activity didn't stop (Berberian and Berberian, 1981). The studied volcanic rocks are andesite, dacite and minor rhyodacite. The andesite rocks as lava flow contain abundant plagioclase, orthopyroxene, clinopyroxene and opaque oxides, which can be accompanied by amphibole and biotite. The dacites are constituted by plagioclase, orthopyroxene, amphibole, biotite, quartz and opaque oxides. Geochemical studies show these rocks are a medium to high K calc-alkaline suite and meta-aluminous. These rocks have Adakite-like characteristics. Adakites form suites of intermediate to felsic rocks with compositions ranging from andesite to dacite and rhyolite. The models for generation of adakitic rocks include partial melting of young, hot subducting slab that extends down to the amphibolite–eclogite transition zone, partial melting of thickened mafic lower crust (Atherton and Petford, 1993), partial melting of delaminated lower continental crust (Xu et al., 2006) and partial melting of underplated basaltic lower crust. Adakitic magmas are encountered in active continental margins and collision zones .These volcanic rocks are characterized by SiO_2 > 56 wt%, Al_2O_3 > 15 wt%, high Na_2O contents (3.5 wt% ,<Na_2O < 7.5 wt%), low K_2O/Na_2O ratio (≈0.42), high Sr content (>300 ppm), high LILE (>400–3000 ppm) and low HREE contents (Yb < 1.8 ppm, Y < 18 ppm) (Defant and Drummond,1990; Martin, 1999). Primitive mantle normalized multi-element and chondrite-normalized rare earth element patterns in adakites display a characteristic positive Sr peaks and absence of significant Eu anomalies.

The studied volcanic rocks have SiO_2 contents higher than 57wt%. The most rock also has a low content of compatible elements such as Ni (6-28ppm) and Cr (34-20.5ppm. Zr is in the range 92-175 ppm while Nb varies from 3.9 to 7.7 ppm. Large ion lithophile elements (LILE), Rb, Ba, Th and especially Pb, show enrichment in these samples. LILE elements, Sr (381-1039 ppm) Ba (446-1283ppm), Th (3.3-26ppm) and Rb (157-37.5 ppm) display a wide range of concentrations. Among the trace elements, They show LILE and LREE enriched normalized multi-element patterns, and negative Nb, Ti, Ta and P. These characteristics are consistent with ratios obtained from subduction related volcanic rocks and in collision setting. Chondrite-normalized REE patterns, display a steep decrease from LREE to HREE without any Eu anomaly.

HREE and Y depleted pattern suggest the existence of garnet as a residue in the source. The enrichment of Sr and absence of negative Eu anomalies indicate that the residual source was plagioclase free. The Nb and Ti are strongly depleted in the studied samples, which suggest that the source also has residual Ti bearing phase and amphibole and thus was most probably garnet-amphibolite or amphibole-eclogite.Major, trace element and REE data indicate that these adakite-like rocks may have been produced by partial melting of thickened lower continental crust. It is expected that crustal thickening caused by Arabian–Iranian continental collision. Partial melting resulting from thickened lower crust, with garnet ± amphibole as the residual phase and loss of plagioclase in the source, could form rocks that would have high Sr/Y, La/Yb ratios display clear trends of fractional crystallization.

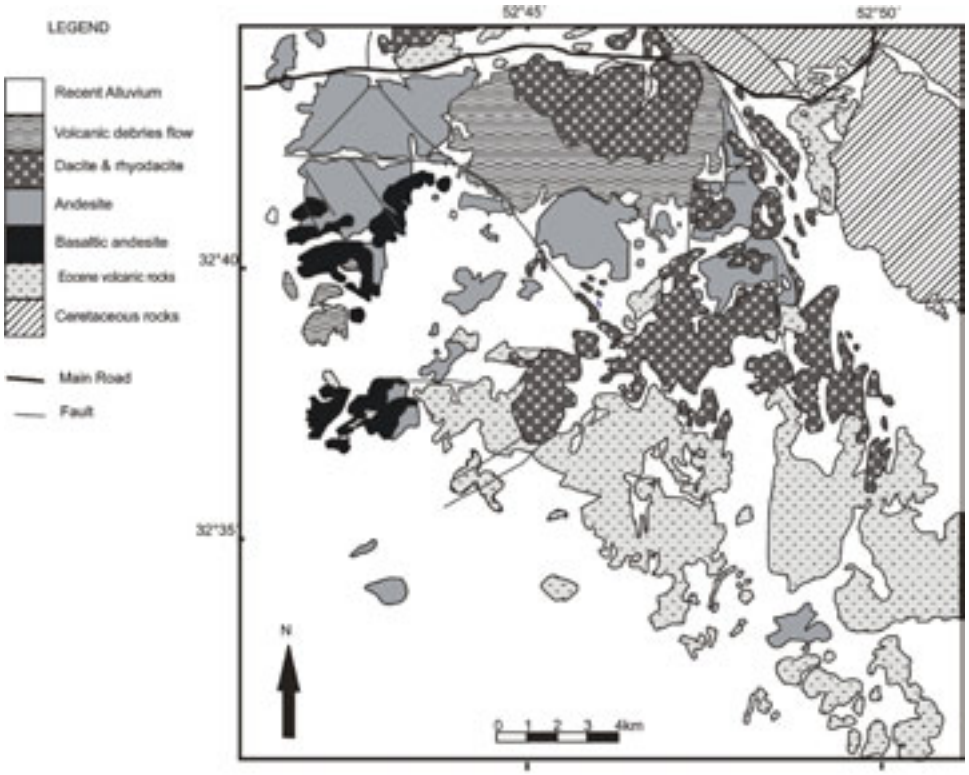

Figure1.Geological map of the studied area (Simplified from the geological map of 1:100,000 Kajan)

REFERENCES

Atherton, M.P., Petford, N. 1993: Generation of sodium-rich magmas from newly underplated basaltic crust. Nature 362, 144–146.

Berberian, F. and Berberian, M. 1981: Tectono-plutonic episodes in Iran. In: Gupta, H.K. & Delany, F.M. (Eds.), Zagros, Hindukosh, Himalaya Geodynamic Evolution. American Geophysical Union, Washington DC, 5–32.

Martin, H., 1999: Adakitic magmas: modern analogues of Archean granitoids. Lithos 46, 411–429.

Varol,E., Temel,A., Gourgaud, A. & Bellon,H. 2007: Early Miocene adakite-like volcanism in the Balkuyumcu region, central Anatolia, Turkey: Petrology and geochemistry. Journal of Asian Earth Sciences 30, 613–628.

Xu, W.L., Wang, Q.H., Wang, D.Y., Guo, J.H. & Pei, F.P. 2006: Mesozoic adakitic rocks from the Xuzhou-Suzhou area, eastern China: evidence for partial melting of delaminated lower continental crust. Journal of Asian Earth Science 27, 454–464.

2.22

Age determinations of the Fitz Roy Plutonic Complex, Southern Patagonia (Argentina)

Ramírez de Arellano Cristóbal*, Putlitz Benita*, Müntener Othmar*, Cosca Mike* **

*Institut de Minéralogie et Géochimie, Université de Lausanne. Batiment Anthropole CH-1015 Lausanne, Suisse (cristobal.ramirez@unil.ch)
** now at U.S. Geological Survey MS 963 Denver, CO 80225 USA*

The Fitz Roy plutonic complex belongs to a chain of isolated Miocene plutons in Patagonia, Southern South America, located in an “exotic” position between the active volcanic arc and the Patagonian plateau basalts, in the eastern side of the Magallanes fold and thrust belt. Here, we present field observations, petrological and geochronological data to decipher the igneous history of this complex.

The host rocks are composed of: Paleozoic metamorphic basement (Bahia de la Lancha Fm.), Jurassic rhyolitic-dacitic volcano-sedimentary rocks (El Quemado Complex), sandstones (Springhill Fm.), lower Cretaceous dark shales (Rio Mayer Fm.), and a surrounding mylonite (Mojón Rojo mylonite) in the South-Eastern part of the intrusive. The structure in the host rock consists of thrusts and strike-slip faults in Paleozoic and Jurassic rocks, folding in the shales and shearing in the mylonite. The extent of contact metamorphism around the plutonic rocks is poorly constrained and is characterized by cordierite and andalusite-bearing metapelites, calcsilicates and a garnet-bearing mylonite (Mojón Rojo mylonite).

Detailed field work allowed to distinguish four different plutonic units: (i) an ultramafic unit; (ii) a mafic unit (including diorites and various gabbros); (iii) a tonalite unit, and (iv) granitoid rocks (granodiorite and granites). The ultramafic rocks show brecciated contacts with tonalites and gabbros. The mafic unit is characterized by mingling textures and syn-magmatic deformation and, locally, by igneous breccias and layered textures. Many of the mafic rocks show alteration (chl, ep, qtz, ser). Some gabbros are deformed by ductile shear zones, consisting of a secondary mineralogy (amph, bt, fsp, qz). The tonalite is fresh, contains abundant xenoliths of diorite and gabbro and exhibits a pervasive syn-magmatic foliation. The granitoids are relatively fresh and clearly not deformed.

The Fitz Roy plutonic complex has been dated by whole rock K-Ar to 18 ± 3 Ma (Nullo et al. 1978). This age data do not permit to correlate Fitz Roy magmatism to other regional events, neither to define the internal history of the complex. Here we present preliminary results of new Ar-Ar step heating dating of Hbl and Bt that are consistent with the sequence of intrusions derived from the intrusive relationships. For the gabbro (Hbl) we obtain an isochron age of 19.3 ± 0.4 Ma. Hbl from a tonalite sample gave an isochron age of 18.1 ± 0.5 Ma. One granodiorite sample gave plateau ages of 16.1 ± 0.1 Ma in Bt and 16.7 ± 0.1 Ma in Hbl. We interpret the Hbl age as being close to the crystallization age suggesting a cooling rate of 0.3°/ ky for the granodiorite. This data suggest a difference of around 3 My between the gabbro intrusions and the granitic rocks. The wide range of ages confirms our suggestion of a protracted magmatic history overlapping with deformation and metamorphic events (Ramírez de Arellano et al. 2007, 2008).

REFERENCES

Nullo, F., Proserpio, C., Ramos, V. A. & Rabassa, J. 1978: Estratigrafía y Tectónica de la vertiente este del Hielo Continental Patagónico, Argentina-Chile. Acta VII Congreso Geológico Argentino, Neuquén, Tomo1, 455-470.

Ramírez de Arellano, C., Putlitz, B., Kosmal, A. & Dessimoz, M. 2007: Preliminary observation on the Fitz Roy Plutonic Complex, 5th Swiss Geosciences Metting, Geneva, Switzerland.

Ramírez de Arellano, C., Putlitz, B. & Müntener, O. 2008: Magmatic history of the Fitz Roy Plutonic Complex, Southern Patagonia (Argentina), European Geosciences Union general Assembly, Vienna, Austria.

2.23

A lot of andesitic rocks but no andesitic melts: the paradox of arc magmatism.

Reubi Olivier*, Blundy Jon**,

* *Institute of Isotope Geochemistry and Mineral Resources, ETH Zurich (olivier.reubi@erdw.ethz.ch)*

** *Dpt. of Earth Sciences, University of Bristol, Bristol, UK*

Andesites are widely considered as the typical product of subduction zone volcanism and are regarded as a major component in the formation of continental crust. In reality, andesites are only the dominant rock type at mature continental volcanoes and the textural complexity of many andesites suggests that magma mixing or mingling plays a key role in their petrogenesis. Theses observations question the abundance of true andesitic melts and raise doubts about the validity of petrogenetic models based on bulk rock compositions. We shade new light on this controversy and present an alternative view of arc magmatism based on a compilation of melt inclusions for arc magma.

Melt inclusions in arc magmas show a bimodal basaltic andesite - high-silica dacite/rhyolite distribution with few compositions in the range 58 to 66 wt% SiO_2. Detailed studies of several arc volcanoes indicate that this compositional gap is neither a sampling artefact nor a bias in the melt inclusion record. Comparison of melt inclusions with liquid lines of descent produced experimentally by crystallization of hydrous basaltic melts over a range of crustal pressures demonstrates that fractionation of mafic magmas reproduces accurately the range of melt inclusions compositions. On the other hand, comparison

of experimentally produced melts with arc bulk rock compositions show a clear mismatch in the range 58 to 66 wt% SiO_2, corroborating the gap recorded by the melt inclusions and suggesting that andesitic bulk compositions are indeed not representative of melts. Volatiles (H_2O, CO_2) contents in melt inclusions record volatile-saturated conditions at pressure <5 Kbar, implying formation in the upper crust, and indicate that volatile-saturated crystallization produces limited melt differentiation (<10 wt% SiO_2). The melt inclusion record shows that melt compositional diversity is produced by differentiation of basaltic melts in the lower crust, but that melts crystallizing in the upper crust are bimodal with few intermediate compositions. We suggest that this compositional gap is related to the shallow temperature-composition slope of the liquidus for andesitic compositions, precluding the widespread extraction of these melts from the deep crust. Consequently melts rising to the upper crust, where they reach volatile saturation, crystallize, and assemble to form subvolcanic magmatic reservoirs or plutons, are essentially bimodal, as recorded by the melt inclusions. The abundance of andesitic rocks does not characterize a primary genetic feature of arc magmatism, but instead reflects effective mingling or mixing in subvolcanic reservoirs of mature continental arc volcanoes. Accordingly, the role of upper crustal magmatic systems needs to be reconsidered as sites of homogenization rather than differentiation.

2.24

Natrocarbonatitic tephrafall from the explosive eruption of Oldoinyo Lengai in September 2007

Reusser Eric* & Mattsson Hannes*

**Institut für Mineralogie und Petrographie, ETH Zürich, CH-8092 Zürich (reusser@erdw.ethz.ch)*

An explosive eruption started at Oldoinyo Lengai in early September 2007 and fresh ashfall from the plume was sampled in, and around, the Engaresero village (≈18 km N of the volcano) three days after the onset of the eruption. Closer inspection of the samples show that the composition of the first erupting magma, i.e. September 7th, was natrocarbonatitic, similar to that commonly reported for the near-continuous effusive volcanism that has been characteristic for Oldoinyo Lengai.

The ashfall is very well-sorted and individual particles display fluidal droplet-shapes containing few vesicles, reflecting the extremely low viscosity of the natrocarbonatitic melt. Accidental lithic fragments consisting of quartz and/or quartz-biotite-plagioclase assemblages are common in the deposits. These lithic fragments have angular shapes and are frequently coated by the natrocarbonatitic melt, suggesting that they were entrained at depth by the ascending magma. The chemical composition of the main phenocryst phases, nyerereite and gregoryite, overlap with previously published analyses (Zaitsev & Keller, 2006). However, it is possible to distinguish two separate populations of both minerals based on the Sr-content, i.e. high and low Sr-varieties.

The natrocarbonatitic ash-droplets and lithic fragments are frequently coated with an array of different microscopic mineral phases (fluorite, halite, sylvite, neighborite, sellaite, apatite, etc.). Many of these adhering minerals probably formed as a result of scavenging of volatile phases present in the eruption column. Fluorine is considerably enriched in the adhering minerals compared to the droplets. Although natrocarbonatites are water-soluble, XRD-analyses show that the extent of subsolidus alteration of the ash is minimal despite the fine-grained character of the ash and transport in a convecting eruption column.

This initial explosive phase of natrocarbonatitic composition was short-lived and later reports suggest that the composition of the erupted magma had shifted to a hybrid formed by the assimilation of natrocarbonatite by a nephelinitic magma by September 24th (Mitchell & Dawson, 2007).

REFERENCES

Mitchell, R.H. & Dawson, J.B., 2007: The 24th September ash eruption of the carbonatite volcano Oldoinyo Lengai, Tanzania: mineralogy of the ash and implication for formation of a new hybrid magma type. Mineralogical Magazine, 71, 483 – 492.

Zaitsev, A.N. & Keller, J., 2006: Mineralogical and chemical transformations of Oldoinyo Lengai natrocarbonatites. Lithos, 91, 191 – 207.

2.25

Advantages of using TEM when analysing asbestos in ambient air

Catheline Reymond*, Laurie Leuthold-Favre*, Antonio Mucciolo**, Michel Bonin***

* *Institut de Santé au Travail, Laboratoire de Minéralogie, rue du Bugnon 21, CH-1011 Lausanne (catheline.reymond@hospvd.ch) (laurie.leuthold@hospvd.ch)*
** *Centre de Microscopie Electronique, Université de Lausanne, rue du Bugnon 27, CH-1005 Lausanne (antonio.mucciolo@unil.ch)*
*** *Departement für Chemie und Biochemie, Universität Bern, Freiestrasse 3, CH-3012 Bern*

Asbestos is an industrial term to describe some fibrous silicate minerals, which belong to the amphiboles or serpentines group. Six minerals are defined as asbestos including: chrysotile (white asbestos), amosite (grunerite, brown asbestos), crocidolite (riebeckite, blue asbestos), anthophyllite, tremolite and actonolite, but only in their fibrous form. In 1973, the IARC (International Agency for Research on Cancer) classified the asbestos minerals as carcinogenic substances (IARC,1973).

The Swiss threshold limit (VME) is 0.01 fibre/ml (SUVA, 2007). Asbestos in Switzerland has been prohibited since 1990, but this doesn't mean we are over asbestos. Up to 20'000 tonnes/year of asbestos was imported between the end of WWII and 1990. Today, all this asbestos is still present in buildings renovated or built during that period of time. During restorations, asbestos fibres can be emitted into the air. The quantification of the emission has to be evaluated accurately. To define the exact risk on workers or on the population is quite hard, as many factors must be considered.

The methods to detect asbestos in the air or in materials are still being discussed today. Even though the EPA 600 method (EPA, 1993) has proved itself for the analysis of bulk materials, the method for air analysis is more problematic. In Switzerland, the recommended method is VDI 3492 using a scanning electron microscopy (SEM), but we have encountered many identifications problems with this method. For instance, overloaded filters or long-term exposed filters cannot be analysed.

This is why the Institute for Work and Health (IST) has adapted the ISO10312 method: ambient air – determination of asbestos fibres – direct-transfer transmission electron microscopy (TEM) method (ISO, 1995). Quality controls have already be done at a French institute (INRS), which validate our practical experiences. The direct-transfer from MEC's filters on TEM's supports (grids) is a delicate part of the preparation for analysis and requires a lot of trials in the laboratory. IST managed to do proper grid preparations after about two years of development.

In addition to the preparation of samples, the micro-analysis (EDX), the micro-diffraction and the morphologic analysis (figure 1.a-c) are also to be mastered. Theses are the three elements, which prove the different features of asbestos identification. The SEM isn't able to associate those three analyses.

The TEM is also able to make the difference between artificial and natural fibres that have very similar chemical compositions as well as differentiate types of asbestos.
Finally the experiments concluded by IST show that TEM is the best method to quantify and identify asbestos in the air.

REFERENCES:

IARC. 1973, Some Inorganic and Organometallic Compounds. IARC Monographs on the Evaluation of Carcinogenic Risk of Chemicals to Humans, vol. 2. Lyon, France: International Agency for Research on Cancer. 181 pp.

ISO 10312:95, Ambient atmospheres: Measurement of asbestos fibres, Direct-transfer transmission electron microscopy method, International Standards Organisation , Geneva, 1995

U.S. EPA-600/R-93/119, July 1993

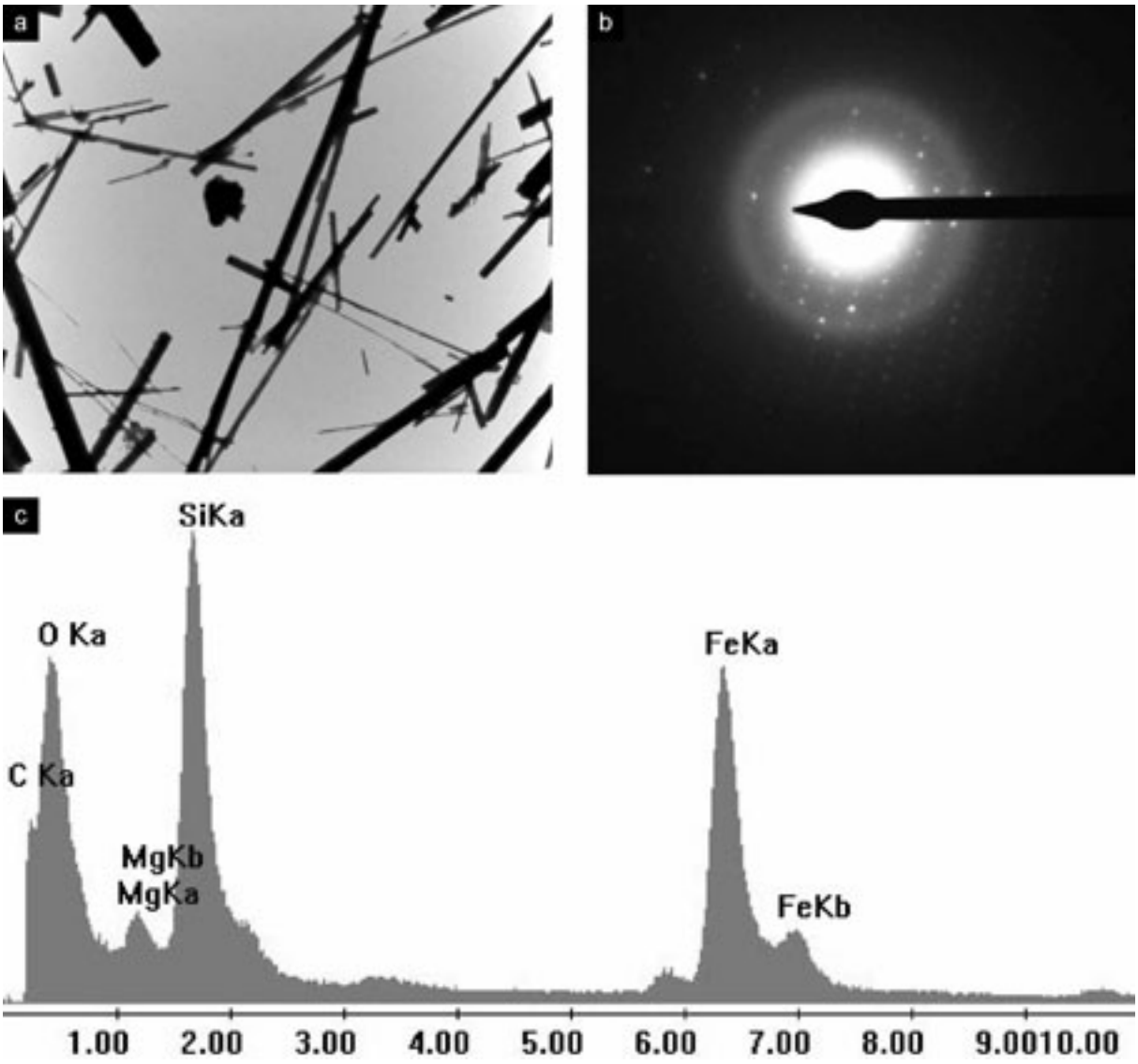

Figure 1. Pictures from TEM (morphology (a), micro-diffraction (b) and EDS (c)) of an amosite fibre

2.26

Textural, chemical and microstructural records during snowball garnets growth

Robyr Martin*, Carlson William**, Passchier Cees*** & Vonlanthen Pierre****

*Institute of Geological Sciences, University of Bern, CH-3012 Bern, (martin.robyr@univie.ac.at)
** Geol Science Dept, the University of Texas at Austin, Austin, TX 78712-0254
***Institut für Geowissenschaften, Johannes Gutenberg Universität, 55099 Mainz
****Institute of Geology and Palaeontology, University of Lausanne, CH-1015 Lausanne

The growth history of two populations of snowball garnets from the Lukmanier Pass area (central Swiss Alps) was examined through a detailed analysis of chemical zoning, crystallographic orientation and 3D geometry. The first population was collected in the hinge of a chevron-type fold and shows an apparent rotation of 360˚. Microstructural and chemical data reveal a modification of the stress field regime during garnet growth occuring after 270˚ of relative rotation and for XMn = 0.009. Crenulated inclusion trails indicate that the last 90˚ of the spiral curvature was formed under a non-rotational regime associated with flexural folding. Electron Backscattered diffraction (EBSD) maps reveal a crystallographic central domain

exhibiting 270˚ of relative rotation and distinct smaller crystallographic domains at the end of the spirals. A second population collected on the limb of the folds exhibits a spiral geometry that does not exceed 270˚. Here, the garnet microstructures do not record any evidence for a modification of the stress field regime during garnet growth, and a single crystallographic orientation is observed for the whole spiral. Local geological data and microstructural elements tend toward a simultaneous growth and rotation for the core region of the snowball garnet, whereas subsequent garnet growth occurs under a non rotational regime. The similarity in geometry between the central sector domains and the geometry acquired by the snowball garnets under the rotational regime strongly suggests that as long as the growth is accompanied by rotation, the primary core orientation is preserved, but once the rotation stops the crystallographic orientation may change.

EBSD data also indicate that the central domain displays a crystallographic orientation characterized by a [001] pole oriented sub-parallel to the symmetry axis of the garnet. Moreover, in most crystallographic sectors, one of the two other [100] poles is (sub)parallel to the orientation of the internal foliation. This feature suggests that the crystallographic orientation across the garnet spiral is not random and that a relation between symmetry axis, internal foliation and crystallographic orientation does exist. Several arguments indicate that EBSD data can represent an indicator of the modification of the growth regime during the formation of the snowball garnet. In this view, EBSD data can potentially be used to distinguish between the rotational and non-rotational models.

2.27

Alkaline mantle melts in the southern Alpine lower crust mark the initiation of late Triassic rifting

Schaltegger Urs*, Antognini Marco**, Girlanda Fabio***, Wiechert Uwe**** & Müntener Othmar*****

*Section des Sciences de la Terre, Université de Genève, rue des Maraîchers 13, 1205 Genève
**Museo Cantonale di Storia Naturale, Via Carlo Cattaneo 4, 6900 Lugano
***Cesura, 6653 Verscio
****Fachbereich Geowissenschaften, Freie Universität Berlin, Malteserstrasse 74-100, D-12249 Berlin
*****5Institut de Minéralogie et Géochimie, Université de Lausanne, l'Anthropôle, 1015 Lausanne

Introduction: The mafic-ultramafic Finero complex is situated at the eastern end of the Ivrea Zone in the Centovalli (CH) and Valle Vigezzo (I), and consists of (partially serpentinized) peridotite, pyroxenites and layered gabbros. The body was incorporated into the lower crust and metamorphosed under granulite facies during Paleozoic orogenic processes, and has been intensively metasomatized after its emplacement. The age of the Paleozoic metamorphism is controversial, as large age variations between 300 and 210 Ma are recorded by zircon populations of mafic and differentiated igneous, and metamorphic rocks. A considerable number of late Triassic ages suggest that the lower crust has been overprinted by an important thermal event at around 220-210 Ma: Sm-Nd mineral ages from the internal gabbro of the Finero complex yield ages of 230-210 Ma (Lu et al. 1997). Zircons from alkaline pegmatoid lenses around the Finero complex yield U-Pb ages of 225 ± 13 Ma (Stähle et al. 1990) and 212.5 ± 0.5 Ma (Oppizzi and Schaltegger 1999). A similar U-Pb age of 207.9 +1.7/-1.3 Ma was reported from anhedral zircon in chromitite layers of the Finero peridotite (Grieco et al. 2001). These data coincide with results from zircon and monazite bearing, granulite facies metasediments in the Ivrea zone: Secondary Ionprobe mass spectrometry (SIMS) analyses show scattering results in granulite-facies zircons down to ≈220 Ma (Vavra et al. 1996, 1999), ages that are close to newly formed monazite at ≈210 Ma in the same rocks (Vavra and Schaltegger 1999).
New alkaline pegmatites have recently been described at the eastern termination of the Finero complex. Girlanda et al. (2007) and Weiss et al. (2007) reported the occurrence of large zircon crystals occurring in a nepheline-albite-pegmatite. At the meeting we present new U-Pb age determinations of one of these zircons, review previous data and draw preliminary geodynamic interpretations for these late Triassic alkaline pegmatites.

Age and source of magmatism: Two pegmatites have been dated, both having sinuous, irregular contacts towards the peridotite. They consist of nepheline, albite, biotite, zircon, apatite and a large number of accessory minerals (Weiss et al. 2007). A gem-quality zircon has been fragmented from the lower pegmatite nr. 1 (see Weiss et al. 2007) and yielded a mean $^{206}Pb/^{238}U$ age of 212.5 ± 0.5 Ma (Oppizzi & Schaltegger 1999). Five fragments of one large zircon have been analyzed from the upper pegmatite nr. 2 and yield $^{206}Pb/^{238}U$ ages between 207.5 and 209.5 Ma, pointing to long-lived or episodic zircon growth, already indicated by very variable morphology and REE patterns. This age is younger than the emplacement of pegmatite nr. 1 but closely fits the age of metasomatic zircon-bearing chromite layers in the Finero Peridotite (Grieco et al. 2001). The mineralogical, geochemical and isotopic data suggest that the pegmatites represent differentiated products of low-degree partial melts from enriched subcontinental mantle, preferentially enriched in Na (and K), and possibly saturated in volatiles.

Geodynamic interpretation: The ages around 210 Ma coincide with the beginning of crustal thinning and rifting of the Europe-Adria continent at the locus of the future Piemont ocean. The extensional processes led to low degrees of decompressional melting of the subcontinental mantle, which produced the alkali-rich pegmatoids. The advection of heat caused overprinting of isotopic systems in many different mineral phases in the lower crust (granulite-facies rocks of the Ivrea zone), such as zircon and monazite. Published biotite K-Ar ages range down to 180 Ma (e.g. Hunziker 1974), indicating cooling to ≈300°C during extension-related exhumation of the lower crust. The Ivrea Zone may therefeore not be the ideal place to study the behaviour of isotopic systems during granulite facies, since many of those are overprinted and disturbed by late Triassic heat advection during the first stages of rifting following the continental breakup of the European and Adriatic plates.

REFERENCES

Girlanda F., Antognini M., Weiss S. & Praeger M. (2007) Zirkon aus Nephelin-pegmatiten im Peridotit Finero-Centovalli (Schweiz). Lapis 32/6, 13-23

Grieco G., Ferrario A., von Quadt A., Koeppel V. & Mathez E.A. (2001) The zircon-bearing chromitites of the phlogopite peridotite of Finero (Ivrea Zone, Southern Alps): Evidence and geochronology of a metasomatized mantle slab. J. Petrol. 42, 89-101

Lu M., Hofmann A.W., Mazzucchelli M. & Rivalenti G. (1997) The mafic-ultramafic complex near Finero (Ivrea-Verbano Zone), II. Geochronology and isotope geochemistry. Chem. Geol. 140, 223-235

Oppizzi, P. and Schaltegger, U. (1999) Zircon-bearing plagioclasites from the Finero complex (Ivrea zone): dating a Late Triassic mantle hic-up Schweiz. Mineral. Petrogr. Mitt. 79, 330-331

Stähle, V., Frenzel, G., Kober, B., Michard, A., Puchelt, H. & Schneider, W. (1990) Zircon syenite pegmatites in the Finero peridotite (Ivrea zone): evidence for a syenite from a mantle source. Earth Planet. Sci. Lett. 101, 196-205

Vavra G., Gebauer D., Schmid R. & Compston W. (1996) Multiple zircon growth and recrystallization during polyphase Late Carboniferous to Triassic metamorphism in granulites of the Ivrea zone (Southern Alps): an ion microprobe (SHRIMP) study. Contrib. Mineral. Petrol. 122, 337-358

Vavra G., Schmid R. & Gebauer D. (1999) Internal morphology, habit and U-Th-Pb microanalysis of amphibolite-to-granulite facies zircons: geochronology of the Ivrea zone (Southern Alps). Contrib. Mineral. Petrol. 134, 380-404

Vavra, G. & Schaltegger U. (1999) Post-granulite facies monazite growth and rejuvenation during Permian to Lower Jurassic thermal and fluid events in the Ivrea Zone. Contrib. Mineral. Petrol. 134, 405-414

Weiss S., Fehr T., Ansermet S. & Meisser N. (2007) Zirkonführende Nephelin-pegmatite im Centovalli, Südschweiz: Struktur, Mineralogie und Kristallisationsabfolge. Lapis 32/6, 24-30

2.28

Shocked quartz in Ticino, and beyond

Franz Schenker

SCHENKER KORNER + PARTNER GmbH Geologische Beratung Büttenenhalde 42 6006 Luzern (franz.schenker@fsgeolog.ch)

The Breccia of Arzo (Wiedenmayer 1963) consists mainly of brecciated clasts. Such “breccia within breccia” may be formed by “normal” geological mechanisms such as neptunic dykes, dilatation tectonics or volcanic activities. Today, polymict lithic breccia additionally are considered as one of many clues to recognize terrestrial impact structures (e.g. Masaitis 2005). Definite evidence for shock deformation is, among other, the incidence of planar deformation features (PDFs) in quartz (French 1998). Because our samples from the Breccia of Arzo did not contain any quartz, some quartz bearing formations from Ticino were sampled with regard to find shock-produced features in minerals and rocks.

The Bernardo Gneiss (Reinhard 1953) shows intense fracturing and PDFs in quartz (Figure 1). Further indication of shock metamorphism are coarse flakes of mica (biotite and muscovite) with kink-bands, and glassy spots in feldspars (?maskelynite) and within or at the border of quartz (?diaplectic quartz glass).

PDFs in quartz occur in the Upper Carboniferous Manno Conglomerate, and in the porphyries and granophyres of the Luganese, too (Figure 2). Petrography, geochemistry and spatial occurrence of the “Porfido Luganese” (Buletti 1985) show exiting similarities with impact melt sheets from Sudbury and other impact structures (Therriault et. al. 2002). Years ago, Ernst Niggli pointed to the chemical and mineralogical disaccord between common volcanic rocks and the Porfido Luganese (Niggli 1953).

The Bernardo-Gneiss is an element of the cataclastic Gneiss chiari, which Reinhard (1953) considered to form a thin (500 - 1000 m), but large (100 km, Borgosesia – Pizzo del Diavolo) Variscian nappe on top of the crystalline basement and his metasediments, what remained difficult to explain with modern tectonic models (Schumacher et al. 1997). With its widespread occurrence of shocked quartz, the Gneiss chiari can be interpreted now as cataclastic target rock representing the (par)autothochthonuous floor of an impact crater. Because of the extensiveness of the "nappe", the effects of the impact must have been significant. Further hints of a huge structure give additional occurrences of shocked quartz beyond the Southern Alps, as the "Maranerbreccie" of Arosa (Cadisch 1953) or the "Saluverbreccie" near St. Moritz (Finger 1978). Like the Breccia of Arzo, these formations seem to coincide with processes at the Triassic-Jurassic Boundary.
Due to the Alpine orogenesis and the accompanying alteration and sedimentation, no circular or elliptical impact crater structure has survived. But probabely, the several kilometres of siliceous limestones in the Monte Generoso and Monte Nudo basins (Bernoulli 1964) represent a relic of impact-related debris filling depressions of the TrJ-boundary impact structure.

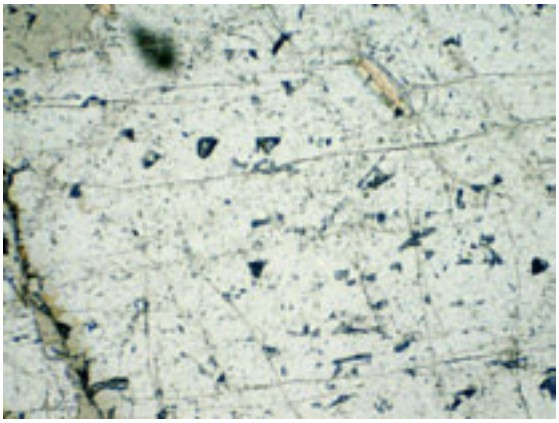

Figure 1. Bernardo-Gneiss from Orlino; Quartz with subparallel planar fractures and with small, high-relief crystals of ?coesite, plane-polarized light, width of picture is 0.3 mm

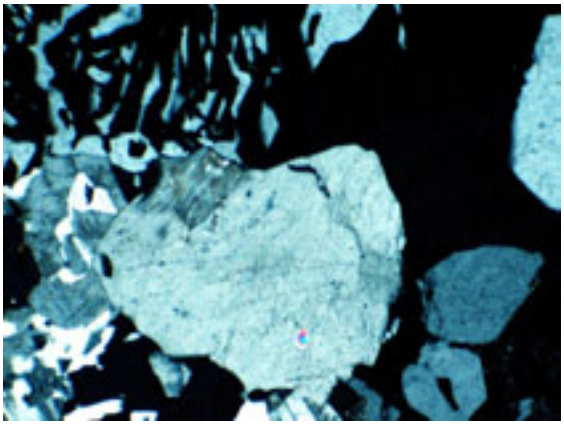

Figure 2. Porfido Luganese from Carona, quartz grain with PDFs in a granophyric matrix, cross-polarized light, width of picture is 0.6 mm

REFERENCES

Bernoulli, D. 1964: Zur Geologie des Monte Generoso, Beitr. Geol. Karte Schweiz, N. F. 118.
Buletti, M. 1985: Petrographisch-geochemische Untersuchungen im Luganer Porphyrgebiet, Diss. Univ. Bern, unpublished.
Cadisch, J. 1953: Geologie der Schweizer Alpen, Verlag Wepf & CO., Basel.
Finger, W. 1978: Die Zone von Samaden und ihre jurassischen Breccien. Diss. ETH Zürich.
French B. M. 1998: Traces of Catastrophe, LPI Contribution No. 954, Lunar and Planetary Institute, Houston.
Masaitis V.L. 2005: Redistribution of Lithologies in Impact-induced Dikes of Impact Structures, in Koeberl, C. & Henkel, H. (Eds.): Impact Tectonics, Springer-Verlag Berlin Heidelberg.
Niggli, E. 1953: Die magmatischen Bildungen, in Cadisch, J.: Geologie der Schweizer Alpen, Verlag Wepf & CO., Basel.
Reinhard, M. 1953: Über das Grundgebirge des Sottoceneri im südlichen Tessin. Eclogae geol. Helv. 46, 214-222.
Schumacher, M. E., Schönborn, G., Bernoulli, D. & Laubscher, H. P. 1997: Rifting and Collision in the Southern Alps, in Pfiffner. A. O. et al. (Eds): Deep Structures of the Swiss Alps, Birkhäuser Verlag, Basel.
Wiedenmayer, F. (1963): Obere Trias bis mittlerer Lias zwischen Saltrio und Tremona (Lombardische Alpen). Eclogae geol. Helv. 56, 529–640.
Therriault A.M., Fowler, A.D & Grieve, R.A.F. 2002: The Sudbury Igneous Complex: A Differentiated Impact Melt Sheet, Economic Geology; November 2002, v. 97, no. 7,1521-1540.

2.29

Comparing carbon and sulfur isotopes in ophiolites and active peridotite-hosted hydrothermal systems

Schwarzenbach Esther M.*, Früh-Green Gretchen L.*, Bernasconi Stefano M.**

* *Institut für Mineralogie und Petrographie, Clausiusstrasse 25, CH-8092 Zürich (esther.schwarzenbach@erdw.ethz.ch)*
** *Geologisches Institut, Universitätstrasse 16, CH-8092 Zürich*

At slow and ultraslow mid-oceanic ridges extensional processes and crustal thinning lead to the exposure of ultramafic rocks on the ocean floor resulting in serpentinization and precipitation of carbonate in open fractures. Serpentini-zation plays a major role in the global marine bio-geochemical cycle and accounts for an important part of the exchange of sulfur and carbon between seawater and the oceanic crust. The opaque mineral assemblage and the sulfur and carbon isotopic composition strongly depend on fluid flux and redox conditions prevailing during serpentinization of the peridotites. Furthermore, the unique conditions prevailing in these systems supports a microbial community with sulfate-reducing, sulfur-oxidizing and methane-oxidizing bacteria leading to characteristic enrichments and depletions of the sulfur and carbon isotopes.
The Lost City Hydrothermal Field (LCHF) is as yet the only known example of an active, low temperature (T = <40°C to 90°C), high pH (9 to 11) system driven by serpentinization processes. Its serpentinite basement, cut by a network of calcite veins, is remarkably similar to ophicalcites found in ophiolite sequences on continents. Ophicalcites can therefore be considered the ancient analogues of peridotite-hosted hydrothermal systems like the LCHF. Here we present a carbon and sulfur geochemical study that compares Lost City with ancient systems preserved in drill cores of the Iberian margin (ODP Leg 149) and ophicalcites from Liguria (northern Apennines, Italy). Petrographic studies and analyses of sulfur, carbon and oxygen isotopes, as well as carbon and sulfur contents have been conducted on serpentinized peridotites and calcite veins to better understand physical and chemical conditions during serpentinization and to determine the origin and speciation of carbon and sulfur, and possible links to microbial activity in these systems.

Petrographic examination revealed the occurrence of sulfides such as pyrite, pyrrhotite, millerite and pentlandite in the samples from Liguria, which is similar to observations of Alt and Shanks (1998) and indicate reducing conditions during serpentinization. Sulfur-contents are in general low, compared to those measured in samples from Leg 149 (Alt & Shanks 1998).

Carbon analyses indicate that samples from Leg 149 show distinct changes with depth: total carbon contents (TC) are dominated by carbonate at the top of the serpentinite unit and strongly decrease with depth. This change corresponds to a shift from more positive $\delta^{13}C_{TC}$ values to strongly negative values downhole. This trend, together with $\delta^{13}C$ of total inorganic carbon (TIC) indicates a decrease in seawater penetration and marine carbonate precipitation with depth. However, oxygen isotope temperature calculations show no distinct trends with depth, with relatively constant carbonate precipitation temperatures of <20°C. Interestingly, carbonates in the Ligurian ophicalcites show similar marine carbon isotope values but have $\delta^{18}O$ values that vary according to vein generation and vein type, and which record temperatures of carbonate precipitation similar to serpentinization temperatures (150°C) at the Iberian margin. Total organic carbon (TOC), calculated from TC and TIC, are up to >4000 ppm in the Iberian Margin serpentinites and are considerably lower in the Ligurian ophicalcites (up to 250 ppm). Values of $\delta^{13}C_{TOC}$ from both localities generally lie within a narrow range of -28 to -24‰, suggesting the presence of organic matter. The range in carbon compositions and a dominance of depleted carbon isotope compositions is similar to trends in serpentinites from Lost City (Delacour 2007) and indicates that organic carbon is an important component of the carbon budget in marine serpentinites, regardless of the tectonic setting.

REFERENCES

Alt, J. C. & Shanks, W. C. 1998: Sulfur in serpentinized oceanic peridotites: Serpentinization processes and microbial sulfate reduction. Journal of geophysical research 103, B5, 9917-9929.

Delacour A. 2007: Ph.D. thesis, No.17198 ETH Zurich, 170-213.

2.30

Petrogenesis of post-collisional granitoid of Ghaleh-Dezh, NW Azna, Sanandaj-Sirjan zone, Iran: Nd–Sr isotope evidence

Shabanian Nahid*, Davoudian Ali Reza** & Khalili Mahmoud*

* *Department of Geology, Faculty of Sciences, Isfahan University, Isfahan, Iran (nahid.shabanian@gmail.com)*
** *Department of Natural Resources, Shahrekord University, Shahrekord, Iran*

The Gahleh-Dezh pluton occurs as an elongated exposure in the northwest of Azna city. The study area is located in the west of Iran, 400 Km west of Tehran and 15 km northeast of the Main Zagros Reverse fault. The Main Zagros reverse fault at the northeastern limit of the High Zagros is the suture between the colliding plates of central Iran and the Arabian passive continental margin (Berberian 1995). In the studied area, Ghaleh-Dezh granitoid has juxtaposited the predominantly metamorphic rocks of both sedimentary and magmatic origins. No contact metamorphism has been observed in the vicinity of the granitoid.

The pluton is essentially composed of biotite granite, and has no compositional zoning. The dominant facies is a grey color, foliated biotite granite with white augen of feldspar. The granite consists of quartz, alkali feldspar (mostly as perthite), plagioclase, biotite and white mica (muscovite and phengitic muscovite). Plagioclase is albite and usually sericitized. Alkali feldspar is also locally sericitized. Biotite is locally altered to chlorite. Accessory phases in the granitoid include tourmaline, zircon, epidote, allanite, apatite, and magnetite. aggregates of white-mica, biotite, quartz and feldspar is wrapped (Shabanian et al. 2008).

Quartz grains show evidence of crystal–plastic deformation. The microstructures observed in quartz include ribbons, subgrains and dynamic recrystallization to very fine-grained quartz. Elongated, preferably oriented, newly recrystallized quartz aggregates suggest dynamic recrystallization. Most of the white-mica and biotite in these rocks show preferred orientation parallel to the main foliation of the rock and sub-parallel or parallel to the margins of the quartz ribbons.

Based on collected geochemical data, the granites have a pronounced A-type affinity: they are mostly metaluminous with high concentrations of Na_2O+K_2O, Rb, HFSE, REE (except Eu), high K_2O/Na_2O and Fe/ (Fe+Mg) ratios, and very low concentrations of MgO, CaO, P_2O_5, and Sr contents (Fig. 1). Moreover, the granites plot in the range of post-collision granites and belong to the A2-type (Eby 1992). The decreasing concentrations of Al_2O_3, TiO_2, Zr, Sr, Ba and, maybe Ga with increasing SiO_2 may be related to fractional crystallization of mainly biotite, K-feldspar, plagioclase, titanite and zircon.

We have collected Sr and Nd isotopic data for the mylonitic granite (Table 1). Based on these data and on Rb/Sr ratios, an approximate age of 278 Ma was calculated with initial Sr and Nd isotopic compositions for three samples ranging from 0.70791-0.7123 and 0.51228-0.51229, respectively. These Sr isotopic compositions would be very high for a mantle source and the Nd isotopic compositions would be very low - even for a source metasomatized long ago. The geochemical data (major and trace elements, and Sr and Nd isotopic ratios) indicate mantle-derived magma that underwent assimilation - fractional crystallization process within the crust.

Table 1. Nd–Sr isotopic data for the Ghaleh-Dezh granitoid from Sanandaj-Sirjan zone, Iran

Sample no.	Rb	Sr	$^{87}Rb/^{86}Sr$	$^{87}Sr/^{86}Sr$	Sm	Nd	$^{147}Sm/^{144}Nd$	$^{143}Nd/^{144}Nd$
N1-2	134.1	104.8	3.699266	0.724650	17.4	91.3	0.174336	0.512491
N1-4	202.9	53	11.067621	0.756381	12.33	61	0.180477	0.512506
N4-2	192.3	53.6	10.372002	0.749149	13.05	73.8	0.167026	0.512487

REFERENCES

Berberian, M., 1995: Master “blind” thrust faults hidden under the Zagros folds: active basement tectonics and surface morphotectonics. Tectonophysics 241, 193–224.

Eby, G. N. (1992): Chemical subdivision of the A-type granitoids: petrogenetic and tectonic implications. Geology 20, 641–644.

Shabanian N., Khalili M. & Davoudian, A.R. 2008: Petrography and geochemistry of mylonitic granite of Ghaleh-Dezh, NW Azna, Sanandaj-Sirjan zone, Iran. Neues Jahrbuch Fur Mineralogie-Abhandlungen, in Press.

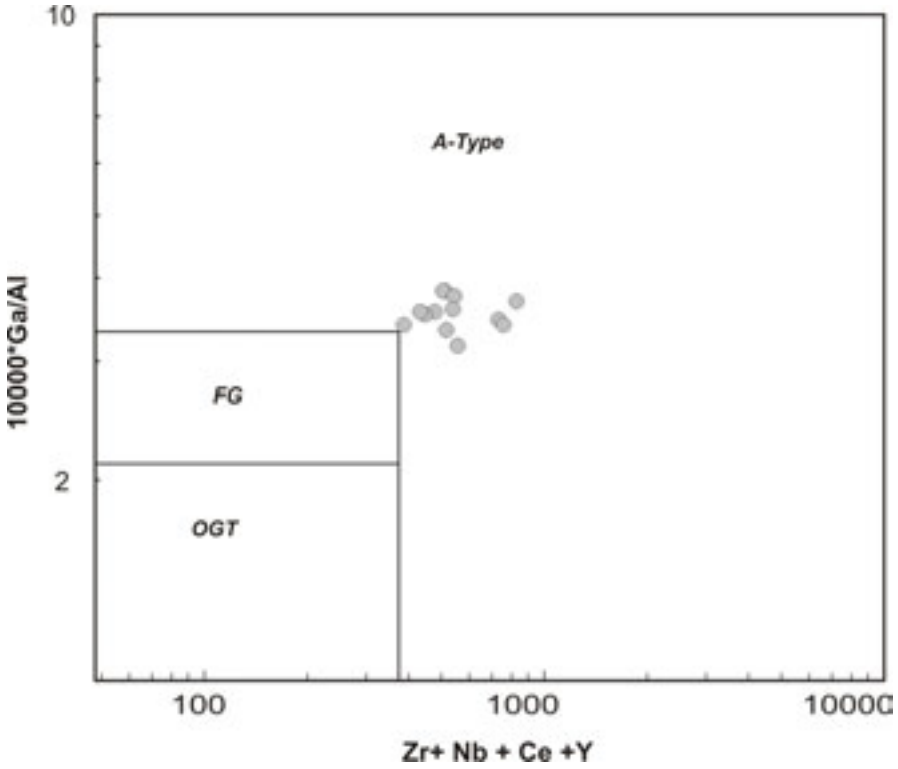

Figure 1. 10000*Ga/Al vs Nb, Ce, Y and Zr in the Ghaleh-Dezh granitoid suggesting their mainly A-type granite character.

2.31

Trace Elements in Miocene Subbituminous Coals from the Swiss Molasse Basin with Special Attention to Uranium and its Mode of Occurrence

Studer Anja*, Kündig Rainer*, Schenker Franz**, Surbeck Heinz***

*Schweizerische Geotechnische Kommission, Universitätstrasse 6, CH-8092 Zürich (studera@student.ethz.ch)
**Geologische Beratung Schenker Korner & Partner GmbH, Büttenenhalde 42, CH-6006 Luzern (franz.schenker@fsgeolog.ch)
***Centre d'Hydrogéologie, Université de Neuchâtel, Rue Emile-Argand 11, CH-2009 Neuchâtel (heinz.surbeck@unine.ch)

Two Miocene subbituminous coals from the Swiss Molasse Basin have been investigated with the goal, to increase the knowledge and data about coals in Switzerland and especially to systematically analyse their trace element composition.

Investigations of the consituents of the Riedhof and Mühlebach coals (located in the cantons of Zürich and Zug, respectively) revealed their deposition in a subaquatic environment. Evidences were found which indicate on the one hand repeated flooding of the area of coal formation and on the other hand the desiccation of the same area. This environment corresponds well with the continental conditions of the Miocene. By means of coal rank analysis the Riedhof coal could be classified as a subbituminous coal (C to B), while the Mühlebach coal either as a subbituminous coal A or a high volatile bituminous coal C. However, from a petrographical point of view, both coals would be classified as a hard coal, i.e. a "Steinkohle" in the German nomenclature.

Mineral impurities of the coals comprise quartz, framboidal pyrite, sheet silicates, clay minerals, calcite, aragonite as well as felspars in the Mühlebach coal and secondary sulfates in the Riedhof coal. Elemental analysis (XRF) show a distinct (one to two order of magnitudes) enrichment of the Riedhof coal in Ag, Ta, Sb and Cd compared to typical Swiss coals (measured by Hügi et al. 1993) and in U, Sb and Ta compared to world-wide coals (data compiled by Swaine 1990). The Mühlebach coal is

clearly enriched in Ag, Sb, Ta and Cd compared to typical Swiss coals and in U, Mo and Ta compared to world-wide coals. Several other elements such as Hf, Pb, Mo, Cu, As, Ga and Ce show a minor enrichment within the two coals.

XRF measurements together with autoradiographies of polished whole-coal samples indicate that the uranium enrichment is limited to the coal. In the hand specimen, the uranium is distributed heterogeneously and occurs mostly within black, shiny coal layers while only minor amounts are contained within (secondary?) pyrite grains. Based on these data, and in combination with the fact that no uranium-minerals have been detected by XRD analyses, an organic mode of occurrence of uranium in coal is suggested. However, an inorganic mode of occurrence of U in coal cannot be excluded due to the possible presence of ultrafine mineral particles intergrown with the organic matter.
The enrichment of uranium occurs in the peat stadium, where it is introduced into the coal swamp as a U-complex in solution. The binding to the coal takes place either by ion-exchange mechanisms, where an uranyl ion is bond to carboxyl-groups, or by the precipitation of inorganic U(IV) species in the reducing environment during coalification (von Borstel 1984).

Radon gas measurements in the coal mine galleries revealed activities around 8'000 to 14'000 Bq/m^3 for the Riedhof mine and around 4'000 to 5'000 Bq/m^3 for the Mühlebach mine.
Water measurements in the Riedhof mine showed increased activities of the radionuclides ^{238}U, ^{234}U and ^{222}Rn together with a low ^{226}Ra activity; however, all these values are below the Swiss limits for drinking water.

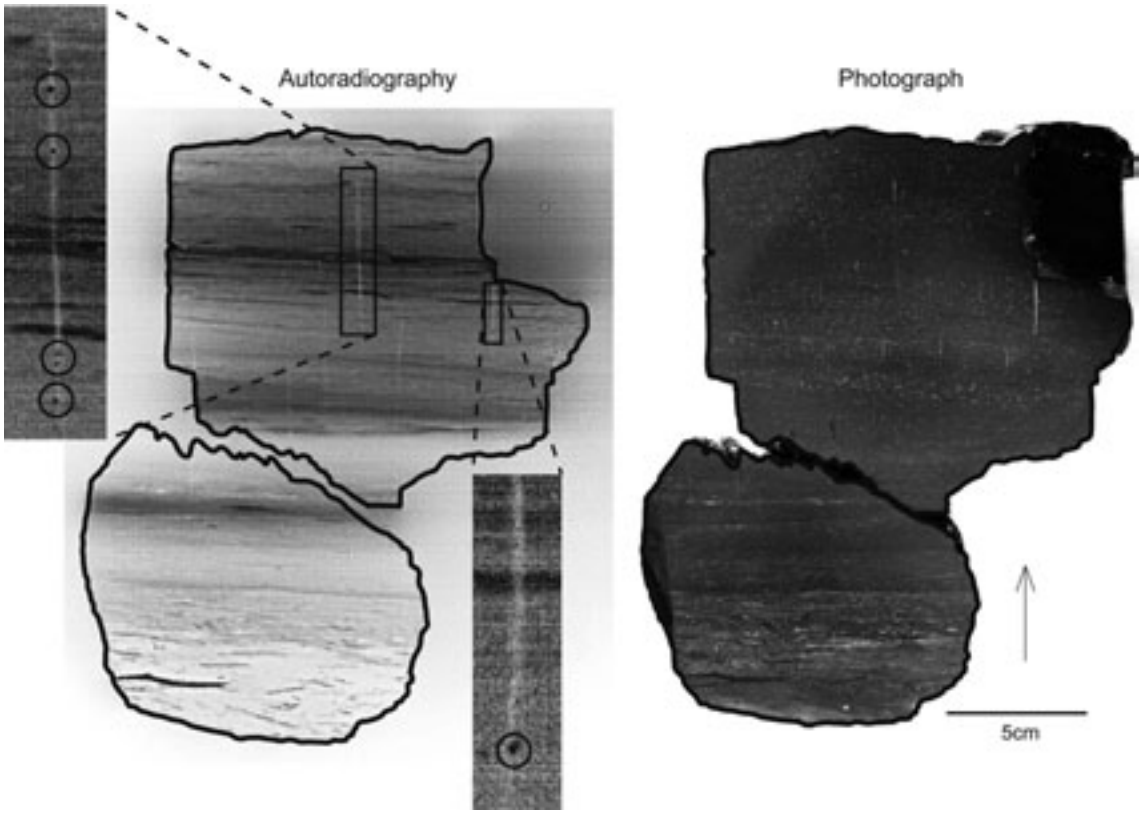

Figure 1: Photograph and autoradiography of the Mühlebach coal. Magnified areas show cracks within the coal containing radioactive pyrite grains. The arrow indicates the younging direction of the sample.

REFERENCES

von Borstel, D. 1984: Bindungsformen von Uran in kohligen Ablagerungen von Sedimenten unterschiedlichen Diagenesegrades. Ein geochemischer Beitrag zur Kenntnis der Bindung von Uran an Stoffgruppen organogener Substanz. PhD thesis, TU Clausthal.

Hügi, T., Fardy, J.J., Morgan, N.C. & Swaine, D.J. 1993: Trace Elements in Some Swiss Coals. Journal and Proceedings, Royal Society of New South Wales 126, 27-36.

Swaine, D.J. 1990: Trace Elements in Coal. Butterworth & Co.

2.32

Physical volcanology of the Lake Natron-Engaruka monogenetic field, Tanzania

Tripoli Barbara* & Mattsson Hannes*

Institut für Mineralogie und Petrographie, ETH Zürich, CH-8092 Zürich (btripoli@student.ethz.ch)

The Lake Natron-Engaruka monogenetic volcanic field is located between the Ketumbeine, Gelai, Kerimasi and Oldoinyo Lengai volcanoes in northern Tanzania (East African Rift System). The field comprises more than 100 monogenetic cones of Quaternary age. Dry magmatic eruptions forming scoria cones are dominating (72%), whereas only 28% of the cones are generated by phreatomagmatic activity (forming tuff cones, tuff rings and maars). The spatial distribution of the phreatomagmatic cones does not correlate with any visible faults or a larger extent of a proto-Lake Natron, thus the source of the external water required to produce these features in a semi-arid climate remain unclear.

In several locations the scoria cones form partially agglutinated deposits consistent with ballistic emplacement of hot magma near the vent (Strombolian-type activity). More explosive basaltic eruptions are recognized by well-stratified, laterally continuous, grain-supported deposits which are generally well-sorted. This suggests near-continuous deposition of clasts from a sustained eruption column. Inversely graded layers surrounded by thin layers of fine lapilli are common and are interpreted to be grain flows accumulated on steep slopes. In at least two locations eruptions have occurred along fissures forming cone-rows. Only 10% of the scoria cones produced lava flows, most of which have a very small volume.

The phreatomagmatic deposits are generally fine-grained and display no direct evidences of wet volcanism other than adhesion of the ash fraction to larger grain-sizes and absence of well developed grain-segregation. During fieldwork only one single accretionary lapillus was found in these deposits. Moreover, plastic deformation of bedding-layers under ballistic impacts is rarely observed, attesting to the relatively dry nature of these phreatomagmatic eruptions.

Mantle xenoliths are found in 13 cones in the area, all of which are phreatomagmatic with a single exception (the Pello Hill scoria cone). This suggests that the magmas involved in the formation of tuff-rings and maars rose quickly to the surface and did not experience extensive fractionation and degassing in crustal magma chambers prior to the eruptions.

2.33

Reaction between tholeiitic melt and residual peridotite in the uppermost mantle: An experimental study at 0.8 GPa

Greg Van den Bleeken*, Othmar Müntener**, Peter Ulmer***

* *Institute of Geological Sciences, University of Bern, Switzerland (greg.vandenbleeken@geo.unibe.ch)*
** *Institute of Mineralogy and Geochemistry, University of Lausanne, Switzerland (othmar.muntener@unil.ch)*
*** *Institute for Mineralogy and Petrology, ETH Zürich, Switzerland (peter.ulmer@erdw.ethz.ch)*

Melt-rock reaction in the upper mantle is known from a variety of ultramafic rocks and is an important process in modifying melt composition on its way from the source to the surface. Evidence for depletion or enrichment by melt percolation is found in ophiolites, mantle xenoliths, and mantle sections exposed along MOR's. It includes disequilibrium textures, changes in major-to-trace element compositions and isotopic ratios.

In order to simulate melt-peridotite reaction processes, we perform nominally dry piston cylinder experiments with a 3-layered setup: a bottom layer composed of vitreous carbon spheres (serving as a melt trap) overlain by a peridotite layer and on top a "melt layer" corresponding to a primitive MORB composition. The peridotite layer is mixed from pure separates of orthopyroxene, clinopyroxene and spinel (Balmuccia peridotite), and San Carlos olivine. Two tholeiitic melt compositions with compositions in equilibrium with lherzolitic (ol, opx, cpx) and harzburgitic (ol, opx) residues after partial melting of KLB-1 at 1.5GPa (cf. Runs 19 and 20 of Hirose & Kushiro, 1993) were used respectively. Melt from the melt layer is 'forced' to move through the peridotite layer into the melt trap.

Experiments have been conducted at 0.8 GPa with peridotite of variable grain sizes, in the temperature range 1200 to 1320°C and for run durations of 10min to 92h. In this P-T range, representing conditions encountered in the transition zone between

the thermal boundary layer and the top of the asthenosphere beneath MOR's, melt is subjected to fractionation, whereas the peridotite is partially melting (T_s ≈1260°C). Results show a strong dependence between phase relations in the melt layer and changes in the modal composition of the peridotite layer, both as a function of temperature and melt composition. Textural and compositional evidence demonstrate that reaction between percolating melt and peridotite occurs by a combination of dissolution-reprecipitation and solid-state diffusion. Dissolution-reprecipitation leads to well-equilibrated phases whereas diffusional equilibration introduces zoning. As a result of these reaction and equilibration processes, the infiltrating melt and initial phases undergo significant compositional changes. We will present a combination of textural, modal and compositional observations to illustrate the implications of melt-peridotite reaction in the upper mantle.

2.34

Late Cretaceous history of the western Colombian Andes

Villagómez Diego*, Spikings Richard*, Magna Tomas**, & Winkler Wilfred***

* *Département de Minéralogie – Université de Genève. 13 Rue des Maraichers, 1205 Genève, Switzerland (Diego.Villagomez@unige.ch)*
** *Correnssstrasse 24 D-48149 Münster, Germany*
*** *Geologisches Institut – ETH-Zurich, 8092 Zürich, Switzerland.*

Mafic oceanic rocks which crop out in the western Colombian Andes are juxtaposed against continental rocks along the Cauca-Almaguer Fault. Several studies have proposed that these oceanic rocks may form part of the large Caribbean Colombian Oceanic Plateau formed above the Galapagos hotspot (e.g. Kerr et al., 1997); its accretion to the continental margin of Colombia is not well established, with proposed ages ranging from Aptian-Albian (Cediel et al., 2003) to Eocene (Gomez et al., 2007).

In order to define the origin and nature of the oceanic province we dated and geochemically constrained several mafic fragments within this unit. Our results agree with most authors (e.g. Kerr et al., 1997) suggesting that these rocks were formed in an oceanic plateau setting. Our new U/Pb LA-ICPMS data show that these rocks in Colombia range in age from 96 to 90 Ma.

Any attempt to decipher the time of accretion of the oceanic terranes onto the continent must take into account: 1) thermochronological data in the indenting oceanic rocks and buttressing continental rocks, 2) characterization of syn- and post-accretionary sedimentary rocks within the accreted terranes and the continental margin in the peripheral and retro-foreland basins, and 3) geochronological information from arc-related batholiths, which intrude both the allochtonous and autochtonous terranes, thus pre- and post-dating terrane accretion (Kerr et al, 2005).

We have addressed these points by using several geochronological (U/Pb LA-ICPMS) and thermochronological (apatite U-Th/He, multiphase $^{39}Ar/^{40}Ar$, apatite and zircon fission track) techniques to reconstruct an accurate model for the late Cretaceous evolution of western Colombia.

Our data suggest that the allochtonous terranes in Colombia were accreted to the paleocontinental margin at some point between 80 and 75 Ma. The accretion of equivalent, oceanic plateau rocks in Ecuador (south of Colombia) has been tightly constrained at 73-75 Ma (Spikings et al., 2008), suggesting that accretion may have proceeded diachronously along the Northern Andes.

REFERENCES

Cediel, F., Shaw R., & Caceres C. 2003, Tectonic assembly of the Northern Andean Block, in C. Bartolini, R. T. Buffler, and J. Blickwede, eds., The Circum-Gulf of Mexico and the Caribbean: Hydrocarbon habitats, basin formation, and plate tectonics: AAPG Memoir 79, p. 815– 848.

Gómez, J., Nivia, A., Montes, N., Jiménez, D., Tejada, M., Sepúlveda, M., Osorio, J., Gaona, T., Diederix, H., Uribe, H. & Mora, M., compiladores. 2007. Mapa Geológico de Colombia. Escala 1:1'000.000. INGEOMINAS, 2 hojas. Bogotá.

Kerr, A., Marriner, G., Tarney, J., Nivia, A., Saunders, A., Thirlwall, M., & Sinton, C. 1997. Cretaceous Basaltic Terranes in Western Colombia: Elemental, Chronological and Sr-Nd Isotopic Constraints on Petrogenesis. Journal of. Petrology. 38, 677–702.

Kerr, A., Tarney, J. 2005. Tectonic evolution of the Caribbean and northwestern South America: The case for accretion of two Late Cretaceous oceanic plateaus. Geology, 33, 269–272.

Spikings R., Crowhurst P., Winkler W., & Villagomez D. 2008. Syn- and post accretionary cooling history of the Ecuadorian Andes constrained by their in-situ and detrital thermochronometric record. Earth and Planetary Science Letters. (submitted).

2.35

Experimental geochemistry and mineralogy for industrial applications: new membranes for alkaline electrolysers

V. Zakaznova-Herzog*, D. Wiedenmann*, M. Gorbar**, B. Grobéty***, U. Vogt*, A. Züttel*

* *Laboratory "Hydrogen & Energy", EMPA, Überlandstrasse 129, 8600 Dübendorf*
Valentina.Herzog@empa.ch
** *Laboratory for High Performance Ceramics, EMPA, Überlandstrasse 129, 8600 Dübendorf*
*** *Dept. of Geosciences, University of Fribourg, Chemin du Musée 6, Pérolles, CH-1700 Fribourg*

Mineral stability and reactivity with hydrothermal solutions from low to high temperatures and pressures are important issues in petrology and geochemistry. These data may also be of importance Industrial applications of such minerals. An example is the hydrogen production by alkaline electrolysis, for which membranes resisting concentrated KOH solutions are needed. About 1.6 million tonnes per year of world hydrogen production is by means of electrolysis (U.S. Department of energy, http://www.hydrogenassociation.org). Currently, chrysotile asbestos membranes are used to separate hydrogen and oxygen gases during water electrolysis (Fig. 1).

The focus of our project is the study of the currently used asbestos membranes and the development of new membranes to replace asbestos membranes, which are banned due to recent health regulations. The new material needs to be impermeable for O_2 and H_2, ion-conductive, stable in 30% KOH at 90°C and 32 bars, flexible, robust and affordable.. Because of their proven stability in alkaline solutions and low costs, Mg-silicates, such as olivine (Hänchen et al, 2006), are perfect candidates as replacement materials. Chrysotile asbestos membranes have a high ion conductance and gas tightness and sufficient flexibility and mechanical robustness, even for very large dimension i.e. diameters up to 2meters. The reason for these excellent physico-chemical properties are, however, not well understood.

The electrochemical performance of membranes made of replacement materials will be monitor in a prototype test cell. Stability and dissolution behaviour of chrysotile asbestos and a selection of replacement materials will be studied before and after having served in the test cell by means of environmental scanning electron microscopy, X-ray diffraction and X-ray photoelectron spectroscopy (XPS). XPS is one useful technique for probing chemical states at fresh and reacted surfaces, from which insight into the stability and the dissolution mechanisms may be gained (e. g., XPS study of fresh and reacted olivine and pyroxenes, two potential membrane materials, Zakaznova-Herzog et al., 2008). Material solubility will be monitored by the gravimetrical method and ICP MS.

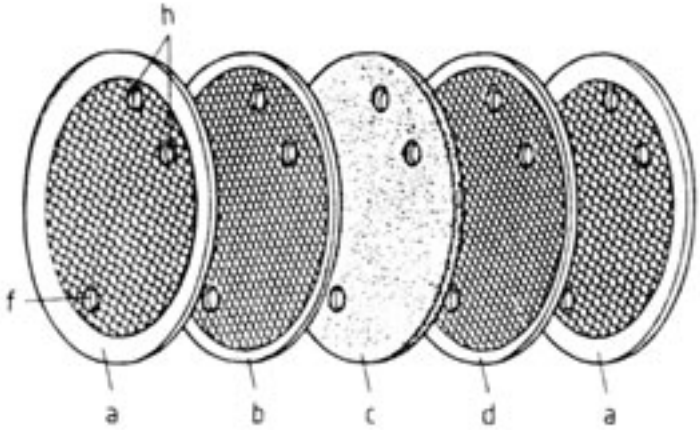

Fig. 1 Exploded view of a pressure electrolysis unit (Lurgi, Zdansky-Lonza pressure electrolysis): (a Bipolar electrodes, dimple plate cell partition; b) Pre-electrodes in the form of nets c)Asbestos diaphragm; d) Cell frame; e) Hydrogen and oxygen ducts (Häussinger P., et al., 2006)

REFERENCES

Häussinger P., Lohmüller R., Watson A. (2006) Ullmann's Encyclopedia of Ind. Chemistry, Chap.: Hydrogen, v.17.

Hänchen, M.; Prigiobbe, V.; Storti, G.; Seward, T. M.; Mazzotti, M.(2006) Dissolution kinetics of fosteritic oli-vine at 90 150 °C including effects of the presence of CO_2 Geochimica et Cosmochimica Acta, Volume 70, Issue 17, p. 4403-4416

Zakaznova-Herzog V.P., H.W. Nesbitt, G.M. Bancroft and J.S. Tse. (2008) Characterization of Leached Layers on Olivine and Pyroxenes using High Resolution XPS and Density Functional Calculations Geochim. Cosmochim. Acta 72, 69-86.

2.36

Geochemistry and Source of the Recent Sediments in Southwestern of Ahvaz, Khouzestan Province, Iran

Zarasvandi. A

Department of Geology, Shahid Chamran University, Ahvaz, Iran zarasvandi_a@scu.ac.ir

The Ahvaz City is located in Khouzestan province in southwest of Iran. This city is the most important geographical and industrial city between Iran and Iraq border. The climate of the study area is considered to be arid and humid. This area is part of Zagros orogenic belt and consists of Cenozoic sedimentary rocks such as Limestone (Asmari Formation), Gypsum (Gachsaran Formation), Sandstone (Aghajari Formation) and Conglomerate (Bakhtiari Formation). This belt is the product of three major geotectonic events during subduction between the Arabian and Iranian plates. The belt consists of there parallel tectonic zones from NE to SW: (1) the volcanic–plutonic zone (Urumieh– Dokhar belt); (2) the Sanandaj-Sirjan metamorphic zone; (3) the Zagros fold belt.

The rock fragments and minerals in the study area derived from erosion of the banks of the rivers and sand dunes in the southwest of the area. The surficial distribution of sediments shows miscellaneous layers and mixture of sands, silts and hard muds. The study area is characterized by the predominance of alluvial and sedimentary rocks of both chemical and detrital origins. Except for some unpublished exploration reports there are no other published literature about the geology, geochemistry, economic geology and genesis of these sediments. The combination of petrography and geochemistry data of the sediments can reveal the nature and tectonic setting of sediments as main indicators for mineral exploration in the surficial sediments. In this way, 30 samples from alluvial deposits and sand dunes were collected for geochemical and petrography using XRF and XRD methods.

Petrographical studies and using major element discrimination diagrams indicate that these sediments are classified as litharenite, sublitharenite, and subarkose types. Petrographic studies using XRD reveal that these sediments are mainly consist of quartz, feldspars, Muscovite, Biotite, clay minerals, heavy minerals and fragments of Igneous and metamorphic rocks. Tectonic setting discrimination diagrams based on major elements show that most of samples fall in an active continental margin. Geochemical characteristics suggest that in addition to quartzose recycled sedimentary rocks plutonic igneous or high-grade metamorphic rocks can be as parent rocks for these sediments. Based on all data can conclude these sediments are result of erosion of sandstone and conglomerate rocks in the study area which are formed by erosion of felsic plutonic and metamorphic rocks of the Sanandaj-Sirjan metamorphic belt. These sedimentary rocks were deposited along the passive marginal coast of the Oligocene-Miocene Zagros foreland basin.

REFERENCES

Alavi, M., 2004, Regional stratigraphy of the Zagros fold-thrust belt of Iran and its proforeland evolution: American Journal of Science, 304, 1–20.

Nesbitt, H.W., Young, G.M., 1982, Early Proterozoic climates and plate motions inferred from major element chemistry of lutites: Nature, 299, 715–717.

Pettijohn, F.J., Potter, P.E., Siever, R., 1972, Sand and Sandstones: New York, Springer-Verlag.

Roser, B.P., Korsch, R.J., 1986, Determination of tectonic setting of sandstone –mudstone suites using SiO_2 content and K_2O/Na_2O ratio:Journal of Geology, 94, 635–650.

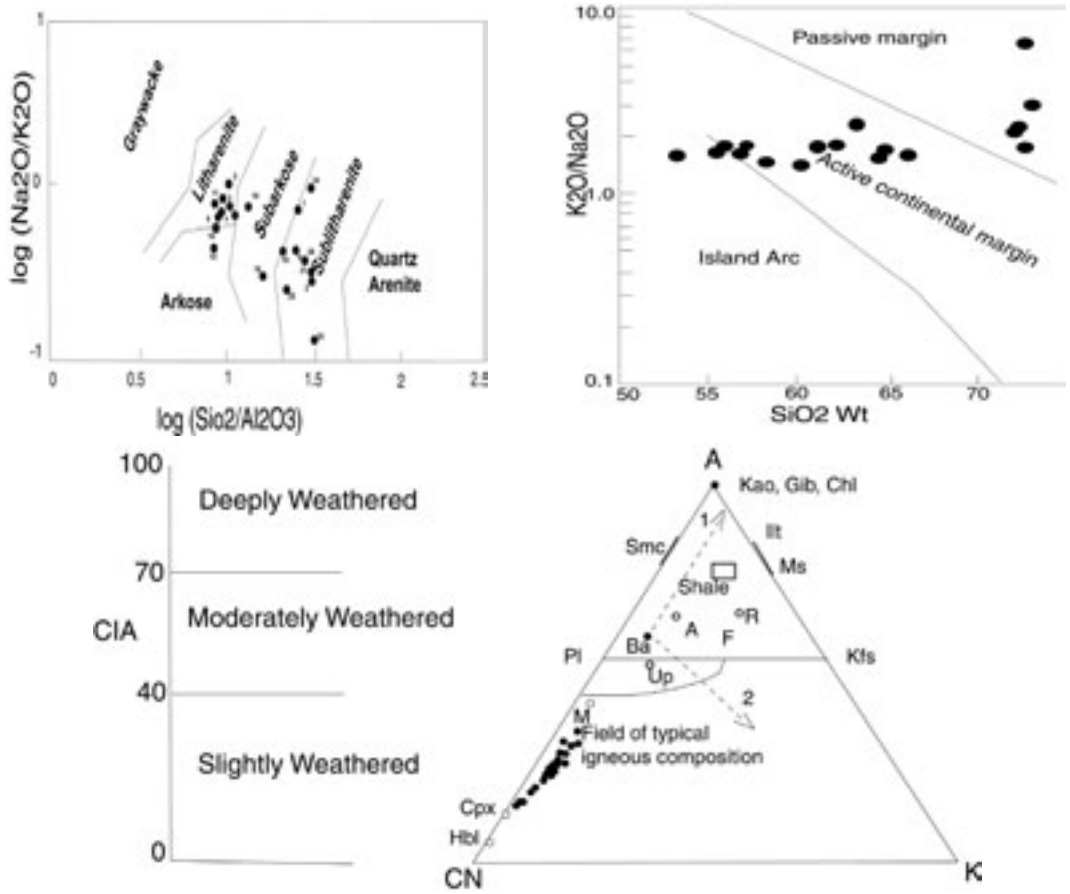

Figure.1 Chemical classification of samples from the sediments based on (A) log (SiO_2/Al_2O_3) vs. log (Na_2O/K_2O) diagram of Pettijohn et al. (1972), and (B) the SiO_2 vs. (Na_2O/K_2O) diagram of Roser and Korsch (1988) and (C) Ternary diagram of the parent rock of the sediments by Nesbitt and Young, 1982.

2.37

Surface water in the Zermatt—Matterhorn area, Switzerland, a hydrogeochemical study

Zhou Wei*, Stober Ingrid & Bucher Kurt

Institute of Mineralogy and Geochemistry University of Freiburg, D-79104, Freiburg, Germany
**wei.zhou@minpet.uni-freiburg.de*

The chemical characteristics of surface runoff have been used to infer the mechanisms of solute acquisition in open system environments. We studied the chemical evolution of surface waters in geologically diverse Alpine catchments of the Zermatt-Matterhorn area. Two hydrogeochemical models have been set up for interpreting the water-rock interaction.

Water samples were collected mainly from small water bodies located in the Findeln glacier area and two river systems, Mattervispa (Theodul) and Mellichenbach (Täsch valley) representing the geographical and lithological diversity. Altitudes of sampling locations were around 1600m to 3200m. Since water samples were from water bodies at high elevation, water-rock interaction was little affected by anthropogenic or biologic contributions.

Temperature, pH, and electric conductivity were measured on site. Charge balance of the analysis was better than 8%. Total dissolved solids was relatively low and varies from 6 to 244 mg/l. Dominant solutes are Ca, Mg, HCO_3, SO_4 and minor components are Na, K, NO_3, Cl and Si, while F and B occur in traces only.

Statistical analysis of the composition data shows that Ca-HCO_3-SO_4 and Na-K-Cl are strongly correlated. Three chemical types of water can be distinguished: Mg-HCO_3, Ca-SO_4 and Ca-HCO_3. The calculation of saturation states with phreeqc shows that all surface waters are undersaturated with respect to all relevant minerals.

A model for the hydrogeochemical evolution has been set up to estimate the contributions of the various rock-forming minerals to the composition of the waters. It shows that: A) The dominant source of solutes is the dissolution of carbonate minerals. B) Sulfate originates mostly from oxidation of sulfide minerals (pyrite and others). C) Two reaction equations relate the dissolution of the most reactive minerals to the observed water compositions. These are (1) Cal + Py + Chl + Pl + Ms + Qtz = Kao + Hem + Water and Cal + Sd + Py + Ab + Chl + Ms + Qtz = Kao + Hem + Water. D) Water compositions can be represented and characterized by the proportion of the minerals that are needed to be dissolved to create the observed water composition. The computed models are shown as pie charts in Fig. 1 and they are related to the background geology of the sampling area.

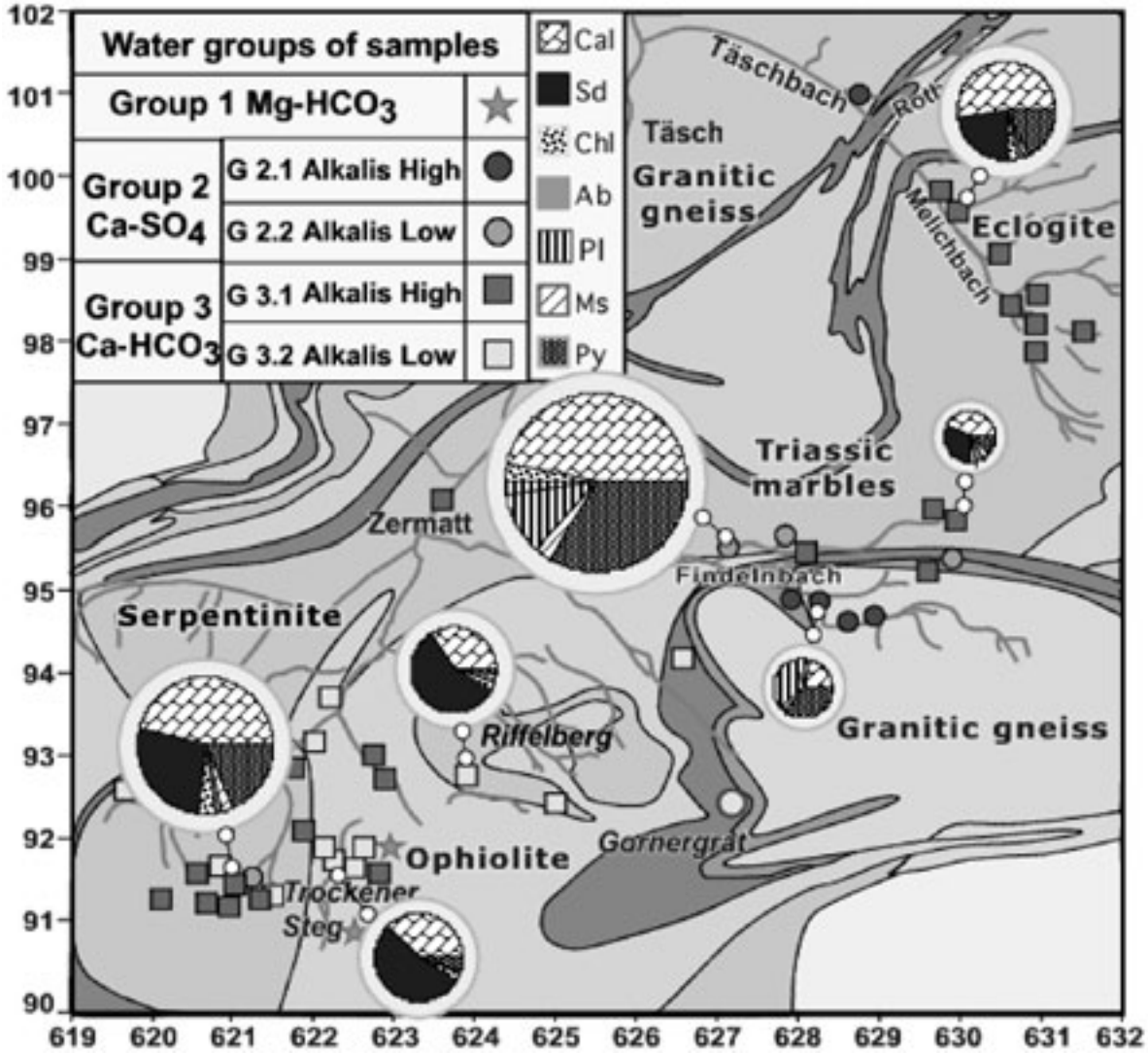

Fig.1: Hydrogeochemical models and background geology of the Zermatt-Matterhorn area. The models show that the composition of the surface waters is controlled by the geology (dominant lithology) of the catchment.

REFERENCE:

Brown G. H., 2002: Glacier meltwater hydrochemistry, Applied Geochemistry, 17, 855-883.

Collins, D. N.,1979: Quantitative determination of the subglacial hydrology of two alpine glacials, Journal of glaciology, 23, 347-361

Drever, J.I., & Zobrist, J., 1992: Chemical weathering of silicate rocks as a function of elevation in the southern Swiss Alps, Geochimica et Cosmochimica Acta, 56, 3209-3216.

Tranter M., Brown, G.H., Hodson, A., & Gurnell, A.M., 1996: Hydrochemistry as an indicator of subglacial drainage system structure: a comparison of Alpine and Sub-Polar environments, Hydrological Processes, 10, 541-556.

White, A.F., & Blum, A.E., 1995: Effects of climate on chemical, weathering in watersheds, Geochimica et Cosmochimica Acta 59(9), 1729-1747.

2.38

New Experiments of Feldspar Hydrolysis and Implications for Interpretations of Weathering Rates

Zhu C.*, Fu, Q.**, Lu P.*, Seyfried W.E.**

*Indiana University, Department of Geological Sciences, Bloomington, IN 47405, USA (chenzhu@indiana.edu)
**Department of Geology and Geophysics, University of Minnesota, Minneapolis, MN 55455, USA

We conducted a series of new batch reactor experiments for alkali-feldspar dissolution and secondary mineral precipitation at 150 – 200 °C and 300 bars. Temporal evolution of fluid chemistry was monitored with a time series of in situ fluid samples (e.g., Fig. 1) following the method discussed in Seyfried et al. (1987). Solid reaction products were retrieved from experiments, some terminated after different durations for identical experiments, to examine the intermediate and final reaction products. FEG-SEM and HR-TEM examinations revealed dissolution features and secondary mineral coverage on feldspar surfaces. Boehmite, kaolinite, and muscovite were identified as secondary minerals by XRD and TEM for different experiments. In order to evaluate the complex interplay between dissolution and precipitation reaction kinetics, we performed speciation and solubility geochemical modelling to compute the saturation indices (SI) and to trace the reaction paths on equilibrium activity-activity diagrams. The speciation and solubility modelling results demonstrated: (1) the experimental aqueous solutions were supersaturated with respect to product minerals for almost the entire duration of the experiments; (2) the aqueous solution chemistry did not evolve along the phase boundaries but crossed the phase boundaries at oblique angles; and (3) the earlier precipitated product minerals did not dissolve but continued to precipitate even after the solution chemistry had evolved into the stability fields of minerals lower in the paragenesis sequence. These three lines of evidence suggest that product mineral precipitation is a slow kinetic process and product minerals were not in partial equilibrium with aqueous solution in these experiments.

The newly acquired experimental data and geochemical modelling results support the new hypothesis put forward by Zhu et al. (2004a,b) on the apparent discrepancy between field derived feldspar dissolution rates and dissolution rates measured in laboratory at purportedly similar conditions (Blum and Stillings, 1995). The new hypothesis proposes that one important mechanism controlling the slow feldspar dissolution rates is the slow precipitation kinetics of clays. The precipitation of clays removes solutes from solution, resulting in undersaturation with respect to feldspars in the aqueous solution and making additional feldspar dissolution possible. This hypothesis, in which clay precipitation kinetics controls the overall feldspar dissolution rate, presents several dilemmas for the traditional application of kinetic theories to weathering and diagenesis systems. The hypothesis shifts the paradigm from the century-old debate about feldspar dissolution rates and mechanisms to the formation mechanisms of secondary phases.

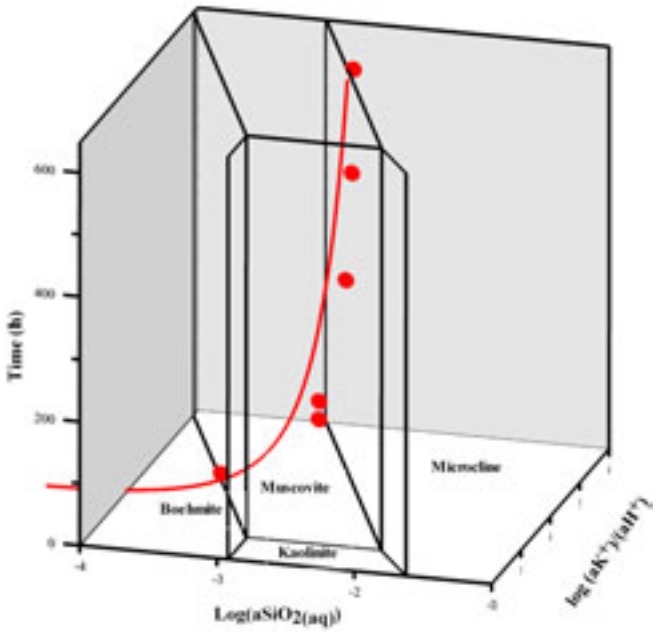

Figure 1. Activity – activity diagram showing the phase relations in the system K_2O-(Al_2O_3)-SiO_2-H_2O-HCl at 200 °C and 300 bars. Symbols represent experimental aqueous solutions of alkali feldspar dissolution in 0.2 m KCl and 0.05 m CO_2 solution at 200 °C and 300 bars. The red line is prediction from reaction path modelling.

REFERENCES

Blum, A. and Stillings, L., 1995. Feldspar dissolution kinetics. In: Brantley, S. L. and White, A. R. Eds.), Chemical Weathering Rates of Silicate Minerals. Mineralogical Society of America, Washington DC..

Seyfried, W. E., Jr., Janecky, D. R., and Berndt, M. E., 1987. Rocking autoclaves for hydrothermal experiments; II, The flexible reaction-cell system. In: Barnes, H. L. e. (Ed.), Hydrothermal Experimental Techniques. Wiley-Intescience. 647.

Zhu, C., Blum, A., and Veblen, D., 2004a. Feldspar dissolution rates and clay precipitation in the Navajo aquifer at Black Mesa, Arizona, USA. In: Wanty, R. B. and Seal, R. R. I. Eds.), Water-Rock Interaction. A.A. Balkema, Saratoga Springs, New York.).

Zhu, C., Blum, A. E., and Veblen, D. R. D., 2004b. A new hypothesis for the slow feldspar dissolution in groundwater aquifers. Geochimica et Cosmochimica Acta 68, A148.

3. Palaeontology (Open Session)

Damien Becker

Swiss Palaeontological Society (SPS)
Kommission des Schweizerischen Paläontologischen Abhandlungen (KSPA)

3.1

Sedimentology and palaeocology of the Banné Member (Late Jurassic, Kimmeridgian): new data from excavations along the Transjurane highway (Canton Jura, Switzerland)

Ayer Jacques*, Comment Gaël*, Adatte Thierry**, Badertscher Christophe***, Boll Samuel****, Fürsich Franz T.*****, Gretz Mélanie*, Hug Wolfgang A.*, Marty Daniel*

*Section d'archéologie et paléontologie, République et Canton du Jura, Office de la culture, Hôtel des Halles, CH-2900 Porrentruy 2. Jacques.ayer@jura.ch
**Institut de géologie et paléontologie, Quartier UNIL-Sorge, Bâtiment Amphipôle, CH-1015 Lausanne
*** Bureau d'Etudes Géologiques S, Rue de la Printse , CH-1994 Aproz
**** Marti Tunnelbau AG, Freiburgstrasse 133, CH-3008 Berne
*****Institut für Paläontologie, Pleicherwall 1, D-97070 Würzburg

The Banné Member defined by Gygi in 2000 was originally called "Marnes à Ptérocères" (Ptérocère=*Harpagodes oceani*), and it was described by Jules Thurmann as "Marnes du Banné" (Thurmann & Etallon 1864). The Banné Member is about a 10 m thick sequence of highly fossiliferous calcareous marls and marly limestones deposited in a shallow, internal lagoon or a shallow, large tidal channel. Most of the levels are so rich in marine invertebrates (mainly Bivalvia, Gastropoda and Brachiopoda) that they are best described as shell beds. Ammonites (*Prorasenia* sp.) date the Banné Member to the late Early Kimmeridgian (Divisum zone, ca. 152 My) and the time interval of its sedimentation, based on sequence stratigraphical and cyclostratigraphical analyses (Colombié 2002, transgressive deposits after Kim 3), corresponds to about 0.2 My.

Between 2001 and 2007, the Palaeontology A16 carried out systematic excavations along the future course of the Transjurane highway (A16) in the Banné Member near Porrentruy (Canton Jura, Switzerland). Based on bulk sampling and detailed documentations of several surfaces of one square meter species richness, abundance and commonness were used to characterize the vertical evolution of the invertebrate assemblages. Larger surfaces were also excavated in order to improve the completeness of the fossil record, including uncommon taxa (echinoids, ammonites, fishes, turtles and crocodiles). A systematic sampling was performed for mineralogical and sedimentological analyses using X-ray diffraction and microfacies descriptions.

The first faunal list of bivalves contains about 100 species (Hicks 2006; Richardt 2006). The surface documentations underline a significant vertical change in the invertebrate assemblages, marked by an increasing diversity. Moreover, clay mineral analysis shows a progressive decrease and then the disappearing of kaolinite in the middle part of the sequence. This study is actually in progress. It seems that we can interpret the preliminary results as a climatic change influencing the weathering regime of the hinterland. The decline in kaolinite abundance, is probably directly controlled by the 'drying-out' of the hinterland (Wignall & Ruffell 1990), but local observations of the Banné Member near Porrentruy may help us even to understand in more detail how climate, sea-level and tectonics interact and influence hydrodynamic changes and the ecological evolution of the depositional environment.

A special effort will be done in statistic analyses to better understand the evolution of the faunal assemblages. Our aim is to characterize the ecological evolution of the fauna of the Banné Member and the associated mineralogical changes in a high resolution stratigraphical frame and to correlate these changes with other regional localities of the same time interval.

REFERENCES

Colombié, C. 2002: Sédimentologie, stratigraphie séquentielle et cyclostratigraphie du Kimméridgien du Jura suisse et du Bassin vocontien (France): relations plate-forme – bassin et facteurs déterminants. GeoFocus 4, 198 pp.

Hicks, S. 2006: Palökologie des Makrobenthos aus dem oberen Jura (Kimmeridge) im Kanton Jura, Nordschweiz. Unpublished master thesis, Institut für Paläontologie, Universität Würzburg, 72 pp.

Richardt, F. 2006: Palökologische Analyse einer oberjurassischen Mergelfolge im Gebiet von Porrentruy, NWSchweiz. Unpublished master thesis, Institut für Paläontologie, Universität Würzburg, 50 pp.

Thurmann J. & Etallon A. 1861-64: Lethea Bruntrutana ou Études paléontologiques et stratigraphiques sur le Jura bernois et en particulier les environs de Porrentruy. Mémoires de la Société hélvétique des Sciences naturelles 18-20, 1-500.

Wignall, P.B. & Ruffell, A.H. 1990: The influence of a sudden climatic change on marine deposition in the Kimmeridgian of north-west Europe. Journal of the Geological Society of London 147, 365-371.

3.2

Palaeocene to Oligocene Foraminifera from the Azuero Peninsula (Panama): The timing of seamount formation, accretion and forearc overlap, along the Mid-American Margin

Baumgartner-Mora Claudia*, Baumgartner Peter O.*, Buchs David,* Bandini Alexandre* & Flores Kennet *

* *Institut de Géologie et Paléontologie, University of Lausanne. Anthropole, CH-1015 Lausanne, Switzerland. (Claudia.Baumgartner@unil.ch)*

Larger benthic and planktonic Foraminifera recovered from limestones and debris flows in the Azuero Peninsula (Panama) allow to date the formation of accreted seamounts, the time of their docking along the Mid-American convergent margin, as well as the diachronous onset of forearc sequences on accreted terranes.

Interflow pelagic to offshore limestones from the Hoya Seamount Unit: Paleocene-early Eocene ages are indicated by *Morozovella*-type planktonic foraminifera and small *Amphistegina* spp. An early Eocene age is indicated by the association of *Discocyclina barkeri, Pseudophragmina* sp., *Euconoloides* sp. cf. E. *wellsi* and *Amphistegina undecima* (Pl.1 Figs.1-4). Calcarenites interbedded with lava flows of the Punta Blanca seamount Unit reveal an early to middle Eocene age by the presence of *Pseudophragmina ancoensis* and *Orthophragmina* sp. (Pl.1 Figs.7-8). These findings document synchronous Late Palaeocene to early-middle Eocene volcanic construction and carbonate sedimentation in at least two pacific seamounts, that outcrop in the SW-corner of the Azuero Peninsula.

Middle to late Eocene ages are indicated by rich assemblages of Larger Benthic Foraminifera both in tectonic mélanges that overly the seamount sequences, as well as at the base of the unconformably overlapping Tonosi forearc-sequence. *Discocyclina* sp. and *Lepidocyclina polylepidina* (Pl.1 Figs. 5-6). suggest a middle Eocene age maximum age for the debris flows found in tectonic mélanges that formed during accretion of the seamounts. *Pseudophragminides* ssp., *Asterocyclina* in the older, paralic facies and abundant *Lepidocyclina* spp., and rare *Operculinoides* sp. (Pl.1 Fig. 9)., in the younger pure carbonate facies suggest a middle to late Eocene age for the unconformable onset of the Tonosi forearc sediments in SW-Azuero.

Oligocene ages are determined from shallow water limestones at the base of Tonosi in central Azuero documenting the progressive onlap of this fore-arc sequence onto the Late Cretaceous plateau and arc “basement”. At least two distinct facies are characterized by: 1. abundant flat *Nummulites* spp. (Pl.1 Figs.10-11) and 2. by dominant large Oligocene *Lepidocyclina* spp. (Pl.1 Figs.12-13).

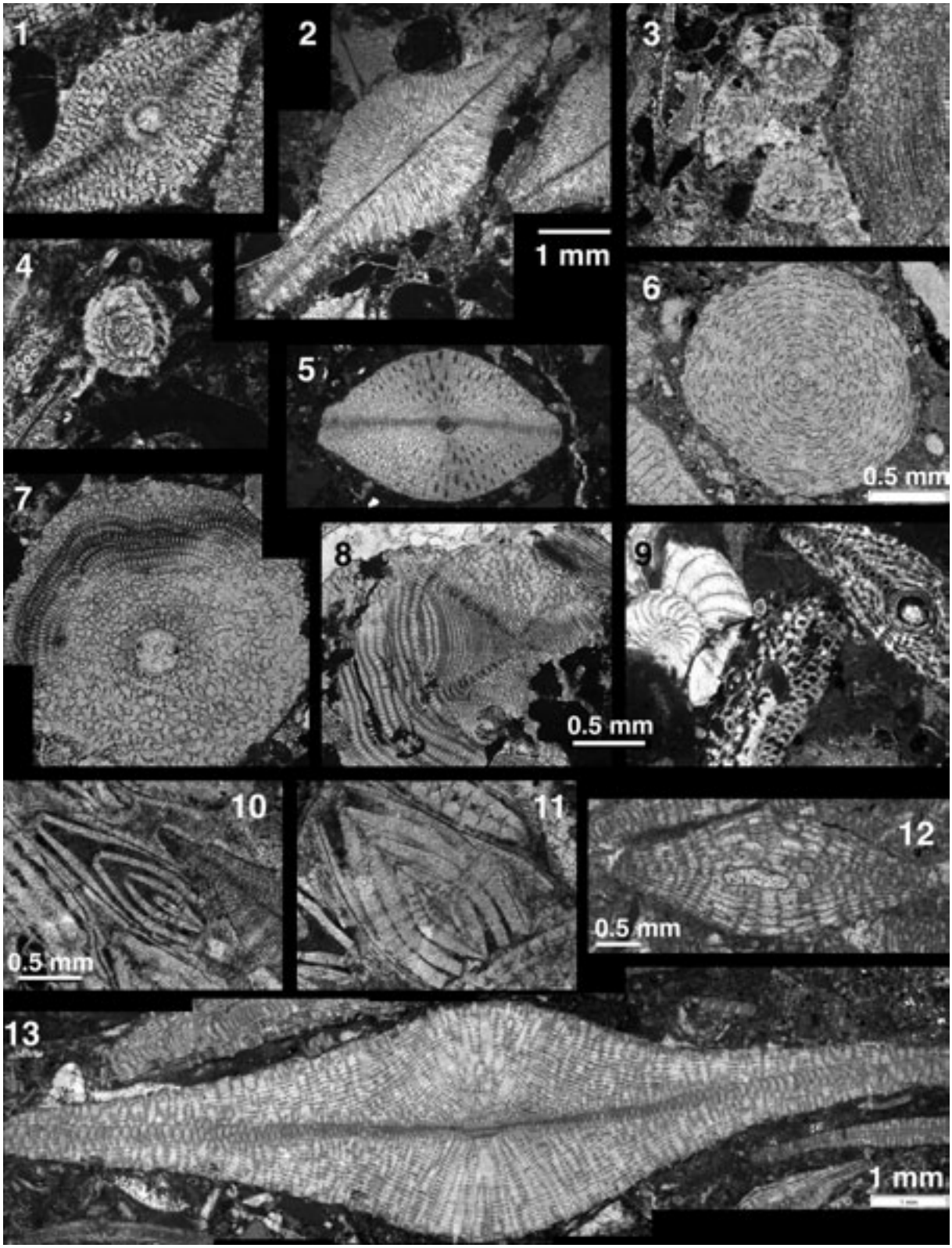

Plate 1. 1-4, lower Eocene larger benthic Foraminifera, inland outcrop (DB07-010b, Rio Pavo) Hoya Seamount Unit, Azuero, Panama.Scale bar = 1 mm.1. *Discocyclina barkeri*, 2. *Pseudophragmina* sp., 3. *Euconoloides* sp. cf. *E. wellsi* and *Amphistegina undecima*., 4. *Amphistegina undecima*. 5-6, middle Eocene, debris flow matrix, Covachon beach (POB06-20). 5. *Discocyclina* sp., scale as for 1-4, 6. *Lepidocyclina polylepidina*. 7-8, lower-middle Eocene forms from calcarenite (DB07-037b, Rio Horcones) interlava, Punta Blanca Seamount, S-Azuero. 7. *Pseudophragmina ancoensis*, 8. *Orthophragmina* sp. 9. *Lepidocyclina* sp. and *Operculinoides* sp. (POB06-022 W of Punta Blanca). Middle-Upper Eocene shallow water limestone at base of Tonosi overlap sequence. 10-13, Oligocene, shallow water lmestones associated with the base of Tonosi forearc sequence, central Azuero. 10. *Nummulites panamensis* and *Discocyclina* sp. (AL026, Rio Guerita), 11. *Nummulites dia* (AL026, Rio Guerita), 12. *Lepidocyclina tournoueri* and 13. *Lepidocyclina undosa* (both AL031, Rio Guerra).

3.3

The Late Pleistocene mammalian fauna from Ajoie (Northwestern Switzerland): stratigraphy, taphonomy, palaeoecology

Becker Damien*,Scherler Laureline*,**,Tütken Thomas***,Aubry Denis* & Detrey Jean*

*Section d'archéologie et paléontologie, Hôtel des Halles, CP64, CH-2900 Porrentruy (damien.becker@palaeojura.ch)
**Department of Geosciences, Institute of Geology, ch. du Musée 6, Pérolles, CH-1700 Fribourg
***Steinmann Institut für Geologie, Mineralogie und Paläontologie, Rheinische Friedrich-Wilhelms-Universität Bonn, Poppelsdorfer Schloss, D-53115 Bonn

The karstic relief of the Ajoie Plateau is formed by many dolines. These dolines functioned as natural traps for skeletal remains of mammoth, woolly rhinoceros and other large terrestrial mammal during the last glaciation. Often the dolines yield a fossil assemblage of the latest Middle Pleniglacial (ca. 30 to 40–45 ka BP) embedded in a loessic matrix (see fig. 1).

Most of the fossil remains have been transported by biological (predation, scavenging) and/or physical (solifluction, gelifluction, withdrawing) processes resulting in sorting, abrasion, weathering and concentration of the bones and teeth. The fossil mammal assemblages are dominated by grazing mega- (>1000 kg) and large herbivores (>100 kg) as well as fossorial rodents. In contrast, forest-dwelling species are only a minor component and intermediate-sized mammals seem to lack in these faunal assemblages. Rare lithic artefacts associated with the mammal fossils support at least an occasional presence of humans, but no long time settlements or hunting.

Based essentially on palaeoecological analyses of the mammal community (e.g., biodiversity, cenograms, ecological histograms) the palaeoenvironmental reconstruction of the Ajoie during the time interval 30 to 40–45 ka BP should correspond to a humid relatively open landscape partially covered by a bush, shrub and forest vegetation. The preliminary results of phosphate oxygen isotope analyses of mammoth tooth enamel (mean $\delta^{18}O_{PO4}$=14.1±1.5‰, n = 14) about 2.5‰ higher than those of mammoth teeth from the 45 ka BP old Niederwenigen site, near Zurich (Tütken et al., 2007) and indicate the ingestion of drinking water with similar $\delta^{18}O$ values as for modern precipitation in Swiss lowland areas. Thus the mammoths probably lived in the Ajoie during an interstadial phase of the latest Middle Pleniglacial (either the Hengelo, Huneborg or Denekamp).

REFERENCES

Aubry, D., Guélat, M., Detrey, J. & Othenin-Girard, B. 2000: Dernier cycle glaciaire et occupations paléolithiques à Alle, Noir Bois (Jura, Suisse). Cahier d'archéologie jurassienne, 10, Office de la culture et Société jurassienne d'Émulation, Porrentruy, 175 pp.

Braillard, L. 2006: Morphogenèse des vallées sèches du Jura tabulaire d'Ajoie (Suisse) : rôle de la fracturation et étude des remplissages quaternaires. PhD Thesis, University of Fribourg, Geofocus, 14, 224 pp.

Guélat, M. 2006: Le Quaternaire dans le canton du Jura. Actes de la Société jurassienne d'Emulation 2005, 9-31.

Tütken, T., Furrer, H. & Vennemann, T.W. 2007: Stable isotope compositions of mammoth teeth from Niederweningen, Switzerland: Implications for the Late Pleistocene climate, environment and diet.Quaternary International 164-165, 139-150.

Vliet-Lanoë van, B. & Guillocheau, F. 1995: Évolution de l'enregistrement pédosédimentaire depuis 150 ka en France du NO et en Belgique: biorhexistasie et bilans sédimentaires. Comptes Rendus de l'Académie des Sciences, 320, 419-426.

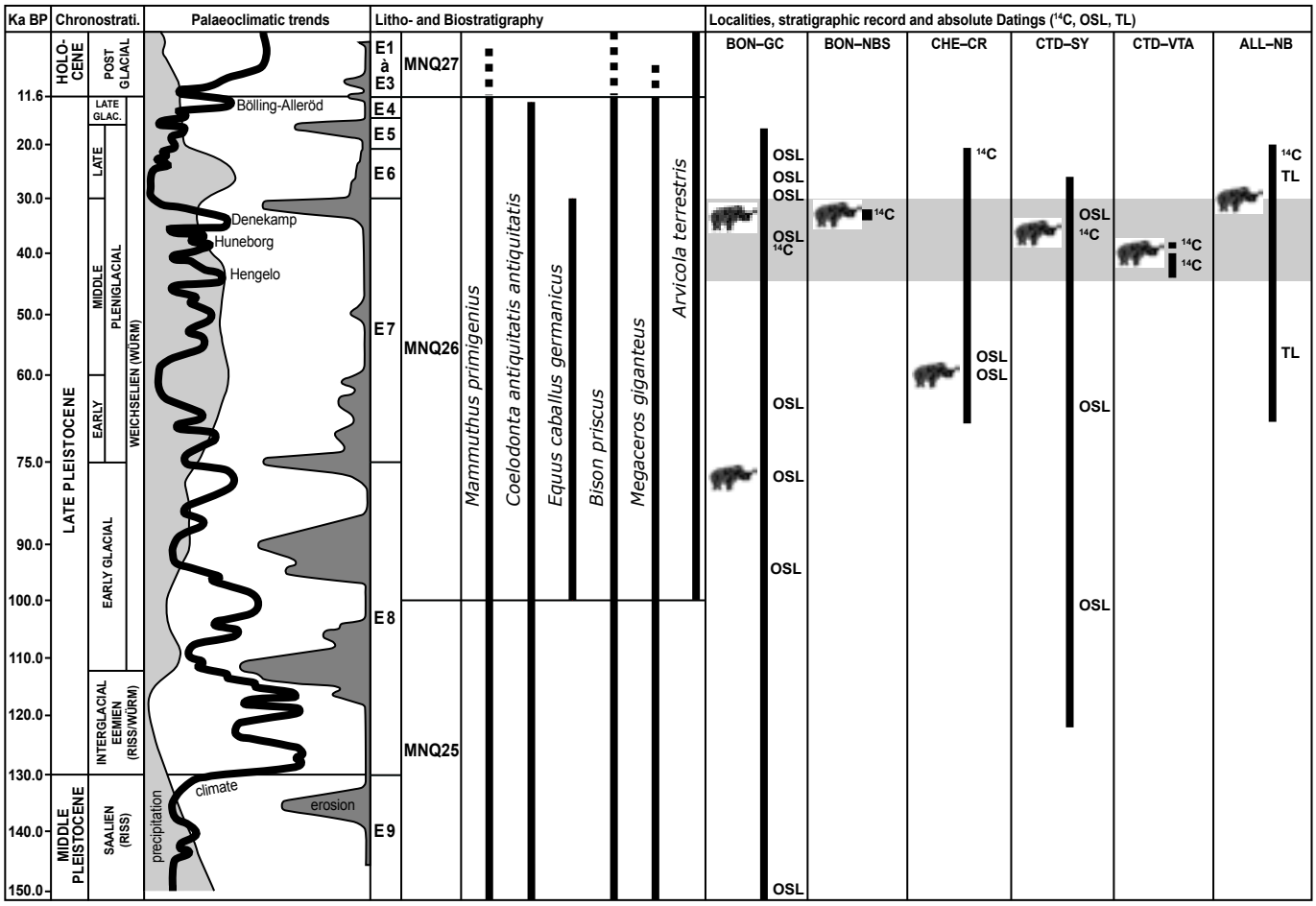

Figure 1. Chronostratigraphy of the large mammal remains of the doline fillings of Ajoie (Late Pleistocene, north-western Switzerland), modified from Van Vliet-Lanoë & Guillocheau (1995), Aubry et al. (2000), Braillard (2006) and Guélat (2006). The grey area underlines the time interval 30 to 40–45 ka BP associated to the most part of mammal remains. TL: Thermoluminescence dating; OSL: Optically Stimulated Luminescence dating; ^{14}C: Radiocarbon dating.

3.4

Inventory of geotopes of national significance : the paleontological record

Berger Jean-Pierre[1], Reynard Emmanuel[2], Constandache Monica[1], Dumas Joëlle[1], Felber Markus[3], Häuselmann Philipp[4], Jeannin Pierre-Yves[4], Martin Simon[2], Regolini Géraldine[2], Scapozza Cristian[2], Schneider Hans[5]

[1]*Département des Géosciences/Géologie, Université de Fribourg, CH–1700 Fribourg*
[2]*Institut de Géographie, Université de Lausanne, CH–1015 Lausanne*
[3]*Consulenze geologiche e ambientali, CH–6834 Morbio Inferiore*
[4]*Institut suisse de spéléologie et de karstologie (ISSKA), CH–2300 La Chaux-de-Fonds*
[5]*Office fédéral de l'environnement, CH–3000 Berne*

Starting in 2006, the revision of the inventory of Geotopes of national significance is in progress (see Berger et al. 2008, Reynard et al 2008). We publish here a complete list of the geotopes presenting a paleontological value. A part of this list has been already accepted by the assembly of the Working group, the other part will be probably accepted in february 2009. The publication of the full inventory is planned for 2010.

AG
01. GIN330 Echinodermensteinbruch Schinznach
02. GIN619 Fossilfundstelle Tongrube Frick
03. GIN981 Molasse Steinbruch Eckwil, Mägenwil
04. GIN627 Herznach
05. GIN738 Schümel
06. GIN221 Aargauer FaltenJura im Staffeleggebiet
Appenzell AI
07. GIN558 Felskuppe Flammeneggzug Rüte
08. GIN902 Flyschgebirge Fäneren, Rüte
Appenzell AR
09. GIN678 Molassekar Rossmoos Urnäsch
10. GIN679 Sturzenegg
11. GIN554 Urnäschtobel, Urnäsch
BE
12. GIN205 Austernriff Scherpfenrain, Häutligen
13. GIN906 Fallantiklinal bei Plaffeien (Fallvorsessli)
14. GIN113 Chaîne des Gastlosen (Jaun, BE/FR)
15. GIN905 Carrière Reuchenette
16. GIN621 Moutier (Cluse + Combe du Pont)
17. GIN431 Cluse de la Birse/Moutier.
18. GIN415 Gorges Pichoux, Undervelier
19. ..... Wischberg, Bumbach, Marbach :
BL
20. GIN10 Ziegelei, Allschwil
21. GIN12 Trias Neue Welt, Münchenstein
22. GIN13 Molasse/Jura Kontakt Schlossgarten
23. GIN14 Huppergruben Lausen
24. GIN15 Fossilfundstelle Rain, Zunzgen
25. GIN16 Molasse Steinbruch Steinholden
26. GIN17 Trias Steingraben Hemmiken
27. GIN19 Tongruben Liesberg-Dorf, Andil
28. GIN20 Tongrube Laufen Uf Saal
29. GIN311 Molasse Tennikerfluh
30. ..... Brochene Fluh bei Waldenburg
BS
——
FR
31. GIN349 Fossiles du Creux de l'Ours
32. GIN393 Molasse de Heitenried
33. GIN620 Crétacé-Tertiaire de Roter Sattel (Jaun)
34. GIN440 Mt. Vully
35. GIN650 Veveyse Fégyre
36. GIN023 Gorges de la Sarine
37. ..... Schiffenen
GE
38. GIN123 Molasse oligocène de la Roulavaz
GL
39. GIN633 Fossillokalität Landesplattenberg, Engi
GR
40. GIN47 Ruchberg-Sandstein (Maienfeld)
41. GIN507 Kesch-Ducan Gebiet mit Prosanto-Fm.
42. GIN964 Dinosaurierfährten am Piz dal Diavel
JU
43. GIN656 Grès vosgiens des Etangs de Bonfol
44. GIN623 Paléokarst de Petite Morée (Glovelier)
45. GIN639 Récifs coralliens de St-Ursanne
46. GIN1035 Traces de dinosaures de Courtedoux
47. ..... Chevenez
48. ..... La Caquerelle
49. ..... Châtillon
50. ..... Soulce
LU
51. GIN130 Molasse (OMM) Ränggloch
52. GIN133 Molasse (OMM) Luzern
53. GIN 479 Hagleren - Schlieren Flysch (LU, OW)
NE
54. GIN743 Localité type du Valanginien (Valangin)
NW
55. GIN372 Bärenhöhle S-4 am Schwalmis
56. .....Risteten-Beckenried Steinbruch
OW
——
SG
57. GIN203 Ries-Impakt Sittertobel, Waldkirch
58. GIN461 Lignit Böllenbergtobel, Uznach
59. GIN532 Molasse Goldach Martinstobel
60. GIN534 Molasse Schrönteller, Thal
61. GIN540 Saugetierlokalität Martinsbrünneli, Jona
62. GIN538 Gufler, Weesen + GIN559 Mättler Höchi
+ GIN560 Brunegg Amden
63. GIN550 Krummenau
SH
64. GIN79 Randen-Biberthal Verwerfung, Biberegg
65. GIN80 Seebi Trias-Steinbruch, Schleitheim
SO
66. GIN338 Liasische Stromatolithe, Passwang
67. GIN345 Sauropodenfährten Oberdorf/Lommiswil
68. GIN347 Typuslok. Solothurner-Schildkrötenkalke St Niklaus
69. GIN618 Liasgrube Unterer Hauenstein
70. ..... Egerkingen
71. ..... Rickenbach Huppergrube

SZ
72. GIN478 Bergsturzgebiet Goldau (SZ/ZG)
73. GIN645 Flysch und Klippendecke, Mythen
74. GIN990 Steinbach, Einsiedlen
TG
75. GIN86 Felsenholz Deckenschotter, Sitterdorf
76. GIN91 Molasse (OSM) Mammern
77. GIN521 Molasse Tongrube Altegg, Mettlen
78. GIN524 Glimmersandgrube Helsighausen
79. GIN526 Deckenschotter Grosswies
80. GIN528 Molasse Sandgrube Schlatt-Paradies
81. GIN90 Bischofszell Bentonite (TG, SG)
TI
82. GIN157 Serie Triassico-Giurassica Lucomagno
83. GIN164 "Bündnerschiefer" 'Alta Valle Bedretto
84. GIN165 Palude della Bedrina (Dalpe)
85. GIN175 Carbonifero di Manno
86. GIN176 Serie stratigrafica del Monte Caslano
87. GIN177 Sito paleontologico Monte San Giorgio
88. GIN178 Gole della Breggia
89. GIN179 Argille di Castel di Sotto (Novazzano)
90. GIN180 Gonfolite Lombarda della Collina Penz
91. GIN185 Conglomerato di Pontegana (Morbio)
92. GIN917 Torbiera al Paü Coldrerio
UR
———
VD
93. GIN624 Gisement fossilifère Rivaz-Monod
94. GIN625 Carrière de St-Triphon
95. GIN685 Crét./Molasse La Chaux-La Vraconne
96. GIN425 La Sarraz-Gorges du Nozon
+ Carrières du Mormont-Eclépens

97. GIN10106 Goufre du Narcoleptique
VS
98. GIN615 Glaciokarst de Tsanfleuron (Savièse)
99. GIN111 Traces dinosaures la Golette
100. GIN153 Empreintes de dinosaures d'Emosson
101. GIN684 Carrière de Miéville
ZG
102. .....Schieferkohlenkomplex Greit (BLN 1307)
ZH
103. GIN458 Deckenschotter Irchel
104. GIN740 Benken
105. GIN600 Käpfnach, Horgen
106. GIN596 Küsnachter Tobel
107. GIN601Tüfels, Chilen
108. GIN121 Lägern- Dielsdorf (= GIN223)

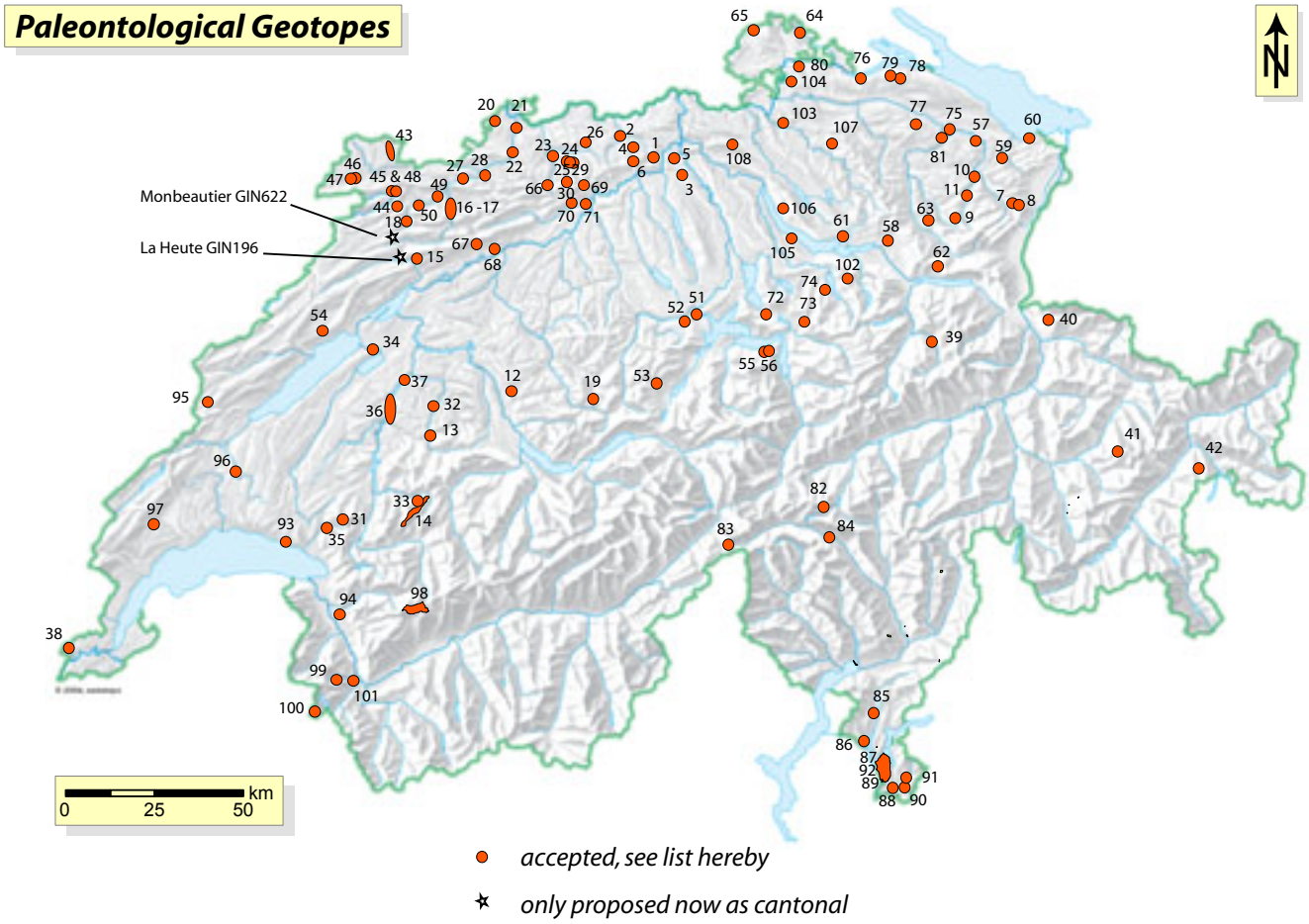

Figure 1. Map of paleontological geotopes of national significance

REFERENCES

Berger J.-P., Reynard E., Bissig G., Constandache M., Dumas J., Felber M., Häuselmann P., Jeannin P.Y., Schneider H. : Révision de la liste des géotopes d'importance nationale : rapport du groupe de travail 2006-2007. – Groupe de Travail pour les Géotopes en Suisse, 22 p.

Reynard E, Berger JP, Constandache M, Dumas J, Felber M, Häuselmann P, Jeannin PY, Martin S, Regolini G, Scapozza C, Schneider H : The revision of the inventory of geotopes of national significance. SGM Lugano, this volume

Special thanks to the BAFU and the Swiss Academy of Sciences (SCNAT) for financial support and to all the colleagues who help us to compile and choice paleontological sites.

3.5

Fossil assemblages from the early Late Cretaceous of southeast Morocco

Cavin Lionel *, Meister Christian*, Piuz André* & Boudad Larbi**

* *Dpt de Géologie et Paléontologie, Muséum de Genève, CP 6434, 1211 Genève 6, Suisse*
** *Faculté des Sciences et Techniques, BP, 509, Boutalamine, Errachidia, Maroc*

The Cretaceous deposits surrounding the northern, eastern and southern borders of the Palaeozoic Tafilalt and Mader basins have yielded numerous fossils for more than fifty years. First surveys by French geologists recorded Cenomano-Turonian ammonite assemblages (Basse & Choubert 1959), fish fragments in Turonian of the High Atlas and Midelt area (Dubar 1949), continental reptiles remains in the 'Grès Infra-cénomaniens', or 'Continental Intercalaire' of the Kem Kem region (Lavocat 1948, 1949).
During the following decades, only few palaeontological data about the 'mid-Cretaceous' of that area have been published. During the last thirty years, however, local people have engaged very active excavation works for collecting Cretaceous fossils for commercial purpose. Beautifully preserved specimens have been discovered by this way, but little information about sedimentological, startigraphic and geographical contexts is usually associated with this material.

Here we present preliminary results of fieldworks conducted by the authors in 2008. The goal of this study is to better understand the palaeoenvironmental and startigraphic contexts of the 'mid-Cretaceous' transgression in North-west Africa. In this study, we focused on microfossils, ammonites and fishes as indicators of age and environment changes.
We sampled in eight main localities along a north-south transect within the basin in order to detect lateral variations. The series started with continental and deltaic deposits (fig. 1), regarded as Albian-Cenomanian in age, which are topped by coastal then open marine deposits (fig. 2) corresponding to the Cenomanian-Turonian major transgression.

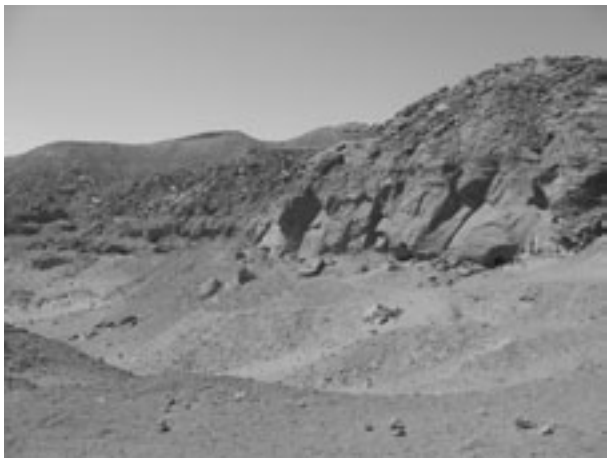

Figure 1. Albian-Cenomanian continental and deltaic deposits at the base of the series, Taouz (photo Cavin, L.).

Figure 2. Cenomanian-Turonian marine deposits at the top of the series, Belkassem (photo Piuz, A.).

REFERENCES
Basse, E., & Choubert, G. 1959: Les faunes d'ammonites du "Cénomano-Turonien" de la partie orientale du domaine atlasique marocain et de ses annexes sahariennes, C. R. 20th International Geological Congress. In L. B. Kellum (ed.) El Sistema Cretacico, 2, 59-81.
Dubar, G. 1949: Carte géologique provisoire du Haut-Atlas de Midelt, notice explicative. In: Notes et Mémoires du Service géologique du Maroc, 1–56.
Lavocat, R., 1948. Découverte de Crétacé à vertébrés dans le soubassement de l'Hammada du Guir (Sud marocain), C. R. Académie des Sciences, Paris 226, 1291–1292.
Lavocat R., 1949. Les gisements de vertébrés crétacés du Sud marocain, C. R. sommaires de la Société Géologique de France, 19, 125–126.

3.6

Correlation between morphology, behaviour and habitat – bivalve burrowing in simulation and robotics

Germann Daniel*, Schatz Wolfgang**, Hadorn Maik*, Fischer Andreas* & Eggenberger Hotz Peter*

*University of Zurich, Department of Informatics, Artificial Intelligence Laboratory, Andreasstrasse 15, CH-8050 Zurich (germann@ifi.uzh.ch)
**University of Lucerne, Pfistergasse 20, CH-6003 Lucerne

Bivalves show a large diversity of shell shapes and sculptures during their long history of evolutionary adaptations to different modes of life. The comparatively dense fossil record of bivalves, the well-defined morphological space and the quite complete picture of bivalvian phylogeny offer basis for an analysis of general evolutionary processes. However, while the fossil record conveys information about the shape and the habitat of bivalves, the interpretation of the functional morphology, locomotion and changes in shell shape is generally vague, as fossils represent only discrete states in the morphological space and suffer from the preservational bias. Thus, the purpose of this project is to extend the knowledge about the evolution of bivalves and their adaptations to burrowing using both a computer simulation and a burrowing robot. The simulation will cover the dynamics of burrowing as well as the evolution in morphology and behaviour, reconstructing a trajectory in the morphological space and analysing the processes inducing these state-shifts.

There already exist mathematical models of sea shells (e.g. Raup & Michelson 1965), models of granular media (e.g. van Wachem & Almstedt 2003), burrowing robots and simulations of artificial evolution, but they have never been combined. Our simulation consists of (i) models of recent, fossil and artificial bivalve morphospecies, (ii) a model of a granular medium including the physical interactions with the shell, (iii) an implementation of the burrowing sequence (cf. Trueman 1966) and (iv) an artificial evolutionary system. The artificial evolution may change parameters controlling the behaviour or the morphology of the bivalves. Using a computer simulation allows an efficient and systematic analysis of the burrowing efficiency by changing just a single parameter at a time.

The virtual shell models are converted into physical objects using a 3D-printer (Fig. 1). As a starting point for the physical experiments, finally leading to a self-sufficient burrowing robot, we will attach the shell to two rods simulating the rocking locomotion of the bivalve during the burrowing process (cf. Stanley 1975). In further steps, the opening and closing of the valves and finally an artificial foot probing into the sediment will be added to complete the robot. The data provided by the robot is used to calibrate the simulation and to assess the coherence of the model and the physical reality. After testing the biological significance of the simulation, we will explore the functional correlations between the shell shapes and sculptures, the burrowing behaviour and the sediment type.

As shown in earlier examples (Hadorn et al. 2004), a close collaboration between palaeontology and evolutionary computation/robotics can return profit for both scientific fields. A possible application of this research may be a tool for palaeontologists to link shell forms and the mode of life of fossil bivalves in a more sophisticated way. The simulation can be used to perform experiments with evolution, to identify functional constraints, to find explanations for aberrant and extinct shell forms and even to create and test shell forms that have never existed. By investigating the functionality not only of recent but also of fossil shells, the field of bionics could be remarkably extended. In industry, the robot might serve as a prototype for autonomous burrowing robots or removable and fixed anchorage of man-made structures in soft sediments.

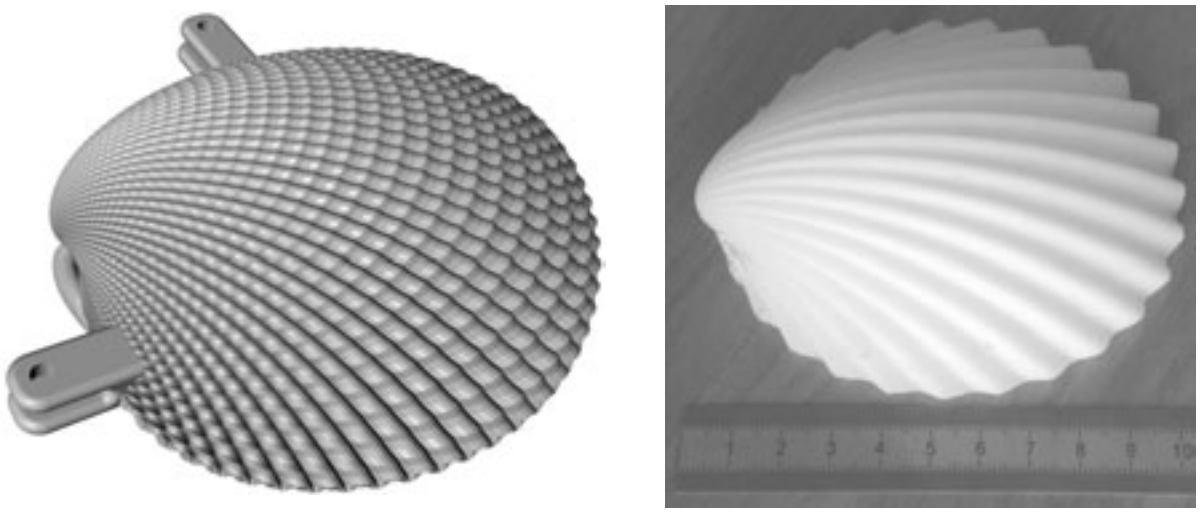

Figure 1. Left: An artificial shell generated by the simulation software with added sockets for the rods. Right: Photo of a valve printed by the 3D-printer (scale in centimetres).

This work is part of the Swiss National Foundation project no. 113934.

REFERENCES

Hadorn, M., Schatz, W. & Eggenberger Hotz, P. 2004: Were Adam and Eve Ediacarans? – A possible sexual dimorphism in Dickinsonia costata, Abstracts of the 2nd Swiss Geoscience Meeting.

Raup, D. & Michelson, A. 1965: Theoretical morphology of the coiled shell, Science, 147, 1294-1295.

Stanley, S. 1975: Why clams have the shape they have; an experimental analysis of burrowing, Paleobiology, 1, 48-58.

Trueman, E. 1966: Bivalve mollusks: Fluid dynamics of burrowing, Science, 152, 523-525.

van Wachem, B. & Almstedt A. 2003: Methods for multiphase computational fluid dynamics, Chemical Engineering Journal, 96, 81-98.

3.7

Smithian-Spathian boundary: the biggest crisis in Triassic conodont history

Goudemand Nicolas*, Orchard Mike**, Bucher Hugo*,***, Brayard Arnaud****, Brühwiler Thomas*, Galfetti Thomas*, Hermann Elke*, Hochuli Peter A.*,*** & Ware David*.

**Paläontologisches Institut und Museum der Universität Zürich, Karl Schmid-Str.4, CH-8006 Zürich (goudemand@pim.uzh.ch).*
***Geological Survey of Canada, Vancouver, Canada.*
****Department of Earth Sciences, ETH Zürich, Switzerland.*
*****LMTG, UMR 5563 CNRS, Université Toulouse IRD, France.*

Ongoing work in California, S-China, Tibet, Pakistan and Oman has led to a refined biochronologic subdivision of the late Early Triassic and allows reconstructing a high resolution diversity time series, partly constrained by new U-Pb ages from S-China (Galfetti et al. 2007a).

Conodonts crossed the PTB without major changes (Orchard 2007). In the Early Triassic the first major conodont faunal turnover occurred during the late Griesbachian - early Dienerian, with the disappearance of Anchignathodontids (*Hindeodus-Isarcicella* group), which were replaced by the emergent *Neospathodus* and *Borinella*? species.

In the earliest Smithian, conodonts experienced a dramatic radiation, which ended in a major extinction during the late Smithian. This extinction was the most severe of the entire Triassic in terms of generic diversity and multi-element apparatuses. In the early Spathian conodonts radiated again explosively and gradually declined during late Spathian times.

These global diversity patterns coincide with large perturbations of the global carbon cycle (Brühwiler et al. 2007; Galfetti et al. 2007b, Payne et al. 2004). As indicated by changes in the latitudinal gradient of generic richness of ammonoids, the boreal palynological record, and a prominent positive δ^{13}C-isotope shift, the late Smithian - early Spathian boundary interval is marked by a severe climatic change.

REFERENCES
Brühwiler T., Goudemand N., Galfetti T. & Bucher H. 2007: Early Triassic ammonoid biostratigraphy and a new high-resolution carbon isotope record from Tulong area, South Tibet. 5th Swiss Geoscience Meeting, Geneva.
Galfetti T., Bucher H., Ovtcharova, M., Schaltegger U., Brayard A., Brühwiler T., Goudemand N., Weissert H., Hochuli P. A., Cordey F. & Guodun K., 2007a: Timing of the Early Triassic carbon cycle perturbations inferred from new U-Pb ages and ammonoid biochronozones. Earth and Planetary Science Letters, 258, 593-604.
Galfetti T., Hochuli P.A., Brayard A., Bucher H., Weissert H. & Vigran O.V. 2007b: Smithian-Spathian boundary event: Evidence for global climatic change in the wake of the end-Permian biotic crisis. Geology 35:291-294.
Orchard M.J., 2007: Conodont diversity and evolution through the latest Permian and Early Triassic upheavals, Palaeogeography Palaeoclimatology Palaeoecology **252** (2007), 93-117.
Payne J.L., Lehrmann D.J., Wei J., Orchard M.J., Schrag D.P. & Knoll A.H., 2004: Large perturbations of the carbon cycle during recovery from the end-Permian extinction, Science **305 (2004)**, 506–509.

3.8

New data on the Bouwxiller Formation (Eocene, Lutetian)

Lavoyer Thibault & Berger Jean-Pierre

Département de Géosciences, Géologie et Paléontologie, Université de Fribourg, chemin du musée 6, CH-1700 Fribourg

The old quarry in Bouxwiller is a historical outcrop studied since the beginning of the XIXe century (Cuvier 1812). It is located in the village of Bouxwiller, in the western part of the North Middle Upper Rhine Graben in Alsace, France (Fig. 1). Previous studies from the marls situated below and above the Bouxwiller limestone dated the deposit to the mammal zone MP 13 (Jaeger 1971). This author postulates that the fauna of the two levels can be considered as homogeneous.

The outcroup consists of fossiliferous limestones and clays with a very small proportion of detrital elements.
All samples come from the “Ensemble supérieur” of the Bouxwiller formation, of the marly levels directly over- (coll. Lavoyer 2006-2007) and underlying (Collected by R. Isenmann during the eighties) the Bouxwiller limestone s.s. (Fig 2).

It has provided new fossils of several species, notably otoliths, mammal and reptilian teeth (crocodiles (with some serrated teeth (pristichampsids)) and lizard), fragments of turtle shells, osteoderms, charophytes (with *Maedleriella embergeri*), gastropods (*Planorbis* sp., *Hydrobia* sp., *Melanopsis* ?) and ostracods.

R. Isenmann has also provided access to his private collection, composed of reptilian and mammal teeth and bones. They originate from the green marls, in the upper part of the limestone/clay alternation just under the Bouxwiller limestone s.s.

The purpose of this work is to compare the various levels of the Bouxwiller Formation (biostratigraphy, paleoecology, taphonomy) and to confront these new data with the existing literature to confirm (or not) the homogeneity of the Bouxwiller fauna.

This study is a part of the PhD of T. Lavoyer and is financed by the SNF Project 200020-109457 and 200020-118025 “Paleontology and Stratigraphy of the South Rhine graben during the Paleogene”.

We thank Mr Rodolphe Isenmann for providing access to his personnal collection.

Figure 1. Location of the outcrop (modified from Berger et al. 2005)

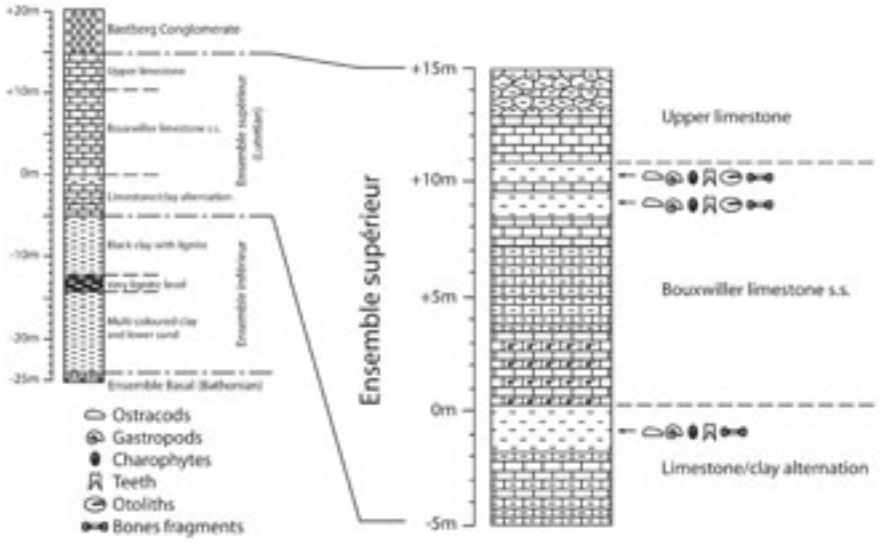

Figure 2. Lithology (modfied from Trauth et al. 1977)

REFERENCES

Berger J.-P. Reichenbacher B., Becker D., Grimm M., Grimm K., Picot L., Storni A., Pirkenseer C., Derer C., Schaefer A., 2005b. Eocene-Pliocene time scale and stratigraphy of the Upper Rhine Graben (URG) and the Swiss Molasse Basin (SMB). International Journal of Earth Sciences, 94(4): 711-731.

Cuvier G. 1812. Recherches sur les ossemens fossiles où l'on rétablit les caractères de plusieurs animaux dont les révolutions du globe ont détruit les espèces. E. d'Ocagne, Paris 3 : 1-436.

Jaeger J.-J.,1971. La faune des mammifères du Lutétien de Bouxwiller (Bas-Rhin) et sa contribution à l'élaboration de l'échelle des zones biochronologiques de l'Eocène européen. Bull Sci géol Alsace Lorraine 24(2-3):93-107

Trauth N., Cavelier C., Sommer F., Tourencq J., Pomerol C., Thiry M., 1977. Aperçu sur la sédimentation paléogène du synclinal de Bouxwiller, comprise entre les Marnes à Rynchonnelles (Bathonien) et le conglomérat du Bastberg (Oligocène). Sci. Géol. Bull, 30, 2, p. 91-100.

3.9

Methodology of systematic excavation and documentation of dinosaur tracksites along the Transjurane highway (Canton Jura, NW Switzerland)

Marty Daniel*, Paratte Géraldine*, Lovis Christel*, Jacquemet Mathilde*, Hug Wolfgang Alexander*, Iberg Andreas*, Oriet Amalric*, Denier Clemens**, Mihajlovic Dragan***

*Palaeontology A16, Section d'archéologie et paléontologie, Office de la culture, Hôtel des Halles, C.P. 64, CH-2900 Porrentruy 2, daniel.marty@palaeojura.ch
**Terradata AG, Mühlestrasse 9, CH-8840 Einsiedeln
***Photogrammetrie Perrinjaquet AG, Worbstrasse 164, CH-3073 Gümligen

Since 2002, the Palaeontology A16 excavates dinosaur tracksites near Porrentruy along the future course of the Transjurane highway A16 (Marty et al., 2007). This resulted in the development of a complex excavation-, documentation-, and protection-methodology of dinosaur tracks and tracksites.

First, tracksites are located by geological surveying followed by palaeontological prospecting with shovel excavators. Large-scale excavations are then planned and scheduled in agreement with the civil engineering office over one to several years prior to the construction of the highway. The tracks are found on multiple superimposed palaeosurfaces within horizontally-bedded biolaminites of Late Kimmeridgian age, which accordingly have to be excavated level-by-level. At the beginning of an excavation as much overburden as possible is removed with the help of shovel excavators. Within the biolaminites, the track-bearing levels are then excavated and cleaned with hand tools. This is often a time-consuming and difficult affair, because of normal faults displacing levels or because levels are amalgamated and cannot be followed laterally.

Tracks are then searched for, identified, and wherever possible attributed to trackways. This includes analyses at night with oblique lighting, indispensable to find and study small tracks and track details. Simultaneously, all tracks are outlined with black chalk and labelled on the surface itself using specified acronyms. Subsequently, the tracks and trackways are analyzed and described, and their parameters are measured in a consistent fashion and gathered in a database. They are also photographed including stereoscopic photographs of selected tracks. Further, macrosedimentary features (e.g., desiccation cracks, ripple marks) are analyzed and the encasing sediment is logged and sampled.

Afterwards, a georeferenced 2x2 meter grid is installed on the surface and tracks and normal faults are drawn at a scale of 1:10 or 1:20. These drawings are vectorized in the office and assembled in a map. Because outline drawings represent one person's simplified interpretation of a complex three-dimensional object, the most important palaeosurfaces are likewise documented with 3D imaging techniques using high-resolution (in the order of 1-2 mm) laser scanning and extreme close-range (2-10 m from camera to object) photogrammetry. These are merged in a virtual 3D model, on the basis of which tracks and trackways can easily be vectorized and their parameters measured in CAD software, if previously they were labelled and outlined with chalk. Similarly assembled data can later also be integrated into a GIS database.

If a surface is going to be destroyed or exposed to weathering after excavation the 3D documentation is the most accurate way to document its original state, especially if applied together with complementary, classical illustrative and descriptive techniques as well as replicas (see also Lockley & Matthews, 2007). Consequently, future generations of researchers will have access to virtually the same database. Nonetheless, judging by our own experience, the 3D methods cannot fully replace careful observations and descriptions of the actual tracks in the field because the interpretation of small tracks or track details (e.g., digital pads, claws, skin impressions), poorly-preserved tracks, and/or crossing trackways (track interferences) is a difficult and subjective task made at best on the original specimens. Also, 3D methods are expensive and cannot always be applied. Another drawback is that adequate safeguarding of the imaging data for posterity may be difficult to guarantee.

After their documentation, the most important tracks and trackways are either recovered as slabs or replicated, and then the underlying level is excavated. Such level-by-level excavation and documentation offer important insight into the formation, taphonomy, and preservation of tracks. Notably the identification of undertracks, true tracks, and overtracks, which is important for the correct ichnological and palaeoecological interpretation of the tracks (Marty, 2008).

At the end of an excavation recovered slabs, samples, and replicas are archived, and the documentation (e.g., photographs, track parameters, etc.) is assembled in a database (collection and documentation management). The main track level of the Transjurane tracksites is commonly located at the top of massive limestone and at the base of biolaminites. Consequently, it cannot be removed and will be either covered or (partially) destroyed by the construction of the highway. The importance of a tracksite has to be evaluated "in context" based on abundance, quality, and uniqueness of the tracks. Whenever possible it has to be preserved as a geotope *in situ*. Actually, at least two tracksites can be preserved for posterity by the construction of additional highway bridges. These outstanding results of cooperation between engineers and palaeontologists are the basic conditions for a public accessibility of the tracksites, managed and financed by the Canton Jura, once the highway will be finished.

REFERENCES
Lockley, M.G. & Matthews, N.A. 2007: Observations on scientific documentation and preservation strategies employed at hominid and other vertebrate tracksites in America and elsewhere. In: Kim, J.Y., Kim, K.S. (eds.), Proceedings of 2007 International symposium on the conservation and application of hominid footprints, 7th-9th December 2007, Jeju Island, Japan, 13-43.
Marty, D. 2008: Sedimentology, taphonomy, and ichnology of Late Jurassic dinosaur tracks from the Jura carbonate platform (Chevenez—Combe Ronde tracksite, NW Switzerland): Insight into the tidal-flat palaeoenvironment and dinosaur diversity, locomotion, and palaeoecology. GeoFocus, 21, 278 pp.
Marty, D., Ayer, J., Becker, D., Berger, J.-P., Billon-Bruyat, J.-P., Braillard, L., Hug, W.A. & Meyer, C.A. 2007: Late Jurassic dinosaur tracksites of the Transjurane highway (Canton Jura, NW Switzerland): overview and measures for their protection and valorization. Bulletin for Applied Geology, 12, 75-89.

3.10

A new Aquitanian fauna in the Jura Molasse (Sur le Mont, Tavannes, Northwestern Switzerland)

Mennecart Bastien*, Zulliger Luca*, Scherler Laureline*,**, Becker Damien**, & Berger Jean-Pierre*

*University of Fribourg, Department of Geosciences, Chemin du Musée 6, Pérolles, CH-1700 Fribourg (bastien.mennecart@unifr.ch)
**Section d'archéologie et paléontologie, Hôtel des Halles, Case Postale 64, CH-2900 Porrentruy

The construction of the Transjurane Highway (A16) in the Jura Mountains gave the opportunity to observe new outcrops in the Tavannes area (Canton Bern). The new vertebrate locality of Sur le Mont, located in the eastern part of the future tunnel of Tavannes, corresponds to three different fossiliferous levels of a fluvial sandy conglomeratic complex rich in mud pebbles. This series of around ten meters of thickness is stratigraphically situated just above the last freshwater deposits of the *Calcaires delémontiens* Formation. The microfossil assemblage essentially contains essentially charophytes. The vertebrate assemblage is composed by turtles, crocodiles, eggshells probably of birds, small carnivores, lagomorphs, and small and large ungulates. The presence of the taxa *Diaceratherium asphaltense* (Rhinocerotidae) and *Dremotherium feignouxi* (Ruminantia) allows to assign this fauna with confidence to the Aquitanian.

The *Calcaires delémontiens* were long time considered by numerous authors as exclusively Oligocene. These last ten years, Picot et al. (1999) and Becker (2003) showed that the top of this formation could correspond to the basal Aquitanian in some rare outcrops. However, this dating is most of time based on charophyte assemblages. Only the locality of SE Pré Godat (Canton Jura) and Waldenburg-Humbel (Canton Basel Land) were ascribed to the biozones MP30-MN1 on the basis of small mammal remains (see Theiler 1998 and Engesser & Mödden 1997). Additionally, Mojon et al. (1985) and Engesser & Mödden (1997) mentioned the well-known Aquitanian localities of Boudry (MN1) and La Chaux 7 (MN2). These localities belong respectively to the *Grès et Marnes grises à Gypse* and the *Calcaires de La Chaux* Formations and are located at the southern boundary of the Western Jura Mountains. Thus the top of the Sur le Mont section could be the youngest record of USM deposits within the Jura Molasse. It should allow to reconsider the classical "Aquitanian" gap within this structural unit and to give some light to the geodynamic evolution of the Jura Mountains (see Berger et al. 2005).

This study is supported by the Swiss National Foundation project (n°115995) on the large mammal evolution in the Swiss Molasse Basin during the Oligocene and early Miocene. More investigations will be made in the taxonomy of the fossil remains and biogeochemical analyses will complete this work. The aim is to better understand the palaeobiogeography and the palaeoenvironmental conditions during the early Miocene in Switzerland.

REFERENCES
Becker, D. 2003: Évolution paléoécologique et paléoclimatologique de la Molasse du Jura et sud-rhénane: utilisation des Périssodactyles (Mammalia) et des Minéraux argileux. PhD Thesis, University of Fribourg, Geofocus 9, 327 pp.
Berger, J.-P., Reichenbacher, B., Becker, D., Grimm, M., Grimm, K., Picot, L., Storni, A., Pirkenseer, C. & Schaefer, A. 2005: Eocene-Pliocene time scale and stratigraphy of the Upper Rhine Graben (URG) and the Swiss Molasse Basin (SMB). International Journal of Earth Sciences 94, 711-731.
Engesser, B. & Mödden, C. 1997: A new version of the biozonation of the Lower Freshwater Molasse (Oligocene and Agenian) of Switzerland and Savoy on the basis of fossil Mammals. In Aguilar, J.-P. et al. (Eds.): Actes du Congrès BiochroM'97.

Mémoires et Travaux de l'Ecole pratique des Hautes Études, Institut de Montpellier 21, 475-499.
Mojon, P.O., Engesser, B., Berger, J.P., Bucher, H. & Weidmann, M. 1985: Sur l'âge de la Molasse d'eau douce inférieure de Boudry, Neuchâtel. Eclogae geologicae. Helvetiae 78, 631-667.
Picot, L., Becker, D. & Berger, J.-P. 1999: Nouvelles données paléoécologiques et biostratigraphiques sur la formation des Calcaires delémontiens (« Delsberger Kalke », Oligocène terminal, Jura Suisse). Neues Jahrbuch für Geologie und Paläontologie Abhandlungen 214, 433-462.
Theiler, E. 1998: Geologie im Gebiet der Tiergartenantiklinale (JU) mit besonderer Berücksichtigung der Molasseeinheiten. Unpublished Master Thesis, University of Fribourg, 93 pp.

3.11

New excavations in the Cassina levels (Monte San Giorgio, Middle Triassic) preliminary reports

Renesto Silvio*, Lombardo Cristina**, Stockar Rudolf***

*Dipartimento di Biologia Strutturale e Funzionale, Università degli Studi dell'Insubria, via Dunant 3 I-21100, Varese, Italy (silvio.renesto@uninsubria.it)
**Dipartimento di Scienze della Terra, Università degli Studi di Milano, via Mangiagalli 34, I-20133 Milano, Italy (cristina.lombardo@unimi.it)
*** Museo Cantonale di Storia Naturale, viale C. Cattaneo 4, CH-6900 Lugano, Switzerland, (rudolf.stockar@ti.ch)

Among the calcilutite sequence of the Early Ladinian Lower Meride Limestone of Monte San Giorgio (Unesco WHL, Switzerland) three fossiliferous beds are known: the Cava inferiore, Cava superiore and Cassina beds. These latter were originally investigated in 1933 by the University of Zürich which carried out further excavations in 1937 and in the period 1971-1975. Along with different reptile taxa (e. g. *Ceresiosaurus lanzi, Neusticosaurus edwardsii, Macrocnemus bassanii* and *Tanystropheus meridensis*) a large fish fauna was collected then, dominated by well preserved *Saurichthys* (S. *curionii* and S. *macrocephalus)*, along with smaller actinopterygians referred to three different species: *Peltopleurus* sp. (one specimen, Bürgin 1992), *Archaeosemionotus* sp. nov. and *Macrosemiidae* gen. et sp. nov. (both listed in Bürgin 1999, but not described so far).

In 2006 the Museo cantonale di storia naturale (Lugano) undertook a new excavation in the Cassina beds at the type locality, to investigate bed by bed on a surface of about 40 m^2 the whole fossiliferous succession. In the new site the fossiliferous beds represent an almost 3m thick interval of mainly interbedded finely laminated, organic-rich shales and limestones with intercalated thicker bituminous micritic and marly limestones. Normal graded calcarenites, showing erosional surfaces and bearing scattered clearly reworked fossil fragments, suggest the instability of the basin margins and the occasional influence of turbidity currents. Volcaniclastic layers (tuffs and bentonites) are frequent throughout the section.

The new excavations revealed profitable, yielding an interesting vertebrate fauna. Besides isolated bones and teeth of sauropterygian reptiles, interesting and well-preserved fossil fishes have been found, providing further information about the extraordinary ichthyofauna from the Monte San Giorgio area.

In the Cassina beds both neopterygians, as *Archaeosemionotus* and *Eosemionotus*, and paleopterygians, as *Saurichthys* and *Peltopleurus*, are represented. The medium-sized *Archaeosemionotus* is characterized by the mosaic-like covering of the cheek and the well-developed dentition, probably adapted to an hemi-durophagous diet; this genus has been found in other levels from Monte San Giorgio, with at least three different species (Bürgin 1999). On the contrary, the smaller *Eosemionotus*, with its typical thin and elongate teeth on premaxillary and dentary bones and the small fins with large fulcra, is reported for the first time in these levels. *Peltopleurus*, is widely represented throughout the different levels of Monte San Giorgio, with a surprising intra- and interspecific variability (Bürgin 1992; Lombardo 1999).

The most abundant findings, however, belong to the large predator actinopterygian fish *Saurichthys*, with many complete and well preserved specimens (mainly S. *curionii*, but S. *macrocephalus* is also present). Among yet prepared material, four *Saurichthys* specimens contained several skulls of small specimens that can be identified as embryos. In one of these specimens, the embryos are very small and each skull is associated to a tiny, narrow and white cylinder (Fig. 1) that is either curled or comma shaped. Chemical investigation revealed that these structures are made of phosphate. The chemical compostion, size and structure of these cylinders compared to the associated skulls, suggests that they may well represent the fossilized musculature of the embryos and each segment corresponding to a somite. This finding is of great scientific relevance because it represents the first case of preservation of soft tissues and even of postcranial structures in embryos of *Saurichthys*.

REFERENCES

Bürgin, T. 1992: Basal Ray-finned fishes (Osteichthyes, Actinopterygii) from the Kalkschieferzone (Uppermost Ladinian) near Meride (Canton Ticino, Southern Switzerland). Eclogae geol. Helv. 88/3, 803-826.

Bürgin, T. 1999: Middle Triassic marine fish faunas from Switzerland. In Arratia G. & Schultze H.-P. (eds.): Mesozoic Fishes 2 – Systematics and Fossil Record. Pfeil, München, 481-494.

Lombardo, C. 1999: Sexual dimorphism in a new species of the Actinopterygian *Peltopleurus* from the Triassic of Northern Italy. Palaeontology, 42/4, 741-760.

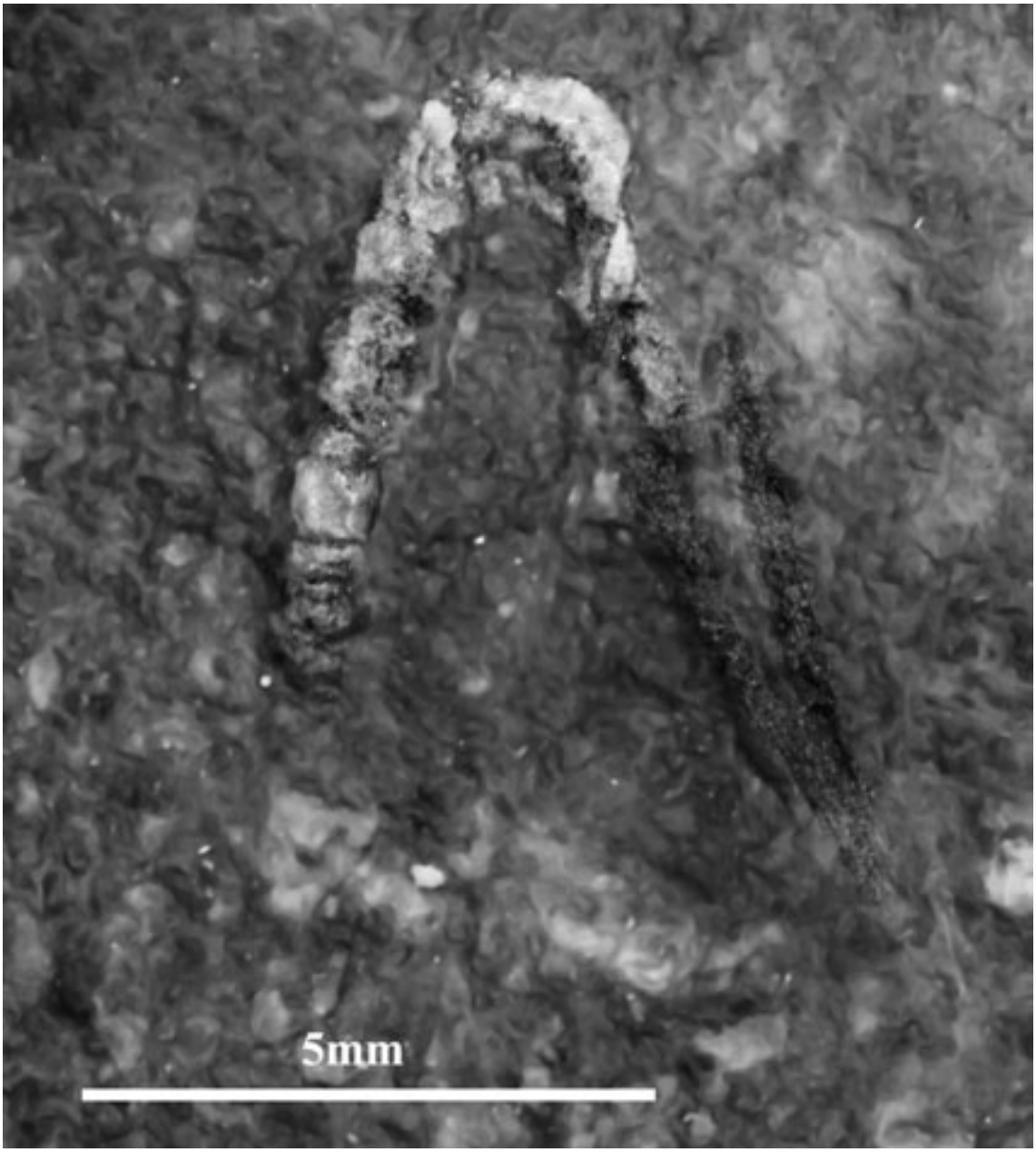

Figure 1. A small *Saurichthys* embryo with axial musculature preserved.

3.12

The revision of the inventory of geotopes of national significance

Reynard Emmanuel*, Berger Jean-Pierre**, Constandache Monica**, Dumas Joëlle**, Felber Markus***, Häuselmann Philipp****, Jeannin Pierre-Yves****, Martin Simon*, Regolini Géraldine*, Scapozza Cristian*, Schneider Hans*****

*Institut de Géographie, Université de Lausanne, CH–1015 Lausanne
(Emmanuel.Reynard@unil.ch)
**Département des Géosciences/Géologie, Université de Fribourg, CH–1700 Fribourg
***Consulenze geologiche e ambientali, CH–6834 Morbio Inferiore
****Institut suisse de spéléologie et de karstologie, CH–2300 La Chaux-de-Fonds
*****Office fédéral de l'environnement, CH–3000 Berne

In the early 1990s, a group of Earth scientists created the *Working Group for the protection of geotopes in Switzerland* (Strasser et al., 1995) and organised a first inventory of geotopes of national significance, published in 1999 (Swiss Academy of Sciences, Working Group for the protection of geotopes, 1999). A call for proposals was sent to Earth scientists, regional services, museums, universities and other interested institutions. From a preliminary list of more than 800 sites, 401 geotopes were selected and partly described and the list was published with a small abstract for each site. A map presenting the location of each geotope was also published but no legal status was given to the inventory. In 2006, a revision of the inventory was launched. The objectives were to re-evaluate each site, to complete the information available and to create a digital database for managing the data. This paper presents the methodology that was used, the different steps of the revision and the problems that the authors faced.

A database was created and each site was described and assessed. The evaluation was carried out by three disciplinary groups of scientists: geology, geomorphology and speleology. The criteria used for assessing the quality of sites are those developed by V. Grandgirard (1999). The scientific quality of the sites was evaluated, based on criteria such as rarity, representativeness and integrity, and information on other interests – educational value, ecological interest, archaeological interest, etc. – were also taken into account. Information on the integration of sites in other federal and cantonal inventories (e.g. mire landscapes, alluvial zones, landscapes of national significance, cantonal inventories of geotopes, etc.) was also collected. For each site, one or more photographies were collected, and a map showing the indicative perimeter and location was created in a GIS environment. For speleological sites, topographic sketches were also integrated in the database.

At the moment, 248 sites have been accepted as geotopes of national significance by the assembly of the working group (fig. 1), about 100 sites necessitate more information and need a new evaluation, and 50 sites were rejected. About 80 supplementary potential geotopes have been proposed by members of the working group and by some cantonal administrations. A second phase of assessment has therefore begun in 2008 and will be completed at the end of 2009. The publication of the full inventory is planned for 2010.

We faced several problems. Because experts based the inventory carried out in the 1990s on proposals, the spatial and thematic representativeness of the current list is not sufficient. Some geological objects (e.g. erratic boulders, morainic systems) are over-represented, whereas others (e.g. rock glaciers, structural or hydrological sites) are not sufficiently taken into account. Thematic and geographical gaps were therefore discussed during a forum organised in June 2008 in Fribourg, where specialists of various Earth science fields could propose new sites. A second important issue is the uniformity and quality of the inventory. Because the assessment was not carried out in a systematic manner, the content of the assessment cards is variable. A quality assessment will therefore be carried out in 2009. The third phase of the project will be to promote the inventory both in the political circles and in the tourist domain, especially by promoting the creation of geoparks in areas where the geological heritage is particularly rich. Data will also be sent to the Cantons, asking them to protect legally the most vulnerable sites.

REFERENCES

Berger, J.-P., Reynard, E., Bissig, G., Constandache, M., Dumas, J., Felber, M., Häuselmann, P., Jeannin, P.-Y. 2008: Révision de la liste des géotopes d'importance nationale: rapport du groupe de travail 2006-2007. Fribourg, Groupe de travail pour les géotopes en Suisse, 17 p.

Grandgirard, V. 1999: L'inventaire des géotopes. Geol. Insubr. 4, 59-66.

Strasser, A., Heitzmann, P., Jordan, P., Stapfer, A., Stürm, B., Vogel, A., Weidmann, M. 1995: Géotopes et la protection des objets géologiques en Suisse. Fribourg, Groupe Suisse pour la protection des géotopes.

Swiss Academy of Sciences, Working group for the protection of geotopes. 1999: Inventory of geotopes of national significance. Geol. Insubr. 4, 25-46.

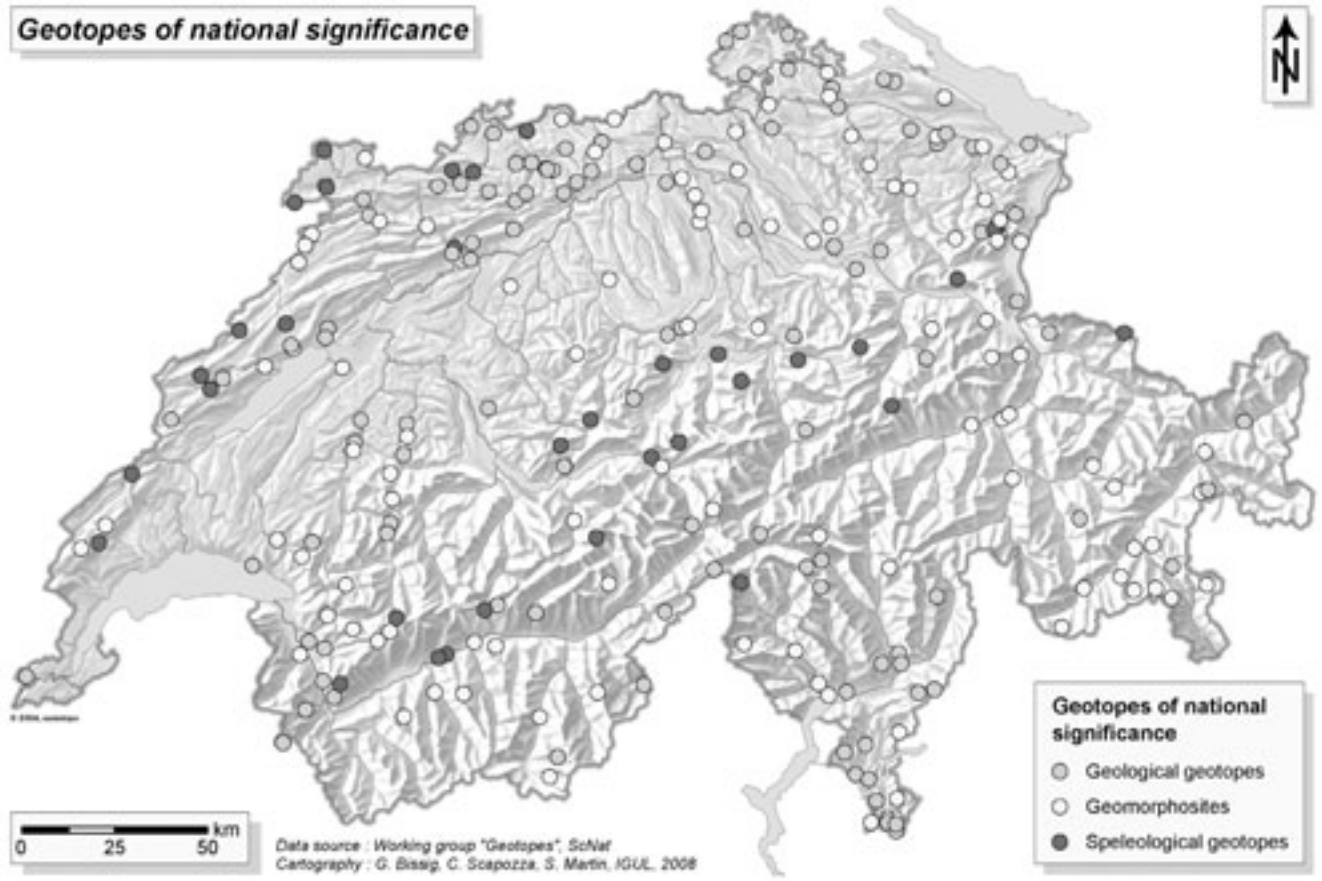

Figure 1. The preliminary map of geotopes of national significance (248 sites). The map will be completed in 2009 with a second round of evaluation.

3.13

Tapiridae (Perissodactyla, Mammalia) of the Swiss Molasse Basin during the Oligo-Miocene transition: taxonomical study and preliminary results.

Scherler Laureline*,**, Mennecart Bastien*, Becker Damien** & Berger Jean-Pierre*

*Department of Geosciences, Institute of Geology, ch. du Musée 6, Pérolles, CH-1700 Fribourg (laureline.scherler@unifr.ch)
**Section d'archéologie et paléontologie, Hôtel des Halles, CP64, CH-2900 Porrentruy

The systematics of the European tapirids has been prone to a major revision in the last few years (Cerdeño & Ginsburg 1988; Heissig 1999). Four genera are present in Europe from the Oligocene to the Pleistocene, where they disappear: *Protapirus, Paratapirus, Eotapirus* and *Tapirus*.

During the Oligo-Miocene transition several localities of the Swiss Molasse Basin record fossils of Tapiridae, such as Aarwangen (MP27), Ebnat-Kappel (MP28), Rüfi bei Schänis (MP29), Haslen (MP30? or MN3?), Wischberg (MN1), Höhronen (MN1-2?) and Brüttelen (MN3a). Their biostratigraphical record ranges from MP27 to MN3, highlighting the Oligo-Miocene transition (see fig. 1).

The tapirid remains are relatively scarce at the end of the Oligocene, represented for example by a mandible of *Tapirus* sp. in Ebnat-Kappel and a fragmented maxilla in Rüfi bei Schänis, or a skull and a mandible of *Paratapirus helvetius* in Haslen. The remains are more abundant in the Early Miocene, with a skull and a mandible of *Eotapirus broennimanni* in Wischberg and some mandibles and maxillas of *Tapirus intermedius* and *T. helveticus* in Höhronen. These determinations must be clarified —

only remains of Haslen and Wischberg have been reviewed — as *Tapirus* is a genus coming in Europe only in the Middle Miocene.

During this time interval, changes in the large mammal faunal record can be observed:

- in the anthracotheriid community with the extinction in MP29 of *Anthracotherium* and *Microbunodon* (N'Guyen 2008, Scherler in progress);
- in the suid community with the appearance in the Early Miocene of *Hyotherium, Aureliachoerus* and *Bunolistriodon* (Scherler in progress);
- and also in the rhinocerotid (Becker 2003) and ruminant (Mennecart in progress) comunities.

The Swiss tapirids are then expected to bring some precisions upon these environmental changes.

As part of a Swiss National Foundation project (n°115995) started in January 2007, the large mammal evolution studies in the Swiss Molasse Basin during the Oligocene and Early Miocene are aiming for a better understanding of the palaeobiogeography and the palaeoenvironmental conditions. These reconstructions will be obtained through taxonomical determinations and different proxies such as biogeochemical or palaeoecological analyses.

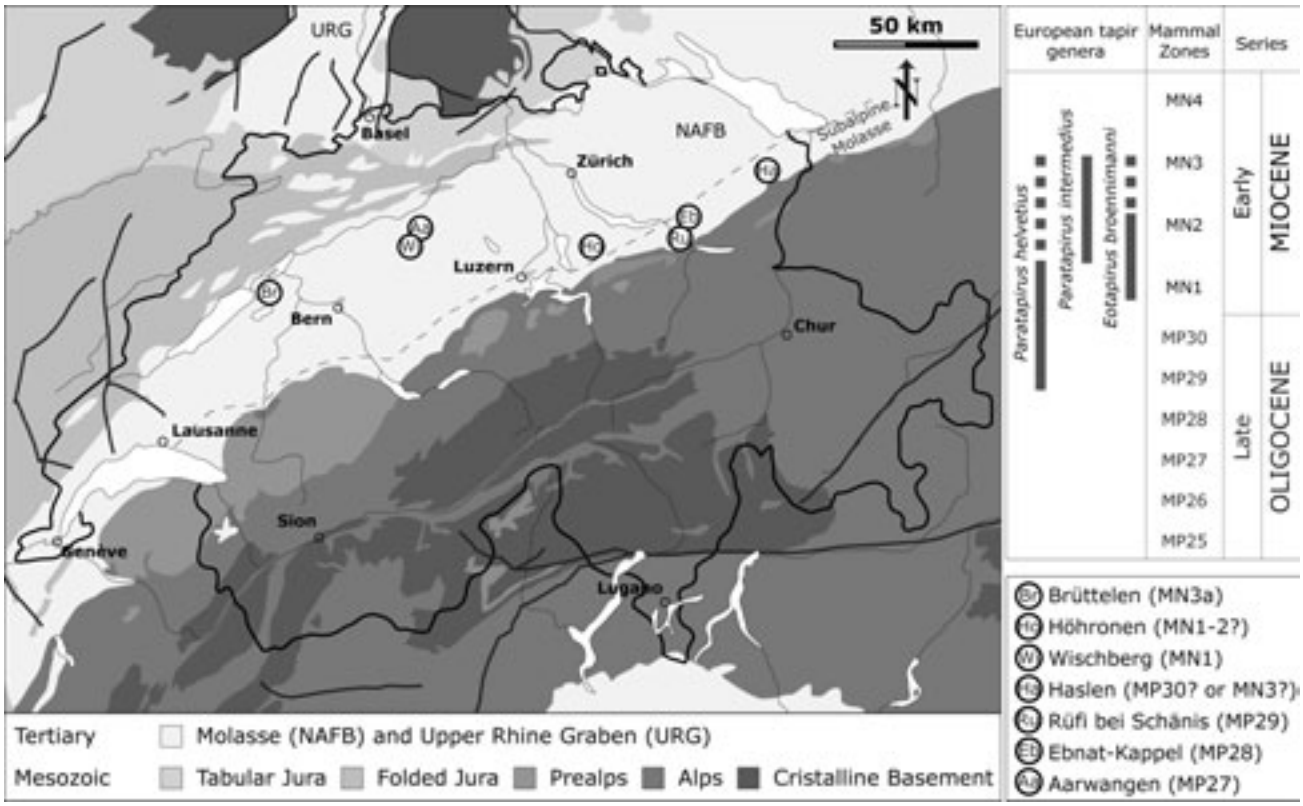

Figure 1. Geographical and geological setting of the Swiss localities recording tapirid remains, with the biostratigraphical extensions of the swiss species.

REFERENCES

Becker, D. 2003: Paléoécologie et paléoclimats de la Molasse du Jura (Oligo-Miocène): apport des Rhinocerotoidea (Mammalia) et des minéraux argileux. GeoFocus, 9, 328 pp.

N'Guyen, T.B. 2008: Die Anthracotherium des Oligozäns der Schweizer Molasse: Stratigraphie, Paläoökologie und Paläoklima. Unpublished Diploma Thesis, University of Fribourg, 138 pp.

Cerdeño, E. & Ginsburg, L. 1988: Les Tapiridae (Perissodactyla, Mammalia) de l'Oligocène et du Miocène inférieur européens. Annales de Paléontologie, 74, 71-96.

Heissig, K. 1999: Family Tapiridae. In: Rössner, G. & Heissig, K. (Eds.): Land Mammals of Europe. Verlag Dr. Friedrich Pfeil, München, 171-174.

Mennecart, B. in progress: The Ruminantia and Cainotheriidae (Mammalia, Artiodactyla) from Oligocene to Early Miocene of Switzerland, reassessment and new data on their phylogeny, palaeoecology and palaeoenvironment. PhD Thesis, University of Fribourg.

Scherler, L. in progress: Large mammal evolution (Anthracotheriidae, Suidae, Tapiridae) from the Swiss Molasse during the Oligo-Miocene: biostratigraphy, biogeochemistry, palaeobiogeography and palaeoecology. PhD Thesis, University of Fribourg.

3.14

How similar are morphological and genetic diversities recognizable on a typical plankton filter?

Schweizer Magali*, Thierstein Hans*, Schulz Hartmut** & Darling Kate***

*Geological Institute, ETHZ & University of Zurich, Universitaetsstrasse 6, CH-8092 Zurich (magali.schweizer@erdw.ethz.ch)
**Institute for Geosciences, Eberhard-Karls-Universitaet Tuebingen, Sigwartstrasse 10, D-72076 Tuebingen
***School of GeoSciences and Institute of Evolutionary Biology, University of Edinburgh, Edinburgh EH9 3JW, UK

Coccolithophore sequences currently available from GenBank concern almost exclusively cultured strains. Recently, it has been shown that it is possible to retrieve DNA from dried filters (Scherrer et al., oral contribution). This opens new perspectives for research on environmental coccolithophore samples collected by filtration.

Here we evaluate how easy it is to link SEM observations of coccolithophores and other organisms with DNA sequences obtained from a single filter piece. For that purpose, we cut small filter fragments containing low numbers of planktic organisms collected in the Arabian Sea. The filter fragments were coated and scanned in a SEM to document all the recognizable organisms on them; DNA was then extracted from each filter piece. The DNA extractions were amplified with universal and specific primers for SSU rDNA and the positive amplifications were cloned. About 60 different clones were sequenced.
None of the coccolith bearing taxa recognizable with the SEM was identified in the DNA sequences. The majority of the sequences belong to Prymnesiophyceae that bear no hard parts and were therefore not identified in the SEM. New primers are currently being developed to specifically amplify coccolith bearing taxa that may have been out-competed by naked ones during amplification.

3.15

Two late Triassic biostroms levels as key beds for controlling sea level changes in central Iran

Yazdi Mehdi * , Mannani Maryam*

*Department of Geology, University of Isfahan, Iran, (yazdimehdi@yahoo.com), *(mannani_m@yahoo.com)

This research focused on a pair of biostrom levels in age of Late Triassic in Central Iran (North of Isfahan, Bagher Abad Area). For the first time the appearance and extinction of Genus Heterastridium traced within these biostrom levels. The increasing depth of water from Bidestan Member to Howz- e- Khan Member prepared a good and nutrial paleoenvironment for near shore biota such as: gastropods, bivalves, corals, sponges and crinoids. The changing of silica clastic continental sediments (Middle Triassic) to carbonate component confirmed the deepening phenomena in Late Triassic as well. A regression or decreasing the depth of water happened after end of Howz- e- Khan member (Rheatian). As a result of regression, a mass extinction had happened (wipe out all biota group) in the end of Rheatian to Liassic. Several researchers reported the presence of Late Triassic biota from Iran such as Hautmann, M.,(2001), Kluyver, H. M., Griffis, R. J., Tirrul, R., Chance, P. N and Meixner, H. M., (1983). *Heterastridium* spp. Can be seen in Bagher Abad, Delijan, Soh, Abyaneh, Kalahroud Ferdus, Tabas, Parvadeh, Kerman, Lakar Kuh and Dige rostam. Some of these localities such as Soh, Abyabeh, Kalahroud, Bagher Abad areas (North of Isfahan) *Heterastridium* spp. (marine environment) can be seen as paralic sea within continental coal bearing environment. Finally we proposed that these biostrumal levels (Bagher Abad Area) can be used as Key beds for correlating Late Triassic deposits in Iran and neighboring countries as well as Alpine Region.

REFERENCES

Hautmann, M. 2001: Die Muschelfauna der Nayband – formation (obertrias, Nor- Rhät) des östlichen Zentraliran: Beringeria, 29: 1- 181.

Kluyver, H. M., Griffis, R. J., Tirrul, R., Chance, P. N & Meixner, H. M. 1983: Explanatory text of the Lakar Kuh Quadrangle Map 1: 250,000: Geological Survey of Iran, J9: 1- 175.

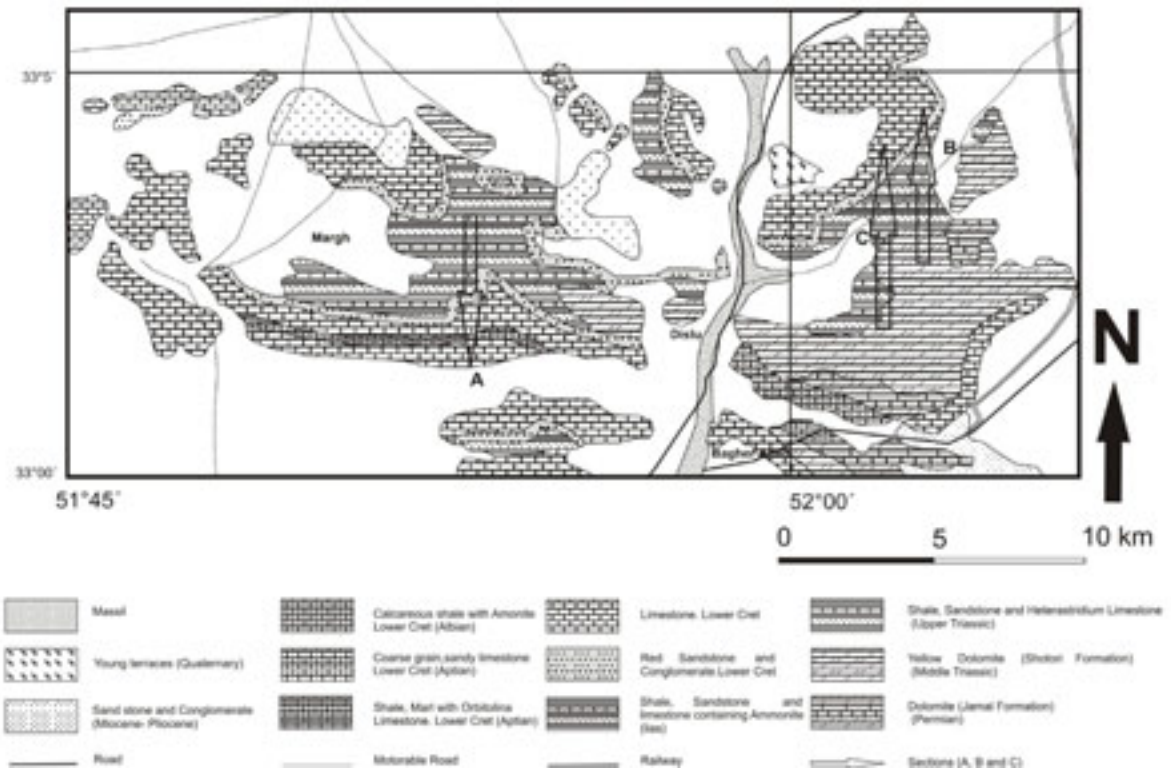

Fig.1 Geological map of north of Isfahan (Central Iran)

4. Meteorology and Climatology (open session)

Rolf Philipona, Markus Furger

Swiss Meteorological Society

4.1

Electron microscopy of aerosols

Barthazy Eszter

ETH Zürich, Institut für Atmosphäre und Klima, Universitätsstrasse 16, 8092 Zürich
Und
Elektronenmikroskopie Zentrum ETH Zürich, Wolfgang-Pauli-Strasse 16, 8093 Zürich
(eszter.barthazy@emez.ethz.ch)

The CIRRUS-III field experiment took place in November 2006 in Northern Germany. The objective of the campaign was to investigate midlatitude frontal cirrus clouds and the environment in which they form in order to better understand their formation mechanisms. Measurements were made with the enviscope Learjet. Six flights were conducted over the altitude range from 7-12 km, corresponding to the upper troposphere/lower stratosphere. Aerosols were sampled on TEM grids for analysis in a transmission electron microscope.

The aerosol samples were investigated with a Philips transmission electron microscope CM30, working with 300 kV. Results are shown of aerosols sampled in dry air, within clouds and from a flight through stratospheric air. Size distributions were analysed as well as the composition according to different aerosol types. Sulfuric acid aerosols were abundant in in-cloud samples. One sample showed almost exclusively soot particles. Organics and mineral dust aerosols were less frequent. The type of the aerosols were determined using EDX (electron dispersive X-ray spectrometer) by identifying the elemental composition of single aerosols.

4.2

Digitization and homogenization of long-term climate series from surface observation stations in Switzerland – DigiHom

Füllemann Christine*, Begert Michael*, Brönnimann Stefan**, Croci-Maspoli Mischa*

*Swiss Federal Office of Meteorology and Climatology MeteoSwiss, Krähbühlstrasse 58, CH-8044 Zurich (christine.fuellemann@meteoswiss.ch)
** Swiss Federal Institute of Technology, Institute for Atmospheric and Climate Science, Universitätstrasse 16, CH-8092 Zurich

The term DigiHom combines the intentions at MeteoSwiss i) to digitize long-term surface time-series from historical paper data and ii) to homogenize the complete data series with respect to make accurate estimates of the dimension of climate change and the corresponding effects. The goal of DigiHom is to make an important contribution to the national and international climate observation system by means of long-term climate series of Switzerland.
DigiHom has a time-frame from 2008-2011 and is accomplished in close collaboration with ETH Zurich who has profound experience in the digitization process (Brönnimann et al., 2006). The homogenization process will be carried out at MeteoSwiss using a well established homogenization procedure (THOMAS, Tool for Homogenization of monthly data series, cf. Begert et al. 2005).
The surface observation stations processed within DigiHom are the long–term climate series of the newly defined Swiss National Basic Climatological Network (Swiss NBCN). This network defines the most valuable climatological stations in Switzerland and accordingly guarantees a long-term perspective of their operation. The Swiss NBCN consists of 28 climatological stations (different parameters), presented in Begert et al. (2007) and 46 precipitations stations (Begert, 2008) covering respectively all climatological regions of Switzerland (Fig. 1). Representative climatological regions for the different surface observation stations have been calculated using the complete-linkage cluster analysis.
After the successful completion of DigiHom in 2010 the following climatological variables will be available electronically and in high-quality back to the year of their origin (most of them before 1900): temperature (mean, minimum, maximum), precipitation and sunshine duration. Although the coverage of stations at different altitudes is quite good, stations with multivariate time series are mainly located below 1000m asl (see Fig. 2). Higher elevated stations generally offer mean temperature and precipitation series. 6 NBCN stations have all parameters starting before 1901.
In this study the technical background to accomplish DigiHom will be presented and first results of homogenized long-term time-series will be introduced.

Figure 1. The 74 NBCN surface observation stations in Switzerland separated as 28 climatological stations (different parameters) and 46 precipitation stations.

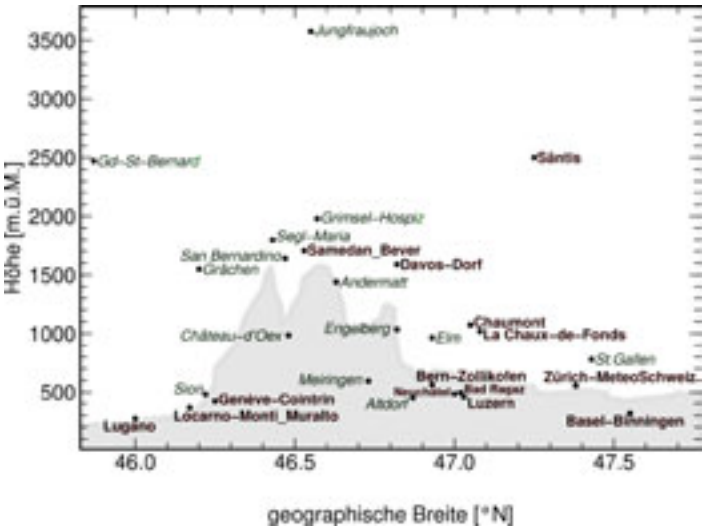

Figure 2. Distribution of the 28 climatological NBCN stations in relation to latitude and altitude.

REFERENCES

Begert M., Schlegel T., Kirchhofer W. 2005: Homogeneous temperature and precipitation series of Switzerland from 1864 to 2000. Int. J. Climatol. 25, 65-80.

Begert, M., Seiz, G., Foppa, N., Schlegel, T., Appenzeller, C., Müller, G. 2007: Die Überführung der klimatologischen Referenzstationen der Schweiz in das Swiss National Climatologial Network (Swiss NBCN), Arbeitsberichte der MeteoSchweiz, 215, 43p.

Begert, M. 2008: Repräsentativität der Stationen im Swiss National Basic Climatological Network. Arbeitsberichte der MeteoSchweiz, 217, 40p.

Brönnimann, S., Annis, J., Dann, W., Ewen, T., Grant, A. N., Griesser, T., Krähenmann, S., Mohr, C., Scherer M., Vogler C. 2006: A guide for digitising manuscript climate data. Climate of the Past, 2, 137-144.

4.3

Operational nowcasting of thunderstorms in the Alps using TRT during MAP D-PHASE

Hering Alessandro, Germann Urs & Boscacci Marco

Swiss Federal Office of Meteorology and Climatology (MeteoSwiss), Via ai Monti 146, CH-6605 Locarno-Monti, (alessandro.hering@meteoswiss.ch)

The MAP Forecast Demonstration Project D-PHASE was an excellent opportunity to demonstrate in real-time the performance of the operational nowcasting system TRT (Thunderstorms Radar Tracking). Since 2003 MeteoSwiss runs this real-time object-oriented nowcasting tool, as a part of its severe thunderstorms nowcasting, warning and information system. TRT is a multiple-radar, multiple-sensor system that uses heuristic and centroid-based methods for the automatic detection, tracking, characterisation and extrapolation of intense convective cells. TRT was used during MAP D-PHASE as one of the operational nowcasting systems in the Alpine area, and was available in real-time on the project visualisation platform.

The current version of TRT fully exploits volumetric reflectivity data of multiple-radar composites to describe the 3D storm structure, and has been expanded to a multiple-sensors system including cloud-to-ground lightning flashes. TRT is tuned to identify individual cells rather than storm systems, hence the evolution of cell-based attributes like e.g. VIL (Vertically Integrated Liquid), 15/45 dBZ echo tops, the altitude of maximum storm reflectivity, and cloud-to-ground lightning flashes is available to the forecasters in real-time.

The latest improvement in TRT is the “cell severity ranking” nowcasting product, developed for MAP D-PHASE and tested in

real-time on the visualisation platform during the demonstration period from June to November 2007. The goal of this product is to find and highlight the most dangerous and strongest cells, and to enhance the reliability and timeliness of severe convection warnings. To this purpose thunderstorm cells are classified into four distinct categories based on their severity and represented by a colour coded ellipse. The severity categories are computed integrating the three cell-based attributes VIL, mean of 45 dBZ Echo Top altitude, and maximum cell reflectivity, with a weighting scheme.

The new product includes also a 60 minutes position forecast. The estimated future position of the thunderstorms is computed based on the motion of individual cells, using their weighted displacement velocities. The expected position is shown with a colour coded ellipse and takes into account the spread (standard deviation) of the velocity vectors from the last three 5min time steps. The size of the ellipse is proportional to the uncertainty of the position forecast.

The presentation will focus on the added value of the new cell severity ranking product, which combines together the 3D-radar attributes VIL, 45 dBZ Echo Top, and maximum reflectivity.

4.4

Assessing fossil fuel CO_2 fluxes in the urban atmosphere of the city using combined measurements of CO_2, CO and $^{14}CO_2/^{12}CO_2$ mixing ratios

Jelen Dorota, Kuc Tadeusz, Necki Jaroslaw, Rozanski Kazimierz, Zimnoch Miroslaw

AGH University of Science and Technology, Al. Mickiewicza 30, 30 − 059 Krakow, Poland (djelen@novell.ftj.agh.edu.pl)

Emissions of carbon dioxide related to burning of fossil fuels constitute an important component of the carbon budget, both on global and regional scales. For heavily industrialized and populated areas such as western and central Europe, a large proportion of the total CO_2 flux entering the atmosphere is attributed to this source. Global and regional models of carbon cycle rely mainly on emission statistics to quantify the magnitude and variability of the fossil CO_2 flux into the atmosphere.

Krakow (50°04'N, 19°55'E, 220 m a.s.l.) is a large urban agglomeration located in the southern Poland, with about 1 million inhabitants, rapidly growing car traffic and significant industrial activities. Consumption of coal, gas and oil for communal and transport purposes generates major fluxes of anthropogenic carbon dioxide and carbon monoxide within the region. In addition, due to prevailing westerly air circulation, the Krakow region is under substantial influence of a large coal mining and industrial centre (Upper Silesia) located approximately 60 km west of the city.

The $^{14}CO_2/^{12}CO_2$ ratios measured in Krakow since 1983 testify major changes in economy of the region which have occurred since 1989. The ^{14}C signature of atmospheric CO_2 reflects significant changes in anthropogenic CO_2 fluxes released into the atmosphere both on local and regional scales. The contribution of fossil-fuel derived CO_2 in the total CO_2 load of the lower atmosphere in Krakow decreased from approximately 21 ppm in 1989 to around 10-12 ppm in the last few years. This change is linked with major reduction in coal consumption in Poland, from ca. 160 Mt in 1985 to 84 Mt in 2004.

The measurements of CO concentrations in urban atmosphere can serve as a substitute for costly determinations of $^{14}CO_2/^{12}CO_2$ mixing ratios, provided that the ratio CO/CO_2(fossil) is determined for the given area and its variability is adequately characterized. The average value of CO/CO_2(fossil) ratio derived for the period April 2003 - April 2006 for Krakow region is equal 27.6 ± 4.2 ppb CO per ppm of fossil CO_2. No distinct seasonal changes of this ratio were detected so far. Occasionally, very high (above 70 ppb/ppm) and very low (below 10 ppb/ppm) values of the CO/CO_2(fossil) ratio have been observed. The emission-based CO/CO_2 ratios reported for the period 1998-2005 for major industrial sources in the Krakow region are in the range between 7.3 and 10.8 ppb CO per ppm of fossil CO_2. However, they do not comprise emissions related to car traffic which is an important source of fossil fuel CO_2.

REFERENCES

Kuc, T. Rozanski, K., Zimnoch, M., Necki, J., Chmura, L., Jelen, D. 2007. Two decades of regular observations of $^{14}CO_2$, and $^{13}CO_2$ content in atmospheric carbon dioxide in central Europe: long-term changes of regional anthropogenic fossil CO_2 emissions. Radiocarbon, 49(2), 807-816.

Levin, I., Kromer, B., Schmidt, M. and Sartorius, H. 2003. A novel approach for independent budgeting of fossil fuels CO_2 over Europe by $^{14}CO_2$ observation. Geophys. Lett., 30(23); 2194.

4.5

Changes in integrated water vapor above Switzerland over the last 12 years

Morland June*, Collaud Coen Martine**, Hocke Klemens*, Jeannet Pierre**, Mätzler Christian*

*Institute of Applied Physics, University of Bern, Sidlerstrasse 5, CH-3012 Bern, Switzerland (June.Morland@iap.unibe.ch)
**MétéoSuisse, Station aérologique, CH-1530 Payerne, Switzerland

Water vapour is the strongest natural greenhouse gas. Under the assumption of constant relative humidity, the Clausius Clapeyron equation predicts a water vapor increase of 6 % per degree Kelvin increase in atmospheric temperature. Model simulations have shown that the water vapor feedback effect increases the climate sensitivity to rising greenhouse gas concentrations Studies with radiosonde (Ross and Elliott, 2001) and ERA40 (Trenberth et al., 2005) datasets showed large scale trends in Integrated Water Vapour (IWV) of up to +0.04 mmyr^{-1} (+0.13 %yr^{-1}) for the 1975-1995 and 1988-2003 periods, respectively. However, no significant trends were detected over Europe . On the other hand, a study of IWV from 33 ground-based GPS receivers in Sweden and Finland indicated trends of between -0.05 and +0.1 mmyr^{-1} (-0.14 and +0.75 %) with errors of around 0.04 mmyr^{-1} (Nilsson and Elgered, 2008).
Ground based microwave radiometers offer an independent source of atmospheric information from both radiosonde and analysis data. In the present study, IWV was calculated from the TROWARA (TROpospheric WAter RAdiometer) microwave radiometer in Bern for the period 1996-2007. Standard homogenisation techniques (Vincent, 1998) were used to correct for biases caused by instrument problems in the initial period up to 2002. IWV between 850 and 200 hPa was calculated from ECMWF analysis data for the closest gridpoint to Bern. IWV between 850 and 200 hPa, RS (850-200), as well as between the surface and 200 hPa, RS (s-200), was calculated from the Payerne radiosonde data.
Annual trends were calculated using the Least Squares Analysis (LSA) and monthly trends were calculated using the seasonal Mann Kendall (MK) technique following the methods described in Collaud Coen et al, 2007. In the following discussion, trends are given in mm or %yr^{-1} and the standard error is given afterwards in square brackets. Figure 1 shows the annual trends for all data, midnight and midday datasets calculated using LSA. The TROWARA midday trends are larger than all day or midnight trends, whilst RS and ECMWF data show higher midnight trends. The fact that RS and ECMWF agree more closely than RS and TROWARA is not surprising given the fact that the Payerne radiosonde is assimilated in the ECMWF analysis.
The RS (s-200) midnight trend of +0.087 [0.046] mmyr^{-1} or 0.55 [0.29] %yr^{-1} is significant at the 90 % level. The TROWARA midday trend (+0.098 [0.061] mmyr^{-1} or 0.70 [0.43] %yr^{-1}) and RS (s -200) trend (+0.068 [0.043] mmyr^{-1} or +0.45 [0.29] %yr^{-1}) for all observations are statistically significant at the 89 % level. These findings are within the range of trends reported by Ross and Elliott (2001), Trenberth et al. (2003) and Nilsson and Elgered (2008). Analysis with the MK technique showed a significant positive trend in July of +0.19 [0.14] to +0.34 [0.25] mmyr^{-1} (+1.2 [0.8] to +1.6 [1.1] %yr^{-1}) for all three datasets. In December, ECMWF and TROWARA indicated a significant negative trend of -0.20 [0.14] and -0.36 [0.24] mmyr^{-1} (-3.6 [2.5] and -4.3 [2.9] %yr^{-1}), respectively. This is consistent with the findings of Nilsson and Elgered (2008), who observed the strongest positive IWV trends in summer and frequently observed negative trends in winter.
The three datasets showed consistent positive annual trends from 1996 to 2007. A longer observing period is needed in order to establish significance, whist observations over several decades are required to distinguish anthropogenic influences from decadal oscillations in the climate system.

REFERENCES

Collaud Coen M., Weingartner, E., Nyeki, S., Cozic, J., Henning, S., Verheggen, B., Gehrig, R. & Baltensperger U. 2007:, Long-term trend analysis of aerosol variables at the high-alpine site Jungfraujoch, J. Geophys. Res., 112, D13213, doi:10.1029/2006JD007995.

Nilsson, T. & Elgered G. 2008: Long Term Trends in the Atmospheric Water Vapor Content Estimated from Ground-Based GPS Data, in Measuring and modelling variations in the distribution of atmospheric water vapour using GPS, Tobias Nilsson, PhD Thesis, Chalmers University of Technology, Göteborg, Sweden.

Ross, R. J.& Elliott W. P. 2001: Radiosonde-Based Northern Hemisphere Tropospheric Water Vapor Trends, J. Clim., 14, 1602-1612.

Trenberth, K. E., Fasullo, J. & Smith L. 2005: Trends and variability in column-integrated atmospheric water vapor, Clim. Dynam, 24(7-8),741-758m doi:10.1007/s00382-005-0017-4.

Vincent, L. A. 1998: A Technique for the Identification of Inhomogeneities in Canadian Temperature Series, J. Clim., 11, 1094-1104.

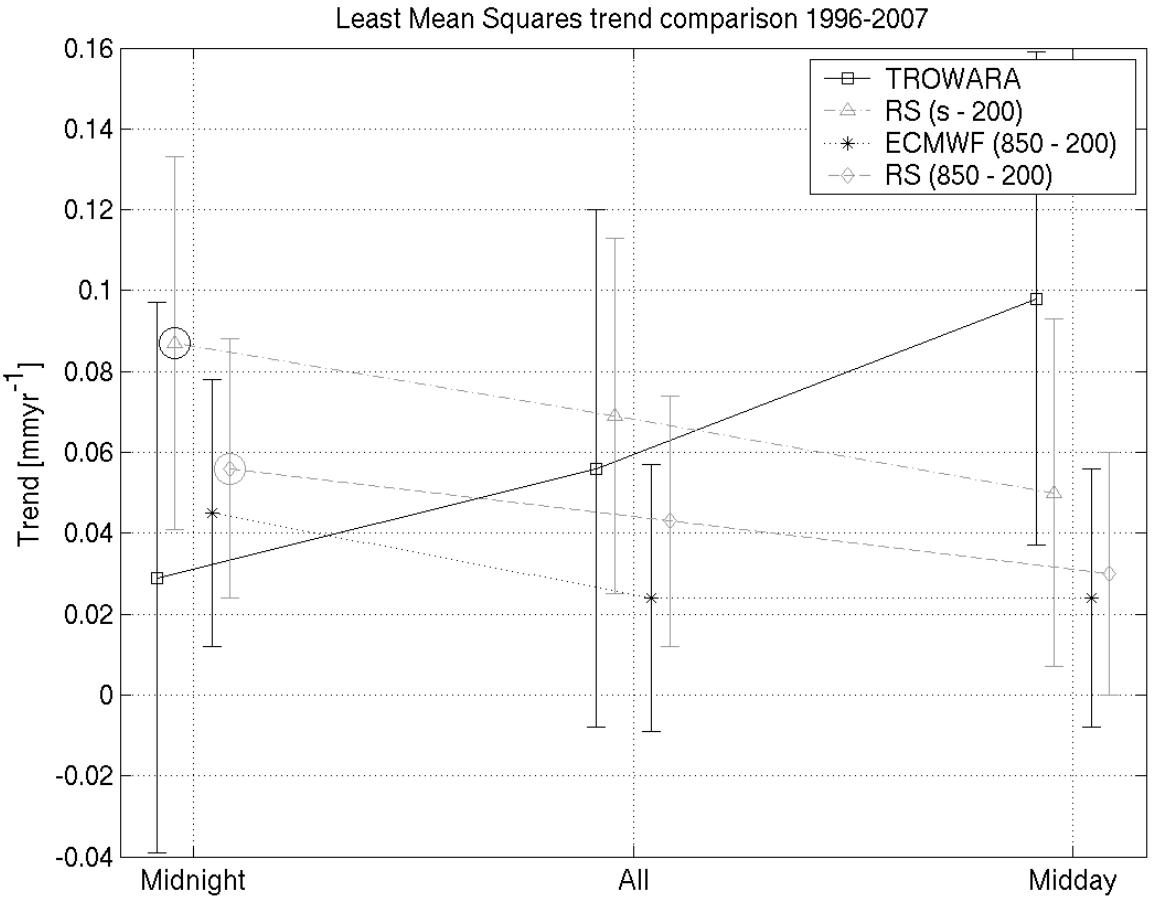

Figure 1. Yearly trends in IWV in mm calculated for the 1996-2007 period. The error bars show the standard error and the large circles indicate that a trend is significant at the 90 % level.

4.6

Impact of GNSS Network Design on Water Vapour Tomography

Perler Donat*, Geiger Alain*, Leuenberger Daniel**, Brockmann Elmar***, Kahle Hans-Gert*

*Institute of Geodesy and Photogrammetry, ETH Zurich, Schafmattstrasse 34, CH-8093 Zurich (donat.perler@geod.baug.ethz.ch)
**Federal Office of Meteorology and Climatology MeteoSwiss, Kraehbuehlstrasse 58, CH-8044 Zurich
***Federal Office of Topography swisstopo, Seftigenstrasse 264, CH-3084 Wabern

In the last decades, substantial progress is made in Numerical Weather Prediction (NWP). Thanks to the increasing computing power, the model resolution has been continuously ameliorated. In contrast to this, the number of meteorological observations for initialising the models has not evolved to the same extent especially concerning the water vapour measurements over land. The lack of high-resolution water vapour measurements is seen as a major limit for further improvements of the NWPs. With GNSS-tomography, this gap can be filled. GNSS-tomography provides a three dimensional water vapour field with high resolution. Thereby, the setup of the GNSS network is an essential factor for the resolution and for the quality of the provided measurements. Sensitivity analyses are carried out to assess the influence of network configuration and of the visibility of the satellites. Results of network optimisation in view of water vapour tomography will be discussed and presented. The advent and extension of new and existing GNSS, respectively, will allow to simultaneously collect signals from several systems such as GPS, Galileo and GLONASS. The impact of the use of several systems on the result of water vapour tomography is investigated and presented.

4.7

How declining aerosols and rising greenhouse gases forced rapid warming in Europe since the 1980s

Philipona Rolf*, Behrens Klaus**, Ruckstuhl Christian***

* *Federal Office of Meteorology and Climatology MeteoSwiss, Aerological Station, CH-1530 Payerne, Switzerland (rolf.philipona@meteoswiss.ch)*
** *Meteorologisches Observatorium Lindenberg, Deutscher Wetterdienst, D-15848 Lindenberg, Germany*
*** *Institute for Atmospheric and Climate Science, ETH Zürich, CH-8057-Zürich, Switzerland*

Mainland Europe's temperature rise of about 1°C since the 1980s is considerably larger than expected from anthropogenic greenhouse warming. Aerosol optical depth and surface irradiance measurements from radiation sites in Switzerland and Northern Germany, recently showed a 60 % decline of aerosol concentration, which led to a significant increase of solar irradiance under cloud-free skies since the 1980s confirming solar brightening. Here we analyse all shortwave and longwave surface forcings and relate them to humidity- and temperature increases through the radiation- and energy budget over Mainland Europe. Shortwave climate forcings from direct- and indirect- aerosol effects combined are found to be two to three times larger than the longwave forcing from rising anthropogenic greenhouse gases. Almost tree quarters of the energy of these forcings goes into the turbulent fluxes, which increase humidity and hence the longwave forcing by water vapour feedback. However, with respect to the initial anthropogenic forcings the analysis shows that about two thirds of the rapid temperature rise since 1980 is forced by declining aerosols and only one third by rising greenhouse gases. The results explain the recent rapid temperature rise in Europe and demonstrate experimentally how manmade climate forcings increase surface temperature. With aerosol concentrations now reaching low levels in Europe solar brightening likely subsides, and temperature will henceforth mainly increase due to anthropogenic greenhouse warming.

REFERENCES

Ruckstuhl, C., Philipona, R., Behrens, K., Collaud Coen, M., Dürr, B., Heimo, A., Mätzler, C., Nyeki, S., Ohmura, A., Vuilleumier, L., Weller, M., Wehrli, C., and Zelenka, A., 2008: Aerosol and cloud effects on solar brightening and the recent rapid warming, Geophys. Res. Letters, 35, L12708, doi:10.1029/2008GL034228.

4.8

Monitoring weather/climate related and other phenomena by simple RGB compositing of multispectral imagery from Meteosat Second Generation

Roseli HansPeter

via Monte Brè 5, CH-6605 Locarno

Meteosat Second Generation's (MSG) Spinning Enhanced Visible and InfraRed Imager (SEVIRI) provides operationally multispectral imagery at high repetition rate from the geostationary orbit. MSG and SEVIRI have been at their inception in 2002, and still are, a first world-wide in geostationary imaging of the Earth. Since this summer, using the back-up satellite, the northern hemisphere is scanned not only every 15 minutes (full Earth disc by Meteosat-9 at 0° longitude), but also at 5-minute intervals (Meteosat-8 at 9.5° East). The continuous data flow from both satellites allows for excellent monitoring of a wide range of weather/climate related and other phenomena.

Display of individual channels or images of channel differences from a multi-spectral imager falls short of imparting in a concise way to the user the wealth of pertinent information buried in the image data content. Based on experience with AVHRR and MODIS products, the application on SEVIRI image data of the RGB compositing technique offers the possibility of compression of the multi-spectral information content for optimum visualisation, while preserving pattern and texture

of cloud, atmosphere and surface features as well as continuity in the time domain. Also, by a careful choice of the inputs to an RGB composite scheme a multitude of phenomena may be captured in one go. Adequately re-projected RGB composites may be used right out to regions on the limb of the SEVIRI coverage. Thus, the RGB compositing technique is an efficient way for a continuous monitoring of phenomena in the atmosphere and on the Earth surface. It preserves the "natural-look-and-feel" of mono-channel imagery many users are used to from earlier satellite generations, in particular when viewing image sequences.

RGB compositing also has its drawbacks. The number of channels invites to a confusing number of possible combinations. There are individual (subtle or more serious) colour perception problems and difficulties in memorising the resulting colour schemes, i.e. in relating colour shades to particular meteorological or non-meteorological features.

For operational applications and for training it is important to reduce the set of RGB schemes to a minimum while maximising the number of identifiable phenomena relevant to the application. At the same time the selected RGB schemes should often cover 24-hours/7-days including twilight conditions with at most small changes in colouring. Most importantly, RGB composting schemes should be based on physical considerations as regards the selection of the channel combinations as well as the attribution of them to the individual colour planes of the RGB display device. This assists in understanding and memorising the image content and its relation to the resulting colour landscape.

A typical RGB example is the 24-hour cloud microphysics RGB. It allows for the identification of fog and low cloud night and day including twilight conditions, while still differentiating among mid/high-level stratiform and convective cloud. In Jython (language used in the display freeware IDV by Unidata) the RGB is coded as follows:

```
# 24-hour cloud microphysics
# units: K
#R:      IR120-IR108      -4K ...   2K
#G:      IR108-IR87         0K ...   6K
#B       IR108            248K ... 303K

def ACMP_RGB(IR87,IR108,IR120):
 R = 255.*max_data(min_data((IR120-IR108+4.)/6.,1.),0.)
 G = 255.*(max_data(min_data((IR108-IR87)/6.,1.),0.)**(1./1.2))
 B = 255.*max_data(min_data((IR108-248.)/55.,1.),0.)
 return combineRGB(R,G,B)
```

RGB composites from SEVIRI data support the identification and monitoring of a multitude of features like:

- solid and liquid water particles (snow – ice crystals – cloud droplets) and of their relative size at, close to, the cloud tops;
- weak-moderate and strong convection;
- air mass type in middle and high troposphere;
- snow and vegetation cover;
- extended flooding;
- dust storms and long-range transport;
- volcanic ash and SO_2 eruption and long-range transport;
- industrial SO_2 release;
- Industrial/wild fire and smoke.

The verbal presentation will show SEVIRI RGB composited images and image sequences covering phenomena from the above list.

4.9

Eddy covariance measurement of CO_2 fluxes in Cairo/Egypt

Vogt Roland, Frey Corinne M., Burri Susanne, Harhash Maha, Parlow Eberhard

Institute of Meteorology, Climatology and Remote Sensing, Basel University
email: Roland.Vogt@unibas.ch

Measurements of CO_2 fluxes in urban areas are still rare, especially when it comes to megacities. As part of a ground truth campaign for a remote sensing project, surface energy balance fluxes were measured at three stations (urban, rural, desert) in and around Cairo, Egypt. At two sites CO_2 fluxes were measured, for details see Frey et al., same conference. In this presentation results from the urban station are reported. It was located at the southern border of the campus of Cairo University in Gizeh (30°01'33.4N, 31°12'27.7E). A 12 m mast was erected on a 20 m high building and attached to a 4.5 m buildup on the flat roof. The flux instrumentation (sonic: Campbell CSAT3, open path gas analyzer: LiCOR LI7500) was mounted on top of the mast. It additionally carried a 4-component net radiometer (Kipp & Zonen CNR1) and a psychrometer. Fluxes were calculated and corrected online, but raw data were also stored for subsequent analysis. The measurement period was from November 10, 2007 to February 26, 2008.
The area north of the station was urban, the area south, south-west was dominated by agricultural use (up to 1 km). To the South-East, there was a sports ground and 400 m to the East the zoo of Cairo was located. The area of the zoo is roughly a 500x1000 m N-S oriented vegetated rectangle. The western bank of the river Nile was 1 km east of the site.
The wind was blowing dominantly from North (60% from N ± 60°, 20% from S ± 40°, from W 16%, from E 4%). Preliminary results show, that on average, the CO_2 flux is upward directed. With winds from South, the magnitude is reduced and can even be downward directed during daytime. Peak values are reached during midday and are in the range of 0.5 to 1.5 mg m^{-2} s^{-1}. Nocturnal values are around 0.2 mg m^{-2} s^{-1}. The weekly traffic intensity can be seen in the CO_2 fluxes. On Fridays there is no distinct diurnal course. Afternoon values are below 0.5 mg m^{-2} s^{-1}. On Saturdays the peaks are slightly reduced with values below 1 mg m^{-2} s^{-1}.

4.10

Temporal variability of Radon-222 in near-ground atmosphere

Wach Paulina*, Zimnoch Miroslaw*, Rozanski Kazimierz*, Kozak Krzysztof**

**AGH University of Science and Technology, Faculty of Physics and Applied Computer Science, al. Mickiewicza 30, 30-059 Krakow, Poland*
***Institute of Nuclear Physics, Laboratory of Radiometric Expertise,*
Radzikowskiego 152, 31-342 Krakow, Poland

Radon-222 is an alpha-emitting radioactive inert gas with the half-life of 3.8 days. It is a product of decay of ^{226}Ra which belongs to ^{238}U-decay series. Uranium-238 and its decay product ^{226}Ra are ubiquitous in the upper Earth's crust and in the soils. Radon-222 which is being released into the pore space of soils, diffuses into the atmosphere where it decays to lead ^{210}Pb through intermediate chain of short-lived radionuclides (^{218}Po-^{214}Pb-^{214}Bi-^{214}Po). The release rate of ^{222}Rn is controlled by source term (^{226}Ra content in the soil and its vertical distribution) and by physical properties of the upper soil layer (mineral structure, porosity, water content).
Concentration of ^{222}Rn has been measured quasi-continuously in Krakow since June 2004 with the aid of radon monitor based on detection of daughter products of this gas. The radon monitor has been calibrated against AlphaGUARD detector. The air intake is located ca. 20 meters above the ground, on the roof of the Faculty building. The radon monitor provides individual readings every 30 minutes, representing average activities of ^{222}Rn over 30-minute sampling intervals. In the same location, quasi-continuous measurements of CO_2 and CH_4 mixing ratios in the local atmosphere are performed.
Rn-222 exhibits substantial seasonal and diurnal fluctuations. The absolute amplitude of the recorded individual ^{222}Rn concentrations reached during the 4-year observation period approximately 40 Bqm^{-3}. The maximum of monthly mean ^{222}Rn concentration occurs usually in October (ca. 10 Bqm^{-3}), while the minimum is recorded in March or April (ca. 2.5 Bqm^{-3}). Daily mean values of ^{222}Rn concentration fluctuate between ca. 1Bqm^{-3} and 18 Bqm^{-3}.
Influence of various factors on the observed variability of ^{222}Rn concentration in the near-ground atmosphere in Krakow on different time scales (diurnal, synoptic, seasonal) was investigated. The following parameters were considered: (I) stability of the lower atmosphere largely controlling diurnal variability, (II) wind speed, (III) temperature, (IV) fluctuations of atmospheric pressure, (V) history of air masses, (VI) fluctuations of water table and water content of the soil column.

4.11
Effect of clouds on erythemal UV radiation

Walker Daniel[*] [**], Vuilleumier Laurent[*]

[*] *Federal Office of Meteorology and Climatology MeteoSwiss, Payerne, Switzerland (daniel.walker@meteoswiss.ch)*
[**] *Institute for Atmospheric and Climate Science, ETH Zurich, Switzerland*

Ultraviolet (UV) radiation is known to have strong and potentially adverse effects on human health, ecosystems and materials. Erythemal UV irradiance has been defined as a measure to quantify such effects on human skin. The medical community and public health policy makers are interested in detailed information about the spatial distribution and temporal evolution of UV radiation.

UV time-series in Switzerland are spatially sparse and temporally too short to answer current needs including trend analyses. Therefore, radiative transfer models are used to substitute for missing data. However, simulating the effect of clouds on UV is very difficult, but being able to handle both clear-sky situations and various cloud conditions is crucial in assessing changes in UV radiation. An alternative way of describing the influences of clouds is the use of global shortwave radiation (SW_{glo}) as a proxy. This parameter holds information about the transmittance of the atmosphere and describes the cloud effect over the whole solar spectra. Furthermore, the advantages of SW_{glo} are the vast availability of measurements and the long time-series available in Switzerland.

We present a model that calculates global erythemal UV radiation for all-sky conditions. This model combines the accuracy of radiative transfer models for clear-sky conditions with semi-empiric information describing the influence of clouds. For this purpose cloud modification factors in the UV and SW range are inferred from data. The dependencies of this model on environmental conditions such as solar position, total ozone, and surface reflectance are analyzed. Resulting estimated UV doses are validated against UV observations at four locations in Switzerland. A fine time resolution of 10 minutes allows a validation of various aggregated UV doses (10', 1h, and daily doses).

The model is able to describe the short-term variability in the UV radiation due to changing cloud coverage. Depending on the location, RMS errors between 10.6 and 14.4% for the 10'-data have been found. The correlation exceeds 0.99. Better correspondence is obtained for daily UV doses with RMS errors between 6.3 and 9.5%. The performance of the method is generally better for higher solar elevations. The skills are lower at the high alpine station Jungfraujoch due to measurement problems, such as icing.

5. Quaternary Research (Open Session)

Irka Hajdas, Susan Ivy-Ochs

Swiss Society for Quaternary Research (CH-Quat)

5.1

Anthropogenic impact on 'Findlinge' (erratic boulders) in the Alpine foreland and its implications for surface exposure dating

Akçar Naki*, Ivy-Ochs Susan**, Kubik Peter W.*** & Schlüchter Christian*

*University of Bern, Institute of Geological Sciences, Baltzerstrasse 1-3, 3012 Bern
(akcar@geo.unibe.ch, christian.schluechter@geo.unibe.ch)
**Institute of Particle Physics, ETH Hönggerberg, 8093 Zürich (ivy@phys.ethz.ch)
***Paul Scherrer Institute c/o Institute of Particle Physics, ETH Hönggerberg, 8093 Zürich (kubik@phys.ethz.ch)

'Findlinge' are allochthonous huge erratic boulders which contributed to the understanding that the Alpine glaciers advanced hundreds of kilometers into the Alpine foreland (Ivy-Ochs et al., 2004). They were once delineating the maximum extent of LGM (Last Glacial Maximum) and MEG (Most Extensive Glaciation) glaciers. Following the final retreat of LGM glaciers, the 'findlinge' were subjected to intensive anthropogenic activity, i.e. most of them have been quarried and used as construction material and/or building stone since Roman times. They have been also destroyed by dynamite in order to 'clean-up' the farmlands in modern times.

For instance, pieces of erratic boulders are generally observed in walls of the buildings and gardens, and several boulders were quarried to construct fountains (e.g. Graf et al., in prep.). Most of the survivors are now located either in the forests or at the boundary of two farms. During the last decade, few available 'findlinge' were surface exposure dated by cosmogenic nuclides (Ivy-Ochs et al., 2006; Graf et al., 2007).

In this study, we focus on the three erratic boulders on Möschberg hill close to Grosshöchstetten (BE). According to our first results, only one ^{10}Be cosmogenic exposure age of around 19 kyr correlates well with timing of LGM (sample ER1 in Ivy-Ochs et al., 2004). The second boulder exposure date reflects exhumation. The third boulder shows evidence of quarrying as it is surrounded by fragments. Thus, most of the 'findlinge' in the Alpine foreland are not suitable for surface exposure dating, show strong anthropogenic impact or have been exhumed.

REFERENCES

Graf, A.A., Strasky, S., Ivy-Ochs, S., Akçar, N., Kubik, P.W., Burkhard, M. & Schlüchter, C. 2007: First results of cosmogenic dated pre-last glaciation erratics from the Montoz area, Jura Mountains, Switzerland Quaternary International 164-65, 43-52.

Graf, A.A., Akçar, N., Ivy-Ochs, S., Strasky, S., Kubik, P.W., Christl, M., Burkhard, M., Wieler, R., & Schlüchter, C. in prep: Surface exposure dating confirms multiple extensions of Rhône glacier into the Jura Mountains.

Ivy-Ochs, S., Schafer, J., Kubik, P.W., Synal, H.A., & Schluchter, C. 2004: Timing of deglaciation on the northern Alpine foreland (Switzerland) Eclogae Geologicae Helvetiae 97 (1), 47-55.

Ivy-Ochs, S., Kerschner, H., Reuther, A., Maisch, M., Sailer, R., Schafer, J., Kubik, P.W., Synal, H.A., Schluchter, C. 2006: The timing of glacier advances in the northern European Alps based on surface exposure dating with cosmogenic ^{10}Be, ^{26}Al, ^{36}Cl, and ^{21}Ne. Geological Society of America Special Paper no. 415, 43-60.

5.2

Glacier erosion rates since Little Ice age during advance and retreat of a Norwegian outlet glacier

Burki Valentin*,**, Hansen Louise**, Fredin Ola**, Beylich Achim**,*** & Larsen Eiliv**

*Department of Geography, University of Zurich - Irchel, Winterthurerstrasse 190, CH-8057 Zürich, Switzerland (valentin.burki@geo.uzh.ch)
**Geological Survey of Norway, N-7491 Trondheim, Norway
***Department of Geography, Norwegian University of Science and Technology (NTNU), Dragvoll, N-7491 Trondheim, Norway

The Jostedalsbreen ice field is situated at the eastern end of the Nordfjord valley-fjord system. One of its outlet glaciers is the Bødalsbreen glacier. The proglacial basin is a glacially eroded and bedrock-confined basin of up to 80 m depth. The sediments in the basin are divided into four units (A-D), based on a grid of georadar profiles and Quaternary geological mapping. Unit A contains different glacial and glacio-fluvial sediments deposited during and subsequent to the deglaciation. Unit B is composed of till and morainal deposits and was formed between AD 1755 and AD 1930. Unit C consists of glaciodeltaic to glaciolacustrine sediments that accumulated in lake Sætrevatnet. Unit D is a glaciofluvial fan situated in front of the present-day glacier front of Bødalsbreen glacier. The last two units were deposited between AD 1930 and AD 2005.

As a result of the volume estimations and the corresponding catchment area, the total erosion rates are calculated to 0.8 ±0.4 mm yr^{-1} (Unit B) and 0.7 ±0.3 mm yr^{-1} (unit C/D). The total erosion rate is considered as the sum of subglacial bedrock erosion and the evacuation of subglacially stored sediment. Considering the glaciation history, two major subglacial depressions in the catchment of the glacier, and the clast maturity distribution in the lateral moraines, we conclude: (i) the total erosion rate is time dependent; (ii) the two quantities representing the total erosion rate seem to be in the same order of magnitude at present; and (iii) the estimated values of glacial erosion rates are in the same order of magnitude as other ones obtained from the region.

5.3

Glacier erosion: processes and quantification

Burki Valentin*, Haeberli Wilfried*, Schlunegger Fritz**, & Schnellmann Michael***

*Department of Geography, University of Zurich-Irchel, Winterthurerstrasse 190, CH-8057 Zürich
**Institut für Geologie, Universität Bern, Baltzerstrasse 1-3, CH-3012 Bern
***Nagra, Hardstrasse 73, CH-5430 Wettingen

The impact of glacier erosion is manifested by a variety of erosional and depositional landforms indicating the former presence of glaciers. Processes of abrasion, plucking, and meltwater erosion have been widely described (e.g. Benn and Evans, 1996). During a cycle of a glacier advance and retreat, it is challenging (i) to reveal the spatial and temporal distribution of different erosional processes, and (ii) to quantify them (e.g. Sugden and John, 1976; Drewry, 1986; Benn and Evans, 1996). Answers to these questions are important in order to understand the development of single glacial-erosional landforms and the evolution of an entire glacierized landscape.
Based on a detailed literature investigation, we discuss glacial-erosional processes and models for their quantification, with the aim to better understand the processes and to evaluate their impact during future ice ages. A special focus is on linear landforms formed by subglacial meltwater erosion. By investigating gorges with a potential subglacial formation, the knowledge about their formation process will be increased. These investigations will allow more detailed predictions regarding the safety of deep depositories for nuclear waste during future ice ages (Haeberli, 2004).

REFERENCES

Benn, D.I., & Evans D.J.A. 1996: Glaciers and Glaciations, Arnold, London, 734pp.
Drewry, D. 1996: Glacial geological processes, Edward Arnold, 276pp.
Haeberli, W. 2004: Eishaus +106a. Zu Klima und Erdoberfläche im Zürcher Weinland während der kommenden Million Jahre. Geographisches Institut Universität Zürich, 39pp.
Sugden, D.E., & John, B.R. 1984: Glaciers and Landscape. Edward Arnold, London, 376pp.

5.4

Differentiation of rock avalanche deposits from lateglacial moraines in Val Ferret (Mont Blanc Massif, Italy) using cosmogenic ^{10}Be

Deline Philip*, Akçar Naki**, Ivy-Ochs Susan***, Kubik Peter W.**** & Schlüchter Christian**

*EDYTEM Lab, Université de Savoie, CNRS, 73376 Le Bourget-du-Lac, France (pdeli@univ-savoie.fr)
**University of Bern, Institute of Geological Sciences, Baltzerstrasse 1-3, 3012 Bern (akcar@geo.unibe.ch, christian.schluechter@geo.unibe.ch)
***Institute of Particle Physics, ETH Hönggerberg, 8093 Zürich (ivy@phys.ethz.ch)
****Paul Scherrer Institute c/o Institute of Particle Physics, ETH Hönggerberg, 8093 Zürich (kubik@phys.ethz.ch)

On September 12th 1717 AD, inhabitants of the upper Ferret valley (Mont Blanc Massif, Italy) witnessed one of the largest rock avalanches of the Alps, destroying two small settlements with 2 causalities and lost of their cattle. This avalanche mobilized a rock volume of larger than 10 millions m^3 and huge volume of ice from Triolet glacier. This mass, composed of ice and sediment, moved more than 7.5 km down valley and reached lower part of the valley. Although this natural hazard is historically recorded, extend of its deposits in the Ferret Valley is still under discussion due to the insufficient number of absolute dates.

Quaternary deposits in the upper Ferret valley have been attributed for a long time to glacier advances (Figure 1). In the 1960's it has been suggested that rock avalanche sediments was forming only a small part of these deposits (e.g. Mayr, 1969). Later Aeschlimann (1983) argued for lateglacial moraines whereas
Orombelli and Porter (1988) controversially stated that the whole valley was covered by this rock avalanche. Using the new findings, and relative and absolute ages, Deline and Kirkbride (2008) have recently shown that 1717 AD rock avalanche was deflected along northern side of the valley floor, preserving older slope and glacial sediments along the southern side (Figure 1). Moreover, deposits of an earlier rock avalanche onto the Triolet Glacier, probably occurred before 1000 AD, was also identified (Deline & Kirkbride, 2008). Despite several radiocarbon dates on peat and wood buried in or overlying the avalanche deposit, the extend of avalanche deposits in the valley floor still remains undetermined, which in fact delimits the modeling of its propagation.

Our study focuses on the surface exposure dating of Quaternary deposits of Ferret valley with ^{10}Be. Such exposure dates would allow us to differentiate these deposits and build up their chronology. With this aim, nine samples from the granite boulders were collected (Figure 1) and prepared for AMS analysis. The first results of this study will be presented.

REFERENCES

Mayr, F. 1969: Die postglazialen Gletscherschwankungen des Mont Blanc-Gebietes.

Orombelli, G., & Porter, S.C. 1988: Boulder deposit of upper Val Ferret (Courmayeur, Aosta valley): Deposit of a historic giant rockfall and debris avalanche or a lateglacial moraine? Eclogae Geologicae Helvetiae, 81, 365-371.

Aeschlimann, H. 1983: Zur Gletschergeschichte des italienischen Mont Blanc Gebietes: Val Veni – Val Ferret – Ruitor. Ph.D. thesis, Universität Zürich, Switzerland.

Deline, P., & Kirkbride, M.P. 2008: Rock avalanches on a glacier and morainic complex in Haut Val Ferret (Mont Blanc Massif, Italy), Geomorphology, in press. doi:10.1016/j.geomorph.2007.10.020

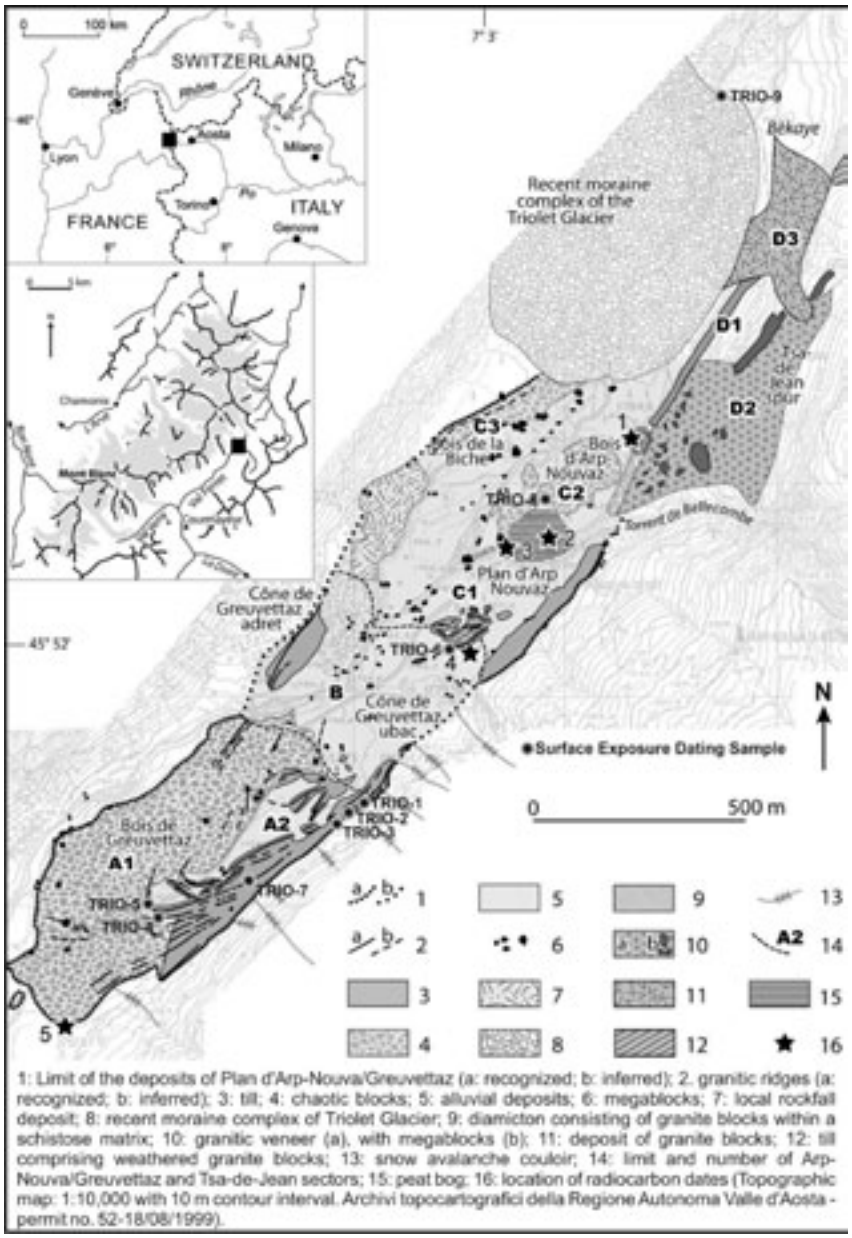

Figure 1. Map of the deposits of Haut Val Ferret and location of the surface exposure dating samples (modified from Deline & Kirkbride, 2008).

5.5

Environmental and climatic history of an overdeepened and filled glacial basin in Northern Switzerland

Furrer Heinz*, Riedi Marc Andri**, Anselmetti Flavio***, Drescher-Schneider Ruth****, Graf Hansruedi*****, Hajdas Irka******
Lowick Sally******* & Preusser Frank*******

* *Paläontologisches Institut und Museum Universität Zürich, Karl Schmid-Strasse 4, CH-8006 Zürich (heinz.furrer@pim.uzh.ch)*
** *Geologisches Institut, Departement Erdwissenschaften ETH, CH-8092 Zürich*
*** *Eawag, Swiss Federal Institute of Aquatic Science and Technology*
Überlandstrasse 133, CH-8600 Dübendorf
**** *Schillingsdorfer Straße 27, A-8010 Kainbach bei Graz*
***** *matousek, baumann & niggli ag, beratende geologen usic, Postfach,*
CH-5401 Baden
****** *Ion Beam Physics, ETH and PSI Zürich, Schafmattstrasse 20, CH-8093 Zürich*
******* *Geologisches Institut Universität Bern, Baltzerstrasse 1-3, CH-3012 Bern*

Origin, age and sedimentation history of overdepeened glacial valleys in the alpine foreland are still intensely debated. Geological studies in the Wehntal, 20 km northwest of Zürich suggest the presence of a deep trough cut by Pleistocene glacial erosion into Neogene Molasse beds; containing a sedimentary archive covering several glacial-interglacial cycles. Most of the narrow valley was filled by lake sediments and peat deposits. Between 2003 and 2006 an interdisciplinary project investigated a mammoth remains-bearing peat horizon exposed in construction pits at Niederweningen (3–5 m below surface). Results proved that the peat with its famous mammal fauna was deposited during the last glacial cycle (45–65 ka ago, Middle Würmian) in a shoaling lake (Furrer et al. 2007, Drescher-Schneider et al. 2007, Coope 2007, Preusser & Degering 2007, Tütken et al. 2007). In October 2007, a 30 m-deep core was drilled nearby to investigate the depositional, palaeoenvironmental and climatic history of the upper part of this glacial basin in the foreland of the Swiss Alps. A first study has been recently finished (Riedi 2008), other results are in a preliminary stage.

The mammoth peat was drilled between 4.6 and 5.3 m, underlain by silty and sandy lake sediments (5.3–12 m, OSL ages of ≈65–100 ka). Another peat was recovered in 12–14 m depth, which was deposited at the end of the last interglacial (late Middle–Late Eemian, MIS 5e) suggesting a hiatus of several thousand years (Early-early Middle Eemian) at its base. The uppermost beds of the underlying silts yield a mollusc fauna and many characeans together with a typical 'late glacial' palynoflora (≈130 ka). The lower part down to 30 m with mainly laminated silts is nearly free of organic material and coarser layers, suggesting a depositional environment in a distal location of a cold proglacial lake. The OSL age from the base of the core is 190 ka. Deformed layers, increased shear strength and erosional unconformities between 18.5 and 20 m suggest an important event at about ≈150 ka (MIS 6), probably caused by overriding of the sediments by an advancing glacier.

The interpretation of a recently completed seismic campaign in the Wehntal (summer 2008) provides new insights into the deeper structure of the valley down to 70–140 m depth. A proposed deep drill core in the most promising section of the valley, planned for winter 2008/09, will shed new light on the sedimentary infilling history of this glacial basin and potentially recover a unprecedented archive of multiple glacial-interglacial successions.

REFERENCES

Coope, R. 2007: Coleoptera from the 2003 excavations of the mammoth skeleton at Niederweningen, Switzerland. Quaternary International 164–165, 130–138.

Drescher-Schneider, R., Jacquat, C. & Schoch, W. 2007: Palaeobotanical investigations of the mammoth site of Niederweningen (Kanton Zürich), Switzerland. Quaternary International 164–165, 113–129.

Furrer, H., Graf, H.R. & Mäder, A. 2007: The mammoth site of Niederweningen, Switzerland. Quaternary International 164–165, 85–97.

Hajdas, I., Bonani, G., Furrer, H., Mäder, A. & Schoch, W. 2007: Radiocarbon chronology of the mammoth site at Niederweningen, Switzerland: Results from dating bones, teeth, wood, and peat. Quaternary International 164–165, 98–105.

Preusser, F. & Degering, D. 2007: Luminescence dating of the Niederweningen mammoth site, Switzerland. Quaternary International 164–165, 106–112.

Riedi, M.A. 2008: Die Sedimentologie der "Mammut"-Bohrung des Wehntals: Ein Archiv der Glazialzyklen der vergangenen 180'000 Jahre. Unpubl. Bachelorarbeit DERDW ETH, 35 S.

5.6

Dating old bones: Study case mammoth from Niederweningen, ZH

Hajdas Irka*, Michczynski Adam**, Bonani Georges*, Wacker Lukas* & Furrer Heinz***

* *Ion Beam Physics, ETH and PSI Zürich, Schafmattstrasse. 20, 8093 Zürich, Switzerland (hajdas@phys.ethz.ch)*
** *Silesian University of Technology, Institute of Physics, Radiocarbon Laboratory, GADAM Centre of Excellence, Boles awa Krzywoustego 2, 44-100 Gliwice, Poland*
*** *Paläontologisches Institut und Museum der Universität Zürich, Karl Schmid-Strasse 4, 8006 Zurich, Switzerland*

Preparation of bone material for radiocarbon dating is still a subject of investigation. In the past the most problematic ages appeared to be the very old bones i.e., with ages close to the limit of the dating method. Development of preparative methods requires sufficient amounts of bone material as well as possibility of verification of the ages. In the peat section at Niederweningen, ZH Switzerland numerous bones of mammoth and other animals were found in the late 19th century. The first AMS radiocarbon ages of those bones from 1890/1891 excavations placed the age between 33,000 BP and 35,000 BP. The excavations in 2003/2004 provided additional material for radiocarbon dating. The age of 45,870±1080 BP was obtained on base cleaned gelatine from mammoth bone, which was very close to the age of 45,430±1020 BP obtained for the peat layer that buried the mammoths (Hajdas et al. 2007). This study shows that three pre-treatment methods base+Longin, Longin+Ultra-filtration, and Base+Longin+Ultraflitration (Fig. 1) give the ages consistent with each other and also consistent with the age of peat section.

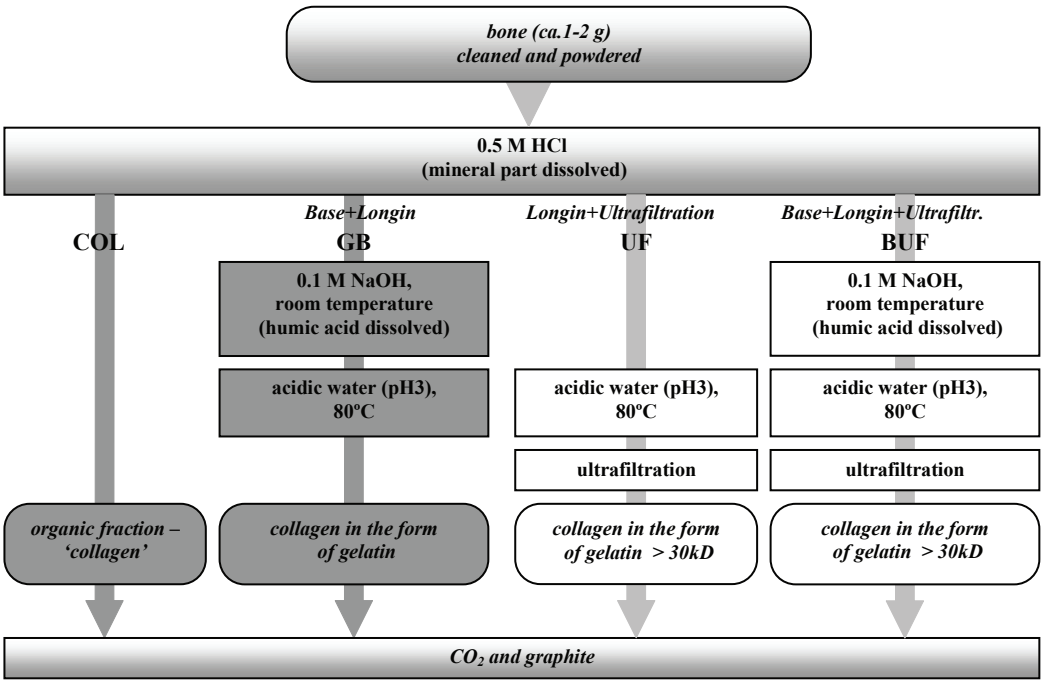

Figure 1. Schematic diagram of the chemical preparation of the dated bones. Grey colour marks steps of preparation methods applied in previous studies (Hajdas et al. 2007), while white colour indicates steps of methods used in this study.

REFERENCES

Hajdas, I., Bonani, G., Furrer, H., Mäder, A. & Schoch, W. 2007: Radiocarbon chronology of the mammoth site at Niederweningen, Switzerland: Results from dating bones, teeth, wood, and peat. Quaternary International 164-65, 98-105.

5.7

Chronology and development of the postglacial beach plain NE of Lake Neuchâtel on Swiss Plateau, using OSL*- and ^{14}C-Data.

*Optically Stimulated Luminescence

Heer Aleksandra 1*, Hajdas Irka2, Lowick Sally 3, Preusser Frank 3 & Veit Heinz 1

1 Institute of Geography, University of Bern, Hallerstrasse 12, CH-3012 Bern,
*heer@giub.unibe.ch * corresponding author, veit@giub.unibe.ch*
2 Ion Beam Physics, Swiss Federal Institute of Technology (ETH Zürich), Schafmattstr. 20, CH-8093 Zürich, hajdas@phys.ethz.ch
3 Institut für Geologiel, Universität Bern, Baltzerstrasse 1+3, CH-3012 Bern, lowick@geo.unibe.ch , preusser@geo.unibe.ch

After the LGM-glaciers melted down, they left behind plains which were successively infilled with erosional debris transported by big Alpine rivers (Rhone, Aare, Rhine and Reus). These plains have been influenced by Late Pleistocene and Holocene climate change, by lake level and shore line shifting, and also by human settlement and rural land use during the last 9.0 ka. Within the plains sand ridges have been recognized at different sites in the NW Alpine foreland in Switzerland and France (Rhine Valley, Swiss Plateau, Lower Wallis Valley and south of Lake Geneva). The sand ridges mount glacio-fluvial or limnic deposits and are located within the outer limits of the LGM – moraine belt. This project is aiming at highlighting the remaining open questions about the interrelation of landscape forming factors, as mentioned above, and also at better understanding of the processes and times which control the creation and preservation of the fossil beach landscapes in the NW Alpine foreland. New results derived from six excavations in Grosses Moos, a fossil beach plain NE of Lake Neuchâtel, as well as from OSL- and ^{14}C-dating, will be presented.

The sedimentary structures as well as the OSL- and ^{14}C- ages suggest continues sedimentation and marsh development responsible for silting up the NE part of the Lake Neuchâtel and for the construction of the Grosses Moos beach plain. The beach plain grows from the NE towards the present shore line of Lake Neuchâtel. Climatic oscillations and changes of the hydrological regime are assumed to be responsible for rapid emergence and drying of the pre-existing littoral ridges. Subsequently they have been wind reworked and accumulated as a dune. Hence, as their shape along the present NE lake shore already suggested, the sand ridges of Grosses Moos give evidence for the stepwise regression of Lake Neuchâtel since the Bölling-Alleröd period. Paleochannel infilled with "Seelandschotter" (13.3 ± 1.1 ka) and peat (12.5 – 13.3 cal ka) underlying the "Islerendüne" (the most NE-stern sand ridge) provides evidence of this sedimentary period. The Younger Dryas cold period gave rise to building of the "Islerendüne" sand ridge (12.9 ± 1.1 ka) which continued into the Boreal (9.8 ± 0.9 ka). On few spots on the "Islerendüne" the original Luvisol has been preserved, whereas Cambisol and Arenosol are predominant. As the OSL-ages suggest, the formation of the aeolian sequence of the "Islerendüne" started in the Younger Dryas consequently, the Luvisol must be of Holocene age.

As the "Rundidüne" (next SW to the "Islerendüne") hasn't been sampled yet, the only hint at its age is provided by the archaeological finds dated to about 9.0 ka BP (Nielsen 1991). Those human settlements may also be responsible for the reshaping and the widespread erosion of the Luvisol on the "Islerendüne".

The profile of the "Nusshofdüne" (next SW to the "Rundidüne") revealed Younger Dryas lake sediments (10.95 ± 0.8 ka) covered by reeds (age not yet determined) and organic - rich littoral sediments of early middle Holocene age (7.2 ± 0.7 / 6.4 ± 0.9 ka). Lake regression created a dune (5.5 ± 0.5 ka) on the top of this formation. The ^{14}C – data suggest an input of older organic material into the littoral sequence due to peat erosion in the hinterland. The "Witzwilerdüne 1" – profile (next SW to the "Nusshofdüne) reveals Roman Period marsh (2.5 ± 0.2 ka / 2.4 – 2.2 cal ka) covered by coastal dune accentuating a lake regression at the turn to the past millennium (2.07 ± 0.3 ka). In the "Witzwilerdüne 2"-profile (a small sand ridge close to the lake shore) a small dune mount over Little Ice Age lake deposits (0.5 ± 0.06 ka). The dune developed after the lake level had gone down due to the JGK* (0.15 ± 0.03 ka), as the OSL-ages suggest.

* Jura Gewässer Korrektur

REFERENCES

Ivy-Ochs, S. et al. (2004). Timing of deglaciation on the northern Alpine foreland (Switzerland). Eclogae geologicae Helvetiae 97, 47-55.

Meyer-Wohlfahrt, B. (1987). Das jüngere Quartär im Westschweizer Seeland. Revue de Paléobiol. 6/1, 55-80

Nielsen, E.H. (1991). Gampelen-Jänet 3. Eine mesolithische Siedlungsstelle im westlichen Seeland. 151. Bern: Lehrmittelverlag.

van der Meer, J.J.M. (1982). The Fribourg area, Switzerland. A study in quaternary geology and soil development. Diss. Univ. Amsterdam. Publ. Fys. Geogr. Bodemk. Lab. Univ. Amsterdam, 32, 203 pp.

5.8

Exposure dating of the Chironico landslide, Leventina, Switzerland

Ivy-Ochs Susan*, Kober Florian**, Kubik Peter W.*** & Schlüchter Christian****

*Ion Beam Physics, Particle Physics, ETH Zürich, CH-8093 Zürich and
Department of Geography, University of Zürich, CH-8057 Zürich
**Geological Institute, ETH Zürich, CH-8092 Zürich
***Ion Beam Physics, Particle Physics, ETH Zürich, CH-8093 Züich
****Institute of Geological Sciences, University of Bern, CH-3012 Bern

The Chironico landslide is composed of several million cubic meters of granitic gneiss that detached from the eastern wall of the Ticino River valley along 25-30 degree dip slopes and was deposited along the western valley side up to elevations of around 800 m. ^{14}C ages from wood fragments in lake sediments in a former lake north of and dammed by the landslide yield a minimum age of about 13,500 cal yr BP (Antognini and Volpers, 2002). Samples for cosmogenic ^{10}Be exposure dating were taken from quartz veins on upper surfaces of huge boulders in both lobes of the landslide to the north and south of Ticinetto stream. The study will be presented in the framework of other dated landslides in the Alps. After Koefels (Tyrol Austria), which is 9800 yr old, the Chironico slide is one of the largest slides in crystalline rock in the Alps. The Chironico slide is also one of the oldest, with only the Almtal slide (Upper Austria) being older at 15,600 yr (van Husen et al., 2007). In contrast most of the identified large landslides in the Alps (Koefels, Flims) occurred during the early Holocene (Ivy-Ochs et al., 2008).

REFERENCES

Antognini, M., & Volpers, R. 2002: A late Pleistocene age for the Chironico rockslide (Central Alps, Ticino, Switzerland). Buletin of Applied Geology 7, 113-125.

Ivy-Ochs, S., Poschinger, A.v., Synal, H.-A., & Maisch, M. Surface exposure dating of the Flims landslide, Graubünden, Switzerland. Geomorphology (in press).

van Husen, D., Ivy-Ochs, S., & Alfimov, V. 2007: Mechanism and age of Late Glacial landslides in the Calcareous Alps; The Almtal landslide, Upper Austria. Austrian Journal of Earth Sciences 100, 114-126.

5.9

Late glacial tree-ring chronologies reflecting environmental changes - last steps towards an absolute chronology back to 14,250 cal BP

Kaiser Klaus Felix 1, 2, Schaub Matthias 1, 2, Friedrich Michael3,4, Kromer Bernd4, Talamo Sahra4, Miramont Cécile5, Guibal Frédéric5

1 Swiss Federal Research Institute WSL, CH-8903 Birmensdorf, Switzerland
2 Geographic Department, University of Zurich, CH-8057 Zurich, Switzerland
3 Institute of Botany (210), University Stuttgart Hohenheim , 70593 Stuttgart, Germany
4 Heidelberg Academy of Sciences, INF 229, 69120 Heidelberg, Germany
5 IMEP - UMR 6116 - CNRS, Europôle Méditerranéen de l'Arbois, 13545 Aix-en-Provence, France

During the last years, significant progress has been made in the development of Lateglacial tree-ring chronologies in Switzerland, Germany and Southern France with different sites to combine existing chronologies of fossil Scots pines and to extend these throughout the whole Bølling-Alledrød Interstadials [BØ, AL] into the Younger Dryas Stadial [YD].
In France finds along Durance River and tributaries have yielded several floating chronologies extending back into the very important first half of YD ant the end of AL. In Germany the chronology from Reichwalde spans 864 years between approx. 14,080 and 13,220 cal BP. Parallel to it run two chronologies from Danube valley (709 yrs) and Warendorf (465 yrs). Two further chronologies from Danube valley (334 and 190 yrs) extend towards the end of AL at approx. 12,750 cal BP. A series from Northern Italy (Carmagnola, Turin) incorporates the BØ back to 14,250 cal BP spanning 308 yrs.
In Switzerland new series built with trees from two highway-tunnel construction sites (Zurich Gaenziloh and Zurich Landikon) afforded to combine most of the floating chronologies from Daettnau (Winterthur) and Wiedikon (Zurich) to a extensive one that spans 1605 years between approx. 14,250 and 12,650 cal BP. Both series from Switzerland and Germany

have been built independently but have been dendro matched to each other.
Additional radiocarbon dated floating chronologies from Zurich, the floaters from Durance Valley and several single trees appear to bridge the ≈200 year gap between the absolute chronology (12,593 cal BP). The filling of this gap will result in nearly a two millennia extension of the absolute chronology.
Lateglacial pines usually grew under geomorphic stress and were gradually buried by loamy alluvia until the aggrading sediment killed the trees. Crossdating is complicated by both growth disturbances during the first 100 years of a trees life and the poorer preservation of the outer sapwood cells. Crossdating is normally based on an overlap of 50 up to 100 rings. Numerous decadal high precision ^{14}C-age determinations assisted and verified the dendrochronological crossdating. While fluctuations in the chronology are driven in part by local geomorphic activities, fluctuations may also coincide with short stadials and interruptions such as Older Dryas [OD], volcanic events (e.g., Laacher See eruption) and the Gerzensee deviation. Splitting the spline-detrended dataset from Zurich into subgroups demonstrates the potential for detecting common environmental signals. Variations in age-related trends indicate changes in environmental conditions over the 2500 years of AL, YD and Preboreal. Comparisons of tree growth and life span of trees between AL and YD suggest the YD to be rather a period of reduced winter temperatures than of low temperatures during the growing season.
The dendroclimatic-style analyses presented are the first performed on Lateglacial tree-ring chronologies. Future efforts should focus on robustly preserving lower-frequency environmental variations and comparisons with other high resolution archives to quantify and calendrically date the main climatic fluctuations during Lateglacial and early Holocene.

5.10

Oxygen isotopic composition of lacustrine cellulose and authigenic calcite – new insight into Late Glacial and Holocene temperature changes in central Poland

Klisch* M.A., Rozanski* K., Edwards** T.W.D.

* AGH-University of Science and Technology, Krakow, Poland (monikaklisch@gmail.com)
** University of Waterloo, Waterloo, Ontario, Canada

The $\delta^{18}O$ of lacustrine calcite potentially provides information about both temperature and $\delta^{18}O$ of lake water. If the $\delta^{18}O$ of lakewater is strongly controlled by the $\delta^{18}O$ of local precipitation, such as in a groundwater-fed lake having rapid throughflow, and lakewater temperature covaries with climatic temperature, then $\delta^{18}O_{calcite}$ may serve as a direct palaeothermometer.
The "calibration" of the thermometer will be determined by two opposing relationships: temperature-dependent changes in the $\delta^{18}O_{precipitation}$ (c. +0.64‰/K for Poland; Duliński et al., 2001) and changes in the temperature-dependent equilibrium fractionation between calcite and water (c. – 0.23‰/K; Craig, 1965):

$$\Delta\delta^{18}O_{calcite}/\Delta T = 0.64‰/K - 0.23‰/K \approx 0.4‰/K \quad (1)$$

Equations like (1) have been used in many situations to reconstruct palaeotemperatures, including, for example, the development of a Holocene palaeotemperature record from $\delta^{18}O_{calcite}$ in the sediments of Lake Gosciaz. A source of significant uncertainty in this approach, however, is the possibility that changes in the hydrologic balance of a lake may alter the relation between $\delta^{18}O_{precipitation}$ and $\delta^{18}O_{lakewater}$, potentially adding spurious non-temperature-dependent signals.

Here we report results from a pilot study to test the $\delta^{18}O_{calcite}$ thermometer in Lake Gosciaz sediments by using aquatic cellulose $\delta^{18}O$ to directly estimate the $\delta^{18}O$ of lakewater at times in the past. Since the isotopic fractionation between cellulose and lakewater is believed to be constant (Edwards and McAndrews, 1989; Wolfe et al., 2007), this allows us to isolate the effects of temperature-dependent calcite-water fractionation to obtain estimates of absolute temperature changes during and between selected intervals over the past 12,000 years, without interference from possible changes in the hydrologic balance of the lake. The calibration of the cellulose-calcite thermometer in this case is described by:

$$\Delta T = (\Delta\delta^{18}O_{calcite} - \Delta\delta^{18}O_{cellulose})/(-0.23\ ‰/K) \quad (2)$$

Our data from Lake Gosciaz yield some striking differences in estimated temperature changes. For example, for the Younger Dryas/Preboreal transition, equation (1) gives an increase in lakewater temperature of about +5K, meanwhile equation (2) suggests +20 K, because of the incorporation of a pronounced shift of +6.5 ‰ observed in $\delta^{18}O_{cellulose}$. This shift in $\delta^{18}O_{cellulose}$ almost certainly reflects the influence of increased evaporative enrichment of the lakewater in response to drier conditions, which obviously cannot be accommodated by equation (1).

REFERENCES
Craig H., 1965: The measurement of oxygen isotopes paleotemperatures, In Tongiorgi, E. (ed.): Stable Isotopes in Oceanographic Studies and Paleotemperatures. Spoleto, Consiglio Nazionale delle Ricerche, Laboratorio di Geologia Nucleare, Pisa, Italy, 161-182
Duliński, M., Florkowski, T., Grabczak, J.& Różański, K. 2001: Twenty-five years of systematic measurements of isotopic composition of precipitation in Poland, Przegląd Geologiczny 49, 250-256 (in Polish)
Edwards, T.W.D & McAndrews, J.H. 1989: Paleohydrology of a Canadian Shield lake inferred from ^{18}O in sediment cellulose, Can.J.Earth Sci.26, 1850-1859
Wolfe, B.B., Falcone, M.D., Clogg-Wright, K.P., Mongeon, C.L., Yi Yi, Brock, B.E., St Amour, N.A., Mark, W.A., Edwards, T. W.D. 2007: Progress in isotope paleohydrology using lake sediment cellulose, Journal of Paleolimnology, Vol 37, No 2, 221-231

5.11

Variation of denudation rates in the partially fluvially and partially glacially scupltured Hörnli region, Switzerland

Kober, F. *, Abbühl, L.**, Ivy-Ochs, S.***, Schlunegger, F.**, Kubik, P.W.****,Baur, H*****, Wieler, R. *****,

*Geological Institute, ETH Zürich, CH-8092 Zürich (kober@erdw.ethz.ch)
** University of Bern, Baltzerstrasse 1+3, CH-3012 Bern
***Ion Beam Physics, Particle Physics, ETH Zürich, CH-8093 Zürich and
Department of Geography, University of Zürich, CH-8057 Zürich
****Ion Beam Physics, Particle Physics, ETH Zürich, CH-8093 Züich
*****Isotope Geology and Mineral Resources, ETH Zürich, CH-8092 Zürich

The Hörnli region has long been recognized for its landscape with opposite appearance: the lower regions (mainly the western Hörnli/Glatt valley and eastern Hörnli/Thur valley) are glacially overprinted and have smooth surface expressions; whereas the inner part of the Hörnli region (the Töss valley and surrounding highs) is a fluvial overprinted landscape. This fact is a result of an ice free "Hörnli-nunataker", at least during the Würm glaciation (Hantke, 1980). Slopes, relief, river longitudinal and cross profiles complement this view, being U-shaped, subdued and partially filled with terraces or V-shaped and steep, in glacial or fluvial settings, respectively. Currently, U-shaped valleys are getting incised due to the lowering of the base-level further outward and transmission of this base-level change headward, producing step-morphologies. This is a common feature observed in the Alps. Such morphologies are characterized as being in a transient stage - in the transition from the glacial to a fluvial dominated system (Schlunegger et al., 2002).
However, it is controversial to what extend and with what rates the inherited shape and form of a landscape (glacial vs. fluvial) or a transient stage of a valley form controls short and long-term denudation rates.

The Hörnli region is an ideally suited field area to study those denudation processes because it is uniform in lithology (Upper Sweetwater Mollasse), tectonics (being very slow but uniform uplifted) and climate. As such, crucial parameters in controlling denudation rates can be ignored and focus can be given to isolate parameters such as inherited topography and relief (von Blanckenburg, 2006).

In order to quantify denudation rates in such a two-process dominated landscape we have sampled various rivers around the Hörnli region for catchment-wide denudation rate estimations using cosmogenic nuclides (^{10}Be, ^{21}Ne; in a second step we aim to analyze ^{14}C to capture short-term variations in a steady or transient stages of erosion). The dataset comprises samples from rivers which show completely fluvial, glacial or a combination of both morphologies. Sample analysis however is ongoing. Preliminary results from samples of the Töss river and tributaries yield denudation rates that are on the order of rates previously acquired for Swiss Middleland rivers (Norton et al., 2008; Wittmann et al., 2007), though denudation rates tend to be higher in glacially compared to fluvial overprinted catchments. Additionally, local variations occur which are not directly linkable to a glacial or fluvial origin. So far ^{10}Be and ^{21}Ne concentrations and denudation rates correlate poorly, which is largely due to obtain precise low ^{21}Ne-concentration in our samples.

REFERENCES
Hantke, R., 1980. Eiszeitalter, 1-3. Ott Thun Verlag, Thun.
Norton, K.P., von Blanckenburg, F., Schlunegger, F., Schwab, M. and Kubik, P.W., 2008. Cosmogenic nuclide-based investigation of spatial erosion and hillslope channel coupling in the transient foreland of the Swiss Alps.

Geomorphology, 95(3-4): 474-486.
Schlunegger, F., Detzner, K. and Olsson, D., 2002. The evolution towards steady state erosion in a soil-mantled drainage basin: semi-quantitative data from a transient landscape in the Swiss Alps. Geomorphology, 43: 55-76.
von Blanckenburg, F., 2006. The control mechanisms of erosion and weathering at basin scale from cosmogenic nuclides in river sediment. Earth and Planetary Science Letters, 242(3-4): 224-239.
Wittmann, H., von Blanckenburg, F., Kruesmann, T., Norton, K.P. and Kubik, P.W., 2007. Relation between rock uplift and denudation from cosmogenic nuclides in river sediment in the Central Alps of Switzerland. Journal of Geophysical Research- Earth Surface, 112: F04010, doi:10.1029/2006JF000729.

5.12

Regional synthesis of Mediterranean atmospheric circulation during the Last Glacial Maximum

Kuhlemann Joachim1,5, Rohling Eelco J. 2, Krumrei Ingrid1, Kubik Peter3, Ivy-Ochs Susan4, Kucera Michal1

1 Inst. for Geosciences, Univ. of Tuebingen, Sigwartstr. 10, D-72076 Tuebingen, Germany (kuhlemann@uni-tuebingen.de)
2 School of Ocean and Earth Science, National Oceanography Centre, Southampton, SO14 3ZH, U.K.
3 Institute of Particle Physics, HPK H30, ETH Zurich, CH-8093 Zurich, Switzerland
4 Institute of Particle Physics, HPK H27, ETH Zurich, CH-8093 Zurich, Switzerland
5 HSK/ENSI, CH-Villigen-HSK (Joachim.Kuhlemann@hsk.ch)

Atmospheric circulation leaves few direct traces in the geological record, making reconstructions of this crucial element of the climate system inherently difficult. Here, we produce a regional Mediterranean synthesis of palaeo-proxy data from sea-surface to alpine altitudes. This provides a detailed observational context of change in the 3-dimensional structure of atmospheric circulation between the Last Glacial Maximum (LGM; ≈23-19 ka) and Present. The synthesis reveals evidence for frequent cold polar air incursions, topographically channelled into the northwestern Mediterranean. Anomalously steep vertical temperature gradients in the central Mediterranean imply local convective precipitation. We find the LGM patterns to be analogous, though amplified, to previously reconstructed phases of enhanced meridional winter circulation during the Maunder Minimum (Little Ice Age).

The equilibrium line altitude (ELA) of glaciers contains information on the vertical structure of the atmosphere, which can be reconstructed by in-situ dating of glacial advances and retreats. Small temperate glaciers in circum-Mediterranean mountain chains are (and were) exposed to well-mixed air masses and are known to have been sensitive to even small changes of the ELA, typically responding by advance or retreat within several years to decades. The ELA responds to both temperature and precipitation change, and it is possible to differentiate between these two factors only in particularly well-studied regions, such as Corsica (Kuhlemann et al. 2008). For this island, we present new information on the LGM ELA, including a deconvolution of the two main controlling processes. For the ELA depression of LGM glaciers in the wider Mediterranean region, we use previously published information, which – as a first-order end-member solution – we calculate as pure temperature change, using a standard free atmospheric lapse rate of 6.5 °C decrease per km of increasing elevation. The potential overprint of precipitation changes is then considered where anomalous results are found. The error ranges on the resultant ELA reconstructions amount to up to +100 m in Corsica and +150 m in other Mediterranean mountains. We thus develop a regional synthesis of glacial vertical temperature gradients in the lower atmosphere. Next, we compare the ELA-based LGM cooling at alpine altitudes with estimates of LGM reduction of Mediterranean sea-surface temperatures (SST) derived from the difference between foraminiferal assemblages and alkenone data. When comparing the temperature equivalent of the ELA depression with SST reduction in the LGM relative to the present (Fig. 1), we consider that a shift of similar magnitude would indicate a constant atmospheric lapse rate.

Our analysis reveals an LGM pattern of southward extending lobes of ELA depression in mountainous regions of Italy and the Dinarides, which suggests frequent higher-altitude southward advances of polar air. Iberia is characterized by a steep gradient from the northern and northwestern coastlines towards the interior and southeast, which likely results predominantly from barrier effects of near-coastal mountain ranges. Especially the data from Corsica identify a lobe of ELA depression that extends over the Gulf of Lions towards the south and east, indicating significant invasion of polar air from the north. The temperature difference inferred from the recent ELA and our LGM reconstruction generally decreases from north (10-11 °C) to south (6-7 °C) (Fig. 1). Both SST and ELA-determined atmospheric temperatures (T_{ELA}) underwent similar (within +2 ºC) changes, relative to the present, across the northern Bay of Biscay and western sector of the western Mediterranean. LGM SST seems less reduced than T_{ELA} in the Atlantic Ocean offshore Iberia and Morocco, which likely reflects the southward displacement of the relatively warm Gulf Stream during glacial times. The warm anomaly in the central Mediterranean basin, however, can hardly be attributed to advection of warm surface waters from the western basin because of land barriers.

We propose that advection of warm desert air from the Sahara and relatively cloud-free subtropical conditions over the central/eastern basin largely account for the minor LGM cooling of SSTs in this region.

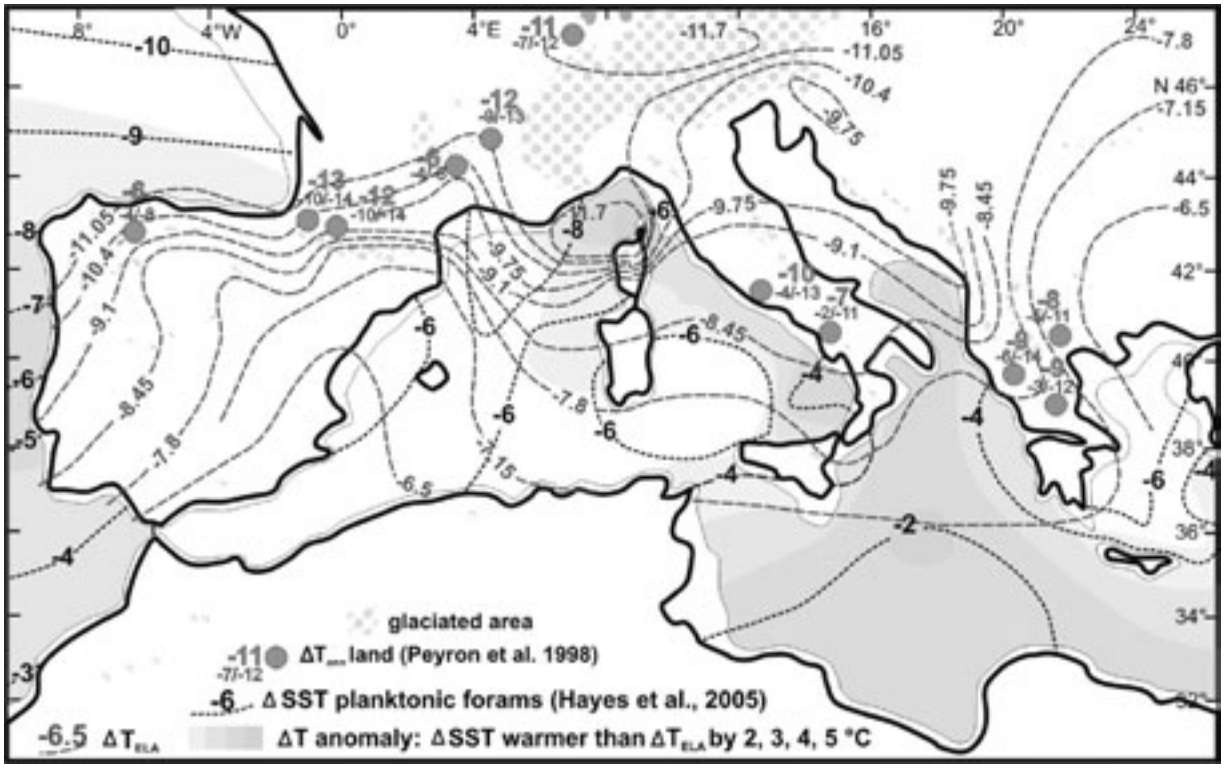

Figure 1: Map of the temperature difference between recent and LGM SST, and temperature equivalent of the ELA depression (6.5 ºC km^{-1} lapse rate), respectively. The error range of this estimate is +1°C for the Mediterranean in general, and +0.7°C in Corsica.

REFERENCES:
Kuhlemann, J., Krumrei, I., Rohling E., Kubik, P., Ivy-Ochs S., Kucera, M. 2008. Regional synthesis of Mediterranean atmospheric circulation during the Last Glacial Maximum. Science DOI: 10.1126/science.1157638

5.13

Reconstructing the fluvial history of the Llanos de Moxos, NE Bolivia – approaches, challenges and first results

May Jan-Hendrik*, Lombardo Umberto & Veit Heinz

Geographisches Institut, Universität Bern, Hallerstr. 12, CH-3012 Bern
**(may@giub.unibe.ch)*

The reconstruction of past fluvial environments and their changes over time is a major issue in Quaternary sciences. This is particularly true for the lowlands of South America where the late Quaternary history of many extensive fluvial systems has remained virtually unexplored. The Moxos plains (Llanos de Moxos), NE Bolivia, are among the largest inundated savanna landscapes in the world (Fig. 1A). They are drained by the large meandering fluvial systems of the Río Beni and the Río Mamoré, and are subject to annual flooding (e.g. Hamilton et al. 2004). Frequency and magnitude of these flood events, however, have varied significantly over the last centuries, probably in relation to larger scale atmospheric phenomena (e.g. Aalto et al. 2003; Ronchail et al. 2005). However, no data exist regarding changes on millennial or late Quaternary time scales.

Therefore, this study aims at i) documenting the large complexity inherent to the fluvial systems in the Llanos de Moxos, ii) discussing selected approaches and possibilities for their reconstruction, and iii) presenting and interpreting preliminary field data from the Río Mamoré area:

Outcrops along the *active Río Mamoré meander belt* (Fig. 1B) represent an archive of Río Mamoré overbank deposition and flooding activity. Several profiles extend into the late Pleistocene, even though ^{14}C dating of these sedimentary sequences still bears some limitations. The analyses of paleosols and geochemical parameters (grains size, total elements and mineralogy) indicate reduced flooding intensities during the early to mid-Holocene.
Several abandoned meander belts and paleochannels testify to large scale channel avulsions and changes of fluvial regime in the past. These meander belts are considered valuable archives for paleoenvironmental reconstruction: i) Their fluvial geometries were measured along the paleo-Mamoré (Fig. 1C) and compared to the present floodplain, pointing to markedly reduced channel forming discharges in the past. ii) Partly filled oxbows may serve as an excellent archive for reconstruction by means of higher-resolution proxies and the analysis of a first coring transect is currently in progress. iii) Rectangular lake basins, canals and dams are features of possible anthropic origin (e.g. Mann 2000), which are superposed onto the abandoned Río Mamoré meander belt. The dating of the underlying fluvial and lacustrine sediments provides maximum ages for these features, and thereby allows for the first time the establishment of a chronological framework for the late Holocene pre-Columbian human interference into the hydrological system of the Llanos de Moxos.

In conclusion, the presented work documents a dynamic fluvial history of the Llanos de Moxos since the late Pleistocene. Thus, this new information adds valuable data to questions regarding the paleoenvironmental evolution as well as the degree and type of pre-Columbian human impact in lowland Amazonia.

REFERENCES

Aalto, R., Maurice-Bourgoin, L., Dunne, T., Montgomery, D.R., Nittrouer, C.A. and Guyot, J.L. 2003. Episodic sediment accumulation on Amazonian flood plains influenced by El Niño/Southern Oscillation. Nature, 425, 493 - 497.

Hamilton, S.K., Sippel, S.J. and Melack, J.M. 2004. Seasonal inundation patterns in two large savanna floodplains of South America: the Llanos de Moxos (Bolivia) and the Llanos del Orinoco (Venezuela and Colombia). Hydrological Processes, 18, 2103-2116.

Mann, C.C. 2000. Earthmovers of the Amazon. Science, 287(5454), 786-789.

Ronchail, J., Bourrel, L., Cochonneau, G., Vauchel, P., Phillips, L., Castro, A., Guyot, J.-L. and de Oliveira, E. 2005. Inundations in the Mamore basin (south-western Amazon–Bolivia) and sea-surface temperature in the Pacific and Atlantic Oceans. Journal of Hydrology, 302(1-4), 223-238.

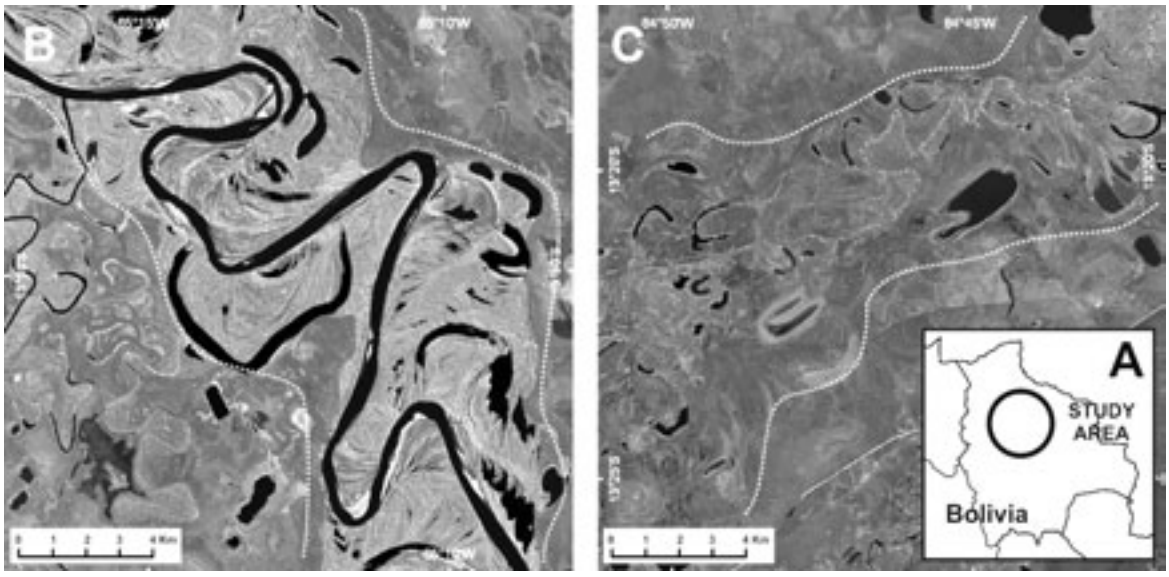

Figure 1: A) Location of the study area (Llanos de Moxos) in Bolivia; B – Landsat image of the modern Río Mamoré meander belt outline by white dotted line (232-70, RGB 742, 19/9/2001, Source: http://edcsns17.cr.usgs.gov/Earth Explorer); C – Landsat image of the Paleo-Mamoré meander belt outlined by white dotted line including several partly infilled oxbow lakes and other lakes (232-69, RGB 742, 19/9/2001, Source: http://edcsns17.cr.usgs.gov/Earth Explorer/).

5.14

Chronostratigraphy of the Quaternary of Switzerland

Preusser Frank & Schlüchter Christian

Institut für Geologie, Universität Bern, Baltzerstrasse 1+3, CH-3012 Bern

While Early Quaternary glacial deposits are exposed in northern Switzerland (Deckenschotter complex, cf. Graf 1993), the so far best investigated and dated Middle to Late Pleistocene record is known from the Aare Valley and surrounding regions. The oldest unit here is the water-lain till from the base of the Thalgut drilling, followed by lake deposits that are, based on palynostratigrapy (40 % Fagus, Pterocarya), attributed to the Holsteinian Interglacial. The Holsteinian corresponds to either Marine Isotope Stage (MIS) 11 (≈ 400 ka) or MIS 9 (≈ 300 ka). A glacial advance subsequent to this interglacial is recorded in the Thalgut sequence. A prominent discontinuity following this glaciation is interpreted to result from interglacial weathering and erosion (cf. Schlüchter 1989). Sediments presumably corresponding to this time gap have been identified at Meikirch (Preusser et al., 2005). According to sedimentology, luminescence dating and re-interpretation of pollen data originally published by Welten (1982, 1988) the Meikirch Complex represents three warm phases with interglacial character that belong to MIS 7. A similar tripartition of MIS 7 has been identified in the loess sections of Sierentz (Upper Rhine Graben, Rentzel et al., submitted) and Wels (Austria, Preusser and Fiebig, 2008).

Controversially discussed has been the question if glaciers reached the Swiss lowlands during MIS 6. With the re-interpretation of Meikirch, an important argument against such a glacial advance, for which substantial evidence is available from other parts of the planet, has ceased to exist (cf. Preusser et al. 2005). Furthermore, two recent studies provide dating evidence for an extensive glaciation of the Swiss lowlands. Graf et al. (2007) present first surface exposure ages implying that at least some of the erratic boulders from the Jura Mountains may be deposited during MIS 6 and luminescence dating of high lying gravel deposits ("Höhenschotter") from Emmental support extensive glaciation during that time (Preusser, unpubl. data).

The chronology of the last glacial cycle has been discussed in detail by Preusser (2004) and will only be summarised here. Welten (1982, 1988) und Wegmüller (1992) identified two stadials and two interstadials during the Early Würmian in Swiss pollen records. Cold but relatively humid conditions during MIS 5d (ca. 105 ka) may have triggered a glacial advance beyond the boarder of the Alps at that time (Welten 1982, Preusser et al. 2003). A further glacial advance during MIS 4 (ca. 65 ka) has been dated by Preusser et al. (2007) in Seeland. The Middle Würmian (MIS 3, ca. 55-30 ka) is best recorded in the Gossau section, showing an alternation between cool and temperate conditions. Peat deposits with vertebrate remains from Niederweningen with an age of ca. 45 ka are probably on of the best investigated terrestrial MIS 3 deposits world-wide (Furrer et al. 2007), although reflecting only are quite short period of time. The last glacial advance reached the Swiss lowlands shortly after 30 ka and this area was ice-free by 20 ka ago (Ivy-Ochs et al. 2004).

REFERENCES

Furrer, H., Graf, H.R., & Mäder, A. 2007: The mammoth site of Niederwenigen, Switzerland. Quaternary International 164-165, 85-97.

Graf, H.R. 1993: Die Deckenschotter der zentralen Nordschweiz. – Diss. ETH Nr. 10205 1-151.

Graf, A.,A., Strasky, S., Ivy-Ochs, S., Akcar, N., Kubik, P.W., Burkhard, M., & Schlüchter, C. 2007: First results of cosmogenic dated pre-Last Glaciation erratices from the Montoz area, Jura Mountains, Switzerland. Quaternary International 164-165, 43-52.

Ivy-Ochs, S., Schäfer, J., Kubik, P.W., Synal, H.-A., & Schlüchter, C. 2004: Timing of deglaciation on the northern alpine foreland (Switzerland). Eclogae geolgicae Helvetiae 97, 47-55.

Preusser, F. 2004: Towards a chronology of the Late Pleistocene in the northern Alpine Foreland. Boreas 33, 195-210.

Preusser, F., Drescher-Schneider, R., Fiebig, M., Schlüchter, C. 2005: Re-interpretation of the Meikirch pollen record, Swiss Alpine Foreland, and implications for Middle Pleistocene chronostratigraphy. Journal of Quaternary Science 20, 607-620.

Preusser, F., Geyh., M.A., Schlüchter, Ch. 2003: Timing of Late Pleistocene climate change in lowland Switzerland. Quaternary Science Reviews 22, 1435-1445m.

Preusser, F., Blei, A., Graf, H.R., Schlüchter, C. 2007: Luminescence dating of Würmian (Weichselian) proglacial sediments from Switzerland: methodological aspects and stratigraphical conclusions. Boreas 36, 130-142.

Preusser, F., Fiebig, M. 2008. European Middle Pleistocene loess chronostratigraphy: Some considerations based on evidence from the Wels site, Austria. Quaternary International. doi:10.1016/j.quaint.2008.07.006

Rentzel, P., Preusser, F., Pümpin, Ch., Wolf, J.-J.: Cover sediments and palaeosols on the High Terrace at Sierentz, France, and implications for the chronology of terrace formation in the southern Upper Rhine Graben. – Swiss Journal of Geosciences. (submitted)

Schlüchter, C. 1989: The most complete Quaternary record of the Swiss Alpine Foreland. Palaeogeography, Palaeoclimatology, Palaeoecology 72, 141-146.

Wegmüller, S. 1992: Vegetationsgeschichtliche und stratigraphische Untersuchungen an Schieferkohlen des nördlichen

Alpenvorlandes. Denkschrift der Schweizer Akademie für Naturwissenschaften 102, 1-82, Birkhäuser, Basel.
Welten, M. 1982: Pollenanalytische Untersuchungen im Jüngeren Quartär des nördlichen Alpenvorlandes der Schweiz. – Beiträge zur Geologischen Karte der Schweiz – Neue Folge 156.
Welten, M. 1988: Neue pollenanalytische Ergebnisse über Jüngeren Quartär des nördlichen Alpenvorlandes der Schweiz. Beiträge zur Geologischen Karte der Schweiz – Neue Folge 162.

5.15

Reconstruction of Jordan palaeoenvironments (≈25 000 BP - present day): the Water Life and Civilisation project

Rambeau Claire*, Inglis Robyn**, Smith Sam*, Finlayson Bill*** & Black Stuart*

* *School of Human & Environmental Sciences, The University of Reading, Geoscience building, Whiteknights, P.O. Box 277, Reading RG6 6AB, UK (c.m.c.rambeau@reading.ac.uk)*
** *Department of Archaeology, The University of Cambridge, Downing Street, Cambridge CB2 3DZ, UK*
*** *Council for British Research in the Levant (CBRL), British Institute, PO Box 519, Jubaiha 11941, Amman, Jordan*

Early Holocene climatic variations have frequently been cited as 'prime movers' in the transitions to sedentism and agriculture in the Near East. Variations in water availability, which has probably played a crucial role in the development of the first permanent settlements and first farming communities, are strongly dependant on climatic conditions, which underwent significant changes throughout the Late Quaternary period. The Levant, and more particularly the Jordan Valley, represents an ideal context for studying the impact of late Quaternary climate change on past human settlements, in particular in nowadays arid to semi-arid areas.

As part of the Water, Life and Civilisation (WLC) project based in Reading (UK), our group aims to reconstruct prehistoric, historic and modern palaeoenvironmental conditions for parts of the Jordan Valley and south Jordan using a range of techniques including the study of isotopes (stable and radiogenic) in carbonate systems. Data obtained are integrated with results from other WLC groups (hydrology, climate modelling, social geography and archaeology) to explore the relationship between water, environment and human society within Jordan from ≈25,000 BP to the present day, and beyond.
Our current work focuses on case studies investigating the potential for spring-related carbonate sequences outcropping near archaeological sites (especially in southern Jordan) to record environmental variations, which may be linked to contemporaneous histories of human occupations.

Research into the local environment at Beidha, the famous Neolithic site near Petra in southern Jordan excavated by Diana Kirkbride in the 1960s, encompasses studies of landscape feature variations, a reconstruction of local climatic variations via stable isotopic (oxygen and carbon) contents of spring-carbonates and soil carbonate concretions, and the obtention of new radiocarbon dates from the archaeological site early occupation layers. Beidha was occupied during Natufian (two discreet phases) and Pre-Pottery Neolithic B (PPNB) times. The new dates help in refining the time-scale of human settlement at Beidha for the Late Natufian and the start of the Neolithic occupation, and in comparing it with the environmental records.
Selected root-related and other carbonate concretions from the landscape features surrounding the site were dated by U-series. The results, alongside a geomorphological reconstruction of the area including indices of riverine aggradation and down-cutting, were integrated into an initial reconstruction of environment at Beidha during human occupation. A sequence of carbonate precipitations related to a fossil spring, outcropping <100 m W of the site, allowed us to reconstruct climatic variations between <16,500 years BP and ≈8,400 years BP (U-series dating) by the use of carbon and oxygen stable isotope analyses.
The results of the palaeoenvironmental study were compared with the archaeological evidence, to provide a detailed picture of the relationship between human occupation and local climatic variability.
Overall, periods of human occupation, both during the Natufian and Neolithic times, seem to correspond to more favourable environmental conditions. The fossil spring itself stopped flowing around 8,500 years BP, coeval with the abandonment of the PPNB settlement. A phase of extended vegetation colonization, marked by the presence of large root concretions, took place on top of wind-blown sand dunes around 11,500 years BP. Wetter conditions therefore appear to have been present at Beidha before the PPNB, which may raise the question of a possible Pre-Pottery Neolithic A (PPNA: ≈12,000 – 10,600 cal. BP) occupation at Beidha.

Similar investigations are ongoing at Wadi Faynan, where a study of the isotopic composition of carbonate precipitations adjacent to PPNA to Byzantine settlements is being compared to archaeological information and hydrological models for this

site.
Information gained from these case studies are being integrated with other available data sets (e.g., lake and sea levels, botanical and sedimentological studies, paleosols occurrences) on a broader regional scale. This review contributes to our understanding of the past environments of the Levant, and especially of its most arid regions, and therefore helps to refine palaeo-climatic models.

5.16

Proposing IR stimulated luminescence to date Quaternary phreatomagmatic eruptions from central Madagascar

Rufer Daniel*, Preusser Frank & Schreurs Guido

Institut für Geologie, Universität Bern, Baltzerstrasse 1 + 3, CH-3012 Bern
** Corresponding author: rufer@geo.unibe.ch*

The Ankaratra volcanic field in central Madagascar is closely linked to extensional tectonics that affects the area since the middle Miocene. This intracontinental rifting in Madagascar possibly represents a continuation of the East African Rift (Bertil and Regnoult, 1998). The latest phase of the rift-related volcanism in central Madagascar occurred in the southern part of the Ankaratra volcanic field during the late Quaternary. The existing dates for the eruptions in this region are only of indirect nature or based on geomorphological observations and absolute ages are lacking. It is therefore of great interest to directly date the Quaternary volcanism in order to establish a reliable temporal framework for the youngest neotectonic and magmatic events in central Madagascar.
Unfortunately, the available methods for directly dating volcanic rocks of quaternary, especially late Pleistocene to Holocene age, are rather scarce and possess some inherent pitfalls like the necessity of closed system behaviour, usable estimations of initial ratios (U/Th disequilibria) or finding suitable sample material (e.g. organic material for ^{14}C). The young age and the geochemical and petrological composition causes further problems for radiogenic dating with K/Ar or Ar/Ar methods, as the bulk of the potassium is dispersed in the vitreous to aphanitic matrix and a noted absence of juvenile sanidine is observed. Luminescence dating would be a potential target technique for acquiring ages in the timeframe in question, and Tsukamoto et al. (2007) have shown that red isothermal TL on volcanic quartz can be used to date rhyolitic tephras back to 388 ± 25ka. However, as the alkaline ultramafic volcanic rocks of the Ankaratra region are mostly silica undersaturated and alkaline feldspars are scarce or occur only as microcrysts in an aphanitic matrix, neither quartz nor suitable feldspars are available for luminescence dating. However, at least one phreatomagmatic eruption occurred during the early stages of most Quaternary volcanic centres. Due to the nature and the immense energy release of the explosive eruptions, large volumes of crystalline basement material were disintegrated and ejected as ash and sand sized particles over large areas of several tens to hundreds of square kilometres. The bleaching potential during the relatively long aerial transit-time of up to several hours (Bonadonna et al., 2005) and the potential resetting of the luminescence signal by hydrostatic pressure or frictional heating during the eruption (Zöller et al., 2007) suggests that quartz or feldspar grains from this kind of deposit might be suitable for luminescence dating.
In this study we test the potential of IR stimulated luminescence (IRSL) for directly dating phreatomagmatic explosion layers from late Quaternary eruptions from the Ankaratra volcanic field. Multiple feldspar samples from several volcano-stratigraphically linked explosion horizons were studied by single aliquot regenerative IRSL. The quartz samples were not measured, as they exhibited an unusually low saturation level for laboratory irradiation, the cause of which is not clear, but might be related to the violent fragmentation process of the eruption.

REFERENCES

Bertil, D. and Regnoult, J.M. 1998: Seismotectonics of Madagascar. Tectonophysics, 294(1-2): 57-74.
Bonadonna, C., Connor, C. B., Houghton, B. F., Connor, L., Byrne, M., Laing, A., Hincks, T. K. 2005: Probabilistic modeling of tephra dispersal: Hazard assessment of a multiphase rhyolitic eruption at Tarawera, New Zealand. Journal of Geophysical Research-Solid Earth, 110(B3).
Tsukamoto S., Murray A.S., Huot S., Watanuki T., Denby P.M., Bøtter-Jensen L. 2007: Luminescence property of volcanic quartz and the use of red isothermal TL for dating tephras. Radiat. Meas. 42, 190-197.
Zoeller, L., Blanachard, H., McCammon, C. 2007: The partial heat - longest plateau technique for TL dating of Middle and Upper Quaternary volcanic eruptions. Chemical Geology, submitted.

5.17

Glacier advances during the Lateglacial to Holocene transition in the Swiss Alps

Schindelwig Inga*, Akçar Naki*, Lukas Sven**, Kubik Peter W.*** & Schlüchter Christian*

*Institute of Geological Sciences, University of Bern, Baltzerstr. 1 & 3, 3012 Bern (schindelwig@geo.unibe.ch)
**Department of Geography, Queen Mary, University of London, Mile End Road, London
***Paul Scherrer Institute, c/o Institute of Particle Physics, ETH Zurich, 8093 Zurich

Dating of glacial deposits (e.g. erratic boulders) through surface exposure dating (SED) can provide important information concerning the mechanisms and rates of climate change and hence, can improve the chronology of climate records. During the Lateglacial, stadial and interstadial transitions are abundant (e.g. Björck et al. 1998). Glacial response to rather short lived climatic fluctuations seems to be dependent on various factors such as type of glacier (valley or cirque glacier), exposition of the individual glacier system or size of the catchment area.

Focussing on the end of the Lateglacial, the Gschnitz stadial (≈15.4 to 17 ka, Ivy-Ochs et al. 2008) is the first distinct post-Late Würmian readvance of mountain glaciers, followed by the Clavadel/Senders, the Daun and the Egesen stadial and subsequent advances during the early Holocene (Preboreal). The Egesen stadial in the European Alps is assumed to be related to the Younger Dryas (YD) event. In the Northern Alpine Foreland the YD chron was dated at 12100-11000 cal. yr BP (Hajdas et al. 2004) and represents the last recurrence to near glacial conditions prior to the onset of the Holocene. It is characterized, amongst other things, by significant shifts in temperature at its onset and termination (Dansgaard et al. 1989). At several sites the Egesen stage comprises two or three phases, whereas two of them (Egesen 1 – Maximum, Egesen 2 - Bocktentälli) may directly be associated with the YD (Ivy-Ochs et al. 1996, 2008). For an occasionally appearing third phase of glacial deposits from the Egesen (Kartell stage) it still remains controversial whether it may be associated with the late YD chron or with the early Preboreal chron (11550-10180 cal. yr BP, Ivy-Ochs et al. 2008).

In order to understand different glacier response times and mechanisms, the adjacent valleys of (a) Belalp and Great Aletsch and (b) Val Cristallina and Val la Buora are investigated and compared to each other.
The slow responding Great Aletsch valley glacier shows only one confirmed moraine ridge related to the Lateglacial (Egesen stadial, Kelly et al. 2004). However, the rather fast responding small Unterbächl cirque glacier at the Belalp, a similarly exposed - and tributary valley to the Great Aletsch valley, features up to 6 individual moraine ridges related to Lateglacial and early Holocene times. In contrast, the latter two valleys, also similarly exposed, but interestingly the Val Cristallina with the larger catchment area features up to 6 moraine ridges whereas the smaller Val la Buora seems to have only one prominent moraine ridge related to the Lateglacial.
These results are based on geomorphological mapping and surface exposure ^{10}Be dating of glacially transported boulders or deglaciated bedrock. All ^{10}Be/^{9}Be measurements were carried out at the accelerator mass spectrometer at the ETH/PSI tandem facility in Zurich.

REFERENCES

Björck, S., Walker, M.J.C., Cwynar, L.C., Johnson, S., Knudsen, K-L., Lowe, J.J. & Wohlfarth, B. 1998: An event stratigraphy for the Last Termination in the North Atlantic region based on the Greenland ice-core record: a proposal by the INTIMATE group. Journal of Quarternary Science, 13, 283-292.

Dansgaard, W., White, J.W.C. & Johnsen, S.J. 1989: The abrupt termination of the Younger Dryas climate event. Nature, 339, 532-534.

Hajdas, I., Bonani, G., Hadorn, P., Thew, N., Coope, G.R. & Lemdahl, G. 2004: Radiocarbon and absolute chronology of the Late-Glacial record from Hauterive/ Rouges-Terres, Lake Neuchâtel (CH). Nuclear Instruments and Methods in Physics Research Section B: Beam Interactions with Materials and Atoms, 223-224, 308-312.

Ivy-Ochs, S., Kerschner, H., Reuther, A., Preusser, F., Heine, K., Maisch, M., Kubik, P.W. & Schlüchter, C. 2008: Chronology of the last glacial cycle in the European Alps. Journal of Quaternary Science, 23, 559-573.

Ivy-Ochs, S., Schlüchter, C., Kubik, P.W., Synal, H-A., Beer, J. & Kerschner, H. 1996: The exposure age of an Egesen moraine at Julier Pass, Switzerland, measured with the cosmogenic radionuclides ^{10}Be, ^{26}Al and ^{36}Cl. Eclogae geol. Helv., 89, 1049-1063.

Kelly, M.A., Kubik, P.W., von Blanckenburg, F. & Schlüchter, C. 2004: Surface exposure dating of the Great Aletsch Glacier Egesen moraine system, western Swiss Alps, using the cosmogenic nuclide ^{10}Be. Journal of Quarternary Science, 19, 431-441.

5.18

Application of "clumped-isotope" thermometry to paleotemperature reconstructions in lacustrine carbonates.

Schmid Thomas W. & Bernasconi Stefano M.

Geologisches Institut, ETH Zürich, Universitätsstrasse 16, CH-8092 Zürich (schmidth@erdw.ethz.ch)

"Clumped-Isotope" Geochemistry (Eiler, 2007) is a novel method for temperature determination form carbonate minerals. It is based on the measurement of the abundance of carbonate molecules containing the two rare isotopes ^{13}C and ^{18}O. Gosh et al. (2006) have shown that the difference in abundance of the ^{13}C-^{18}O bonds from a stochastic distribution in carbonate minerals is dependent on the temperature of mineral formation and independent from the $\delta\ ^{18}O$ of the water and the δ13C of the dissolved inorganic carbon. Therefore, with this method it is possible to obtain a temperature estimate that can be used in combination with the $\delta\ ^{18}O$ of the carbonate to precisely reconstruct the oxygen isotope composition of the water. This method, and the necessary analytical techniques are still in development and its application to various climate archives still has to be tested to further reveal its potential and limitations.

We will present first data obtained from the successful application of "clumped-isotope" thermometry to lacustrine carbonates from Lake Zurich. Lacustrine carbonates, because of their wide distribution, are important archives of climate change on the continents. However, the extraction of climatic information from carbonate oxygen isotope records is difficult due to the dependency of $\delta^{18}O$ of the carbonates from both the temperature and the isotopic composition of the lake water. These two parameters are important because water temperatures are correlated with air temperatures and the $\delta\ ^{18}O$ of the lake reflects the $\delta^{18}O$ of precipitation and thus is also dependent on mean annual temperature and atmospheric circulation. "Clumped-isotope" thermometry is independent from the $\delta\ ^{18}O$ of the water and the $\delta^{13}C$ of the DIC and therefore allows an independent temperature determination and $\delta^{18}O$ calculation of the original water body.
We are evaluating the potential of the method by analysing lake Zurich sediments and comparing it with historical water temperature measurements for the last 60 years. In addition we are collecting authigenic calcites in the surface waters to establish a calibration for lacustrine carbonates. We have analysed samples from a short core collected at the deepest point of the lake and annual varves were sampled from the years 1907 to 2000. The measurements were carried out with a Thermo Finnigan Kiel IV Carbonate Device connected to a Delta V plus dual inlet mass spectrometer, equipped with a Faraday cup configuration, designed to measure simultaneously CO_2 of masses 44 to 48, which allows to measure up to 46 samples in a totally automated run. The sample weight is ≈200μg and the external reproducibility of δ47 lies between 0.04‰ and 0.1‰.
We will show a comparison from the annual mean temperature of the Lake Zurich surface water derived by "clumped-isotope thermometry" from measured varves compared to recorded temperatures as well as first data from the authigenic carbonates, precipitated this year in the surface water of Lake Zurich.
This will represent the first calibration of clumped isotope thermometry for lacustrine carbonates and we are planning to apply this method for paleoclimatic reconstructions to other lakes and paleolakes in the future.

REFERENCES

Eiler, J. M., 2007. "Clumped-isotope" geochemistry - The study of naturally-occurring, multiply-substituted isotopologues. Earth and Planetary Science Letters 262, 309-327.

Ghosh, P., Adkins, J., Affek, H., Balta, B., Guo, W., Schauble, E. A., Schrag, D., and Eiler, J. M., 2006. 13C-18O bonds in carbonate minerals: A new kind of paleothermometer. Geochimica et Cosmochimica Acta 70, 1439-1456.

5.19

Soil carbon dynamics on annual to millennial timescales – the experimental approach

Smittenberg Rienk*, Birkholz Axel* Gierga Merle, Hajdas Irka**, Hagedorn Frank***, Guelland Kathi*** Christl Iso****, Bernasconi Stefano M.*,

*Geologisches Institut, ETH Zürich, Universiätstrasse 16, 8092 Zürich (smittenberg@ erdw.ethz.ch)
** Ion Beam Physics AMS ^{14}C lab, ETH Zürich, Schafmattstr. 20, 8093 Zürich
*** Swiss Federal Institute of Forest, Snow and Landscape Research, Zürcher Str. 111, 8903 Birmensdorf.
**** Dept. Environmental Sciences, ETH Zürich, Universitätstrasse 16, 8092 Zürich, Switzerland

Knowledge of soil organic matter (SOM) turnover rates is very important for the quantification of soils as sources and sinks of atmospheric CO_2. Research on the dynamics of especially the recalcitrant fraction of soil organic carbon (SOC) – ultimately responsible for long-term carbon storage - is challenging due to its complex nature, the multitude of physical and chemical processes, and the timescales involved. We present the methods and first results of two different approaches to gain further understanding of the dynamics of especially the recalcitrant SOC fraction:

1. Newly formed or exposed landscapes provide a natural experiment to investigate the roles various mechanisms of OM stabilization play. We present insights in the early development of alpine soils that were gradually exposed after glacier retreat in Central Switzerland, thereby creating a chronosquence of very young to 140 year old soils. First, an inventory of the total carbon content in the forefield as well as the measurement of CO_2 fluxes and the export as dissolved inorganic and organic carbon gives further insight in the carbon dynamics of these young developing soils. Followed over the chronosequence, initial SOM accumulation is clearly present, which shows an exponential increase in TOC content (Figure 1). Second, chemical and physical separation techniques combined with chemical fingerprinting techniques of size and density fractions along the chronosequence, as well as analysis of specific compounds, gives further insight in the build-up and relative importance of the various SOM 'pools' (e.g. chemically stable, or protected by mineral adsorption) over time. More specifically, the use of radiocarbon analysis as natural tracer for the age of various organic carbon pools is explored. Comparison of the total carbon content and ^{14}C content of various physically and chemically separated fractions, including specific compounds, provides further insight in the mechanisms that play a role in carbon dynamics.

2. We build further on the successful approach of Smittenberg et al. (2006), where the terrestrial SOC pool is followed through a well-preserved and well-dated sedimentary sequence covering the Holocene (Figure 2). More specifically, the radiocarbon ages of soil-derived molecular compounds and organic matter fractions are compared to those with the actual age of deposition of the sediment. In this way, the build-up of the terrestrial SOC pool can be reconstructed, providing for instance information whether some 'steady state' has been reached or if there is still a continuous and ongoing accumulation of recalcitrant SOC. We have started to investigate laminated and well-dated sediments from the Meerfelder Maar, Germany, and lakes from the Lofoten, Norway, both spanning approximately the last 15,000 year, from which we will present some first results.

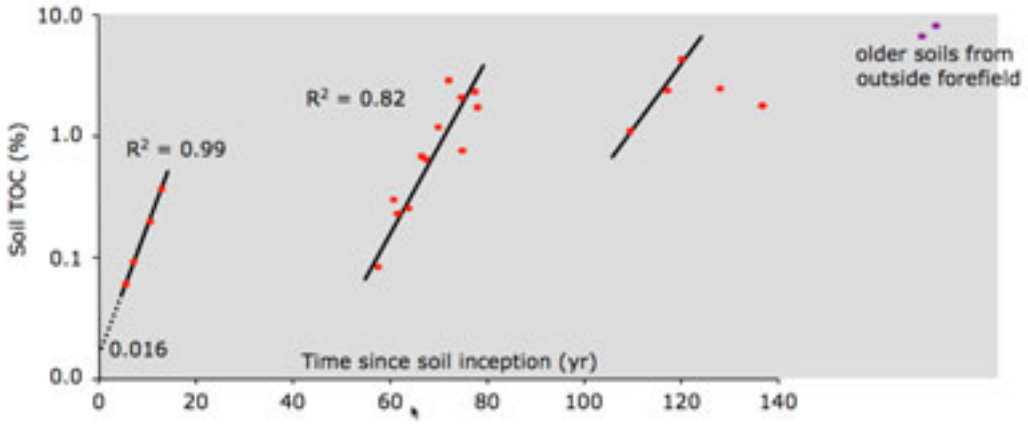

Figure 1. Exponential increase of Total Soil Carbon over the 140yr long chronosequence of the Damma forefield, Switzerland, Kanton Uri.

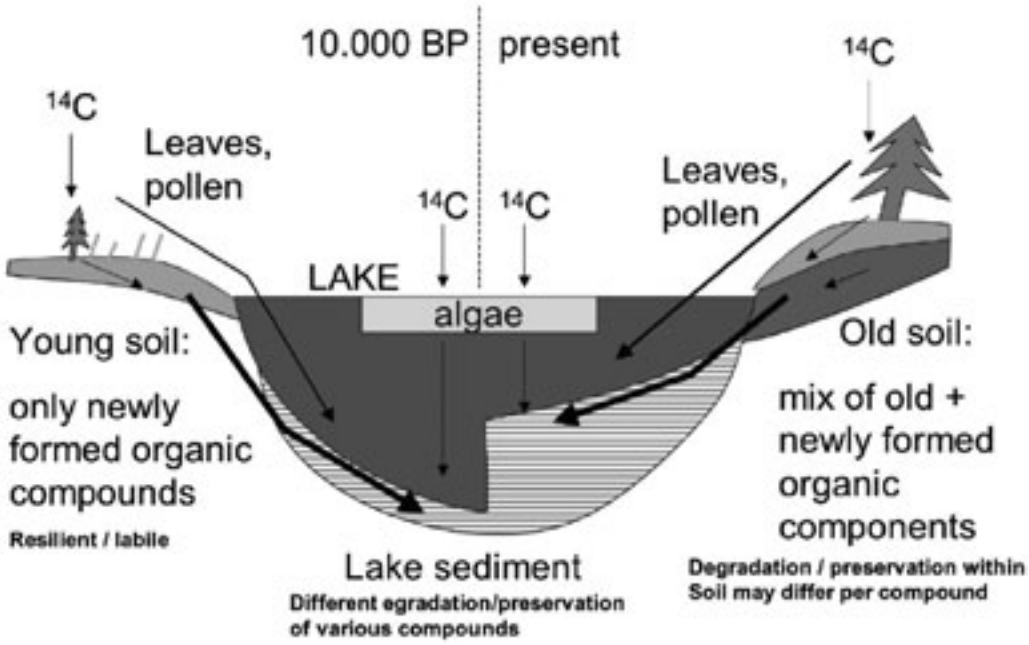

Figure 2. Cartoon of carbon fluxes into a lake sediment. Resilient organic matter builds up in soils. In the past, as well as at present, a small fraction of the soil erodes, and the sediment receives thus each year a 'snapshot' of the soil carbon pool, that can be dated using ^{14}C.

REFERENCES

Smittenberg, R.H., T.I. Eglinton, S. Schouten, J.S. Sinninghe Damsté, 2006, Ongoing build-up of refractory organic carbon in boreal soils during the Holocene. Science 314, 1283

5.20

Record of past environmental and climatic changes in the sediments of Lake Pfafforet (Valais, Switzerland)

Straub Marietta*, Wick Lucia**, Anselmetti Flavio***, Gilli Adrian*, Guélat Michel****, Mottet Manuel*****, Paccolat Olivier******, Rentzel Philippe**

* *Department of Earth Science, Swiss Federal Institute of Technology (ETH) Zürich*
** *Institute for Prehistory and Archaeological Science, IPAS, University Basel, Spalenring 145, 4055 Basel*
*** *Eawag, Swiss Federal Institute of Aquatic Science & Technology*
**** *Géologue, Creux de la Terre 11, 2800 Delémont*
***** *Bureau ARIA, Rue de Loèche 11, 1950Sion*
****** *Bureau TERA, Rue du Pré-Fleuri 12, 1950 Sion*

A 5 m long sediment record of Lake Pfafforet (Valais, Switzerland) indicates significant changes in paleo-climate, paleo-vegetation and paleo-hydrology over the last ≈4000 yrs BP in the Pfyn-Forest. These changes are correlated to nearby situated archaeological sites, which show a long history of human occupation in the area.

Lake Pfafforet is situated within the Pfyn-Forest in the Rhone valley between Leuk and Sierre. The Pfyn-Forest is characterised by a special micro-climate, with very hot summers and cold winters that are more extreme than average. The undulating and irregular morphology of the area is built up by slide deposits from the rockslide of Sierre, which is estimated to be ≈15'000 years old (Burri 1997), although no precise dating exists today. Within the Pfyn-Area, archaeological excavations on relicts from the Iron Age, the Roman Period and Mediaeval Period were carried out, which triggered interest in the climatic and the environmental situation during these historic times. As Lake Pfafforet is the deepest natural lake in the Pfyn-Forest (Bendel et al., 2006), its sediment record was targeted to get information about the past climatic and environmental evolution.

Sediment cores were taken at four different sites in the lake. Several chemical, physical and biologic analysis were carried out, including MSCL (density and magnetic susceptibility), XRF & XRD (elemental and mineralogical composition), carbon and oxygen isotopes, carbon content, smear slides, pollen and grain size measurements. The sediment consists of a complex succession of organic-rich, authigenic lake sediments intercalated by light-coloured, detrital layers. These detrital layers consist mainly of quartz, calcite and mica and they are interpreted as Rhone sediments, probably brought into the lake by floods. Together with the age model (C-14 datings), a detailed reconstruction of the climatic and environmental changes in the past is proposed. The longest sediment core Pf07-1_2, taken in the middle of the lake, shows a complete sediment record of the last ≈4000 yBP and reveals the climatic cold phases from Löbben (≈3000 yBP and older) to the Little Ice Age (13th-19th century). The end of the Iron Age, the Roman Period, as well as the mediaeval times could be identified in the pollen and C-14 data, indicating human impacts like forest fires, pasturing, agriculture and forest-clearings. The whole sediment record could additionally be correlated in detail with the glacial advance and retreat curve of the Aletsch glacier (Holzhauser, 1995) and other glacial data (Maisch 2000, Röthlisberger 1986) showing the influence of the Central Alpine climate to the sedimentation regime in Lake Pfafforet. The advance periods of the Aletsch glacier correlate well with the deposition of detrital sediment layers, indicating a connection between detrital sediment input into the lake and cold climate phases.

REFERENCES

Bendel M.; Tinner W.; Amman B. (2006): Forest dynamics in the Pfyn forest in recent centuries (Valais, Switzerland,Central Alps): interaction of pine (Pinus sylvestris) and oak (Quercus sp.) under changing land use and fire frequency. The Holocene 16, 81-89

Burri M. (1997): Géologie de Finges et de ses environs (VS). Bulletin de la Murithienne, 115, Sion, 5-27

Holzhauser H. (1995): Gleschterschwankungen innerhalb der letzten 3200 Jahre am Beispiel des grossen Aletsch- und des Gornergletschers. Jubiläums-Symposium der Schweiz, Gletscherkommission 1993 in Verbier (VS). Zürich, 218 S.

Maisch M.; Wipf A.;Denneler B. (2000): Die Gletscher der Schweizer Alpen-Gletscherhochstand 1850, Aktuelle Vergletscherungen, Gletscherschwund-Szenarien. 2. Auflage, Geographisches Institut der Universität Zürich

Röthlisberger F. (1986): 10000 Jahre Gletschergeschichte der Erde. Verlag Sauerländer, Aarau, Frankfurt am Main. 416 pages

5.21

Evidence for climatic cooling at Grizzly Lake (Alaska) around 2800 cal. yr. BP

van Raden Ulrike *, Beer Ruth**, Tinner Willy **, Gilli Adrian *, Clegg Ben***, Bigler Christian****, Hu Feng Sheng ***, Haug Gerald*

Geological Institute, ETH Zurich, Universitätstrasse 16, CH-8092 Zürich, Switzerland, (vanraden@erdw.ethz.ch)
Oeschger Centre for Climate Change Research & Institute of Plant Sciences, University of Bern, Altenbergrain 21, CH-3013 Bern, Switzerland
Program in Ecology and Evolutionary Biology, University of Illinois, 265 Morrill Hall, 505 S. Goodwin Ave, Urbana, IL 61801, USA
Department of Ecology and Environmental Science, KBC plan 5, Umeå University, S-901 87 Umeå, Sweden

Recent studies revealed climatic changes at about 2800 BP in several regions of the northern and southern hemisphere (e.g. Chambers et al. 2007; Swindles et al. 2007). In order to understand environmental and climatic changes as manifestations of this event in northern high latitudes, we investigated a 20 cm sediment core section from Grizzly Lake (Alaska) covering about 900 years of sedimentation. We conducted a high-resolution multiproxy study to reconstruct vegetation and climate changes with a focus on interrelations of different ecosystem aspects and climate. The sediment archive of Grizzly Lake is particularly suitable for paleoenvironmental studies as direct anthropogenic influence is negligible before ≈1950 AD. The high-resolution measurements of numerous proxies enable detailed investigation of leads and lags within the environment.

Analyses on pollen, plant macrofossils, charcoal, chironomids and diatoms allude to a potential cooling event similar to the Little Ice Age (Tinner et al. 2008) just before 2800 cal. yr. BP. Preliminary chironomid-assemblage analysis indicates a dramatic change at a core depth of 95.5 cm (about 2900 yrs. cal. BP) where cold stenotherm taxa such as *Micropsectra, Corynocera oliveri, Tanytarsus lugens* and *Heterotrissocladius* emerge or increase in abundance. Interestingly, tree pollen (especially *Picea glauca*) increase at the same time. At 92.75 cm (about 2750 yrs. cal. BP) a marked decrease in tree pollen abundance (*Picea mariana, Picea glauca*, and *Betula*) coincides with an increase in pollen from shrub taxa, such as *Alnus viridis*, a species highly adapted to disturbance (e.g. landslides, avalanches, fire, windthrow).

Optical core descriptions classified the sediment mainly as dark brown gyttja with a light brown silt layer at 94-91.5 cm (about 2800-2680 cal. yr. BP). Complementary sedimentological, mineralogical and geochemical analyses were conducted to verify the macroscopic and paleoecological observations. Ultra-high-resolution XRF scans were used to analyse the elemental composition along the core section. These data, combined with thin section and XRD analyses, reveal constant quiet sedimentation with very little autochthonous material within the dark sediment of the core section.

The pale silt interval consists of at least seven event layers, each between 1.5 and 5.5 mm in thickness and some with an erosional base. Every layer shows a gradation with coarse bottom depositions containing high amounts of Si and Ca (evidence for quartz and carbonate) and fine top layers with high amounts of Fe, K, Ti and Al (evidence for feldspars and clays). We interpret these sediments to be washed into the lake from the Alaska Range in the North as a result of the preceding cooling event and associated reduction in forest cover and emerging higher erosion. A potential increase of precipitation that may have altered the hydrological cycle and the lake thermal stratification will be further tested by diatom-assemblage analysis.

We suggest that these inferred changes in vegetation and concurrent higher erosion mark the final stage of the cold event. Pollen data and preliminary chironomid analysis reveal a fast recovery of the ecosystem after this series of erosion events and organic rich sediments prevail again after 91.5 cm (about 2680 yrs. cal. BP).

All hitherto existing results consolidate the conclusion that the chironomid assemblage denotes the beginning of a cold event. With a lag of about 150 years the vegetation finally responded and forests collapsed, possibly in response to high frost-induced mortality of trees, which were close to their upper distributional limit (see interpretation for Little Ice Age, Tinner et al. 2008). The collapse of forests induced a phase of high erosion events marking the final stage of this period. Taken together our data suggests that the cooling event around 2800 cal. yr. BP had distinct impacts on the environment around Grizzly Lake and presumably large areas of south-central Alaska.

REFERENCES

Chambers, F.M., Mauquoy, D., Brain, S.A., Blaauw, M. & Daniell, J.R.G. (2007), Globally synchronous climate change 2800 years ago: Proxy data from peat in South America, Earth and Planetary Science Letters, 253 (3-4), 439-444.

Swindles, G. T., Plunkett, G., Roe, H. M. (2007), A delayed climatic response to solar forcing at 2800 cal. BP: multiproxy evidence from three Irish peatlands, Holocene, 17 (2), 177-182.

Tinner, W., Bigler, C., Gedye, S., Gregory-Eaves, I., Jones, R. T., Kaltenrieder, P., Krahenbuhl, U. & Hu, F. S. (2008), A 700-year paleoecological record of boreal ecosystem responses to climatic variation from Alaska, Ecology, 89 (3), 729-743.

5.22

From the 'Kanderschnitt' to the 21st century: Human impact and natural hazards in the Lake Thun sediment record

Wirth Stefanie*, Girardclos Stéphanie*,** & Anselmetti Flavio S.***

*Geological Institute, ETH Zurich, 8092 Zürich (wirths@student.ethz.ch)
**new address: Dept Geology and Paleontology, University of Geneva, Rue des Maraîchers 13, 1205 Geneva
***Eawag, Swiss Federal Institute of Aquatic Science and Technology, Dübendorf, Switzerland

Lake Thun sediments provide an excellent archive to reconstruct the history of human impact and natural disasters occurring in the lake and the watershed during the last 300 years. 1714 AD is a key year in this history, as it marks the deviation of the sediment load- and carbonate-rich Kander river as new major sediment input to the lake (also called 'Kanderschnitt'). On the basis of a high-resolution reflection seismic survey and sediment cores (2.5 m maximum length) the consequences of this human-induced change in the lake sedimentary system are investigated.

On seismic data, the onset of the Kander input is characterised by proximally deposited sediments imaged on seismic data by chaotic/transparent facies, indicating frequent subaquatic mass-movements certainly released from the overloaded Kander delta slopes. This mass-movement material is deposited distally in the form of turbidite beds imaged seismically with onlapping high amplitude reflections. In the sediment record, the onset of the Kander river input is detected by a relative increase in carbonate elements as Ca, inorganic carbon and Sr, and a decrease in magnetic susceptibility, all reflecting the carbonate-rich input of the Kander river.

Around 1850 AD, a second sedimentological change in the lake system occurred, expressed in the seismic data as a general substitution of 'mass-movement' facies with parallel and continuous reflections. In the sediment record, a change towards finer-grained flood turbidites and very fine- and in the main part homogeneously-grained mass-movement-related turbidite deposits in the core material. The factors responsible for this change are presumably lake-level regulations, Kander river corrections and gravel withdrawal at the Kander delta and in the Kander river, all contributing to a stabilisation of the Kander delta slopes. The Kander is the source for the majority of Lake Thun flood events (Röthlisberger, 1991) and their corresponding flood-related turbidite deposits. However, small tributaries along the lake north shore can locally generate coarse grained flood-related turbidite deposits.

Known earthquakes events (Fäh et al., 2003) could be correlated to deformation structures and mass-movement-related turbidite deposits in sediment cores. An earthquake in Kandersteg 1898 (M = 4.8, I = VII) is with high probability responsible for deformation structures and a 'homogenite' bed. Earthquakes in Wengen 1825 (M = 4.3, I = VI) and Interlaken 1937 (M = 4.2, I = VI) can be correlated to coarse-grained mass-movement-related turbidites. These events were not of large magnitude but probably strong enough to trigger subaquatic mass-movements on the instable Kander delta slopes. The biggest registered earthquake in the Lake Thun region (Frutigen 1729; M = 5.6, I = VI) could not be assigned to a particular deposit because of frequently occurring subaquatic mass-movements in the decades after the 'Kanderschnitt'.

The Lake Thun sediment record of the last 300 years presents an interrelation of human impact and natural disasters. In fact, human activities in the catchment area and the lake influence the properties and frequency of deposits provoked by natural disasters as flood events or earthquakes.

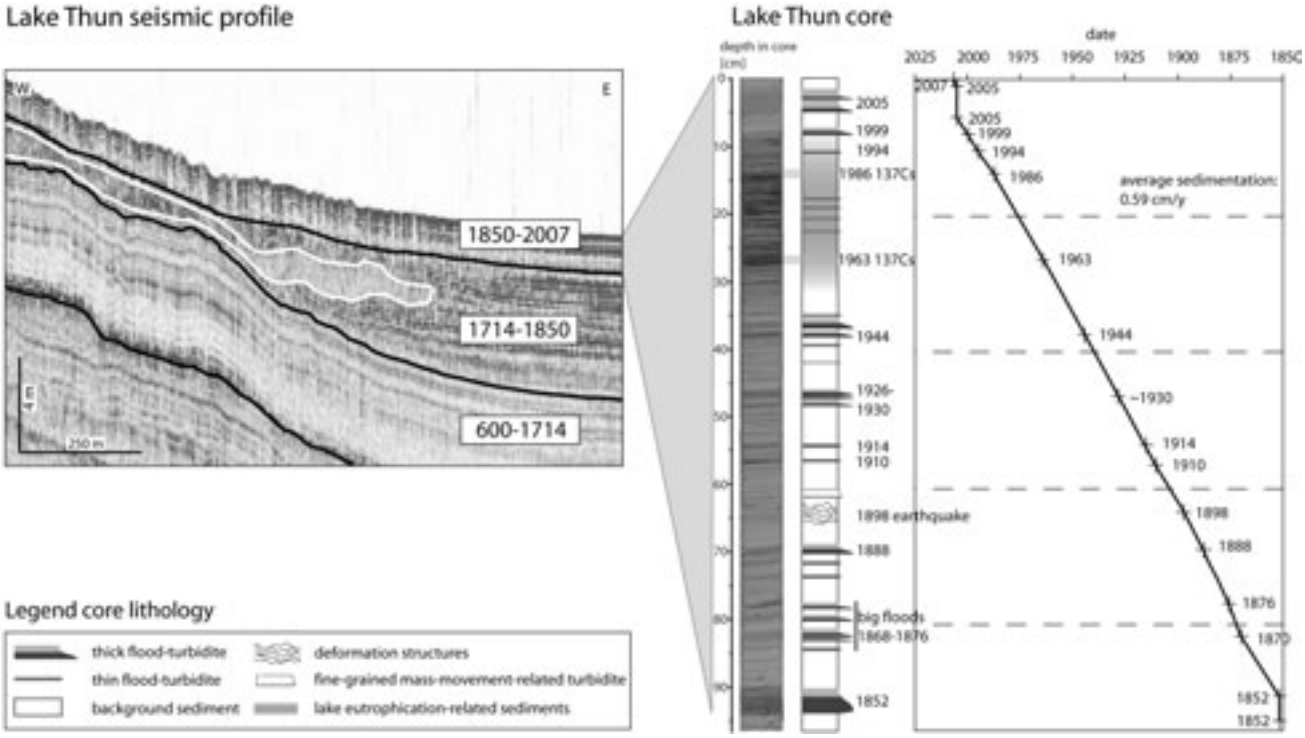

Figure 1. Lake Thun seismic profile and sediment core illustrating constant sedimentation rate from 1850 to 2007 and instable sedimentation with mass-movements (white on seismic profile) from 1714 to 1850.

REFERENCES

Fäh, D., Giardini, D., Bay, F., Bernardi, F., Braunmiller, J., Deichmann, N., Furrer, M., Gantner, L., Gisler, M., Isenegger, D., Jimenez, M.J., Kästli, P., Koglin, R., Masciadri, V., Rutz, M., Scheidegger, C., Schibler, R., Schorlemmer, D., Schwarz-Zanetti, G., Steimen, S., Sellami, S., Wiemer, S. and Wössner, J. 2003: Earthquake Catalogue Of Switzerland (ECOS) and the related macroseismic database. Eclogae geol. Helv., 96: 219-236.

Röthlisberger, G. 1991: Chronik der Unwetterschäden in der Schweiz. Berichte der Eidgenössischen Forschungsanstalt für Wald, Schnee und Landschaft, 330, Birmensdorf, 122 pp.

5.23

Paleoclimates since the MIS 3 on the NE Qinghai-Tibet Plateau: a comparison with SCS and European records

Yu Junqing, Zhang Lisa, Zhan Dapeng & Gao Chunliang

Institute of Salt Lake Studies, Chinese Academy of Sciences, Xinning Street 18, 810008 Xining, China (junqyu@isl.ac.cn)

Seismic profiles, piston cores and a 26m drill core were recovered from Lake Qinghai by the Sino-Swiss limnogeological expedition in 1985 and 1987 (Kelts et al. 1989; Lister et al. 1991; Yu & Kelts 2002). The reconstructed history of lake-level fluctuation and paleoenvironmental change for the China's largest closed-basin lake is an indispensably important record not only for the study of the Asian monsoon changes but also for an intercontinental correlation of paleoclimate records since the MIS 3.

Lake Qinghai lies on the NE corner of the Qinghai-Tibet Plateau at 3194m above sea level. As located at the outer margin of the Asian summer monsoon, the lake and its large catchment are climatically under a conjunct influence of the monsoon circulation and prevailing westerly winds. Because the large lake lacks surface outlets and groundwater discharge, past changes in water chemistry and lake level are the sensitive indicator of paleoclimate changes. Results from investigation on paleoshorelines, cores from the central subbasins of the lake and seismic profiles indicate that both lake size and temperature during the MIS 3 did not exceed those of the Holocene and the MIS 3 environment was neither fully glacial nor fully interglacial (Yu 2008). The paleo-lake during the LGM separated into smaller lakes and windblown loess-like sediments deposited, indicating an extremely cold and arid climate. The arid Younger Dryas equivalent at 10.7-10 ka (AMS ^{14}C age) was followed by an abrupt onset of a warm early-Holocene climate. The effective moisture at 10-8 ka was however much lower than that of today. A permanent expansion of Lake Qinghai occurred at 10 ka and the lake began to increase towards the present-day dimension from about 8 ka. This reflects a stepwise enhancement of summer rainfall on the NE Qinghai-Tibet Plateau.

The G. *rubber* δ^{18}O record from a northern South China Sea (SCS) core suggests that the main pattern of climate change since the MIS 3 is consistent with that documented in the Greenland GISP2 δ^{18}O record. The SCS during the MIS 3 was overall under the conditions of a strong winter monsoon and weak summer monsoon precipitation, as also indicated by low fluvial clay content and high modal grain size. The proxy record clearly indicates deteriorated conditions during the LGM. The correlation of the SCS record with Lake Qinghai suggests that the paleoenvironmental conditions of the western Pacific marginal seas and the WPWP had a substantial impact of moisture availability on the outer margin of the Asian summer monsoon, which determined that the strength of the summer monsoon during the MIS 3 was weaker than the Holocene. During the LGM, a combined impact of southward-shifted polar front and an about 100 m decrease of the WP marginal sea levels resulted in a further increase of aridity on the NE Qinghai-Tibet Plateau.

The MIS 3 and LGM conditions in terms of temperature change on the NE Qinghai-Tibet Plateau were in general consistent with the European record. A short-term setback to cold climate conditions at the YD chronozone is however uncertain. The Lake Qinghai record implies that mountainous glaciers on the NE plateau advanced during the period of MIS 3 more than the cold and arid period of the LGM. This indicates that the difference of atmospheric circulation between Europe and East Asia existed during the MIS 3 and LGM.

REFERENCES

Kelts, K., Chen, K., Lister, G., Yu, J. Q., Gao, Z., Niessen, F., Bonani, J. 1989: Geological fingerprints of climate history: a cooperative study of Qinghai Lake, China. Eclogae geol. Helv., 82, 167–182.

Lister, G., Kelts, K., Chen, K. Z., Yu, J. Q., Niessen, F. 1991: Lake Qinghai, China: closed-basin lake levels and the oxygen isotopic record for ostracoda since the latest Pleistocene. Palaeogeography, Palaeoclimatology, Palaeoecology, 84, 141–162.

Yu, J. Q. & Kelts, K. 2002: Abrupt changes in climatic conditions across the late-glacial/Holocene transition on the N. E. Tibet-Qinghai Plateau: evidence from Lake Qinghai, China. Journal of Paleolimnology, 28, 195–206.

Yu, J. Q. 2008: LAKE QINGHAI: Paleoenvironment and Paleoclimate. Beijing: Science Press, 128pp.

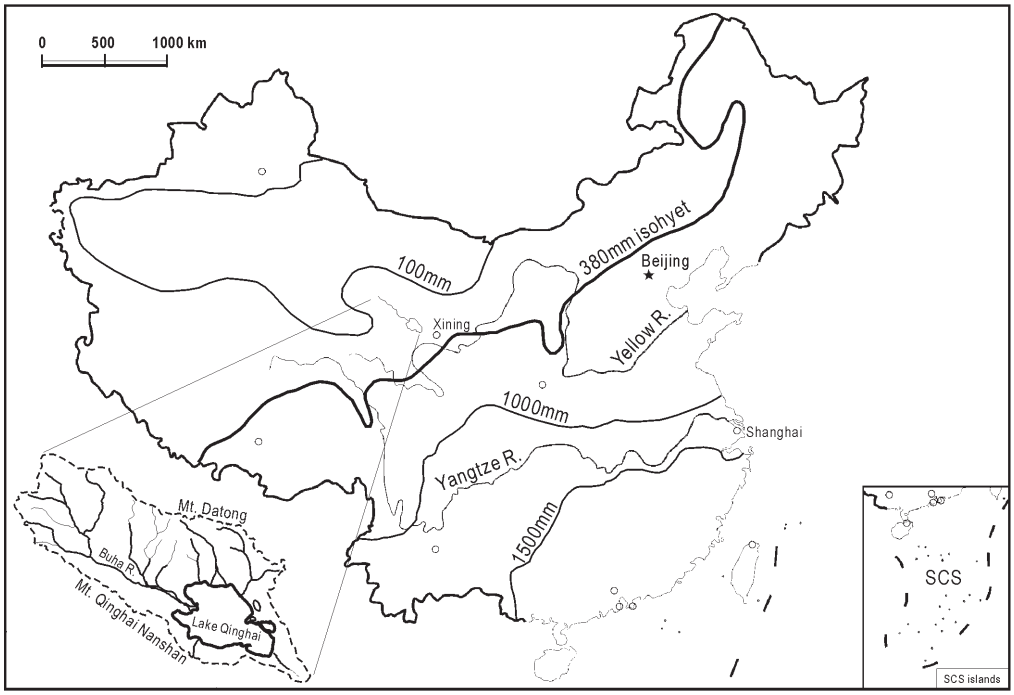

Figure 1. Precipitation gradient to the northwest decreasing steadily from the southeast coast of China towards the drainage basin of Lake Qinghai, reflecting the pattern of the East Asian monsoon rainfall.

6. Apply! Snow, Ice and Permafrost Science + Geomorphology (Open Session)

M. Hoelzle, A. Bauder, B. Krummenacher, C. Lambiel, M. Lüthi, M. Phillips, J. Schweizer, M. Schwikowski + M. Bollschweiler, G. R. Bezzola, R. Delaloye, C. Graf., N. Kuhn, E. Reynard

Swiss Snow, Ice and Permafrost Society + Swiss Geomorphological Society

6.21 Paul F. & Haeberli W.: Spatial variability of glacier elevation changes in the Alps obtained from differencing two DEMs

6.22 Paul F., Kääb A., Rott H., Shepherd A., Strozzi T. : GlobGlacier: A new ESA project to map the world's glaciers from space

6.23 Phillips M., Zenklusen Mutter E., Kern-Luetschg M.: Rapid permafrost degradation induced by non-conductive heat transfer within a talus slope at Flüela Pass, Swiss Alps.

6.24 Roer I., Hoelzle M., Haeberli W., Kääb A.: Rockglacier dynamics in the Swiss Alps – comparing kinematics and thermal regimes in the Murtèl-Corvatsch region

6.25 Scapozza C., Gex P., Lambiel C., Reynard E. : Electromagnetic prospecting in alpine permafrost: examples from the Southern Swiss Alps

6.26 Scapozza C., Mari S., Valenti G., Strozzi T., Gex P., Fontana G., Müller G., Lambiel C., Delaloye R., Reynard E. : Permafrost map of the Eastern Ticino Alps

6.27 Theler D., Bardou E., Reynard E. : Conceptualising sediment cascades to enhance dynamic geomorphological mapping

6.28 Worni R., Pulgarín B., Agudelo A., Huggel C. : Glacier volcano interactions and related hazards during the 2007 eruptive crisis at Nevado del Huila, Colombia

6.29 Wüthrich C., Begert M., Scherrer S.C., Croci-Maspoli M., Appenzeller C., Weingartner R.: Analyses of newly digitised snow series over the last 100 years+ in Switzerland

6.30 Zenklusen Mutter E., Phillips M., Blanchet J. : Evidence of warming in disturbed and undisturbed permafrost terrain at Schafberg (Pontresina, Eastern Swiss Alps)

6.1

Long term point observations of seasonal mass balance: a key to understanding 20th century climate change

Bauder Andreas and Huss Matthias

Versuchsanstalt für Wasserbau, Hydrologie and Glaziologie (VAW), ETH Zürich, Gloriastrasse 37-39, CH-8092 Zürich (bauder@vaw.baug.ethz.ch)

Point observations of glacier surface mass balance at fixed locations directly reflect climatic variations and are not biased by uncertain spatial interpolation of mass balance or the change in glacier surface area. Thus, they are considered to be the best indicator for changes in the climatic forcing on glaciers (Vincent and others, 2004; Ohmura and others, 2007). Four long term time series of seasonal mass balance observations (Fig. 1) at fixed locations have been compiled for two stakes on Claridenfirn and one stake on Grosser Aletschgletscher and Silvrettagletscher, Switzerland, all starting in 1914 (Huss and Bauder, in press). These data represent the longest series of direct mass balance measurements worldwide.

Using a mass balance model based on the temperature-index approach, the field observations are corrected for varying dates, inconsistency, systematic errors and data gaps. The resulting homogenized continuous 93-year time series from the three glaciers cover most of the 20th century and enable to investigate temporal, regional and altitudinal variability of mass balance and fluctuations in the climatic forcing on glaciers.

Long term variations in mass balance are mainly driven by changes in summer ablation. Three stakes (Clariden, Silvretta) located near the equilibrium line display significantly lower summer balances in the mid 1960s to mid 1980s, whereas the high altitude site (Aletsch) shows opposite trends. Two periods of enhanced climatic forcing are detected, 1943-1953 and 1987-2007. At all stakes the energy consumed for melt was higher in the 1940s in spite of lower air temperatures than during the last two decades.

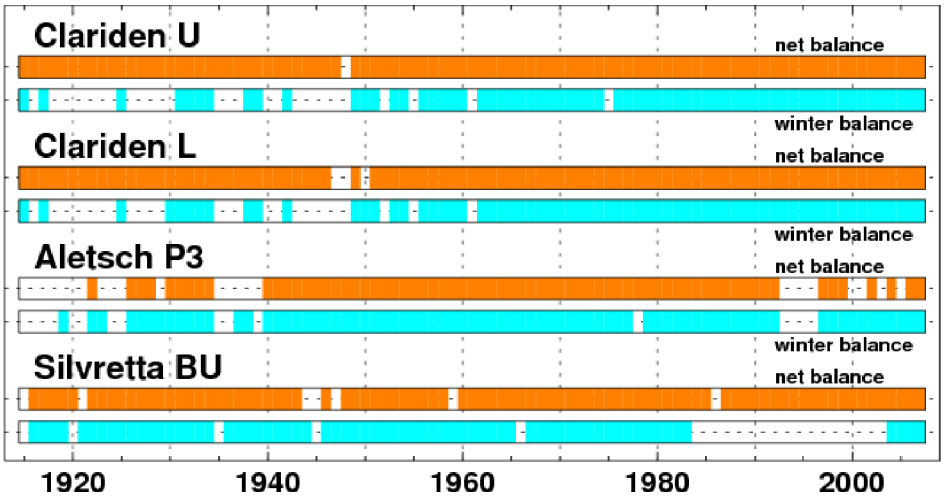

Figure 1. Seasonal observations of point based net and winter balance since 1914 from four sites in the Swiss Alps.

REFERENCES

Huss, M. and Bauder, A. (in press). Twentieth century climate change inferred from four long≈term point observations of seasonal mass balance. Annals of Glaciology, 50.

Ohmura, A., Bauder, A.,≈Müller, H. and Kappenberger, G. (2007). Long-term change of mass balance and the role of radiation, Annals of Glaciology, 46, 367–374.

Vincent, C., Kappenberger, G., Valla, F., Bauder, A., Funk, M. and Le Meur, E. (2004). Influence of climate change over the 20th Century on four French glacier mass balances. Geophysical Research Letters, 109, D10104. (10.1029/2003JD003857.)

6.2

Towards a first assessment of the permafrost distribution in the French Alps

Bodin X.*, Schoeneich P.*, Lhotellier R.*, Gruber S.**, Deline P.***, Ravanel L.***, Monnier S.****

* *Institut de Géographie Alpine, Université de Grenoble*
** *Institut de Géographie, Université de Zurich*
*** *EDYTEM, Université de Savoie*
**** *Laboratoire de Géographie Physique, Université de Paris 12*

In mountain regions, permafrost is important for the geomorphology of high altitudes areas as well for the water resources of inhabited watersheds. Under the present Global Warming, the possible degradation of permafrost during the coming decades could hence provoke various kind of slope instability and change drastically the hydrological functioning (Kääb et al., 2006). A better understanding of the distribution of the permafrost is therefore a necessary prerequisite for further analysis and mitigation of those hazards.

As permafrost is in most cases invisible and, though covering large areas, its distribution is largely unknown. Extensive permafrost "mapping" can be approached only through either empirical, statistical or physically based modelling (Riseborough et al., 2008). Permafrost maps have been produced this way for the Swiss Alps.

As no such map existed yet for the French Alps, this paper thus intends to present an overview of the main available datasets on the presence of permafrost, in rockfaces as well within debris accumulations: inventories of geomorphological indicators (rockglaciers and other creeping landforms related to the presence of ground ice) and in-situ measurements (BTS, geophysical soundings ...).

Among various types of available models, a statistico-empirical one has been set up: it is based on the relation between the two most important topoclimatic controls (solar radiation and air temperature) of the rockglaciers presence. This relation was computed on a lithologically, geomorphologically and climatically homogeneous small massif (Combeynot Massif, ≈ 45° N, 40km) which presents numerous rockglaciers in various topoclimatic contexts (Bodin, 2007). Two versions of the model, one for the root of rockglaciers, one for their frontal part, have been combined to assess the potential presence of permafrost in the entire French Alps.

Two validation procedures have been performed using independent rockglaciers inventories: one in the Mercantour Massif (lat. ≈ 44° N), one in the Vanoise Massif (lat. ≈ 45.5° N). The comparison between training set and validation set shows a good correspondence of the altitude and aspect of the actual rockglaciers and of the modelled front and root areas. Those first results are thus encouraging as they already provide to public and to decision-makers usable new information about permafrost presence in their territory. At fine scales (lower than the watershed), more investigations are nevertheless necessary to detect and characterise precisely the permafrost, either in debris accumulation or in rock-face.

REFERENCES

Bodin, X. 2007: Géodynamique du pergélisol de montagne : fonctionnement, distribution et évolution récente. L'exemple du massif du Combeynot (Hautes Alpes). PhD, Geography, University of Paris-Diderot Paris 7, 272 p.

Kääb, A., M. Chiarle, B. Raup & C. Schneider. 2006: Climate change impacts on mountain glaciers and permafrost. Global and Planetary Change.

Riseborough, D. W., N. I. Shiklamonov, B. Etzelmüller, S. Gruber & S. S. Marchenko. 2008: Recent advances in permafrost modeling. Permafrost and Periglacial Processes 19(2).

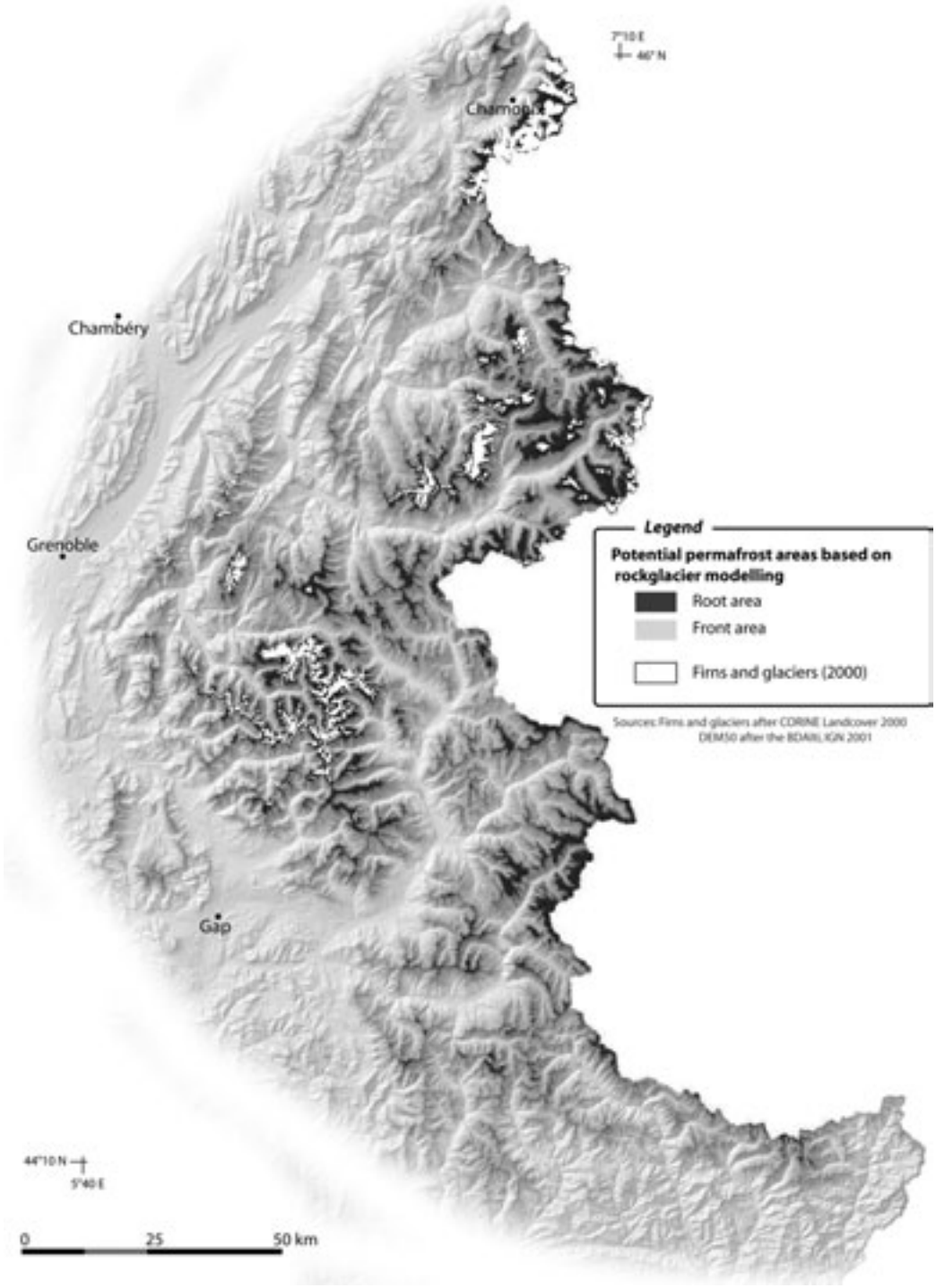

Figure 1. Map of the potential permafrost distribution in the French Alps.

6.3

The Flims Rockslide 3D terrain modelling and volume calculations with GIS-application

Caprez Jürg*, Maisch Max*, von Poschinger Andreas**

* *Geographisches Institut, Universität Zürich-Irchel, Winterthurerstr. 190, CH-8057 Zürich, (j.caprez@geo.unizh.ch), (max.maisch@geo.uzh.ch)*
** *LfU, Lazarettstr. 67, D-80636 München, (Andreas.Poschinger@lfu.bayern.de)*

The Flims rockslide is to be known as the largest mass movement in the Alps. Recent studies support the hypothesis of an early Holocene age of this mega-event by radiocarbon dates centred around cal. 9450 BP (Deplazes, Anselmetti & Hajdas 2007). At that Preboreal time climate already has changed to warmer conditions and therefore a readvance of the main valley glacier of Vorderrhein as well as from small local glaciers can be excluded from having reworked the rockslide area (Poschinger et al. 2006). Despite of various new findings up to now the paleogeographic framework, especially the former shape of the pre-existing Flimserstein is poorly established.

Based on geologic evidence (geol. maps, profiles) and geomorphologic considerations (i.e. extrapolation of slopes) in this study a new effort was made to rebuild and reconstruct the former 3D-topography of the Flims area within a GIS (Geographic Information System). This approach allows to determine with enhanced precision the dimensions of this extraordinary rockslide event and to reveal in more details the various processes involved.

The 3D terrain models yielded a total volume ranging from 7 km^3 up to 7.3 km^3 for the breakout zone of the rockslide. The volume of the deposition zone on the other hand gave, according to different scenarios, values between 8.6 km^3 to 9.3 km^3. In addition about 1.5 km^3 of the rockmass was eroded later on by the Vorderrhein river.

During the Flims rockslide the pre-existing valley infill, supposedly saturated completely by water, was squeezed out and mobilised between Sagens and Bonaduz, subsequently being deposited as a special facies type, known as "Bonaduzer Schotter" (Abele 1997). Approximately 20 percent of the alluvial valley fill was evacuated directly by the impact of the rockslide. Accordingly, the debris mass does not reach the basement of the Vorderrhein valley but seems to rest on a layer of relict alluvial sediments. The 3D-reconstructions of the Flims topography resulted also in modelling former lakes with their maximum levels, triggered and dammed by the rockslide event. Various 3D-visualizations of the study area certainly will launch fruitful discussions on the dynamics, the processes and the geologic consequences of this famous Flims event.

REFERENCES

Abele, G. 1997: Rockslide movement supported by the mobilisation of groundwater-saturated vally floor sediments. Zeitschrift für Geomorphologie, N.F., 41/1 , 1-20.

Deplazes, G., Anselmetti, F. & Hajdas, I. 2007: Lake sediments deposited on the Flims rockslide mass: the key to date the largest mass movement of the Alps. Terra Nova, Vol 19, No. 4 , 252–258.

Poschinger, A. v., Wassmer P. & Maisch, M. 2006: The Flims Rockslide: History of interpretation and new insights. In: Evans, S.G., Sacarascia-Mugnozza, G., Strom, A. & Hermanns, R.L. (eds.), Massive Rock Slope Failure. Kluwer Academic Publishers , 341-369.

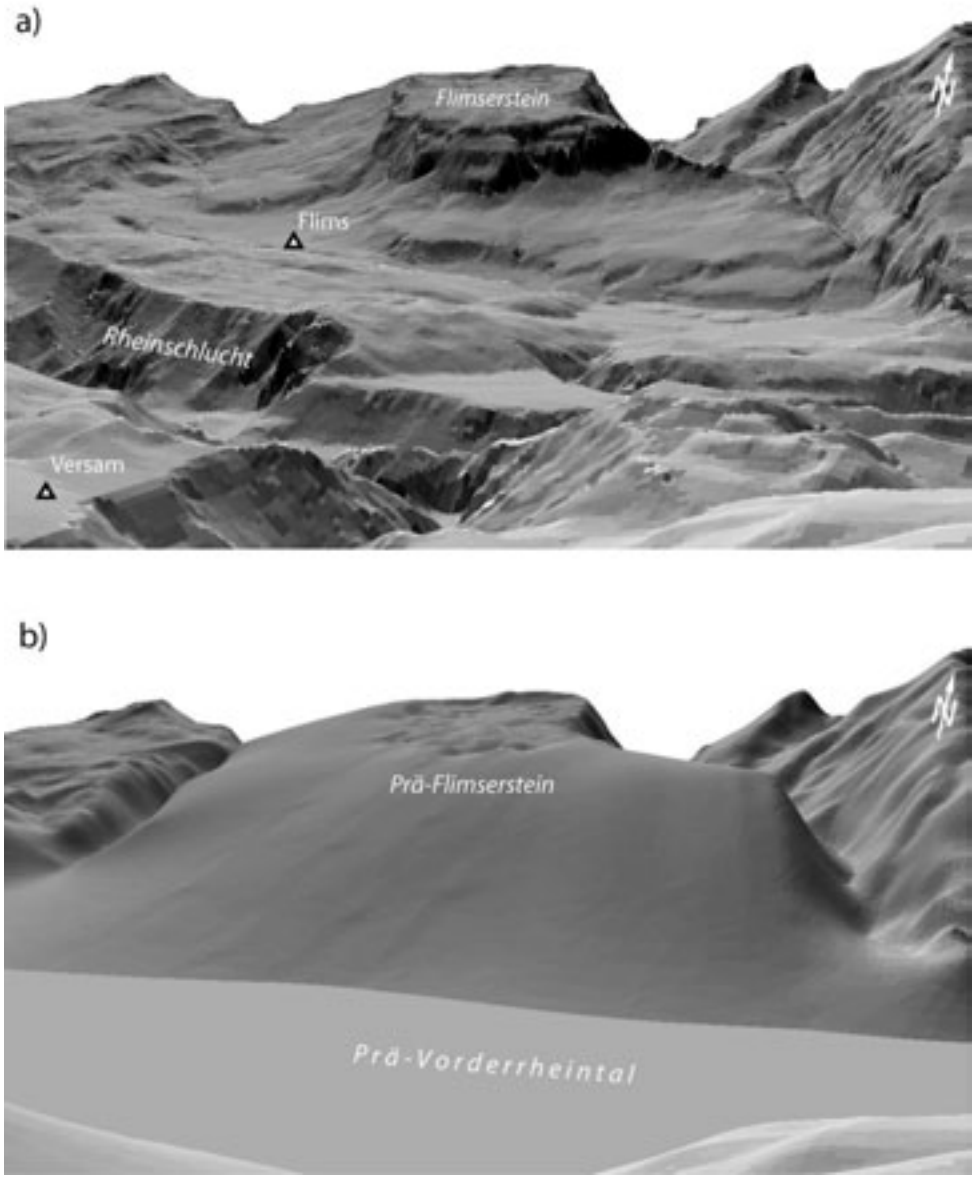

Figure 1: 3D-reconstructed terrain surface of the Pre-Flimserstein. a) Digital terrain model of the Flims rockslide area with the Flimserstein in the background and the partially eroded rock mass in the foreground. b) Reconstruction of the Pre-Flimserstein and the Vorderrhein valley before the rockslide event.

6.4

Erosion-driven uplift of the modern Central Alps

Champagnac Jean-Daniel*, Schlunegger Fritz **, Norton Kevin*, von Blanckenburg Friedhelm *, Abbühl Luca** & Schwab Marco**

* *Institut für Mineralogie, Universitat Hannover, Callinstrasse 1, D-30167 Hannover, champagnac@gmail.com*
** *Institute of Geological Sciences, University of Bern, Baltzerstrasse 1-3, CH-3012 Bern.*

We present a compilation of four sets of data of modern tectono-geomorphic processes in the Central Alps of Switzerland that appear to suggest that rock uplift is a response to climate-driven denudation in the absence of active convergence. These are (1) basin-averaged Late Holocene denudation rates determined from cosmogenic nuclides and from suspended river loads; these slightly exceed, but spatially mimic the pattern of rock uplift rates as determined by geodetic leveling; (2) the geodetic reference point is also the geomorphic base level with respect to erosion; we further present (3) a compilation of

modern plate motion velocities shows that the rotation pole of the Adriatic plate is located within the area, hence the area is not under convergence; finally (4), we illustrate that the Central Alps have acted as a closed system for Holocene sediment redistribution up to the peri-Alpine lakes which have operated as a sink for the erosion products of the inner Alps.

While a variety of hypotheses have been put forward to explain the Central Alpine uplift (e.g. lithospheric forcing by convergence or mantle processes; ice melting) we show with a numerical isostatic model that the correlation between erosion and crustal uplift rates reflects a positive feedback between denudation and the associated isostatic response to unloading. Therefore erosion does not passively respond to advection of crustal material as might be the case in actively converging orogens. Other forces need to be considered to drive surface erosion. We suggest that the geomorphic response of the Alpine topography to glacial erosion and the resulting disequilibrium for modern channelized and associated hillslope processes explains much of the pattern of modern denudation and hence rock uplift. Therefore, in a non-convergent orogen such as the Central European Alps, the observed vertical rock uplift is primarily a consequence of passive unloading due to erosion.

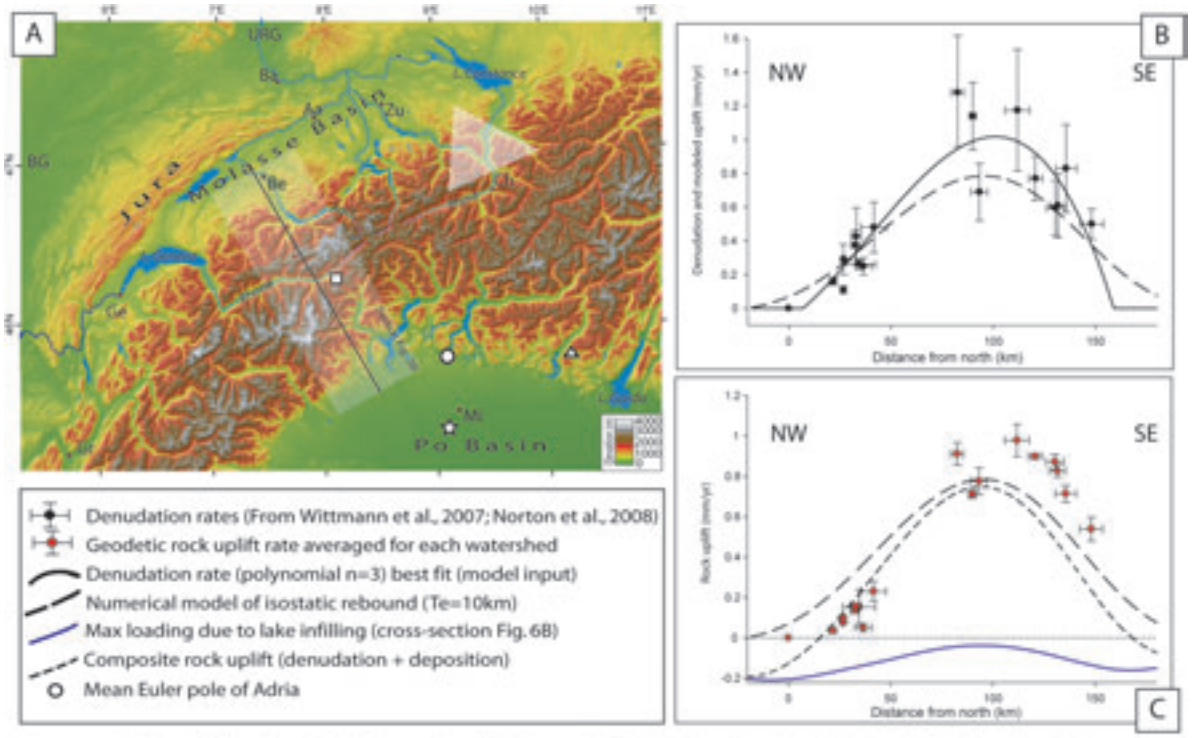

Figure 1. A) DEM of the Central Alps, location of Euler pole of Adriatic microplate (white circle), based on the average of 3 kinematic studies (white triangles, Anderson and Jackson, 1987, square, Battaglia et al., 2004, and star, Calais et al., 2002). Also shown is the section across the belt used in numerical models.
B) Modern denudation rates from cosmogenic radionuclides (Wittmann et al., 2007, Norton et al., 2008) and polynomial best fit to the data. Dashed line is the numerical solution of erosional unloading.
C) Models of isostatic rock uplift induced by modern erosion (long-dashed line) and lake deposition (blue line). The composite solution (short-dashed line, erosion + deposition) is compared with geodetic rock uplift (red dots).

REFERENCES:

Anderson, H. and Jackson, J., 1987. Active tectonics in the Adriatic region. Geophysical Journal Royal Astronomical Society 91, 937–983.

Battaglia, M., Murray, M.H., Serpelloni, E. and Burgmann, R., 2004. The Adriatic region: An independent microplate within the Africa-Eurasia collision zone. Geophysical Research Letter 31, L09605, doi:10.1029/2004GL019723.

Calais, E., Nocquet, J., Jouanne, F. and Tardy, M., 2002. Current strain regime in the Western Alps from continuous Global Positioning System measurements, 1996 – 2001. Geology 30, 651-654.

Norton, K.P., von Blanckenburg, F., Schlunegger, F., Schwab, M. and Kubik, P.W., 2008. Cosmogenic nuclide-based investigation of spatial erosion and hillslope channel coupling in the transient foreland of the Swiss Alps. Geomorphology, 95, 474–486

Wittmann, H., von Blanckenburg, F., Kruesmann, T., Norton, K.P., and Kubik, P., 2007. The relation between rock uplift and denudation from cosmogenic nuclides in river sediment in the Central Alps of Switzerland. Journal of Geophysical Research-Earth Surface 112, doi:10.1029/2006JF000729.

6.5

First results of firn temperature measurements in 2008 on Colle Gnifetti, Monte Rosa, Switzerland

Darms Gian*, Hoelzle Martin**

**Glaciology, Geomorphodynamics & Geochronology, Department of Geography, University of Zurich, Winterthurerstrasse 190, CH-8057 Zurich (gian.darms@gmail.com)*
***Department of Geosciences, University of Fribourg, Chémin de Musée 4, CH-1700 Fribourg (martin.hoelzle@unifr.ch)*

At the end of the 19th century and into the beginning of the 20th century, it was assumed that all glaciers in the Alps are temperate, although (Vallot 1893, 1913) observed in the Mont Blanc area that cold firn on high altitude mountain tops is widespread. In the 1950s, Fisher published several articles (1953, 1954, 1955, 1963) about cold firn observations in the Monte Rosa area as did Haefeli & Brentani (1955) for the Jungfrau area. In the 1970s (Lliboutry et al. 1976) and (Haeberli 1976) were the first scientists who systematically investigated the distribution of cold ice and firn in the Alps. In the last 20 years, research activities have started to increase in the cold high-mountain accumulation areas in the Alps, many studies have been undertaken in connection with hazards and core drillings (Alean et al. 1983, Böhlert 2005, Haeberli & Funk 1991, Laternser 1992, Lüthi & Funk 1997, Lüthi & Funk 2000, 2001, Oeschger et al. 1977, Schwerzmann 2006, Suter 1995, Suter et al. 2001a, Suter et al. 2001b, Suter 2002, Suter & Hoelzle 2002, 2004, Suter et al. 2004, Vincent et al. 1997, 2007).
Currently, there are two sites where such measurements have been repeatedly made: Col du Dôme in the Mont Blanc area (Vincent et al. 2007) and Colle Gnifetti in the Monte Rosa area. Colle Gnifetti is a very wind-exposed firn saddle with accumulation rates of 0.3 to 1.2 m water equivalent per year (Lüthi 2000).
On Colle Gnifetti, several boreholes were drilled in vicinity of the saddle point and, until now, measurements were made in 1976, 1982, 1991, 1994, 1995, 1999, 2000, 2003 and 2007. This summer (2008), new field-work has been carried out on Colle Gnifetti. Nine boreholes were drilled with a steam drill and borehole temperatures were measured. These temperatures are now ready to be compared with some older data to detect possible changes.

6.6

Snow temperatures: measurement and modelling

Fierz Charles & Lehning Michael

WSL Institute for Snow and Avalanche Research SLF, Flüelastrasse 11, CH-7260 Davos Dorf (fierz@slf.ch)

Both measuring and modelling snow temperatures within the topmost centimetres of the snowpack is a challenge. Snowpack evolution, and in particular snow metamorphism, heavily depend on the temperature distribution near the surface of the snowpack.

Short wave radiation penetrating the snowpack is picked-up by the sensors that heat up. A careful sensor design is thus required and we present two of them: the first allows for highly depth-resolved temperature profiles while the second is suitable for accurate continuous measurements over a few days.

Daily temperature cycles within the top 30 to 50 cm are due to both energy exchanges at the surface and to short wave radiation penetrating the snow. SNOWPACK, the Swiss snow-cover model, treats the latter as a volume source of heat, alike refreezing. We will show how the multi-band parameterization of short wave absorption implemented in SNOWPACK can be optimized by comparing model outputs to reliable measurements of snow temperatures.

6.7

Combined LiDAR and photogrammetry for stability-related change detection in glacierised and frozen rock walls - A case study in the Monte Rosa east face

Fischer Luzia *, Eisenbeiss Henri**, Kääb Andreas***, Huggel Christian* & Haeberli Wilfried *

* *Glaciology, Geomorphodynamics & Geochronology, Department of Geography, University of Zurich, Switzerland (luzia.fischer@geo.uzh.ch)*
** *Institute of Geodesy and Photogrammetry, ETH Zurich, Switzerland*
*** *Department of Geosciences, University of Oslo, Norway*

Often, rock walls in high-mountain areas are in large parts covered by steep glaciers and firn fields and are under permafrost conditions. Impacts on surface and subsurface ice in such flanks from climatic and other changes strongly influence stress and thermal fields in rock and ice, geotechnical parameters as well as the hydraulic and hydrological regime and may eventually lead to slope instabilities and enhanced mass movement activity such as major ice and rock avalanches (Gruber and Haeberli, 2007; Fischer and Huggel, 2008). The dynamics and changes of steep glaciers and ice cover in high-mountain rock walls and their interactions with the underlying bedrock are very complex and still incompletely understood (Wegmann et al., 1998; Pralong and Funk, 2006; Fischer et al., 2006).

The Monte Rosa east face, Italian Alps, is the highest flank in the European Alps (2200–4600m a.s.l.) and is a prominent example for strong changes and instabilities in a high alpine rock wall. Steep glaciers and firn fields cover large parts of the wall. Since the last glaciations maximum during the Little Ice Age (i.e. since approximately 1850) until the 1980s, the glaciation has changed little. During recent decades, however, the ice cover experienced an accelerated and drastic loss in extent and thickness and some glaciers have completely disappeared within short time (Kääb et al., 2004; Fischer et al., 2006). Over the recent two decades, new instabilities developed in bedrock as well as in ice. The mass movement activity increased drastically since about 1990, culminating in major mass movements in August 2005, with an ice avalanche of more than 1x106 m^3, and in April 2007, with a rock avalanche of about 0.3x106 m^3.

Acquisition of high-quality data is essential to better understand the predominant processes and hazards but is a major challenge in such high-mountain rock walls are very difficult due to topographic conditions, ice cover, and terrain that is difficult and dangerous to access. Therefore, remote-sensing based investigations are fundamental for an integrative assessment of changes in ice cover and bedrock as well as of slope instabilities in such flanks.

The main objective of the presented study is the investigation of changes in bedrock and glaciation in the Monte Rosa east face based on multi-temporal digital terrain models (DTMs) and terrestrial and aerial photographs. For this purpose, high-resolution DTMs of the Monte Rosa east face were photogrammetrically generated from aerial photographs of the years 1956, 1988 and 2001.
In 2007, a helicopter-borne light detection and ranging (LiDAR) scan of the entire Monte Rosa east face could be achieved. Further high-resolution DTM data stems from an airplane –borne LiDAR campaign in 2005. Based on the comparisons of DTMs and photographs over the last 50 years, the spatio-temporal changes in surface topography are evaluated and quantitative assessments of mass wasting and mass accumulation are performed. This unique multi-temporal data set gives an insight in the complex stability, dynamics and mass balance cycles of steep glaciers. Additionally, complex process interactions between different processes in bedrock and ice can be detected from the image data available.

REFERENCES

Fischer, L. & Huggel, C. 2008: Methodical Design for Stability Assessments of Permafrost Affected High-Mountain Rock Walls, Proceedings of the 9th International Conference on Permafrost 2008, Fairbanks, Alaska, USA, 29.6.-3.7.2008, 1, 439-444.

Fischer, L., Kääb, A., Huggel, C. & Noetzli, J. 2006: Geology, glacier retreat and permafrost degradation as controlling factors of slope instabilities in a high-mountain rock wall: the Monte Rosa east face, Natural Hazards and Earth System Sciences, 6, 761-772.

Gruber, S. & Haeberli, W. 2007: Permafrost in steep bedrock slopes and its temperature-related destabilization following climate change, Journal of Geophysical Research, 112, F02S18, doi:10.1029/2006JF000547.

Kääb, A., Huggel, C., Barbero, S., Chiarle, M., Cordola, M., Epinfani, F., Haeberli, W., Mortara, G., Semino, P., Tamburini, A. & Viazzo, G. 2004: Glacier hazards at Belvedere glacier and the Monte Rosa east face, Italian Alps: Processes and mitigation, Proceedings of the Interpraevent 2004 – Riva/Trient, 1, 67-78.

Pralong, A. & Funk, M. 2006: On the instability of avalanching glacier, Journal of Glaciology 52(176), 31-48.

Wegmann, M., Gudmundsson, G. H., & Haeberli, W. 1998: Permafrost changes in rock walls and the retreat of Alpine glaciers: a thermal modelling approach, Permafrost and Periglacial Processes, 9, 23–33.

6.8

Lateglacial glacier evolution of the Greina region (Central Swiss Alps)

Fontana Georgia*, Scapozza Cristian*, Reynard Emmanuel*

*Institut de Géographie, Université de Lausanne, Anthropole, CH−1015 Lausanne (Georgia.Fontana@unil.ch)

The Greina region is well known because of its importance in the Swiss nature protection history. In spite of the interesting natural features of the region, only few scientific researches were carried out until now, particularly in the field of geomorphology. The aim of this research (Fontana 2008) was to reconstitute the lateglacial glacier evolution of the Greina region, in order to fill a gap in the geomorphological knowledge of the Central Swiss Alps and to make available basis scientific information for the promotion of the Greina geomorphological heritage.

A large-scale geomorphological map of the whole region was first realised; special attention was accorded to the cartography of glacial landforms. On the basis of the cartography of moraines and other glacier-related deposits, a reconstitution of the lateglacial positions of glaciers was realised.

Four main lateglacial glacier positions were identified (Figure 1). One of these positions is characterised by a complex ice origin, whereas the other ones correspond to ancient positions of the Gaglianera glacier and of a disappeared glacier located NE of the Pizzo Coroi. For each glacier position, the Equilibrium Line Altitude (ELA) depression related to the reference phase of 1850 (Maisch, 1992) was calculated. The comparison of the ELA depression of each glacier position allowed us to establish a regional regression sequence including three phases (Table 1). The results were then compared with regional regression sequences established by Maisch (1981) in the Eastern Swiss Alps and by Renner (1982) in the Gothard region (Table1).

Greina	***ELA dep. (m)***	***Eastern Swiss Alps***	***ELA dep. (m)***	***Gothard***	***ELA dep. (m)***
(Fontana, 2008)		*(Maisch, 1981)*		*(Renner, 1982)*	
Greina 1a	110	*Bockten*	100-150	*Alpe di Cruina*	116
Greina 1b	210	*Egesen*	170-240	*Manio*	200-240
Greina 2	310-350	*Daun*	250-350	*All'Acqua*	280-315

Table 1: Comparison of the Greina regional regression sequence with regional regression sequences established by Maisch (1981) and Renner (1982).

The glacier positions and the regional regression sequence allowed the reconstitution of a general lateglacial glacier evolution of the Greina region. An important change in the general ice-flow directions certainly happened between the Last Glacial Maximum (LGM) and the Lateglacial. The general ice-flow coming from the Rhin-source ice-cap recognised by Florineth & Schlüchter (1998) was certainly substituted by a regional ice-flow. The general ice-flow had a NNE-SSW direction in the Plaun la Greina region during the LGM and a SSW-NNE direction during the Lateglacial. During the Greina 2 phase, the Gaglianera, Coroi and Terri glaciers were confluent and formed a front in the middle of the Plaun la Greina region. During this phase, a glacier located NE of Pizzo Coroi occupied the Crap la Crusch depression. Concerning the Greina 1a and Greina 1b phases, only the positions of the Gaglianera glacier could be reconstituted. The front of the glacier was certainly located W of the Plaun la Greina region during both phases.

REFERENCES

Florineth, D., Schlüchter, C. 1998: Reconstructing the Last Glacial Maximum (LGM) ice surface geometry and flowlines in the Central Swiss Alps, Eclogae geol. Helv., 91, 391-407.

Fontana, G. 2008: Analyse et propositions de valorisation d'un paysage géomorphologique. Le cas de la Greina. Lausanne, Institut de Géographie (Master thesis published on February 28, 2008, on http://doc.rero.ch).

Maisch M. 1981: Glazialmorphologische und gletschergeschichtliche Untersuchungen im Gebiet zwischen Landwasser und Albulatal (Kt. Graubünden, Schweiz). Zürich, Geographisches Institut.

Maisch, M. 1992: Die Gletscher Graubündens. Zürich, Geographisches Institut.

Renner, F. 1982: Beiträge zur Gletscher-Geschichte des Gotthardgebietes und dendroclimatologischen Analysen an fossilen Hölzern. Zürich, Geographisches Institut.

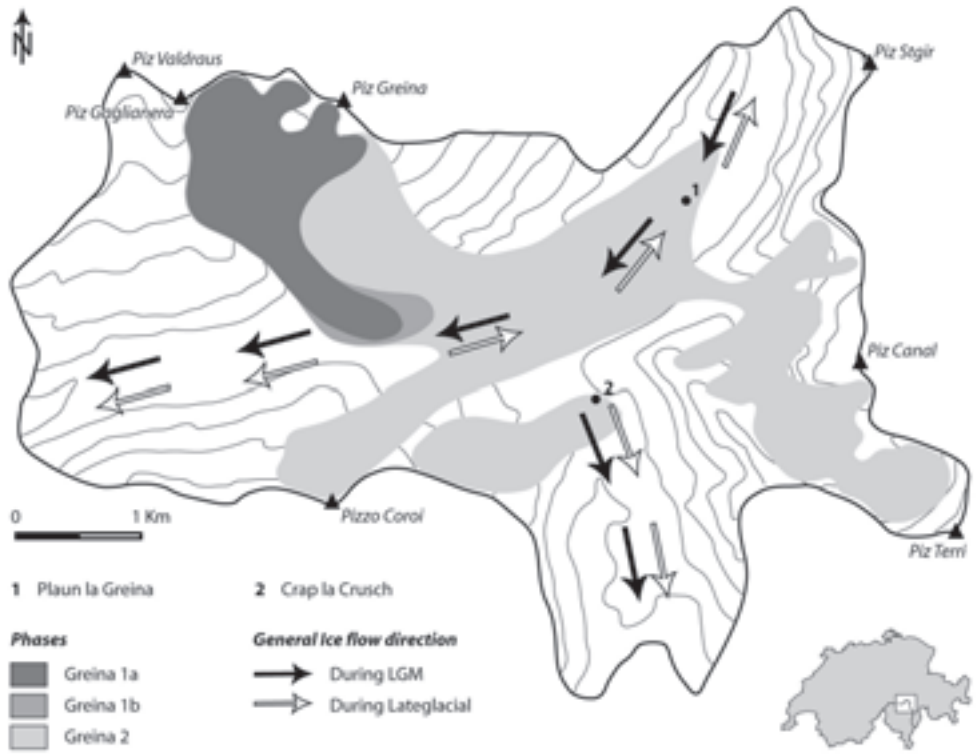

Figure 1. General ice flow direction during LGM and lateglacial phases in the Greina region.

6.9

Geomorphological map of the Greina region (Central Swiss Alps)

Fontana Georgia*, Scapozza Cristian*, Reynard Emmanuel*

*Institut de Géographie, Université de Lausanne, Anthropole, CH–1015 Lausanne (Georgia.Fontana@unil.ch)

The Greina is a high mountain region located in the Central Swiss Alps. In spite of the interesting geomorphological features of the region, no scientific research was carried out in this field until now. The aim of this research was to realise a geomorphological map of the Greina region, in order to reconstitute the morphogenesis of the area and to make available basis information for the promotion of the geomorphological heritage of the Greina region (Fontana 2008).

The geomorphological map was realised using the guidelines developed at the Institute of Geography of Lausanne University (Schoeneich et al. 1998). The method allows the realisation of morphogenetic maps and is particularly interesting for morphogenesis reconstitutions.

The Greina region presents a rich geomorphological diversity including structural, fluvial, gravitative, karstic, glacial, periglacial and organic landforms. The landform distribution is largely dependent on geological structure. From a tectonic point of view, the northern part of the study area belongs to the Gothard Massiv. This tectonic unit is composed of crystalline rocks, especially gneiss. Crystalline rocks are quite resistant to erosion and still conserve the traces of glacial erosion. Roches moutonnées and striations are therefore very frequent. The tectonic units situated southern of the Gothard Massiv include its sedimentary cover and some lower Penninic nappes. The autochthon sedimentary cover is mostly composed of dolomitic rocks, which present several karstic landforms, like dolines and residual landforms. The parautochton sedimentary cover and the lower Penninic nappes include several lithologies. Calcschists are very frequent: as these rocks are sensitive to the action of frost, erosional glacial landforms are quite rare, whereas talus slopes are very frequent. As clays are a product of calcschists weathering, well-developed solifluxion lobes are also visible.

Thanks to the geomorphological map and to other field observations, the general morphogenesis of the Greina region during the Lateglacial and the Holocene could be reconstituted (for the Lateglacial, see Fontana et al. 2008). During the Holocene, glacial processes became less important, whereas gravitative, fluvial and periglacial processes strongly shape the current

evolution of landscape. At the beginning of Holocene, the whole region should have been concerned by a paraglacial morphogenetic crisis. An important glacial sedimentary stock should have been reworked by fluvio-glacial and fluvial processes, while rockfalls and landslides should have been numerous. The fluvial rework of glacial sediments is at the origin of two relict paraglacial alluvial fans outside of the Gaglianera (Figure 1) and Canal valleys. At the same time, the frost and gravity action should have contributed to the talus slope formation. The rivers also shaped progressively their talwegs and the dissolution of dolomite rocks shaped karstic landforms. The current sedimentation level is lower than it was at the beginnings of Holocene and corresponds to the Piano della Greina, Plaun la Greina and Alpe di Motterascio alluvial plains. Concerning glaciers, their Holocene evolution is not well known. Since 1850, they present a strong regression (Maisch 1992) and occupy today a very small part of their glacial cirque (Fontana 2008).

Figure 1. The Gaglianera paraglacial alluvial fan (on the right), and the current alluvial fan (on the left).

REFERENCES

Fontana, G. 2008: Analyse et propositions de valorisation d'un paysage géomorphologique. Le cas de la Greina. Lausanne, Institut de Géographie (Master thesis published on February 28, 2008, on http://doc.rero.ch).

Fontana, G., Scapozza, C., Reynard, E. 2008: Lateglacial glacier evolution of the Greina region, Proceedings of the 6th Swiss Geoscience Meeting, this volume.

Maisch, M. 1992: Die Gletscher Graubündens, Zürich, Geographisches Institut.

Schoeneich, P., Reynard, E., Pierrehumbert, G. 1998: Geomorphological mapping in the Swiss Alps and Prealps, Wiener Schriften zur Geographie und Kartographie, 11, 145-153.

6.10

Observation of the Cryosphere – Switzerland's contri-bution to the Global Climate Observing System GCOS

Foppa Nando*, Seiz Gabriela*, Walterspiel Julia*

**Swiss GCOS Office, Federal Office of Meteorology and Climatology MeteoSwiss Kraehbuehlstr. 58, CH-8044 Zurich, (Nando.Foppa@meteoswiss.ch), www.gcos.ch*

In recent decades – especially following the adoption of the UN Framework Convention of Climate Change (UNFCCC) in 1992 – the demand for observations of climate change and the closer links between climate observation and climate research/modeling has steadily increased, leading to the establishment of the Global Climate Observing System (GCOS).

GCOS is an initiative of the World Meteorological Organization (WMO), the Intergovernmental Oceanographic Commission (IOC) of the UNESCO, the UN Environmental Programme (UNEP) and the International Council of Science (ICSU). GCOS is

designed to ensure that the observations and information needed to address climate-related issues are obtained systematically and made available to all potential users. In particular, GCOS follows the aims and requirements of systematic observation as specified in the UNFCCC and the Kyoto Protocol.

In Switzerland, the Swiss GCOS Office at the Federal Office of Meteorology and Climatology MeteoSwiss was established in 2006, following the ratification of the Kyoto Protocol in 2003, to coordinate climate observations at the national level and to foster information exchange and collaboration among the various institutions. In 2007, the Swiss GCOS Office has compiled the first-ever inventory of the country's long-term climatological data series of the atmosphere and the land surface, entitled "National Climate Observing System (GCOS Switzerland)" (Seiz & Foppa, 2007). Switzerland has a long tradition in the observation of cryospheric parameters, including more than 100 years of glacier and snow depth measurements, the longest Central European lake ice cover records, the permafrost monitoring network PERMOS, the world's longest snow water equivalent series for catchment areas, and is additionally hosting the important World Glacier Monitoring Service.

Our presentation will give an overview about GCOS in general and about the Swiss GCOS activities. It will highlight how local measurements of different cryospheric parameters in Switzerland contribute to the Global Climate Observing System and the added-value of satellite-based observations of the cryosphere within GCOS.

REFERENCES

Seiz, G., & Foppa, N. 2007: National Climate Observing System (GCOS Switzerland). Publication of MeteoSwiss and ProClim, 92 p., (available in German, French and English under http://www.gcos.ch)

6.11

Replica method for three-dimensional X-ray microtomographic imaging of snow

Frei Esther, Heggli Martin & Schneebeli Martin

WSL Institute for Snow and Avalanche Reserach SLF, Flüelastrasse 11, CH-7260 Davos Dorf (heggli@slf.ch)

Snow microstructure is a crucial factor determining many properties such as mechanical strength, thermal conductivity, or optical properties. There are basically three techniques used to measure the full three-dimensional microstructure of snow samples: serial sectioning, direct X-ray computer tomography (micro-CT), or micro-CT of 1-chloronaphthalene cast snow. Samples that need to be transported or stored must be conserved by casting the snow with a solidifying substance, e.g. 1-chloronaphthalene or diethyl phthalate (DEP). Chloronaphthalene, while having a good X-ray contrast, is quite toxic and smells bad.

Image processing of serial sections of DEP cast snow is often very difficult, due to the formation of DEP crystals that appear optically very similar to ice crystals. Micro-CT was so far not applicable to DEP cast snow samples because there is hardly any absorption contrast between ice and DEP.

We developed a new replica method that allows investigating the microstructure of DEP cast samples by micro-CT. The sampling and casting process can be done as usual. Before the micro-CT measurement, the ice needs to be removed from the cast samples. The vapour pressure of DEP is about a million times smaller than that of ice, which allows sublimating the ice selectively. Keeping the sample under vacuum accelerates the sublimation process drastically to a few days. This leaves behind the DEP, which forms an exact negative image of the snow. The porous structure can now be measured in the micro-CT. A numerical inversion of the segmented micro-CT images yields a digital replica of the original snow structure.

The accuracy of replication was tested by comparing the digital replica to the original snow structure. The structural parameters of the two structures were compared to each other. The replication of the snow microstructure was very good with relative errors below 5%. The presented replica method is comparably straightforward and, for the snow types tested, the microstructure is accurately reproduced.

6.12

The ice ridge at Murtèl/Corvatsch: Studying a (c)old archive

Frey Holger*, Busarello Claudio**, Frauenfelder Regula***, Haeberli Wilfried*, Hoelzle Martin****, May Barbara*****, Rau Sebastian*****, Wagenbach Dietmar***** & Wagner Stefan******

*University of Zurich, Department of Geography, Winterthurerstr. 190, CH-8057 Zurich (holger.frey@geo.uzh.ch)
**SwissRE, Mythenquai 50/60 P.O. Box, CH-8022 Zurich
***Norwegian Geotechnical Institute, P.O. Box 3930 Ullevål Stadion, NO-0806 Oslo, Norway
****University of Fribourg, Department of Geosciences, Chemin du Musée 4, CH-1700 Fribourg
*****University of Heidelberg, Institute of Environmental Physics, Im Neuheimer Feld 229, D-69120 Heidelberg,
******Bitzi-Bendel, CH-9642 Ebnat-Kappel

Cold cornice-, crest- and plateau-type miniature ice caps of the northern hemisphere are known to contain old (Holocene to even Pleistocene) ice layers. These small but highly interesting paleoglaciological and paleoclimatical archives, however, are still largely unexplored and their future response to the rapid warming of the atmosphere remains to be investigated. On the north-south-oriented ice ridge Murtèl/Corvatsch (3300 – 3500 m.a.s.l) in the Upper Engadin, systematic studies are performed since several years (Haeberli et al. 2004). In this contribution we like to sum up the investigations and findings, present new results and discuss potential future research questions.

Refreezing of melt water is the main accumulation process, resulting in small accumulation rates. Temperatures in boreholes and at the marginal ice/rock-contact reveal that the ridge consists of cold ice and is frozen to the permafrost-bedrock (no basal sliding). Finite elements modelling shows that only very small flow velocities can be expected under the ridge where the surface slope tends towards zero. These two findings (small accumulation rates and probable ice velocities close to zero at the ice/rock interface) indicate that basal ice layers may have a considerable age (millennia). These assumptions are supported by a C14 date from an ice core drilled down to the bedrock in 2007, which however, since being a preliminary result, needs to be confirmed by further analyses.

A GPS survey was performed in 2000 and repeated in 2007. Comparison of the two digital elevation models (DEM) showed an average subsidence of the surface of about 5m (≈0.7m/y) with a maximum lowering of > 15 m and a geometric distortion of the ridge. Analyses of the Tritium content show that the ice at the surface in 2007 dates back to around 1960, which means that the ice accumulated in the last four to five decades has already melted away. Ground penetrating radar (GPR) measurements from 2001 indicate ice thicknesses of about 30m (±20m) under the ridge and more shallow parts at the glacier margins. Continuation or even acceleration of recent thinning rates would, hence, lead to vanishing of the glacier within decades.

REFERENCES

Haeberli, W., Frauenfelder, R., Kääb, A. & Wagner, S. 2004: Characteristics and potential climatic significance of “miniature ice caps” (crest- and cornice-type low-altitude ice archives). Journal of Glaciology, 50 (168), 129-136.

6.13

Application of operational geophysical monitoring systems on alpine permafrost

Hauck Christian* & Hilbich Christin**

*Department of Geosciences, University of Fribourg, Chemin de Musée 4, CH-1700 Fribourg (christian.hauck@unifr.ch)
**Geographical Institute, University of Jena, Löbdergraben 32, D-07743 Jena

Determining the subsurface ice and unfrozen water content in cold regions are important tasks in all kind of cryospheric studies, but especially on perennial (permafrost) or seasonal frozen ground, where little insights can be gained from direct observations at the surface. In the absence of boreholes, geophysical methods are often the only possibility for “visualising” the subsurface characteristics, and their successful application in recent years lead to more and more sophisticated ap-

proaches including 2- and 3-dimensional monitoring and even quantifying the ice and unfrozen water content evolution within the subsurface (for an overview see Hauck & Kneisel 2008).

Due to the strong sensitivity of electrical resistivity and permittivity to the phase change from unfrozen water to ice, the application of electrical and electromagnetic techniques has been especially successful. Within these methods, Electrical Resistivity Tomography (ERT) is often favoured due to its comparatively easy and fast data processing, its robustness against ambient noise and its good performance even in harsh, cold and irregular environments. Numerous recent studies have now shown that ERT is principally suitable to spatially delineate ground ice, differentiate between ice-poor and ice-rich occurrences, monitor freezing, thawing and infiltration processes, and even determine the origin of the ice, i.e. a differentiation between buried glacier ice and segregation ice, due to their different ion contents (yielding a reduced electrical resistivity for the latter).

In the context of a possible increased frequency of extreme weather periods, such as the hot summer 2003 in the European Alps, a monitoring of cryospheric components such as the mountain permafrost evolution becomes more and more important (Hilbich et al. 2008a). Common observation techniques are usually based on the thermal aspects, as in existing permafrost borehole temperature monitoring networks. Concerning the impacts of changing climate parameters, not only temperature but especially the ice and water content of the subsurface plays an important role, especially for permafrost observation purposes.

In summer 2006 the installation of a semi-automatic ERT monitoring system has been completed at 4 permafrost sites in the Swiss Alps (in co-operation with the Swiss permafrost network PERMOS, Vonder Mühll et al. 2007). This geophysical monitoring network serves to investigate the sensitivity of characteristic morphological sites to extreme atmospheric forcing in order to estimate the long-term evolution due to climate induced warming. Monitoring profiles are located at a rockglacier (Murtél, Upper Engadine), steep slope (Schilthorn, Bernese Alps), talus slope (Lapires, Valais) and frozen bedrock (Stockhorn plateau, Valais)(Hilbich et al. 2008b). The geophysical monitoring strategy includes repeated ERT measurements with a monthly to seasonal resolution over several years, as well as annual refraction seismic measurements at all sites. Whereas relative resistivity changes with time can be attributed to freeze and thaw processes, combined ERT and refraction seismic tomography will serve to determine total fractions of ice, unfrozen water and air within the pore space of the respective subsurface sections (Hauck et al. 2008).

REFERENCES

Hauck, C. & Kneisel, C. (Eds) 2008: Applied geophysics in periglacial environments. Cambridge University Press.

Hauck, C., Bach, M. & Hilbich, C. 2008: A 4-phase model to quantify subsurface ice and water content in permafrost regions based on geophysical data sets. Ninth Internat. Conf. on Permafrost, Fairbanks, Alaska, 2008, 6pp.

Hilbich, C., Hauck, C., Hoelzle, M., Scherler, M., Schudel, L., Völksch, I., Vonder Mühll, D. & Mäusbacher R. 2008: Monitoring mountain permafrost evolution using electrical resistivity tomography: A 7-year study of seasonal, annual, and long-term variations at Schilthorn, Swiss Alps, J. Geophys. Res., 113, F01S90, doi:10.1029/2007JF000799.

Hilbich, C., Hauck, C., Delaloye, R. & Hoelzle, M. 2008: A geoelectric monitoring network and resistivity-temperature relationships of different mountain permafrost sites in the Swiss Alps. Ninth Internat. Conf. on Permafrost, Fairbanks, Alaska, 2008, 6pp.

Vonder Mühll, D., Noetzli, J., Roer, I., Makowski, K. & Delaloye, R. 2007. Permafrost in Switzerland 2002/2003 and 2003/2004, Glaciological Report (Permafrost) No. 4/5 of the Cryospheric Commission (CC) of the Swiss Academy of Sciences (SCNAT) and Department of Geography, University of Zurich, 106 pp.

6.14

Thermal conductivity of snow: How to find a better parameterisation?

Heggli Martin, Köchle Bernadette, Pinzer Bernd & Schneebeli Martin

WSL Institute for Snow and Avalanche Reserach SLF, Flüelastrasse 11, CH-7260 Davos Dorf (heggli@slf.ch)

The thermal conductivity of snow is an important parameter in the energy balance of snow-covered areas. This energy balance is a key to understanding the response of arctic regions to changing global climate. The thermal conductivity and the heat flow through snow also determine the temperature gradient metamorphism which modifies the microstructure of snow (Schneebeli & Sokratov 2004; Kaempfer et al. 2005). As a consequence, mechanical, thermophysical, chemical, and optical properties of the snow are changed. For modelling the metamorphism of snow, it is essential to use a realistic parameterisa-

tion for the thermal conductivity. An understanding of the relationship between heat flow and snow microstructure is crucial for improving models in climatology, interpretations of chemical signals in firn and ice, and for avalanche research.

Available data for the effective thermal conductivity of snow, k_{eff}, are mostly based on measurements with a transient method using a needle probe (e.g. Sturm et al. 1997). They relate keff empirically to the density. However, the measured values differ by up to a factor of five for snow with the same density and the same grain shape. Thus, a large uncertainty is introduced into models that use a parameterisation based on these measurements. Furthermore, new measurements using a steady state method with heat flux plates suggest values of k_{eff} that are significantly higher than those measured by Sturm et al. (1997). For snow samples with a density of 200-300 kgm^{-3}, a k_{eff} of 0.2-0.3 $Wm^{-1}K^{-1}$ was measured.

In our study, we systematically compare measurements of k_{eff} with a needle probe (transient method) and with heat flux plates (steady state method) for different snow types and snow densities. The microstructure of the snow samples is characterized with micro computer tomography (micro-CT). Based on the assumption that the bonds between grains are more important than the density of the snow, Dadic et al. (2008) suggest a correlation between the penetration resistance and the thermal conductivity of snow. We test this correlation by measuring the penetration resistance of the different snow types using the SnowMicroPen (SMP), a high resolution penetrometer (Schneebeli & Johnson 1998), and correlating these measurements to the measured thermal conductivity.

Contact problems between the probe and the snow sample may be a potential explanation for the observed differences between the measurement methods. This effect is expected to be especially pronounced in fragile snow types such as depth hoar. The contact geometry between the probe and the snow sample is investigated using micro-CT.

REFERENCES

Dadic, R., Schneebeli, M., Lehning, M., Hutterli, M.A. & Ohmura A. 2008: Impact of the microstructure of snow on its temperature: A model validation with measurements from Summit, Greenland. J. Geophys. Res. 113, D14303.

Kaempfer, T.U., Schneebeli, M. & Sokratov, S.A. 2005. A microstructural approach to model heat transfer in snow. Geophys. Res. Lett. 32, L21503.

Schneebeli, M. & Johnson, J.B. 1998. A constant speed penetrometer for high-resolution snow stratigraphy. Ann. Glaciol. 26, 107-111.

Schneebeli, M. & Sokartov, S.A. 2004. Tomography of temperature gradient metamorphism of snow and associated changes in heat conductivity. Hydrol. Process. 18, 3655-3665.

Sturm, M., Holmgren, J., König, M. & Morris, K. 1997: The thermal conductivity of seasonal snow. J. Glaciol. 43, 26-41.

6.15

Thermal and electrical properties of a periglacial talus slope

Lambiel Christophe*, Scapozza Cristian*, Pieracci Kim*, Baron Ludovic** & Marescot Laurent***

*Institute of Geography, University of Lausanne, Anthropole, CH-1015 Lausanne (christophe.lambiel@unil.ch)
**Institute of Geophysics, University of Lausanne, Amphipôle, CH-1015 Lausanne
***Institute of Geophysics, ETH-Swiss Federal Institute of Technology, 8093 Zurich

Les Attelas talus slope is located on the western flank of the Mont Gelé (3023 m a.s.l.), in Verbier area. This cone-shaped landform is affected by solifluction in the upper-mid part of the slope, whereas bulging suggests the presence of creeping permafrost in the lower part of the slope.

In order to determine the spatial extension and the characteristics of the permafrost within the slope, several thermal and geoelectrical measurements have been carried out (Lambiel 2006).

Ground surface temperatures measured in March 2005 at the base of the snow cover (BTS method) displayed values colder than -6°C below 2700 m a.s.l. (Fig. 1). In the upper portion of the slope, temperatures were warmer (up to -1°C). According to these values, permafrost may be present in the lower part of the slope, whereas the probability of its presence decreases upslope.

In summer 2007, 48 permanent electrodes were installed each 4 meters along an upslope-downslope profile in order to monitor the underground resistivity using the Electrical Resistivity Tomography (ERT) technique (Fig. 1). The ERT profile (Fig. 2) shows that the highest resistivities are located in the lower part of the slope. From the distance of 85 meters to the foot of

the slope, a resistive body with values higher than 25 kΩm and thickness of about 15 meters has been imaged by both apparent resistivity and inversed resistivity. It corresponds to the cold BTS temperatures (Fig. 1) and can be interpreted as a permafrost lens. In the middle of the ERT profile, the lower resistivities (<10 kΩm) measured below 15-20 m depth are interpreted as unfrozen sediments. In the upper section, the resistive body is still present, but is found at greater depth and the resistivity values are lower (12-20 kΩm). This may be interpreted either as low-resistivity permafrost or as porous sediments. In the uppermost part of the profile, the resistivities lower than 4 kΩm indicate the absence of frozen sediments.

The permafrost distribution pattern evidenced in Les Attelas talus slope is conform to the measurements carried out in other alpine talus slopes (e.g. Otto and Sass 2006, Lambiel and Pieracci 2008). Permafrost appears likely in the lower part of the slopes, whereas it is generally absent upslope. In order to get direct information on the ground characteristics and thermal regime, 3 boreholes will be drilled along the ERT profile.

REFERENCES

Lambiel, C. 2006: Le pergélisol dans les terrains sédimentaires à forte déclivité: distribution, régime thermique et instabilités. Thèse, Université de Lausanne, Institut de Géographie, coll. "Travaux et Recherches" n° 33, 260 p.

Lambiel, C., Pieracci, K. 2008: Permafrost distribution in talus slopes located within the alpine periglacial belt, Swiss Alps. Permafrost and Periglacial Processes, 19: 293–304.

Otto, J.C., Sass, O. 2006: Comparing geophysical methods for talus slope investigations in the Turtmann valley (Swiss Alps). Geomorphology 76: 257-272.

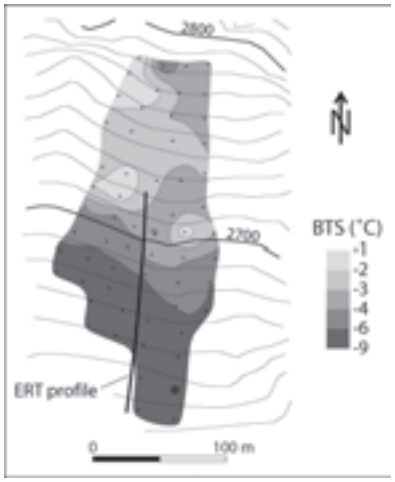

Figure 1. BTS measurements in March 2005 (black dots) and location of the Electrical Resistivity Tomography profile (black line) in Les Attelas talus slope.

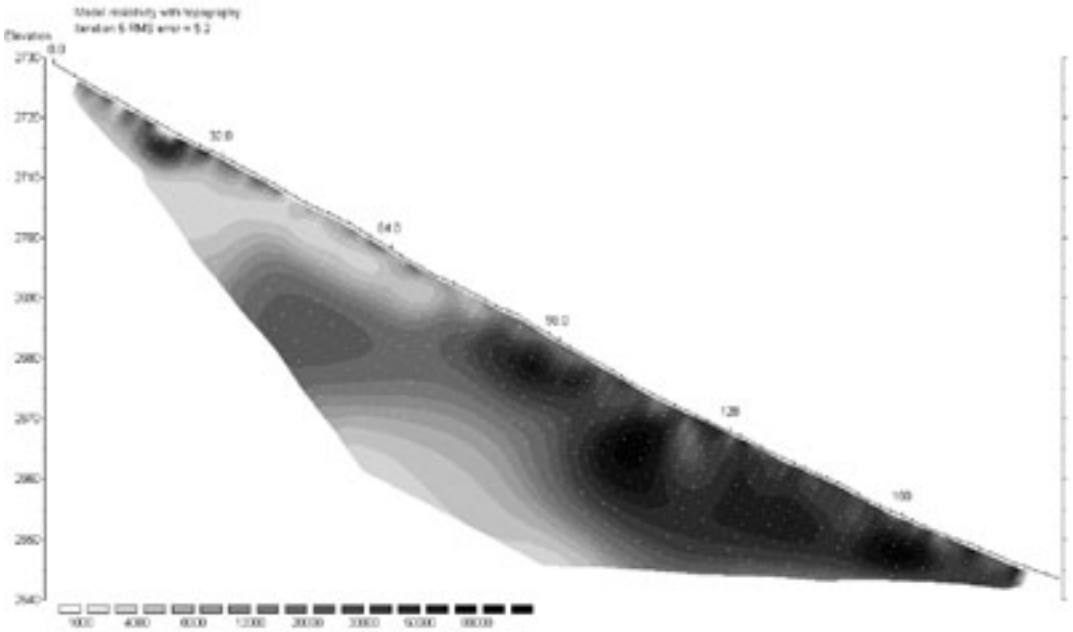

Figure 2. Electrical resistivity tomogram in Les Attelas talus slope, July 2008. The colour scale represents inverted resistivities in Ωm.

6.16

Modelling of glacier bed topography from glacier outlines and DEM data in a GIS

Linsbauer Andreas*, Paul Frank*, Hoelzle Martin* & Haeberli Wilfried*

* *Department of Geography, University of Zurich, Winterthurerstr. 190, CH-8057 Zürich (alinsbau@geo.uzh.ch)*

Due to the ongoing and expected future increase in global mean temperature, the Alpine environment will continue to get further away from equilibrium. This could have large environmental and societal impacts. Glaciers are a part of the high-mountain cryosphere, and their changes are considered to be the best natural indicators of climatic changes. The observation of the high-mountain environment and its glaciers forms thus an important part in global climate related observing programs. The calculation and visualization of future glacier development is thus an important task of communicating climate change effects to a wider public (Paul et al., 2007).

One of the most challenging topics in the assessment of climate change impacts on future glacier development is the unknown glacier bed and the related uncertainties in glacier volume estimations (Driedger and Kennard, 1986). In this respect, an estimated topography of the glacier bed would facilitate the calculation of glacier volume, the detection of local depressions, and the visualization of future ice-free grounds. While several methods exist to obtain a glacier bed from modelling combined with measurements (e.g. Huss et al., 2008), the goal of this study is the application of a simple but robust method which automatically approximates a glacier bed for a large sample of glaciers, using only few input data such as a digital elevation model (DEM), glacier outlines, and a set of flow lines for each glacier (Fig. 1). It is based on the calculation of the ice thickness along selected points of the flow line from the shallow ice approximation (SIA) following Haeberli and Hoelzle (1995) and subsequent spatial interpolation using a routine (topogrid) that is implemented in a geographic information system (GIS) and was developed by Hutchinson (1989).

Sensitivity tests with simple geometric forms on flat and inclined surfaces helped to constrain the model parameters. This includes the specifications for topogrid as well as the rules for digitizing the flow lines. For Switzerland, they form the only part of the input data that have to be newly created. The model was tested with real data from the Bernina region which lead to some modifications of the flow line digitizing and interpolation process. Finally, the reconstructed beds are compared to glacier beds or thickness measurements for three glaciers (Morteratsch, Gorner and Zinal) which have been obtained in previous studies.

The comparison revealed that the method has a large potential, but further improvements could be integrated as well. The general depth distribution of the reconstructed glacier beds is in a fairly good agreement with the results from the other studies and calculated glacier volumes or the location of local depressions do agree as well. However, there is a tendency to underestimate glacier thickness and locally some strong deviations exist. Currently, mean slope is the only (and thus a very sensitive) variable for the ice thickness calculation. Hence, it might be possible to improve the performance of the method by integrating some basic laws of glacier flow and further geomorphometry-dependent smoothing of the glacier surface (e. g. Huss et al., 2008). However, the method as a whole should stay as simple as possible to facilitate its automated and large scale application.

The application of the (improved and locally calibrated) method to all glaciers in the Swiss Alps does only require that glacier flow lines are digitized according to the rules outlined in this study. In combination with further GIS-based models (e.g. Paul et al., 2007) the here presented method would allow to calculate and visualize impacts of climate change on glaciers and their role as a water resource for Switzerland.

REFERENCES

Driedger, C. & Kennard, P. 1986: Glacier volume estimation on cascade volcanos: an analysis and comparison with other methods. Annals of Glaciology, 8, 59–64.

Haeberli, W. & Hoelzle, M. 1995: Application of inventory data for estimating characteristics of and regional climate-change effects on mountain glaciers: a pilot study with the European Alps. Annals of Glaciology, 21, 206–212.

Huss, M., Farinotti, D., Bauder, A. & Funk, M. 2008: Modelling runoff from highly glacierized alpine drainage basins in a changing climate. Hydrological Processes, 22 (19), 3888–3902.

Hutchinson, M. 1989: A new procedure for gridding elevation and stream line data with automatic removal of spurious pits. Journal of Hydrology, 106, 211–232.

Paul, F., Maisch, M., Rothenbühler, C., Hoelzle, M. & Haeberli, W. 2007: Calculation and visualisation of future glacier extent in the Swiss Alps by means of hypsographic modelling. Global and Planetary Change, 55, 343–357.

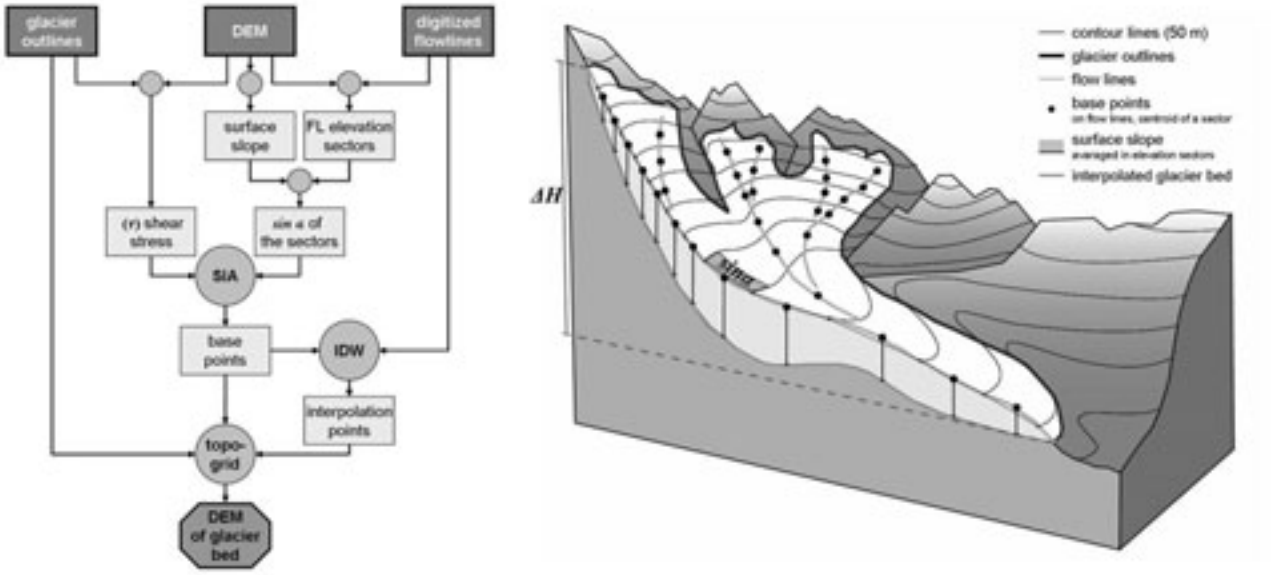

Figure 1: Schematic flowchart and details of the glacier bed modelling.

6.17

Transient response of idealized glaciers to climate variations

Martin Lüthi

VAW Glaciology, ETH Zürich, CH-4092 Zürich (luethi@vaw.baug.ethz.ch)

Variations of glacier length and volume under climate variations are investigated with model glaciers on a simple bedrock geometry. Under periodic climate oscillations the well-known phase lags of length and volume are obtained, after initial transients have died out. The relation between glacier mass balance (local or total) and climate is strongly influenced by the transient response for forcing periods shorter than the volume time scale. These transients are surprisingly large, and lead to unexpected trajectories in phase space. Under periodic oscillations the local ice thickness follows the climate forcing with a typical phase delay of 60° (accumulation area) to 180° (glacier terminus), while glacier length is completely out of phase for forcing periods below the volume time scale. The evolution of the model glacier can be approximately described with a forced, linearly damped harmonic oscillator which is typically underdamped. Approximate expressions for the volume- and area time scales are explicitly derived, as are volume-length scaling relations.

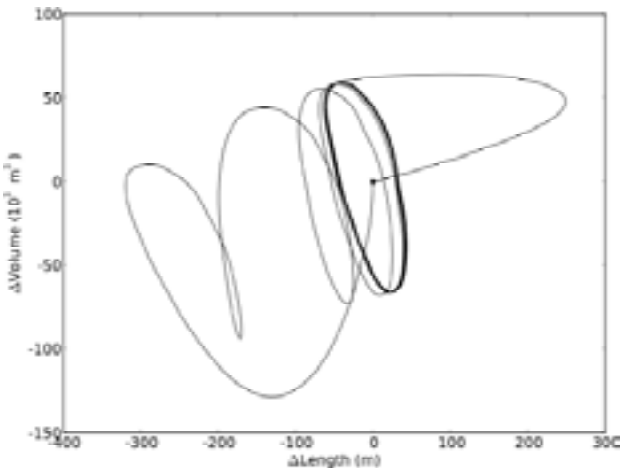

Phase space diagram of volume change vs. length change of a model glacier under climate forcing with 50 year period. Only after 5 climate cycles the glacier response approaches the limiting cycle around the steady state (black dot). Obviously climate and glacier reaction are not closely related.

6.18

Airflow velocity measurements in ventilated porous debris accumulations

Morard Sebastien*, Delaloye Reynald*

**Geography, Dept. Geosciences, University of Fribourg, Chemin du Musée 4, CH-1700 Fribourg (sebastien.morard@unifr.ch, reynald.delaloye@unifr.ch)*

The mechanism of deep air circulation (the "chimney effect") is known to be a frequent phenomenon maintaining very cold ground conditions, and sometimes permafrost, in porous debris accumulations (talus slope, relict rock glacier) located several hundred meters below the regional permafrost limit. Temperature measurements at the ground surface (Morard et al. 2008) and in borehole (Delaloye & Lambiel 2007) revealed that the ground thermal regime is strongly influenced by the advective-heat effect of the airflow.
In order to better understand the processes by which internal ventilation causes a strong overcooling of the lower part of debris accumulations, experimental continuous airflow velocity measurements (using anemometers and an air differential pressure sensor) have been carried out recently in three sites : in the Creux-du-Van talus slope (Jura mountains, 1250 m a.s.l.), in the Dreveneuse-d'en Bas talus slope (Valais Prealps, 1560 m a.s.l.) (Delaloye & Lambiel 2007) and in the Gros Chadoua relict rock glacier – talus slope complex (Fribourg Prealps, 1570 m a.s.l.).

Windmill and sonic anemometers were placed in wind holes located in the lower part of the ventilation system. In the Dreveneuse-d'en Bas talus slope, the windmill sensor recorded a velocity of 0.1 – 0.4 m/s in summertime, but stronger aspiration (up to 0.8 m/s) by very cold weather during a snow free period in late fall. In the Creux-du-Van talus slope, data from the sonic anemometer were very noisy, but seem also range between 0.05 - 0.5 m/s and sometimes 1 m/s.
In the Gros Chadoua, both wind sensors recorded outflow values between 0.5 to 1.7 m/s in summer, with faster velocities when the external temperature rises. In fall, before the onset of a snow cover, when the external air temperature crossed a threshold of about +4°C, airflow direction changes rapidly. Airflow reversibility occurred several times during this period, depending on the outside air evolution (figure 1). The wind sensors did not work properly during winter.
The relation between airflow velocity (U) and the outside air temperature is not linear, but can be expressed as : $U = c \sqrt{(\text{Outside Air Temperature} - \text{Reversibility Threshold Temperature})}$ (Ohata et al. 1994). C is an empirical coefficient depending upon structural conditions. For the Gros Chadoua, the results fit well with a coefficient c between 0.25 and 0.5. For Dreveneuse-d'en Bas, results are better with a smaller coefficient (0.10).

When the wind hole was disconnected from the open air environment by a snowcover, the differential pressure sensors revealed for most of all the winter season that the pressure contrast between the inside and the outside was dependant on the external temperature. This pressure low at the base of the snow cover is assumed to be caused dynamically by the ascent of relatively warmer light air throughout the debris accumulation. This process forces the external air to penetrate in the ground through the snow cover in the lowermost part of the system.

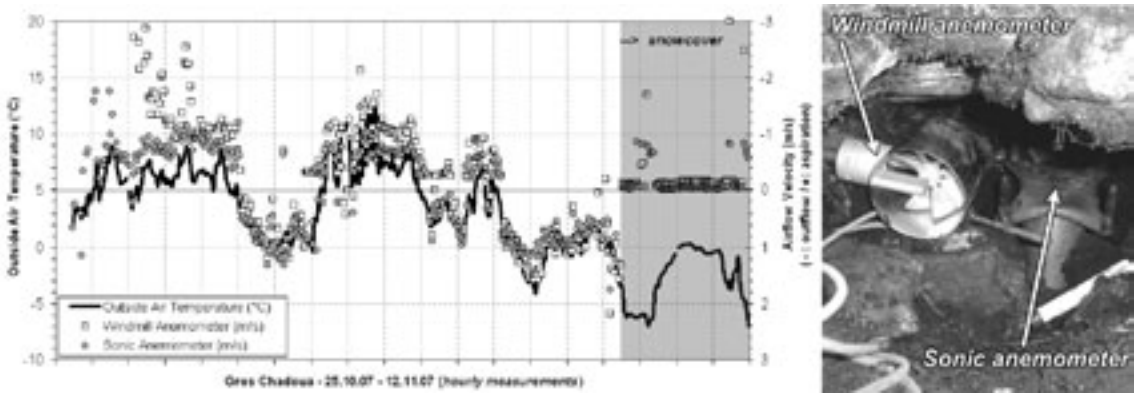

Figure 1. Air flow velocity and direction (outflow or aspiration) linked with the outside air temperature in the Gros Chadoua, between 25. October and 12. November 2007.

Despite these instruments were normally intended for open-air measurements, a range of airflow velocity has been determined. The results show that the airflow is maintained by a simple relation determined by the pressure gradient resulting from temperature difference between the inside and the outside air. The circulation of air inside porous debris accumulation is also a continuous process, even after the development of a snowcover.

REFERENCES
Delaloye, R., & Lambiel C. 2007: Drilling in a low elevation cold talus slope (Dreveneuse, Swiss Prealps). Geophysical Research Abstracts 9: 10907.
Morard, S., Delaloye, R. & Dorthe J. 2008: Seasonal thermal regime of a mid-latitude ventilated debris accumulation. Proceedings of the Ninth International Conference on Permafrost, July 2008, Fairbanks, Alaska, 1233-1238.
Ohata, T., Furukawa, T. & Higuchi K. 1994: Glacioclimatological study of perennial ice in the Fuji ice cave, Japan, Part 1, Seasonal variation and mechanism of maintenance. Arctic and Alpine Research, vol. 26, 3. 227-237.

6.19

Inventory of geomorphosites of Bavona and Rovana valleys (Ticino)

Pagano Luca

6670 Avegno, luca.pagano@gmail.com

During the last decade, research on geomorphological heritage has improved due to the development of geotourism and geoparks and to the activity of the Working group on Geomorphosites of the International Association of Geomorphologists. Several methods (see Reynard and Coratza, 2007) were developed for assessing the quality of geomorphosites – that is landforms to which a value can be given due to human perception and/or utilization (Panizza, 2001). The aim is to reduce subjectivity and to facilitate the selection of the most representative sites, worth to be protected and/or promoted.
Inspired by several approaches developed during the last decade, Reynard et al. (2007) developed at the Institute of Geography of Lausanne University an assessment method of geomorphosites. The method allows assessing the scientific, ecological, aesthetic, cultural and economic values of geomorphosites and to note more descriptive data in order to set up a site inventory. The assessment is divided in two categories of criteria: the central (scientific value) and additional (ecological, economic, aesthetic and cultural) values.
The assessment method was applied on two alpine valleys in the Southern Swiss Alps. More precisely, we focused on the selection and the assessment of Bavona and Rovana valleys' geomorphosites (Maggia Valley, Ticino). 28 landforms with a scientific central value were identified and studied. Results show that Calnegia hanging valley obtains the most important score and is just followed by the Basòdino Glacier, a small ice cap glacier. One site, the fossil proglacial margin of the Basòdino Glacier W, represents an incredible geodiversity due to the glacio-karstic origin of Pian del Ghiacciaios polje.
After the inventory stage, we noted that, on the ground, geomorphology is not much known in comparison with the high value of some geomorphosites. Thus, in order to acknowledge them by the general public, we offered some perspectives with the intention of promoting the geomorphological heritage of the region. Firstly, the definition of categories of protection would contribute to preserve the vulnerable geomorphosites towards human impacts. Secondly, we underline the value of some interesting sites of the inventory with the idea of promoting a sustainable tourist development. Geodiversity is indeed poorly taken into account for the (geo)tourist development of the region.

REFERENCES:
Pagano, L. 2008: Inventaire des géotopes géomorphologiques du Val Bavona et du Val Rovana. Sélection, evaluation et perspectives. Mémoire de Licence. Université de Lausanne.
Panizza, M. 2001: Geomorphosites, concepts, methods and examples of geomorphological survey. Chinese science bulletin 46, Suppl. Vol., 4-6.
Reynard, E. & Coratza, P. 2007: Geomorphosites and geodiversity: a new domain of research. Geographica Helvetica 62, 3: 138-139.
Reynard, E. Fontana, G. Kozlic, L. Scapozza, C 2007: A method for assessing « scientific » and « additional values » of geomorphosites. Geographica Helvetica, 62, 3: 148-158.

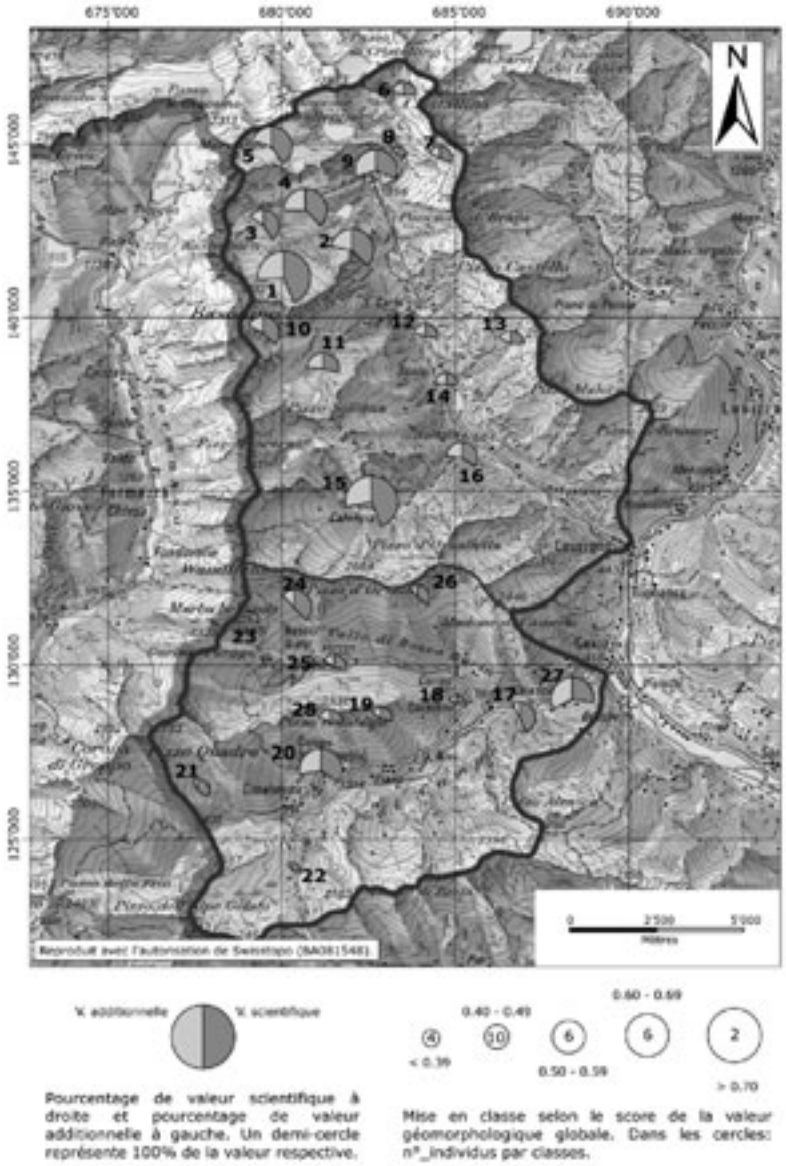

6.20

Evaluation des effets de l'enneigement artificiel sur la chimie du sol: Cas de Crans-Montana-Aminona, Valais

Parisod Julien*, Senn Claudia*, Pfeifer Hans-Rudolf * & Vennemann Torsten*

**Institut de Minéralogie et de Géochimie, Faculté des Géosciences et de l'Environnement, Université de Lausanne, Anthropole, CH-1015 Lausanne, Suisse.*

Ce travail traite des éventuels impacts sur la chimie du sol dû à l'utilisation de l'enneigement artificiel, ainsi qu'à celle d'additif qui permet une production de neige de culture à des températures plus hautes. Le but est de déterminer s'il existe des impacts sur la chimie du sol, par comparaison des résultats d'analyse entre différents profils de sols, soumis et non soumis à l'enneigement artificiel, et d'évaluer l'ampleur de ces derniers s'il existe. La neige artificielle est produite par pulvérisation d'eau mélangée à de l'air comprimée, ce qui forme des microgouttelettes qui vont s'agglomérer sur des noyaux de congélations pour former des cristaux de neige (Brillaud et al., 2005 et Campion, 2002). Il ne semble donc pas qu'un apport en élément, de surcroît polluant, soit à craindre, pour autant que l'eau utilisée ne soit pas polluée (ou que n'y retrouve pas un ou plusieurs éléments dans des concentrations anormalement élevées). Cependant, l'utilisation d'un additif est parfois

présente, ce qui était le cas pour une partie des installations du domaine skiable de Cran-Montana-Aminona jusqu'en 2007. L'additif le plus souvent utilisé est une protéine bactérienne appelée INP (Ice Nucleation Protein, Graether et Jia, 2001) produite par Snowmax®. Cette protéine joue le rôle de noyau de congélation, et favorise ainsi la formation de cristaux de neige à des températures plus élevées (soit environ − 2°C au lieu de -4°C sans). Une utilisation croissante de l'enneigement artificielle, lié à l'utilisation, dans certains cas, d'un additif d'origine bactérienne, est bien souvent à l'origine de craintes vis-à-vis de l'environnement. Ce travail ne prétend pas répondre à la question « L'utilisation de l'enneigement artificielle, avec ou sans additif, est-il à l'origine d'une pollution des sols ? », mais, se place plutôt comme un point de départ, afin de déterminer si des impacts directs ou indirects sur la chimie du sols sont imputable à l'utilisation de cette technologie, notamment un apport en composés azotés qui serait lié à la présence de l'additif d'origine protéinique. Nous avons échantillonné trois « types» de sols : soumis à l'enneigement uniquement naturel, à l'enneigement artificiel sans additif et naturel et à l'enneigement artificiel avec additif et naturel, ainsi que différents «types» de neige afin de vérifier l'origine l'apport en certains éléments: neige naturel, neige artificielle sans additif et avec, neige mixte naturelle-artificielle sans additif et avec. Nous avons également échantillonné différentes eaux provenant de ruisseaux alimentés par la fonte de neige naturelle, artificielle avec et sans additif afin d'éventuellement constaté un transfert dans ces eaux (Fig. 1). Dans le but de passer en revue un maximum d'éléments (chimiques) ainsi que les propriétés de base (pH, granulométrie), présents dans le sol, nous avons effectué les analyses suivantes :

- composition en éléments majeurs et traces par fluorescence X
- composition ionique par chromatographie sur extractions
- dosage du carbone total, organique et minéral par coulométrie (sur échantillons solides) et analyseur élémentaire de C dissout (sur extractions)
- analyses CHN (sur échantillons solides)
- analyses qualitatives spécifiquement des composés protéiniques par spectroscopie par fluorescence UV-Visible et absorbance
- dosage de protéines totales par la méthode de Bradford (sur les extractions).

Les résultats montrent que globalement, il existe peu de variations de concentrations des éléments analysés pouvant être corrélés avec l'utilisation de l'enneigement artificiel que ce soit avec ou sans additif. Il n'y a notamment pas d'apports flagrants en composés azotés malgré l'utilisation d'un additif de nature protéinique et d'origine bactérienne. Les seuls éléments dont on peut redouter un apport, du fait que des concentrations relativement élevées dans les échantillons de neige artificielle avec et sans additif, sont le magnésium, le calcium ainsi que le sulfate. Cependant, ce dernier étant un anion, une retention dans les sols est peu probable. Ce dernier se retrouve en concentrations plus élevées dans les eaux de ruisseaux, alimentés par les eaux de fonte de neige mixte, donc avec présence de neige artificielle avec et sans additif. Il est toutefois difficile de corréler ces concentrations plus élevées avec un apport direct dû à l'utilisation de l'enneigement artificiel, aux vues de la dynamique des systèmes d'alimentation des ruisseaux, et de la date de prélèvement des échantillons. Nous pouvons donc conclure qu'un impact sur la chimie du sol (pour la part de ce domaine exploré dans ce travail), n'est pas clairement observable, et est dans tous les cas pas d'une ampleur importante. Cependant, nos résultats nous montrent également qu'il serait intéressant de faire des recherches se dirigeant dans le domaine de la biochimie du sol, plus particulièrement le développement et l'activité bactérienne.

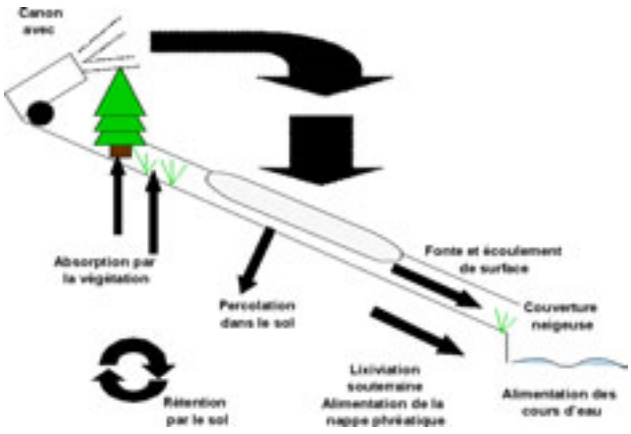

Figure : 1 : Schéma des différentes voies possibles de transfert des composés chimiques de la neige artificielle dans les différents compartiments

REFERENCES

Brillaud M-A., Luez A., Rodicq M. (2005), Neige de culture et Snowmax : quels impacts sur la santé, Rapport Atelier Santé-Environnement Ecole Nationale de la Santé Publique, Rennes. Récupéré sur http://www.tourisme.gouv.fr/fr/navd/mediatheque/publication.

Campion T (2002), Impact de la neige de culture, Rapport de l'Agence de l'Eau Rhône Méditerrannée Corse.

Graether S.P., Zongchao Jia. (2001), "Modeling Pseudomonas syringae ice-nucleation protein as a β-helical protein". Biophysical Journal, 80, pp. 1169-1173.

6.21

Spatial variability of glacier elevation changes in the Swiss Alps obtained from differencing two DEMs

Paul Frank* & Haeberli Wilfried*

* *Department of Geography, University of Zurich, Winterthurerstr. 190, CH-8057 Zurich (frank.paul@geo.uzh.ch)*

During the past 25 years massive glacier thinning has been observed in the Alps. This is documented by direct mass balance measurements on nine regularly observed glaciers as well as field evidence (e.g. disintegration of glacier tongues, increased areas of rock outcrops, collapsing rock walls, revised hiking trails) at several sites (Paul et al., 2007). However, it remained uncertain how representative the nine directly measured glaciers are for the volume change of the entire Alps. A possible way of assessing the representativity is to subtract two digital elevation models (DEMs) from two points in time which are of sufficient accuracy with respect to the expected changes.

For the Swiss Alps, a DEM with 25 m spatial resolution (DEM25) was generated by swisstopo around 1985. In February 2000 a near-global DEM was acquired by interferometric techniques during the Shuttle Radar Topography Mission (SRTM). This DEM is available for free from an ftp-server at 90 m (or 3") spatial resolution. It offers now the unique opportunity to assess glacier elevation changes over the entire Alps by subtracting it from an earlier DEM (like the DEM25 in Switzerland). It has to be noted that both DEMs could have larger errors in the (snow-covered) accumulation area of glaciers. For the DEM25, the stereo matching of optical aerial photography suffers from poor contrast over snow and the SRTM DEM has some uncertainty due to a variable snow penetration depth of the C-band radar beam.

For mainly two reasons we have not corrected the elevation dependent bias of the SRTM elevations which was reported in earlier studies. One reason is that a similar bias results as an artefact when DEMs of different cell size are subtracted (Paul, in press), the other is that a huge portion of glaciers would get positive elevation changes (mass gains) in the accumulation area, which is highly unlikely during the period 1985 to 1999.

For this study we have calculated glacier specific elevation changes from 1985 to 1999 for about 1050 glaciers larger than 0.1 km^2 in the Swiss Alps (Paul and Haeberli, 2008). The changes refer to the glacier geometry of 1973 which is close to the 1985 glacier extent (Paul et al., 2004) and digitally available for all glaciers in Switzerland. In order to compare the results with the direct measurements, two mean volume change values (in meter water equivalent, m w.e.) are calculated. One is (method A) the arithmetic mean of the individual mean changes of all glaciers and another one is (method B) the mean value for the entire glacierized area that does not consider individual glaciers (all glaciers together are taken as one glacier entity).

The analysis reveals strong thickness losses (partly >80 m) for flat / low-lying glacier tongues and a strong overall surface lowering also for glacier tongues under a thick debris cover. The difference image (Fig. 1) displays fine spatial details of the change.

Apart from the obvious massive downwasting of the tongue of Triftglacier, it clearly reveals that some glaciers (e.g. Stein, Kehlen, Damma) have been larger in 1985 than in 1973 as the zone of thinning is outside the 1973 extent. The mean cumulative mass balance of the nine glaciers with direct measurements (-10.8 m w.e.) agrees well with the mean change (method B) for the Swiss Alps from DEM differencing (-11 m w.e.) and can thus be considered to be representative for the Alps. Mean thickness change of individual glaciers is correlated with their size, elevation, and exposure to solar irradiation. This implies that mass losses of large glaciers can be underestimated when they are directly inferred from values measured at the generally much smaller glaciers in the mass balance network. Indeed, the mean change with method (A) is only -7.0 m w.e. and thus much less negative than the field derived value. In particular the large regions at low elevations from the largest ice masses contribute to the stronger loss.

REFERENCES

Paul, F. In press: Calculation of glacier elevation changes with SRTM: Is there an elevation dependent bias? Journal of Glaciology.

Paul, F. & Haeberli, W. 2008: Spatial variability of glacier elevation changes in the Swiss Alps obtained from two digital elevation models. Geophysical Research Letters, doi:10.1029/2008GL034718.

Paul, F., Kääb, A. & Haeberli, W. 2007: Recent glacier changes in the Alps observed from satellite: Consequences for future monitoring strategies. Global and Planetary Change, 56, 111-122.

Paul, F., Kääb, A., Maisch, M., Kellenberger, T. W. & Haeberli, W. 2004: Rapid disintegration of Alpine glaciers observed with satellite data. Geophysical Research Letters, 31, L21402, doi:10.1029/2004GL020816.

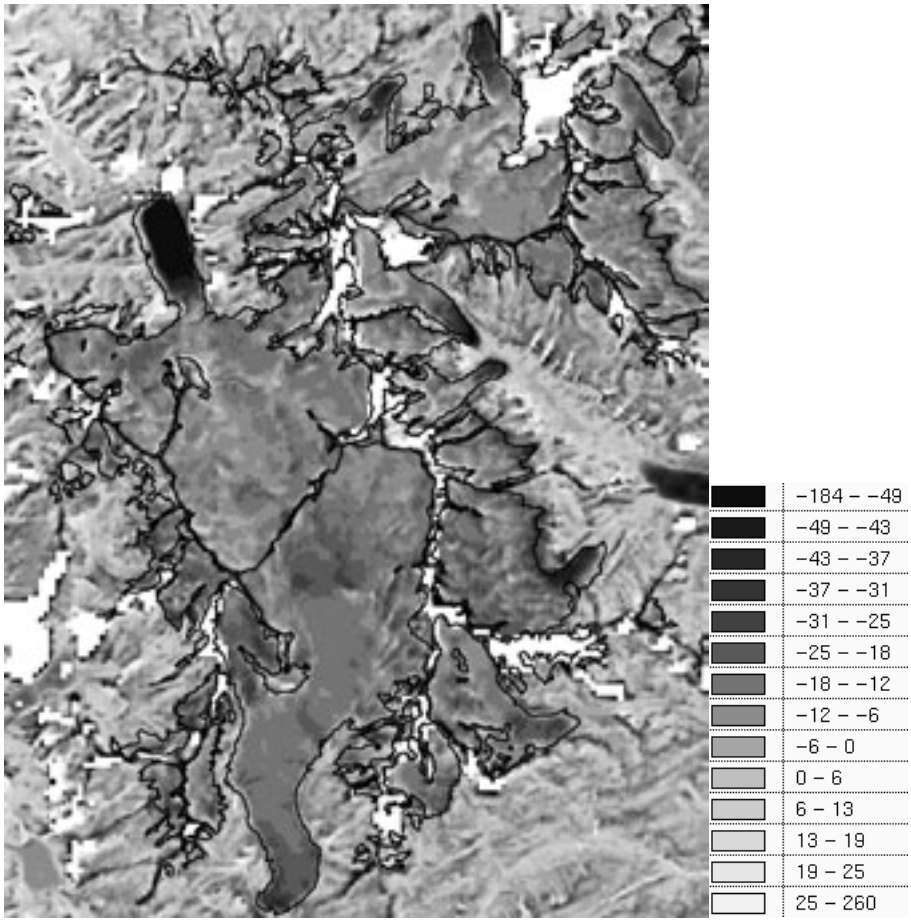

6.22

GlobGlacier: A new ESA project to map the world's glaciers from space

Paul Frank*, Kääb Andreas**, Rott Helmut***, Shepherd Andrew**** & Strozzi Tazio*****

* *Department of Geography, University of Zurich, Winterthurerstr. 190, CH-8057 Zurich (frank.paul@geo.uzh.ch)*
** *Department of Geosciences, University of Oslo, Oslo, Norway*
*** *Environmental Earth Observation (Enveo), Innsbruck, Austria*
**** *School of Geosciences, University of Edinburgh, Edinburgh, Great Britain*
***** *Gamma Remote Sensing, Gümligen, Switzerland*

Changes of glaciers and ice caps are key indicators of climatic change, mostly due to their enhanced and well recognizable reaction to small climatic variations. They have thus been selected as one of the essential climate variables (ECVs) in the global climate observing system (GCOS) and their monitoring is organized in a tiered strategy within the global terrestrial network for glaciers (GTN-G). Within GTN-G, annual measurements of mass balance (c. 50 glaciers) and length changes (c. 550 glaciers) are performed and in the world glacier inventory (WGI) detailed data exist as point information for about 71'000 glaciers, which is c. 40% of the estimated 160'000 glaciers worldwide. Thus, (1) the current sample of glaciers with annual measurements is very small and might be not representative for the changes at a global scale and (2) the WGI is not complete and difficult to use for change assessment (point data). As melting glaciers and ice caps might provide an even larger contribution to global sea level rise in the coming decades than the two continental ice sheets, there is an urgent necessity to generate more complete and representative data sets (GCOS, 2006).

While the large potential of multispectral satellite data for glacier mapping is already utilized by the GLIMS initiative to create a digital database of glacier outlines, the full potential of satellite data for determination of glacier mass balance or length changes in a systematic way remain to be explored. As the required techniques for mapping glacier snow lines, topography, elevation changes or velocity fields (all indicative for mass balance) do already exist, a remaining challenge is their integrated and systematic application to a large set of glaciers (IGOS, 2007). The here presented new ESA project GlobGlacier aims at exploring and applying the existing methods to already archived satellite data in order to contribute to existing

databases (GLIMS, WGI) and observation programs (WGMS). GlobGlacier is one of ESAs data user element (DUE) activities that responds to the needs of some major users groups, which are actively involved in defining the products and assessment of the service (Volden, 2007).

The products that will be generated by GlobGlacier include (see Fig. 1): glacier outlines and terminus positions for 20'000 units each, snowlines and topographic information for 5000 units each, elevation changes for 1000 units and velocity fields for 200 units. The techniques to be applied vary with the product and the sensor and include optical and microwave satellite data as well as laser altimetry (cf. Paul et al., subm.). Glacier **outlines** will be derived from multispectral sensors (mainly Landsat TM/ETM+) using well established methods (band ratios with threshold) combined with manual editing and GIS-based data fusion at three different levels of detail: Level 0 (L0): outlines enclosing contiguous ice masses that are corrected for misclassification (e.g. debris, shadow, water); L1: individual glaciers that result from combining L0 outlines with hydrologic divides; L2: outlines from L1 combined with DEM data to obtain a detailed glacier inventory. The **terminus position** will be marked where the central flowline crosses the glacier terminus. **Snow lines** will also be derived from optical imagery based on terrain and atmospherically corrected albedo values. The **topography** information is basically derived from the freely available SRTM DEM and complemented by DEMs from optical stereo sensors (e.g. ASTER, SPOT) and interferometric techniques (e.g. using ERS1/2 SAR data) in regions outside the SRTM coverage. **Elevation changes** will be calculated by differencing DEMs from two points in time and by comparing spot elevations from laser altimeters at orbit crossing points. Finally, **velocity** fields will be derived from feature tracking of repeat pass optical imagery or from microwave sensors using differential SAR interferometry or offset-tracking. The time period analysed will depend on the available satellite data and vary from seasonal to annual means.

REFERENCES

GCOS 2006: Systematic Observation Requirements for Satellite-based Products for Climate - Supplemental details to the satellite-based component of the Implementation Plan for the Global Observing System for Climate in Support of the UNFCCC. GCOS Report 107, WMO/TD No. 1338, 103 pp.

IGOS 2007: Integrated Global Observing Strategy Cryosphere Theme Report - For the Monitoring of our Environment from Space and from Earth. Geneva: World Meteorological Organization. WMO/TD-No. 1405. 100 pp.

Paul, F., A. Kääb, H. Rott, A. Shepherd, T. Strozzi, & E. Volden subm.: GlobGlacier: Mapping the worlds glaciers and ice caps from space. Earsel eProceedings.

Volden, E. 2007: ESAs GlobGlacier project. In: CliC Ice and Climate News, Issue 9, 8.

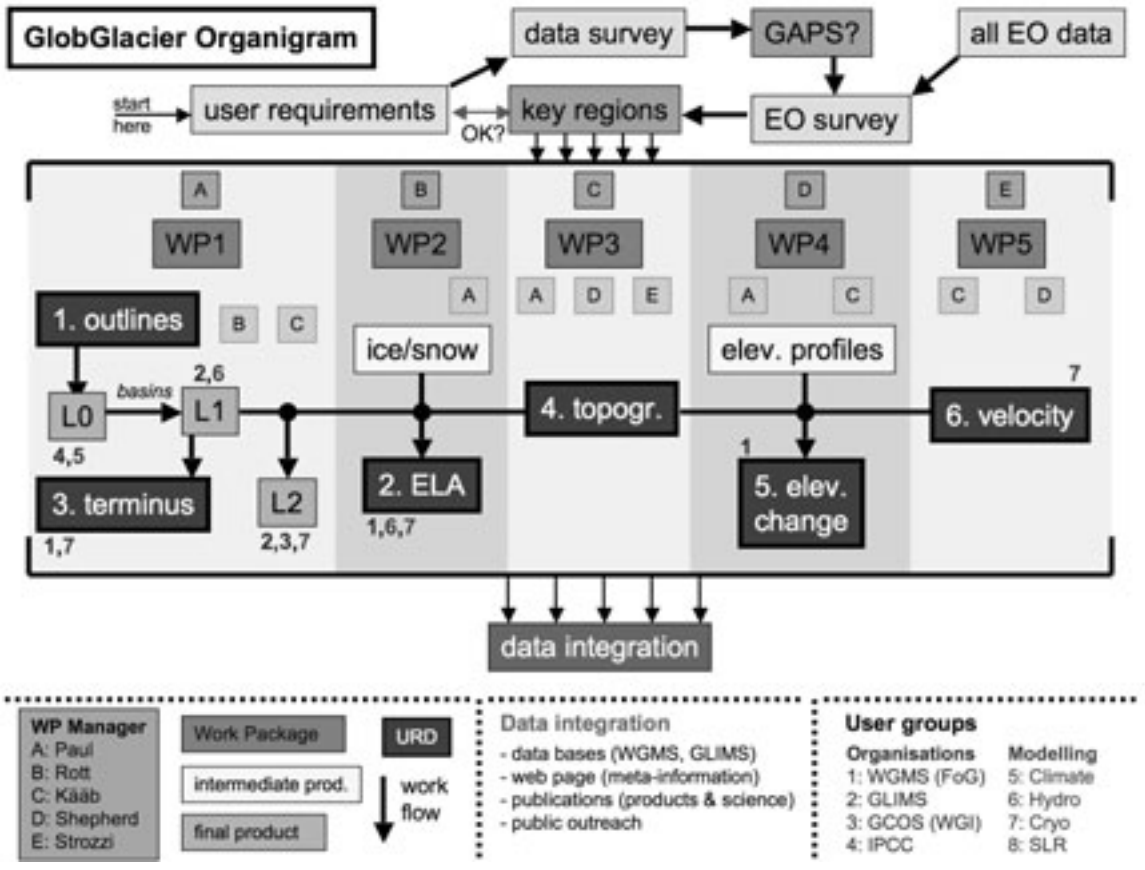

Figure 1. Schematic overview of the workflow, the workpackages and the generated products of the GlobGlacier project.

6.23

Rapid permafrost degradation induced by non-conductive heat transfer within a talus slope at Flüela Pass, Swiss Alps.

Phillips Marcia*, Zenklusen Mutter Evelyn*, Kern-Luetschg Martina*

WSL Institute for Snow and Avalanche Research SLF Davos (phillips@slf.ch)

Talus formations are an important type of debris storage in mountain environments and the degradation of ice within them can lead to the triggering of mass movements or to structure instability (Phillips and Margreth 2008). Numerous surface investigations have shown that the inner structure of talus formations and hence the processes occurring there can be complex. However, few direct measurements exist, for example in boreholes. One of the earliest studied talus slopes in the Swiss Alps is a NE oriented, 25-35° slope located at Flüela Pass, ranging between 2380 and 2600 m asl. The slope is bounded by a rock wall at the top and by a lake at the base. Geophysical investigations in the 1970s indicated the presence of ground ice at the base of the slope, thinning upslope and not occurring at the top (Haeberli 1975). The presence of permafrost was attributed to the persistence of avalanche debris at the base of the slope in summer and later also to local differences in surface roughness (Lerjen et al. 2003).

Two 20 m deep boreholes were drilled at the site in 2002, confirming the presence of ice at the base of the slope (Luetschg et al. 2004). Borehole B1 is located at 2501 m asl (midslope) and B2 is at 2394 m (near the base of the slope). Borehole stratigraphies showed the presence of varying amounts of ice between 3 and 10 m depth and the occurrence of coarse blocks interspersed with large voids at 9 – 14 m depth in B1 and at 10 –17 m depth in B2; the material presumably originates from para-/postglacial rockfall deposits or blocky Egesen moraines, which were subsequently covered with firn/ice and finer clasts.

Borehole temperature measurements have been carried out in B1 and B2 since 2002, using 12 YSI 44008 thermistors and Campbell CR10X loggers in each borehole. Meteorological data was obtained near to the slope in a flat area of Flüela Pass. During the measurement period (2002-2007) active layer depths have remained very constant at 3 m, even during the summer 2003 heat wave, pointing to the ongoing presence of ice below 3m. In 2003 the permafrost body in B2 was 7 m thick, between 3 and 10 m depth. By July 2008 its thickness had halved and was located between 3 and 6.5 m depth. This rapid permafrost degradation was triggered from below.

Borehole temperature data also indicate the occurrence of thermal anomalies at around 10 m depth in B1 and around 15 m depth in B2. The temperature curves here display a much higher variability and amplitude than those measured just above and below. This suggests the occurrence of intra-talus ventilation through the large voids within the coarse blocky material, a phenomenon driven by the expulsion of the relatively warmer and less dense intra-talus air in winter, leading to the aspiration of cold external air into the base of the slope (Delaloye and Lambiel 2005). The phenomenon is particularly effective with cold air temperatures and low snow depths and can also occur in summer when air temperatures are below 0°C.

The presence of voids and the evidence of the occurrence of intra-talus ventilation suggest that non-conductive heat-transfer processes, in particular latent heat effects, are contributing to the extremely rapid thinning of the permafrost ice from below. As the intra-talus air is drawn through the snow cover into the voids and because temperature gradient induced vapour migration occurs from below, the intra-talus air must have a high moisture content; when this air comes into contact with the frozen ground and the dew point is reached, condensation will occur, releasing energy and enhancing permafrost degradation. The latent heat of condensation is high (2.5 MJ kg^{-1}), so little vapour is required to cause significant warming.

Further investigations such as gas-tracer experiments, local microclimatological measurements and more detailed borehole temperature measurements will be required to analyze the causes and effects of the intra-talus ventilation in detail. The existing measurements deliver interesting information on possible mechanisms of currently occurring permafrost degradation in alpine talus slopes.

REFERENCES

Delaloye, R., and Lambiel, C. 2005. Evidences of winter ascending air circulation throughout talus slopes and rock glaciers situated in the lower belt of alpine discontinuous permafrost (Swiss Alps). Norsk geogr. Tidsskr., 59: 194-201.

Haeberli, W. 1975. Untersuchungen zur Verbreitung von Permafrost zwischen Flüelapass und Piz Grialetsch (Graubünden). Zurich.

Lerjen, M., Kääb, A., Hoelzle, M., and Haeberli, W. 2003. Local distribution of discontinuous mountain permafrost. A process study at Flüela Pass, Swiss Alps. In Eighth International Conference on Permafrost. Edited by S.A. Phillips. Zurich. Swets & Zeitlinger, Vol.1, pp. 667-672.

Luetschg, M., Stoeckli, V., Lehning, M., Haeberli, W., and Ammann, W. 2004. Temperatures in two boreholes at Flüela Pass, Eastern Swiss Alps: the effect of snow redistribution on permafrost distribution patterns in high mountain areas. Permafrost and Periglacial Processes, 15: 283-297.

Phillips, M., and Margreth, S. 2008. Effects of ground temperature and slope deformation on the service life of snow-supporting structures in mountain permafrost: Wisse Schijen, Randa, Swiss Alps. In 9th International Conference on Permafrost. Edited by D.L. Kane and K.M. Hinkel. Fairbanks, Alaska. Institute of Northern Engineering, University of Alaska Fairbanks, Vol.2, pp. 1417-1422.

6.24

Rockglacier dynamics in the Swiss Alps – comparing kinematics and thermal regimes in the Murtèl-Corvatsch region

Roer Isabelle*, Hoelzle Martin*,**, Haeberli Wilfried* & Kääb Andreas ***

* *Glaciology, Geomorphodynamics & Geochronology; Geography Department, University of Zurich, Winterthurerstrasse 190, CH − 8057 Zürich (iroer@geo.uzh.ch)*

** *Department of Geosciences, University of Fribourg, Chemiin du musée 6, CH − 1700 Fribourg*

*** *Department of Geosciences, University of Oslo, Postbox 1047 Blindern, NO - 0316 Oslo*

In the context of the recent climatic changes and their impact on the cryosphere, permafrost environments play a key role due to their sensitivity towards thermal changes and resulting geomorphological response. The indicative role of rockglaciers in these geosystems was emphasized only recently (e.g., Haeberli et al. 2006), but was up to now mainly restricted to temperature variations within the permafrost body as well as variations in active layer thickness. Within the last decade, an increasing number of studies monitored and quantified the creep behaviour of rockglaciers in the European Alps and observed increasing surface displacements since the 1990s (e.g., Schneider & Schneider 2001, Lambiel & Delaloye 2004, Kääb et al. 2007). In this context it is described, that the Alpine rockglaciers show a rather synchronous behaviour and respond sensitively to recent temperature increase (Roer et al. 2005, Kääb et al. 2007, Delaloye et al. 2008). There seems to be a strong indication that the observations are related to a warming of the shearzone within the individual rockglaciers (Arenson et al. 2002).

The presentation aims at the combined analysis of rockglacier kinematics and thermal characteristics in the Murtèl-Corvatsch region, one of the best equipped permafrost research sites.

REFERENCES

Arenson, L.U., Hoelzle, M. & Springman, S. 2002: Borehole deformation measurements and internal structure of some rock glaciers in Switzerland. Permafrost and Periglacial Processes 13: 117-135.

Delaloye, R., Perruchoud, E., Avian, M., Kaufmann, V., Bodin, X., Hausmann, H., Ikeda, A., Kääb, A., Kellerer-Pirklbauer, A., Krainer, K., Lambiel, C., Mihajlovic, D., Staub, B., Roer, I. & Thibert, E. 2008: Recent interannual variations of rock glacier creep in the European Alps. In: Kane, D.L. & K.M. Hinkel (eds.) Ninth International Conference on Permafrost (Fairbanks, Alaska) 1: 343-348.

Haeberli, W., Hallet, B., Arenson, L., Elconin, R., Humlum, O., Kääb, A., Kaufmann, V., Ladanyi, B., Matusoka, N., Springman, S. & Vonder Mühll, D. 2006: Permafrost creep and rock glacier dynamics. Permafrost and Periglacial Processes 17: 189-214.

Kääb, A., Frauenfelder, R. & Roer, I. 2007: On the response of rockglacier creep to surface temperature increase. Global and Planetary Change 56: 172-187.

Lambiel, C. & Delaloye, R. 2004: Contribution of real-time kinematic GPPS in the study of creeping mountain permafrost: examples from the Western Swiss Alps. Permafrost and Periglacial Processes 15: 229-241.

Roer, I., Avian, M., Delaloye, R., Lambiel, C., Bodin, X., Thibert, E., Kääb, A., Kaufmann, V., Damm, B. & Langer, M. 2005: Rockglacier „speed-up" throughout European Alps − a climatic signal? Proceedings of the Second European Conference on Permafrost, Potsdam, Germany, June 2005: 101-102.

Schneider, B. & Schneider, H. 2001: Zur 60jährigen Messreihe der kurzfristigen Geschwindigkeits-schwankungen am Blockgletscher im Äusseren Hochebenkar, Ötztaler Alpen, Tirol. Zeitschrift für Gletscherkunde und Glazialgeologie 37, 1: 1-33.

6.25

Electromagnetic Prospecting in Alpine Permafrost: Examples from the Southern Swiss Alps

Scapozza Cristian*, Gex Pierre**, Lambiel Christophe* & Reynard Emmanuel*

*Institut de Géographie, Université de Lausanne, Anthropole, CH-1015 Lausanne (Cristian.Scapozza@unil.ch)
**Institut de Géophysique de l'Université de Lausanne, Amphipôle, CH-1015 Lausanne

Within the framework of geomorphological and glaciological investigations of the Lateglacial and Holocene glacier/permafrost evolution in the Canton Ticino (Southern Swiss Alps), several geophysical methods (frequency-domain electromagnetic lateral mapping and 2D resistivity profiling, direct-current resistivity soundings, self-potential measurements and thermal prospecting) have been used for mapping the permafrost distribution at the local scale (Scapozza 2008; Scapozza et al. 2008). In this context, the application of electromagnetic geophysical methods in the prospecting of alpine permafrost is a recent and not well-developed approach (see, for example, Hauck 2001).

In this study, two frequency-domain electromagnetic methods were used: the field ground conductivity-meter Geonics EM-31 and the VLF-R (Very-Low Frequency Resistivity) resistivity-meter Geonics EM-16R. The Geonics EM-31 operates at a fixed frequency and allows to determine the spatial apparent conductivity and inphase variations in the survey area (McNeill 1980). The inphase is proportional to the magnetic susceptibility of the ground. The depth of investigation depends to the spacing between transmitter and receiver (3.66 m for the EM-31) and to the frequency (9.8 kHz). According to the polarisation of the instrument, the depth of investigations is around 6 m with the vertical dipoles (VD) and around 3 m with the horizontal dipoles (VH). The VLF-R technique uses electromagnetic energy radiated by a very low frequency (VLF) transmitter (Cagniard 1953). In this study the Rhauderfehn transmitter (23.4 kHz) located in Germany (near Bremen) was used. The measurement of the horizontal component of the electric field (E) and of the horizontal magnetic component (H) perpendicular to the azimuth of the transmitting station allows to know the apparent resistivity of the near surface. The ratio between H and E gives a phase angle that changes according to variations of resistivity with the depth. The combined inversion of apparent resistivity and phase angle data allows us to realize 2D VLF-R tomography with a two-layer resolution.

The measurement carried out on the Piancabella rockglacier (Blenio Valley) (Fig. 1A) show that permafrost occurrence is probable, with maximal resistivities at the front of the rockglacier and a decrease of the values toward upslope, as expected by geomorphological observations and other geophysical measurements (see Scapozza 2008). In particular, the electromagnetic prospecting allows us to know approximately the active layer depth and the permafrost resistivity, as shown in the VLF-R tomography (Fig. 1B). This example shows that electromagnetic prospecting in alpine permafrost offers good possibilities to map the spatial apparent resistivity (i.e. the permafrost distribution) (EM-31 and VLF-R) and/or to obtain information concerning the structure of the prospected terrains (VLF-R tomography).

REFERENCES

Cagniard, L. 1953: Basic theory of the magneto-telluric method of geophysical prospecting. Geophysics 18, 605-635.

Hauck, C. 2001: Geophysical methods for detecting permafrost in high mountains. Mitteilungen der VAW-ETH Zürich No. 171.

McNeill, J.D. 1980: Electromagnetic terrain conductivity measurements at Low Induction Numbers. Mississauga, Geonics Ltd., Technical Note TN-6.

Scapozza, C. 2008: Contribution à l'étude géomorphologique et géophysique des environnements périglaciaires des Alpes Tessinoises orientales. Lausanne, Institut de Géographie (MSc Thesis, published on February 28, 2008, on http://doc.rero.ch/).

Scapozza, C., Gex, P., Lambiel, C. & Reynard, E. 2008: Contribution of self-potential (SP) measurements in the study of alpine periglacial landforms: examples from the Southern Swiss Alps. Proceedings of the 9th International Conference on Permafrost, Fairbanks, AK, 29 June – 3 July 2008, 1583-1588.

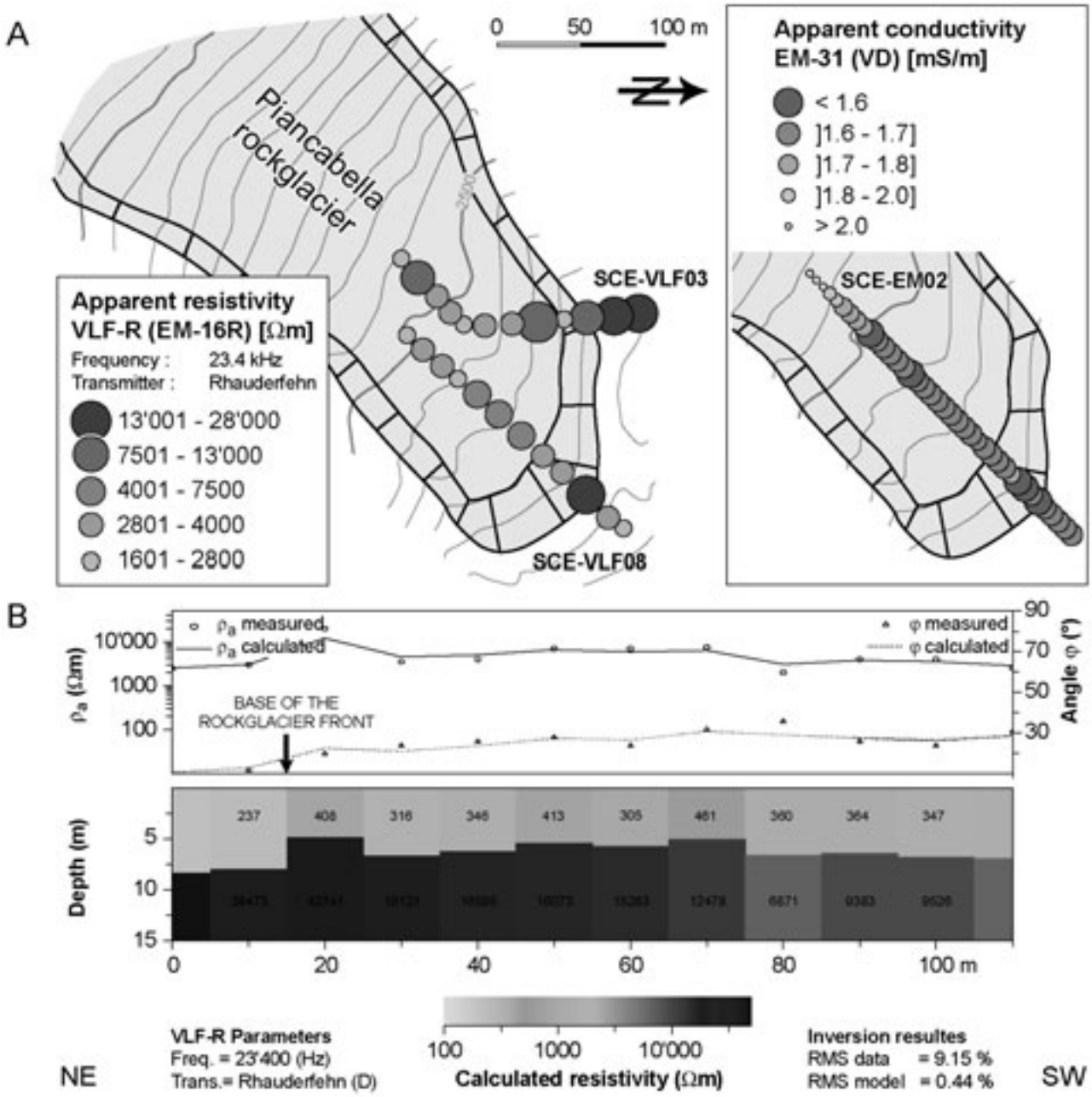

Figure 1. A: VLF-R (EM-16R) and EM-31 profiles along the Piancabella rockglacier. B: VLF-R tomography of the profile SCE-VLF08.

6.26

Permafrost Map of the Eastern Ticino Alps

Scapozza Cristian*, Mari Stefano**, Valenti Giorgio***, Strozzi Tazio****, Gex Pierre*****, Fontana Georgia*, Müller Guy*, Lambiel Christophe*, Delaloye Reynald** & Reynard Emmanuel*

*Institut de Géographie, Université de Lausanne, Anthropole, CH-1015 Lausanne (Cristian.Scapozza@unil.ch)
**Département des Géosciences, Géographie, Université de Fribourg, Chemin du Musée 4, CH-1700 Fribourg
***Sezione Forestale Cantonale, Viale Franscini 17, CH-6500 Bellinzona
****GAMMA Remote Sensing, Worbstrasse 225, CH-3073 Gümlingen
*****Institut de Géophysique, Université de Lausanne, Amphipôle, CH-1015 Lausanne

The permafrost distribution and characteristics in the Southern Swiss Alps are poorly known because of lack of research dedicated to this morphoclimatic context of the Alps during the last decades. In spite of the interest for the cryosphere reactions to climate warming, only few scientific studies were carried out until now in the periglacial belt of the Ticino Alps. Within the framework of geomorphological and geophysical investigations on the Lateglacial and Holocene glacier/permafrost evolution in the Southern Swiss Alps (see Scapozza & Reynard 2007; Scapozza 2008; Scapozza et al. 2008), a regional model based on an inventory of 75 rockglaciers was developed to simulate the permafrost distribution in the Eastern Alps of the Canton Ticino (Fig. 1). The model used is based on the assumption that the permafrost distribution at the regional scale depends mainly on altitude and orientation (topoclimatic parameters) and that the minimal altitude of active/inactive rockglaciers can be used as an indicator of the lower limit of discontinuous permafrost. The model was calibrated by thermal and geophysical prospecting, in order to asses the permafrost distribution at the local scale. Moreover, several sites were equipped for long-term studies. At the moment, in the Eastern Ticino Alps (Fig. 1), the followings studies are carried out:

- Geomorphological mapping and geophysical prospecting and monitoring in the Sceru Valley. The geophysical prospecting was carried out with frequency-domain electromagnetic lateral mapping and 2D resistivity profiling (Geonics EM-16R and EM-31), direct-current (DC) resistivity soundings, self-potential measurements, and thermal prospecting (miniature ground temperature data loggers and spring temperatures) (Scapozza 2008; Scapozza et al. 2008). On the Piancabella rockglacier and on the Gana Rossa talus slope, a ground- surface temperature and self-potential monitoring network was set up.
- Geomorphological mapping, direct-current (DC) resistivity soundings, ground-surface temperatures and real-time kinematic (RTK) GPS monitoring for studying the dynamics of creeping permafrost in the Northern side of the Cima di Gana Bianca, particularly on the Stabbio di Largario rockglacier (Valenti 2006; Müller, in prep.).
- ERS InSAR (space-borne synthetic aperture radar interferometry) signatures inventory to estimate both magnitude and spatial pattern of slope motion in the periglacial belt of the Ticino Alps, in particular in the Gothard region and in the Blenio Valley.

In the next years, the study and the equipment of others sites for permafrost research and monitoring is planned in the Val Bedretto region and in the Greina region. The goal is to better known the cryosphere reaction to recent climate warming in order to assess and quantify the processes related with permafrost degradation in high mountain environments.

REFERENCES

Müller, G. in prep.: La dégradation du pergélisol liée aux changements climatiques et les risques associés. Le cas du versant Nord de Cima di Gana Bianca (Val di Blenio, Tessin). Lausanne, Institut de Géographie (MSc Thesis).

Scapozza, C. 2008: Contribution à l'étude géomorphologique et géophysique des environnements périglaciaires des Alpes Tessinoises orientales. Lausanne, Institut de Géographie (MSc Thesis, published on February 28, 2008, on http://doc.rero.ch/).

Scapozza, C. & Reynard, E. 2007: Rock glaciers e limite inferiore del permafrost discontinuo tra la Cima di Gana Bianca e la Cima di Piancabella (Val Blenio, TI). Geologia Insubrica 10, 21-32.

Scapozza, C., Gex, P., Lambiel, C. & Reynard, E. 2008: Contribution of self-potential (SP) measurements in the study of alpine periglacial landforms: examples from the Southern Swiss Alps. Proceedings of the 9th International Conference on Permafrost, Fairbanks, AK, 29 June – 3 July 2008, 1583-1588.

Valenti, G. 2006: Il permafrost in Ticino. Dati, statistiche e società 6(2), 46-50.

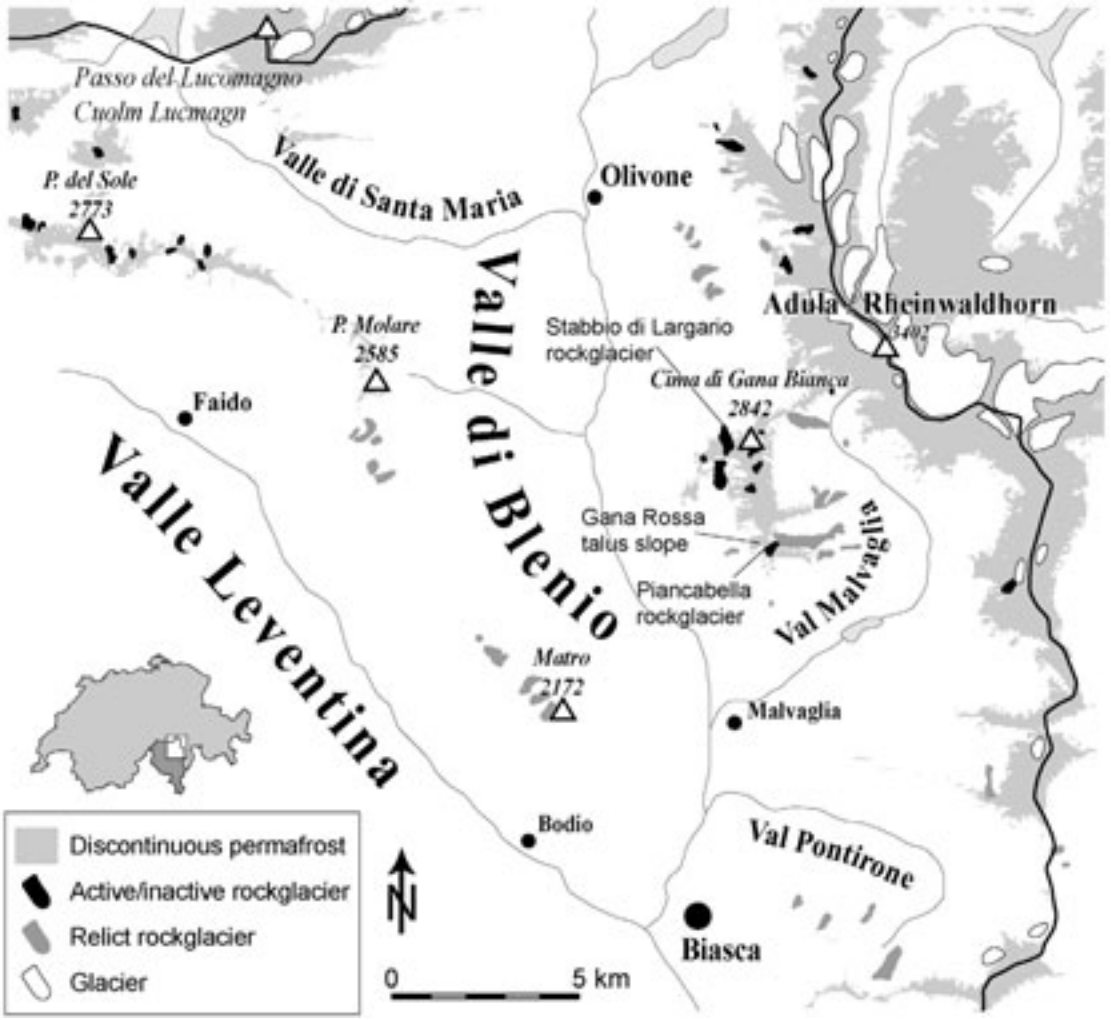

Figure 1. Permafrost and rockglaciers distribution in the Eastern Ticino Alps.

6.27

Conceptualising sediment cascades to enhance dynamic geomorphological mapping

Theler David*, Bardou Eric**, Reynard Emmanuel*

*Institut de Géographie, Université de Lausanne, Quartier Dorigny, CH-1015 Lausanne (david.theler@unil.ch)
**Bureau IDEALP Ingénieurs Sàrl, Rue de la Marjorie 8, CH-1950 Sion

Research focusing on geomorphological mapping often concerns the establishment of landforms inventories at large scales. The main disadvantage of the maps produced is their static character. In fact, available geomorphological legend systems are not always sufficient for mapping alpine environments with high geomorphological activity. A good example is illustrated by torrential systems where dynamic processes like channelised debris flows occur and where landforms associated to these processes may change very fast in time and space scales. Assessing sediment volumes that supply debris flow channels is one of the key parameters to mitigate disasters on places geomorphologically concerned by fluvial processes (Zimmermann et al. 1997). Data derived through GIS spatial analysis based on high accuracy digital elevation models (slopes, aspect, hydrographic network and delineation of subwatersheds) might be of high interest for mapping dynamic geomorphological processes as shown by an attempt done for Bruchi torrential system in the Swiss Alps (Theler et al. in press). This paper proposes to use GIS tools coupled with a qualitative conceptualisation of the system, what should open new opportunities for geomorphological mapping. An example is presented for a torrential system in the Swiss Alps.

The different parts of the system are conceptualised in order to depict the sediment transfers on a mountain flank (Fig. 1,

2). Sediment transfer starts from the hillslopes (1), where physical weathering followed by gravitational processes are predominant. The time of residence of sediments is very variable depending on the topographic setting and the intensity of processes and could be related to a complex stochastic function (e.g. Hegg, 1997). Sediments may have a second repository when they reach the active gully (2). Here, the time of residence depends on water runoff. It could be explained by less complex functions, because transfer is done only through two processes – debris flow or bed load transport. These two phenomena transfer sediments very actively and therefore do not store them for long (3). When they reach the fan (4) sediments transported by active geomorphic phenomena could either be stored (5) or transit directly to the effluent (6). Following these previous observations debris transfer are then replaced into the global erosion system. This could help to highlight with which part of the system volume assessment model are playing. The global scheme can be summarised by a tank cascade as depicted in Figure 2. The size of the tank is referred to the potential residence time of sediments (the difference in size on the graph must be seen in a logarithm perspective).

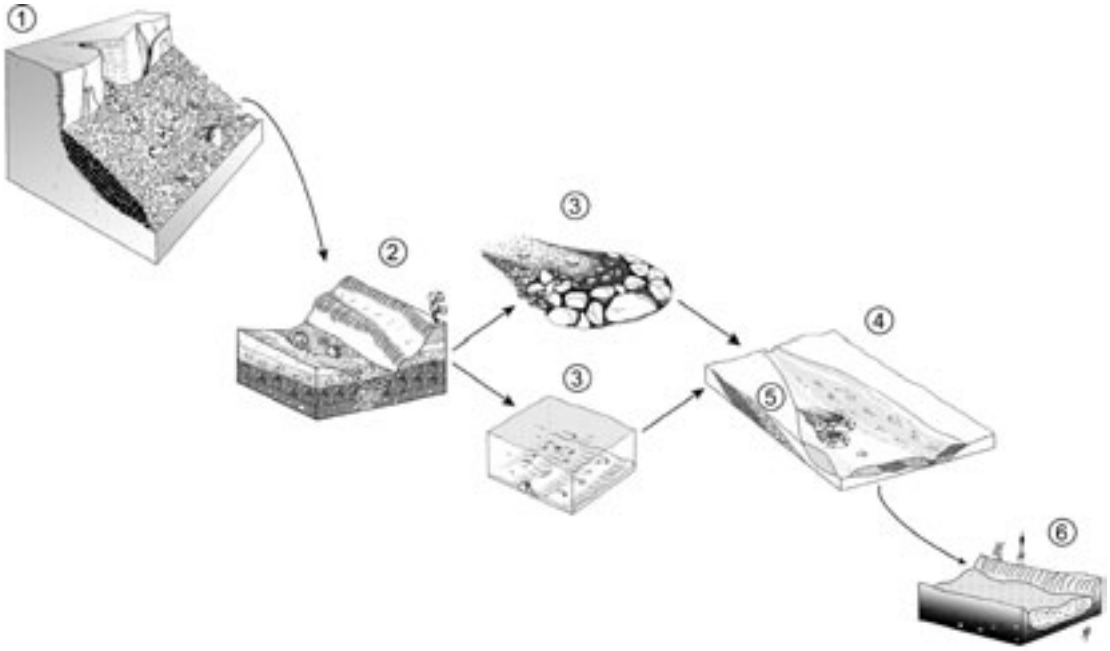

Figure 1. Place of debris flow and bed load transport into the erosive system.

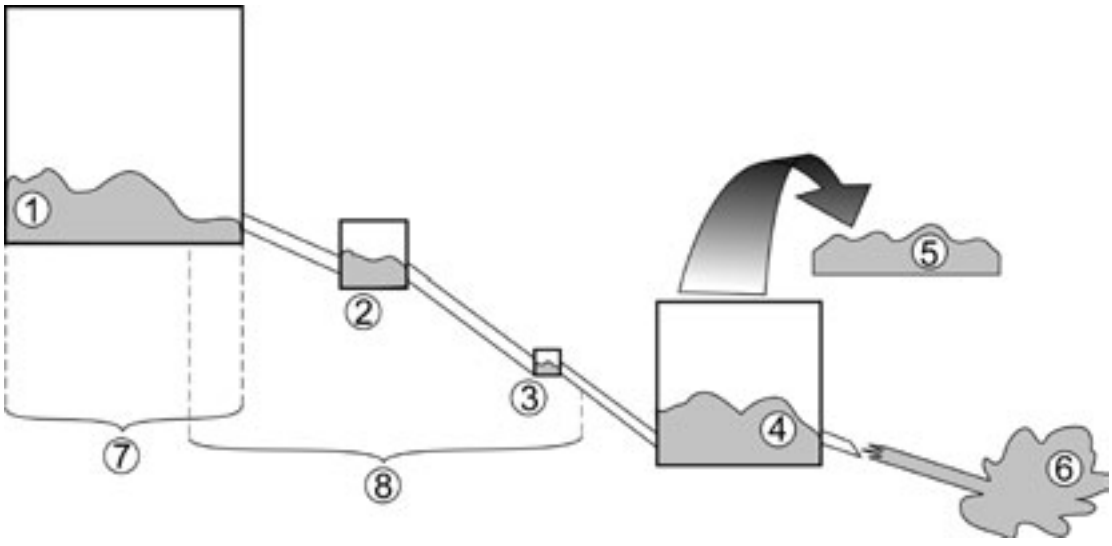

Figure 2. Tank cascade for sediment transfer and landscape elements where the different formula are applied.

REFERENCES

Theler, D. & Reynard, E. in press: Assessing sediment transfer dynamics from geomorphological maps: Bruchi torrential system, Swiss Alps. Journal of Maps 2008.

Hegg, C., 1997. Zur Erfassung und Modellierung von gefährlichen Prozessen in steilen Wildbacheinzugsgebieten, G 52. Geographisches Institut der Universität Bern, Bern.

Zimmermann, M., Mani, P. & Romang, H. 1997: Magnitude-frequency aspects of alpine debris flows. Eclogae geol. Helv., 90, 415–420.

6.28

Glacier volcano interactions and related hazards during the 2007 eruptive crisis at Nevado del Huila, Colombia

Worni Raphael*, Pulgarín Bernardo**, Agudelo Adriana**, Huggel Christian*

*Department of Geography, University of Zurich, Switzerland (raphael_worni@gmx.net)
**INGEOMINAS Popayán, Colombia

Nevado del Huila, a glacier-covered volcano in the South of Colombia's Cordillera Central, has not experienced any historical eruptions. In February and April 2007 the volcano erupted with two comparably small phreatic events. Each eruption was accompanied by the formation of large fissures in the Huila summit region of 2 km length and 50-80 m width with continued strong fumarolic activity after the eruptions. The eruptions produced lahars that travelled 150 km down the Paez River, with flow volumes of several million m^3 and ≈40 million m^3 for the February and April events, respectively. The water content of the April flow is estimated at ≈25 million m^3.

The eruption and glacier related dynamics were analyzed using air-borne photography, QuickBird and Aster satellite imagery. It was found that glaciers were not affected by the eruptions in a magnitude that would correspond to the amount of ice-melt generated water necessary to produce the observed lahar flow volumes. Instead, indications of flow paths suggested that most of the water that formed the lahars was expelled from the fissures, stemming from hydrothermal water reservoirs. Channels of a few meters depth incised in glacier ice provided evidence of water flow over the glaciers with temperatures likely exceeding 80°C. Sediment was deposited on the glaciers and further downstream. During the April eruption the lowermost part of the El Oso glacier failed, probably as an avalanche with about 0.5 million m^3 of ice. The mechanism that caused this glacier failure is not yet well understood but could be related to hot water released from the summit fissures that entered the base of the glacier and provoked a sudden reduction of shear strength at the glacier-bedrock interface.

The understanding of the volcano-ice interactions on Nevado del Huila and related formation of large lahars is important in view of the resulting severe hazards. The particularly large dimension of the lahars associated with the 2007 eruptions leave space for discussion as to the origin of such large amounts of water. A literature review suggested that drainage of similarly large hydrothermal water reservoirs during eruptive activity is very rare. More investigations are therefore needed to better constrain the relevant processes.
As to the future conditions at Nevado del Huila, it is most likely that glaciers will continue to respond to ongoing atmospheric warming. In the last 20 years glaciers were found to have shrunk by 30% to a current size of 10.7 km^2, with an estimated ice volume equivalent to 410 million m^3 of water. The current rate of retreat suggests glaciers could disappear completely in the second half of the 21st century, and hence still represent a major source of hazard when interacting with volcanic activity resulting large lahars.

6.29

Analyses of newly digitised snow series over the last 100 years+ in Switzerland

Wüthrich Christian*, Begert Michael*, Scherrer Simon C.*, Croci-Maspoli Mischa*, Appenzeller Christof*, Weingartner Rolf**

*Bundesamt für Meteorologie und Klimatologie MeteoSchweiz, Krähbühlstrasse 58, Postfach 514, CH-8044 Zürich, christian.wuethrich@meteoswiss.ch
**Geographisches Institut der Universität Bern, Gruppe für Hydrologie, Hallerstrasse 12, CH-3012 Bern

Snow is on the one hand an important commercial factor especially in the Swiss Alpine region (tourism, hydro-electricity, drinking water) and on the other hand responsible for considerable hazards like avalanches. In addition, snow is an excellent indicator to detect climate change. Hence, high-quality long-term snow series are crucial for reliable analyses.
In the presented study 12 Swiss snow series with daily measurements since at least 1910 (one dating back to 1864, cf. Fig. 1) and altitudes between 450 and 2500 m asl have been analysed. The objectives were twofold. First, suitable long-term snow series have been selected, missing data digitized and the entire series quality checked. Second, the long-term snow series

have been used for trend analyses over a time period >100 years. A snow depth reconstruction with the method of Brown and Braaten (1998) using daily new snow, temperature and precipitation as input variables performed well and made it possible to analyse days with snow pack (Fig. 2).
The results show that the snow cover is varying substantially on seasonal and decadal time scales, which is in line with Scherrer (2006). The analyses of the decadal new snow trends during the last 100 years shows unprecedented low new snow sums in the winter seasons (DJF) of the 1990s. The 100 year trend of days with snow pack reveals a significant decrease for stations below 800 m asl in the winter season (DJF) and for stations around 1800 m asl in the spring season (MAM). Similar results were found for seasonal new snow sums. Finally the results of the trend analyses are discussed with respect to the temperature trends.

REFERENCES

Brown, R.; Braaten, R.; 1998: Spatial and Temporal Variability of Canadian Monthly Snow Depths (1946-1995); Atmosphere Ocean 36 (1), 37-54.

Scherrer, S.C.; 2006: Interannual climate variability in the European and Alpine region; Veröffentlichung Nr. 67 der MeteoSchweiz, Zürich.

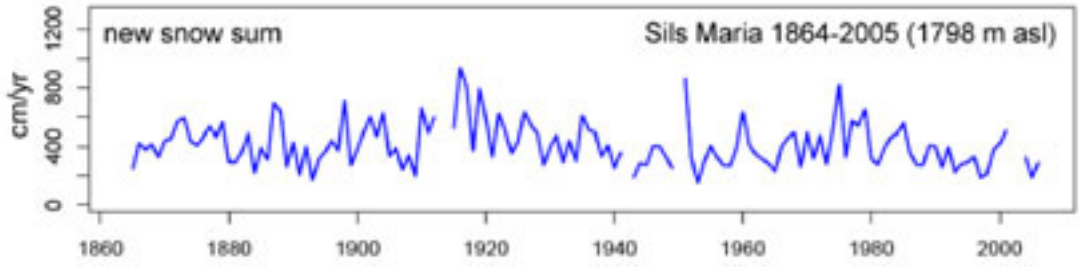

Figure 1. New snow sum series for Sils Maria (1798 m asl) 1864-2005

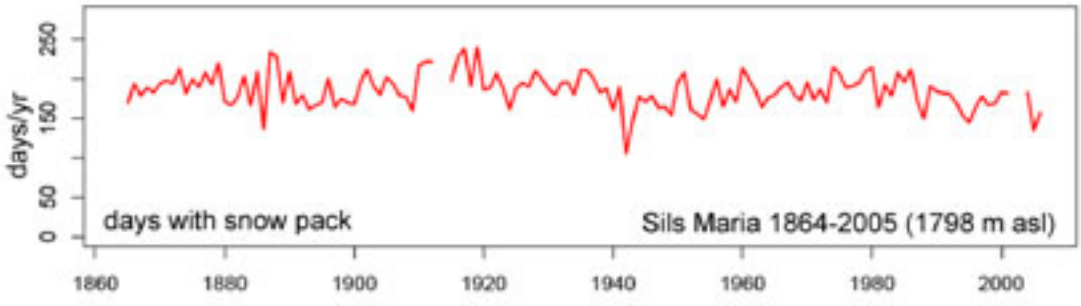

Figure 2. Days with snow pack based on reconstructed snow depth for Sils Maria (1798 m asl) 1864-2005.

6.30

Evidence of warming in disturbed and undisturbed permafrost terrain at Schafberg (Pontresina, Eastern Swiss Alps)

Zenklusen Mutter Evelyn*, Phillips Marcia*, Blanchet Juliette*

WSL, Institute for Snow and Avalanche Research SLF, CH-7260 Davos, Switzerland (zenklusen@slf.ch)

Both climate and human influences in the form of technical structures may alter ground temperatures in mountain permafrost soils (Phillips 2006). In 1996 several boreholes were drilled into the permafrost of the Muot da Barba Peider (Schafberg) ridge above Pontresina in the Eastern Swiss Alps. This study investigates and compares the ground temperatures measured in two of these boreholes, B1 and B2.

The boreholes are located 50m apart at 2960m asl in a NW oriented steep scree slope and are instrumented with 10 thermistors between 0.5m and 17.5m depth. Both locations are very similar from a climatological and geological point of view. The

main difference between the two boreholes is that borehole B1 is located between snow-retaining avalanche defense structures whereas B2 is in the undisturbed scree slope. As a consequence, the snow cover persists longer at B1 than at B2 in early summer, thus modifying ground temperatures there.

11 complete years (1997-2007) of daily borehole temperature measurements at Schafberg (Fig.1) and data delivered by a nearby meteorological station offer a first view of possible influences of climate change and technical structures on permafrost ground temperatures.

For both boreholes, temporal trend analyses show significant warming for annual minimum, mean and median temperatures at depths below 10m and for annual maximum temperatures in all depths. The magnitude of these trends are all similar and at both borehole locations approximately 0.02 – 0.03°C per year, which is less than those registered for example during the same period in Scandinavian mountain permafrost (Isaksen et al. 2007), reflecting the influence of the ridge topography, highly variable snow cover and the presence of coarse blocks at the ground surface at our study site.

Analyses of the maximum annual active layer depth (defined as being the maximum annual penetration of the 0°C isotherm, (Burn 1998)) reveal that the active layer in B2 (around 2m) is almost twice as thick as in B1, due to small local differences in stratigraphy, hydrology and solar radiation (Rist and Phillips 2005). During the 11-year measurement period, the active layer depths in both boreholes have remained quite constant with a temporary deepening during the extremely hot summer 2003. Concerning the annual duration of the active layer, significant positive trends were found for both boreholes. Although the annual duration of the active layer at B2 is about 50% longer than at B1, the increase of the annual active layer duration at B2 (5 days per year) is lower than at B1 (6 days per year).

The comparison of the temporal occurrence of annual maximum/minimum temperature in different depths gives an insight into how fast the ground reacts to seasonal warming/cooling. Cooling in winter occurs similarly at both borehole locations and near-surface warming in summer is delayed due to the presence of the insulating scree cover. Summer warming can additionally be delayed by 1 to 2 months due to the longer lasting snow cover at B1 compared to B2 (e.g. years 1999 to 2001).

In summary, similar warming trends over the period 1997-2007 are visible in both boreholes, indicating the registration of a common warming influence at depth, despite the cooling effect of avalanche defence structures at B1 in summer through the delay of snow melt at the end of snow-rich winters.

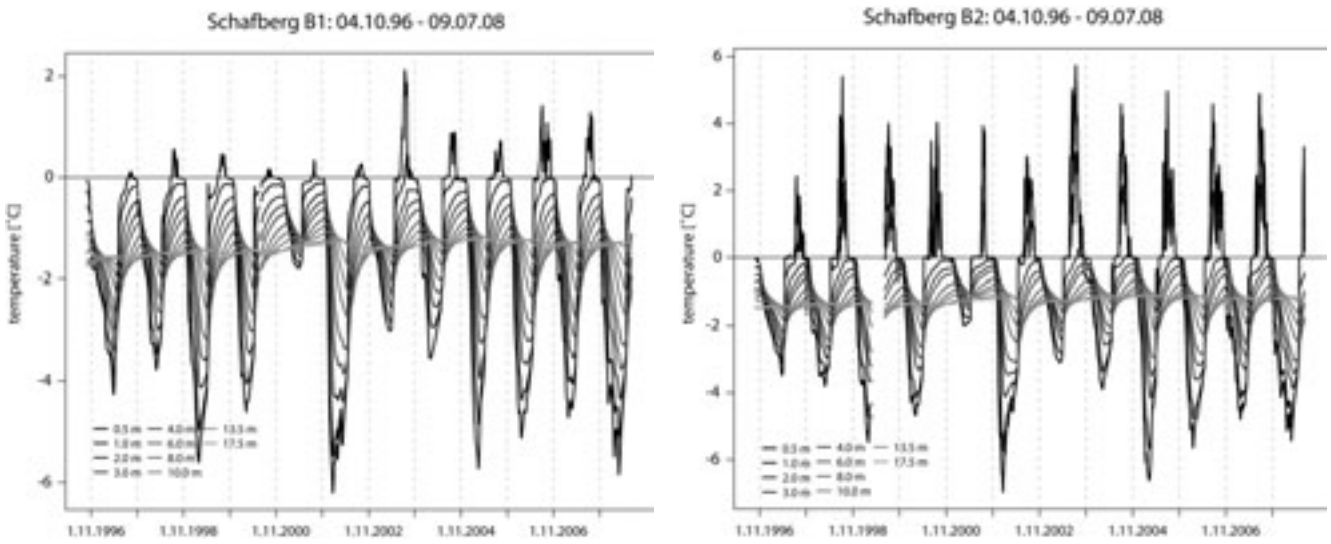

Fig. 1: Ground temperature series in the Schafberg boreholes B1 (left) and B2 (right), 1996-2008

REFERENCES

Burn, C.R. 1998. The active layer: two contrasting definitions. Permafrost and Periglacial Processes, 9: 411-416.

Isaksen, K., Sollid, J.L., Holmlund, P., and Harris, C. 2007. Recent warming of mountain permafrost in Svalbard and Scandinavia. Journal of Geophysical Research, 112(F02S04, doi: 10.1029/2006JF000522).

Phillips, M. 2006. Avalanche defence strategies and monitoring of two sites in mountain permafrost terrain, Pontresina, Eastern Swiss Alps. Natural Hazards, 39: 353-379.

Rist, A., and Phillips, M. 2005. First results of investigations on hydrothermal processes within the active layer above alpine permafrost in steep terrain. Norsk geogr. Tidsskr., 59: 177-183.

7. Geofluids and related mineralization: from shallow to deep

Robert Moritz, Thomas Wagner

Swiss Society for Mineralogy and Petrology (SSMP)

7.1

Low temperature fluid phase relations of granitic solutions and implications for crustal mass transport.

Maarten Aerts*, Alistair C. Hack, Peter Ulmer and Alan B. Thompson

Institute for Mineralogy and Petrology, Clausiusstrasse 25, CH-8092 Zürich, Switzerland (maarten.aerts@erdw.ethz.ch)*

Aqueous fluids transport and precipitate dissolved silicate components in natural hydrothermal processes throughout the earth's crust. To understand the solubility of significant mineral assemblages over large ranges of P-T, we have employed the diamond-trap technique to investigate aqueous fluids in equilibrium with K-feldspar, muscovite and quartz (KMQ) from 0.5-2.5 GPa and 600-700 °C. Fluids were found to be highly peralkaline (K_2O/Al_2O_3 up to 9, by weight) despite relatively high concentrations of dissolved aluminum (>0.04 mAl at 1 GPa, 700°C) in these fluids, compared to corundum ± kyanite solubility in the absence of alkalis [1].
Over the P-conditions investigated, measured fluid compositions have K:Si=1:3, which is higher than HKF* aqueous speciation calculations predict (extrapolated to the investigated PT-conditions, following [2]).
Our KMQ solubility data indicate K-Si species are significantly more abundant than aluminous 'feldspar-like' complexes [3]. Further experiments, involving synthesis of quartz-hosted fluid inclusions, were conducted to investigate fluid/melt immiscibility and bracket the wet melting reaction quartz + muscovite + K-feldspar + V = L. Inclusion petrography and microthermometry indicate that the occurrence of (supercritical) melt-fluid miscibility in simplified granitic systems is sensitive to the compositional evolution of the fluid and might actually be encountered upon cooling (and not heating) of the system.
Our experimental results reveal retrograde solubility patterns governing the evolution of residual granitic solutions that may be linked to the possible occurrence of continuous solubility between fluid and melt in peralkaline granitic systems, as Bowen postulated 80 years ago [4]. Moreover, the results indicate paths leading to enhanced mass mobilization in natural fluids at low-temperatures.

REFERENCES:
[1] Manning (2007) Geofluids 7, 258-269.
[2] Manning (1998) Schweiz. Mineral. Petrogr. Mitt. 78, 225-242.
[3] Anderson and Burnham (1983) Am. J. Sci. 283A, 283-297.
[4] Tuttle and Bowen (1958) Geol. Soc. Am. Memoir 74.

7.2

Mineralogy and Fluid inclusions investigations of carbonate hosted Pb-Zn-Ba-(Cu) deposits in Jebel Ajered, Central Tunisia.

Jaloul Bejaoui*, Salah Bouhlel *, Esteve Cardellach**, Angels Pique*** & Àngels Canals***.

**Laboratoire de Minéralogie et Géochimie, Département de Géologie, Faculté des Sciences de Tunis, Université de Tunis El Manar, 2092 Tunis. (bjaoui_geo@yahoo.fr)*
*** Departament de Geologia, Universitat Autònoma de Barcelona, Spain.*
****Dept. de Cristallografia, Mineralogía i Dipòsits Minerals, Universitat de Barcelona, Spain.*

Carbonate-hosted Pb-Zn-Ba-(Cu) epigenetic deposits in Jebel Ajered, is located in the Central Tunisia (300Km from Tunis). The deposits are hosted by Upper Aptian carbonate Unconformity. The potential reserve estimated of 1.2Mt grading 8% Zn, 4% Pb and 2% Ba.
This study presents the results of a geological, mineralogical, and geochemical investigation of the carbonate-hosted Pb-Zn deposits.
This mineralization is hosted by hydraulic breccias related to extensive dolomitized and silicified limestone, collapse cavities and karsts generated with dissolution of host rock (Fig. 1-A, 1-C, 1-F and 1-D). These mineralizations have different shapes ranging from mineralized breccias to stratabound and concordant with host rocks and fault-related. (Bouhlel et al., 1988 and Bejaoui et al., 2006 and 2007)

The metalliferous mineral association is formed by galena, sphalerite, pyrite, chalcopyrite, goethite and covellite. Minerals non-metalliferous are; dolomite, quartz and Barite.

In this study we measured inclusions in sphalerite and in quartz from Jebel Ajered. Two-phase inclusions were observed in studied minerals. They consist of vapor and aqueous solution of NaCl with small amount of $MgCl_2$ and $CaCl_2$ (Fig. 1).

Inclusions in sphalerite consist of vapor and aqueous solution of NaCl with small amount of $MgCl_2$ and $CaCl_2$. They are located in growth surface and their size is less than 100μm. Melting temperature of ice (Tmi) varies from -11°C to -14.5°C. Homogenization temperature (Th) varies from 125°C to 140°C. Calculated salinity varies from 15 to 18 wt. % NaCl equiv. and densities vary between 1, 07 g/cm^3 and 1, 12 g/cm^3.

Homogenization temperature in quartz1 (Fig. 1-B and 1-D), gangue of sphalerite varies from 128°C and 147°C. Salinity range from 15 to 19 wt.% NaCl. Fluid inclusions in quartz cogenitic with barite consist of vapour and aqueous solution of NaCl with small amount of $MgCl_2$ and $CaCl_2$. Eutectic temperature (Te) varies from -40°C to -22°C. Their size is less than 80μm. Tmi varies from -19°C to -15°C (Fig. 2). Inclusions were homogenized on liquid in temperature from 155°C to 171°C. Salinity varies from 18 to 21wt. % NaCl equiv. We can observe decreasing salinity with the gradual decreasing temperature (Th) from quartz cogenetic with barite to sphalerite. These features of mineralogical and fluid inclusions study suggest a possible contribution of basinal brines mineralizing fluids in ore formation. The Ajered stratabound ore deposits are similar to Mississippi valley type deposits. Isotopic and trace elements are in progress.

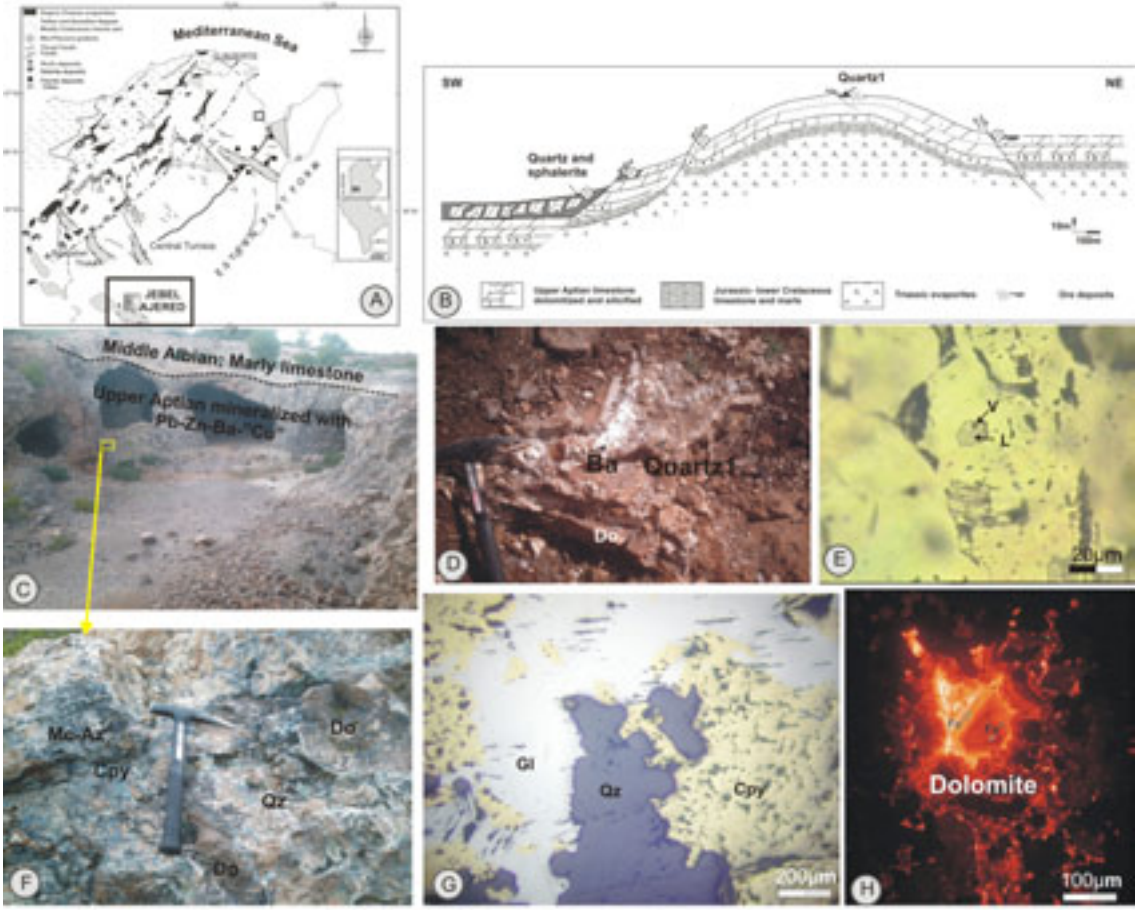

Fig. 1. A: Localization of study area in Tunisian structural map, B: distribution of ore bodies in cross section, C: Ajered old mine where ore deposits are located, D: Geodic quartz collapsed with barite. E: primary aqueous fluid inclusions in sphaleite, F: Hydraulic breccias mineralized with chalcopyrite and galena, G: coarse-grained quartz associated with chalcopyrite and galena, H: Cathodoluminescence photomicrograph of dolomite, in contrast to the dolomite crystals, this cement shows a bright orange color with well developed zoning with different iron content. (Do;dolomite, Ba: Barite, Cpy: Chalcopyrite, Qz: Quartz, Mc-Az: Malachite and azurite , Gl: Galena, V:Vapor, L: Liquid).

REFERENCES

Bejaoui, J. & Bouhlel S. 2007: Carbonate-hosted Mississipi Valley Type Zn-Pb-Ba Deposits in Upper Aptian of Jebel El Hamra, Central Tunisia. Oral presentation in Swis Geoscience Meeting (SGM) 2007, 21-22

Bejaoui. J. et Bouhlel S. 2006: Les inclusions fluides comme indicateur du type de gisement: Cas des minerais de Pb-Zn-Ba du Jebel El Hamra, Tunisie centrale. Communication Sem. Internationale ; Géosciences au Service du développement durable. Tébessa, Algérie, 166-170.

Bouhlel S., Fortuné J. P., Guilhaumou N. et Touray J.C. 1988 : Les minéralisations stratiformes à F-Ba de Hammam Zriba Jebel Guebli (Tunisie nord-orientale) : l'apport des études d'inclusions fluides à la modélisation génétiques. Miner. Deposita, 23, 166-173.

7.3

Miocene magmatism and related porphyry and polymetallic mineralization in the Morococha district, central Peru

Bendezú Aldo*, Catchpole Honza*, Kouzmanov Kalin*, Fontboté Lluís*, Alexey Ulianov** & Astorga Carlos***

*University of Geneva, Department of Mineralogy, Rue des Maraîchers 13, 1205 Genève
**University of Lausanne, Institute of Mineralogy and Geochemistry, Lausanne
***Pan American Silver Corp, Lima, Peru

The Morococha mining district in central Peru displays a complex magmatic and hydrothermal history where several intrusive events and spatially associated mineralization and alteration styles are recognized. At least nine main intrusions form several magmatic clusters and four ore body types: porphyry mineralization, massive pyrite-quartz bodies, polymetallic replacement bodies, and polymetallic veins crossing the entire district, have been distinguished. Porphyry mineralization and alteration are restricted to the vicinity of certain intrusions, whereas replacement bodies and polymetallic veins do not seem to show any spatial relationship to a particular intrusion. The geology of the district consists of Permian continental volcanic rocks and red beds, Triassic-Jurassic sedimentary carbonate, volcanic rocks and basalts, Late Cretaceous silicoclastic and carbonate rocks, cut by several Miocene intrusions. The oldest intrusion (14.1 Ma; Kouzmanov et al., 2008) covers a large area in the western part of the district. The mineralization, however, is related to the emplacement of younger Miocene intrusions (7-9 Ma; Beuchat, 2003, Kouzmanov et al., 2008). The polymetallic mineralization postdates both intrusive events.

Porphyry style alteration and mineralization was recognized in three areas: (1) the Toromocho porphyry Cu-Mo deposit in the central part of the district; (2) the Codiciada Cu-Mo porphyry in the north-eastern part, and (3) the Ticlio Cu-Au porphyry in the westernmost area. Only the latter two are included in this study. Other mineralization styles, partly in the epithermal range, in the Morococha district include (a) endo- and exoskarns; (b) pyrite-quartz bodies; (c) replacement polymetallic bodies, and (d) polymetallic veins.

The *Codiciada Cu-Mo porphyry system* comprises an igneous suite of microdiorite, porphyritic microdiorite, quartz-feldspar porphyry, and amphibole-biotite porphyry intrusions. The petrochemical analyses of intrusions in the Codiciada area display negative Nb, Ta, and Ti anomalies indicating a magmatic arc setting. Chondrite-normalized REE patterns show weak negative Eu anomalies suggesting minor plagioclase fractionation, probably at shallow crustal levels. Strong LREE fractionation (high Ce/Yb ratios) and associated intra-HREE fractionation (e.g. Dy/Yb) suggest a combination of hornblende and garnet fractionation in the magma source. The rocks consistently display Sr contents >600-700 ppm and Y contents <18 ppm allowing their classification as adakite-like (Richards and Kerrich, 2007). This is consistent with initial evolution of the magma at the base of a thickened continental crust. The alteration styles in this system consist of pervasive Na-Ca, selective pervasive potassic and phyllic alterations, as well as silicification. Porphyry style veinlets are quartz-pyrite-chalcopyrite±pyrrhotite, quartz-molybdenite and quartz-pyrite-sericite in composition. Molybdenite, chalcopyrite and pyrite, occur in much lower quantities, disseminated in the altered rock.

The *Ticlio Cu-Au porphyry* is a single granodiorite intrusion showing a pronounced zonation pattern with respect to mineralization and alteration. Its central part is characterized by the occurrence of high-density quartz-magnetite±K-feldspar stockwork. The zone rimming the core shows strong K-feldspar alteration with low-density magnetite and quartz-magnetite veining. This zone hosts small amounts of chalcopyrite and bornite as disseminations and in veinlets. Native Au is observed as small inclusions in chalcopyrite. The peripheral parts of the system show weak biotite, K-feldspar and actinolite alteration, as well as weak chalcopyrite and pyrite mineralization. The most distal part of the porphyry system is characterized by weak propylitic alteration.

In the Morococha district steeply dipping (N 110° E to N 150° E) porphyry quartz-molybdenite and quartz veinlets have been observed at several locations. This suggests a possible structural relationship with the emplacement of quartz-feldspar porphyry dykes with the same trend found in the Codiciada area. The late porphyry-stage pyrite-quartz-sericite veinlets cut the quartz-molybdenite veins. These veinlets show, a not well defined N 70° E orientation and dip from 80° to 90° NW-SE.

The epithermal polymetallic veins in the district are fault-controlled and belong to two main systems: (a) normal dextral or sinistral faults striking N60-80, and (b) normal dextral faults striking N20-30. Field evidence suggests that the N60-80 system predates the N20-30 one. Both systems are enriched in base-metals, whereas the N60-80 has higher contents in quartz and pyrite. Polymetallic mineral association can be found as well in some re-opened N 70° E trending pyrite-quartz-sericite porphyry veinlets.

Both, the Ticlio (Cu-Au) and the Codiciada (Cu-Mo) porphyry systems in the Morococha district are genetically related to Late-Miocene subvolcanic intrusions with similar petrochemical characteristics; however they show different alteration and

mineralization styles, suggesting different depth of emplacement and/or different P-T-X conditions of ore-formation. The Ticlio porphyry is most probably more deeply eroded than the Codiciada system. Both porphyries are crosscut by the lately formed polymetallic veins.

REFERENCES

Beuchat, S. 2003. Geochronological, structural, isotope and fluid inclusions constrains of the polymetallic Domo de Yauli district, Peru. Terre & Environnement, University of Geneva, vol. 41, 130 p.

Kouzmanov, K., Ovtcharova, M., von Quadt, A., Guillong, M., Spikings, R., Schaltegger, U., Fontboté, L. & Rivera, L. 2008. U-Pb and $^{40}Ar/^{39}Ar$ constraints for the timing of magmatism and mineralization in the giant Toromocho porphyry Cu-Mo deposit, central Peru. XIV Congreso Peruano de Geologia.

Richards, J.P. & Kerrich, R. 2007. Special paper: Adakite-like rocks: their diverse origins and questionable role in metallogenesis. Economic Geology, vol. 102 (4), 537-576.

7.4

Paragenesis and preliminary fluid inclusion data of porphyry-related base metal mineralisation styles in the Miocene Morococha district, central Peru

Catchpole Honza*, Bendezú Aldo*, Kouzmanov Kalin*, Fontboté Lluís* & Edgar Román**

*Département de Minéralogie, Rue des Maraîchers 13, CH-1205 Genève (Honza.Catchpole@terre.unige.ch)
** Pan American Silver Corp., Lima, Peru

The Morococha district, located in the western Cordillera of the Central Peruvian Andes, is characterised by barren and Cu-Mo porphyry bodies of Miocene age, ranging from 14.1 – 7.7 My (Beuchat, 2003; Kouzmanov et al., 2008), intruded into volcanic and sedimentary rocks. Good outcrop conditions and superimposing of different hydrothermal mineralisation styles make Morococha an ideal location for the study of a porphyry-related hydrothermal mineralisation system. In Morococha, mineralisation processes from porphyry-dominated (Bendezú et al., 2008) to near-surface epithermal environment can be studied in detail (Fig. 1).

Following main mineralisation styles post-date porphyry ore formation in the Morococha district: (a) massive magnetite–serpentine exoskarns and diopside-garnet endoskarns, partly hydrated to epidote, amphibole and chlorite, often bearing polymetallic mineralisation; these are found where mainly Jurassic dolomitic carbonates of the Pucará Group are in contact with porphyry intrusions; (b) massive pyrite-quartz bodies with phyllic alteration halos found in the fringe areas of certain intrusives and/or as replacement of previously formed breccia zones such as in the base of the Pucará Group just overlying Permian volcanics; (c) polymetallic manto-type bodies occurring mainly as a replacement of tectonic and dissolution breccias within the Pucará Group, overthrust-related breccias, and skarnified beds of particular horizons of limestones within the lower units of the Pucará Group. In composition, the replacement bodies range from magnetite, chalcopyrite, sphalerite, and galena-bearing pyrrhotite- and pyrite-dominated bodies to quartz-carbonate-sulphosalts bodies; (d) steeply dipping epithermal Zn-Pb-Ag-Cu-bearing veins with phyllic alteration halos hosted by NNE to ENE trending fractures and cutting the previous ore styles. Zn-Pb-Ag-Cu-bearing veins cross-cut at district scale/district-wide the intrusive bodies, the surrounding sediments, as well as the skarn and pyrite-quartz bodies. They are well distinguished into two stages within the vein. A (i) quartz-pyrite-rich stage with arsenopyrite, Fe-rich sphalerite and pyrite with inclusions of pyrrhotite, galena, chalcopyrite, and minor amounts of Bi-Ag-sulphosalts, stannite, scheelite, and bismuthinite, is followed by a base metal stage (ii), rich in Cu-sulphosalts, sphalerite, galena and Mn-carbonates, including economically important Ag-bearing minerals of the fahlore group. The Mn-rich carbonate zones have abundant quartz and rhodochrosite, and in minor quantities rhodonite, pyrite, fahlore and alabandite with inclusions of native Te and Ag-tellurides. Copper values in the polymetallic veins increase from Zn-Pb-rich veins in external parts of the district towards the central parts of the district, as the importance of sphalerite, galena and Mn-bearing minerals decreases, while that of chalcopyrite, tennantite, enargite, and Cu-Sn-bearing sulphides increases, indicating a higher sulphidation-state in the central part of the Morococha district.

First fluid inclusions data from quartz crystals of the pyrite-quartz stage from a polymetallic vein cutting the Potosí Miocene microdiorite show intermediate salinities of up to 13 wt% eq. NaCl and homogenisation temperatures of up to 380°C. A maximum hydrostatic pressure of 210 bar for the earliest precipitation of the crystals has been calculated. These results are consistent with magmatic ore-forming fluids at mesothermal to epithermal conditions. Towards younger growth zones of the quartz crystals, salinities and homogenisation temperatures decrease down to about 1 wt% eq. NaCl and 265°C, respectively, a trend ascribed to increasing influence of mixing with meteoric fluids.

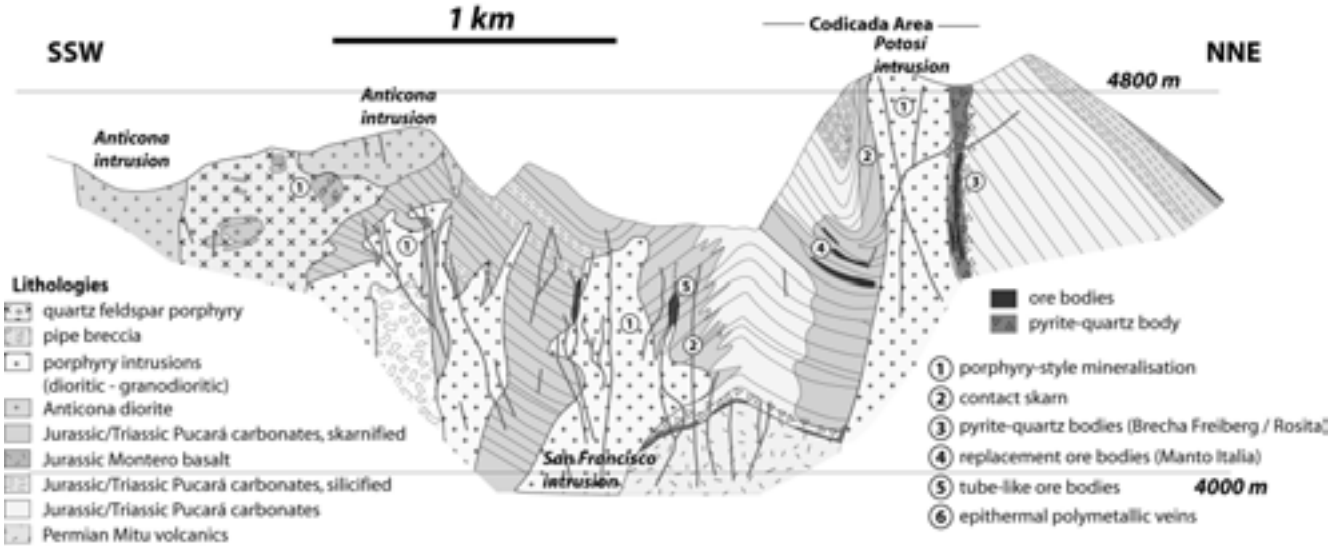

Figure 1: Schematic cross-section through the Morococha district including lithologies and mineralisation styles (vertically exaggerated, southern section modified after León, 2006 based on geological maps from the Cerro de Pasco Copper Corporation; northern section modified after geological maps from Pan American Silver Corp.).

REFERENCES

Kouzmanov, K., M. Ovtcharova, A. von Quadt, M. Guillong, R. Spikings, U. Schaltegger, L. Fontboté, and L. Rivera, 2008, U-Pb and $^{40}Ar/^{39}Ar$ age constraints for the timing of magmatism and mineralization in the giant Toromocho porphyry Cu-Mo deposit, Central Peru: XIII Congreso Latinoamericano de Geología.

Beuchat, S., 2003, Geochronological, structural, isotopes and fluid inclusion contraints of the polymetallic Domo de Yauli District, Peru: Terre & Environnement, v. 41, p. 130.

Bendezú, A., H. Catchpole, K. Kouzmanov, L. Fontboté, and C. Astorga, 2008, Miocene magmatism and related porphyry and polymetallic mineralization in the Morococha district, Central Peru: XIII Congreso Latinoamericano de Geología.

León, J., 2006, Relación espacial y temporal entre el sistema pórfido-skarn Toromocho y la sobreimpresión de las posteriores vetas cordilleranas de metales base, Universidad Nacional de Ingeniería, Lima, Peru, 158 p.

7.5

Formation of sphalerite mineralisations and cadmium enrichments in the Hauptrogenstein formation (Upper Bajocian) of Jura Mountains (Switzerland): geological, geochemical and isotopic (O, C, S) evidence

Natalia Efimenko*, Jorge E. Spangenberg**, Virginie Matera***, Thierry Adatte*, & Karl B. Föllmi*

*Institut de Géologie et Paléontologie, Université de Lausanne, Anthropole, CH-1015 Lausanne, Switzerland
** Institut de Minéralogie et Géochimie, Université de Lausanne, Building Anthropole, CH-1015 Lausanne, Switzerland
***Institut de géologie et d'hydrogéologie, Université de Neuchâtel, Rue Emile-Argand 11, CH-2007 Neuchâtel, Switzerland

Disseminated sphalerite (ZnS) mineralisations occur in carbonates of Triassic and Jurassic ages in the Jura Mountains (Holenweg, 1967; Hofmann, 1989 and 1993). The cadmium content in sphalerite crystals reaches values of 6000 mg/kg (Graeser, 1971). Cadmium concentrations of up to 21.4 mg/kg was also observed in carbonates of Bajocian and Oxfordian ages (Prudente, 1999; Benitez-Vasquez, 1999; Veuve, 2000; Dubois et al., 2002; Rambeau, 2006), which exceed the mean marine carbonate value of 0.03 mg/kg (Gong et al., 1977; Tuchschmid, 1995). These elevated cadmium contents in the rock substratum lead to cadmium enrichments in the corresponding soils of up to 16 mg/kg, which largely exceed the Swiss official tolerance guideline values for non-polluted soils fixed at 0.8 mg/kg.

In order to develop a predictive tool to identify Cd-enriched soils related to Jurassic rock substrata we need to reconstruct the pathways along which Cd was transfered and concentrated inside the carbonate rock and construct the model of Cd incorporation. Previous research (Veuve, 2000; Rambeau, 2006) established a model of synsedimentary and early diagenetic enrichment in Cd of shallow-water carbonate rocks in Jura mountains with organic matter as a vector of Cd transport.

We propose a model of formation of Cd-bearing sphalerite mineralisations and cadmium incorporation into the Jurassic

rocks during periods of tectonic and hydrothermal activity in the region. Basement rocks are inferred to be the source of zinc and cadmium, amongst other elements, and fluid flow controlled by the permeability of the different formations of Jurassic carbonates the principal vector of Cd transfer.

To test our model we study the samples of shallow-marine oolitic carbonates of Bajocian age (Hauptrogenstein formation) including sphalerite crystals sampled by H. Holenweg in Auenstein (AG, Jura Mountains). Optical thin-section microscopy, XRD and ICP-MS and sulphur, carbon and oxygen isotope geochemistry analyses are presently performed on these samples to clarify the conditions of sphalerite mineralisation and Cd distribution inside the rock.

REFERENCES

Benitez-Vasquez N. 1999: Cadmium speciation and phyto-availability in soils of the Swiss Jura: hypothesis about its dynamics. PhD thesis n° 2066, EPFL, Lausanne, 132 p.

Dubois J.P., Benitez N., Liebig T., Baudraz M., Okopnik F. 2002 : Le cadmium dans les sols du haut Jura suisse. In : Les éléments traces métalliques dans les sols. Approches fonctionnelles et spatiales (D. Baize et M. Tercé, eds) INRA Editions, Paris, 33-52.

Gong H., Rose A.W., Suhr N.H. 1977: The geochemistry of cadmium in some sedimentary rocks. Geochimica et Cosmochimica Acta, 41, 1687-1692.

Graeser S. 1971: Mineralogisch-geochemische Untersuchungen an Bleiglanz und Zinkblende. Schweiz. Mineralogische und Petrographische Mitteilungen, 51, 414-442.

Holenweg H. 1967: Mineralparagenesen im Schweizer Jura. Tätigkeitsberichten der Naturforschenden Gesellschaft Baselland, 25, 303-308.

Hofmann B. 1989: Erzmineralien in paläozoischen, mesozoischen und tertären Sedimenten der Nordschweiz und Südwestdeutschlands. Schweiz. Mineralogische und Petrographische Mitteilungen, 69, 345-357.

Hofmann B. 1993: Formation of stratiform sulfide mineralisations in the Lower Muschelkalk (Middle Triassic) of Southwestern Germany and Northern Switzerland: constraints from sulfur isotope data. Schweiz. Mineralogische und Petrographische Mitteilungen, 73, 365-374.

Prudente D. 1999 : Distribution des teneurs naturelles en cadmium dans les sols de la forêt communale des Fourgs (Doubs – Fr.). PhD thesis EPFL, Lausanne, 68 p. (inédit).

Rambeau C. 2006: Cadmium anomalies in jurassic carbonates (Bajocian, Oxfordian) in western and southern Europe. PhD thesis, University of Neuchâtel, 179 p. (unpubl.).

Tuchschmid M. 1995: Quantifizierung und Regionalisierung von Schwermetallen und Fluorgehalten bodenbildender Gesteine der Schweiz. Umwelt-Materialen, 32, BUWAL, Berne.

Veuve P. 2000 : Etude géochimique et sédimentaire d'un enrichissement en cadmium observé dans les calcaires oolithiques jurassiques du Jura. Diploma thesis, University of Neuchâtel, 56 p. (unpubl.).

7.6

Phosphorites-Hosted Zinc and Lead in the Sekarna Ore Deposit (Central Tunisia)

Hechmi Garnit* & Salah Bouhlel*.

**Department of Geology, Applied Mineralogy and Geochemistry Unit, Faculté des Sciences de Tunis, El Manar University, 2092 Tunis, Tunisia. (garnit1hechmi@yahoo.fr)*

The Sekarna Zn-Pb deposit is located in Central Tunisia, at the north-eastern edge of the Rohia graben. The deposit is composed with sulfide and non-sulfide zinc–lead ore bodies. Mineralization form two major ore types: (1) Disseminated Zn-Pb sulfides forming lenses in sedimentary phosphorite layers, and (2) cavity-filling zinc oxides ore (calamine-type ore) cross-cutting Upper Cretaceous and Lower Eocene limestone.

In this abstract we focus on the sulfide Zn ore body of Saint Pierre, which is hosted in a sedimentary phosphorites unit, 5 meter in thickness, Lower Eocene in age. Mineralizations occur as stratiform lenses sphalerite-rich, with minor galena, Fe-sulfides and barite. The sulphide mineralization occurs as replacement of carbonate cements of phosphorite pellets and post-date four diagentic events that are: phosphatogenesis, glauconitization, compaction and silicification.

Microthermometric analyses of fluid inclusions in sphalerite give a homogenization temperature in the range of 80° to 130°C. The final ice melting temperatures were in the range of -22°C to -11°C corresponding to salinities of 15 to 24-weight % NaCl eq. This fluid is typical of basinal brines.

The sulphur isotope compositions of sphalerite have homogeneous $\delta^{34}S$ values forming a narrow range between -11.2 ‰ and -9.3 ‰, mean at -10.22 ‰. The sulphur isotope compositions of galena have homogeneous $\delta^{34}S$ values forming a narrow range between -16 ‰ and -12.3 ‰, mean at -13.85 ‰.
Barite from Sekarna deposit has $\delta^{34}S$ values between 24.9 ‰ and 25.3 ‰, mean at 25.1 ‰. Barite is enriched of about 4 % when compared to the Tertiary sea water.
Fluid inclusion homogenization temperature and sulphur isotopes indicate that the reduced sulphur in sulfides was derived throw reduction of marine sulphate by bacterial sulphate-reduction process using organic matter from phosphorite source rocks.
In terms of global classifications of mineral deposits, mineralization in the Sekarna shares some characteristics of both Mississippi Valley Type (MVT) deposits and Sedimentary Exhalative (SEDEX) deposits. The features of the Sekarna deposit that are akin to MVT deposits are: Simple mineralogy, replacement of carbonates, fluid inclusions characteristics (low to moderate homogenisation temperatures and high salinities). The features of the Sekarna deposit that are akin to Sedex type are: disseminated sulfide textures, hosted within specific phosphorites beds, organic-rich.

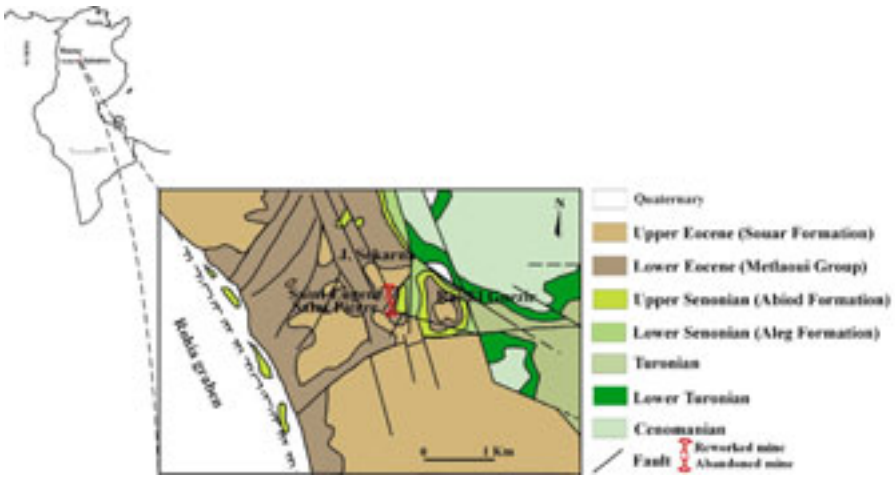

Figure 1. Location and geological map of the Sekarna area, showing the main Zn-Pb deposits. (modified from Zaïer 1999)

REFERENCES

Bouhlel, S. 2005: Carbonate-Hosted Mississippi Valley-type Pb-Zn deposits in Tunisia (Eastern Atlasic belt). Mineral Deposit Research, Meeting the Global Challenge China, 3, 19-22.

Leach, DL., Sangster, DF., Kelly, KD., Large, RR., Carven, G., Allen, CR., Gutzmen, J. & Walters, S. 2005: Sediment- Hosted Lead-Zinc Deposits: a Global Perspective. Economic Geology 100th Anniversary volume, 561-607.

Zaïer, A. 1999 : Evolution tectno- sédimentaire du bassin phosphate du centre-Ouest de la Tunisie minéralogie, pétrographie, géochimie et genèse des phosphorites. Thèse Doct. Es-Sci. Univ. Tunis II

7.7

Numerical modelling of fluid flow in submarine hydrothermal systems

Grün Gillian*, Coumou Dim**, de Ronde Cornel***, Driesner Thomas*, Weis Philipp* & Heinrich Christoph*

*Institute of Isotope Geochemistry and Mineral Resources, ETH Zürich, Clausiusstrasse 25, 8092 Zürich, Switzerland (gruen@erdw.ethz.ch)
**Potsdam Institute for Climate Impact Research (PIK), Telegraphenberg A 31, 14473 Potsdam, Germany
***GNS Science, 1 Fairway Drive, Avalon, Lower Hutt 5040, New Zealand

Fluid flow through submarine hydrothermal systems transports a major part of the Earth's heat to its surface and greatly impacts the chemistry of the crust and overlying ocean. Associated high-temperature "black smokers" are manifestations of active ore-forming systems and can be regarded as modern analogues of massive sulphide deposits whose ancient equivalents have been exploited as world-class mines onshore.

The physics of these systems is complex because seawater can phase-separate, either via boiling or condensation, into a low-salinity vapour and a high-salinity brine. In order to model the sub-seafloor hydrology with numerical transport simulation techniques, a new pressure-enthalpy-salinity scheme has been developed which includes the full phase relations of the NaCl-H_2O system up to 1000 °C and 5000 bars and accurately captures boiling, condensation, and salt precipitation. Simulations with homogeneous permeability representing mid-ocean ridge systems show that many of the key-observations at black smoker systems can be explained by the non-linear dependence of the fluid properties on temperature, pressure, and salinity (Coumou 2008).

Research cruises dedicated to seafloor hydrothermal activity along the intra-oceanic Kermadec arc have systematically surveyed and sampled numerous hydrothermal plumes. Venting ranges from relatively high temperature (≈300°C), metal-rich fluids to lower temperature, gas-rich and metal-poor fluids. In contrast to black smoker systems at mid-ocean ridges, some vent sites found at arc-related hydrothermal systems show evidence for significant contributions from magmatic sources (e.g., de Ronde et al. 2005).

We will develop a new numerical model, based on observations in currently active arc-related systems, to assess the influence of first-order physical parameters, seafloor topography, and the contribution of magmatic fluids to fluid flow patterns, thermal structure, and phase-separation (Figure 1). We aim to predict the optimal conditions for which metal-rich magmatic vapour may cool and contract to an aqueous liquid, which in turn is likely to generate particularly Cu- and Au-rich mineralization on the seafloor.

REFERENCES

Coumou, D. 2008: Numerical modeling of mid-ocean ridge hydrothermal systems. Unpublished PhD thesis, ETH Zürich.

de Ronde, C. E. J., Hannington, M. D., Stoffers, P., Wright, I. C., Ditchburn, R. G., Reyes, A. G., Baker, E. T., Massoth, G. J., Lupton, J. E., Walker, S. L., Greene, R. R., Soong, C. W. R., Ishibashi, J., Lebon, G. T., Bray, C. J. & Resing, J. A. 2005: Evolution of a submarine magmatic-hydrothermal system: Brothers volcano, southern Kermadec arc, New Zealand. Economic Geology 100, 1097-1133.

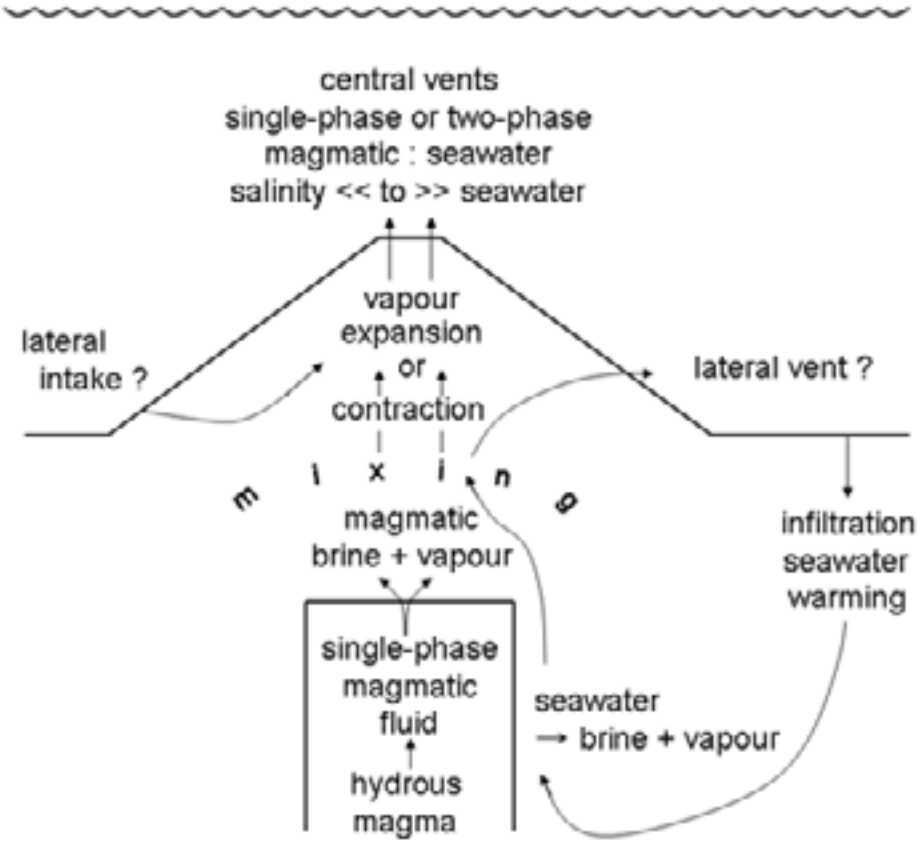

Figure 1. Schematic concept of hydrothermal fluid processes that may occur inside a submarine volcano underlain by a magmatic intrusion. Saline, single-phase fluids exsolved by crystallizing magma may separate into magmatic brine and vapour, selectively carrying certain ore metals and volatile components. The size of the magmatic heat and fluid sources, water depth, large-scale rock permeability and the intrinsic properties of the salt-water fluid system are likely key controls on the dynamic fluid evolution in space and time.

7.8

Maureen unconformity-related U-Mo-F deposit, Georgetown, QLD, Australia

Hurtig Nicole C.*, Driesner Thomas*, Heinrich Christoph A.*, Wall Vic** and Matthison Ian**

*Institute of Isotope Geochemistry and Mineral Resources, Clausiusstrasse 25, CH-8092 Zurich, Switzerland (nhurtig@student.ethz.ch)
**Mega Georgetown Ltd Pty, c/- Taylor Wall & Associates, Ground Level, 67 St Pauls Tce, Spring Hill, QLD 4000, Australia

Maureen deposit is situated about 290 km south-west of Cairns and 35 km by north-north-west of Georgetown. The general lithofacies can be subdivided into a Proterozoic metamorphic complex (Bain et al., 1978; Oversby et al., 1975), namely the Robert River Subgroup which is unconformably underlying the Maureen Volcanic Group of Carboniferous age, which in turn unconformably underlays the Mesozoic Gilbert River Formation. The Maureen Volcanic Group is subdivided into the basal Fiery Creek Formation, which is hosting the U-Mo-F mineralisation, the Lower Volcanic Unit and the Upper Volcanic Unit (Bain and Withnall, 1980; O'Rourke, 1975).

The deposit has a calculated grade of 0.12 % U_3O_8, 13.1 % CaF_2 and 0.07 % molybdenum. The geological setting of Maureen deposit shows characteristics of unconformity-type uranium deposits. Uranium is supposed to be transported in the hexavalent state in oxidized basinal fluids. Along deeply rooted fractures and faults reduced basement fluids rise. Where mixing between these two fluids occurs uranium is reduced and precipitates. The aim of this study is to identify the transporting fluid of uranium and other relevant ore forming components and to find evidence for mixing of reduced and oxidized fluids.

The precipitation of U, Mo and F was spatially related to the intersection of steeply dipping faults with the Precambrian – Palaeozoic unconformity and occurred preferentially in coarse grained and pebbly sandstone or conglomerate beds of the Fiery Creek Formation. Mineralised zones appear as elongated narrow bodies showing a close relationship to EW oriented structures. Mineral contours of U, Mo and fluorite are shown in Figure 2 along an EW cross section through the Southern mineralisation zone. Typical alteration assemblages include fluorite, dickite, chamosite and disseminated pyrite. In low to intermediate mineralized samples muscovite shows enrichment in Mg where it occurs in contact with chlorite. Such mineral assemblages show characteristics of hydrothermal deposits where the mineralizing fluids have compositions that are drastically different from the country rock assemblages (Komninou and Sverjensky, 1995). During early mineralisation, fluorite matrix replacement stays within narrow zones surrounding fractures. With progressive mineralisation grain replacement, veining and finally chemical brecciation dominate. Sulfide-rich mineral assemblages located in deeper parts of the deposit near the unconformity represent the reduced end member of the system, whereas assemblages containing anatase, trögerite and other oxides are supposed to represent the oxidized end member. Further constraints on mixing of oxidized basinal fluid with reduced basement fluids were obtained from fluid inclusion analysis. Figure 2 illustrates the result of LA-ICP-MS analysis and microthermometry on a fluid inclusion sample from Maureen deposit.

This study combined field observations with fluid inclusion analysis and mineral geochemistry providing important insights into transport and precipitation processes of unconformity-related uranium deposits.

REFERENCES

Bain, J. H. C., Oversby, B. S., Withnall, I. W., and Mackenzie, D. E., 1978, Precambrian and Palaeozoic geology of the Georgetown region, Queensland.; Third Australian geological convention; excursions handbook, p. 1-27.

Bain, J. H. C., and Withnall, I. W., 1980, Mineral deposits of the Georgetown region, Northeast Queensland.; The geology and geophysics of northeastern Australia, p. 129-148.

Komninou, A., and Sverjensky, D. A., 1995, Pre-ore hydrothermal alteration in an unconformity-type uranium deposit.: Contributions to Mineralogy and Petrology, v. 121, p. 99-114.

O'Rourke, P. J., 1975, Maureen Uranium Fluorine Molybdenum Prospect, Georgetown, Economic Geology of Australia and Papua New Guinea, 1. Metals: Victoria, The Australiasian Institute of Minin and Metallurgy, p. 764 - 769.

Oversby, B. S., Palfreyman, W. D., Black, L. P., Cooper, J. A., and Bain, J. H. C., 1975, Georgetown, Yambo and Coen inliers; regional geology: Monograph Series Australasian Institute of Mining and Metallurgy, v. 5, p. 511-515.

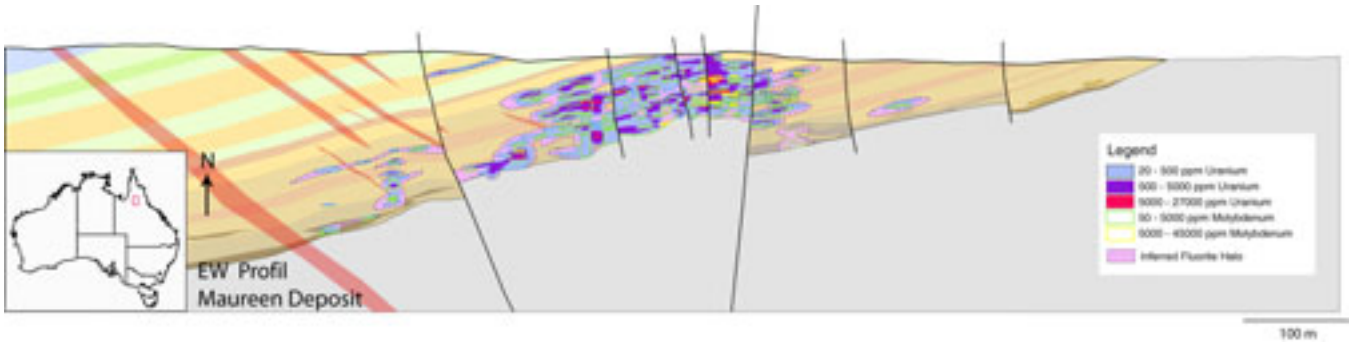

Figure 1. EW cross-section though the Southern mineralisation at Maureen deposit. Mineral contouring based on drill hole data provided by Mega Georgetown showing the distribution of U, Mo and Fluorite. The contour lines of U, Mo and F overlap, but differ in their extensions. Fluorite forms an extensive halo surrounding high grade ore bodies.

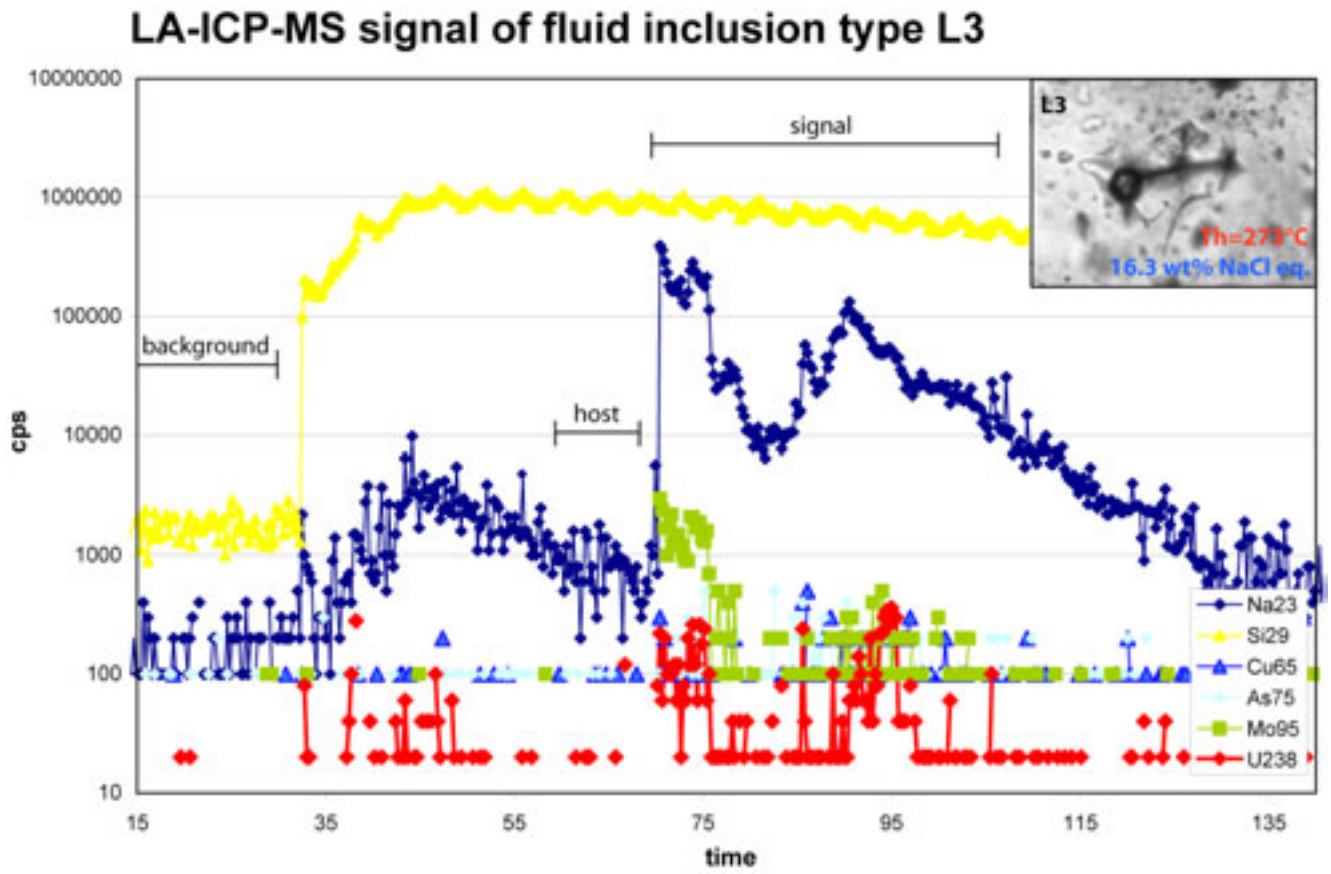

Figure 2. LA-ICP-MS signal of a saline 2 phase fluid inclusion (L3-type) showing corresponding peaks for U, Mo, As, Cu and Na. The uranium concentration is 11 ppm and Mo has a much higher concentration of 702 ppm, which is very unusual.

7.9

Olivine-Ti-clinohumite veins and their relation to partial dehydration of high pressure serpentinites

János Kodolányi*, Carl Spandler*, Timm John**, Marco Scambelluri*** and Thomas Pettke*

* *Institute of Geological Sciences, University of Berne, 1-3 Baltzerstrasse, Berne, CH-3012, Switzerland (janos@geo.unibe.ch)*
** *Physics of Geological Processes, University of Oslo*
*** *Dipartimento per lo Studio del Territorio e delle sue Risorse, University of Genova*

A major question concerning the dehydration of subducted ultramafic (UM) rocks is whether they have the potential to leave a chemical fingerprint on the mantle wedge above them. Fluids released by UM rocks at high P and T are not directly accessible. However, they can be traced by studying the chemistry of serpentinites that were subducted to depths of serpentinite dehydration. In the present study we explore peak-metamorphic veining in high pressure (HP) serpentinites of the Erro-Tobbio Unit (ET), Ligurian Alps, Italy, in order to learn about the chemical composition of the fluid released by these rocks during partial dehydration.
The ET Unit represents ultramafic mantle (UM) that was hydrated on the Tethys ocean floor. The UM rocks were then subducted to depths of 65-80 km at around 550-600°C and developed olivine (Ol) + Ti-clinohumite (Ti-Cl) + antigorite (Atg) + clinopyroxene (Cpx) + magnetite (Mag) peak mineral assemblage. The same minerals dominate adjacent HP veins, but their proportions are different. The ET HP serpentinites went through partial dehydration to form Ol + Atg from brucite (Brc) + low-T serpentine polymorph (Srp) (Scambelluri et al., 2001). Olivine has abundant polyphase (serpentine ± magnetite ± methane) inclusions in wall rocks as well as in the veins, and is often accompanied by inclusion-rich Ti-Cl. The abundance and appearance of these inclusions and the presence of methane indicate that these polyphase inclusions represent fluid inclusions modified by post-entrapment modification(s) during exhumation. Trace element analysis of these inclusions reveals subtle but significant differences in dehydration fluid chemistry, which can be linked to different mineral proportions and water/rock ratios during fluid release and migration.
Fluid in the ET rocks was partly channelized and migrated as attested by the veins. Vein bulk rock trace element concentrations show enrichment in Ti, Ba, Nb, Li, HREE and Cu relative to the wall rocks, accompanied by depletion in Cr. Based on trace element distribution in Srp of recent ocean-floor serpentinites decomposition of Brc + Srp produces relatively dilute fluids. This requires high net fluid flux to produce HFSE-rich veins. However, disequilibrium in and around fluid conduits may enhance reactions and trace element uptake from the fluid. High concentration of certain trace elements in vein Cpx (e.g. Sr 191-202 μg/g) and Ol (e.g. Li 9.8-35.5 μg/g) are therefore not necessarily indicative of significant addition of these elements from an external source. Our study emphasizes the importance of mineral stability and trace element chemistry in influencing bulk rock and fluid geochemical evolution.

REFERENCES

Scambelluri M., Rampone, E. and Piccardo, G.B. 2001 Fluid and Element Cycling in Subducted Serpentinite: a Trace Element Study of the Erro-Tobbio High Pressure Ultramafites (Western Alps, NW Italy) Journal of Petrology 42, 55-67.

7.10

Trace element uptake into quartz cement – a function of temperature or fluid characteristics?

Lehmann Katja*, Driehorst Frauke*, Ramseyer Karl*, Pettke Thomas*, Wiedenbeck Michael**

**Institut für Geologie, Baltzerstr. 1+3, CH-3012 Bern (katja.lehmann@geo.unibe.ch)*
***GeoForschungszentrum Potsdam, Telegrafenberg 326, D-14473 Potsdam*

In the Interior Oman Sedimentary Basin (Fig. 1) siliciclastic sediments of the Permo-Carbonifereous Haushi Group were deposited under both glacial (Al Khlata Formation) and temperate to semi-arid (Gharif Formation) conditions. Due to a varied subsidence, these sediments today cover depths ranging from surface outcrop in the SE to almost 5000 m in the NW. Burial is maximal in the NW part of the basin, whereas in the SE uplift of up to 2000 m is indicated from basin modeling results. Basin-wide authigenic quartz cementation began concurrent with the Late Cretaceous obduction of the Oman Mountains,

and thus, independent of burial depth or temperature (Juhasz-Bodnar, 1999). Crystallization temperatures vary between 85 and 150°C. Pressure solution is the major source of silica since no other cogenetic reactions occurred which could release silica.

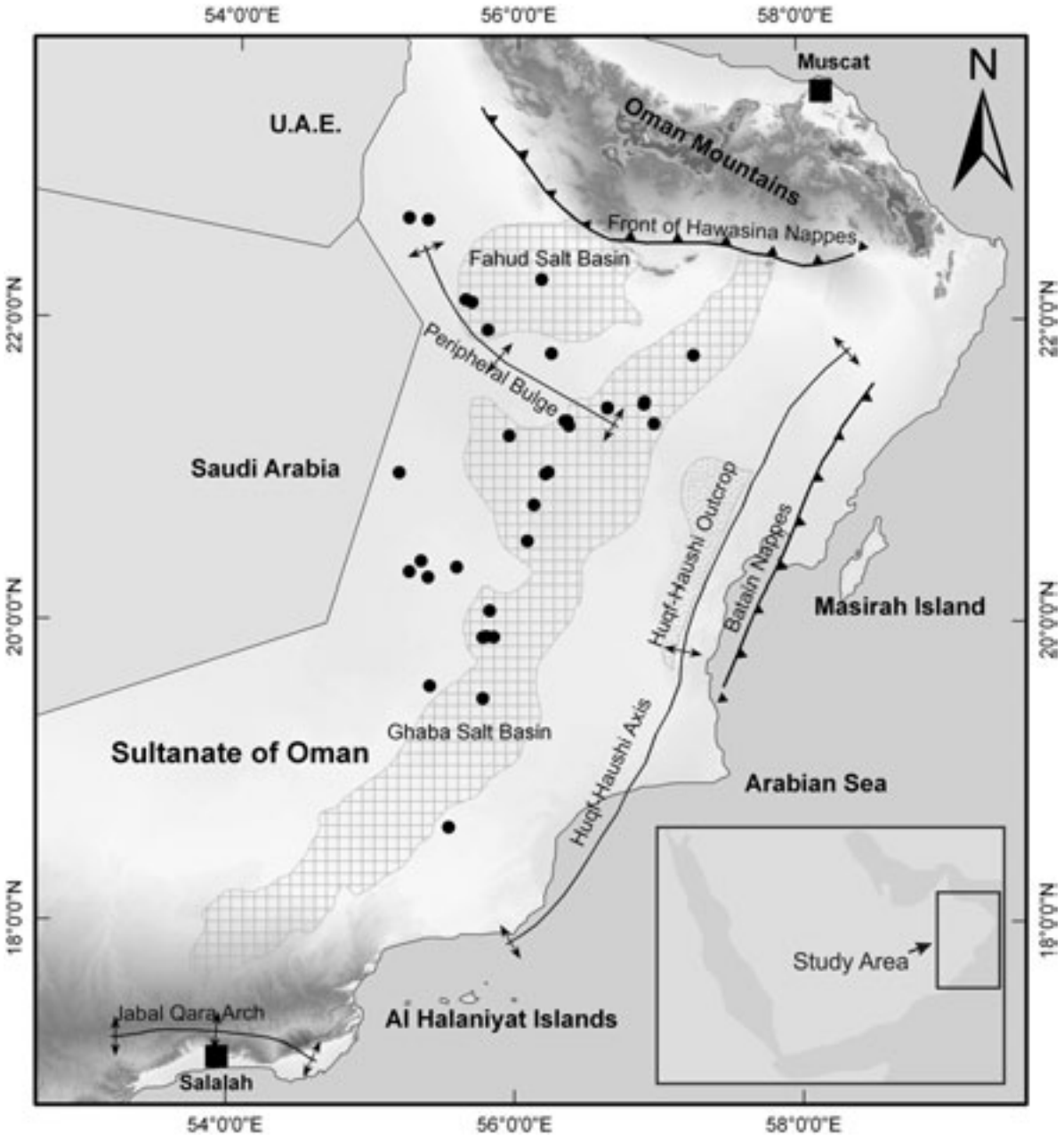

Fig. 1: Map of the sampling area. Well locations are marked by black dots.

LA-ICPMS and SIMS analyses of authigenic quartz reveal Al and charge balancing Li as the predominant impurities ranging from 60 to 1700 µg/g and 0.5 to 60 µg/g, respectively. Li and Al are correlated with an atomic ratio of 0.11 (R^2=0.94) in the Al Khlata Formation and 0.14 (R^2=0.80) in the Gharif Formation. SIMS analyses indicate a positive correlation between H and Al. Na is below 10 µg/g and not correlated with any other trace element. Be, B, K, Ti and Fe are below the element-specific limits of detection of ca. 0.5 µg/g (using a 32 µm spot for analysis).
The mean Al concentration is independent of the stratigraphy and crystallization temperature but the Al concentration varies by a factor of 3 on a regional scale. Additionally, the measured Li/Al ratio is higher than published values for quartz cement formed between 80 and 120°C (Demars et al., 1996), but is lower than ratios in hydrothermal vein quartz formed at temperatures between 200 and 300°C (Perny et al., 1992).

The low Al/Li atomic ratio and the absence of significant other cations required for charge balancing Al in quartz implies the presence of additional positive charged ions such as H^+, which was only semi-quantitatively determined by SIMS. In addition, the highly variable concentrations of Al and Li and hence H, at constant atomic ratios indicate a regionally and temporally variable pH-value. This variability suggests that pH-value is not buffered internally (Landtwing and Pettke, 2005) but externally by processes such as organic matter maturation and/or hydrocarbon migration.

REFERENCES
Demars, C., Pagel, M., Deloule, E., and Blanc, P., 1996, Cathodoluminescence of quartz from sandstones: Interpretation of the UV range by determination of trace element distributions and fluid inclusion P-T-X properties in authigenic quartz: American Mineralogist, v. 81, p. 891-901.
Juhasz-Bodnar, K., 1999, Diagenesis and pore-water evolution of the Permo-Carboniferous Al Khlata Formation, Interior Oman Sedimentary Basin, Sultanate of Oman [phD thesis]: Bern, Universität Bern.
Landtwing, M.R., and Pettke, T., 2005, Relationships between SEM-cathodoluminescence response and trace-element composition of hydrothermal vein quartz: American Mineralogist, v. 90, p. 122-131.
Perny, B., Eberhardt, P., Ramseyer, K., Mullis, J., and Pankrath, R., 1992, Microdistribution of Al, Li and Na in quartz: Possible causes and correlation with short-lived cathodoluminescence: American Mineralogist, v. 77, p. 534-544.

7.11

PVTx properties of H_2O-NaCl fluids using Brillouin scattering spectroscopy

Mantegazzi Davide*, Sanchez-Valle Carmen*, Driesner Thomas**

*Inst. for Mineralogy and Petrology, ETH Zurich, CH-8092 Zurich, (davide.mantegazzi@erdw.ethz.ch)
** Inst. of Isotope Geochemistry and Mineral Resources, ETH Zurich, CH-8092 Zurich

Saline-rich aqueous fluids play a very important role in a wide range of geological events in the Earth's crust and mantle. These processes include, for example, metamorphic reactions, the magma production in the mantle wedge beneath active volcanoes at subduction zones, the transport of chemical components in several geological settings, the alteration of the seafloor and the formation of ore deposits. Mixtures in the H_2O-NaCl binary system are a good proxy for these saline-rich aqueous fluids. Essential for quantitative modelling of phase equilibria related to such geological processes is the knowledge of the thermodynamic properties of these fluids at geologically relevant pressure and temperature conditions. Despite the important role of these geological fluids, very few experimental data on aqueous saline-rich fluids other than pure H_2O are available at pressures higher than 0.1-0.5 GPa. For instance, the equations of state (EoS) for H_2O-NaCl are restricted to 0.5 GPa. Therefore, the interpretation of subduction-related fluid processes and other fluid-mediated geological events requires the extrapolation of thermodynamic properties through over an order of magnitude in pressure.

In this contribution we present the PVTx properties of H_2O-NaCl binary mixtures with different NaCl concentrations up to high P-T conditions, calculated from sound velocity measurements in the external heated membrane diamond anvil cell using Brillouin scattering spectroscopy.

Brillouin scattering spectroscopy allows the direct measurement of sound velocities of compressional waves (V_P) propagating in the fluid and hence, the evaluation of the equation of state $\rho(P,T)$. The obtained sound velocities and densities are compared with available data in the literature.
The results are combined with previous experimental and theoretical EoS to provide the thermodynamical properties of the most relevant aqueous systems involved in geological fluid-mediated processes in the Earth's crust and mantle.

REFERENCES
Wagner, W., and Pruss, A. 2002: The IAPWS formulation 1995 for the thermodynamic properties of ordinary water substance for general and scientific use, J. Phys. Chem. Ref. Data, 31, 387−535.
Abramson, E., and Brown, M.J. (2004): Equation of state of water based on speeds of sound measured in the diamond-anvil cell, Geochim. Cosmochim. Acta, 68, 1827-1835.
Sanchez-Valle, C., and Bass, J.D. (2007) Equation of state of H_2O from sound velocity measurements in the diamond anvil cell, Geochim. Cosmochim. Acta, 71, A873-A873.
Driesner, T. 2007: The system H_2O-NaCl. Part II: Correlations for molar volume, enthalpy, and isobaric heat capacity from 0 to 1000 degrees C, 1 to 5000 bar, and 0 to 1 X-NaCl, Geochim. Cosmochim. Acta, 71, 4902-4919.

7.12

Low-Salinity fluids at the Bajo de la Alumbrera porphyry Cu-Au deposit, Argentina

Dimitri L. Meier *, Christoph A. Heinrich *, Marcel Guillong * & M. Florencia Marquez-Zavalía **

*Institute of Isotope Geochemistry and Mineral Resources, ETH Zürich, Clausiusstrasse 25, CH-8092 Zürich (christoph.heinrich@erdw.ethz.ch)
** CONICET, IANIGLA – CCT Mendoza, Av. Ruiz Leal s/n - Parque Gral. San Martin, ARG-5500 Mendoza

New evidence from several major porphyry copper and epithermal deposits concerning the role of low-salinity fluids has been published. In contrast to earlier interpretations, the parental magmatic fluid is considered to have an intermediate density and salinity. Several metals including copper and gold are mainly transported by a vapor-like fluid, not by a high-salinity brine. This vapor can then contract and carry significant amounts of metal to the low-temperature epithermal regime.

The Bajo de la Alumbrera porphyry copper-gold deposit in north western Argentina is well studied in terms of geology, alteration geochemistry and fluid characteristics, but low-salinity fluids are not documented extensively. In this study, samples particularly from the earliest and latest veins have been taken, to test these new findings at Alumbrera. The aim of the study was not a complete reassessment of the fluid evolution but to fill gaps of previous studies. The mean to investigate fluid characteristics are inclusions in vein minerals, whose salinities and temperatures are measured by microthermometry, and which are then chemically analyzed using LA-ICP-MS.

A very copper-rich, intermediate-density fluid with high homogenization temperatures, as well as high-density vapor inclusions, have been found and analyzed, surprisingly not in the earliest but in a texturally late vein. Nevertheless, similarities to the original magmatic fluids from other deposits indicate that also at Alumbrera the parental fluid was not a high-salinity brine, as inferred by previous studies, but a fluid with intermediate density and salinity.

In late veins, aqueous fluids have been investigated which could easily be the ore fluids for an epithermal deposit, as for example the nearby Farallón Negro deposit. The analytical method has been adapted to measure gold with very low detection limits, and indeed, gold has been detected with a high confidence in those very low-salinity fluids.

In addition to that, attempts to characterize the fluid belonging to relatively late pyrite-chalcopyrite veins occurring in many deposits but never investigated properly have been made, but compositional results are sparse. However, microthermometry indicates aqueous fluids with low salinity being the type of fluid responsible for those veins. Few boiling assemblages have also been analyzed, showing that in a phase separation copper, sulfur and gold partition preferentially into the vapor phase, confirming observations on other deposits. The transition from the vapor-like fluid to an aqueous liquid, called contraction, which is assumed to be responsible for high gold concentrations in ore fluid for epithermal deposits, has not been found in fluid inclusions.

The results presented here are not sufficient to document the whole fluid evolution of the Bajo de la Alumbrera deposit, more samples and analyses would be necessary. Nevertheless, evidence has been found that the new models can be applied to Alumbrera as well and low-salinity fluids indeed are responsible for many processes forming porphyry copper deposits.

7.13

The Pb-Zn-Sr-Ba deposits in Northern Tunisia: trace elements, rare earth elements and Sr geochemical evidence for their origin

Souissi Fouad*, Jemmali Nejib*, Souissi Radhia**, & Dandurand Jean-Louis***

*Laboratoire des Ressources Minérales et Environnement, Faculté des Sciences de Tunis, Campus universitaire, 2092 Tunis, Tunisie (souissi_foued@yahoo.fr).
**Institut National d'Analyses Physico-chimiques, Sidi Thabet, 2020 Ariana, Tunisie.
**Laboratoire MTG, 14 Avenue E. Belin, 31400 Toulouse Cedex, France.

Several Pb-Zn-Sr-Ba deposits are known in the North of Tunisia (Figure 1). Although, several works have been interested in their genetic conditions (Rouvier et al. 1985; Orgeval, 1994; Sheppard et al., 1996; Souissi et al., 2007), the source of metals is yet to be debated.

According to the geological context, the Triassic series may be divided into three dominating facies (i) a megabreccia made of micritic black dolostones with variegated clays and altered basalt fragments (Jalta mine in the Nappes Zone). (ii) a thick bedded dolomitic series, interlayered with thin marly layers (Bechateur quarry in the Nappe Zone), (iii) a chaotic mixture of gypsum, variegated clays and lenticular bodies or isolated blocks of black micritic dolostones that crop out along major faults (J. Ressas in the Tunisian Dorsale) or as diapirs (Boukhil, Lakhouat, Fej Lahdoum, Kebbouch, Guern Halfaya, Fej Hassene, Doghra in the Dome zone).

The mineralizations (stratiform bodies, cavity fillings, karsts, disseminations, veins, stockworks) may be hosted in the Triassic carbonated series (Jalta mine, Guern Halfaya, Jebel Ghozlane), but mainly in the younger carbonated units mechanically in contact with the Triassic: the Upper Jurassic (J. Ressas), The Upper Cretaceous (Boukhil, Lakhouat, Fej Lahdoum, Kebbouch, Guern Halfaya, Fej Hassene, Doghra), the Eocene (Boukhil) and the Mio-Pliocene (Jalta mine, Jebel Ghozlane).

The Geochemical investigation is based on metallic trace elements (MTE), rare earth elements and Sr isotopes analysis. The MTE geochemistry, conducted on the different Triassic lithologic facies, shows that, apart from the barren series of the Bechateur quarry area, strong anomalies in these elements are recorded either in clays (Pb, Zn, Cd) or carbonates (Pb, Zn, Cd, Cr, Co, Cu). REE and Sr isotopes analyses have been conducted on celestite samples and their carbonated (dolomite, calcite) hosts collected along the Triassic-Upper Cretaceous contact. The results show that the total REE contents are too high in the carbonates with respect to those in the celestite samples. In addition to that, the REE spectra of the two mineral species are quite different from each other: carbonates are characterized by nearly flat spectra, the LREE being slightly more concentrated than the HREE, while celestites are characterized by negative Ce and Er anomalies along with strong positive Eu anomalies. Such a result shows that the mineralizing fluids may be assimilated to deep basinal brines which have been equilibrated with detrital sedimentary series or rock units rich in feldspars (Taylor and McLennan, 1985). On another respect, Sr isotopes analyses conducted on the Triassic rocks (dolomite: 0,708152 ± 8 to 0,708908 ± 9, gypsum: 0,708090 ± 9) and on celestite samples (0,708706 ± 9 to 0,710225 ± 9) show that $^{87}Sr/^{86}Sr$ ratios are anomalous with respect to the Triassic (0,70690 to 0,70794), Jurassic (0,70677 to 0,70778) or Cretaceous (0,7071 to 0,7077) sea water. Orgeval (1994) and Sheppard et al. (1996) supposed that fluids enriched in ^{87}Sr have been, continually, in contact with the Triassic diapirs.

Taking into account the positive anomalies of the MTE in the Triassic rocks, part of these elements could be sourced from these units. However, the geological contexts (diapirs or major faults deeply rooted in the basement, both associated to positive geothermal gradients), the REE and the Sr isotopes data as well as the presence of a Pb-(Zn-Ba) mineralization hosted in the Permian "Upper Dolostones" in the South of Tunisia, strongly support the hypothesis that all the elements should be deeply sourced. So, the Paleozoic series (siliciclastics or primary ore deposits) seem to be favourite potential sources.

REFERENCES

Orgeval, J.J. (1994). - Peridiapiric metal concentration : example of the Bougrine deposit (Tunisian Atlas). - Spec. Publ. N° 10, Soc. Geol. Applied to Mineral Deposists. Fontboté/Boni (Eds), Sediment-hosted Zn-Pb ores. Springer-Verlag, Heidelberg.

Rouvier, H., Perthuisot, V. & Mansouri A. 1985: Pb-Zn Deposits and Salt-Bearing Diapirs in Southern Europe and North Africa. Economic Geology 80, 666-687.

Sheppard, S.M.F., Charef, A. & Bouhlel S. 1996: Diapirs and Zn-Pb mineralizations : a general model based on Tunisian (N. Africa) and Gulf Coast (U.S.A.) deposits. Society of the Economic Geologists, special publication N° 4, pp. 30-243.

Souissi, F., Sassi, R., Bouhlel, S., Dandurand, J-L. & Ben Hamda, S. 2007: Fluid inclusion microthermometry and rare earth element distribution in the celestite of the Jebel Doghra ore deposit (Dome zone, Northern Tunisia): towards a new genetic model. Bull. Soc. Géol. Fr., t. 178, n° 6, pp. 459-471.

Taylor S.R. & McLennan S.M. 1985: The continental crust: its composition and evolution. An examination of the geochemical

record preserved in sedimentary rocks. Blackwell, Oxford, 312p.

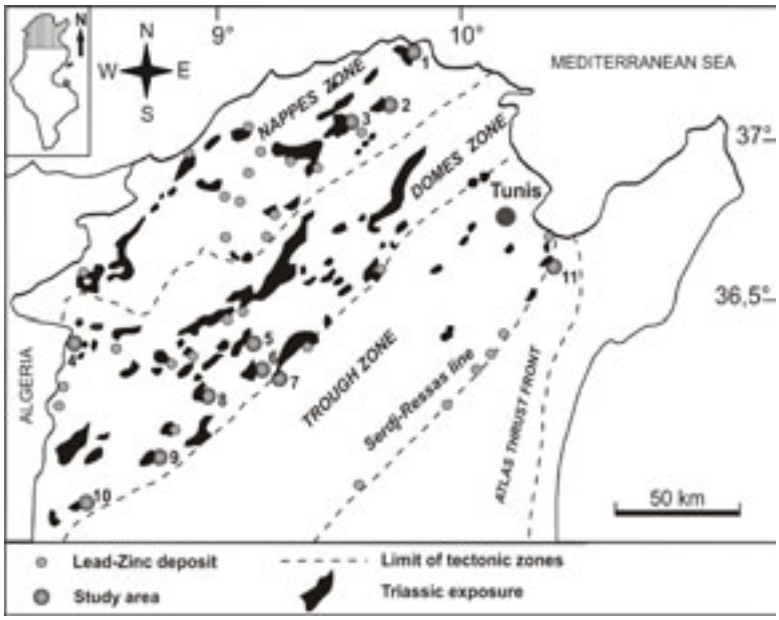

Figure1. The Triassic exposures and Pb-Zn deposits in Northern Tunisia
1 Bechateur; 2 Jebel Ichkeul; 3 Jalta; 4 Fej Hassene; 5 Fej Lahdoum; 6 Boukhil; 7 Lakhouat; 8 Kebbouch; 9 Doghra; 10 Guern Halfaya; 11 Jebel Ressas.

7.14

The Mississippi Valley type fluorite ore of Jebel Stah (North-Eastern Tunisia) II: contribution of the REE and Sr isotopes geochemistry to the genetic model

Souissi Foued*, Souissi Radhia**, Dandurand Jean-Louis***

**Laboratoire des Ressources Minérales et Environnement, Faculté des Sciences de Tunis, Campus universitaire, 2092 Tunis, Tunisie (souissi_foued@yahoo.fr).*
***Institut National d'Analyses Physico-chimiques, Sidi Thabet, 2020 Ariana, Tunisie.*
***Laboratoire MTG, 14 Avenue E. Belin, 31400 Toulouse Cedex, France.*

Several F-(Ba-Pb-Zn) belong to the fluorite district of Zaghouan (FDZ) in the north-east of Tunisia. They are associated to Lower Liassic and Upper Jurassic carbonate formations (Oust and Ressas formations, respectively). Unconformities (paleoreliefs, hard grounds, phosphatic condensed layers, karstification, sedimentary gaps) separate them from the overlying sedimentary cover. These formations run along a major fault considered to be a major tectonic lineament which cuts the basement and its sedimentary cover, trending in the atlasic (NE-SW) direction. Chaotic masses of the Triassic (evaporates, clays and dolostones) crop out frequently along this fault (Fig. 1).

The mineralizations occur either as stratoid bodies along the unconformity surfaces or located at the top of the Oust (Stah, Kohol) or the Ressas formations (Zriba-Guebli, Mecella). They may be also associated to a fracture network which cuts the carbonated formations and their marly-calcareous cover (H. Jedidi, J . Oust, Sidi Taya). .

Souisssi et al. (1997, 1998) have pointed out the epigenetic character of the mineralization of J. Stah, which is rattached to the MVT group of deposits dominated by fluorite. The deposition has resulted from the hydrothermal (135 ± 20 Wt % NaCl equiv.) circulation of a Na-Ca-Cl brine (20 ±1 Wt % NaCl equiv.) in depth. Subsequent circulations are responsible of the remobilisation in deeper conditions of the fluorite (185 ± 20°C, 10 ± 1 Wt % NaCl equiv.) followed by the deposition of the massive

quartz within fractures (225 ± 20°C, 5,5 ± 1 Wt % NaCl equiv.). This study is conducted to provide the genetic model with new arguments in the light of REE and Sr isotopes geochemistry.

The results of the REE geochemistry allow to conclude that the epigenetic dolomites and the finely crystallized fluorite replacing the carbonated matrix (laminated karst deposits and dark layers of the banded ore) exhibit similar REE spectra showing a slight enrichement in LREE with respect to the HREE along with weak cerium and europium anomalies. The coarse crystalline petrographic types of fluorite (open space fillings, veins, geodes) and the associated calcite are characterized by REE spectra showing a depletion in the LREE and a weak negative Eu anomaly. Such a geochemical character allows to conclude that fluorites, in this case, have crystallized from the residual fraction of the same ore fluid.

Strontium isotopes analysis, conducted on different fluorite ore samples show that all the strontium isotope ratios fall in the narrow range 0,708154 ± 8 to 0,708333 ± 8. So, one can deduce that fluoride has been carried by a basinal fluid which is more radiogenic than both of the Triassic (0,70690 to 0,70794) and the Jurassic (0,70677 to 0,70778) sea water (Burke et al., 1982; Koepnick et al., 1990). The migration of this fluid could have been released by a hydraulic fracturing during a post Jurassic major extensional phase. It is noteworthy, however, that several intra-paleozoic fluorite ores hosted in sedimentary series to which magmatic events may be associated are documented all around the Mediterranean basin: in France (the Tarn, the Pyrénées atlantiques, the Cordesse), in Spain (the Asturian province, the Valle De Tena in the Huesca Province) and in Italia (the Sarrabus area of Sardinia). This kind of deposits exists also elsewhere in the world: in England (the North Pennine ore field and the Derbyshire Province, in Canada (the Saint Lawrence deposits of Southern Newfoundland and in the Mississippi Valley, USA (Southern Illinois-Western Kentucky and Sweetwater-Tennessee). For this reason, the authors strongly support the idea that the basinal brines trapped in the underlying Paleozoic sedimentary column, which is rich in siliciclastics, could account for the radiogenic 87Sr/86Sr signature recorded for the fluorite ore of Jebel Stah. Fluoride should come from the lixiviation of primary deposits hosted in this series.

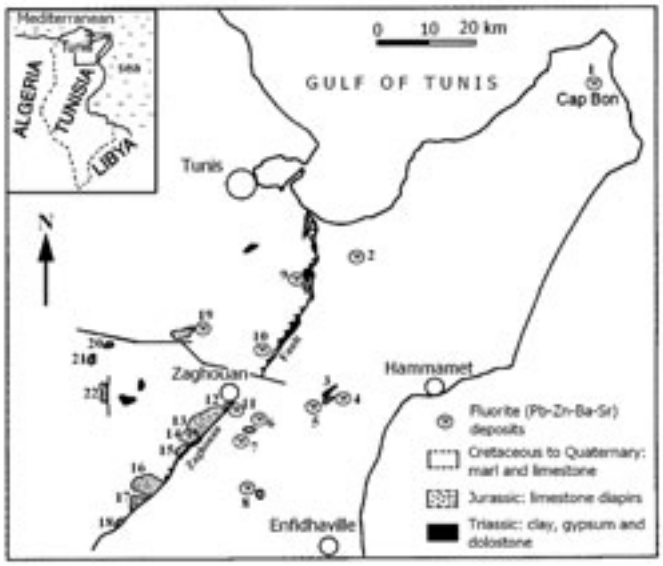

Fig. 1: Location map of the Jurassic diapirs in north-eastern Tunisia and the associated F-(Pb-Zn-Ba) deposits. 1 Oued M'tak, 2 J. Mokta, 3 Ore deposit running along the side of the Triassic outcrop of Hammam Jedidi, 4 J. Azreg, 5 J. el Hammam, 6 Hammam Zriba, 7 J. Guebli, 8 J. M'dekker, 9 J. Ressas, 10 J. Messella, 11 Sidi Taya, 12 Poste Optique, 13 J. Stah, 14 J. Kohol, 15 J. el Azeiz, 16 J. Bent Saidane, 17 J. Fkirine, 18 J. Zaress, 19 J. Oust, 20 J. Aziz, 21 J. Bou Kornine, 22 J. Rouas.

REFERENCES

Burke, W.H., Denison, R.E., Hetherington, E.A., Koepnick, R.B., Nelson, H.F. & Otto, J.B., 1982: Variation of sea water 87Sr/86Sr throughout Phanerozoic time. Geol. 10, 516-519.

Koepnick, R.B., Denison, R.E., Burke, W.H., Hetherington, E.A. & Dahl, D.A., 1990: Construction of the Triassic and Jurassic portion of the Phanerozoic curve of sea water 87Sr/86Sr. Chem. Geol., (Isot. Geosci. Sect.), 80: 327-349.

Souissi, F., Dandurand, J-L. & Fortune, J-P., 1997: Thermal and chemical evolution of the fluids during fluorite deposition in the Province of Zaghouan (north-eastern Tunisia). Mineral. Deposita, 32: 257-270.

Souissi, F., Fortune, J-P. & Sassi, R., 1998 : Le gisement de type Mississippi Valley du Jebel Stah (Tunisie nord-orientale). Bull. Soc. Géol. Fr., n°2, t. 169, p. 163-175.

7.15

Towards a quantitative process model of a porphyry Cu-Mo-Au deposit at the example of Bingham, Utah.

Steinberger Ingo*, Driesner Thomas*, Weis Philipp*, Heinrich Christoph*.

*ETH Zürich, Institut für Isotopengeologie und Mineralische Rohstoffe, Clausiusstrasse 25, CH-8092 Zürich (steinberger@erdw.ethz.ch)

Porphyry copper deposits form from magmatic hydrothermal systems. Dissolved metals are transported in both, vapour and liquid phases and precipitated by rapid changes in temperature and pressure. The driving forces for fluid flow in these systems are fluid density variations generated by the thermal energy released by a magmatic intrusion. In our previous generic models (Driesner and Geiger, 2007) we have been able to predict zones, where temperature and/or pressure change over a short distance, therefore leading to precipitation of metals in a limited volume. The second prerequisite for ore concentration is the amount of fluid passing through this volume. The time scale of these processes may vary between a few 10'000 or several 100'000 years.

Landtwing (2004) demonstrated from fluid inclusion data that ore deposition in Bingham took place at temperatures between 350 and 425°C and pressures between 14 and 21 MPa (about 1.4-2.1 km paleodepth assuming hydrostatic conditions). She concluded from textural observations that vein and ore formation was driven by a single source of magmatic-hydrothermal fluid originating from a porphyry quarz monzonite. The overpressure from the boiling fluid also induced hydrofracturing, creating the initial pathways for the fluid. Because the ore deposition temperature was in the field of quartz dissolution by vapour, she explained the observed two quartz generations in the veins (one before, one after Cu deposition) by the generation of secondary permeability by quartz dissolution. Ore precipitation from a vapour phase took place in a temporal narrow phase of increased permeability. These findings concur with the results from Heinrich et al. (1999), who identified a vapour-like fluid responsible for Cu and Au transport.

Furrer (2006) proved with compositional analysis that the fluids are not convecting around the intrusion, due to missing evidence of fluid dilution. Therefore the fluid originates from the intrusion and is not modified by fluid mixing at the depths determined by Landtwing (2004).

With the availability of these data and our in house finite element code (CSMP++), which is able to model mass conservative hydrothermal saline multiphase fluid flow (Driesner and Geiger, 2007), we will test the predictions from the generic models using the Bingham deposit as a field example. Being supplied with detailed 3D mine data by Kennecott Copper Exploration including ore grades and lithology, we are now capable to set up a model of the ore body, reconstruct the palaeoenvironment and compute the flow paths, the likely ore deposition areas and porosities generated by hydrofracturing. These porosities must correlate with vein density data measured by Grün (2007). From the calculated P-T conditions we can predict ore precipitation zones, which must correlate with the observed field data.

If simulated values are in agreement with observed data, conclusions about the duration of ore forming hydrothermal systems and predictions about the estimated size of unexplored porphyries can be made. As a further step, we are considering extending the model area to batholite scale and try to explain why nearby intrusions a barren, while in bingham a world class deposit has formed.

REFERENCES

Driesner, T. and Geiger, S., 2007. Numerical simulation of multiphase fluid flow in hydrothermal systems. In: A. Liebscher and C.A. Heinrich (Editors), Fluid-Fluid Interactions. Reviews in Mineralogy and Geochemistry. Mineralogical Society of America, Geochemical Society, pp. 187-212.

Furrer, C., 2006. Fluid evolution and metal zonation at the Bingham porphyry Cu-Au-Mo deposit, Utah: constraints from microthermometry and LA-ICPMS analysis of fluid inclusions. M.Sc. Thesis, ETH Zurich, Zurich, 96 pp.

Grün, G., 2007. Distribution and orientation of veins in the Bingham Canyon porphyry Cu-Mo-Au deposit, Utah. M.Sc. Thesis, ETH Zurich, Zurich, 123 pp.

Heinrich, C.A., Günther, D., Audétat, A., Ulrich, T. and Frischknecht, R., 1999. Metal fractionation between magmatic brine and vapor, determined by microanalysis of fluid inclusions. Geology, 27(8): 755-758.

Landtwing, M.R., 2004. Fluid evolution and ore mineral precipitation at the Bingham porphyry Cu-Au-Mo deposit, Utah, deduced from cathodoluminescence imaging and LA-ICPMS microanalysis of fluid inclusions. PhD Thesis, ETH Zurich, Zurich, 260 pp.

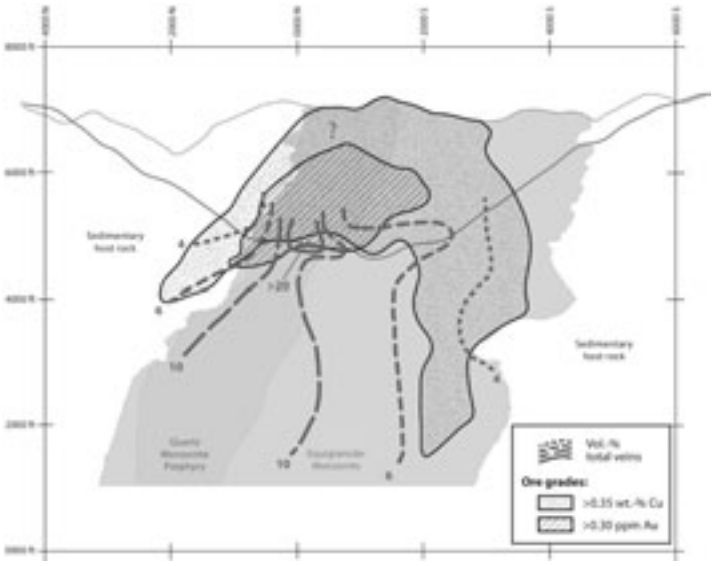

Figure 1: Vein density and Cu as well as Au ore grades in Bingham after Grün (2007)

7.16

Fluid chemical characterisation of the Pataz, Marsa and Parcoy mineralized districts in the Peruvian Eastern Cordillera

Vágó Edina*, Moritz Robert*

Département de Minéralogie, Rue de Maraîchers 13, CH-1205 Genève

During the Carboniferous a widely extended plutonism occurred on the north-western coast of the South-American terrain which is represented today by a large number of granodioritic-monzogranitic intrusions along the Peruvian Eastern Cordillera. These granitoid intrusions contain structurally controlled, shear zone hosted vein type deposits, with several distinct stages of quartz-pyrite-galena-sphalerite-arsenopyrite-gold mineralization. The strike directions of the mineralized veins are corresponding with the main fault directions from ≈N100° to ≈N165° of the area (Haeberlin et al., 2002). Pataz, Marsa and Parcoy mining districts enclose two main contemporaneous auriferous vein systems, which can be distinguished by their dip directions: (a) steeply dipping (≈45°-60° to the E), (b) subhorizontal (≈10°-15° to the E) veins.

New fluid inclusion analysis is being carried out on the three quartz stages of the subhorizontal veins of Pataz, Marsa and Parcoy mining districts (Jimena, Glorita 2, Valeria, Michauara, Rosa Orquidea and Sambuca veins). The result will be compared to previous microthermometric measurements on the steeply dipping vein system of Pataz mineralization (La Lima 2, Choloque) (Heaberlin, 2002). The variability in the sulphide mineral precipitation capacity of the fluid system is represented by a significant decrease in the salinity, from the primary, coarse pyrite (up to 5mm in diameter) bearing, barren quartz stage, through the gold bearing sulphide mineralization to the late stage quartz-carbonate veining. The O isotope analysis based on extended sampling following lateral and vertical dimensions are devoted to show any possible meteoric fluid input into the circulating (magmatic-)hydrothermal system.

There are several different theories on the formation of the Pataz mineralized bodies. Previous investigation interpreted these auriferous vein systems as orogenic gold deposits however there is still an open debate about any possible magmatic link. This study is addressing the issue on the chemical properties of the fluids involved in the formation of the gold deposits and their relationships with any possible contemporaneous magmatic event.

REFERENCES

Haeberlin, Y. 2002: Geological and structural setting, age and geochemistry of the orogenic gold deposits at Pataz Province, Eastern Andean Cordillera, Peru, Doctoral Thesis, University of Geneva, Terre et Environnement 36: 182 p.

Haeberlin Y., Moritz, R., Fontboté, L., 2002: Paleozoic orogenic gold deposits in the Eastern Central Andes and its foreland, South America, Ore Geology Reviews 22, p. 41-59.

8. Building Stones - application, suitability, research

Rainer Kündig, Konrad Zehnder, Andreas Küng

Schweizerische Geotechnische Kommission (SGTK), Scuola universtitaria professionale della Svizzera italiana (SUPSI)

8.1

Geological methods in everyday conservation of monuments and sites

Bläuer Christine*, Rousset Bénédicte*

**CSC Sàrl, Rue de l'Industrie 10, 1700 Fribourg (csc@conservation-science.ch)*

Investigations in the field of conservation of heritage buildings and historic sites are manifold. They can be classified into five groups:

- analysis of original materials,
- analysis of degradation products,
- characterization of the interactions between the building materials and environment prevailing at the monument or the site in question,
- estimating the compatibility between the original materials and the conservation materials
- optimizing the treatment methods or the preventive conservation measures.

The naturalist approach and some simple methods commonly used by geologists are an essential basis for these investigations and generally provide practical results quickly acquired and useable.

Among these methods, field observations are crucial. Sometimes accompanied by mapping materials and degradations, they allow locating the problems, to draw up the state of conservation and to establish an initial list of potential causes of degradation. They allow also to determine what methods of investigation are most relevant in the studied case and to intelligently select the shape, size and locations of sampling when it is needed.

Samples from one to a few cubic millimeters may be sufficient to make observations of dispersions with polarizing light microscopy. These observations, together with microchemical tests extensively used in the early 20th century (Chamot & Mason, 1989) and then adapted by the Swiss geologist Andreas Arnold (1984), are a useful tool to identify the nature of soluble salts responsible for damage or to identify the mineralogical nature of the pigments of wall paintings and polychromies (Plesters, 1956).

On samples from one to a few cubic centimeters of natural stone or mortar the classical mineralogical identifications by means of thin sections can be made (Bläuer & Küng, 2007). But the analysis of a thin section also provides significant information on the form and distribution of pores of the stony materials.

Samples from ten to several tens of cubic centimeters are needed for petrophysical measurements (total porosity, capillary porosity, water absorption and drying kinetics, hydric and hygric dilation, characterization of the hygroscopicity and permeability to water vapor, ...) that characterize the building materials and the conservation materials (Jeannette 1997).
These petrophysical measurements allow us also and especially to determine the physical compatibility between the original materials and the conservation materials (Rousset et al., 2005). This can be tested e.g. by determining the ability of liquid water and vapour to pass from one material to the other, or by trying to find the optimal conditions for a conservation treatment by determining the optimal amount of product to be applied to get the desired result while avoiding as much as possible side effects due to too drastic changes of physical and mechanical properties between the treated and not treated areas.

Based on case studies, we show how we use these geological methods regularly as a part of our consulting activities.

REFERENCES

Arnold A. (1984). Determination of mineral salts from monuments - Studies in Conservation, 29/3, 129-138.
Bläuer C., Küng A., 2007. Examples of microscopic analysis of historic mortars by means of polarising light microscopy of dispersions and thin sections. Materials Characterization 58 (2007), 1199-1207
Chamot E. M. and C. W. Mason (1989). "Handbook of Chemical Microscopy. Volume II. Chemical Methods and Inorganic Qualitative Analysis" Second Ed, Chicago, IL. McCrone Research Institute.
Jeannette, D., 1997. Structures de porosité, mécanismes de transfert des solutions et principales altérations des roches des monuments. La pietra dei monumenti in ambiente fisico e culturale. Atti del 2° Corso Intensivo Europeo tenuto a Ravello e a Firenze dal 10 al 24 aprile 1994, 49-77.
Plesters J., 1956. Cross-sections and chemical analysis of paint samples. Studies in conservation 1, 110-155.
Rousset B., S. Gentile, J. James, B. Pozzi, 2005. Injection grouts for molasse sandstones: preliminary assessments. Proceedings RILEM workshop "Repair mortars for historic masonry", Delft University of Technology, Delft, the Netherlands, 26-28 January 2005.

8.2

The use of ornamental stones from Arzo (Ticino) in the italian architecture

Bugini Roberto* and Folli Luisa

**Istituto CNR Conservazione e Valorizzazione dei Beni Culturali - "Gino Bozza"*
via Cozzi 53, 20125 MILANO (r.bugini@icvbc.cnr.it)

Three different stones, called Broccatello, Macchiavecchia and Rosso di Arzo, were quarried in southern part of Canton Ticino. The stones belong to a Mesozoic sedimentary series outcropping in a large area from lake Maggiore to lake Como (Bernoulli 1964). Broccatello, a bioclastic micritic limestone, together with Macchiavecchia, a syngenetic breccia (Sinemurian, Lower Jurassic) pertaining to the "Lugano swell", outcrops south of lake Lugano close to the Italian border. Broccatello is purple-red with skeletal grains (Brachiopoda, Crinoidea) and some grey veins, Macchiavecchia is multicoloured with white calcite veins on a red, grey or yellow ground, Rosso is dark red with white calcite veins. All the stones are perfectly polishable.
The Arzo quarries are located north-east of the village and they are connected with the italian quarry area of Viggiù, Brenno and Saltrio whose brown or grey clastic limestones were quarried since the Roman times.
The Arzo "marbles" were widely used as ornamental stones either locally or in Northern Italy and in many other italians towns. The first use of Arzo marbles for architectural purpose probably dates back from the 13th century (cut stones for the piers of Broletto, Como) or for ornamental purpose from 15th century, as seen in a milanese church (St Maria delle Grazie - portal of Sacrestia vecchia, 1499). But it's difficult to ascertain the exact year of the marble setting because of the multiple remakes or restorations carried out on the buildings. A witness brought by Vasari in his book (1568) where two Macchiavecchia columns of the Medici funerary monument (sculptor Leone Leoni, Milan Duomo, 1560-63) were described as made of "*pietra macchiata simile al diaspro*" [a spotted stone like jasper]: so the Macchiavecchia was unknown to the Author.
The Macchiavecchia, on the contrary, was well known by Scamozzi, about fifty years later, and it was compared with roman coloured marbles. Scamozzi wrote in his architectural treatise (1615): "*Hanno parimente in Lombardia quella sorte di misto di color*

canellato, e verdiccio corneo più bello di quello della Porta Santa di Roma" [They also have in Lombardy a stone mixed brown to greenish in colour, nicer than the Portasanta in Rome]. The Portasanta is a brecciated limestone from Hios island (Greece) widely used by the Romans for flooring and wall veneering and reused for the enframements of the Porta Santa (Holy Door) of St Peter basilica (early 17th century) in Rome. So the Arzo marbles replaced the roman coloured ones whose quarries were unreachable for a long time.

The Arzo marbles were almost entirely devoted to the altar ornamentations for more than two centuries (17th and 18th). The construction of new altars in the churches was supported by the liturgical renewal in consequence of the Tridentine Council (1545 - 1563). Generally the Arzo marbles were mixed with different coloured marbles coming from Lombardy and from abroad: Arabescato orobico, red and grey limestone from Val Brembana (Bergamo); black limestone from lake Como (Varenna - Lecco); *Occhiadino*, grey and white limestone from Val Camonica (Brescia); white marble from Apuanian Alps (Tuscany); *Rosso di Francia*, red and white limestone from Aude department (France) and few others. The use in the course of the centuries was ubiquitous in milanese churches (St Alessandro, St Ambrogio, St Lorenzo, etc.) and it's very well illustrated in the Duomo: the baptistery (architect P. Tibaldi, 1580), different altars and the crypt (also by P. Tibaldi, end of 16th century), the St Carlo funerary chapel called Scurolo (1606), the St Giovanni Bono altar (late 17th century), the mixed marbles flooring (18th century), the crypt vestibule (1810), the high altar (1985). The marbles were used as: column shaft (monolithic, maximum length about 3 metres, Macchiavecchia), moulding (Macchiavecchia), balustrade (Macchiavecchia, Rosso), veneering or inlay (Macchiavecchia, Broccatello) and flooring (Rosso).

The inlay was made of thin slabs (about 1 cm thick), sometimes in different pieces with curved cuts to enhance the colour variegation and to counterfeit a monolithic slab. Each slab was placed in a shallow pocket carved into the main material (black limestone or white marble) and fixed by an adhesive made of different components as colophony, turpentine, beeswax, etc. mixed with quartz sand or crushed marble.

The marbles were also used in civil buildings, mainly in the balustrades of the main staircases of palaces: Litta (Milan, 1740), Affaitati (Cremona, 1769), Villa Olmo (Como, 1782-97). At least, another important use includes furniture (flat slabs for tables or consoles) and fireplace (Villa La Gallia, Como).

The geographical extent of the use of Arzo marbles was wide; the following list, based on direct observations, is significant but incomplete. Canton Ticino: Arzo, Ascona, Bissone, Brissago, Ligornetto, Locarno, Lugano, Mendrisio, Riva San Vitale. Lombardy: Bergamo, Breno, Busto Arsizio, Cairate, Carpiano, Castelleone, Como, Legnano, Lodi, Melegnano, Morbegno, Pavia, Saltrio, Saronno, Vezza d'Oglio, Vigevano, Viggiù, Villa Pasquali. Piedmont: Aosta, Baveno, Ivrea, Novara, Turin, Varallo. Venetian: Venice. Emilia-Romagna: Bologna, Ferrara, Parma. Liguria: Genoa. Latium: Rome. Campania: Cava dei Tirreni, Neaples.

The decline of these altar ornamentations, called "architectural absurd" by Francesco Milizia, involved the decline of Arzo marbles in the 19th century. But some important accomplishments are still present in Milan: the columns of St Giorgio al Palazzo (1800-21); the basement of the St Simpliciano high altar (1835); the portal of St Carlo al Corso (1839-47); the columns in the atrium of Bagatti - Valsecchi palace (1878). The Arzo marbles were thereafter reported by the architecture and marble treatises in this century, despite their foreign provenance: Milizia - Antolini (1817), Amati (1830), Stoppani (1857), Curioni (1877) and Salmojraghi (1892).

The Arzo marbles were mainly referred to the inside use, so the state of conservation is generally good. But these coloured marbles exposed to weathering are always affected by surface roughening and chromatic alteration. The first one is caused by rain washing dissolving the calcite crystals; the second one fades the colourful surfaces turning them to a brownish or pinkish hue. An example of these decay phenomena are the Macchiavecchia elements in the columned portal of St Maria dei Miracoli (Milan, late 16th century) and in the portal of Monastero Maggiore (Milan, 1683).

REFERENCES

Amati, C. 1830: Dell'architettura di M. Vitruvio Pollione. Milano [book 2, chap. 7, p. 50].

Bernoulli, D. 1964: Zur Geologie des M. Generoso. Beit. Geol. Kar. Schweiz, N.F. 118.

Milizia, F. 1817: Principi di architettura. Milano [Osservazioni, p. 1, c. 12, art. 3, p. 79].

Scamozzi, V. 1615: L'idea dell'architettura. Venezia [part 2, b. 7, chap. 5, p. 189].

Vasari, G. 1568: Le vite. Firenze [vol. 6, Vita di Lione Lioni Aretino (...), p. 202].

8.3

The natural stones used on the Romanesque north wall of the St. Martino church in Mendrisio

Cavallo Giovanni*, Corredig Guido**, Dell'Oro Davide**, Galimberti Lucia**, Rodeghiero Franco**, Vezzoni Bruno*

*University of Applied Sciences of Southern Switzerland, Dept. Environment, Construction and Design, LTS, PO Box 12 CH-6952 Canobbio (Tessin) giovanni.cavallo@supsi.ch
** University of Milan Bicocca, Dept. of Geology, Piazza delle Scienze 4 Milan (Italy)

The Romanesque north wall of the St. Martino church in Mendrisio (fig. 1) has been chosen as model for an applied research project called OSMATER (http://istgis.ist.supsi.ch:8001/osmater/) aimed to link the original materials used, the quarries and the possible routes.

Irregular scabbled stones of silicified limestones have been largely used for the wall corresponding to the oldest one. This stone is locally called Pietra di Salorino (Salorino stone) being the village part of the mining district.
The upper part of the wall is decorated with small arches in Travertine called Tufo Lombardo (Lombard Tuff). The final cornice is in individual decorated blocks of sandstone.

The correlation between the microstructure and the composition of the raw materials and the stones used on the wall allows to refer the silicified limestone to the quarry located at Monte Casima close to the Salorino village and the church. The rock belongs to the Moltrasio stone formation (Low and Middle Lias). It is a marly limestone, pale grey in colour, with veins filled up with coarse grains of calcite and nodules of flint.
The Quaternary Travertine is locally called Tuff for its analogies with the volcanic rocks. The petrographic examination allows to refer this material to the Travertine deposits located in Rancate, a village close to Mendrisio.
The sandstone belongs to the formation Conglomerate of Como (Oligocene); it comes from the quarries located in Malnate and is locally known as *Pietra Molera*. The colour ranges from grey to greenish, the grain size from medium to fine, the mineral phases are quartz, feldspars, biotite and muscovite. Grains of metamorphic and carbonatic rocks are also present. The matrix is siliceous.
The source of the silicified limestones and the travertine is just close to the building. The sandstone quarry is a little bit far from the church.

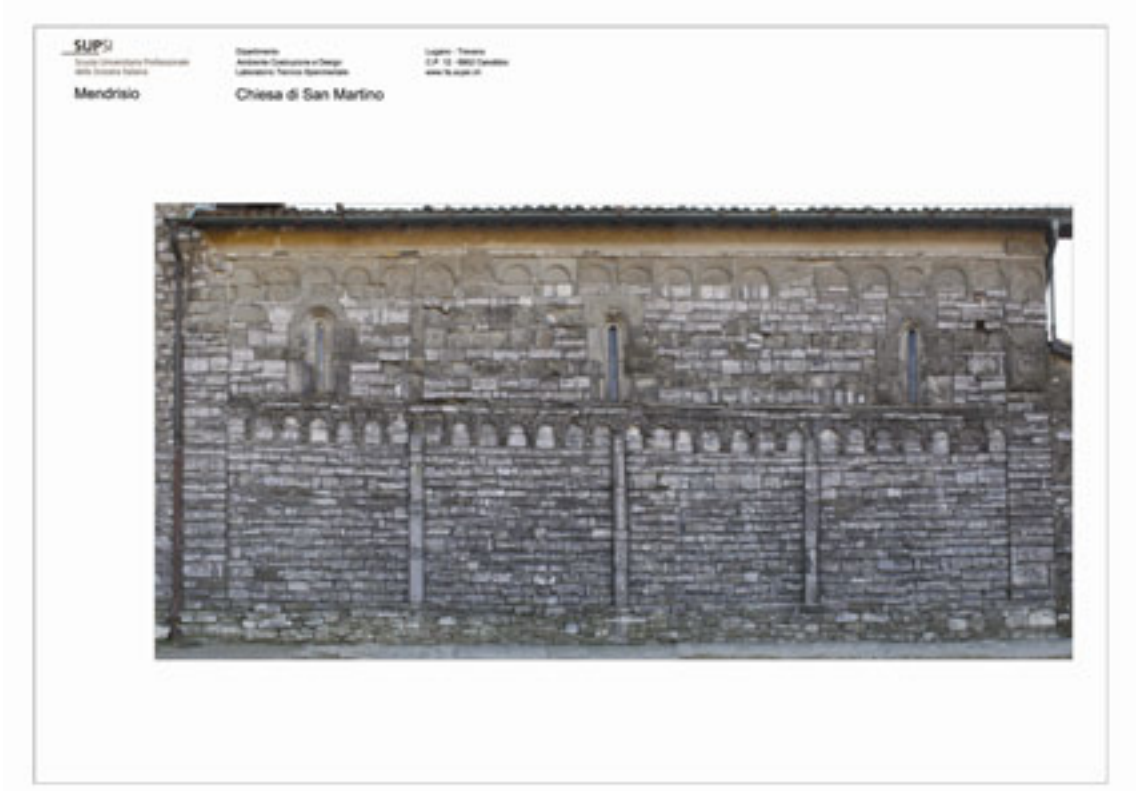

Figure 1. The Romanesque north wall of the St. Martino church in Mendrisio (orthophoto).

8.4

The soapstone of the Romanesque church of San Nicolao in Giornico, Canton Ticino (Switzerland)

Küng Andreas*, Vezzoni Bruno*

*University of Applied Sciences of Southern Switzerland, Dept. Environment, Construction and Design, LTS, PO Box 12, CH-6952 Canobbio (Ticino) andreas.kueng@supsi.ch

The Romanesque church of San Nicolao in Giornico is well known for its architectural and decorative elements made of soapstone and has therefore been chosen for an applied research project called OSMATER (http://istgis.ist.supsi.ch:8001/osmater/) which is dealing with the provenance (quarries) and the transportation routes of stones used for constructions in the past.
First of all a mapping of the soapstone present on external and internal parts of the church has been established. Apart from the sculpted consoles and capitals of the crypt and of the main and side entrance, soapstone has been used for four animals situated at the bottom of the western facade. Parts of the entrance arches, the blind arches and the window frames, as well as the large hexagonal baptismal font and a round holy water stoup inside the church, are also made of soapstone. The next step consisted in trying to characterize macroscopically the soapstone in situ and to establish a classification of different types of soapstone, following and comparing with studies performed on soapstone of the Canton Ticino. Subsequently small samples of every macroscopically established type of soapstone have been taken and examined by means of polarizing microscopy.
The preliminary results revealed that the macroscopically established types of soapstone did not fit the microscopical characteristics. Hence the primary concept consisting in establishing first the type(s) of soapstone and afterwards searching specifically for possible cave(s) of provenience by means of existing literature did not work. As sampling of soapstone from historical monuments is very restricted if at all possible other potential analytical techniques have to take into consideration to get information about its provenance.

Figure 1. Lower part of western facade with main entrance of the San Nicolao church in Giornico. The soapstones are marked with red colour.

REFERENCES

Pfeifer, H.R., Serneels, V.: Inventaire des gisements de pierre ollaire au Tessin et dans les regions voisines: aspects minéralogiques et miniers. Quaderni d'informazione, n. 11, p. 147 - 235. 2000 anni di pietra ollare. Dipartimento dell'Ambiente, Ufficio Monumenti Storici, Ufficio Musei. Bellinzona 1986.

8.5

Spatial and temporal evolution of physico-chemical properties of polymer-modified mortar at the interfaces of large-sized tiles

A. Wetzel*, M. Herwegh*, R. Zurbriggen**,

*Institute of Geological Sciences, University of Berne, Berne, Switzerland
**Elotex AG, Sempach Station, Switzerland

A basic setup for dynamic and spatially resolved investigations of microstructures at the tile-mortar interface of large-sized tiles was described by Wetzel et al. (this volume). In addition, spatially resolved shrinkage and adhesion measurements over sample series allow to reconstruct the evolution of the mortar-tile system. Results indicate that spatially resolved adhesion strength differs from medium values in the centre of the tile over maximum values in-between core and rim reaching minimum values in the vicinity of the rim. This relationship between strength and location was consistent over the entire hardening time. After 6 weeks, a belt of delamination formed few cm away from the rim and grows thenceforward. Dimensional variations of concrete substrate and tile were measured during mortar hardening over a broad mesh and showed differences from tile to substrate. Such variations may affect shear-stresses and its distribution in the mortar, a fact that is critical for local material failure owing to fracturing. The results of this study confirm the typical field observation of tiles, which are only bounded in the centre region and are loose at the edges – a critical situation in the evolution of a potential damage.

8.6

Setup for investigations of tile-mortar interface of large-sized tiles

A. Wetzel*, R. Zurbriggen**, M. Herwegh*

*Institute of Geological Sciences, University of Berne, Berne, Switzerland
**Elotex AG, Sempach Station, Switzerland

In order to reduce the risk of damages, the outdoor application of large-sized fully vitrified ceramic tiles asks for high quality mortars. However, dry-wet, freeze-thaw and hot-cold cycles lead to local cracking of the mortar-tile interface, which in certain cases can result in complete failure. The purpose of the research program (a collaboration of Elotex with the University of Bern, the Empa Dübendorf and CTI the Swiss Commission for Technology and Innovation) is to unravel the evolution of microstructures and the resulting material properties. Here, we describe the basic setup, which allows (i) the reproducible application of large-sized tiles (30 x 30 x 0.8 cm) and (ii) the systematic imaging (through glass tiles) of different aspects such as wetting (mainly as a function of trowel geometry and skin formation), drying, cracking and water ingress. By a quadratic light frame the glass tiles are illuminated from all four sides. This allows to contrast and image microstructures at the mortar-tile interface and to perform in-situ observations as a function of time and distance from the rim. First results of such dynamic studies in combination with the spatially resolved evolution of adhesion strength are presented by Wetzel et al. (this volume).

8.7

Stones on historic buildings and artworks of Switzerland – actual stage of the database

Zehnder Konrad, Kündig Rainer, Baumeler Andreas

Schweizerische Geotechnische Kommission, ETH-Zentrum, 8092 Zürich (konrad.zehnder@erdw.ethz.ch)

The database "Stones on historic buildings and artworks of Switzerland" compiles petrographic and geologic information of the built heritage. It has been collected by Francis de Quervain from the 1950's to the 1980's (F. de Quervain 1983/84; a short presentation of the project was given at the Swiss Geoscience Meeting 2007). The database structure is shown in Figure 1. Presently about 50% of the data (covering the cantons AG, BE, BL, BS, FR, GE, JU, NE, SH, TI, VS, ZH) has been implemented, i.e. about 2500 objects (buildings and sites), 5000 sub-objects (building parts), 230 rocks and 1000 proveniences. Figures 2 and 3 give an example of analysis by geographic distributions of particular rocks on historic buildings. It is important to keep in mind that this information does not represent a statistical distribution. Rather is it an intentional selection which has focused on prominent, typical or easily accessible buildings and works of art. The aim of providing this information in a database is to republish it in an modern way. As a consequence, it can be used more extensively. That will help to better understand and maintain the monuments. It is also intended to update and supplement de-Quervain's collection by new data from various sources. Thus new data can be linked to old data, and architectural or historical information can be related to geographic, petrographic and geologic data in a local as well as in a broader context.

REFERENCES

de Quervain, F. 1983/84: Gesteinsarten an historischen Bau- und Bildwerken der Schweiz, Institut für Denkmalpflege, ETH, Zürich (vol. 1 - 10).

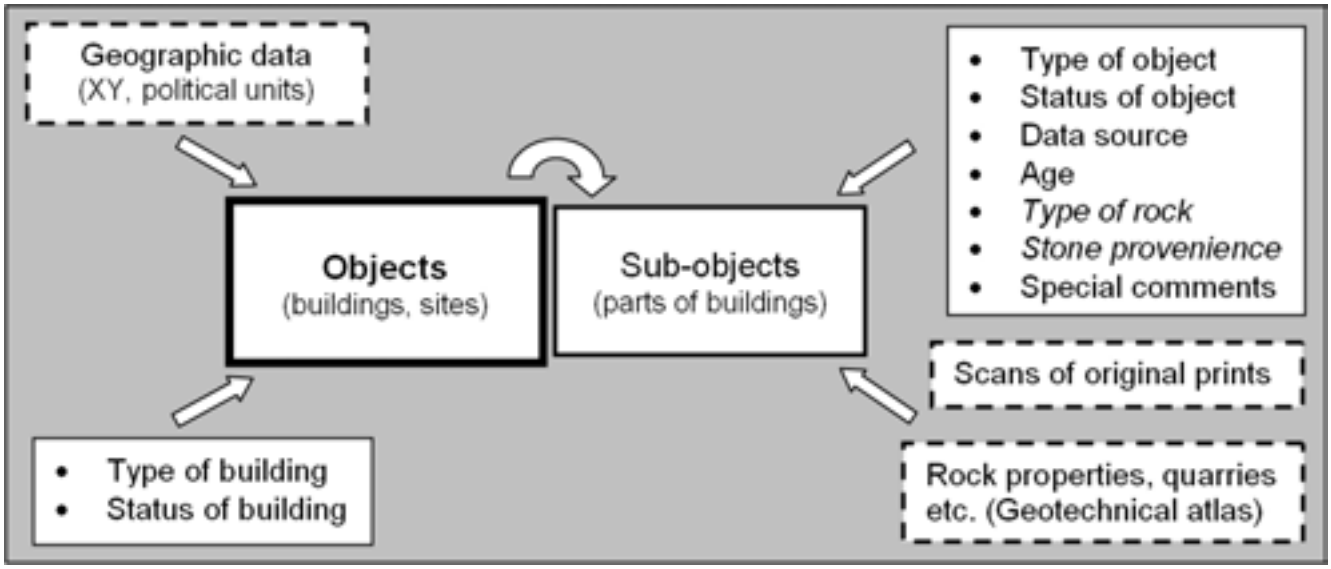

Figure 1. Schematic database structure. The table of georeferenced objects (buildings, sites) is central. It is linked with a sub-table of the relevant building parts and with further tables of specific data, such as rock type etc. Boxes with dashed outlines indicate related data sources and external information.

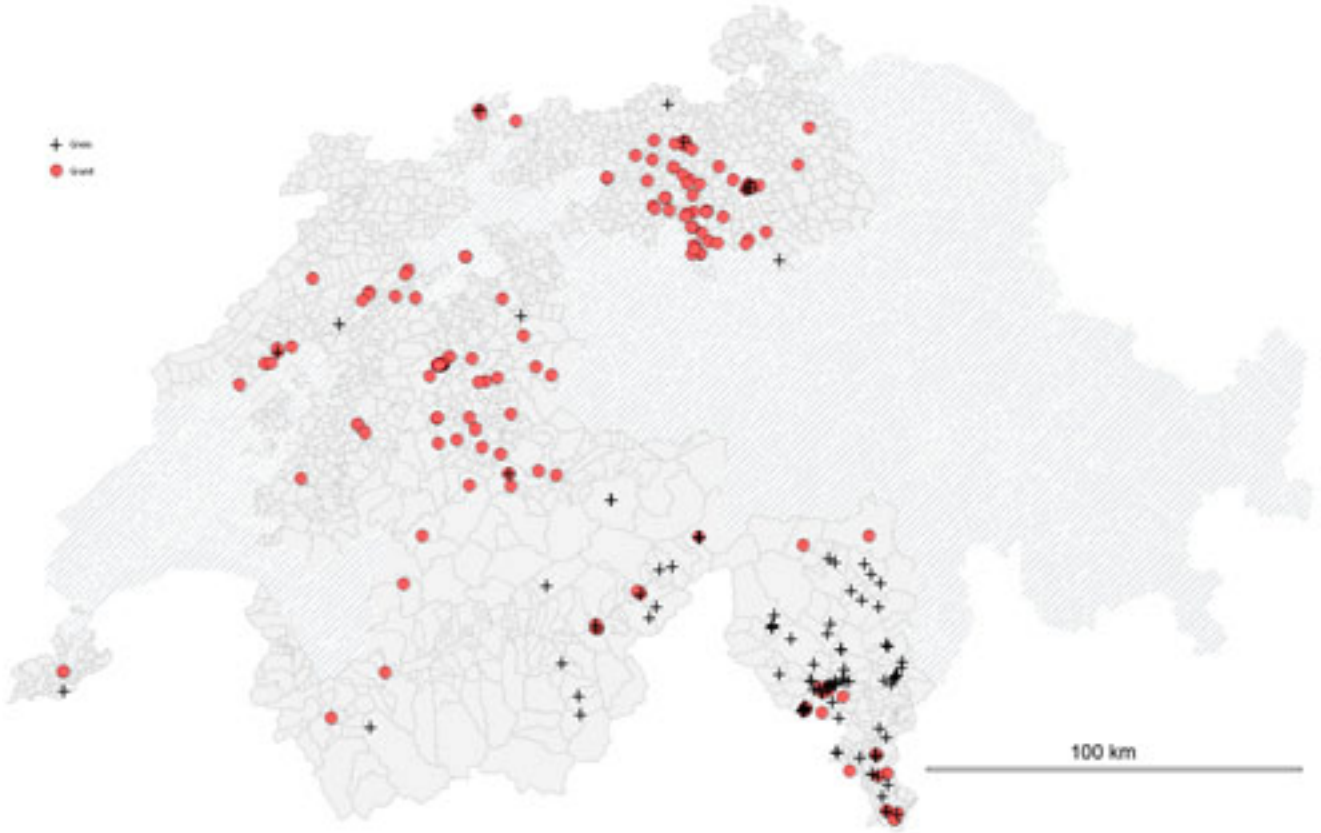

Figure 2. Example of spacial distribution of stones used on historic buildings in Switzerland. Generally, the distribution corresponds to the local and regional availability of stones, i.e. to the nature of the bedrock. In this example, granite (circles) relates to moraines in the northern part of Switzerland and gneiss (crosses) to local debris in southern parts of the Alps. Hatched area is not yet implemented in the database.

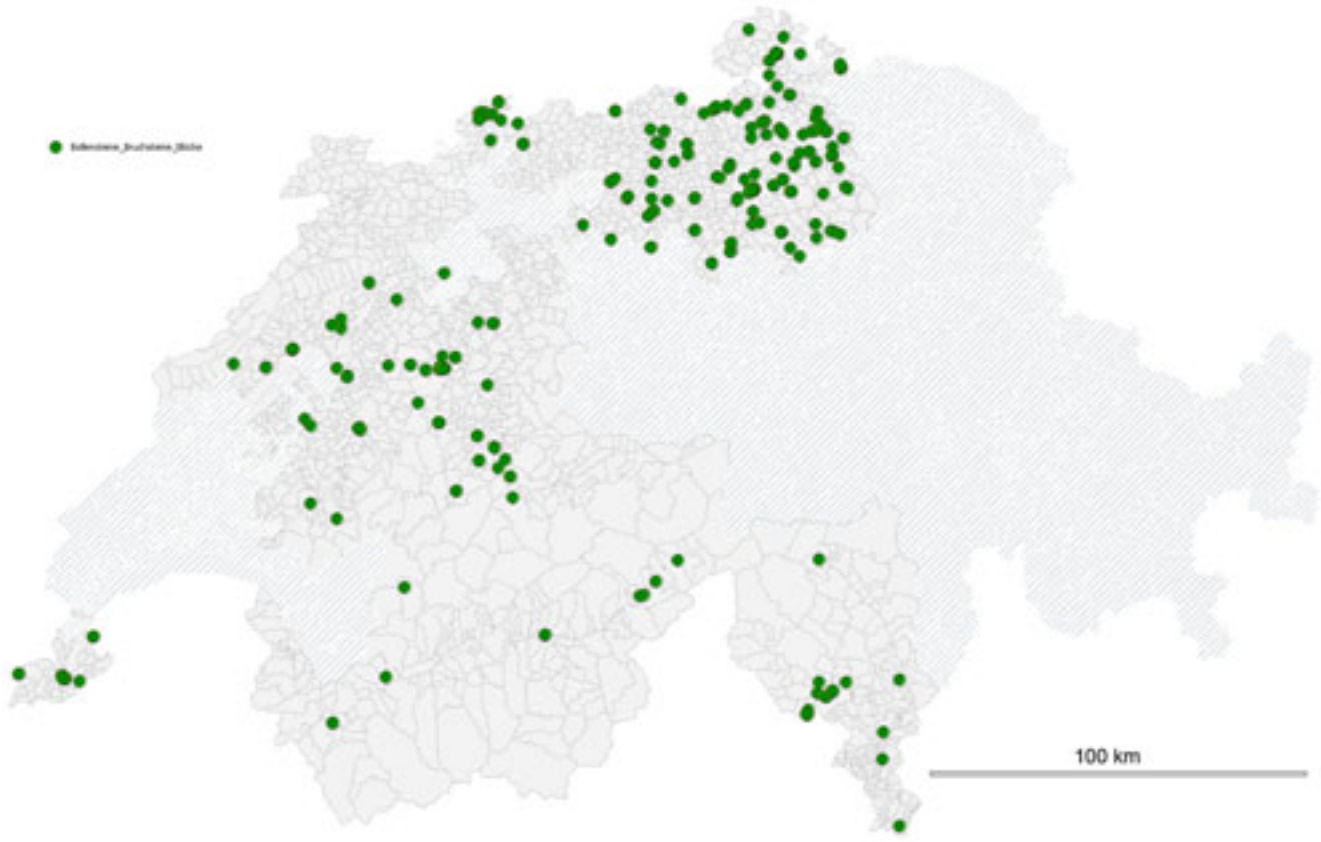

Figure 2. Pebble and rubble stone is widely used in the Alps as well as in surrounding areas according to abundant neogenic sediments of moraines and rivers.

8.8

Construction en pierre massive en Suisse. Le cas des Tre Valli au Canton du Tessin.

Zerbi Stefano*

**Laboratoire de Construction et Conservation 2, Institut d'architecture, Ecole Polytechnique Fédérale de Lausanne, CH-1015 Lausanne (stefano.zerbi@epfl.ch)*

L'intervention porte sur le projet "La Via della Pietra", réalisé à l'EPFL en 2006 et successivement développé pour la Comunità della Riviera. En particulier, on traite de la conception d'une auberge de deux étages et d'un atelier d'expérimentation situés dans la commune de Lodrino. Le système constructif de ces bâtiments est constitué par des éléments en gneiss de 2,2x1,1x0,55m (voir Figure 1).

La méthode choisie se base sur une approche globale au matériau "pierre naturelle": de la ressource jusqu'à sa mise en oeuvre.
Les études géologique, pétrographique et des caractéristiques techniques des roches des Tre Valli, basée sur des sources documentaires (Niggli et al. 1915, Kündig et al. 1997) et sur les informations fournies par les entreprises, ont permis d'établir leur aptitude à l'application structurelle massive.
La connaissance directe de la carrière contemporaine et des techniques d'extraction et de transformation est la base pour une nouvelle stéréotomie qui vise à la production d'éléments modulaires de grandes dimensions. La préfabrication, toujours présente dans le monde de la pierre naturelle, peut aujourd'hui devenir une des clés pour la valorisation de ce matériau de construction.
L'utilisation d'éléments massifs permet d'exploiter des pierres de qualité jugée aujourd'hui inférieure, ce qui est en accord avec une gestion durable de la ressource tendant vers une utilisation totale des matériaux extraits (Dino & Fornaro 2005).
Le développement des solutions constructives répond à un certain nombre de contraintes dont les principales sont celles liées au confort intérieur, à la résistance de la structure en cas de séisme et à l'établissement d'éléments modulaires issus des blocs extraits. Les choix opérés au niveau des détails de construction, de la physique du bâtiment et de la conception de la structure sont présentés ainsi que leurs vérifications.

L'étude ici présentée se situe dans le cadre d'une recherche soutenue par le Fond National Suisse de la Recherche Scientifique visant à démontrer la possibilité actuelle de réaliser des structures porteuses en pierre massive (*Construction en pierre massive en Suisse*, FN-100012-176509).

L'utilisation de matériaux locaux pour la construction est une nécessité non seulement pour réduire l'énergie grise des mêmes, mais aussi afin de favoriser le développement économique et social régional ainsi qu'un plus grand enracinement des bâtisses dans le territoire.
Ce mode de construction, dans un pays comme la Suisse où la pierre naturelle est une ressource disponible, permettrait d'un côté sa valorisation et de l'autre de participer à la sauvegarde de ce secteur économique.
La pierre naturelle comme matériau de construction est aussi un sujet de recherche qui, en Suisse, est désormais en déclin.

REFERENCES

Dino, G.A & Fornaro, M. 2005: L'utilizzo integrale di risorse lapidee negli aspetti estrattivi, di lavorazione e di recupero ambientale dei siti. Giornale di Geologia Applicata 2, 320-327.

Kündig, R. et al. 1997: Die mineralischen Rohstoffe der Schweiz. Schweizerische Geotechnische Kommission. Zürich, Schweizerische Geotechnische Kommission.

Niggli, P. et al. 1915: Die natürlichen Bausteine und Dachschiefer der Schweiz. Bern, Francke.

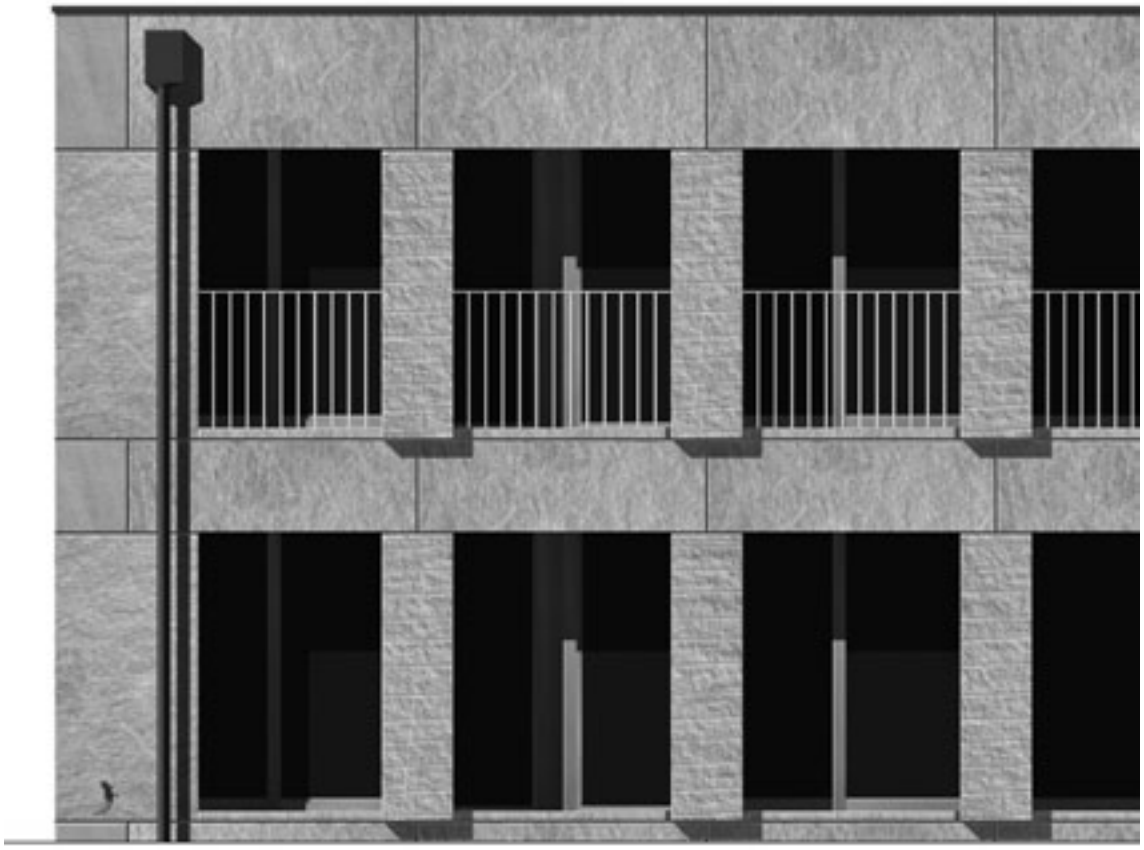

Figure 1. Détail de la façade Sud du bâtiment projété à Lodrino.

9. Natural Hazards and Risks

Giovanni Crosta, Michel Jaboyedoff

Institut de géomatique et d'analyse du risque, Université de Lausanne
Dipartimento Scienze Geologiche e Geotechnologiche, Università di Milano-Bicocca

9.1

Paleoseismological studies on Yedisu seismic gap, eastern part of North Anatolian Fault, Turkey

H. Serdar Akyüz*, Taylan Sançar**, Cengiz Zabcı*, Pınar Gutsuz**, Volkan Karabacak***, Erhan Altunel***, Ziyadin Çakır*, Çağlar Yalçıner***

*Istanbul Technical University, Faculty of Mines, Department of Geology, 34469, Maslak, Istanbul (akyuz@itu.edu.tr)
** Istanbul Technical University, Eurasia Institute of Earth Sciences, 34469, Maslak, Istanbul
***Eskisehir Osmangazi University, Engineering Faculty, Department of Geology, 26480, Eskisehir

North Anatolian Fault (NAF) is one of the most active major faults in Europe. It has a general E-W trend with about 1500 km length throughout northern Turkey and 22 ± 3 mm / year slip rate. During 20th century it is almost totally broken except two important seismic gaps; Marmara Seismic Segment in the west and Yedisu Seismic Segment in the east (Figure 1). This paper presents paleoseimological studies on Yedisu Seismic Segment (YSS).

YSS locates on eastern part of North Anatolian Fault between Erzincan city and Yedisu town of Bingöl city (Figure 2). Western part of the YSS was broken in 1992 with a Ms=6.8 earthquake while eastern part was broken in 1949 with Ms=6.7 earthquake (Figure 1). A 80 km-long fault is remained unbroken between eastern part of Erzincan Basin and Yedisu town. According to Ambraseys & Finkel (1995) this part of the fault was broken lastly in 1784, i.e. 224 years ago. The aim of this study which is supported by TUBITAK (The Scientific & Technological Research Council of Turkey, Project no: 106Y174) is to reveal seismic risk of YSS with paleoseismological data.

The fault geometry, segmentation and offset structures were analysed firstly on aerial photographs and topographical maps, then observed and drown in the field on a 1/25000 topographical map. Three trench sites were also defined in convenient places. First site was chosen in the western part of the YSS, Sarikaya site (Figure 2). Trench was opened perpendicular to the fault trace and trench wall was logged. Fine grained slope deposits and fault branches indicate two earthquake evidences. Second and third trench sites are close to eastern end of YSS (Figure 2). Karapolat Trench was opened perpendicular to fault on distal part of a large recent fan deposits. Trench stratigraphy evidenced two past earthquakes as well. The last trench, named as Tokmanik, was digged deeper due to convenient underground water level. At least 5 past earthquake events were determined on the trench walls. Charcoal samples collected in critical level in all trenches were sent to Arizona University Radiocarbon Laboratory for dating. Dating results together with historical records will give us earthquake recurrence period of Yedisu Seismic Segment. If the date of past earthquakes have periodical behaviour, this will help to predict the date of future earthquake on Yedisu Fault.

REFERENCES

Ambraseys, N.N. & Finkel, C.F. 1995: The Seismicity of Turkey and adjacent areas: a historical review, 1500-1800. Eren, Istanbul, p 240.

Barka, A., Akyüz, H.S., & 18 others, 2002: The surface rupture and slip distribution of the August 17, 1999 zmit earthquake, M=7.4, North Anatolian Fault. Bull. Seism. Soc. Amer. 92, 43-60.

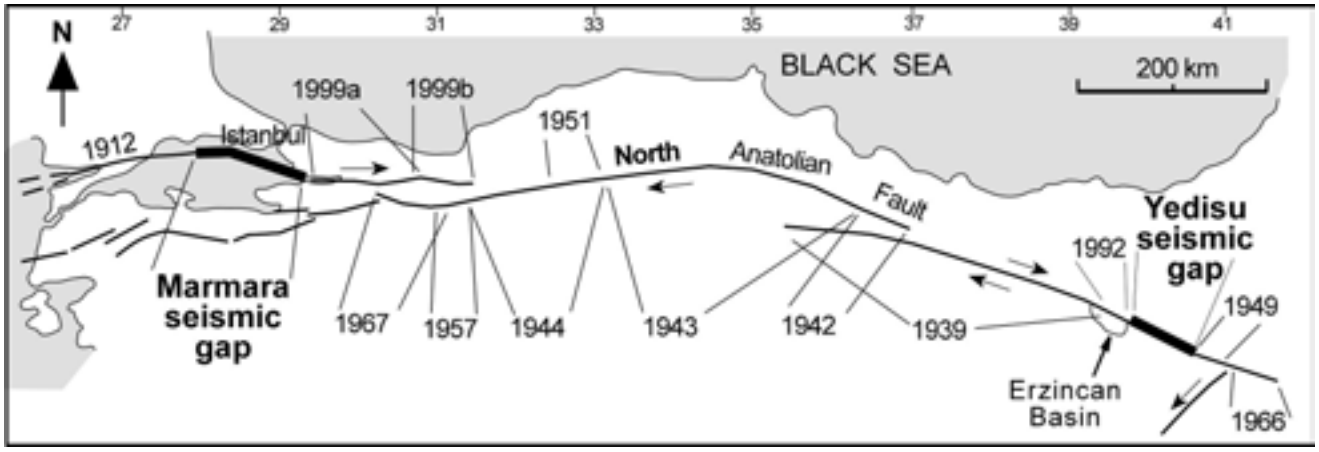

Figure 1. 20th century destructive earthquakes (Barka et al. 2002) and seismic gaps on North Anatolian Fault.

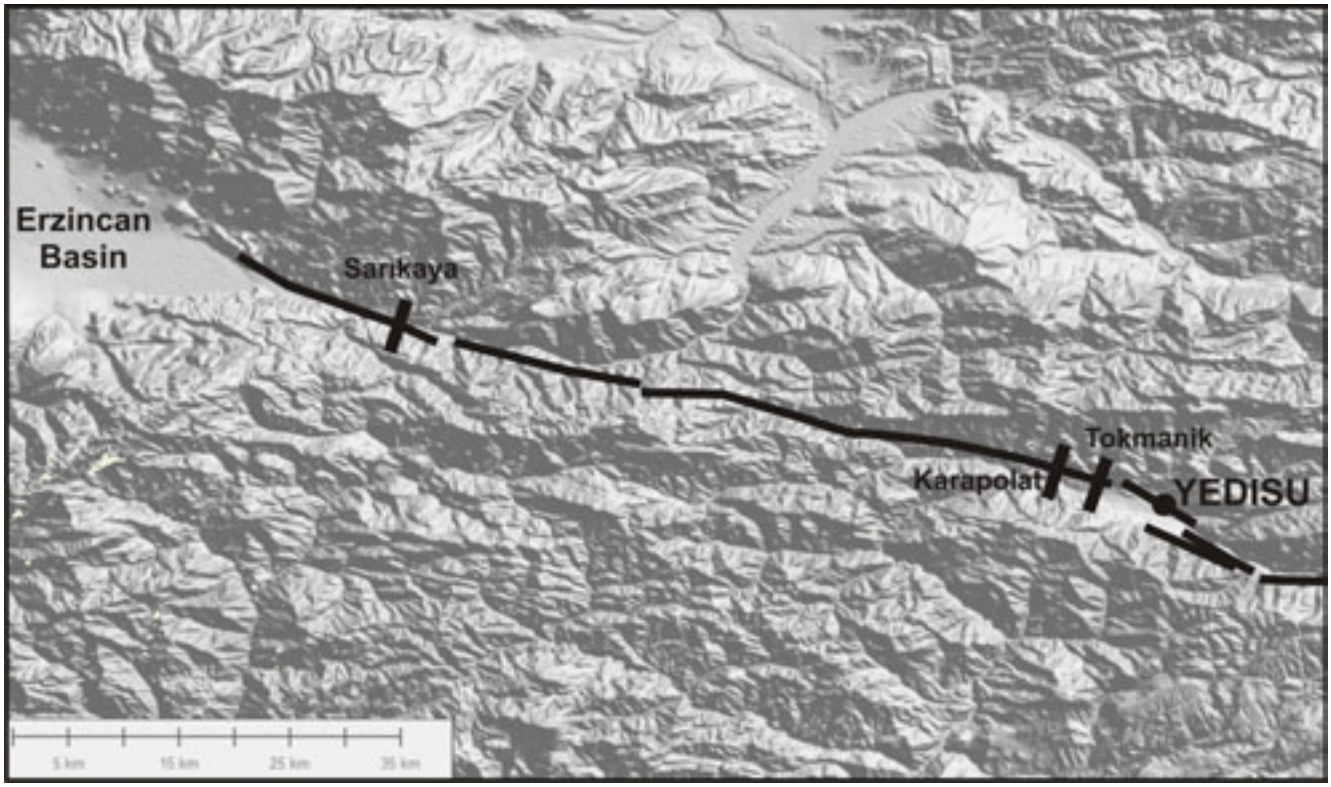

Figure 2. The geometry of Yedisu Seismic Segment and location of trench sites.

9.2

Biomarkers as effective and beneficial tools in petroleum caused natural hazards

Alizadeh Bahram*, Bagheri Soheila* & Hoseini Seyed Hossein *

*Department of Geology, Faculty of Science, S. Chamran University, Ahvaz, Iran. (alizadeh@scu.ac.ir)

In the Zagros oil rich basin comprising more than 40 huge and ten giant oilfields, unavoidebla natural hazards sometimes even force people to evacuate their homes. The aim of this study was to determine the genetic origin of oil seepages occurring in Masjid-e-Soleiman (MIS) oilfield and in Dalaki river near Nargesi oilfield. In order to inject gas in the Nargesi Oilfield (South Dezful Embayment), and at the same time prevent natural disaster it is necessary to establish the origin of oil seeps polluted with H_2S in Dalaki area.

Numerous oil seep polluted with H_2S have been found in Masjid-e-Soleiman oilfield (first oilfield in the Middle East, North

Dezful Embayment), which polluted some areas, forcing local people to leave their houses.

Asmari oil samples from Masjid-e-Soleiman oilfield correlated with oil seeps from Seeberenj and Dare-Khersan and Asmari/ Jahrum reservoir oil from Naregsi oilfield correlated with Dalaki's oil seepages by Gas Chromatography and Gas Chromatography-Mass Spectrometry.

Dalaki's oil seeps exhibit evidences of biodegradation and mix kerogens, this explains the low saturate fraction (29-38 %), the aromatic-asphaltic nature of the oil seeps and an important depletion in the homohopane series. The oil seeps are characterized by high predominance C_{29} to C_{30} hopane ratios (1.25-1.8), low ratios of C_{34} over C_{35} (1.42-1.62), and the low diasterane abundance (C_{27}-C_{29} Dia/Reg Steranes: 0.33-0.44). These characteristics suggest that the oil seeps originate from carbonate marine source rocks (Sañchez, C. & Permanyer, A., 2006). On the other hand the reservoir oil samples of Nargesi oilfield are characterized by high contents of saturates, Pr/Ph ratios below 2, the dominance of C_{30} hopanes over the C_{29} hopane (C_{29}/ C_{30}<1), low ratios of C_{34}/C_{35} (1.02- 1.4) homohopanes and diasteranes are more abundant. These properties suggest that the oils were generated mainly from marine shale facies. The C_{29}/C_{30} hopane and Dia/Reg sterane ratios and a relatively high abundance of oleanane in the oil seepages gives the best evidence of different source rocks for oil and oil seep samples. This is also supported with thermal maturity parameters such αα 20/(20S+20R) sterane and T_s/T_m ratios.

The discrepancy in the biomarker indicators gives the assurance of diverse origin of oils from reservoir and from Seepages (Fig. 1a). Finally the constant seepage discharge even after gas injection into the reservoir proved the oil correlation to be very reliable and trustworthy.

In MIS oilfield, geochemical parameters, such as high ratio of C_{27} over C_{29} sterane (1.01-1.2), the low ratio of C_{29} to C_{30} hopanes (0.63-0.71), as well as the star diagram of tricyclic terpane showed the best similarity between oil and oil seeps. For the Asmari oil and oil seepages, high ratios of steranes to hopanes are very typical (0.60 for oil and 0.48-0.63 for oil seeps) and low ratio of C_{34} over C_{35} homohopanes (0.84-1.15) that are characteristics for algae organic matter deposited within anoxic environment (Alimi et al., 2007). This is also supported by low amounts of C_{30} moretane relative to C_{30} hopane (C_{30}βα/C_{30}αβ: 0.09–0.11), indicative of strong marine input to the source rock. Both oil and oil seeps present low C_{26} over C_{25} (0.66-0.95) and C_{24}/C_{23} (0.45-0.68) tricyclic terpane ratios (less than 1), low abundance of C_{29}/C_{30} hopane (0.63-0.71) and the occurrence of diasteranes, suggest carbonate-marl source facies for oil and oil seeps.The ratios of 20S/(20S+20R) for ααα C_{29} steranes (0.48-0.51) and ββ/ (αα+ββ) for 5α-C_{29} steranes(0.5-0.54) have been evaluated together with the ratios of 22S/ (22S+22R) for C_{32} homohopanes (0.52-0.54). Based on these ratios, all samples are well within the oil window (Rogers et al., 1999). Age-specific biological marker including, Extended Tricyclic Ratio (0.5-0.52), C_{28}/C_{29} (0.79-0.89) sterane ratios, and Oleanane Index (<0.2) show that oil seeps have similar source age as Upper Jurassic-Cretaceous.

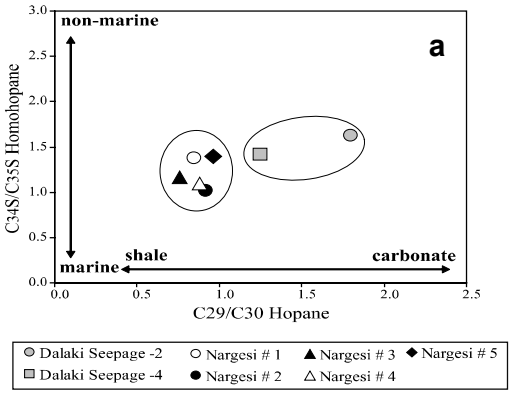

Figure1. Cross plot of C_{29}/C_{30} hopane and C_{34}/C_{35} homohopane, a, clearly indicating two different organic facies.The triangle diagram of diasterane distribution in MIS oilfield, b, demonstrating similar depositional environment for both reservoir oils and oil sepages.

The geochemical parameters showed that the oils and oil seeps were formed in similar depositional environment and have identical thermal maturity level (early oil window). In triangle diagram, (Fig. 1b), the C_{27}-C_{28}-C_{29} diasterane distribution for Asmari oil and oil seeps are located in the same vicinity indicating the source of initial organic matter being one and the same. Finally it can be concluded that the source of pollution in the area is Asmari reservoir oil and due to its pressure drop, the previously condensed H_2S poisonous gas is now free to escape through cap rock fractures, forcing people to evacuate their houses. All these well demonstrate the proficiency of geochemical parameters in predicting and managing natural hazards.

REFERENCES

Alimi, H., Alizadeh, B., Jarvie, D.M., Adabi, M.H., Tezheh, F., Jarvei, B. (2007). Geochemical Evaluation of Crude Oils from Asmari and Bangestan Reservoirs in Marun Oilfield, SW IRAN. 23rd International meeting on Organic Geochemistry, IMOG, Torquay, United Kingdom Sep. 2007.

Sa´nchez, C., Permanyer, A., 2006. Origin and alteration of oils and oil seeps from the Sinu´-San Jacinto Basin, Colombia. Organic Geochemistry, v. 37, p.1831-1845.

Rogers, K. M., Collen, J.D., Johnston, J.H., Elgar, N.E., 1999. A Geochemical appraisal of oil seeps from the East Coast Basin, New Zealand, Organic Geochemistry, v. 30 p. 593-605.

9.3

Sar Interferometric Point Target analysis and interpretation of aerial photographs for landslides investigations in southern switzerland

Ambrosi Christian*, Strozzi Tazio**

* *SUPSI, Istituto Scienze della Terra CP 72, CH 6952 Canobbio (christian.ambrosi@supsi.ch)*
** *GAMMA Remote Sensing, Worbstrasse 225, CH 3073 Gümligen (strozzi@gamma-rs.ch)*

Information on landslide displacement from SAR Interferometric Point Target Analysis (IPTA) and sketch maps from aerial photography interpretation are combined for the study of landslides in Ticino, Southern Switzerland. For current ITPA investigations, ENVISAT and RADARSAT SAR acquisitions over the Swiss territory are used. Numerous unstable phenomena are considered in this mountainous region, with an elevation range from approximately 200 m a.s.l. to more than 3000 m a.s.l. The results achieved with IPTA are attractive to complement aerial photographs interpretation for the evaluation of the state of activity of landslides over villages and in sparsely vegetated areas with numerous exposed rocks. On the other hand, over vegetated areas (forests and meadows) IPTA failed to retrieve displacement information. Because displacement from InSAR is recorded along the satellite line-of-sight direction, IPTA cannot be directly use for the determination of the intensity of landslides in hazard mapping. In general, the actual displacement rate is larger than that recorded with InSAR. Over alpine areas characterized by sparse vegetation, where snow cover limits the availability of a large number of SAR acquisitions, conventional InSAR was successfully applied to estimate the motion of rockglaciers and other periglacial phenomena. For vegetated areas and relatively rapid landslides L-band InSAR (JERS-1 SAR and ALOS PALSAR) has been found to be an efficient solution.

9.4

Interdisciplinary approaches to recognition, analysis and modelling in sackung system and large landslides in southern Swiss Alps

Ambrosi Christian*, Pera Sebastian*

* *SUPSI, Istituto Scienze della Terra CP 72, CH 6952 Canobbio (christian.ambrosi@supsi.ch)*

A very large Deep-Seated Gravitational Slope Deformations and large landslides, affecting the slopes of Swiss Southern Alps, have been recognised and mapped. Several active rotational and translational deep seated landslides occur in the lower part of the slopes, often in association with rockslides at different scale. These phenomena show a different stage of evolution along the flanks of the ridges.
Some of these landslides (Pontirone, Osco, Faido) has been recognised through different techniques. In particular, it has been characterised by aerial photo interpretation, field surveys, tracer tests and analysis of detailed airborne Lidar DEM.
Rock masses, including poly-deformed orthogneisses, paragneisses and dolostones, are affected by systems of impressive gravitational morpho-structures including ENE trending open trenches, scarps and counterscarps forming graben-like structures.
Geodetic measurements (optical targets and GPS points) and satellite radar interferometry (DinSAR) data demonstrate the activity of the gravitational features affecting both the upper and lower part of the slopes.
The analysis of geological, geomorphological, hydrogeological, in situ stress, geodetic and uplift data, have been used to demonstrate the possible relationships among geological, structural, topographic and gravitational features. Numerical 2D modelling have been used to evaluate failure in presence of elastic, elasto-plastic materials and groundwater flow. This allow to verify “model” sensitivity to some factors as slope geometry, structural features, groundwater conditions and to determinate the triggers factors of these instabilities.
On this basis we discuss the possibility that the geological, tectonic and hydrogeological framework can play an active/passive role in the onset and development of the sackung system and related landslides.

9.5
A GIS-tool for risk assessment due to natural hazards in mountain regions

Baruffini Mirko*, Baruffini Moreno* & Thüring Manfred*

*Istituto Scienze della Terra IST-SUPSI, C.P. 72, CH-6952 Canobbio (ist@supsi.ch)

During the last decades land-use increased significantly in the Swiss (and European) mountain regions. Due to the scarceness of areas suitable for development, anthropic activities were extended into areas prone to natural hazards such as avalanches, debris flows and rockfalls (Smith 2001). Consequently, an increase in losses due to hazards can be observed. To mitigate these associated losses, both traditional protective measures and land-use planning policies are to be developed and implemented to optimize future investments. Efficient protection alternatives can be obtained considering the concept of integral risk management.

Risk analysis, as the central part of risk management, has become gradually a generally accepted approach for the assessment of current and future scenarios (Loat & Zimmermann 2004). The procedure aims at risk reduction which can be reached by conventional mitigation on one hand and the implementation of land-use planning on the other hand: a combination of active and passive mitigation measures is applied to prevent damage to buildings, people and infrastructures.

Considering different hazard processes and their impact on the built environment, multiple solutions for the protection of new buildings and infrastructures and the upgrade of existing inventory exist. Consequently, the concept of local protection should be embedded within the framework of integral risk management strategies. Planned early, expenditures for the implementation of local structural measures are comparatively low related to the total cost of the planned construction. Recent studies suggested a considerable decrease in vulnerability, if local structural protection is implemented (Holub & Fuchs 2008).

As part of the Swiss National Science Foundation Project 54 “Evaluation of the optimal resilience for vulnerable infrastructure networks - An interdisciplinary pilot study on the transalpine transportation corridors” we study the vulnerability of infrastructures due to natural hazards.

The Swiss system for risk analysis of gravitational natural hazards (BUWAL 1999) offers a complete framework for the analysis and assessment of risks due to natural hazards, ranging from hazard assessment for gravitational natural hazards, such as landslides, collapse, rockfall, flooding, debris flows and avalanches, to vulnerability assessment and risk analysis, and the integration into land use planning at the cantonal and municipality level. The scheme is limited to the direct consequences of natural hazards.

We conduct a research referred to the concept of the evaluation of the resilience within the framework of integral risk management with the aim to develop a system which integrates the procedures for a complete risk analysis in a Geographic Information System (GIS) toolbox, in order to be applied to our testbed, the Alps-crossing corridor of St. Gotthard.

A simulation environment, RiskBox, is developed within the open-source GIS environment GRASS (Geographic Resources Analysis Support System) and a database (PostgreSQL) in order to manage a infrastructure data catalog. The targeted simulation environment includes the elements that identify the consecutive steps of risk analysis: hazard – vulnerability – risk.

Module hazard integrates applications to simulate natural hazard processes in order to assess their degree of hazard. Module vulnerability integrates vulnerable objects and attributes them with the necessary meta-data. Module risk integrates the necessary analysis approaches in order to conduct the risk analysis based on the former two modules.

The final goal of RiskBox is a versatile tool for risk analysis which can be applied to other situations. There are specific needs for an improvement of the level of information for affected people, legal regulations and risk transfer mechanisms (ARMONIA Project 2007). These needs would not only result in an increased risk awareness of people concerned, but also in an enhanced enforceability of necessary legal regulations, such as land-use planning rules and building codes. So, the individual responsibility could be strengthened and the society will be enabled to an alternatively use of the resources in a more cost-efficient way.

The initial results of the experimental case study shows how useful a GIS-based system can be for effective and efficient disaster response management.
We present the concept and current state of development of RiskBox and its application to the testbed, the Alps-crossing corridor of St. Gotthard.

REFERENCES
ARMONIA Project 2007: Land use plans in Risky areas fro Unwise to Wise Practices – Materials 2nd conference. Politecnico di Milano.
BUWAL 1999: Risikoanalyse bei gravitativen Naturgefahren - Methode, Fallbeispiele und Daten (Risk analyses for gravitational natural hazards). Bundesamt für Umwelt, Wald und Landschaft (BUWAL). Umwelt-Materialen Nr. 107, 1-244.
Holub, M. & Fuchs S. 2008: Benefits of local structural protection to mitigate torrent-related hazards. In: Brebbia, C.A. & Beritatos, E. (eds) 2008: Risk Analysis VI: Simulation and Hazard Mitigation. Institute of Technology, UK and University of Thessaly, Greece, 401-411.
Loat, R. & Zimmermann, M. 2004 : La gestion des risques en Suisse (Risk Management in Switzerland). In: Veyret, Y., Garry, G., Meschinet de Richemont, N. & Armand Colin (eds) 2002: Colloque Arche de la Défense 22–24 octobre 2002, dans Risques naturels et aménagement en Europe, 108-120.
Smith, K. 2001: Environmental hazards. Assessing the risk and reducing disaster. Third edition. London

9.6

Multidisciplinary investigations and back-analysis of a periglacial rock fall event: Tschierva rock fall

Fischer Luzia *, Amann Florian**, & Huggel Christian*

* *Glaciology, Geomorphodynamics & Geochronology, Department of Geography, University of Zurich, Switzerland (luzia.fischer@geo.uzh.ch)*
** *Group of Engineering Geology, Department of Earth Science, ETH Zurich, Switzerland*

Slope stability of steep rock walls in glacierised and permafrost-affected high-mountain regions is controlled by many different factors such as geological and geomechanical characteristics, topography, hydrology and also glaciation and permafrost occurrence. Changes in one or more of these factors may reduce the slope stability and eventually lead to a rock fall event. The atmospheric warming during the 20th century has caused pronounced effects in the glacial and periglacial belts of high mountain areas. The changes are made strikingly evident by, for example, the retreat of Alpine glaciers and less immediately visible but also very significant are changes in mountain permafrost distribution and temperature. Therefore, cryospheric factors are most prone to ongoing climate changes. In this study the influence of different factors and mechanisms determining slope stability is investigated, based on a case study of the Tschierva rock fall event.

The Tschierva rock fall occurred on October 19, 1988 from the western flank of Piz Morteratsch (3751 m asl, Engadin, Switzerland) on Tschierva glacier with an estimated volume of approximately 0.3x10^6 m^3. The rock mass detached at about 3200 m a.s.l. and fell on the Tschierva glacier probably incorporating additional rock-debris from the slope below the detachment zone and stopped on the glacier at an elevation of about 2700 m a.s.l.

The primary objective of the presented study is the back-analysis of the Tschierva rock fall and the investigation of possible geological, geomechanical and climate-related glaciological disposition factors. Therefore, the detachment zone is investigated in a multidisciplinary approach based on in-situ geological field work, associated geotechnical investigations, morphometric analyses, permafrost modelling, glaciation history and subsequent numerical stability modelling with UDEC (Universal Distinct Element Code by Itasca). Based on these analyses, the influence and sensitivity of the different factors and processes on the slope failures is assessed.

Numerical slope stability modeling was performed to examine different scenarios of possible failure mechanisms. Modelling of the unloading of the pleistocene glacial overburden showed that subsequent redistribution of stress and strain fields in the flank have a strongly controlling influence on the geometry of the detachment zone by the opening of unloading joints. A sensitivity analysis of geotechnical parameters additionally showed that the cohesion of the discontinuities was a fundamental parameter. Coupled hydro-mechanical modeling demonstrated that slope stability was very sensitive to changes in water pressure. The existing fault zone crossing the rock slope induced an elevated water inflow due to the higher permeability and might therefore be, together with the long-lasting effects of ice unloading, a main factor for the slope instability.

In conclusion, our analysis could identify some essential factors of slope stability in relation with the geological setting, glacier retreat and permafrost degradation. However, it has also shown that the understanding of the physical processes and the adequate integration in numerical slope stability models needs more research, in particular in view of the hazards that are to be faced.

9.7

Applying altimetry and in-situ data to compute point-wise MSL for inland waters, case study: Caspian Sea

Forootan Ehsan*, Sharifi Mohammad Ali*, Nikkhoo Mehdi**, & Dodge Somayeh***

* *Surveying and Geomatics Engineering Department, College of Engineering, University of Tehran. Northern Amirabad St, Tehran, Iran, Tel:00982161114251, Fax:00982188008837 ({eforootan | sharifi }@ut.ac.ir)*
** *Surveying and Geomatics Engineering Department, KNT University of Technology, Iran. mehdi_nikkhoo@yahoo.com*
***University of Zurich, Winterthurerstr. 190, CH-8057 Zurich*

The Caspian Sea is the largest enclosed body of water on the Earth by area, variously classed as the world's largest lake or a full-fledged sea. The sea is fed by numerous rivers including the Volga, Ural, Terek, and Kura rivers. In the last 25 years, the total surface area has varied from 360000 to 400000 km^2 due to high water level variations. These variations have shown oscillations between -26 and -29 meters (with respect to the zero ocean level) during the last hundreds years.
The largest uncertainty for the Caspian Sea is concerning with the average water level, which by itself is not subject to a statistical distribution, but rather more to a trend. Hence, we applied two major datasets to compute the water fluctuations: 1) in- situ measurements; in this case provided by the Iranian Caspian environmental study center. 2) derived water levels from satellite altimetry mission; we used T/P altimeter data, which are performed, at the Jet Propulsion Laboratory, California and cover repeated T/P mission cycles 11 to 400, spanning more than 10 years. The results of these observations are considered as a set of virtual tide gauges, with a sample rate of every 9.915625 days. Beside that, we applied in-situ observations to reveal the trend and evaluate the altimetry results.
Analysis of T/P observations show that there is a phase differences between various locations in the Sea. In fact, 80% of the input side of the water balance influx comes from the Volga River. It seems that the cause of these differences is related to the distance between locations to the River of Volga. Change in discharge of Volga does not expand all over the sea immediately but the locations that are nearer to the outfall of the river are influenced sooner than the other locations. Therefore, it is necessary to investigate the variations of each point in the Caspian Sea separately in order to discover the environmental variables using time series analysis and then computing the point-wise MSL.
In short the results of our analysis proved that between January 1993 and March 1995 the Caspian mean sea level rose at an average rate of 15 mm/month then followed by a fall at a rate of -5.5 mm/month until January 2003. Beside that, a point-wise MSL is computed for the Caspian Sea during 1993 to 2002. The results will be discussed in more detail in the full paper.

REFERENCES

Avakian, A. B. and V. M. Shirokov. 1994. Rational Use and Protection of Water Resources. Ekaterinburg: Publ. House "Victor" (in Russian).

Benada, J. R., 1997, TOPEX/POSEIDON User's Handbook , Generation B (MGDR-B) Version 2.0, D-11007, Jet Propulsion Laboratory, California Institute of Technology under contract with the National Aeronautics and Space Administration.

Birkett, C.M., 1995a: The contribution of TOPEX/POSEIDON to the global monitoring of climatically sensitive lakes, JGR-Oceans, Vol.100, C12, pp.25, 179-25, 204

Caspian TDA, report volume 2, 2002., Transboundary diagnostic analysis for the Caspian sea. The Caspian sea environment programme., Baku, Azerbaijan. www.caspianenvironment.org

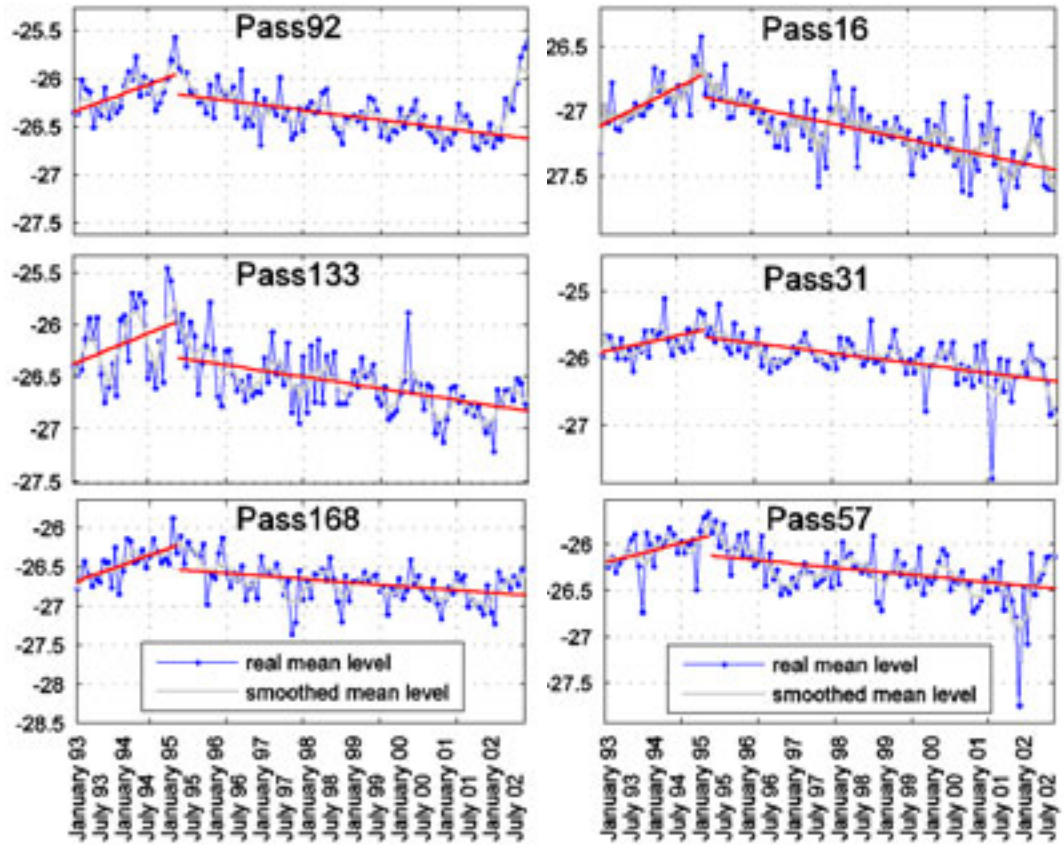

Figure 1. Mean level variations of SSH along 6 passes in Caspian Sea.

9.8

The Deep Seated Gravitational Slope Deformation of Landarenca (Graubünden, Switzerland): A Geological-Geotechnical Analysis

Fossati David*, Kos Andrew*

*Group of Engineering Geology, Geological Institute, Wolfgang-Pauli-Str. 15, 8093 Zürich (fossatid@student.ethz.ch)

A complex deep seated gravitational slope deformation (DSGSD) located in the south western part of the Calanca valley (Graubünden, Switzerland), in the area of Landarenca will be described using an multi-disciplinary approach, where field surveys, remote sensing and geodetic measurements are applied to the site for the first time. The DSGSD lies within isoclinally folded gneisses and mica schists of the Adula and Simano nappes. Geomorphologic features such as terraces, steep rock cliffs, tension cracks, scarps, counterscarps and combined scarp-tension crack structures characterize the area. The area of the DSGSD involves at least 1 square kilometre with an approximate volume of 185 million cubic meters. An integration of results indicate the DSGSD to be slightly active with velocities of up to 8mm per year. Movements involve discontinuous creeping, i.e. a combination of creeping and sliding and the DSGSD can be defined as a slightly active, deep seated kink band slumping, in a developed stage.

REFERENCES

Amann, F. 2006: Grosshangbewegung Cuolm da Vi (Graubünden, Schweiz) – geologisch-geotechnische Befunde und numerische Untersuchungen zur Klärung des Phänomens. Diss. Univ. Erlangen-Nürnberg.

Agliardi, F., Crosta, G. & Zanchi, A. 2001: Structural constraints on deep-seated slope deformation kinematics. Eng. Geol. 59 (1-2), 83-102.

Kieffer, D. S. 1998: Rock slumping: A compound failure mode of jointed hard rock slopes. PhD Thesis. University of California, Berkeley.

9.9

Recent experiences from Swiss projects in risk reduction in South America

Christian Huggel*, Sebastian Eugster**, Juan Manuel Ramírez***, Raphael Worni*, ****

Glaziologie, Geomorphodynamik & Geochronologie, Geographisches Institut, Universität Zürich, Winterthurerstrasse 190, 8057 Zürich (christian.huggel@geo.uzh.ch)
**Swiss Agency for Development and Cooperation, Lima, Peru*
***Swiss Agency for Development and Cooperation, Bogotá, Colombia*
****Department of Environmental Sciences, ETH Zürich*

Extensive parts of South America are characterized by mountain topography and seasonally intense rainfall. Accordingly many regions suffer from repeated landslides, debris flows, floods. These hazards are partly linked, and exacerbated by volcanic activity along the Andean mountain chain. Additionally, in some regions of the Andes, disasters related to glaciers have claimed thousands of victims. Such extreme events occurred in the 1970s in Peru with an ice-rock avalanche from Huascaran and in the 1980s in Colombia with lahars from Nevado del Ruiz. Since the time of these disasters important advances in disaster risk reduction have been made on the national levels. In Colombia, for instance, the failures related to the Ruiz disaster triggered the creation of a National System for Prevention and Attention of Disasters (SNPAD).
However, it continues to be important to improve the current situations to avoid any significant type of disaster. Critical improvements can be made on an institutional and community-based level, combined with the implementation of advanced technological and scientific know-how. Effective disaster risk reduction takes place on a local level but is embedded in the regional and national institutional context.
Here we report on recent experiences from projects of the Swiss Government (Swiss Agency for Development and Cooperation, SDC) in collaboration with the University of Zurich and several national institutions in Colombia and Peru. In Peru, a Peruvian – Swiss programme on adaptation to climate change (PACC) has recently been initiated and aims at identifying climate change impacts in the Andean Cuzco and Apurimac regions in Peru, and to implement a set of adaptation measures to reduce adverse effects of climate change. The PACC focuses on three major areas: (i) disaster risk reduction; (ii) water resource management; and (iii) food security. In a climate change context it is particularly important to approach risk reduction in an integrated perspective considering the related areas and combined effects.
In Colombia, activities have focused on volcanoes, glaciers and rainfall triggered landslides. The 2007 crisis and eruption of Huila Volcano has made necessary a close collaboration of science and civil authorities to avoid disasters that could have been caused by major debris flows originating from volcano-ice interaction. With respect to landslides important experiences have been gained with the implementation of an early warning system.
An effective landslide early warning system is a major challenge in practice. Difficulties are found on a technical-scientific level (e.g. application of rainfall-landslide thresholds) but also on an institutional and community-based level. The early warning system is only successful if the inter-institutional coordination works smoothly in an emergency and if it is also borne by the local population. The perception of the risk by the local people in their livelihood context exerts a significant control on the response to risk reduction efforts. Their views are often diverging from those of public authorities and experts, which has to be taken into account for more effective disaster reduction.

9.10

Theoretical basis for shadow angle variability and implications

Jaboyedoff Michel*, Pedrazzini Andrea*

* *Institute of Geomatics and Analysis of Risk, Faculté des géosciences et de l'environnement, University of Lausanne, CH-1015 Lausanne - Switzerland (michel.jaboyedoff@unil.ch)*

Since Heim (1932) the shadow angle or Farböschung has been widely studied to estimate runout distance of landslides (Corominas, 1996). The distance used to determine the shadow angle is based either on the maximum of runout distance or on a threshold distance (Evans and Hungr, 1993; Toppe, 1987). This discrepancy for empirical approach has to be explained.

In the present paper we inspected the uncertainty on the parameters of the simple model of the energy line. The uncertainty that is relevant comes essentially from the friction parameter. As a consequence the friction coefficient can be assumed as a random variable along the landslide path. As it is a sum of random variables it must follow a normal distribution owing to the central limit theorem.

This hypothesis can be verified on several landslide data sets such as rock falls, shallow landslides, snow avalanches, etc. In any case, this permits to unify all the different approaches taking into account the difference between energy line and Farböschung.

REFERENCES

Corominas J. 1996: The angle of reach as mobility index for small and large landslides. Can Geotech J 33:260–271.
Heim A. 1932: Bergsturz und Menschenleben - Fretz und Wasmuth, Zurich, 218 pp.
Evans, S., Hungr, O., 1993: The assessment of rockfall hazard at the base of talus slopes. Canadian Geotechnical Journal, 30, 620-636.
Toppe, R. 1987: Terrain models: a tool for natural hazard mapping. In: Avalanche formation, movement and effects. Edited by B. Salm &H. Gubler. International Association of Hydrological Sciences. Wallingford, UK. Publication 162, pp. 629-638.
297, 269-281.

9.11

Machine learning algorithms for spatial data. Case studies: environmental pollution, natural hazards, renewable resources

Kanevski Mikhail*, Pozdnoukhov Alexei*, Timonin Vadim*

**Institute of Geomatics and Analysis of Risk (IGAR), University of Lausanne, CH-1015 (Mikhail.Kanevski@unil.ch)*

This paper presents general problems and approaches for the spatial data analysis using machine learning algorithms. Machine learning is a very powerful approach to adaptive data analysis, modelling and visualisation. The key feature of the machine learning algorithms is that they learn from empirical data and can be used in cases when the modelled environmental phenomena are hidden, nonlinear, noisy and highly variable in space and in time. Most of the machines learning algorithms are universal and adaptive modelling tools developed to solve basic problems of learning from data: classification/pattern recognition, regression/mapping and probability density modelling.

In the present report some of the widely used machine learning algorithms, namely artificial neural networks (ANN) of different architectures and Support Vector Machines (SVM), are adapted to the problems of the analysis and modelling of geo-spatial data. Machine learning algorithms have an important advantage over traditional models of spatial statistics when problems are considered in a high dimensional geo-feature spaces, when the dimension of space exceeds 5. Such features are usually generated, for example, from digital elevation models, remote sensing images, etc. An important extension of models concerns considering of real space constrains like geomorphology, networks, and other natural structures. Recent developments in semi-supervised learning can improve modelling of environmental phenomena taking into account on geo-manifolds. An important part of the study deals with the analysis of relevant variables and models' inputs. This problem is approached by using different feature selection/feature extraction nonlinear tools.

To demonstrate the application of machine learning algorithms several interesting case studies are considered: digital soil mapping using SVM, automatic mapping of soil and water system pollution using ANN; natural hazards risk analysis (avalanches, landslides), assessments of renewable resources (wind fields) with SVM and ANN models, etc. The dimensionality of spaces considered varies from 2 to more than 30.

Figures 1, 2, 3 demonstrate some results of the studies and their outputs.

Finally, the results of environmental mapping are discussed and compared with traditional models of geostatistics.

Acknowledgements. The study was partially supported by the Swiss National Science Foundation projects GeoKernels (project No 200021-113944) and Clusterville (project No 100012-113506).

REFERENCES

Kanevski, M. (Editor), 2008. Advanced Mapping of Environmental Data. ISTE Ltd., John Wiley & Sons Inc, 313 pp.

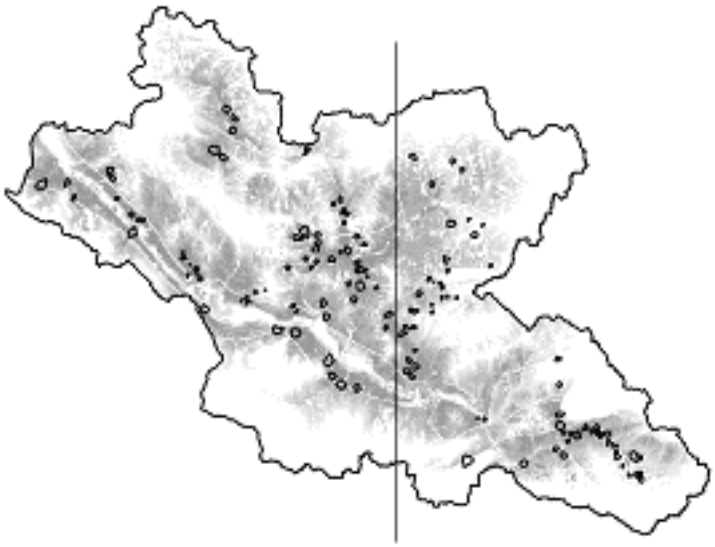

Figure 1. Map of potential areas where landslides can occur (region of the study - northwest China). Darker colours present regions with higher probability of danger. Training areas (outlined by polygons) are also presented.

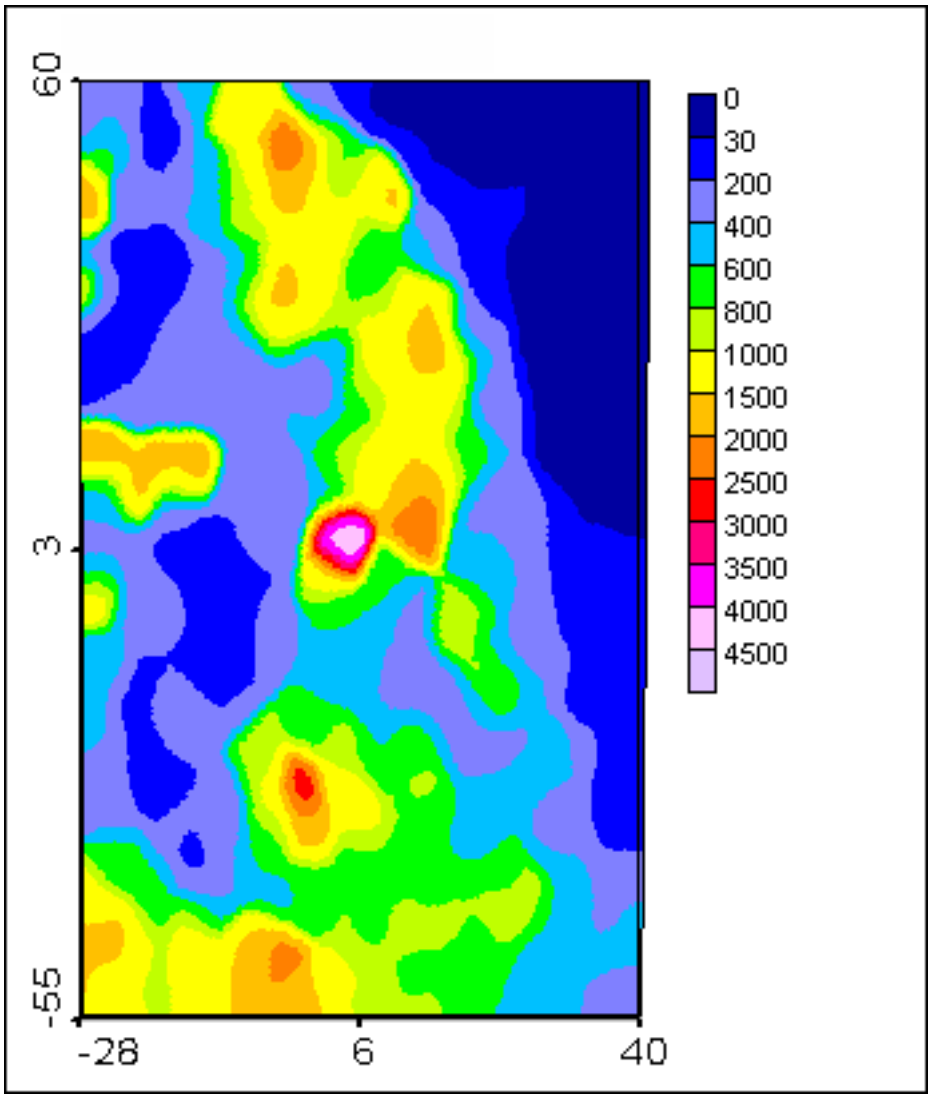

Figure 2. Map of soil pollution automatically generated by ANN.

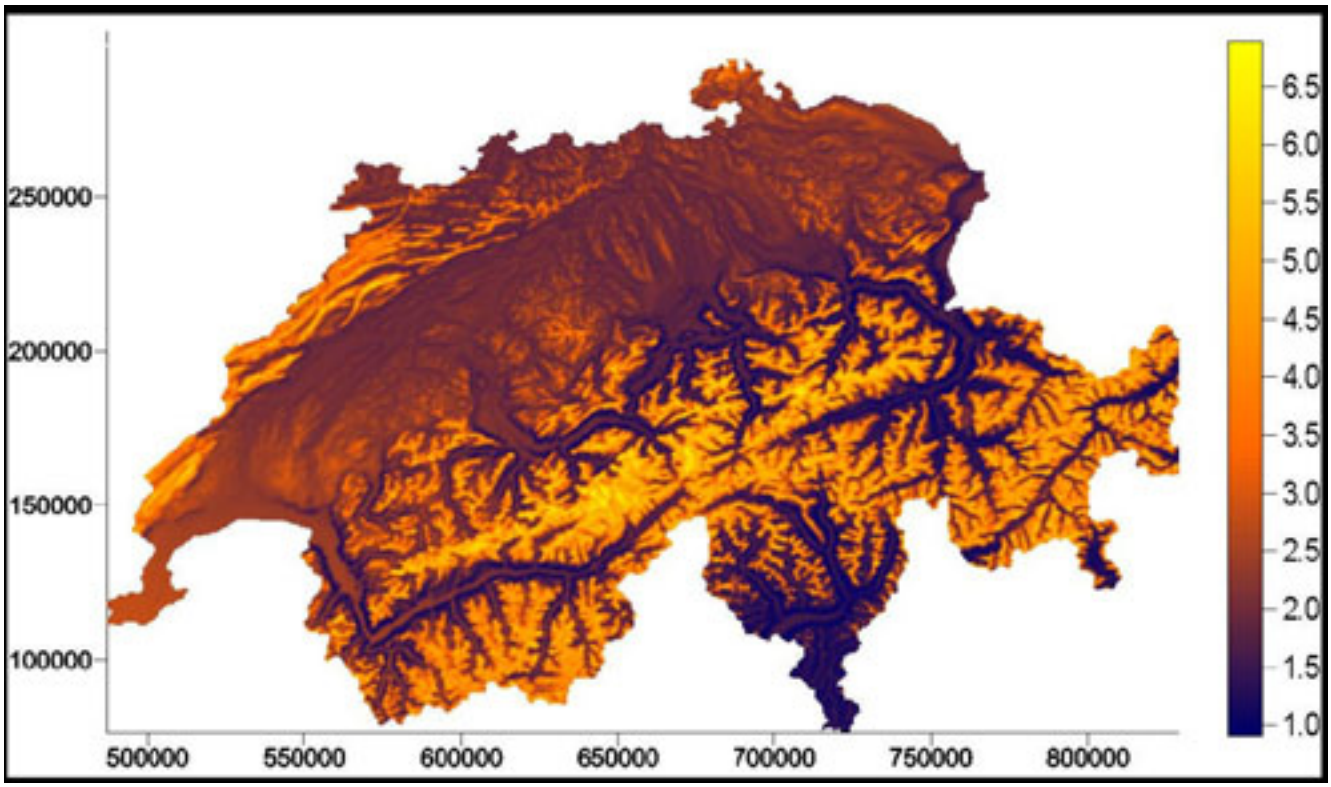

Figure 3. Map of wind fields in Switzerland.

9.12

A method for risk analysis related to lahars and floods – a case study at Nevado del Tolima volcano, Colombia

Künzler Matthias*, Huggel Christian*, Ramírez Juan Manuel**

*Department of Geography, University of Zurich, Winterthurerstrasse 190, CH-8057 Zurich (mkuenzler@access.unizh.ch, christian.huggel@geo.uzh.ch)
**Swiss Agency for Development and Cooperation, Bogotá, Colombia

The glacier-covered Nevado del Tolima located in the Colombian Cordillera Central (Figure 1) is an active volcano with potential lahar hazards similar to those on Nevado del Ruiz (Thouret et al., 1995). For effective disaster prevention a risk analysis is an important tool. We present here a methodology that allows for a relatively rapid assessment of the risk based on a first-order analysis of lahar and rainfall related flood hazards, and vulnerability. The methodology is performed for five villages in the Combeima Valley and the regional capital Ibagué (≈450,000 inhabitants).

Firstly, the models LAHARZ for lahars and HEC-RAS for floods were applied to generate hazard maps. Lahar scenarios are based on melting of 0.5, 1, 5, and 15 m of glacier ice due to volcanic activity, resulting in lahar volumes of 0.5, 1, 5, and 15 million m^3. For flood modelling, design floods with a return period of 10 and 100 years were calculated. A second step involves the analysis of different vulnerabilities. Physical vulnerability is operationalised by market values of dwelling parcels and population density, whereas social vulnerability is expressed by population age and poverty. Thirdly, hazard H and vulnerably V values are both transformed into a scale from 0 to 1 and subsequently multiplied following the risk equation $R = H * V$ (Varnes, 1984). The results are qualitatively risk values per parcel level and quantitative damage estimates. Figure 2 schematically illustrates the risk analysis concept. The left side refers to the vulnerability and the right side to the hazard, respectively. Grey parallelograms are GIS layers.

Whereas flood hazard has limited effects on population and infrastructure, the impact of lahars is more serious. An assumed lahar volume of 15 million m^3 may lead to lahar heights of 19 m and a maximum horizontal cross section of ca. 450 m. Over 20,000 people may be affected.

While uncertainties yet prevail with respect to the topographic basis and hazard mapping in general, the overall methodology has proven to be a suitable tool to provide a first overview of spatial distribution of risk, helpful for decision-makers. We should consider, however, that the weighting of the different vulnerabilities has an important control on resulting risks and should therefore be performed in coordination with the responsible authorities.

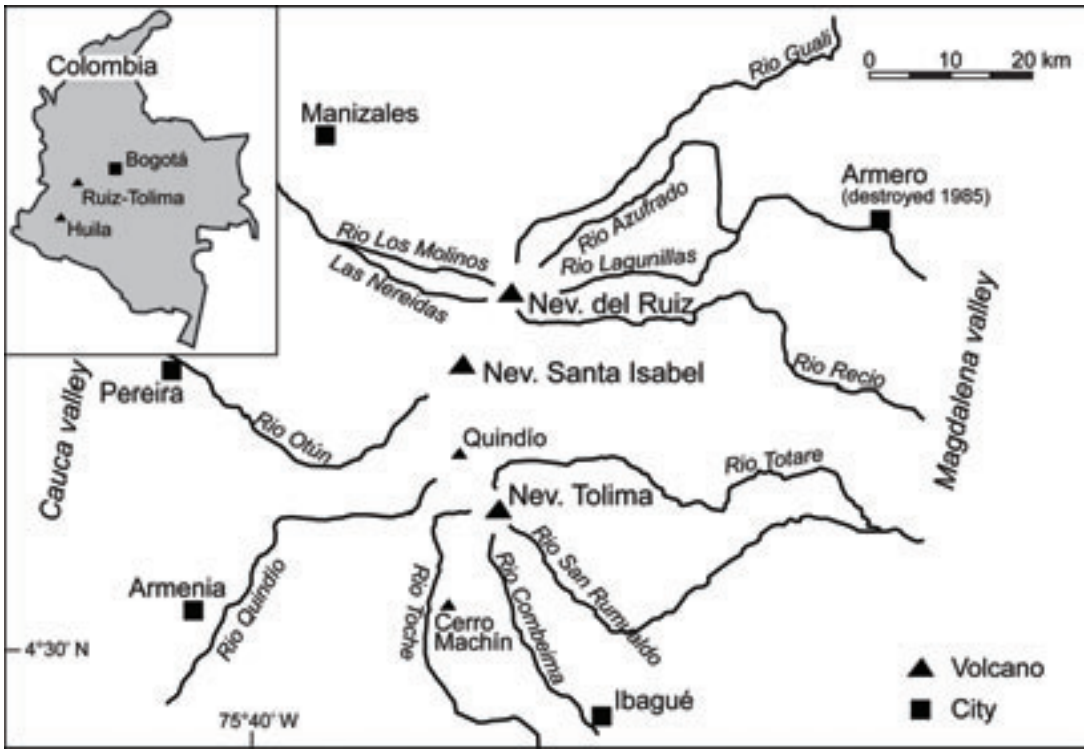

Figure 1. Cordillera Central with Nevado del Tolima and Nevado del Ruiz (from Huggel et al., 2007).

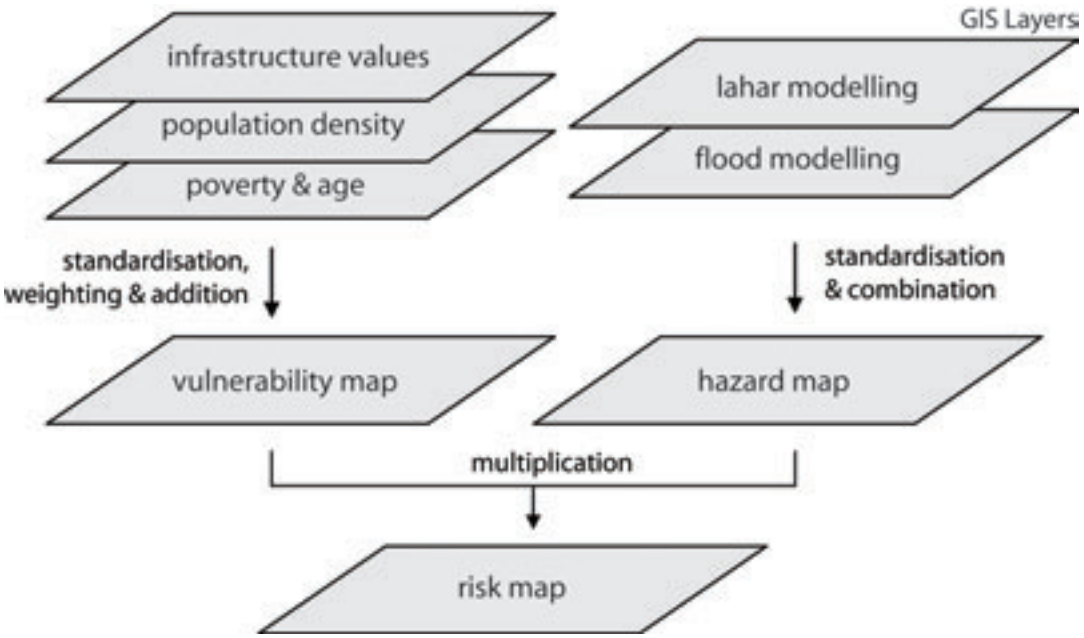

Figure 2. Flow chart of the risk analysis concept based on a $R=V*H$ approach.

REFERENCES

Huggel, C., Ceballos, J.L., Pulgarín, B., Ramírez, J. & Touret, J.-C. 2007: Review and reassessment of hazards owing to volcano-glacier interactions in Colombia. Annals of Glaciology, 45, 128-136.

Thouret, J.-C., Cantagrel, J.-M., Robin, C., Murcia, A., Salinas, R. & Cepeda, H. 1995: Quaternary history and hazard-zone model at Nevado del Tolima and Cerro Machin Volcanoes, Colombia. Journal of Volcanology and Geothermal Research, 66, 397-426.

Varnes, D.J. 1984: Landslide hazard zonation: a review of principles and practice. United Nations Educational, Scientific and Cultural Organisation, Paris. 63 pp.

9.13

Geological heterogeneity in landslides: Characterization and flow modelling

Boris Matti

SUPSI, Istituto Scienze della Terra CP 72, CH 6952 Canobbio (boris.matti@supsi.ch)

Significant progress has been made these last decades in the development of hydrogeological numerical flow modelling for describing the hydrodynamic behaviour of landslides. However, these new sophisticated methods are still very seldom used in the problems of slope instability in particular because of the hydrogeological complexity which characterizes them; thin aquifers, discontinuous media, succession of saturated and unsaturated zones, low permeabilities, high hydraulic gradients, lithological heterogeneity, strong contrasts of permeabilities and heterogeneous infiltration.

Predictive models of flow in the subsurface, which are often based on homogeneous porous media types of representation, are badly adapted to natural systems that are characterized by highly heterogeneous media such as landslides. These models are good and reliable on a landslide scale (regional scale), but their quality may be affected on a local scale by strong geological heterogeneities. Geological heterogeneities of the subsurface take part in determining the hydrodynamical and geomechanical behaviour of landslides. However, their spatial distribution is partially unknown.

Thus, the principal objectives of this work are: (i) To carry out an integrated multidisciplinary characterization study on the internal structure of landslides in flysch and Quaternary environments, in order to clarify the organisation of the geological heterogeneities and to identify the hydrodynamic implications. (ii) To propose a conceptual model representing the geological architecture and the hydrogeological functioning. (iii) To examine the effects of heterogeneity and anisotropy on flow systems. (iv) To better understand the influence of geological heterogeneities on the mechanical behaviour of large landslides by performing numerical sensitivity analyses, by means of different heterogeneity scenarios on the field parameters. (v) Finally, to test the incidences on slope stabilization techniques; evaluation of the efficiency of a drainage gallery work. The main test site of *la Frasse landslide* (VD, Switzerland) was chosen, and completed with additional landslide cases.

The main results are the following:

In most of the case studies, the landslide mass is composed of an old prehistoric stabilized mass, pinched between the active sliding mass and the bedrock, and playing an important hydrologic role. The stabilized mass and the bedrock form the substratum of the landslide.

Landslides occurring in these types of media are defined by an organized heterogeneous environment with “fracture” flows and discontinuity porosity. The overall hydraulic conductivity is low, and locally high permeable zones exist. Regional groundwater circulations are limited and form local interconnected aquicludes organised in thin aquifers, and presenting saturated and unsaturated zones.
The hydrogeological analyses showed that the system presents a bimodal permeability; (i) Low hydraulic conductivities characterizing the global matrix and defining the capacitive fraction, and (ii) high permeable features, with high hydraulic conductivities defining the conductive fraction, and favouring strong channelling effects. Besides, the observation shows that the aquifer system is generally very reactive with important magnitudes. Often, there is a straight correlation between water level variation and climatic conditions (rainy events).
Landslides are characterized by two important inflows namely effective infiltration from the surface and lateral inflows from the neighbouring units. Water transfer between the stabilized mass and the active mass may be important and thus have to be considered. The existence of water transfer between the bedrock and the landslide mass (stabilized and active) is not well established. The bedrock and the landslide mass present a hydrological behavioural independence.

Theoretical two- and three-dimensional flow models are used to investigate the effects of the spatial variability of the hydraulic conductivity on the underground flows. The role of the connectivity in generating flow channelling is examined thanks to the observation of close relations between the permeability and the hydraulic pressures. The sensitivity analysis shows clearly that the relation between local permeability and hydraulic pressures is not straight, and that the organization of the flows depends on the heterogeneity of the hydraulic properties and their spatial correlation. Strong channelling effects are observed in highly heterogeneous porous media. The development of flow channelling as a function of the variance of the natural log permeability values and the correlation lengths is demonstrated.

The integrated multi-disciplinary geological characterization at the *La Frasse* test site combined with the hydrogeological and lithological data of several additional case studies led to the proposal of a global conceptual model. The following assumptions are considered to enable a subsequent quantification of flow components:

- The flow occurs under confined to leaky conditions, with leakage varying in space;
- The flow framework is controlled by a complex multi-layer system, isolated lenses or perched aquifer;
- The aquifer system is divided into interconnected hydrological zones presenting various degrees of saturation;
- Each hydrological zone may function individually from the others;
- Horizontally and vertically, the flow direction in the porous matrix is affected by prevailing structural patterns generating channeling effects;
- The flow is multidirectional, free and channelized, and is affected by temporal and spatial changes;
- The aquifer is under an unsteady flow regime due to seasonal variation of natural gradients.

9.14

Simulation for a volcano monitoring network

Mautz Rainer*

* *Swiss Federal Institute of Technology (ETH), Institute of Geodesy and Photogrammetry, Wolfgang-Pauli-Str. 15, CH-8093 Zurich (mautz@geod.baug.ethz.ch)*

This paper investigates the capability of GNSS aided smart sensor network positioning based on Wireless Local Area Network (WLAN) signals incorporating access points, to monitor 3D deformation associated with volcanic activity and other comparable hazardous events. Many of the world's volcanoes that erupt, experience significant pre-eruption surface deformation. Internal magma pressure makes the surface bulge upwards and outwards. Thus, precise monitoring of surface deformation has the potential to contribute significantly to the realisation of a predictive capability of volcanic eruption. In particular, eruption source depth and evolution time can be estimated from surface deformation. The scale of this deformation is typically centimetric to decimetric over tens of square kilometres and over periods of weeks to years. Horizontal displacements show a radial pattern of movement of up to 10 cm with the displacement of the vertical components typically in the range of 4 to 6 cm per year.

In addition to the use of precise positioning information to facilitate deformation monitoring, the positioning function is vital for spatio-temporal referencing of the relevant multiple and complementary data types for volcano monitoring (e.g., seismicity, ground surface deformation, geothermal, gravity, and geomagnetic).

In architectural terms the monitoring network should consist of an array of distributed intelligent nodes (sensor motes), consisting of low-cost, commercially available, and off-the-shelf components (as far as possible) with built-in local memory and intelligence, with self-configuration, communication, interaction and cooperative networking capabilities. The nodes should be able to identify the type, intensity, and location of the parameters being measured, and collaborate in an internodal manner with each other to perform distributed sensing for event confirmation and significance.

Because of the requirement for high accuracy positioning and the need to keep costs down (both in terms of technical complexity and power consumption), building carrier phase GNSS chips into all WLAN should be avoided. A compromise scenario is to have both types of nodes, some equipped with WLAN as well as carrier phase chips that are used for absolute coordinate referencing but with the majority of nodes with only WLAN communication and ranging capabilities. The limited GNSS aiding proposed should enable WLAN positioning to deliver centimetre level positioning. The sensors equipped with GNSS chips calculate their positions in a higher reference frame with high accuracy, and serve as anchor (= control or reference) points for the monitoring network. The communication function of the network should enable the exchange of the data required for positioning within the monitoring network. This should enable the WLAN nodes to position themselves exploiting inter-node distance measurements.

Such a monitoring system requires multiple key features including construction of the hardware that fulfil the requirements in terms of size, battery life and robustness, the extraction of ranges (distances) between sensor nodes, appropriate supporting network communications, protocol development, optimal routing and positioning. This paper addresses specifically the position function and characterises the performance of a novel high positioning algorithm using simulated range measurements. The 3D positioning algorithm uses the range observations for multilateration, clusterisation and geodetic network adjustment.

The novel algorithm is used to investigate various simulated positioning scenarios. The challenges associated with the use of wireless sensor networks are that ideally, the sensors (nodes) should have reliable positioning data, even in the presence of measurement noise, low inter-node connectivity and badly constrained geometry. This paper presents a strategy to enable

high integrity positioning and assesses its performance based on various parameters such as the node density, maximal signal range, required fraction of anchor nodes (which have GNSS positioning capability), range measurement errors, and locations of the nodes.

Presented are results from large simulated networks (i.e. 400 nodes) and the optimal network parameters are quantified. The requirement to have direct line of sights between stations can be solved by locating the nodes for a maximum number of directs sights. The number of required nodes depends on the transmission range. The required fraction of GNSS enabled reference nodes will be around 10%, depending on the network density.

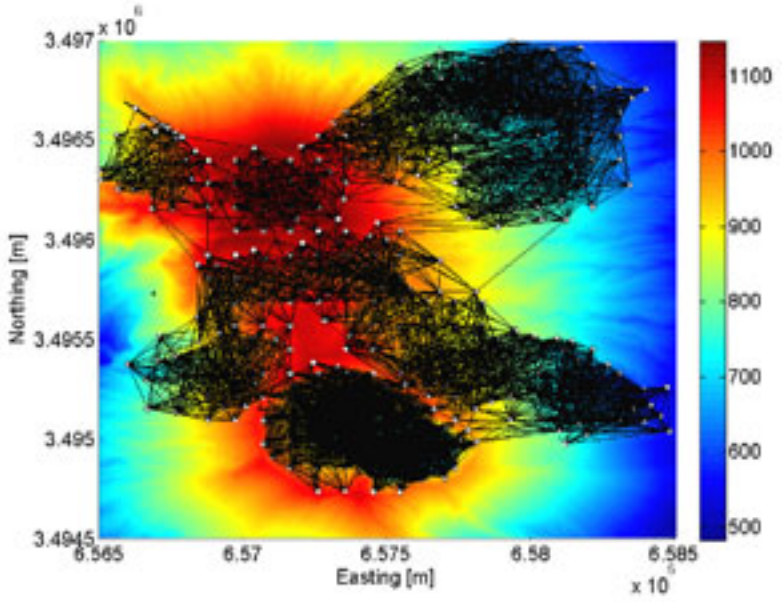

Figure 1. Optimised positions of 400 sensor nodes at volcano Sakurajima.

REFERENCES

Mautz, R., Ochieng, W.Y., Brodin, G. & Kemp, A. 2007:. 3D Wireless Network Localization from Inconsistent Distance Observations, Ad Hoc & Sensor Wireless Networks, Vol. 3, No. 2–3, pp. 141–170.

9.15

Systematic recording and analysis of natural hazards along railway lines using GIS

Andreas Meier, Christina Willi

SBB Infrastruktur, Umwelt; Naturrisiken; Schanzenstrasse 5, 3000 Bern 65

Due to the topographical conditions in Switzerland the SBB railway lines frequently are exposed to natural hazards as rockfall, debris flow, landslide, wind and others. The safe and high disposable train service is very sensitive to changes in the terrain. This asks for a high level of surveillance and preservation in the slopes along the railway lines.
Natural hazard data over the past 100 years and data about the currently prevailing risks exist in a variety of analogue and digital archives or databases. Therefore it is necessary to survey the data in time and space.
With the Geographical Information System for Natural Risks (GIS NR) consisting of the tools DERI NR and WebGIS the SBB established an important system for managing natural risks.

Figure 1. Graphical user interface of DERI NR

Data recording using DERI NR

DERI NR (Dérangements à l'Infrastructure „Natural Risks") is an instrument to report, record and document natural hazards. Events are continuously recorded in a central database (based on @enterprise technology; see figure 1) by the people in charge of maintaining safety.
In addition, during the next years historic data will be added. Thereby DERI NR becomes a constantly updated database of natural risks along the railway lines.

DERI NR is a workflow instrument with a two-step recording process. Train drivers, route inspectors and vegetation keepers register the key data of an event such as natural hazard type, route number and route position. The low number of obligatory data fields helps to report as many events as possible. Photographs and text documents can be attached.

Depending on the operating point and the type of hazard, the system forwards the report to the specialist for natural hazards. As a second step the event is fully documented. The recording ends with the evaluation weather more protection against natural hazards is needed. The recording process can be reactivated at any time, e.g. to add data from external risk calculations.

Visualisation in WebGIS

WebGIS is an application of Intergraph (BM3) and is open to all employees of SBB. It visualises the data from DERI NR on maps or orthophotos.
As a result of the second recording step the record appears in WebGIS. The user can select a specific area to overview previous hazards in the region. Natural hazards can be searched directly in WebGIS using DERI NR. Vice-versa, a double click on the visualised events opens the corresponding documentation in DERI NR.
The constantly updated risk map (figure 2) shows all sites that require more protection against natural hazards.

Figure 2. Map of current risk sites

Figure 3. Natural hazards in WebGIS

Further extensions

Today GIS NR mainly centralises the documentation of natural hazards. Additionally the system offers queries about ice falls and avalanches at the Gotthard line and provides natural hazard maps from SILVAPROTECT.

In the coming years GIS NR will be a data base containing all information needed for the evaluation of risk sites.
Henceforth GIS NR provides the inventory and the condition of protective systems such as dams, warning systems, monitors, protection forests and others as well as calculated risk data, hazard maps and protection targets.
GIS NR helps inspectors and the technical management to decide about protection measures. In addition to the visualisation, tools for spatial data analysis will be available.

REFERENCES

Meier, A. 2008: Naturgefahren: Herausforderung für die SBB. Geomatik Schweiz, 5, 242-243.

9.16

Glass and magnetitic Spherules associated whit The bolid impact and mass extinction in D/C boundary in Central Alborz mountain north of Iran

Mahin Mohamadi

Geology Department, Payame Noor University, PNU.Iran .P.O.Box 19395-4697, Tehran, Iran. Mahin_mohamadi@pnu.ac.ir

Many glass spherules and tear like and also magnetitic and metallic spherules and dumb bell have income in upper part of Geirud Formation in central Alborz mountain. The grey marly limestone bed in upper part of geirud formation (upper Devonian) in Geirud valley, north of Tehran consist of many tear and spherule like yellow glass and also plentiful numbers of metallic and magnetitic spherules and dumb bells whith high density. Lower Carboniferous Mobarak Formation cover this bed in area.
All of these particles is collected and have been photographed by SEM. The form of These particles are similar, (but in different stratigraphic level) to those previously described from F/F boundary in many part of the world and from Kellewaser mass extinction, Claeys, P.,1994-1996, Sandberg,C. and all,1988 and McLaren,D.and all,1982. The biostratigraphy of this bed based on conodont is upper famennian (younger than expanasa zone). (mohammadi and all, in prep.) These spherules are likely to be produced by bolid impact event and may caused big mass extinction at that time which is marked by Hangenberge event .This is the first report of the presence of tektite and magnetitic spherules in D/C boundary layers of Iran and more inspection is needed from other equal layer from other part of country and also chemical and XRD analysis will be done as soon as possible for campaign whit the world samples.

REFRENCES :

Claeys,P.and all,1996 : Geochemistry of the Frasnian_ Famennian Boundary In Belgium : Mass extinction, anoxic ocean and microtektite layer, but not much iridium? Geological Society of America,Special paper 307 .pp,491-505

Claeys,P.and all,1994 :Microtektite-like impact glass associated whit the Frasnian-Famennian Boundary mass extinction, Earth and Planetary Science Lettres,V.22,Issues 3-4, pp,303-315

McLaren,D.and all,1982: Frasnian –Famennian extinction.in Silver,L., T., and Schultz,P.H., eds., Geological implication of Impacts of large asteroids and comets on the earth, Geological Society of America,Special paper 190,pp.477-483

Sandberg,C.A.and all,1988 : Late Frasnian mass extinction : Conodont event stratigraphy global changes and possible causes : Courier Forschungsinstitut Senkenberg, v.102, PP 267-307.

9.17

Geological and structural model of the Åknes rockslide (Norway)

Oppikofer Thierry*, Martina Böhme**, Lars Harald Blikra**, Marc-Henri Derron**, Michel Jaboyedoff*, Saintot Aline**

*Institute of Geomatics and Risk Analysis, University of Lausanne, Amphipôle, CH-1015 Lausanne (thierry.oppikofer@unil.ch)
**Geological Survey of Norway, Leif Eiriksons vei 39, NO-7040 Trondheim

Åknes is a complex rockslide situated on the flank of a famous fjord in Western Norway (Fig. 1a). The rockslide has a volume of >35 million m^3 (Derron et al., 2005) and is investigated and monitored within the Åknes/Tafjord Project, since its failure might cause a catastrophic tsunami in the fjord. A large series of geological, structural, geophysical and borehole investigations and several slope movement monitoring techniques make the Åknes rockslide one of the most intensively studied sites in the world (Ganerød et al., in press).

This study focuses on the conceptual model of the Åknes rockslide based on displacement measurements, digital elevation model analysis, terrestrial laser scanning, and field investigations. The understanding of the mechanism is crucial to implement suitable monitoring and early-warning systems.

Towards the SW and the NE, the rockslide body is delineated by two regional NNW-SSE faults (Fig. 1b). Sub-vertical NNE-SSW trending faults laterally delimit rockslide compartments and act as transfer surfaces. The main folds have a gently plunging ESE-trending axis crossing obliquely the landslide body. Vertical gneiss foliation (S1) near the hinge zones creates weaknesses and favourably orientated planes that lead to the formation of extension failures acting as back-cracks. Such a fracture led to the creation of a fast-moving ridge and a 30 m wide trench in the upper rockslide part and several rockslide scars on the slope are exactly located at the folds hinges with sub-vertical S1.

The observed displacements permit to divide the rockslide into several parts that move with different velocities and/or directions (Fig. 1c). Since most of the sliding surfaces reactivate S1, variations in the orientation of S1 – due to folds and undulations – create changes in the sliding direction between SE and SSW. The sliding surface is not continuous, but stepped by sub-vertical fractures perpendicular to the main sliding direction, that have been clearly identified on the topography in the vicinity of Åknes landslide (Oppikofer & Jaboyedoff, 2007). A model for this upper-most part of the rockslide implies a combination of planar sliding along S1, subsidence due to stepped failure surface and toppling towards the opened graben structure (Fig. 1d) (Oppikofer et al., 2008).

This interpretation gives a coherent framework of the movements obtained by various methods and leads to a reinterpretation of the morphology, indicating that several rockslides occurred in the past. These findings enable to establish the failure surface topography and to define blocks most susceptible to failure.

Figure 1. a) Picture of the Åknes rockslide (Derron et al. (2005)); b) Rockslide morphology displaying the back-scars, lateral transfer zones and the regional faults; c) Annual displacement vectors (data from Ganerød et al. (in press)); d) Instability model for the fast-moving ridge (from Oppikofer et al. (2008)).

REFERENCES

Derron, M.; Blikra, L. H. & Jaboyedoff, M. 2005: High resolution digital elevation model analysis for landslide hazard assessment (Åkerneset, Norway). In: Landslides and Avalanches: ICFL 2005 Norway, 101-106. Taylor & Francis Group, London.

Ganerød, G. V., Grøneng, G., Rønning, J. S., Dalsegg, E., Elvebakk, H., Tønnesen, J. F., Kveldsvik, V., Eiken, T., Blikra, L. H., & Braathen, A. in press: Geological Model of the Åknes Rockslide, western Norway. Eng. Geol.

Oppikofer, T., & Jaboyedoff, M. 2007: Åknes/Tafjord project: DEM analysis of the Rundefjellet/Tårnet area. Report, University of Lausanne, Switzerland, p.44.

Oppikofer, T., Jaboyedoff, M., Blikra, L. H., & Derron, M.-H. 2008: Characterization and monitoring of the Åknes landslide using terrestrial laser scanning. Proceedings of the 4th Canadian Conference on Geohazards, 211–218. Presse de l'Université Laval, Québec, Canada.

9.18

A new approach to dating carbonate-lithic rockslides

Ostermann Marc* & Sanders Diethard*,

*Geologisch-Paläontologisches Institut, Innrain 52, A-6020 Innsbruck
(marc.ostermann@uibk.ac.at)

Large-scale rockslides exceeding 106 m^3 in volume not only are a major process of mountain erosion and orogenic mass balance but, in densely populated regions such as the Alps, also represent a major threat to humans and facilities. Establishing the distribution of rockslides in time is a prerequisite of hazard assessment for future events and for a better understanding of potential triggers, such as climatic change or phases of enhanced earthquake frequency and post-glacial stress relaxation (e.g. Erismann & Abele, 2001).

In the last decades, rockslide deposits were dated by ^{14}C age determination of wood fragments that are preserved (a) in lacustrine or fluvial successions underneath the rockslide mass, (b) within the rockslide mass, or (c) in newly-formed lakes on top of the sturzstrom (e.g. Wassmer et al., 2004). In each case, the ^{14}C age provides a different constraint for the age of the rockslide event, that is, in case (a) the ^{14}C age represents a maximum age limit for the event, in case (b), which is very rare, the ^{14}C age is a good proxy age of the event, and in case (c) the ^{14}C age provides a minimum age limit. Unfortunately, the ^{14}C approach to age-dating often cannot be applied because of absence of suited deposits or exposures thereof, lack of organic remnants or of remnants suited for age-dating, and/or because the resulting ^{14}C age is fraught with marked imprecision (e. g. Prager et al., 2008).

In the past decade, an increasing number of sturzstroms have been dated by ^{36}Cl exposure dating of detachment scars and/or of surfaces of boulders within the sturzstrom deposit (Ivy-Ochs et al., 1998). At the present state, thus, an increasing number of the numerous Alpine rockslides that hitherto could not be determined by the ^{14}C method will foreseeably be dated by exposure dating, but a cross-check with another method of age determination is desirable in each case.

Our preliminary investigations of major carbonate-lithic rockslides of the Alps revealed that indeed nearly all of them contain pockets, thicker crusts and patches wherein the rockslide material underwent cementation into a breccia. These breccia cements can provide a proxy age of the sturzstrom event by dating the cement with the $^{234}U/^{230}Th$ disequilibrium method (Ostermann et al., 2007). To this end, careful petrographic analysis of samples is necessary to distinguish different generations and types of cement.

Within the research project: Catastrophic Rockslides in the Alps, funded by the Austrian Science Fund, age determination of 17 selected rockslides (Fig.1) shall be done by both U/Th dating of cements and by surface exposition dating with cosmogenic radionuclides. Yet exposition dating has the undisputed advantage that it is the only method that veers for the 'real' age of a sturzstrom event. Combining the precision of U/Th ages with the correctness of (often more blurred) exposition ages was, therefore, the ideal approach to determine most precise ages for selected Alpine landslides.

REFERENCES

Erismann, H. T. & Abele, G. 2001: Dynamics of Rockslides and Rockfalls. Springer, Berlin, Heidelberg, New York, 316pp.

Ivy-Ochs, S., Heuberger, H., Kubik, P.W., Kerschner, H., Bonani, G., Frank, M. & Schlüchter, C. 1998:The age of the Koefels event - relative, 14C and cosmogenic isotope dating of an early Holocene landslide in the Central alps (Tyrol, Austria), Zeitschrift f. Gletscherkunde u. Glazialgeologie 34, 57-70.

Prager, C., Ivy-Ochs, S., Ostermann, M., Synal, H.-A. & Patzelt, G. 2008: Geology and radiometric ^{14}C-, ^{36}Cl- and Th-/U-dating of the Fernpass rockslide (Tyrol, Austria). Geomorphology, in press.

Ostermann, M., Sanders, D., Prager, C. & Kramers, J. 2007: Aragonite and calcite cementation in 'boulder-controlled' meteoric environments on the Fern Pass rockslide (Austria): implications for radiometric age-dating of catastrophic mass movements. Facies 53, 189-208.

Wassmer, P., Schneider, J. L., Pollet, N. & Schmitter-Voirin, C. 2004: Effects of the internal structure of a rock-avalanche dam on the drainage mechanism of its impoundment, Flims Sturzstrom and Ilanz paleo-lake, Swiss Alps. Geomorphology 61, 3-17.

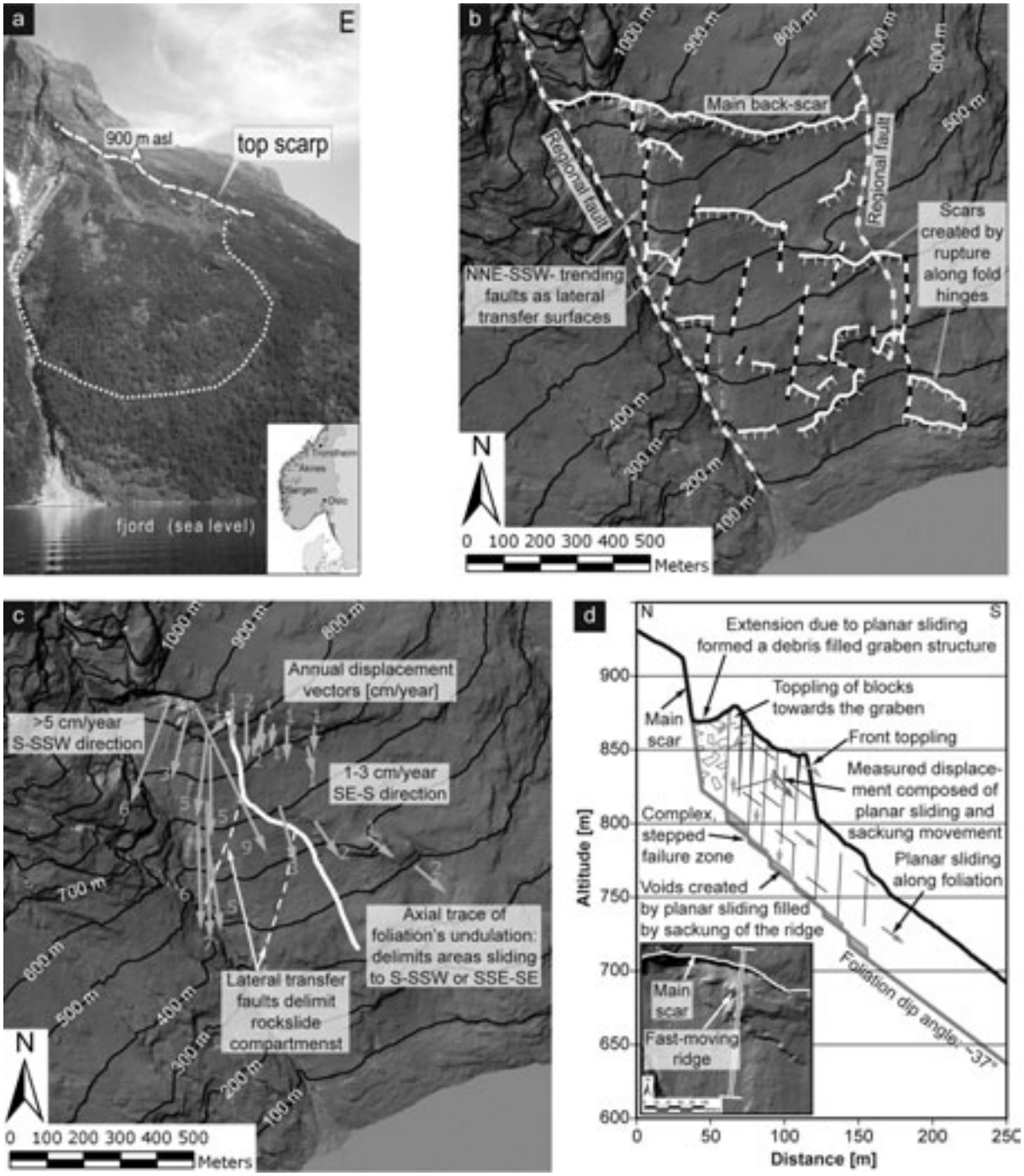

Figure 1. Overview map of the Eastern, Southern and most of the Western Alps with prominent carbonatelithic rockslide deposits. Rockslide deposits chosen for further investigation are highlighted by white framed pentagons.

9.19

The role of regional fault and fold-related fractures in the development of rock slope failure

Pedrazzini Andrea*, Jaboyedoff Michel*, Froese Corey **, Humair Florian *, Langenberg Willem**, & Francisco Moreno**

*Institute of Geomatics and Risk Analysis, University of Lausanne, Amphipôle (andrea.pedrazzini@unil.ch)
**Alberta Geological Survey, Edmonton, Alberta, Canada

Large rock slope failures in fracturated rock are often controlled by the combination of pre-existing tectonic fracture and brittle fracture propagation in the intact rock mass during pre−failure phase (Brideau et al, in press). Tectonic features such fold and large fault have in important influence on the frequency and the spatial distribution of large rock slope failure (Ambrosi and Crosta, 2006). In this paper, we focus on the influence of the tectonic features in the kinematic release but also on the control of the local reduction of rock mass proprieties induced by tectonic damage.

We present here the case study of Turtle Mountain, south-western Alberta, Canada. This area is characterized by the presence of the famous Frank slide, occurred in 1903 and involving 30 mio of m^3 of massif limestone. From a structural point of view the area is characterized be the presence of the Turtle Mountain anticline and the Turtle Mountain thrust. The Turtle Mountain fold could be described as a modified fault-propagation fold.
A detailed field mapping and the morpho-structural analysis (Jaboyedoff et al., in press) the high resolution digital elevation model (HRDEM) allows identifying at least 5 discontinuity sets. Based on the location their orientation three joint sets (J2, J3, and J4) could be related to the folding phase:

1) A persistent extensional joint, sub-parallel to the fold axis and mainly persistent in the hinge area.
2) Two strike-slip conjugate fractures manly persistent in the western fold limb.

The other two joint sets (J1 and J5) have with a dominant feature and cutting the entire Turtle Mountain anticline. The large persistence and their occurrence suggest that these discontinuities are post-folding and related to the NE-SW transpression during Eocene (Price et al., 1986).
In order to quantify the rock mass quality in the different portions of the Turtle Mountain anticline the Geological Strength Index (GSI) was estimated (Hoek and Brown, 1997). In the fold limbs the GSI value range between 35 to 55. the GSI decrease progressively in the hinge area and ranges between 20 to 35. The variation of the GSI values along the fold could by explain an increasing of fracturation (especially discontinuity sets J2) near the hinge zone due to the strain concentration during the folding phase. At the same time an increasing of fracturation in this area increase the susceptibility of the rock mass to weathering or freeze and thaw cycle.
Field mapping shows that hinge area correspond also the area were most of the past and potential instability are concentrated (Figure 1).
In this context two main potential failure mechanisms have been detected:

1) A planar sliding on bedding planes or persistent J1 discontinuity set with the rear release following extensional or the wedge formed by strike-slipe conjugate faults.
2) A toppling-sliding mechanism developed on the extensional fracture.

All this observations have been taking into account in order to asses the stability of the potential unstable areas in Turtle Mountain and to reexaminate the Frank slide mechanism.

REFERENCES

Brideau, M-A., Ming Y., Stead, D. (in press).The role of tectonic damage and brittle rock fracture in the development of large rock slope failure. Geomorphology (2008), doi:101016/j.geomorph.2008.04.010

Ambrosi C. and Crosta G.B. (2006): Large sackung along major tectonic features in the Central Italian Alps. Engineering Geology, 83 183-200.

Jaboyedoff, M., Couture, R. and Locat, P. (in press): Structural analysis of Turtle Mountain (Alberta) using digital elevation model: toward a progressive failure. Geomorphology. (2008). doi:10.1016/j.geomorph.2008.04.012

Price R.A. 1994. Geological history of the Peace River Arch [accessed June 2004]; In Geological Atlas of the Western Canada Sedimentary Basin, Mossop G.D., Shetson I. (comp.), Canadian Society of Petroleum Geologists and Alberta Research Council, Calgary, Alberta, URL http://www.ags.gov.ab.ca/publications/ATLAS_WWW/ATLAS.shtml.

Hoek, E., Brown, E.T., 1997. Practical estimates of rock mass strength. International Journal of Rock Mechanics and Mining Sciences 34, 1165−1186.

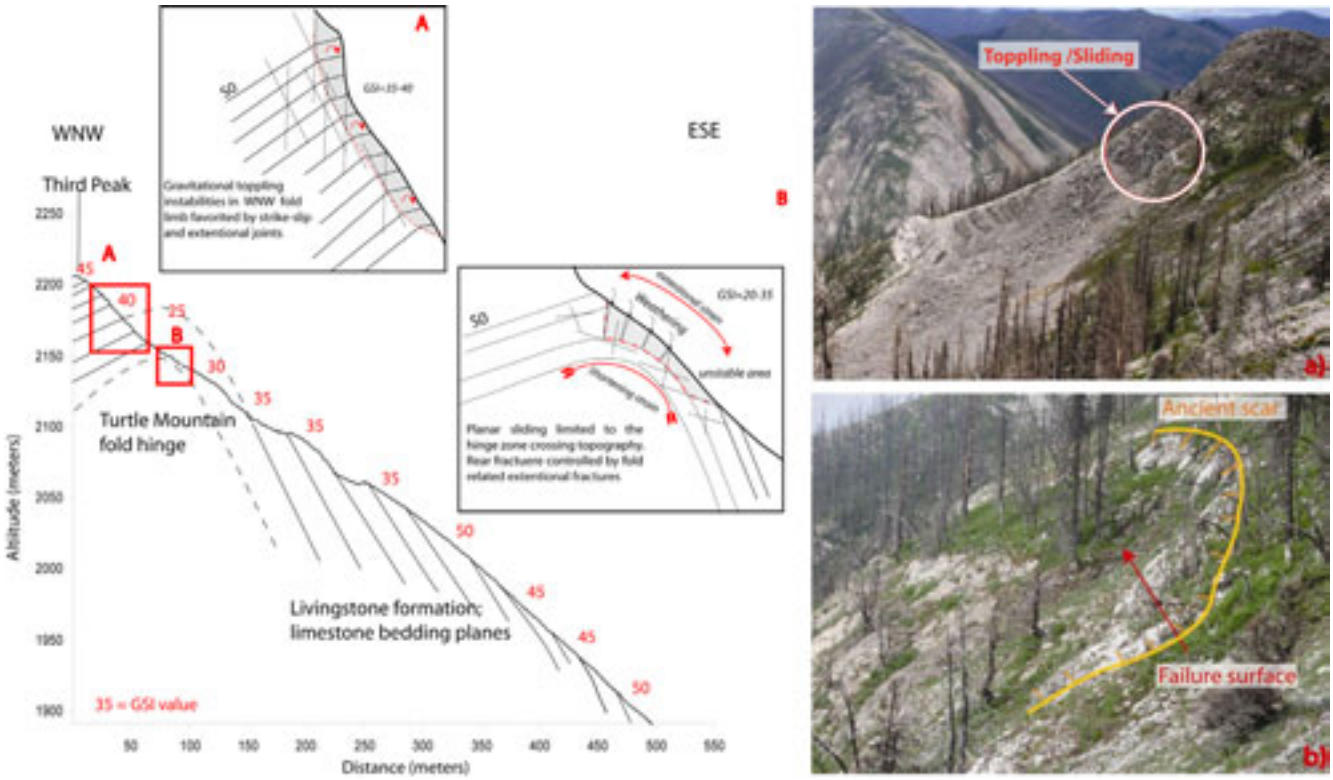

Figure 1: (left) Failure mechanisms driven by fold related fractures affecting the hinge zone of Turtle Mountain anticline. The numbers on the profile correspond to the evolution of the GSI value. (right) Pictures show field evidence of past instabilities related to the fold location.

9.20

The earthquake loss estimating tool QLARM: Applications in real-time and for predictions

Rosset Philippe*, Bonjour Cyrill**, Cua Georgia**, Kaestli Philipp**, Trendafiloski Goran*, Wiemer Stefan** & Wyss Max*

**World Agency for Planetary Monitoring and Earthquake Risk Reduction (WAPMERR), 2 rue de Jargonnant, CH-1207 Genève (p_rosset@wapmerr.org)*
***Swiss Seismological Service, ETH Hönggerberg CH-8093 Zürich*

QLARM is a loss-estimating tool being constructed jointly by WAPMERR and the Swiss Seismological Service. This computer program and its standard world dataset will be available for use by any professional. Its purpose is to calculate mean damage to the built environment and human losses in case of earthquakes anywhere in the world. The world data sets we are currently updating include: Population, building stock, attenuation of seismic waves, local soil conditions, critical facilities, and regional earthquake source properties.

The population is given by number of inhabitants down to the smallest settlements available for each country. QLARM is thus able to rank settlements according to the severity of losses, which is useful for rescue teams in earthquake disasters.

The building stock is distributed in vulnerability classes of the EMS-98 scale. This distribution is a function of the region and of the settlement size. The information on building quality comes from the World Housing Encyclopedia, from the literature, satellite images, ground surveys, and expert opinion.

Attenuation functions are taken from the literature and by calibration. Although it is clear that regional differences exist, they are not well quantified. In some areas we may need to modify the attenuation relationship such that intensities observed in past earthquakes are matched.

Soil properties are defined in varying detail for important cities worldwide in the literature. We derive amplification factors (for intensity or acceleration) as well as we can from published data on soil properties, microzonation maps, geological maps, and topography.

The most probable depth for shallow earthquakes is a parameter we are mapping by region because the need for this parameter arises in real-time loss estimates. We calculate losses for large earthquakes worldwide within less than an hour of their occurrence when there is only a teleseismic estimate of the depth available, with its large error. This poses a problem because losses depend crucially on the hypocentral depth.

An example of a loss estimate in real time is the Sichuan earthquake of the 12 May 2008. At first the magnitude was given as M7.5. Based on this, we distributed an email 28 minutes after the quake, giving 3,000 +/-1,000 as the most probable number of fatalities. As soon as information reached us that the magnitude may be M7.9, we revised our estimate to 40,000 to 100,000 fatalities (50 minutes after the event). Our alerts by email are distributed to anyone who requests them. Figure 1A shows the map of mean damage to settlements that we placed on our website for public viewing 52 minutes after the Sichuan earthquake (www.wapmerr.org).

Predictions of several earthquakes of class M8+ are currently in effect worldwide based on the MSc algorithm (Kossobokov, personal communication). We calculated losses that are expected to result in two of these cases, if the respective predictions should come true. The damage state resulting from a possible future large earthquake in central Chile is shown in Figure 1B. We expect that a major earthquake disaster is likely to occur in central Chile in the future with more than 1,000 fatalities.

To have some confidence in these results, we calibrated QLARM by verifying that the selected attenuation function and the building stock properties yield the intensities and human losses observed in past earthquakes in the region in question. Calibrating QLARM for different parts of the globe is an important ongoing activity. The parameters we consider modifying regionally include vulnerability curves, attenuation functions, distribution of buildings into classes, and the casualty matrix on which the number of fatalities and injured is derived for a given damage state.

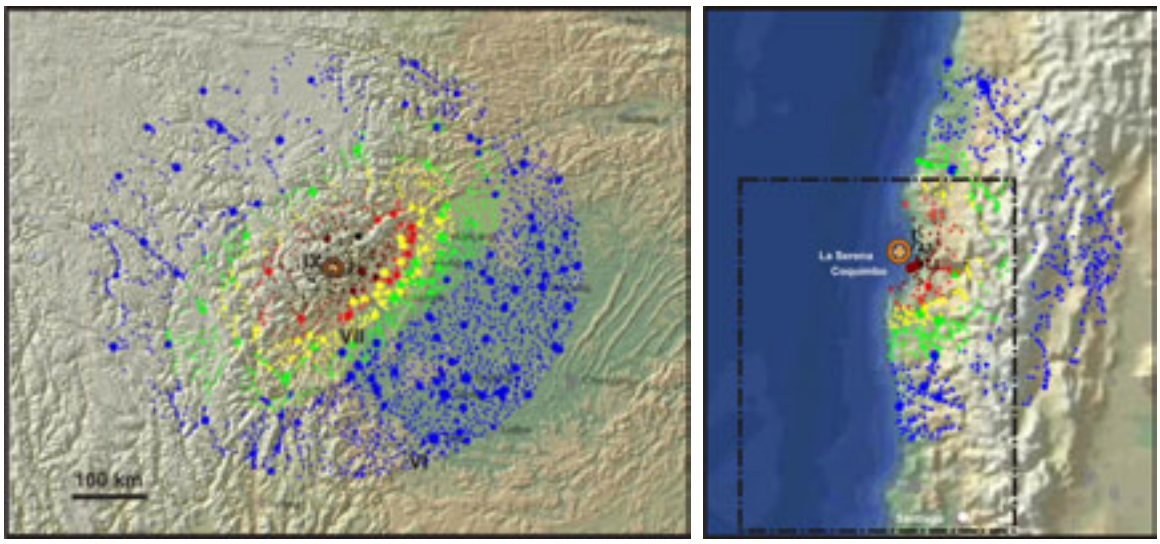

(A) (B)

Figure 1. Maps of mean damage state of buildings in settlements, (A) in the case of the Sichuan earthquake M7.9, May 12 2008, and (B) in a hypothetical scenario that may result in the future from a likely M8.5 earthquake off the coast of central Chile near a location for which a prediction is in effect.
The colour of the dots corresponds to the mean damage in settlements from black (major destruction) to blue (minor damage). The size of the dots is proportional to the population, the epicenter is marked by a ring and roman numerals indicate intensities.

9.21

On the predictability of snow avalanches

Schweizer Jürg

WSL Institute for Snow and Avalanche Research SLF, Flüelastrasse 11, CH-7260 Davos Dorf, email: schweizer@slf.ch

Snow avalanche are rare events and large avalanches that cause damage or harm to people can be called extreme events. In the general context of prediction and predictably of extreme events, we will examine whether snow avalanches are predictable based on a few examples of forecasts at different scales. Clearly, avalanche predictability depends on scale. When the regional avalanche danger is High or Very High, an avalanche is likely somewhere in the region. However, even at such high danger levels, the release probability in a single avalanche path is well below 50% (typically on the order of 1-10%). This means that a single avalanche is a rare event, which is not predictable even when higher danger levels prevail. At the lower danger levels – relevant for backcountry recreation – the release probability is significantly lower. The low release probability does not mean that the risk is low. Even with low occurrence probability the risk might be too high to be acceptable so that comprehensive preventive measures (e.g. temporary road closures) are required. Though the quality of snow avalanche forecasts is typically rather poor, i.e. the skill score in a statistical sense is low, low probability forecasts can be useful if large values are at stake.

9.22

A portable radar interferometer for the measurement of surface deformation

Strozzi Tazio, Werner Charles, Wiesmann Andreas & Wegmüller Urs

Gamma Remote Sensing, Worbstrasse 225, CH-3073 Gümligen ({strozzi,cw,wiesmann,wegmuller}@gamma-rs.ch; www.gamma-rs.ch)

Satellite radar interferometry has been used extensively for ground-motion monitoring with good success. In the case of landslides, glaciers and rock-glaciers, for example, space-borne radar interferometry has a good potential to get an overview on surface deformation. The role of space-borne radar interferometry as an element in a warning system is however constrained by the specific space-borne radar imaging geometry, the typical multiple-week repeat-interval, and uncertainties in the data availability. Most of these limitations can be overcome with an in-situ radar imaging system [1,2].

Gamma Remote Sensing has developed a portable radar interferometer that utilizes real-aperture antennas, each 2 meters in length, to obtain high azimuth resolution [3,4]. Images are acquired line by line while rotating the transmitting and receiving antennas about a vertical axis (Figure 1). The installation effort is relatively small and the instrument is portable and can be battery operated. Individual measurements can be taken in less than 15 minutes and the acquisition time is limited primarily by the speed of the rotational scanner. Each image line is acquired in approximately 2ms hence there is little or no movement of the scene to introduce temporal decorrelation.

Phase differences between successive images acquired from the same location are used to determine line-of-sight displacements δ from the differential phase ϕ via the relationship $\delta = -\lambda \cdot \phi / 4\pi$ where λ is the wavelength. The instrument operates at 17.2 GHz (Ku-Band, λ=17.4 mm) with a displacement measurement sensitivity better than 1 mm. The range resolution of the radar $\delta r = c/2^*B$ is determined by the 200 MHz bandwidth B and is equal to approximately 75 cm. Because this is a real-aperture imaging system, the azimuth resolution is determined by the antenna beamwidth and slant range R, $\delta az = R \sin \theta$. In the case of our terrestrial radar, the azimuth beamwidth is 0.4 degree yielding an azimuth resolution of about 7m at a slant range of 1km.

The instrument uses two receiving antennas with a short baseline to form an interferometer. Phase differences between simultaneous acquisitions by these antennas are used to calculate the precise look angle relative to the baseline, permitting derivation of the surface topography. Expected statistical noise in the height measurements is on the order of 1 meter.

In this contribution the design, measurement principles and characteristics of the portable radar interferometer are presented. Results obtained in a series of experiments started in September 2007 over glaciers (e.g. Rhonegletscher and Gornergletscher) and landslides (e.g. Tessina, Pian San Giacomo) are also discussed.

Figure 1. The portable radar interferometer deployed over the Gornergletscher showing the rotational scanner, antenna support structure, antennas, and microwave assembly.

REFERENCES

[1] Antonello G., N. Casagli, P. Farina, D. Leva, G. Nico, A. J. Sieber and D. Tarchi, Ground-based SAR interferometry for monitoring mass movements, Landslides, 1(1): 21-28, March 2004.

[2] Pieraccini M., L. Noferini, D. Mecatti, C. Atzeni, G. Teza, A. Galgaro and Nicola Zaltron, Integration of Radar Interferometry and Laser Scanning for Remote Monitoring of an Urban Site Built on a Sliding Slope, IEEE Trans. Geosci. Remote Sensing, 44(9): 2335-2342, 2006

[3] Wiesmann A., C. Werner, T. Strozzi and U. Wegmüller, Measuring deformation and topography with a portable radar interferometer, 13th FIG International Symposium on Deformation Measurements and Analysis and 4th IAG Symposium on Geodesy for Geotechnical and Structural Engineering, Lisbon, Portugal, May 12-15 2008.

[4] Werner C., A. Wiesmann, T. Strozzi and U. Wegmüller,Gamma's portable radar interferometer, 13th FIG International Symposium on Deformation Measurements and Analysis and 4th IAG Symposium on Geodesy for Geotechnical and Structural Engineering, Lisbon, Portugal, May 12-15 2008.

9.23

Rockfall modelling applied to rockfall protection design

Thüring Manfred

Istituto Scienze della Terra, Scuola Universitaria Professionale della Svizzera Italiana, CP 72, CH-6952 Canobbio (manfred.thuering@supsi.ch)

Rockfall modeling by computer simulations can be used to plan and design rockfall protection measures. RockSim3D is a recently developed software to simulate the three-dimensional process of rocks falling down a hill slope. The falling rocks are modeled as individual, dimensionless, spherical particles. The interaction with the digital representation of the terrain occurs at the center of the particles.

The computer program is a stand-alone Microsoft Windows application, reads and writes ESRI raster and shapefiles as input and output and needs a GIS (geographic information system) for pre- and post-processing of input and output. The software is developed in Microsoft Visual Studio and uses the open-source library GDAL for reading and writing GIS vector and raster files.

The main input of the software is a raster file which defines the digital terrain and the surface properties, and a shapefile

containing the starting locations of rock elements. A few models are available to simulate the impact phase of rock elements with the underlying terrain. The main outputs are shapefiles containing the three-dimensional rockfall trajectories and particle locations, attributed by information such as elapsed time, velocity, kinetic energy and elevation above terrain.
Recently the functionality to consider rockfall protection measures, such as fences and barriers was introduced in the software. The protective measures are read from a shapefile and are represented as two-dimensional structures in three dimensions. The protections have characteristics, such as height and maximum mechanical resistance against penetration.
During the down-slope movement of a rock element, impacts with the protective measures are searched for and recognized. Three cases can occur, when a rock element approaches a protection: (i) the protection is not high enough and the rock element jumps over the protection and continues its down slope trajectory (ii) an impact occurs between the rock element and the protection and the kinetic energy of the rock element is below the mechanical resistance of the protection, and the rock element is stopped, (iii) the kinetic energy of the rock element exceeds the resistance of the protection and the rock element penetrates the protection, continuing its downhill trajectory with a residual velocity. As a variant, low-angle impacts between rock elements and protections can lead to a reflection of the rock element.
For each protective measure important information, such as number of impacts, or maximum encountered impact energy is saved and can be used for later analysis.
The introduction of protection fences and barriers enables the modeler to place these elements on the digital terrain and assess their efficiency by conducting rockfall simulations. In an iterative process, both the rock elements (i. e. their starting position, number and mass), and the protective measures (position, extension, height and maximum mechanical resistance) can be varied to determine their optimal position and design.
A case study is presented where the software is used to optimize the design and position of rockfall protection fences.

9.24

Hazard and risk assessment of landslides on accumulation reservoirs – a field applicable scheme

Thüring Manfred*, Cannata Massimiliano*, Hammer Jürg**

*Istituto Scienze della Terra, Scuola Universitaria Professionale della Svizzera Italiana, CP 72, CH-6952 Canobbio (ist@supsi.ch)
**DRM Switzerland SA, CH-6952 Canobbio (hammerj@vt.edu)

Slope instabilities are a threat to accumulation reservoirs and corresponding down-stream areas due to possible slope collapse, generation of flood waves, dam overtopping and flooding of downstream areas. A simple and field-applicable assessment scheme, based on existing approaches, is presented to evaluate hazards and risks due to landslide collapse, in order to obtain a first and preliminary overview. The outcomes are used to support planning of further investigations.

The hazards that arise from the presence of landslides on the slopes of accumulation reservoirs are (Figure 1): (i) The slope instability damages the dam itself and buildings and infrastructure. (ii) The masses of a partial or complete slope collapse reach the reservoir lake and cause a pulse wave, which travels to and damages the dam and buildings and infrastructures. (iii) The pulse wave overtops the dam and causes flooding in the areas below the dam. These three hazard situations are discussed briefly and field-applicable assessment schemes are presented to preliminarily evaluate the hazards and estimate the connected risks in terms of worst case scenarios.

In a first step the primary hazard needs to be assessed, estimating the characteristics of the landslide mass and its path down slope. This is mainly done by field evidence. Key information needed is type of material of landslide, volume, elevation above lake level, inclination of trajectory and width of landslide. The maximum run-out of the hazard is estimated by the Fahrböschung-approach or is modeled, evaluating if the slope instability reaches the reservoir lake (Eisbacher & Clague 1984, Hungr 1995). With the previously obtained information the characteristics of the pulse wave which may be generated due to a slope collapse is estimated, using simple calculations (Huber 1997, Huber & Hager 1997). For this purpose a map view of the reservoir and a cross section of the dam is needed, where dam height and geometry, water depths, freeboard, and distances can be read from. From the calculations it is possible to estimate if dam overtopping occurs.

If the calculated wave is likely to overtop the dam, the consequences of dam collapse and flooding are estimated using methodologies that predict flood heights and velocities in downstream areas (Beffa 2000, BWG 2002). Data obtained from maps or by field inspections is needed, such as valley geometry, roughness and inclination. The vulnerability assessment of the flooded areas is done based on maps or field inspections, such as number and type of flooded objects. The assessment gives an estimate of values and fatalities at risk.

The scheme is field-applicable with data usually available or that can be produced on-site and delivers a preliminary assessment of hazards and risks connected to the presence of landslides on the slopes of accumulation reservoirs. We present and discuss the scheme and show its application in a project in Romania, where a preliminary screening on a number of reservoirs was conducted to identify key characteristics in terms of hazard and risk.

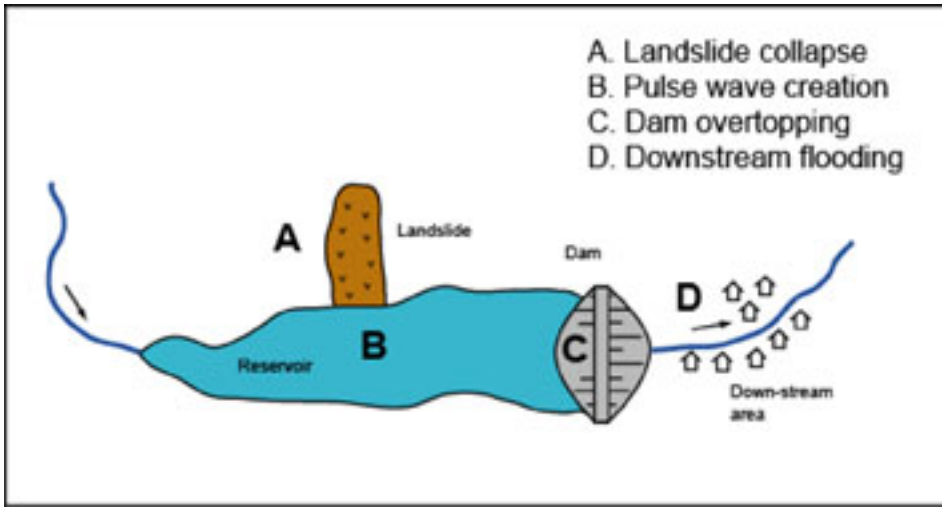

Figure 1. Hazard and risk situations due to the presence of a landslide on an accumulation reservoir.

REFERENCES

Beffa C. (2000): Ein Parameterverfahren zur Bestimmung der flächigen Ausbreitung von Breschenabflüssen, Wasser, Energie, Luft, No. 93, Heft 3/4.

BWG (2002): Sicherheit der Stauanlagen, Basisdokument zu den Unterstellungskriterien. Berichte des BWG, Serie Wasser.

Eisbacher G.H., Clague J.J. (1984): Destructive Mass Movements in High Mountains: Hazard and Management. Geological Survey of Canada, Paper 84-16.

Huber A. (1997): Quantifying impulse wave effects in reservoirs. 19 ICOLD Congress Florence Q.74(R.35), pp. 563-581.

Huber A., Hager W.H. (1997): Forecasting impulse waves in reservoirs. 19 ICOLD Congress Florence C(31), pp. 993-1005.

Hungr O. (1995): A model for the runout analysis of rapid flow slides, debris flows and avalanches. Canadian Geotechnical Journal, 32(4):610-623.

9.25

Landslide investigation by means of PSiNSARTM radar interferometry: the Piemonte experience

Carlo Troisi

ARPA Piemonte, Centro Regionale per le Ricerche Territoriali e Geologiche, via Pio VII 9, 10135 Torino, carlo.troisi@regione.piemonte.it , carlo.troisi@arpa.piemonte.it

PSiNSARTM technique (hereinafter PS technique) is a registered patent of Politecnico di Milano, Italy, and it is one of the Persistent Scatterers Methods, i.e. a group of applications which allow the use of satellite-born radar SAR (Synthetic Aperture Radar) interferometry to detect and measure ground deformations.

The PS Technique identifies single coherent benchmarks, referred to as Permanent Scatterers or PS, and reconstructs their displacement history. PS's are natural "radar targets" that are located across the earth's surface and can be monitored by satellites. When PS remain coherent within a multi-temporal radar data-set, it is possible to detect and measure millimeter variations in the sensor-target distance over time. PS's typically correspond to objects on man-made structures such as buildings, bridges, dams, water-pipelines, antennae, as well as to stable natural reflectors (typically bare exposed rocks faces). Starting with the identification of such PS's, the technique analyzes thousands of square kilometers of territory, within an extremely short time. Indeed, the PS's comprise a sort of "natural geodetic network" for accurately monitoring surface deformation phenomena, as well as the stability of individual structures.

Wherever PS's are present, it is possible to:

- Establish their geographic coordinates.
- Estimate their displacement rate along the Line of Sight (LOS) connecting the satellite and the radar ground target, with a precision which can be as good as 0.1 mm/a, depending on the amount of available data and the PS density.
- Reconstruct the displacement history of an individual PS where the precision can be as good as 1 mm on a single measurements.

All PS measurements can be easily downloaded onto Geographical Information Systems (GIS) and compared with other information layers, for better interpretation of results.
PS technique proved to be excellent for landslide investigation; since the maximum velocity which may be recorded by PS's is in the order of 10 cm/a, the technique is useful basically for slow-moving landslides. The main advantages are:

- Satellite radar images are available since 1992, so that it is possible to obtain displacement data since that year.
- A large number of slow-moving landslide can be cheaply identified and monitored over a wide area.
- There is no need for any field device, benchmark, monument etc., neither the monitored area needs to be accessible.
- Data are easily imported in GIS.

There are also, however, some problems:

- The method records only one component of the displacement, along the line-of-sight (LOS) between the satellite and the PS. The determination of total 3D displacements is not straightforward and may be troublesome.
- The method is not suitable to detect landslides with displacement rates exceeding about 10 cm/a along the LOS.
- The technique works as long as good radar reflectors are present (buildings, bare rocks etc.); in wooded or grass-covered areas it is not applicable. Moreover, unfavourable slope attitude, with respect to satellite acquisition geometries, leads to radar "shadowing" of wide areas. As a result, large portions of a given territory may be unsuited for PS technique. In the Piemonte experience (see below), about one third of the overall surface was totally blind to PS.
- Since satellite orbits are NS oriented, displacements along EW oriented slopes are difficult to detect.
- Since radar satellites pass over the same area once every 35 days (average), real-time landslide monitoring is not possible.
- PS analysis is no trivial matter. Few companies in the world provide this type of analysis
- If the target is affected by LOS displacement values approaching 14 mm between two successive acquisitions, measurements can be "aliased" and the estimation of the displacement may no longer be correct.

In the period 2005-2007 Arpa made a PS survey over the entire Piemonte, about 25000 km^2, the first case in the world of such a wide area surveyed with this technique. The survey was made using data from European radar satellites ERS 1 and 2, covering the time span 1992-2001. Since the main aim of the Arpa survey is landslide detection, this time span is extremely meaningful, for this period was affected by at least seven periods of very heavy or prolonged rains causing both floods and landslides. The survey identified about 2.2 millions PS, out of which about 10% show some displacement. To present the data for diffusion by a web-gis service on Arpa site (www.arpa.piemonte.it) we devised a method based on what we defined area anomala (anomalous area). An area anomala is defined as a polygon containing at least 3 PS's showing a displacement rate exceeding ± 2mm/a and likely to refer to a single definite phenomenon (landslide, subsidence, structural failure etc.). Up to now we defined about 2200 aree anomale. For each area it is possible to download a form describing all the relevant features.

The PS survey is proving extremely useful for the integration of the Piemonte landslide inventory, which includes, up to now, about 35000 landslides, mapped at the scale 1:10k (http://marcopolo.arpa.piemonte.it/website/geo_dissesto/arpa_ib_iffi/viewer.htm).

Up to now we mainly used PS's for:

- Identification and definition of formerly unknown landslides.
- Better definition of landslide limits.
- Definition of the state of activity.
- Zoning of large landslides.

Last, Arpa Piemonte is also experimenting the use of PS's for identification and definition of recent tectonic displacements. The first results are extremely promising.

9.26

Microzonage sismique du Canton de Fribourg: Carte de Sol de fondations

Vouillamoz Naomi* & Mosar Jon*

* *Département de Géosciences Université de Fribourg, Chemin du Musée 6, CH-1700 Fribourg (naomi.vouillamoz@unifr.ch)*

La coordination des cartes de sols de fondation à l'échelle 1 : 25'000 du canton de Fribourg vient terminer en juillet 2008 une étude de microzonage sismique lancée par l'Établissement cantonal d'assurance des bâtiments (ECAB) en collaboration avec la section Risques géologiques de l'Office fédéral de l'environnement (OFEV).
La norme SIA 261 défini 6 classes de sol de fondation (de A à F) sur la base des caractéristiques (lithologie, épaisseur et vitesse des ondes S) des 30 premiers mètres des couches superficielles. La cartographie des différentes classes de sols de fondation permet ainsi d'établir les données d'aléa sismique local. Ces données sont calculées à partir du potentiel d'amplification des ondes sismiques de chaque classe pour les 3 zones d'aléa sismique régional que comporte le canton de Fribourg (zones 1, 2 et 3a, approximativement du Nord au Sud). Cette démarche permet d'évaluer le risque sismique des agglomérations du canton d'une part et de définir le dimensionnement des bâtiments qui devrait s'en suivre d'autre part.
Les mandataires suivants ont participé à l'élaboration des cartes de sols de fondation pour les différentes parties du territoire cantonal fribourgeois délimitées par les feuilles de l'Atlas topographique suisse au 1 : 25'000 (Figure 1) :

- le bureau ABA-GEOL SA (Fribourg) pour les parts fribourgeoises des feuilles 1164 Neuchâtel, 1165 Morat, 1184 Payerne, 1204 Romont, 1244 Châtel-St.-Denis, 1245 Château-d'Oex, 1264 Montreux et 1265 Les Mosses ;
- le Département de Géosciences – Sciences de la Terre de l'Université de Fribourg pour les feuilles 1185 Fribourg, 1205 Rossens et 1224 Moudon ainsi que pour les klippes ou débordements non mandatés 1145 Bielersee, 1166 Bern, 1183 Granson, 1203 Yverdon-les-Bains et 1246 Zweisimmen ;
- le bureau Institut Géotechnique SA (Berne) pour les parts fribourgeoises des feuilles 1186 Schwarzenburg, 1206 Guggisberg et 1226 Boltigen ;
- le bureau Géoval Ingénieurs-Géologues SA (Sion) pour la feuille 1225 Gruyères.

L'élaboration des cartes se fait par l'interprétation en terme de classes de sols de fondation de différents types de données. Les cartes géologiques, les orthophotos, les modèles numériques de terrain (MNT 1m) et ombrages, servent d'information de base en ce qui concerne la nature du terrain. Les données de forages, la carte des instabilités et glissements de terrains du canton ainsi que des études géophysiques ponctuelles (géothermie, géoélectricité, géoradar, « petite sismique », ...) donnent des indications quand à la profondeur du substrat rocheux.
Les cartes de sols de fondation du canton de Fribourg ont été élaborées sous forme de SIG à l'aide de la suite de logiciels ArcGIS©. Une réactualisation continue est ainsi possible lorsque de nouvelles données sont à disposition. Lors de la synchronisation, une certaine systématique a été appliquée dans le but d'uniformiser les fichiers sources d'une part et de coordonner les bordures des cartes selon les mêmes critères d'autre part.

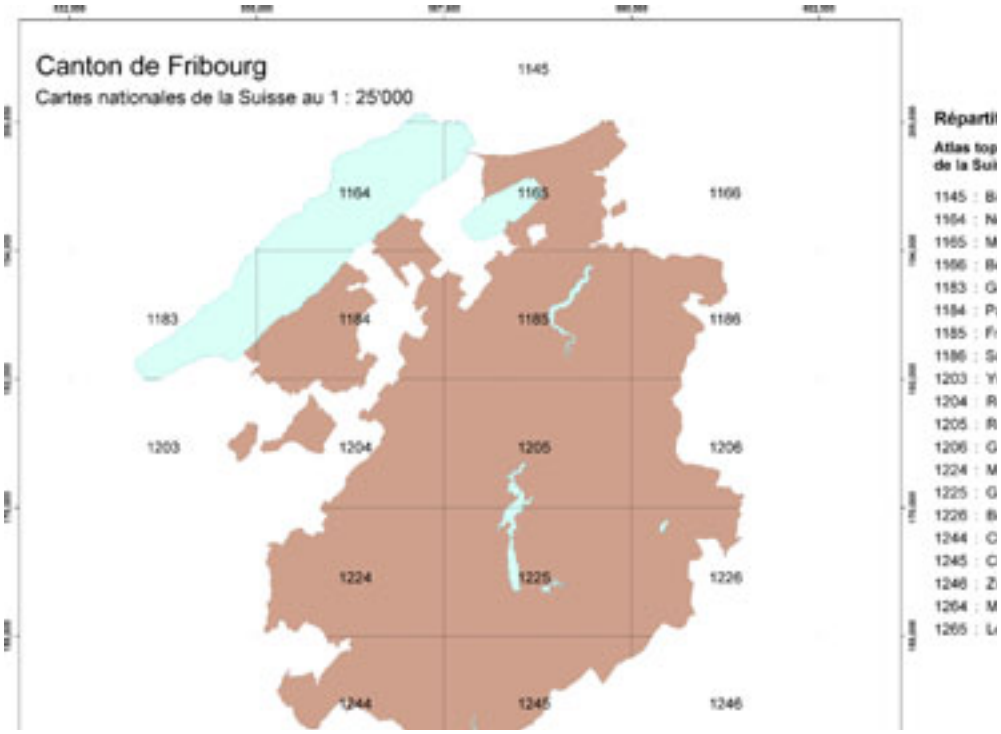

Figure 1. Carte de la répartition des feuilles 1 :25000 couvrant les canton fe Fribourg.

9.27

Effects of tectonic structures, groundwater pumping, and mining activity on evaporite subrosion and resulting land subsidence

Eric Zechner*, Ina Lewin**, Markus Konz*

*Geologisch-Paläontologisches Institut, Universität Basel, Bernoullistrasse 32, CH-4056 Basel (eric.zechner@unibas.ch)
** now at Institut für Angewandte Geowissenschaften, Technische Universität Darmstadt, Schnittspahnstr. 9, D-64287 Darmstadt (change of name from Spottke to Lewin 4/2008)

Evaporites of gypsum or rock salt are widely seen as the most soluble common rock formation. Percolating undersaturated groundwater leads to subsurface dissolution, or subrosion of evaporites and, consequently, to the development of karst. Depending on the hydrogeological setting and the anthropogenic circumstances, the subrosion may cause widespread land subsidence. Even comparably small subsidence rates can significantly affect sensitive urban infrastructure, such as larger buildings, dams, power plants, or the railway tracks for high-speed trains which cross the presented Muttenz-Pratteln site in Northwestern Switzerland.

For the observed widespread land subsidences several causes were considered: (1) natural dissolution of the evaporites of the Middle Muschelkalk (anhydrite and halite), which is induced by the tectonic setting with a set of Horst and Graben structures, (2) salt solution mining, which has been pursued at different locations over the last 150 years, (3) large-scale extraction of groundwater in the Upper Muschelkalk aquifer with successive hydrostatic connection along the normal faults. The tectonic setting of the study area is characterized by horst and graben structures delimited by normal faults. The construction of a 3D geological model included 47 faults and 4 faulted horizons of the main aquifers-aquitards boundaries and provided a basis for numerical groundwater modeling and the comparison with geodetic survey data (Spottke et al. 2005). The 3D numerical groundwater model was used to delineate areas with increased hydrostatic gradients. Intermediate scale laboratory experiments were conducted to understand density-coupled flow mechanisms in porous media. The setup of the density flow experiment was chosen to simulate the geological conditions found at the site (Konz et al. 2008). Recent land subsidences have been surveyed at 6 separate locations within the Muttenz-Pratteln area East of Basel, Switzerland. The diameters of the affected surface areas range from 100 to 1500 m, and corresponding subsidence rates reach more than 100 mm/year. Three sites show elongated shapes of depression cones along a SSW-NNE-oriented axis corresponding to the striking of the Horst and Graben structures, and, therefore, indicating a strong relation to the tectonic setting. The subsidence hazard area above each former or recent solution mining well was estimated based on a model concept, where the collapsed roof of excavated salt propagates with a 45 degrees angle to the surface. For three sites, which are salt solution mining fields, the predicted hazard area corresponds to the observed area of subsidence. One site, where solution mining has stopped more than 100 years ago, shows evidence that the initial cause for subsidence, i.e. solution mining, has been replaced by large-scale groundwater withdrawal initiating a significant hydrostatic gradient, which propagates along the graben normal fault network from the Upper Muschelkalk Aquifer to the evaporites of the Middle Muschelkalk. For the two last sites, a combination of a natural dissolution process due to the tectonic setting and a slightly increased hydrostatic gradient seems the most probable cause for the ongoing land subsidence.

REFERENCES

Konz, M., Ackerer, P., Younes, A., Gechter, D., Zechner, E. & Huggenberger, P. 2008: New homogeneous and heterogeneous laboratory-scale 2-D benchmark experiment for density-coupled flow models. Accepted to Water Resour. Res.

Spottke, I., Zechner, E. & Huggenberger, P. 2005: The southeast border of the Upper Rhine graben: A 3D structural model of geology and its importance for groundwater flow. Int. Jour. Earth Sci., 94, 580–593.

10. Anthropogenic impacts on hydrological regime

Sandro Peduzzi, Andrea Salvetti

Swiss Society for Hydrology and Limnology (SGHL)
Swiss Hydrological Commission (CHy)

10.1

Evaluation of the hydraulic properties of constructed wetlands using geoelectric techniques

Mehdy Al-Zoubaidy*, Alessandro Brovelli*, Luca Rossi*, D. Andrew Barry*, and Klaus Holliger**

* *Ecological Engineering Laboratory, Environmental Sciences and Technologies Institute, EPFL, CH-1015 Lausanne*
** *Institute of Geophysics, University of Lausanne, CH-1015 Lausanne (klaus.holliger@unil.ch)*

Wastewater purification through massive horizontal and/or vertical filtering is increasingly applied throughout the world, albeit with varying success. Different types of systems, commonly referred to as "constructed wetlands" (CWs) can be used to treat wastewaters produced by individual houses, isolated settlements and even small towns provided that the surface area for the treatment is available (Brix, 1993). Among the key advantages of this technology is that CWs require only a small energy input, because they make use of natural biological processes for the degradation of pollutants. Despite their inherent simplicity, these systems are still poorly understood, particularly with regard to the processes responsible for the pollutant degradation and hence, there is significant potential for improving their performances by optimizing the individual subprocesses (Vymazal, 2007). To this end, a well-controlled and extensively instrumented model of a CW system was set up at the Ecological Engineering Laboratory of EPFL (for further information see http://ecol.epfl.ch/research/remieco).

A key prerequisite for studying and characterizing a CW system is to understand and control its hydraulic behavior. Preliminary tests conducted with saline tracers on our laboratory set-up indicated a complex flow field, possibly resulting from the coupled effects of the elevated density of the tracer plume and the inherently non-homogeneous distribution of the hydraulic properties. To investigate these aspects and in attempt to infer the 2D tracer distribution, a set of cross-hole geoelectric resistivity surveys is being conducted. Geoelectric techniques are commonly used to investigate the spatial variability of hydraulic properties and to monitor the evolution of saline plumes (e.g., Slater et al., 2000; Zhou and Greenhalgh, 2000). To obtain reliable and detailed resistivity measurements we constructed an ad hoc device consisting of 2 arrays containing 10 electrodes each. The vertical spacing between the electrodes is about 0.045 m.

The preliminary tests we conducted so far clearly illustrate the potential of the proposed methodology to characterize the hydraulic behavior of our CW model. The left-hand panel of Figure 1 depicts the quasi-1D evolution of apparent electrical resistivity, from time=0h (no tracer) to time=14h (peak of tracer observed in breakthrough curve, not shown). Due to the increased water density as a consequence of the dissolved tracer salt, the vertical profile is not homogeneous but the concentration tends to increase with the depth. The right panel of Figure 1 shows some preliminary 2D time-lapse results obtained by tomographically inverting the measured difference in apparent resistivity data measured at time=0h and time=14h. While the vertical stratification of the resistivity structure seen in the quasi-1D time-lapse profiles shown in the left-hand panel is clearly confirmed, the prominent resistivity anomaly at approximately 5 cm lateral distance and 33 cm depth could indeed be indicative of preferential flow phenomena related to the inherently hydraulic heterogeneity of the materials used to construct typical CWs.

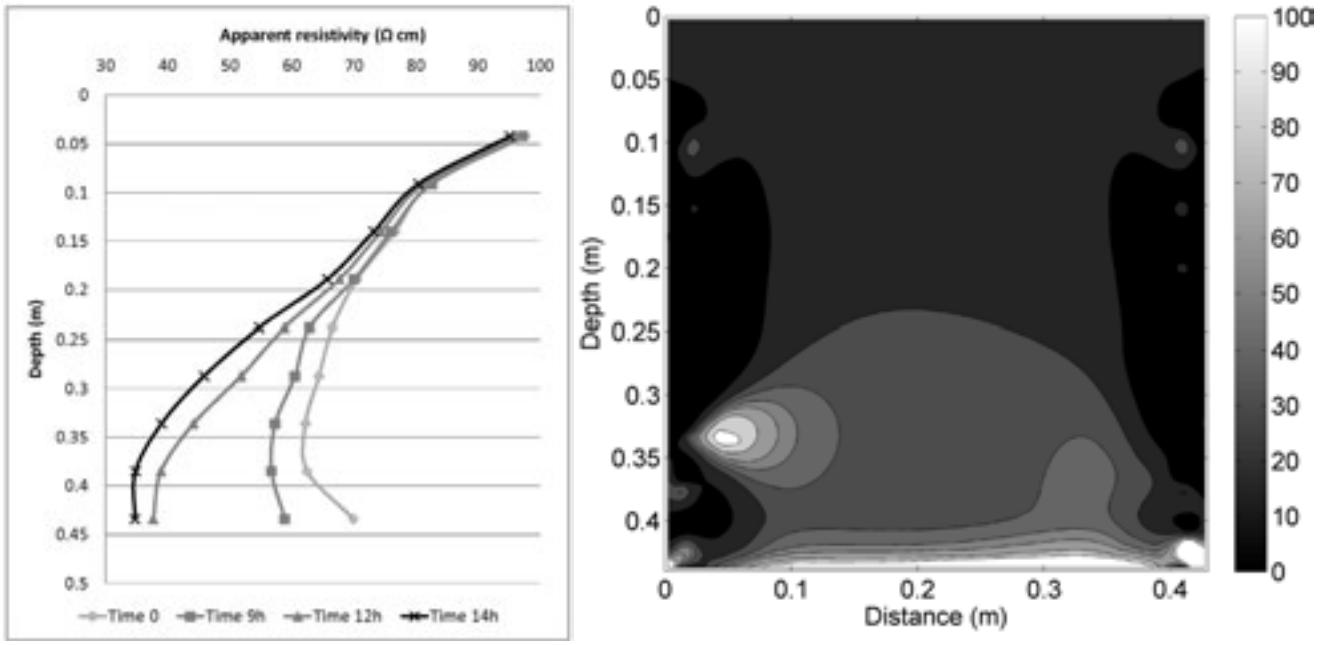

Figure 1. Left: evolution of the resistivity as a function of time and depth in a CW model system during a saline tracer experiment. Right: tomographic reconstruction of the change in resistivity between time=0h and time=14h. The grey-scale range of resistivity variations is given in Ωcm.

REFERENCES

Brix H. 1993: Wastewater treatment in constructed wetlands: system design, removal processes, and treatment performance. In: Moshiri GA, editor. Constructed wetlands for water quality improvement. CRC Press.

Vymazal J. 2007: Removal of nutrients in various types of constructed wetlands. Science of the total environment 380, 48-65.

Slater L., Binley, A.M., Daily, W. & Johnson, R. 2000: Cross-hole electrical imaging of a controlled saline tracer injection, Journal of Applied Geophysics, 44, 85-102.

Zhou B., & Greenhalgh S.A. 2000: Cross-hole resistivity tomography using different electrode configurations, Geophysical Prospecting, 48, 887-912.

10.2

Schwall/Sunk und Morphologie in Fliessgewässern

Peter Baumann

Limnex AG, Zürich

In den letzten Jahren sind die gewässerökologischen Auswirkungen des Schwallbetriebes aus Speicherkraftwerken auch in der Schweiz an einer zunehmenden Zahl von Flüssen untersucht worden. Unter dem Eindruck der so gewonnenen Erkenntnisse wird seit einiger Zeit auch an einer gesetzlichen Regelung dieser Problematik gearbeitet, steht Schwall/Sunk also auf der umweltpolitischen Traktandenliste. Dabei verlangen sowohl die Volksinitiative „Lebendiges Wasser" des Schweizerischen Fischerei-Verbandes als auch die parlamentarischen Initiative „Schutz und Nutzung der Gewässer" der Ständerätlichen Kommission für Umwelt, Raumplanung und Energie, die betroffen Gewässer seien hydrologisch und morphologisch aufzuwerten. Als wesentliche Massnahmen werden dabei, ebenfalls in beiden Fällen, die Revitalisierung der Gewässer, die Verminderung der negativen Auswirkungen von Schwall und Sunk sowie die Reaktivierung des Geschiebehaushaltes ausdrücklich verlangt.
Es stellt sich somit die Frage, wie sich der Schwallbetrieb und die Morphologie in Fliessgewässern gegenseitig beeinflussen. Die Wechselwirkungen von hydrologischen und morphologischen Eingriffen in die Gewässerökologie müssen bekannt sein, um die möglichen Aufwertungsmassnahmen besser aufeinander abstimmen zu können.
Im ersten Teil des vorliegenden Referates wird über die Ergebnisse aus verschiedenen Studien an schwallbeeinflussten Fliessgewässern berichtet und aufgezeigt, was diese Studien über den Zusammenhang zwischen Flussmorphologie und Schwall-Auswirkungen bisher ergeben haben.
In einem zweiten Teil des Referates wird an Beispielen untersucht, wie sich morphologische und/oder hydrologische Veränderungen in verschiedenen Indikatoren für die Beurteilung des Gewässerzustandes niederschlagen. An diesen Beispielen wird schliesslich auch geprüft, wie weit der ökologische Zustand bzw. die ökologische Qualität der untersuchten Schwallstrecken mit theoretischen Vorstellungen über die Auswirkungen von hydrologischen Störungen übereinstimmt.

10.3

Effects of pump storage operations on reservoir turbidity

Bonalumi Matteo*, Anselmetti Flavio*, Kägi Ralf**, Müller Beat*** & Wüest Alfred***

* *Eawag, Swiss Federal Institute of Aquatic Science and Technology, Surface Waters – Research and Management, CH–8600 Dübendorf (matteo.bonalumi@eawag.ch)*
** *Eawag, Urban Water Management, CH–8600 Dübendorf*
*** *Eawag, Surface Waters – Research and Management, CH–6047 Kastanienbaum*

Hydroelectric energy covers in Switzerland about 60 % of the energy requirement. To increase production and to better cover peak demand periods, pump storage operations are becoming more and more important. The effect of hydropower activities on light regime and on primary production in downstream lakes has been studied recently (Finger et al, 2007; Jaun et al., 2007). It is, however, not well understood, how such increased pump activities affect suspended particle load, particle characteristics and sedimentation processes, and whether they may affect also ecologic conditions in downstream areas.

Oberaarsee and Grimselsee, two reservoirs located in a glaciated catchment in the Central Alps, are since 1980 part of a pump storage operations scheme with annual water exchanges amounting to several times the lake volumes. We are currently analyzing this system with the aim to understand how pump storage and turbine operations may influence the water turbidity and sedimentation in the reservoirs. Investigations are undertaken seasonally in different locations and depths of both reservoirs. We determined suspended particle content, combined vertical profiles of temperature and turbidity using a CTD instrument, analyzed composition, number and grain size of particles and used SEM imagery to determine particle shapes. Furthermore, sediment cores provide seasonally-resolved time series of reservoir sedimentation.

For almost all the CTD profiles and analyses of suspended particles collected in Oberaarsee and Grimselsee, a positive correlation exists between turbidity, grain size distribution, particle number and mass concentration. The highest turbidity in both reservoirs occured in summer whereas the lowest was found at the end of winter, when no river inflows and the reservoirs are covered by ice. Moreover, vertical profiles have shown that turbidity generally increases with increasing reservoir depth.

In every season, specific features have been observed related to the annual cycles of climate, runoff and pump storage operations. In summer, when the hypolimnion is characterized by similar conditions in both reservoirs, the epilimnion of Oberaarsee is clearer and warmer in comparison with that of Grimselsee, indicating that a stronger thermal stratification in Oberaarsee may favor the settling of the suspended particles. In winter, higher turbidity has been measured specifically in in the Eastern basin of Grimselsee, where the power operations are continuously exchanging water between the two reservoirs. The decrease in water level of the reservoir causes the emersion of bedrock ridges that impede the flow of this more turbid water of the Eastern basin into the clearer Western part of the reservoir.

A recognized effect of both reservoirs is that they retain sediment that would normally be carried downstream by the River Aare (Anselmetti et al., 2007). Further investigations will try to deepen also the ecological impact down rivers of pump storage operations.

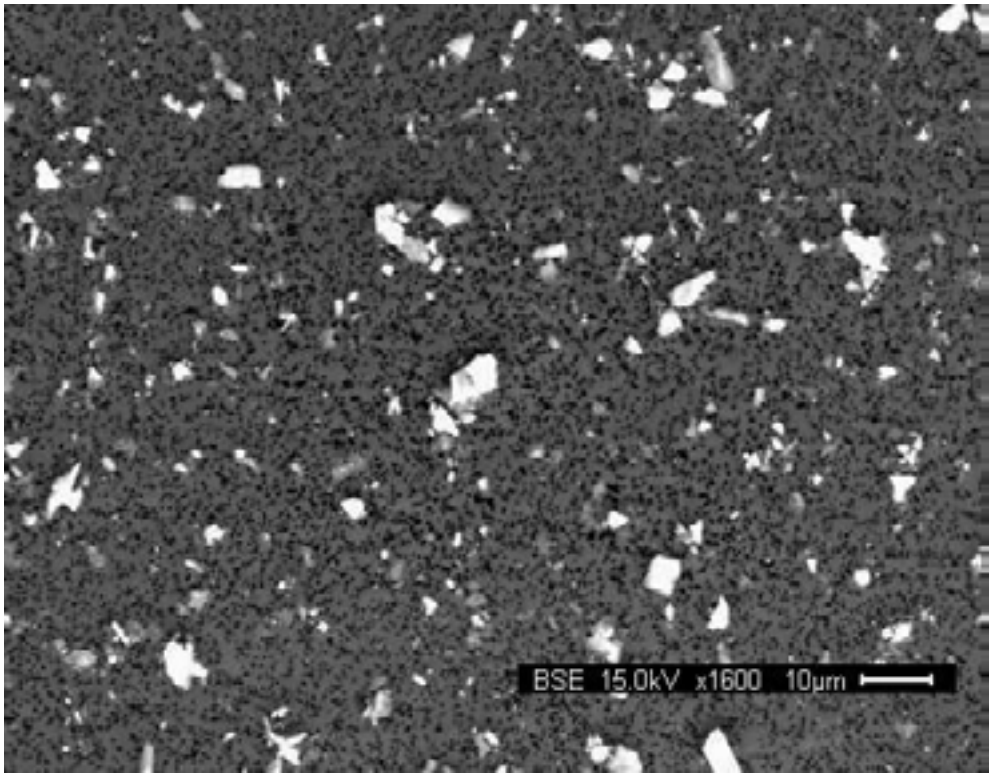

Figure 1. SEM backscattered electron image of clay minerals, feldspar and quartz particles from Grimselsee in 2008, July 28.

REFERENCES

Anselmetti, F. S., Bühler, R., Finger, D., Girardclos, A., Lancini, A., Rellstab, C. & Sturm, M. 2007: Effects of Alpine hydropower dams on particle transport and lacustrine sedimentation. Aquatic Sciences, 69, 179-198.

Finger, D., Bossard, P., Schmid, M., Jaun, L., Müller, B., Steiner, D., Schäffer, E., Zeh, M. & Wüest, A. 2007: Effects of alpine hydropower operations on primary production in a downstream lake. Aquatic Sciences, 69, 240-256

Jaun, L., Finger, D., Zeh, M., Schurter, M. & Wüest, A. 2007: Effects of upstream hydropower operation and oligotrophication on the light-regime of a turbid peri-alpine lake. Aquatic Sciences, 69, 212-226.

10.4

Urban storm water runoff impacts on receiving waters. On the use of continuous modelling and quantitative indicators.

Consuegra David*

**Docteur ès Sciences Appliquées in Rural Engineering of the Swiss Federal Institute of Technology (EPF), Lausanne, CH. Currently scientific director at B+C Engineering SA, Montreux, CH.*

It is widely recognised that urban storm runoff substantially modifies the natural hydrological regime of river systems. Special emphasis is normally given to qualitative impacts, a significant amount of publications deal with the assessment of pollution loads and the modelling of concentrations in storm runoff and receiving water bodies. The quantitative impacts of urbanization are also well documented and can always be summarized by more or less significant increases of runoff volumes and flood peaks and reductions of watershed response times. In urban runoff control studies the priority is normally given to the impacts on floods with moderate to high return periods. The impacts of urbanization on river flooding are normally documented by simple comparisons between present and future design floods and corresponding hydrographs. Most of these comparisons are based on single event modelling based on design storms and/or historical rainfalls selected from intensity-duration-frequency curves.

The increased environmental concern regarding the protection and the restoration of aquatic systems requires the analysis of urban runoff quantitative impacts to be extended to other processes such as river bed and bank erosion, rapid increases and decreases of water levels and velocities, seasonal shifting of flow occurrences as well as clogging of river substratum. The analysis of urban runoff impacts on these processes requires the whole hydrological regime to be assessed; this includes not only flood peaks but also low to medium average flow quantities as well as duration and seasonality.

Simulation techniques need to be adapted to the analysis of the overall hydrological regime. Single event modelling is no longer applicable; long term continuous models have to be used instead. Continuous rainfall inputs must be considered. Suitable approaches to define representative rainfall series have to proposed and applied. Finally, new techniques have to be developed and tested to identify quantitative impacts of urban runoff on simulated hydrological regimes accounting for inter annual variability, climate sensitivity and land use changes.

In the framework of an overall and regional assessment of urban runoff impacts on river systems, the canton of Geneva developed a new methodological framework to describe and model the most determinant characteristics of hydrological regimes. The main features of this methodology include:

Define a global strategy to model hydrological regimes by an appropriate selection of modelling tools and an adequate strategy for model calibration and validation. This concerns both, urban and rural watersheds. The choice of the canton of Geneva refers to deterministic, conceptual and relatively detailed hydrological models.
Define adequate rainfall inputs made of long term continuous series. The canton of Geneva developed several stochastic continuous series; each one covers a period of 20 years with a 10 minutes time step. In conjunction with observed continuous records of precipitation, the rainfall series are used to generate at specific watershed locations several signatures of hydrological regimes. Every time three cases are considered, the first one produces a reference hydrological regime which does not have an urban runoff component while the other two describe the hydrological regime for present and future extents of urbanization.
The various hydrological regimes are analysed with quantitative indicators which are supposed to represent the variations of the most pertinent hydrological regime characteristic with respect to the river process that is analysed, for instance seasonality. Several indicators have been proposed. They are all accompanied with a statistical interpretation framework in order to assess the level of significance of the changes induced by urban runoff accounting for climate sensitivity and variability.

The figure below illustrates the flow series produced for the reference and the future urbanization extents for one of the studied rivers within the canton of Geneva. The analysed indicator is the monthly number of exceedances of a threshold flow value above which sediment transport may occur. The indicator clearly shows the seasonal shift between the reference (rural) hydrological regime and the future one. The statistical framework indicates that the changes are very significant for both the average and the standard deviation of the number of exceedances occurring during the summer period.

ACKNOWLEDGEMENTS
This work is the result of a group effort including the following Geneva cantonal authorities: P. Grandjean, E. Werlen and F. Pasquini from SECOE, A Wyss from SEVAC, F Bachman from SPDE and P. Nirel from former ECOTOX. All modeling developments have been made by D. Consuegra and Gaetan Seguin presently at B+C Ingénieurs, 1820 Montreux.

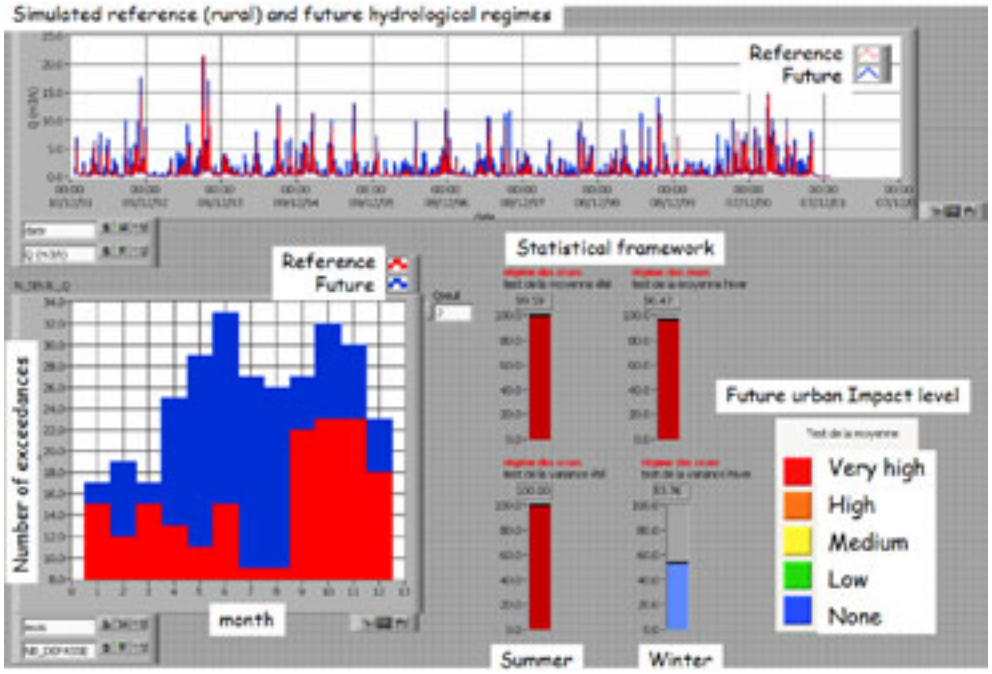

10.5

Schwall-Sunk in der Linth (GL) – ein neuer Ansatz zur Reduktion der Auswirkungen auf das Flussökosystem.

Arthur Kirchhofer, Martina Breitenstein

WFN – Wasser Fisch Natur/, Gümmenen.

Abstract

Die Linth im Kanton Glarus wird von den Kraftwerken Linth Limmern AG (KLL) und von einer grösseren Zahl Kleinwasserkraftwerke genutzt. Für die Anlagen der KLL wurde 2006 ein Gesuch mit UVB 1. Stufe zur vorzeitigen Neukonzessionierung eingereicht und im Juni 2007 mit einem Zusatzbericht zur Schwall-Sunk-Problematik in der Linth ergänzt. Dabei wurde festgestellt, dass mit dem Schwall-Sunk-Betrieb der KLL das Ökosystem der Linth und dessen Organismengemeinschaften negativ beeinflusst werden. Um diese Beeinträchtigungen soweit möglich zu reduzieren, wurden Vorschläge zur Anpassung des Schwall-Sunk-Regimes ausgearbeitet.

Grundlage dieser Vorschläge waren Erkenntnisse aus Untersuchungen der Wirbellosen- und der Fischfauna und umfangreichen hydraulischen Modellierungen der Linth. Es konnte aufgezeigt werden, dass bei jedem Schwall die Flusssohle zwischen Linthal und Schwanden in Bewegung gerät und eine „Katastrophendrift" der aquatischen Wirbellosen stattfindet. Entsprechend gering sind Wirbellosenbiomasse, Fischbestand und fischereiliches Produktionsvermögen des Gewässers.
Die Variantenbeurteilung für einen zukünftigen Schwall-Sunk-Betrieb basierte auf den Habitatansprüchen und dem Flächenbedarf einer Fischpopulation in der Linth, die in etwa derjenigen eines hypothetischen, nicht von der KLL beeinflussten Ausgangszustandes entsprechen würde. Der Vergleich des Flächenbedarfs des aktuellen Fischbestandes mit dem Flächenangebot beim aktuellen Schwall-Sunk-Regime erlaubte die Folgerung, dass heute in erster Linie die für eine natürliche Fortpflanzung der Bachforelle geeigneten Flächen mit stabilem Sohlensubstrat den Fischbestand limitieren. Aufgrund der für die angestrebte Zielpopulation notwendigen Fläche mit stabilem Laichsubstrat wurde ein neues Schwall-Sunk-Regime definiert, das in die im Januar 2008 erteilte Neukonzession übernommen wurde.

10.6

Eco-hydrological impacts of hydropower production in the Adige river system

Maiolini Bruno*, Bruno Maria Cristina**, Carolli Mauro**, Silveri Luana**, Zolezzi Guido***, Bellin Alberto*** & Siviglia Annunziato***

* *Museo Tridentino di Scienze Naturali, Via Calepina, 14, I-38100 Trento*
** *Fondazione E. Mach, Via E. Mach, 1, I-38010 S. Michele all'Adige (Trento)*
*** *Department of Civil and Environmental Engineering, University of Trento, I-38100 Trento*

Most river systems worldwide suffer from loss of ecosystem connectivity, mainly due to dam building and water diversion (Nilsson et al., 2005). In the Alps, the longitudinal, lateral and vertical continuity of riverine ecosystems has been reduced by physical barriers such as dams, canalization, embankments. As a consequence, the disruption of the river continuum has severe effects on the ecological health of rivers and is a major cause of decline in freshwater biodiversity (Bunn & Arthington, 2002).
The historical alteration of the temporal dimension of rivers, i. e. changes of the flow regime at different time scales, has been little investigated. Most of the ecological alterations observed in Alpine rivers are due to hydroelectric power generation, which in the Alps has great economical relevance (Maiolini & Bruno, 2008). Hydropower is a strategic gas-free renewable energy and thus it should be maintained and possibly increased, but given its severe consequences on other benefits and goods deriving from freshwater ecosystems, eco-sustainable approaches to the management of the different phases of hydropower production should be explored.
Long-term changes in the hydrological regime were studied in the Adige River from 1923 to 2006, using different statistical approaches among which the Range of Variability Approach (RVA) (Richter et al., 1997). Severe changes occurred starting from the sixties, when most dams, diversion structures and associated power plants were built (Fig. 1). In more recent years changes in the timing of plant operation, dictated by the energy market, coupled with climate change and other uses such as artificial snow production, have worsened the effects of hydropeaking.
In order to assess in detail the effects of hydropeaking on the river communities, one single hydropeaking event was studied downstream of a representative Alpine power plant on the Noce River, a main tributary to the Adige River. Benthic fauna was affected by catastrophic drift for at least 8 km downstream of the power plant (Fig. 2). Our studies confirmed the well known effects of hydropeaking on the benthic community (i.e. Cereghino et al., 2002); in addition we explored the effects on the hyporheic habitat, where the ratio between stigobite and stigophile taxa was found to be severely affected downstream of the hydropower plant, due to clogging of the interstices.
Further research is being carried on using artificial flumes to analyse separately the physical, hydrological and chemical changes associated with the hydropeaking wave such as discharge, temperature and turbidity variations.

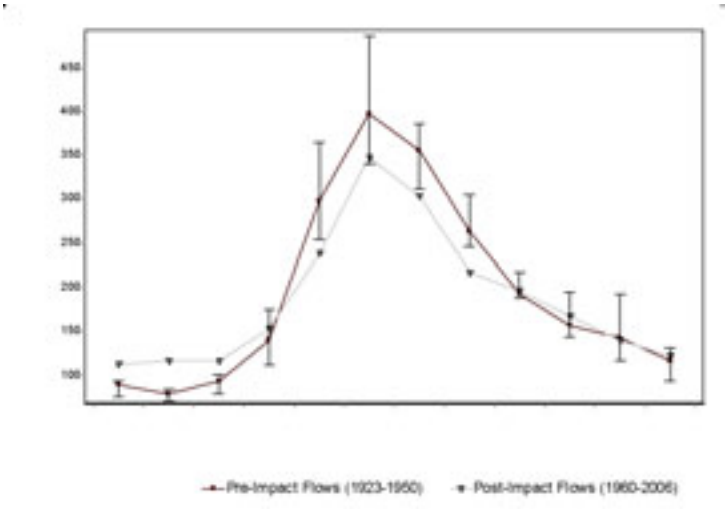

Figure 1. Results of RVA analysis: median monthly flow alterations of the Adige River for pre- and post-regulation periods, measured at Trento San Lorenzo gauging station. Vertical lines represent RVA category boundaries (i.e. the 34th and the 67th percentile of the pre-impact values) into which the post-regulation values should fall.

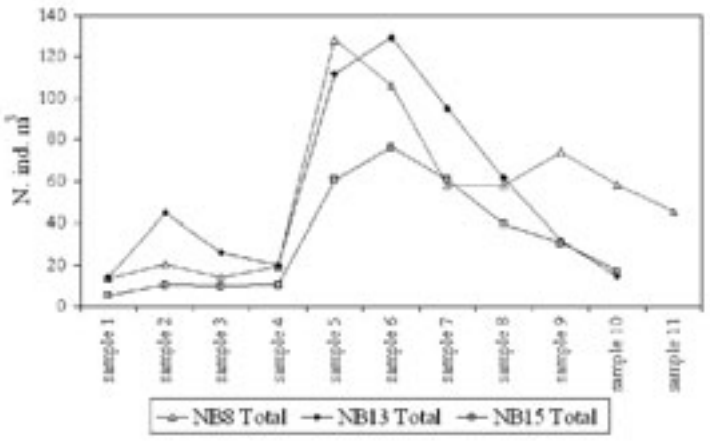

Figure 2. Densities of drifting invertebrates (n. ind./m³) collected at 5 minute intervals at stations NB8 (0.5 km downstream of the power plant), NB13 (6 km), NB15 (8 km). The water release started between sample 4 and 5.

REFERENCES

Bunn, S. E., and A. H. Arthington (2002), Basic principles and ecological consequences of altered flow regimes for aquatic biodiversity, Environ. Manage., 30(4), 492–507.

Céréghino, R., P. Cugny & P. Lavandier, 2002. Influence of intermittent hydropeaking on the longitudinal zonation patterns of benthic invertebrates in a mountain stream. International Review of Hydrobiology 87: 47–60.

Maiolini, B., and M. C. Bruno (2008), The River Continuum Concept revisited: lessons from the Alps. Alpine space - man & environment, vol. 3: The Water Balance of the Alps. Innsbruck University press, pp 21-30.

Nilsson, C., C. A. Reidy, M. Dynesius, and C. Revenga (2005), Fragmentation and Flow Regulation of the World's Large River Systems, Science 308, 405–408.

Richter, B. D., J. V. Baumgartner, J. Powell, and D. P. Braun (1996), A method for assessing hydrologic alteration within ecosystems, Conserv. Biol., 10, 1163–1174.

10.7

Module Hydrology: Assessing the natural status of the flow regime. Methodology and case study Brenno (TI)

Pfaundler Martin*, Salvetti Andrea**

* *Bundesamt für Umwelt (BAFU), CH-3003 Bern (martin.pfaundler@bafu.admin.ch)*
** *Ufficio dei corsi d'acqua Cantone Ticino, Viale Stefano Franscini 17, CH-6500 Bellinzona (andrea.salvetti@ti.ch)*

The flow regime: the driving force of water dynamics

Next to water quality and the ecomorphological status of rivers, the flow regime is the third decisive abiotic influencing factor for the ecological status of watercourses. The "Guiding Principles for Swiss watercourses" (SAEFL and FOWG, 2003) therefore stipulate development goals of "sufficient water quality", "sufficient space for water courses" and "sufficient water flow".

The modular-stepwise-procedure (BUWAL, 1998) develops and provides Swiss-wide standardised methods to assess the ecological status of running waters. So far a module covering hydrological aspects has been missing to yield a comprehensive picture of a river's ecological status.

The Module Hydrology-flow regime (in short HYDMOD) has therefore been developed and conceived as an implementation aid for the Cantons for the above mentioned reasons and also with respect to the requirement of nature-like flow regime conditions as enacted in the federal water protection legislation.

HYDMOD starts with the inventory of water resources management related measures and interventions. Their impacts on the flow regime are evaluated. The result is a classification of the flow regime's natural status for a river system with individual river reaches as spatial reference objects. It is based on nine assessment indicators covering a wide variety of flow regime characteristics from the low flow, medium flow and high flow water regime.

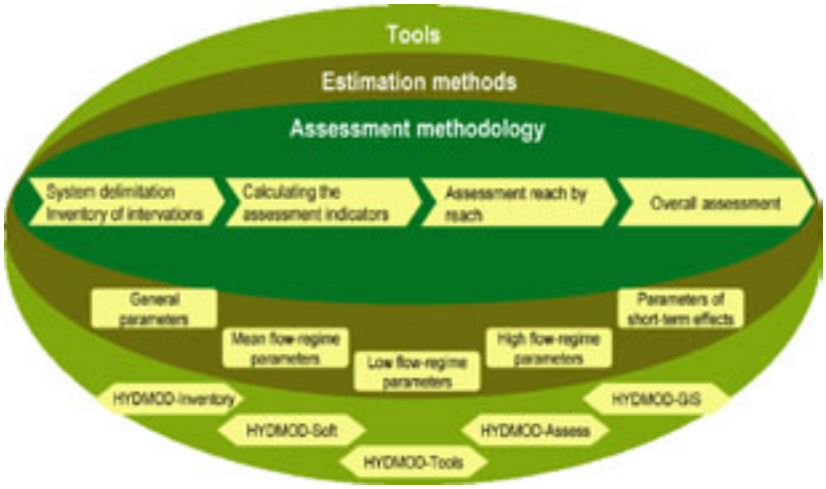

Figure 1. The "package" Module Hydrology – Flow Regime (HYDMOD)

Figure 1 schematically illustrates in the centre the single steps of the assessment method: from (1) inventorying the man-made interventions to (2) calculating the assessment indicators for the significant interventions, then (3) translating the point assessment at the intervention's location to the individual river reaches downstream and finally (4) aggregating the results for the individual indicators to a global classification.

As figure 1 also shows, HYDMOD comes as a package: the use of HYDMOD requires a number of hydrologic parameters. In many cases however, it can be assumed that the data available are scarce. For this reason, in parallel to the method development, a series of hydrologic fundamentals and estimation procedures were worked out that form part of HYDMOD. Finally, a few electronic tools were also developed which should make individual steps in the method's application easier for the user.

Case study Brenno

The method has been tested for the Brenno river basin in the Blenio valley (Canton Ticino) which is influenced by many interventions related to hydro-power exploitation (water abstraction, water deviations, reservoirs etc.). Figure 2 illustrates the cartographic results, left for one of the assessment indicators ("flood frequency"), right the global assessment (aggregation of the nine single indicators).

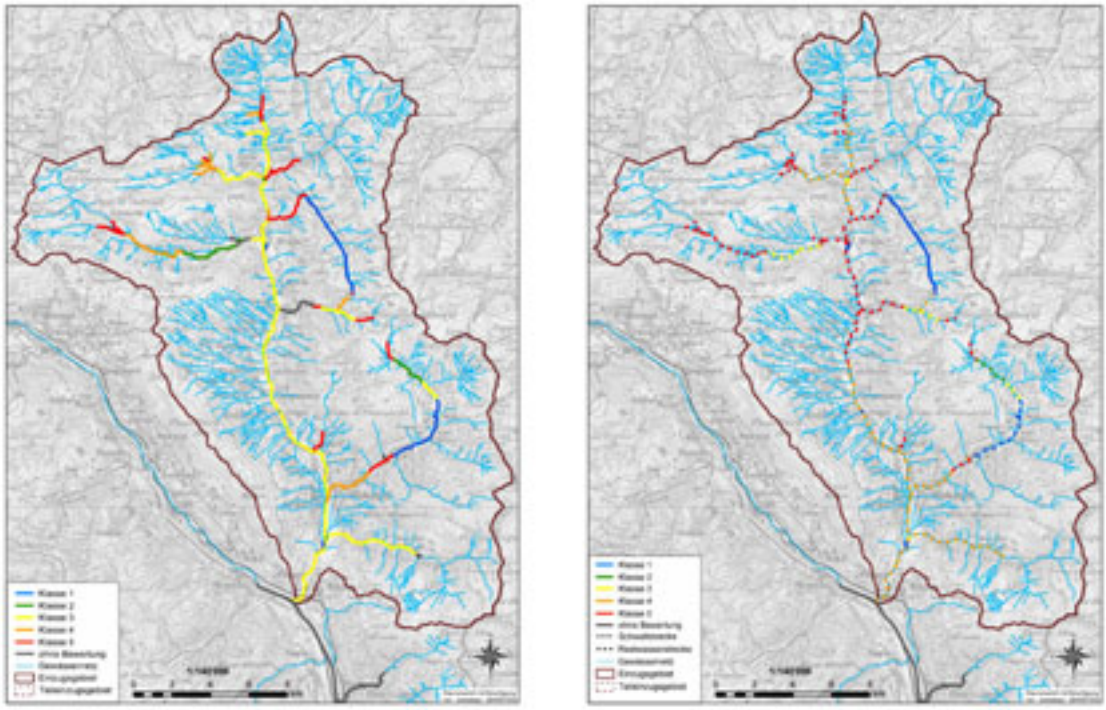

Figure 2. Cartographic results for the Brenno river basin case study. Left: classification for the indicator "flood frequency, right: global classification

The interested parties are invited to apply and test the draft of the method (Pfaundler et al. 2007) until the end of 2009. Based on the feedbacks from the experiences from practical applications, the method will be revised and published in its final version in 2010. The "side-products" and electronic tools developed for HYDMOD can be very useful also for other hydrological tasks. Together with the draft method, they can be ordered and downloaded free of charge via the following URL: http://www.modul-stufen-konzept.ch/e/hydro_startseite_e.htm

REFERENCES

BUWAL, 1998: Modul-Stufen-Konzept. Mitteilungen zum Gewässerschutz Nr. 26. Bundesamt für Umwelt, Wald und Landschaft, Bern. www.modulstufenkonzept.ch]

Pfaundler, M., Dübendorfer, C., Pfammatter, R. und Zysset, A., 2007: Methoden zur Untersuchung und Beurteilung der Fliessgewässer – Hydrologie-Abflussregime. Umwelt-Vollzug. Entwurf vom Oktober 2007. Bundesamt für Umwelt BAFU. Bern, 104 Seiten.

SAEFL/FOWG (Eds.), 2003: Guiding Principles for Swiss watercourses. Promoting sustainable watercourse management. Swiss Agency for the Environment, Forests and Landscapes (SAEFL) and Federal Office for Water and Geology (FOWG), Bern, 12 pp.

10.8

Hydropeaking on the Ticino River: Analysis, Impacts and Mitigation Strategies

Bruno Polli*, Luca Solcà**

* Ufficio caccia e pesca Cantone Ticino, Viale Stefano Franscini 17, CH-6500 Bellinzona, Switzerland (bruno.polli@ti.ch)
** CSD Tre Laghi Lugano, via Lucchini 12, CH-6900 Lugano, Switzerland (l.solca@csd.ch)

The problematic of irregular flow regime caused by the management of hydroelectric power plants has been not analysed at academic level in Switzerland up to the '90 of the last century.
In recent years several studies carried out in Switzerland demonstrate that the artificial variations of the flow regime significantly affect the aquatic biocenosis.
According to the result, the Ticino River is one on the most affected at national scale and, furthermore, a negative trend is observed during the last decades, where the influence of artificial regime is even more pronounced that before.
Starting from 1996 statistical data on the non-professional fishery are collected in Ticino and trends estimated from these data suggest a decrease of the caption in the lower part of the Ticino river.
The cantonal office for hunt and fishery (Ufficio caccia e pesca) decided to start a detailed research study in order to objectively evaluate the impact of hydropeaking activity on the aquatic biocenosis.

The study investigates the impact of anthropological alterations of the hydrological regime on the Ticino River ecosystem with both biological and ecomorphological approaches. The study area range from the embouchure in Lago Maggiore to the hydropower plant AET in Personico.
From a hydrological point of view, the statistical data provided by the Federal Office for the Environment (FOEN) will be completed with data coming from measurement stations specifically installed during this study. This will permit to figure out the hydrological characteristics of the river regime and to extrapolate the potentially alterations caused by the introduction of the "energy market". Physic-chemical parameters will be also collected by means of both punctual and continuous measurements.
Colmatation degree and mobilisation of the river bed during the daily peak of discharge will be studied with an experimental approach. Both phenomena have important influences on the success degree of the natural reproduction of fish populations.
The density and structure of fish populations will be investigated in a qualitative way by means of electrical fish. The target-species are trout (brown trout, lake trout and ev. marmorata) and grayling. In this way, natural reproduction will be quantified by comparing the results obtained before and after the spawn period.
Macro invertebrate populations will be characterized with the help of a biological index called IBGN. Additional collections have the goal to quantify the drift of macro invertebrates induced by the daily increase of the river discharge.
The results of all these activities will provide an exhaustive overview on the actual situation of the river ecosystem, which will allow identifying critical points and possible measures in order to improve the ecological state of the Ticino River.

10.9

Spatio-temporal effects of experimental floods on benthos, drift and seston below reservoirs

CT Robinson*, T Buser*, S Mannes*, D Kelly**, S Larned***

* *Department of Aquatic Ecology, Eawag, 8600 Duebendorf, CH*
** *Department of Conservation, Christchurch, New Zealand*
*** *NIWA, Christchurch, New Zealand.*

We examined the spatio-temporal effects of experimental floods on benthos, drift, and seston in rivers below reservoirs. Studies were conducted on the Spöl River, Switzerland and Opuha River, New Zealand. The flood in the Spöl increased discharge 28X, whereas discharge in the Opuha was increased fourfold. The duration of floods ranged from 4 to 8 hours depending on location along each river. Spatially, benthos was sampled from coarse-scale habitats along the Spöl. Drift and seston were sampled during each flood at sites longitudinally placed along each river. Coarse-scale benthic habitats all showed similar high losses of macroinvertebrates and periphyton regardless of location along the river. During each flood, peaks in drift occurred sooner than peaks in seston. All invertebrate taxa showed similar drift patterns during each flood, and drift density increased downstream during each flood. Seston showed two peaks in the Spöl as bed sediments became mobilized during the flood. Drift/seston displayed typical hysteresis curves during each flood. These data suggest that coarse-scale habitats do not provide refugia during large floods. The drift and seston data further indicate that invertebrates respond sooner to changes in flow than benthic sediments and organic matter, suggesting the role of behaviour in organism response to floods.

10.10

Thermopeaking from power plant releases in regulated Alpine stream

Siviglia Annunziato*, Salvaro Martino*, Zolezzi Guido*, Maiolini Bruno**, Carolli Mauro*** & Bruno Maria Cristina***

* *Department of Civil and Environmental Engineering, University of Trento, I-38100 Trento*
** *Museo Tridentino di Scienze Naturali, Via Calepina, 14, I-38100 Trento*
*** *Fondazione E. Mach, Via Mach, 1, I-38010 S. Michele all'Adige (TN)*

Rapid discharge variations due to hydropower releases are well known to be responsible for a strong impact on the ecological integrity of aquatic ecosystems. Such effect is not only related to sudden increases in water depth and velocity, that cause catastrophic drift and limit the availability of organic matter and refugia for the aquatic organisms. Especially in Alpine areas, in fact, hydropeaking is often associated with "thermopeaking", namely with sharp variations of water temperature induced by relevant temperature differences between the turbinated water and the recipient body.
Despite its ecological relevance, thermopeaking has not been quantified in detail in Alpine areas. A careful field study on the Noce River basin (NE Italy) allowed a first characterization of thermopeaking, providing the basis for the present study.
In order to develop sound mitigation strategies for hydro- and thermopeaking impacted river reaches, it is necessary to distinguish between anthropogenic and natural effects when analyzing the temperature time-series of a stream at a given cross section. This has been achieved through the comparison of temporal and spatial temperature variations due to natural channel confluences with those due to hydropower releases into the stream.
Assessment of existing impacts and of the feasible mitigation strategies requires:
1) quantifing the thermal fluctuations from field observations, and
2) predicting the effects of different release scenarios.

In this work we first quantify the thermopeaking extent in Alpine streams through the analysis of water temperature records and of the derivative of the recorded temperature signal. We compared water temperature regimes between thermopeaking-impacted and unimpacted rivers in order to distinguish daily natural cycles from thermopeaking fluctuations.
Figure 1 shows the marked seasonality of the thermopeaking processes, as a result of hydropower plants releasing cooler than natural water in summer periods, and causing reverse conditions during winter.
In order to predict the downstream effects of thermopeaking waves propagating along the stream a mathematical modelling

framework has been developed. It is a predictive tool based on a fully coupled 1D hydro-thermodynamic numerical model able to deal with natural, irregular geometries. The governing mathematical problem has been conveniently split into a convective problem and a diffusion problem in order to carefully describe rapid temperature and discharge variations. Application of the model can also be of interest to support planning of potential mitigating measures for thermal impacts on the recipient water body.

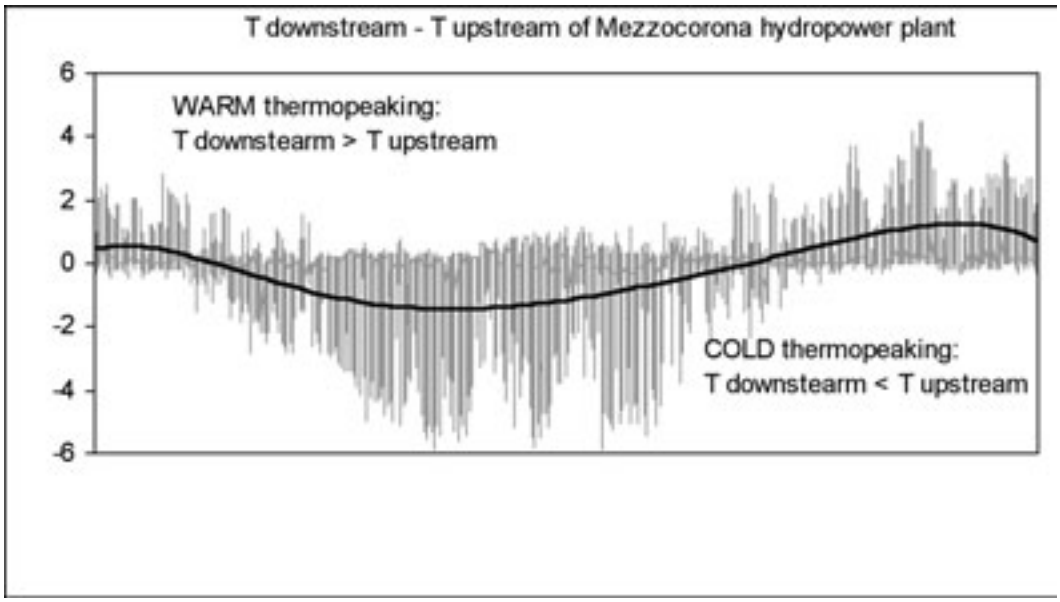

Figure 1. Cold and warm thermopeaking caused by the releases of turbinated water from the Mezzocorona hydropower plant in the Noce River (NE Italy) in the year 2007.

11. Who Cares About Water? - Social Aspects of Water + Environmental Challenges of Border Regions

Walter Leimgruber, Patricia Felber + Doris Wastl-Walter, Béla Filep

Swiss Geography Association
IGU Commission Geography and Public Policy

11.1

Consuming mountain space

Environmental costs of urban sprawl in the French-Swiss Jura.

de Bettignies Gaële

Institut de Géographie de l'Université de Neuchâtel, Espace Louis Agassiz 1, 2000 Neuchâtel, Suisse.
Direction Régionale du Ministère de l'Ecologie, de l'Energie, du Développement durable et de l'Aménagement du territoire, 6 rue Roussillon, 25000 Besançon, France.

The Jura mountain offers geomorphologic continuity on both sides of the border between France and Switzerland: a region characterized by rigourous winters, formerly in a relative isolation due to difficulties of transportation across the mountain relief pleats. The borderline is placed along the crest line of the Jura in the South near Pontarlier, then runs North-East along the Doubs river towards Basel.
The recent growth of the watch industry transforms today the border zone into urban centres in Switzerland, and suburbs in the still-rural France. The cost of life and land is lower in France, and the Swiss salaries higher: therefore more and more employees of firms in Switzerland tend to reside in France, increasing the land pressure. According to the Observatoire Statistique Transfrontalier de l'Arc Jurassien, the number of border zone workers has increased of 55% between 1998 and 2005: the French region, dominated economically by its Swiss mirror (Moine, 2003), welcomes more and more new residents, progressively transforming for this purpose farmland into suburbia.
Thus the French Law (Code de l'Urbanisme and Code de l'Environnement) has a series of instruments to limit or even stop the space consumption: there are laws, so-called “lois paysage”, to avoid urban scattering, urban sprawl, and preserve the quality of town entrances. Additionally to this maine protective frame, special features apply to places recognized for their natural or cultural value, in reference to the notion of heritage: loi montagne, loi littoral, loi de 1930 (sites classés et inscrits), Grands Sites, Unesco, Directives de Paysage, ZPPAUP, ZICO, Natura 2000, ZNIEFF, etc.
In spite of these laws, when pressure is put on the land as here on the border, housing developments multiply rapidly, spreading with similar design and organization regardless of the land's particularities. The low density housing answers the quantitative needs: the demand of private housing meets local political wish of population expansion and economical trans-border opportunity.

In this centralized country that is France, legislative frames are formalized in Paris and then applied in all scales of the national, regional, departemental, communal and then individual (private) level.
A few examples can illustrate differences between the legislator's wish and the result on the field: environmental diagnostics are minimized at the scale of the commune (Plans Locaux d'Urbanisme); urban coherence and adaptation to the ground are absent of housing developments, as well as architecture adequate to the local particularities; landscape integration is neglected almost completely for individual constructions (Permis de Construire).
The environmental costs are of several levels, deriving from space consumption of individual houses in the middle of a gardened parcel. The quantitative level includes energy and primary goods consumption (building the houses and the numerous asphalt roads leading to them, heating and maintenance), water flow acceleration (direct consequence of wide asphalt roads and driveways in mountain areas) or subsidence (topography issues appear when building). The qualitative level is one of preservation of landscape and heritage coherence : it calls for a planning that is larger than the communal level, one that can include both urban centre and rural edges.
The border is so far preventing such an organization: structures authority stop at the borderline, regardless of the evident trans-border logics.
One site, though, offers an alternative to the main pattern: an exceptional natural landscape, visible and accessible from both countries. Identified by both countries as worth protecting, it has brought the French authorities to develop a visiting facility according to national design orientations. Now the Swiss counterpart is engaging into the same process. Although placed directly on the borderline and therefore split into two sets of development codes, this particular place will nevertheless stay one coherent entity.
We propose to discuss the issues of space consumption of low density housing, land pressure and historical landscape, in this case of French-Swiss rural border, with the orientation of town and country planning.
Relationship between sold plots and number of border zone workers.

REFERENCES

Chapuis, R. 2007: Vers des campagnes citadines, le Doubs (1975-2005), Presses Universitaires de Franche-Comté.
Moine, A. 2003: Comprendre et observer les territoires: l'indispensable apport de la systémique, Laboratoire Théma - Université de Franche-Comté.
Ministère de l’Ecologie, de l’Energie, du Développment durable et de l’Aménagement du territoire: www.developpement-durable.gouv.fr.
Observatoire Statistique Transfrontalier de l’Arc Jurassien: http://www.ostaj.org/

11.2

Domestic water as means of masculine domination. An analysis from the High Atlas Mountains

Graefe Olivier

Departement für Geowissenschaften, Université de Fribourg, CH-1700 Fribourg

The domestication of water in the sense of taming and controlling the supply of drinking water on the one hand and making water available at the domicile on the other hand, represents progress to many rural Moroccan households. Especially women do benefit of the new facilities by saving them many efforts of fetching water outside the village. But this undeniable technical improvement for rural areas can also be analyzed in the light of the re-islamization of society and profound social change as a means for men to reify their domination in a context of threatened masculinity. This paper will show, following Bourdieu's and Baudrillard's early works, the political and symbolic logics and meanings which are lying underneath the modernization of rural water supply emphasizing the dialectical relationship between evolving waterscapes and dynamic gender relations.

REFERENCES

Baudrillard, J. 1968, Le système des objets. Paris.
Bourdieu, P. 1972, Esquisse d'une théorie de la pratique. Paris.
Bourdieu, P. 1998, La domination masculine. Paris.
Jackson, C. 1998, Gender, irrigation, and environment: Arguing for agency, Agriculture and Human Values, 15, 313-324.
O'Reilly, K. 2006: "Traditional" women, "modern" water: Linking gender and commodification in Rajasthan, India, Geoforum, 37, 6, 958-972.
Shiva, V. 1989, Staying Alive: Women, Technology and Development. London.

11.3

Increasing sustainability of irrigated urban agriculture in southern countries by Participatory Education and Action Research (PEAR) among small producers: case study of Dakar, Senegal

Chaudhuri Nita*, Gueye Anne**, Pfeifer Hans-Rudolf**, Niang Seydou*** & Cole Donald*

**OISE Coll. Prog. Env.Health, University of Toronto, Canada*
*** IMG - Centre d'Analyse Minérale, Geoscience and Environment, University of Lausanne, Switzerland*
**** Laboratoire de traitement des eaux usées, IFAN-Université Cheikh Anta Diop, Dakar, Senegal*

Urban agriculture in Senegal, as in most developing countries, relies on extremely vulnerable small production units. In the region of Dakar (Fig. 1), the lack of access to adequate water for drinking and irrigation, poor soil fertility and invasive pests, lead to the use of unauthorized fertilizers and pesticides (Fig. 2, Tab. 1): Using untreated waste water for irrigation and excessive pesticide spraying are widespread practices. A participatory education and action research (PEAR) - type process within an ecosystem health framework has been used to investigate different positions of stakeholders and especially the producer issues. Several individual inquiries upon 50 producers revealed the different agricultural practices and the producer perceptions of environment and health before (March 2005) and after educational sessions (March 2006). Results show (Tab. 1 and 2): 1) extremely various agricultural practices (irrigation with waste water or saline ground water, fertilizer and pesticide use) depending mostly on short term decisions, based on financial and market availabilities; 2) low perception of long term soil fertility management and of health impacts associated with pesticide and waste water exposure 3) after interactive workshops and training, significant increase of health risk perception has been observed, marked e.g. by the use of protective equipment when treating with pesticides. The PEAR approach has been shown to be effective. However, several barriers still exist, such as security of land tenure, access to credit, fear related to decrease in productivity, lack of training and information in the use of alternatives to chemical agriculture. Regular workshops will certainly help to reach sustainability.

REFERENCES

Gueye, A. (2006): Swiss National Science Foundation project no. 207021-109689/1, "Use of waste water in urban agriculture in the Dakar area". Intermediate report, Appendix B, 2006-2007.

Chaudhuri, N. (forthcoming): Using Participatory Education and Action Research within an Eco-system Health Framework to Reduce Human Health Risks Related to Wastewater and Pesticide Use, Pikine, Senegal. Ph.D. thesis, International Development Research Centre (IDRC), Canada.

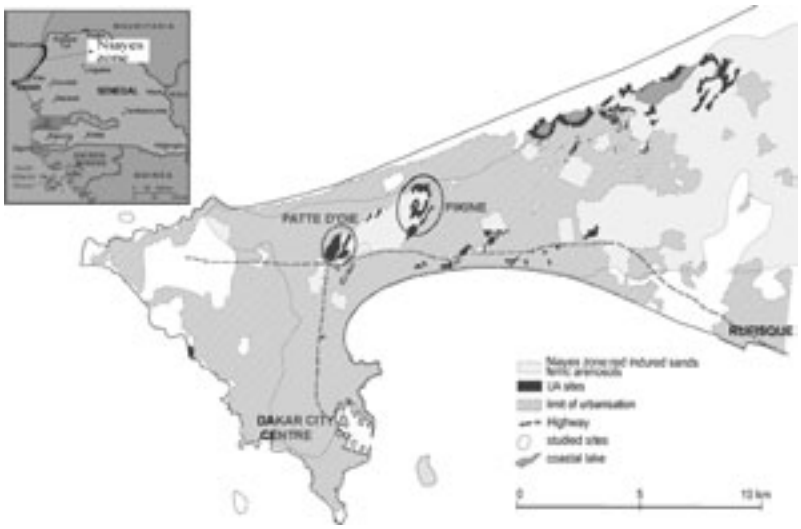

Fig.1. Main areas of urban agriculture in the region of Dakar

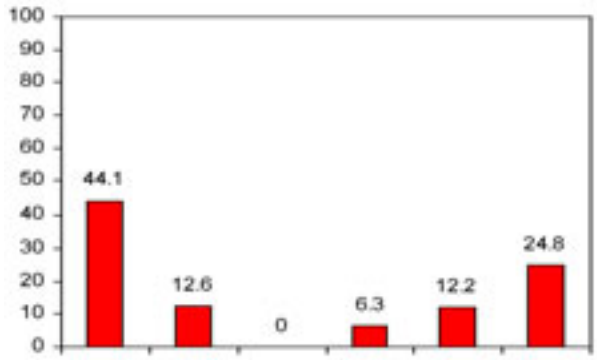

Fig.2. Frequency of pesticides application (%)

Pesticide used	March 2005 N=50	March 2006 N=49
Dimethoate (organophosphorus), II	48 % (24/50)	47 % (23/49)
Dicofol (organochlorine), III	42% (21/50)	29 % (14/49)
Lanate (methomyl, carbamate) IB	40 % (20/50)	29 % (14/49)
Malathion (carborox, carbofos, organochlorine) III	44 % (22/40)	33 % (16/49)
Mocap (ethoprophos)	28 % (14/50)	22 % (11/49)

WHO Hazard Classification: IA-extremely dangerous, IB-highly hazardous,
II-moderately hazardous, III-slightly hazardous,
Tab.1. Change in frequency of pesticide used

Other Methods of Pest Control than Chemical	March 2005 (n=50)	March 2006 (n=49)
Yes	16 % (8/50)	39 % (19/49)
No	82 % (41/50)	31 % (15/49)
sometimes	-	20 % (10/49)
No response	2.0 % (10/49)	10 % (5/49)

Tab.2. Change in the use of alternative methods of pest control

11.4

Nitrogen leaching in groundwater from periurban agrosystems in Senegal: is fertilization contributing to the high nitrate groundwater contamination?

Gueye Anne*, Pfeifer Hans-Rudolf*, Sarr Baba** and Niang Seydou**

*IMG - Centre d'Analyse Minérale, Geoscience and Environment, University of Lausanne, Switzerland
** Laboratoire de traitement des eaux usées, IFAN-Université Cheikh Anta Diop, Dakar, Senegal

Urban Agriculture (UA) can be considered as a border- somehow contentious- region, as urban and rural activities and issues are mixed without regulation. In Dakar, the UA area constitutes the only green belt and provides important fresh food and employment, but it is often perceived as an important source of nitrates, pesticides and pathogenic bacteria and parasite contamination in the environment and foodstuffs. Without integration in urban planification, UA might be banished and transformed in densly inhabited zones. Periurban districts are not equipped with adequate sanitation facilities and therefore contribute to the shallow groundwater contamination in nitrogen, organic matter (Tandia 2000; Becaye, Mbeguere et al. 2005) and possibly in microbial pathogens (Ndiaye 2008). This study deals with the contribution of periurban agriculture to nitrate groundwater contamination and will allow a better comprehension of the nitrogen cycle in UA and fertilizer management.

Several methods were used: 1) The N-balance were calculated with an input and output estimation, based on inquiries about fertilizer use and rotation management, yield data and nutrient analyses. 2) Nitrates from groundwater at dry/rainy season have been sampled in 25 piezometers and wells inside the UA sites and in surrounding townships and analysed with ionic chromatography. 3) The N-leaching rate were simulated with models as a function of soil and crop management caracteristics (soil temperature, moisture content, organic matter, texture, bulk density, fertilization, irrigation, crop rotations). 4) Nitrogen and oxygen isotopes in NO_3 from groundwater are measured to determine the origin of nitrates, according to the method of Silva, Kendall et al. (2000). Specific signatures of mineral fertilizers, manure and sanitation sludge can be distinguished (Shomar, Osenbruck et al. 2008).

Inquiries of 53 smallholders in October 2005 permitted to estimate Nitrogen inputs into the agrosystem of 5 t N ha^{-1} y^{-1} (Tab.1). Groundwater surveys in October 2006 and March 2007 show extremely high contents in nitrates, up to several hundreds mg/L (WHO guideline of 50mg/L for drinking water). More important concentrations are found during the dry season (mean 248 mg/L) than the rainy season (mean 156mg/L). Fig. 1 shows the data from two piezometers sampled before and shortly after N-P-K mineral fertilization (250 kg/ha) on ferric arenosol (hydraulic conductivity: 1.1 m s^{-1}, measured with double ring infiltrometer). NO_3-leaching at 4m depth, in the groundwater, is not immediate. $\delta^{15}N\text{-}NO_3$ from selected piezometer in October 2006 and February 2007 are in the range +8 to + 35‰ (Fig.2) and indicate a major organic origin of N in the township samples. Sludges from septic tanks and animal manure have similar $\delta^{15}N$ signature, but $\delta^{18}O\text{-}NO_3$, actually in progress, will hopefully give more sensitive results. Modelling of nitrogen leaching is in progress, using PHREEQ-CI and MACRO for correlating results.

REFERENCES

Beaudoin, N., B. Mary, et al. (2005). Nitrate concentration in soils and subsoils as affected by farming practices in intensive agricultural areas. N management in agrosystems in relation to the Water Framework Directive, 14th N workshop, oct 2005, Maastricht, The Nederlands.

Becaye, M. Mbeguere, et al. (2005). PLT/PAQPUD/Etude d'impact de l'assainissement autonome sur la nappe phréatique. Dakar, H2Oengineering.

Dasylva, S. (2001). Les bas-fonds des sables dunaires de la région de Dakar. Potentialités agricoles et contraintes urbaines, Université Paris 1-Panthéon-Sorbonne: 405.

Ndiaye, M. L. (2008). Microbiological quality of groundwater related to urban agriculture of the Dakar area (Senegal). 6th Swiss Geoscience Meeting, Lugano.

Shomar, B., K. Osenbruck, et al. (2008). "Elevated nitrate levels in the groundwater of the Gaza Strip: Distribution and sources." Science of the Total Environment 398(1-3): 164-174.

Silva, S. R., C. Kendall, et al. (2000). "A new method for collection of nitrate from fresh water and the analysis of nitrogen and oxygen isotope ratios." Journal of Hydrology 228(1-2): 22-36.

Tandia, A. A. (2000). Origine, évolution et migration des formes de l'azote minéraldans les aquifères situés sous environnement péri-rurbain non assaini : cas de lanappe des sables quaternaires de la région de Dakar (Sénégal).

Vanlauwe, B. and K. E. Giller (2006). "Popular myths around soil fertility management in sub-Saharan Africa." Agriculture, Ecosystems and Environment(116): 34-46.

Table 1. Estimation of annual inputs in Pikine (57ha) and Patte d'Oie (79ha). Source: 53 individual inquiries and field inventory, 2005

N INPUTS	Local aubergine (0.5 y^{-1})	Tomato (0.5 y^{-1})	Salad (5 y^{-1})	TOTAL	Nitrogen input (kg $ha^{-1}y^{-1}$)
Urea (kg $ha^{-1}y^{-1}$)	300	210	40	455	150
NPK (kg $ha^{-1}y^{-1}$)	600	480	60	840	210
Organic manure (t $ha^{-1}y^{-1}$)	20	10	15	90	1800
Irrigation wastewater (m^3 ha^{-1})	23 % total surface 200mg/L N			8500	1700
Irrigation groundwater (m^3 ha^{-1})	77 % total surface 30mg/L N			30000	1000

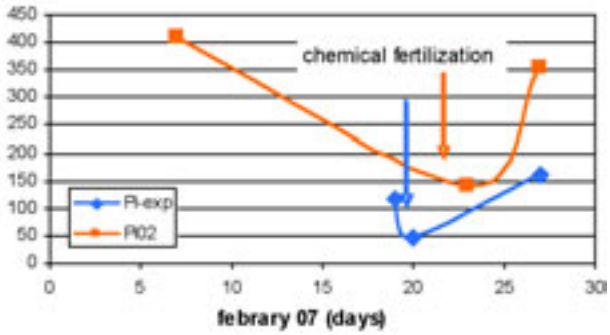

Fig. 1. NO3 in 4m depth-groundwater before and after mineral fertilization

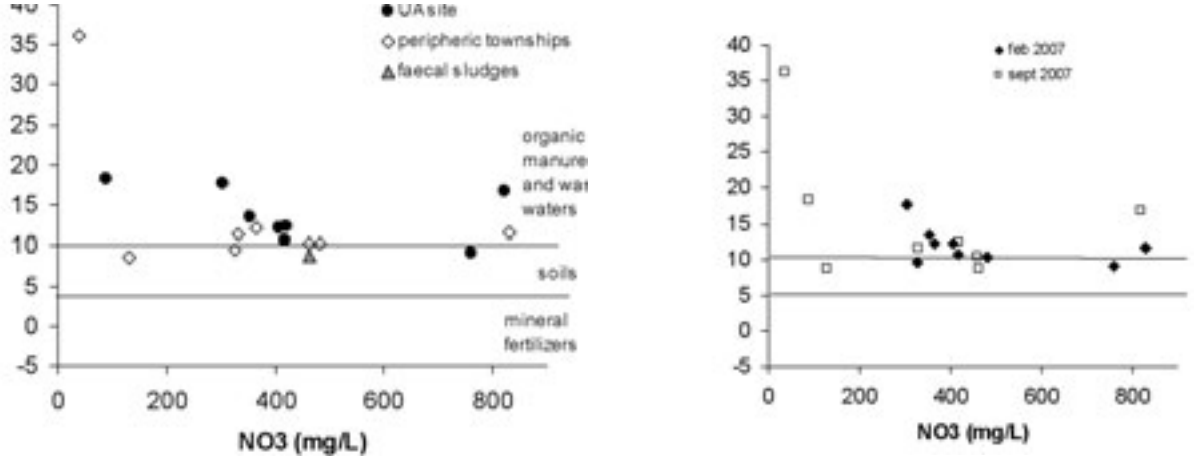

Fig 2. delta 15 N isotopes in nitrates.

11.5

Water violence, governable spaces and the state's frontier

Hagmann Tobias*, Korf Benedikt*

*Geographisches Institut, Universität Zürich, Winterthurerstrasse 190, CH-8057 Zürich (tobias.hagmann@geo.uzh.ch; korf@geo.uzh.ch)

This paper explores the genealogy of water violence in Somali region, Ethiopia, a contested political space at the margins of the Ethiopian state. Somali region has experienced repeated outbursts of violence related to the access to pasture and water among different Somali clans and between Somali clans and the Ethiopian state. Often, such conflicts are attributed to a form of "eco-violence," whereby increasing scarcity of natural resources (due to overpopulation, drought, environmental degradation) fosters contestation between different water user groups. We posit that such approaches under-estimate the political economy of water violence and its historical genealogy. Arguably, two inter-related processes are key in explaining these types of resource related conflicts that we observe in Somali region: first, the increasing penetration of the state into the pastoralist and agro-pastoralist spaces of Somali region as a project of modernization and taming of the state's frontier and, second, new economic opportunities that emerge at the interface of state penetration, porous borders with Somaliland and transnational contraband flows. We illustrate our argument with different case studies stemming from ethnographic research in various parts of Somali region. On the one hand, we will study the "politics of the water pump" whereby competition over the access to irrigation technology becomes a focal point of inter-group conflict. We indicate how such contestation is played out in a complex pattern of clan patronage and the capture of state and aid resources. On the other hand, we scrutinize how privatization of the pastoral commons produces unequal opportunities to monopolize access to water through technical artefacts. While this creates intra-clan resentment, it also disturbs historically long-established inter-clan cooperation around water access in times of distress. Arguably, such examples indicate the political ecology of water violence – it is not material resources or their scarcity that produce social conflict around water, but such conflicts are largely embedded in much longer-term social relationships and political struggles.

11.6

Microbiological quality of groundwater related to urban agriculture of the Dakar area (Senegal)

Ndiaye Mamadou Lamine*,*** ; Peduzzi Raffele**,*** ; Pfeifer Hans-Rudolf**** ; Niang Seydou*; Dieng Yémou ***** & Tonolla Mauro**

LATEU-Laboratoire de traitement des eaux usées, IFAN, Université Cheikh A. Diop, Dakar, Senegal (ndiayma2@etu.unige.ch)
**Istituto cantonale di microbiologia, Via Mirasole 22A, CH- 6500 Bellinzona, Switzerland.*
***Section de Biologie, Faculté des Sciences, Université de Genève, CH- 1211 Genève 4, Switzerland.*
****IMG-Centre d'Analyse Minérale, Faculté de Géosciences et de l'Environnement, Bâtiment Anthropole, CH-1015 Lausanne, Switzerland.*
*****Département de parasitologie et mycologie, Université Cheikh A. Diop Dakar, Senegal.*

Urban agriculture (UA) has existed in the Dakar area since 1937 and plays an important role for food security and local economy. However, due to the lack of water due to climatic change and the increase of the demand, untreated waste water and manure are used by farmers to increase the yield. The agricultural production is mainly based on vegetables with a rapid turnover. The study area is located in the topographically low-laying remnants of the natural Niayes ecosystem, comprising dunes and lakes, 10 to 15km in width, which extends 150 km to north (Fig. 1). About 200 farmers work on 0.5 km^2 surrounded by the rapidly growing town. Several small lakes with elevated salt contents still persist and the groundwater level is shallow, which makes it very vulnerable to contamination. In the town quarters around, water for drinking and cooking still stem largely from hand dug wells and tube pumps. To evaluate the risk for the population and the environment, a long term survey of the microbiological quality of the various waters was started: 1) waters used for irrigation (untreated wastewater, shallow groundwaters called "Ceane" water) and 2) deeper groundwaters from wells, piezometers and pumps were sampled. A fluorescence in situ hybridization (FISH) procedure was developed to analyse viable *Salmonella* spp, and *E. coli* in water samples. The preliminary results show the presence of *E. coli* in all the categories of water within and around the UA sites (Fig. 1). Also, *Salmonella* spp is detected in ground and surface water (≈1.5 m depth) within the site of Patte d'Oie) and around the sites of Patte d'Oie and Pikine (Fig. 2). Although, UA is an important source of food and income for a large city such as

Dakar, the use of untreated wastewater and manure bears considerable risks of microbial contamination for the environment and humans.

REFERENCES

Ndiaye, M.L., Gueye-Girardet, A. & Pfeifer, H.-R. (2006) : Impact des eaux usées sur l'évolution microbiologique des sols : étude de cas à Pikine Dakar-Sénégal. Agrosolutions 17, 33-38.

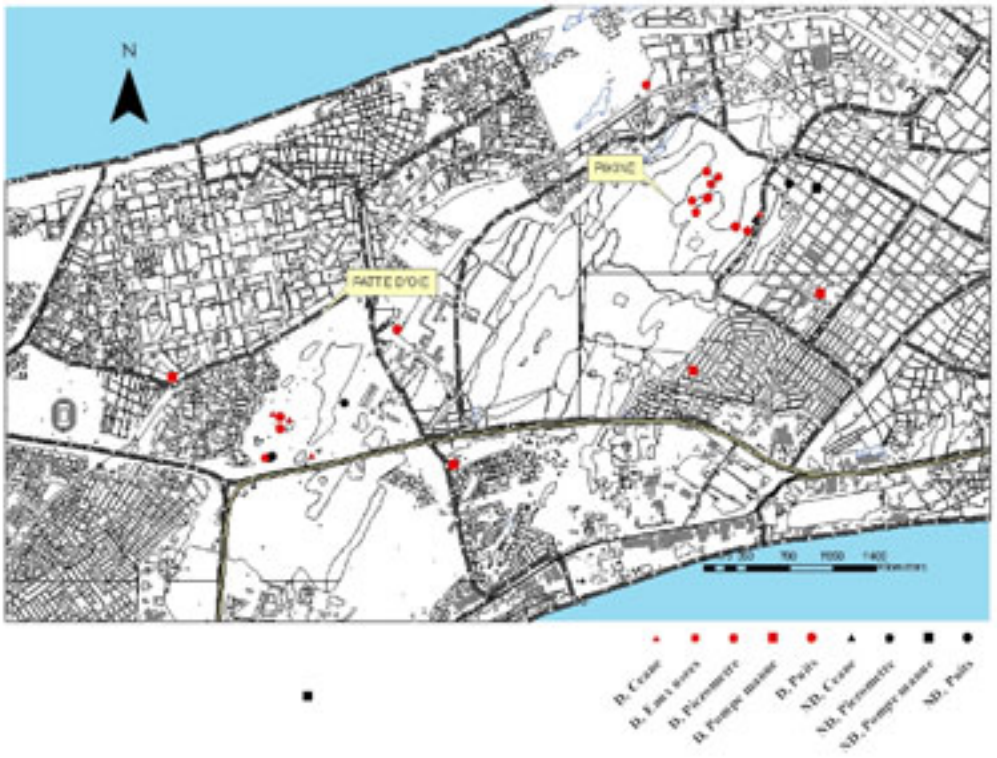

Fig.1. Spatial distribution of E. coli (D: detected, ND : non detected)

Fig.2. Spatial distribution of Salmonella spp

11.7

Recovery of lake Lugano (Switzerland-Italy): a differentiated strategy for a complex challenge

Veronesi Mauro, Pera Sebastian, Simona Marco

Institute of Earth Sciences, University of Applied Sciences of Southern Switzerland
Via Trevano / P.O. Box 72
6952 Canobbio-Lugano, Switzerland

Lake Lugano is a deep, dendritic subalpine lake situated at the border between Switzerland and Italy. The basin is highly eutrophic as a result of the discharge into the lake of waste water from the urban centres in the watershed. The complex morphology and geology of its catchment required a differentiate recovery strategy: in the seventies the first waste water collectors and sewage treatment plants began to be constructed, with the result that there was a sharp drop in the phosphorus load conveyed to the lake. In 1976 sewage produced by the town of Lugano, naturally burdening the northern basin, were diverted to the treatment plant located in the southern basin nearer the outflow. In addition, new legislation was passed in Switzerland to reduce the polyphosphate content of domestic and industrial detergents (1986). All these interventions have halted the eutrophication and are slowly improving the condition of the lake. However, the complete recovery of the lake will depend to a large extent on the behaviour of the nutrient deposits which have been accumulating in the lake for around 50 years, both in the deep hypolimnion of the northern basin and the sediments. Two consecutive cold and windy winters in 2004/2005 and 2005/2006 erased the chemical stratification of the northern basin and led to two exceptionally strong mixing events: for the first time in decades convective mixing reached the bottom of the lake. The consequences of these events were that between 2004 and 2006 in northern basin deep water (layer 100 m–bottom) temperature has lessened by 0.5 °C, total phosphorous content decreased from 642 to 489 t P (-25%), while oxygen balance has become positive increasing by more than 14'000 t O_2. Lake Lugano has now entered a new stage of its long way towards complete recovery.

Figure 1: Lake Lugano (Switzerland-Italy), location of sampling sites

11.8

Cross-border environmental conflicts: Struggling for political participation across borders

Wastl-Walter Doris*, Filep Béla*, Váradi Monika Mária**

*Geographisches Institut der Universität Bern, Hallerstrasse 12, CH-3012 Bern
** Department of Spatial Development Research, Centre for Regional Studies, Hungarian Academy of Sciences, Teréz krt. 13, H-1067 Budapest

The Austrian-Hungarian-Slovenian border region is a remote area constantly undergoing geopolitical change, with the political borders mainly following an ethnic and language border. Over the last century, the region has been subjected to major geopolitical changes, shifting from being the periphery of the Austrian-Hungarian Monarchy to becoming the national border between Austria and Hungary in 1921, to being divided by the so-called Iron Curtain. After the opening of the borders in 1989 and the long period of silence, slowly contacts and economic relations were taken up.
As there had never been any atrocity, war or fighting between the neighbours, the relations of the neighbours were friendly, which allowed joint investments like the Heiligenkreuz-Szentgotthárd Industrial Park to start.
However, after 2006, differences about development and conflicts about future investments arose. In the Austrian part of this border region, the opening of an incinerator is planned. There are clear, legal procedures to be followed for the installation of such a plant, and Austrians see the incinerator only in economic terms and insist on the legality and correctness of the activities. Their Hungarian neighbours, however, see it as an environmental and political issue and claim the right to participate in decision-making as neighbours.
We analyse the competing public discourses and visual representations of the different stakeholders as they express the diverse positions and views of the people involved. The Hungarians' positions are mainly critical, not only about the incinerator, but also because they feel they are neither sufficiently informed nor included in the decision-making, and are now claiming equal rights as citizens of a neighbouring EU state.
As there are also Austrians who are very critical of the planned incinerator, new alliances have been formed across the state borders. This has led to a new neighbourhood concept and neighbourhood discourses across the political, ethnic and language borders that are no longer the main dividing lines. Now, symbolic borders arise from different ideologies and value systems.

REFERENCES

Wastl-Walter, D., & Váradi, M. M. 2004: Ruptures in the Austro-Hungarian Border Region. In: Pavlakovich, V. K., Morehouse, B. & Wastl-Walter, D. (eds.): Challenged Borderlands: Transcending Political and Cultural Boundaries. Hampshire: Ashgate Publishing Limited, 175-192.

Wastl-Walter, D., Váradi M. M. & Veider, F. 2002: Bordering Silence. Border Narratives from the Austro-Hungarian Border. In: Meinhof, U. H. (ed.): Living with Borders. Identity Discourses on East-West Borders in Europe. Hampshire: Ashgate Publishing Limited, 75-93.

11.9

Peasant Border Cases

How peasant principles enhance competencies of farmers at the Swiss-French border to maintain good neighbourhood relationships and the impact of different national agricultural an environmental law on these relationships.

Widmer David

Geographisches Institut der Universität Bern, Hallerstr. 12, 3012 Bern

There are Swiss farmers in the border region to France who also cultivate land in France. This situation has historical reasons and is influenced by the changing legal background of the two states and the financial situation of the farmers. One question is central to the farmers: How can they assure the further cultivation of their land in France? As for some farmers cultivation of this owned or leased land in France is vital. The long-lasting strengthening of the nation-states and more recent the EU-membership of France complicated the informal relationships to the neighbourly farmers in France. Different agricultural and environmental legal foundations intensify the construction of "Self" and the "Other" along the transnational borderline. However, good neighbourhood relationships are crucial for a further cultivation of land in France.

As seen in a qualitative resarch project, using the methods of narrative guided interviews and participant observation, so called peasant principles play an important role in shaping those relationships. By using the theoretical background of structuration theory by A. Giddens (1984), its adaptation for social geography by B. Werlen (1997; 1999) and its extension with the concepts of social and cultural capital by P. Bourdieu (1983) and the empirical findings of R. Girtler (2002) there can be shown the important role of tradition-based knowledge farmers can use today as capital in the maintenance of neighbourly relationships.

This leads to the following conclusion: To enhance the transnational cross-border understanding and cooperation, as a counterbalance to the mentioned separating tendencies by the concept of nation-states and understood as an opportunity for dialogue between the EU and Switzerland, the still existing peasant principles of farmers in the Swiss-French border region should be recognized and strengthened so that they can be used as a source of common identity.

REFERENCES

Bourdieu Pierre 1983. Ökonomisches Kapital, kulturelles Kapital, soziales Kapital In: Kreckel Reinhard (Hg.) 1983. Soziale Ungleichheiten. Schwartz, Göttingen.

Giddens Anthony 1984. The Constitution of Society. Outline of the Theory of Structuration. Polity Press, Cambridge.

Girtler Roland 2002. Echte Bauern. Der Zauber einer alten Kultur; mit einem Beitrag des Vollwertbäckers Hans Gradwohl. Böhlau, Wien.

Werlen Benno 1997. Sozialgeographie alltäglicher Regionalisierungen, Bd.2 Globalisierung, Region und Regionalisierung. Steiner, Stuttgart.

Werlen Benno 1999. Sozialgeographie alltäglicher Regionalisierungen, Bd.1 Zur Ontologie von Gesellschaft und Raum. Zweite Auflage. Steiner, Stuttgart.

12. Data acquisition, Geo-processing, GIS, digital mapping and 3D visualisation

Massimiliano Cannata, Nils Oesterling, Adrian Wiget

Swiss Geological Survey
Swiss Geodetic Commission
Swiss Geotechnical Commission
Swiss Geophysical Commission
Scuola Universitaria Professionale della Svizzera Italiana
Open Source Geospatial Foundation

12.1

Detection of gross-errors into gravity data of IRAN by Kriging approach

Abdollahzadeh Makan*, Najafi Alamdari Mehdi *

**K.N.Toosi University of Technology, Faculty of Geodesy and Geomatics Engineering. 1364 Valiasr Street,Mirdaamaad Intersection,Tehran,Iran*
(m_abdollahzadeh@sina.kntu.ac.ir)

The main aim of this research is to refine Iranian gravity data based on linear prediction method. Iranian gravity dataset has been observed during a long time by different gravimeters and methods. Various kinds of systematic errors have affected the observations due to uncertainty of reference frames and equipments. Hence a refinement process of gravity data seems to be necessary.

Spatially correlated data such as gravity anomaly can be validated first by geographical techniques. It should be low pass filtered (trend removal) and then the map of the filtered data must be inspected. These are done by computing a high degree geopotential model, e.g. *EIGEN04C*, and *RTM* topography effect and then removing from the free air gravity anomaly. A gross error shows up as a chimney or volcano in the countered map. In This step about 1403 points were flagged as outliers.

The size of current gravity database makes it virtually impossible to check and correct the remaining suspected errors. Hence an automatic, or semi-automatic computer based method is needed. Correlations of spatially distributed database are used to detect gross errors. If a value differs more than usual from its neighbouring values, it may be a gross error. This strategy based on *simple Kriging* approach was used with great success. As a result a number of 490 points were eliminated in the numerical process.

The map of the outlier points is presented in figure1. As one can see, there are many blunders in Iranian gravity database. Most of them belong to NCC (Iranian National Carthogeraphic Center) observations, which have been measured along the precise leveling network. These gravity points should be investigated and may need to be remeasured. The new adjustment process seems to be necessary for NCC observed points.

REFERENCES

Bureau Gravimetrique Internation, 1989: Workshop on gravity data validation, Bulletin d' information, No.65, 89-142.

Cressie, N. A. C. 1991: Statistics for Spatial Data, John Wiley and Sons, Inc., New York.

Forsberg, R. 1984: A study of terrain reduction, Density anomalies and geophysical inversion methods in gravity field modelling, Rep. 355, Dept Geod Sci, Ohio state Univ, Columbus.

Journel A.G. & Huijbrects Ch.J 1978: Mining Geostatistics, Academic Press, London, New York, San Francisco.

Tscherning, C.C. 1990b : A strategy for gross-error detection in satellite altimeter data applied in the Baltic-Sea area for enhanced geoid and gravity determination. Proc. 11th General meeting Nordic Geodetic Commission, Copenhagen, 90-106.

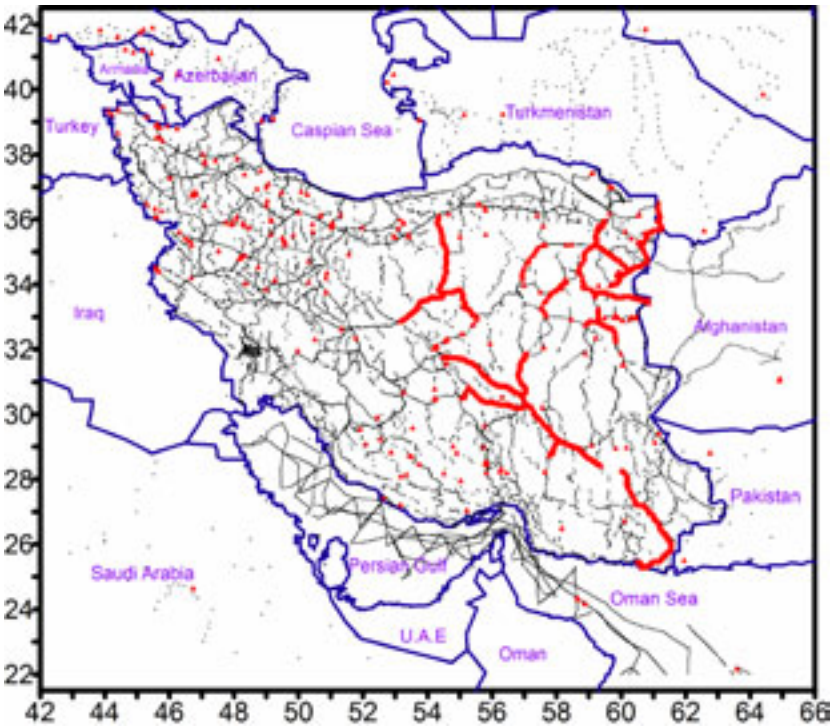

Figure1. Detected outlier gravity points (The red triangles)

12.2

The Sensor Observation Service (SOS)

Milan Antonovic

SUPSI - Institute of Earth Sciences, CH-6952 Canobbio (milan.antonovic@supsi.ch)

The SOS (Sensor Observation Service) aggregates readings from live, in-situ and remote sensors. The service provides an interface to make sensors and sensor data archives accessible via an interoperable web based interface.
The SOS is part of the OGC's SWE (Sensor Web Enablement) group of specifications.
The SWE Working Group, is establishing the interfaces and protocols that will enable a "Sensor Web" through which applications and services will be able to access sensors of all types over the Web.
This presentation introduce the main characteristic of all the SWE specifications and then explain extensively the SOS standard.

The SWE group of specifications are:

1. Observations & Measurements (O&M)
2. Sensor Model Language (SensorML)
3. Transducer Markup Language (TML)
4. Sensor Observation Service (SOS)
5. Sensor Planning Service (SPS)
6. Sensor Alert Service (SAS)
7. Web Notification Service (WNS)

REFERENCES

Arthur Na (IRIS Corp.), Mark Priest (3eTI) 2007: Sensor Observation Service
Mike Botts, 2003: Sensor Model Language (SensorML): XML-Based Language for In-situ and Remote Sensors
Mike Botts, George Percivall, Carl Reed, John Davidson, 2006: OGC® Sensor Web Enablement: Overview And High Level Architecture.
Stefan Falke, 2006: Exploring the Sensor Observation Service (SOS) for Multi-dimensional Atmospheric Science Data

12.3

3D Geological Model of the Mont Terri Rock Laboratory

Roland Baumberger *, P. Bossart *, U. Eichenberger **, A. Kühni *, C. Nussbaum ***, Nils Oesterling *, E. Weber **

* *swisstopo, Swiss Geological Survey, Seftigenstrasse 264, CH-3084 Wabern, Switzerland*
** *Swiss Institute of Speleology and Karst-Research, CH-2301 La Chaux-de-Fonds, Switzerland*
*** *Geotechnical Institute Ltd, Fabrique de Chaux 65, CH - 2882 St-Ursanne, Switzerland*
Contact: roland.baumberger@swisstopo.ch

The Mont Terri Rock Laboratory is located in the Swiss Jura Mountains (Folded Jura, Mont Terri Anticline). It can be accessed via the security gallery of the Mont Terri Highway tunnel. Inside the mechanical, hydrogeological and geochemical properties of the Opalinus Clay Formation, a potential host rock for deep geological disposal in Switzerland, are being investigated. Since 1996 twelve partners from Europe and Japan carry out various kinds of experiments in this facility (developing test methodology, performing demonstrations and understanding processes).

Geological mapping in the region of the Mont Terri anticline was extensively performed during the last century (Laubscher, 1963). A vast amount of surface (geological maps) and sub-surface information (i.e. boreholes, tunnel profile maps) are available. However, these data have never been compiled to a 3D geological model. In order to better understand the regional geological setting around the Mont Terri rock laboratory and to prepare a basis for future hydrogeological and rock-mechanical models, swisstopo has decided to develop a 3D geological model of the Mont Terri anticline.

Using this model the subsurface geological setting of the Mont Terri region and its relationship to the galleries of the rock laboratory can be illustrated.
It is now possible to view stratigraphic boundaries, to follow the propagation of faults and to investigate regional tectonics. All these information can be correlated in a regional scale subsurface view. Additionally, the 3D model also gives important information on the consistency of the geological maps, cross-sections and drill holes.

3D modelling is an iterative and interpretive process, which proceeds over several steps. After data compilation a first, simplified 3D structural model is developed. Using that model, the correlation of structures, the discussion of different concepts, ideas and uncertainties lead to a second, refined interpretation of the geology near the rock laboratory. Subsequent refinement, interpretation and integration of new data are necessary to develop the final, detailed 3D geological model of the region of investigation.

For the successful development of a 3D geological model 1) a conceptual model of the overall geological setting and 2) the clearly defined purpose and application of the model are important prerequisites.

The development of the 3D model of the Mont Terri rock laboratory was a first step of swisstopo in the wide field of 3D geological modelling. Further projects are envisaged (such as a 3D geological information system or hydro-mechanical modelling), for which this first 3D model provides an important basis.

REFERENCES

Laubscher, H.P. (1963): Geologischer Atlas der Schweiz – Erläuterungen zu Blatt 1085 St. Ursanne (Atlasblatt 40); Schweizerische Geologische Kommission (Hrsg.), Bundesamt für Landestopographie swisstopo, Bern.

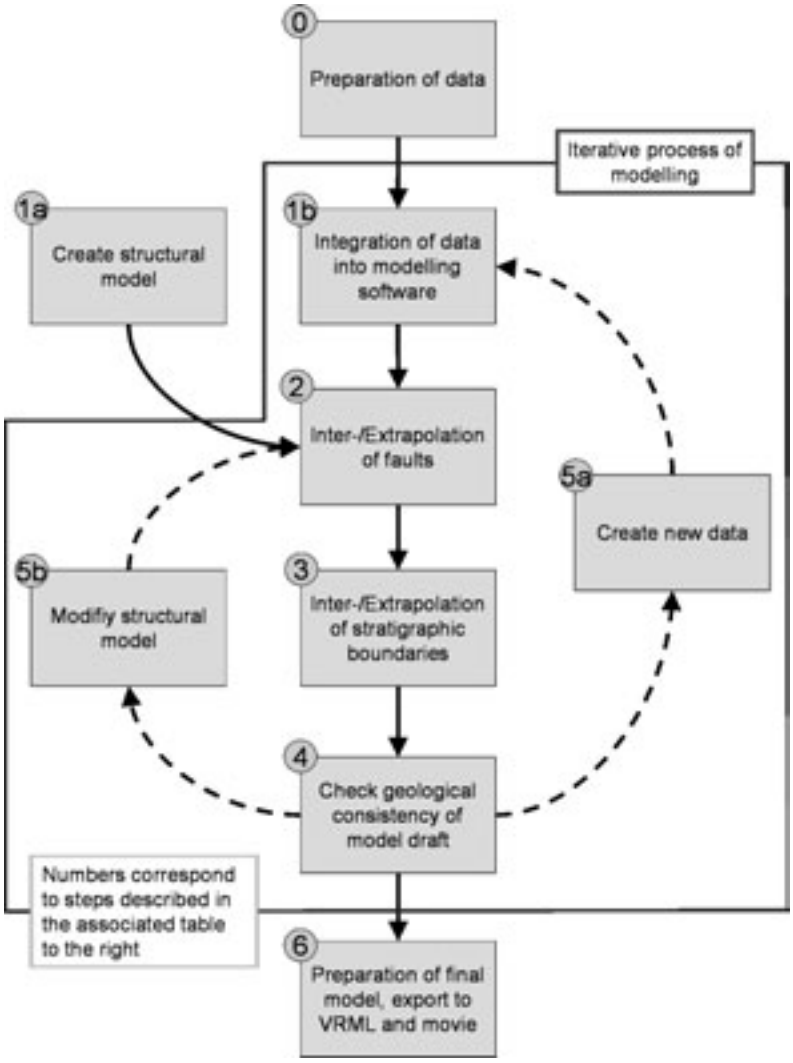

Figure 1. A possible workflow for the development of a 3D geological model (based on the experience of the Mont Terri geological model)

12.4

Bereitstellung digitaler Daten für verschiedene Nutzungen: Modellierung, Internet, Druckprodukte.

Kartografische Anforderungen, Produktions- und Darstellungsprobleme

Baumeler Andreas

Schweizerische Geotechnische Kommission, ETH-Zürich CAB E77, Universitätstrasse 6, 8092 Zürich
(andreas.baumeler@erdw.ethz.ch)

Digitale Daten werden heute vor allem in drei Bereichen verwendet: als Grundlage bei Modellierungen (z.B. Hydrogeologie, 3D-Geologie) sowie für die Datenausgabe über Internet oder als Druckprodukt. Jede dieser Verwendungsmöglichkeiten stellt eigene Ansprüche an die Daten die zum Teil divergent sind (z.B. Lagegenauigkeit und Vollständigkeit der Daten bei der «Modellierung» gegenüber Lesbarkeit bei «Ausgabe Druck»). Die Verwendung eines einzigen unangepassten Datensatzes in allen oben genannten Gebieten ergibt ein suboptimales Ergebnis, da in mindestens einem Nutzungsbereich eine ungenügende wenn nicht falsche Datenrepräsentation auftritt.

Die Datensätze «Modellierung» und «Ausgabe Internet» sind sich recht nahe. Sie unterscheiden sich hauptsächlich durch die Anforderungen bei der Datennutzung. Während bei der eigentlichen Modellierung die vollständigen, lagegenauen Daten

verwendet werden und auf die Darstellung erst in zweiter Linie geachtet wird, muss bei der Ausgabe im Internet primär an die Darstellung bzw. die Lesbarkeit gedacht werden.
Von diesen beiden Datensätzen unterschiedet sich der Datensatz der Stufe «Ausgabe Druck» in stärkerem Masse. Dies ist auf folgende Punkte zurückzuführen:
1) Im Bereich «Modellierung» und «Ausgabe Internet» werden Daten laufend aktualisiert, sie sind im zeitlichen Bezug dynamisch während Druckprodukte einen Zeitauszug darstellen.
2) «Internet-Karten» sind interaktiv; durch die Möglichkeit des Ein- und Ausblendens von Themenebenen sind sie „polythematisch"; es ist möglich den dargestellten Objekten grosse Informationsmengen mitzugeben die bei Bedarf abgerufen werden können. Zudem kann die Symbologie mit dem Darstellungsmassstab verknüpft werden so dass bei Vergrösserung des Bildausschnittes mehr Objekte dargestellt werden können. Gedruckte Karten dagegen sind meistens „monothematisch"; ausgewählte Daten sind in einer festen Grösse dargestellt; die Menge der darstellbaren Objekte ist limitiert durch den Platz der zur Verfügung steht.

Trotz der genannten Einschränkungen sind gedruckte Karten eine unumgängliche Form der Datenpräsentation. Als einziges Medium erlauben sie eine hochauflösende Darstellung weitreichender, zusammenhängender Gebiete in grossem Massstab. Weiter haben sie eine hohe Wichtigkeit durch eine, von technischen Mitteln praktisch unabhängige, Benuzungsmöglichkeit. Nicht zuletzt steht die Tatsache, dass Druckprodukte bislang die einzige wirklich unproblematische Form der langfristigen Datensicherung darstellen.

Bei vorausschauender Projektplanung können die einzelnen Produkte einfach voneinander abgeleitet werden. Die Datenaufnahme mit lagegenauer Objekterfassung bildet die gemeinsame Grundlage. Bei geologischen Karten werden sie durch Ergänzungen (Interpretation) zu einem Gesamtbild vervollständigt. Aus diesem Grunddatensatz, der im Bezug auf die Objektivität den höchsten Grad aufweist, können die Produkte in der Reihenfolge «Datensatz Modellierung» → «Ausgabe Internet» → «Ausgabe Druck» abgeleitet werden.

Die Aufbereitungsschritte sind folgende:
Bei der «Ausgabe Internet» sind für festegelegte Massstabsstufen Generalisierungen der dargestellten Themenebenen abzuleiten. Ebenfalls ist über die Programmsteuerung festzulegen, bei welcher Vergrösserungsstufe welche Daten sichtbar sein sollen.
Für die «Ausgabe Druck» müssen weiterreichende Arbeiten vorgenommen werden. In Druckprodukten kommt der Lesbarkeit ein wesentlich höherer Stellenwert zu als dies bei der «Ausgabe Internet» der Fall ist. Hochqualitative Druckprodukte sind wissenschaftlichen Zeichnungen vergleichbar: sie weisen einen hohen Stilisierungsgrad auf und versuchen damit neben der eigentlichen Widergabe der objektiven Fakten die zugrunde liegende wissenschaftliche Idee klar hervorzuheben. Die Voraussetzung dafür ist eine konsequente Überarbeitung der Daten: Flächen brauchen eine minimale Grösse, Bänder eine minimale Breite. Der Linienverlauf muss klar sein und den Lesefluss lenken. Die dargestellten Punktinformationen müssen so platziert werden, dass sie sich oder andere Objekte nicht abdecken. Diese Schritte erfordern teilweise starke Eingriffe in den ursprünglichen Datensatz: die Lagegenauigkeit der Objekte wird verändert, Objektklassen werden nach dargestelltem Thema gewichtet und damit verstärkt d.h. überdimensioniert dargestellt.

12.5
Digitale Kartografie für GIS und Kartendruck mit Grafikprogrammen

Baumeler Andreas

Schweizerische Geotechnische Kommission, ETH-Zürich CAB E77, Universitätstrasse 6, 8092 Zürich
(andreas.baumeler@erdw.ethz.ch)

Grafikprogramme wurden bisher vor allem für Digitalisierungs- und Gestaltungsarbeiten von Druckprodukten verwendet. Für den Zweck der GIS-Daten-Erfassung wurden sie als ungeeignet betrachtet, da sie zum einen weder über Werkzeuge zur Georeferenzierung oder Attributierung verfügten und es zum anderen nicht möglich war konsistente Daten zu produzieren.
Neuere Entwicklungen in professionellen Grafikprogrammen (Illustrator, Freehand) erlauben eine gleichartige Datenhandhabung und Datenhaltung wie GIS-Programme. Das bedeutet, Flächen, Linien und Punkte können konsequent als Objekte dargestellt werden. Jedes dargestellte Element gehört einer vorgegebenen Klasse an die weiter attributiert werden kann. Die Georeferenzierung erfolgt über eine Programmerweiterung; Geometrie, Klassenzugehörigkeit und Attribute der Objekte können auf diese Weise in GIS-Programme exportiert werden. Ebenso sind Import und Bearbeitung von GIS-Dateien möglich

Die Vorgehensweise der Datenerfassung über Grafikprogramme bietet zwei wesentliche Vorteile:
1) rasche und einfache Datenerfassung durch Verwendung von Bézierlinien
2) freie Gestaltung der kartografischen Elemente, der dargestellten Objekte und der Maquette. Damit ist die Möglichkeit der Druckausgabe in hoher Qualität gegeben

Bézierlinien beschreiben einen Kurvenverlauf mathematisch mit wenigen Ankerpunkten. Damit ist eine präzise Erfassung komplexer Kurvenverläufe möglich Korrekturen und Anpassungen können einfach durchgeführt werden. Für den Export in GIS werden die Bézierlinien in Polylinien konvertiert. Mit Hilfe eines Zusatzprogrammes des Institutes für Kartografie (IKA, ETH-Zürich) kann diese Konvertierung gesteuert und mit hoher Präzision durchgeführt werden.

Abbildung 1: Vergleich der Liniendarstellung durch Bézierlinien (links) und Polylinien (rechts) nach dem Konvertierungschritt.

12.6

The relevance of digital data and techniques to applied geosciences

Beer Christoph* & Beres Milan*

Swiss Geological Survey, Federal Office of Topography swisstopo, Seftigenstrasse 264, CH-3084 Wabern (christoph.beer@swisstopo.ch)

Geoinformation has become one of the most important components of the national economy. An added value is thereby created in economic, administrative and everyday activities. The current market volume of the private geoinformation market is estimated to total 500 Mio. Swiss Francs per year (Fig.1). In comparison to estimates in 2002, the market volume has increased by 300 Mio. Swiss Francs, equivalent to 5% growth per year.

The operational meaning of digital technology is in the making of existing data useful, in the transfer of knowledge and in the networking and co-ordination of data sources down to the customer groups. The most modern technology is essential for handling digital data, particularly in knowledge management. Such technology permits the association of simple datasets for the purpose of recognizing their significance and eventually gaining practical information from them. If this new information is linked with existing information and knowledge, then more knowledge can be generated. Increased knowledge improves the understanding of phenomena and the development of innovative solutions.

Together with the free market use, digital geodata and geoinformation have substantial social and economical uses. They are indispensable for making clear and comprehensible decisions and for engaging the public in important political decisions and social developments. Geoinformation is becoming increasingly important in practically all aspects of life. Various studies of cost-use analyses show that the economical use of digital geoinformation is 4 to 10 times higher than its production cost.

Digital geodata are a raw material with the highest potential in the supply chain. On the one hand there is the one-time profit margin within the value chain of a data-producing enterprise. But since geodata and geoinformation reside in a network of various customers and multiple refinement stages, their added value becomes enormous.

In short, Geodata are a top-ranking good in both political and economical regards.

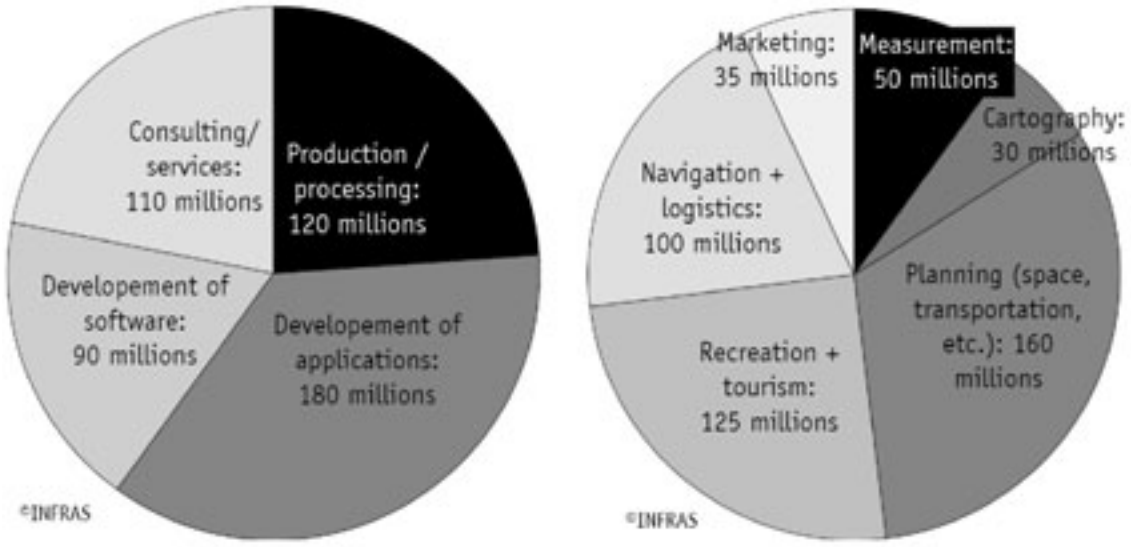

Figure 1: Current market volume categorized by providers (left) and applications (right).

REFERENCES
http://www.swisstopo.admin.ch/internet/swisstopo/de/home/docu/pub/kogis.parsys.5303.downloadList.7391.DownloadFile.tmp/analysegeoinformationsmarkt080813.pdf
http://www.swisstopo.admin.ch/internet/swisstopo/de/home/docu/pub/kogis.parsys.31452.downloadList.83198.DownloadFile.tmp/giflyerde.pdf
http://www.m-spinatsch.ch/d/DetailsPublikationen/Ueberblick/StaatsaufgabeLG-Ueberblick-d.html

12.7

GIS-supported Geology and Fieldwork in the Eastern Greater Caucasus

Bochud Martin*, Mosar Jon*

*Science de la Terre, Département des Géosciences, Université de Fribourg, Chemin du Musée 6, CH-1700 Fribourg (martin.bochud@unifr.ch)

The evolution of new GIS-supported technologies allowed modifying the habits of geologist, especially in the field, during data acquisition and mapping. Sturdy field-computers and GPS have the same importance as field-books and maps.
For the last 5 years, the tectonics group of the University of Fribourg works with portable field-computers and GPS in remote locations of the Eastern Greater Caucasus. Expeditions often require work in areas with no electricity other than supplied by batteries. Presently we use Xplore field-computers equipped with GPS and ArcGIS Desktop capabilities. In addition, we use sophisticated high precision Trimble GeoXH GPS mini-computers with antennas and ArcPad (both from ESRI) to work in the field.

Using this tools makes it possible to introduce all types of measurements directly in a geodatabase. Our geodatabase includes all structural data such as: bedding, schistosity, faults and associated lineations such as striations, axial planes, fold axis, samples location and description as well as pictures. Each datum can be linked with a detailed description, drawings and/or photos. More importantly it allows the geologist in such remote areas to always find its exact position. This is important in regions with no detailed topographic maps and no geology maps. We than rely on satellite imagery and documents scanned and georeferenced. It allows us also at any time to retrieve data already available in the database.

In Azerbaijan the availability of essential data such as topographic maps turned out to be impossible. Especially topographic or geological maps at scales 1:25000 or 1:50000 fall under military restrictions. However the large resources of the www made it possible to find Russian maps at 1:100'000, free satellite images from Landsat (Geocover and ETM+ with the seven spectral bands), digital elevation model at 90 meters from the Shuttle Radar Topography Mission (SRTM) and a geodatabase

with all locality and place names of Azerbaijan. The place name geodatabase allowed to homogenize the place names and to avoid some misunderstanding in papers.

Before leaving to the field, we export the data from the geodatabase to the GPS PDA. In the field we work mostly with the handheld GPS (Trimble GeoXH), and the computer tablets (Explore). At the end of each field day, we transfer new measurements in our geodatabase, where it is than possible to make more detailed annotations, but also modifications or corrections. The updated database is subsequently available for the following days. It can also be used by different groups working in neighbouring areas.
The use of a GIS-database improves the efficiency and extends the boundaries of the geological research, making it possible to share them with co-workers and making them available through the www. The biggest problem with geodatabase is generally not to create, but to fill them with data. Working in the field with PDA and field computer allows filling the geodatabase directly. GIS software now offers numerous possibilities and tools for mapping but also for sophisticated calculations, to compare data, to combine maps and data and to create our own maps.

Similar databases have been developed in international projects such as MEBE in response to the demands and needs of supporting groups from the oil industry. On a more local scale similar needs are expressed by local authorities and other institutions collecting data and surveying the environment.

In addition, we are in the process of implementing these tools for mapping exercises in geology on a bachelor level. It allows the students to develop a multidisciplinary approach to "classic geological mapping"! This is perceived by students as a stimulating exercise otherwise often considered "uninteresting".

5-years experience in field-work in remote areas of the Greater Caucasus have shown that the field computer and GPS handheld computer are rugged enough to tolerate difficult field conditions such as heat and shock as well as rain, or even short immersion in water (student falling into river with equipment!). The only shortcomings are that they cannot (should not!) be used as hammer or as magnifying lens!

12.8
The National Spatial Data Infrastructure

Buogo Alain*, Buser Rolf*, Sonney René*, Wiget Adrian**

Federal Office of Topography swisstopo, Coordination, Geo-Information and Services (COGIS), Seftigenstrasse 264, CH-3084 Wabern
*** Federal Office of Topography swisstopo, Geodesy, Seftigenstrasse 264, CH-3084 Wabern (adrian.wiget@swisstopo.ch)*

Geographical information is data which is spatially referenced by means of coordinates, place names, postal addresses or similar criteria. 60 to 80 percent of all political and economic decisions are of spatial nature. The Swiss federal administration, mandated by the Federal Act on Geoinformation (GeoIG) and lead-managed by COGIS, the Coordination, Geo-Information and Services Division of the federal office of topography swisstopo (www.swisstopo.ch) follows the strategy to facilitate the integration of the widest possible selection of data, to make access easier and to promote the application of this data through the coordination and harmonisation of geographical information. With wider and more intensive usage, greater economic benefit can be achieved from the geographic information which is already available. This will add value for all those involved – federal, cantonal and local government, organisations in the private sector and the scientific community as well as the general public.

The federal strategy for geographical information is also in accordance with the EU directive INSPIRE (Infrastructure for Spatial Information in Europe). In order to implement the strategy and to access the enormous amount of available data, it is proposed to set up a user-friendly, decentralised but networked system. Such a national spatial data infrastructure (NSDI) depends on political, organisational, financial, legal and technical components. First of all it is essential to create an organisational framework for the activities of partners in Switzerland involved in the implementation of the NSDI: Federal, cantonal and local governmental bodies and other organisations like SOGI, the Swiss Organisation for Geographic Information (www.sogi.ch). To this end, the e-geo.ch "impulse programme" was launched in order to build and promote a network of contacts and a project management organisation covering the whole of Switzerland.

REFERENCES

http://www.swisstopo.admin.ch/internet/swisstopo/de/home/topics/geodata_inf.html
http://www.swisstopo.admin.ch/internet/swisstopo/fr/home/topics/geodata_inf.html
http://www.swisstopo.admin.ch/internet/swisstopo/en/home/topics/geodata_inf.html

12.9
FOSS4G: open source tools for geoinformation

Massimiliano Cannata*

**Institute of Earth Scences – SUPSI, Trevano, C.P. 72, CH-6952 Canobbio*

This presentation is an introduction to FOSS4G and what it is about. Introducing the concepts of Open Source Software, Open Source Geospatial foundation, and related geoinformation projects. The goal of the presentation is to welcome newcomers who might like to learn more about FOSS4G and join in the effort.

A large number of geoinformation software has been developed during the last decade. During their evolution often they took inspiration each others and now as a result they are quite similar in capabilities: generally they all (i) manage numerous data format, (ii) produce customizable map visualization, (iii) handle attributes, vector, raster and image data types, (iv) perform general and spatial query/analysis, (v) produce web services, (vi) provide web-GIS interface.
Generally software can be subdivided in two classes: the proprietary software and the Free and Open Sources Software (herein referred to as FOSS).
The first class describes software offered for sale or license, where the users are not allowed to see the source code. Nor are they able to modify the code for their own use or to distribute to others. The vendor is the only proprietary of the software and the user just acquire a licence for use it as it is. On the contrary FOSS denote some user freedom rights such as to run, copy, distribute, study, change and improve the software. As described in the Web-Site of the Free Software Foundation (FSF [1]) the word “free” refers to four kinds of user freedom:

- The freedom to run the program, for any purpose.
- The freedom to study how the program works, and adapt it to any needs.
- The freedom to redistribute copies.
- The freedom to improve the program, and release the improvements to the public, so that the whole community benefits.

For the second and fourth points access to the source code is a precondition.
In order to guarantee this freedom, FOSS are usually licensed under the GNU General Public License (GPL): GPL licence makes restrictions that forbid anyone to deny these rights. Distributed copies of a GPL licensed program, whether gratis or for a fee, must give the recipients all the original rights of freedom; thus the distributor must also make sure that users, too, receive or can get the source code.
While proprietary software grown pushed by commercial goals and concentrated theirs efforts in developing “easy to use” software, FOSS grew to solve problems and develop projects – often governmental or research projects – resulting in high effective but often not friendly software and therefore delegated to a small niche of geoinformation specialists.
The FOSS4G (Free and Open Source Software for Geoinformation) term denote all the FOSS related to geoinformation. Some of them (actually the most diffuse) are today associated in the Open Source Geospatial foundation (OSGeo [2]).
OSGeo, is a not-for-profit organization whose mission is to support and promote the collaborative development of open geospatial technologies and data. The foundation provides financial, organizational and legal support to the broader open source geospatial community. It also serves as an independent legal entity to which community members can contribute code, funding and other resources, secure in the knowledge that their contributions will be maintained for public benefit. OSGeo also serves as an outreach and advocacy organization for the open source geospatial community, and provides a common forum and shared infrastructure for improving cross-project collaboration.
Some of the OSGeo detailed goals are:

- To provide resources for foundation projects - eg. infrastructure, funding, legal.
- To promote freely available geodata - free software is useless without data.
- To promote the use of open source software in the geospatial industry (not just foundation software) - eg. PR, training, outreach.
- To encourage the implementation of open standards and standards-based interoperability in foundation projects.
- To ensure a high degree of quality in foundation projects in order to build and preserve the foundation "brand".
- To make foundation and related software more accessible to end users - eg. binary "stack" builds, cross package documentation.
- To provide support for the use of OSGeo software in education via curriculum development, outreach, and support.
- To encourage communication and cooperation between OSGeo communities on different language (eg. Java/C/Python) and operating system (eg. Win32, Unix, MacOS) platforms.
- To support use and contribution to foundation projects from the worldwide community through internationalization of software and community outreach.

Currently OSGeo Projects include web mapping (deegree, Mapbender, MapBuilder, MapGuide Open Source, MapServer,

OpenLayers), desktop applications (GRASS GIS, OSSIM, Quantum GIS, gvSIG), geospatial libraries (FDO, GDAL/OGR, GEOS, GeoTools), metadata catalog (GeoNetwork), and other projects (Public Geospatial Data, Education and Curriculum).

REFERENCES

[1] FSF, Free Software Foundation, viewed 14 August 2008, <www.fsf.org>
[2] OSGeo, Open Source Geospatial Foundation, viewed 28 August 2008, <www.osgeo.org>

12.10

The "cadastre géologique" of the canton of Vaud: a geoinformatic tool to collect, manage and publish geological data.

Giorgis David*

**Office de l'information sur le territoire (OIT), DINF, Av. de l'Université 5, 1014 Lausanne (david.giorgis@vd.ch)*

The "cadastre géologique" of the canton of Vaud was created to collect, store and distribute systematically, information coming from boreholes and other mechanical underground investigations. An information system was developed, mainly based on web technology. This system contains cartographic overview, borehole insertion (with online e-form) and tracking, as well as the possibility to attach documents. In addition, data extraction and creation of different user's profile is also possible.
This gathering information constitutes part of the geoscience knowledge's base which is then processed by Geographic Information Systems (GIS) to integrate the various sources of information and produce derived graphics, maps and models describing the underground characteristics. It allows the better integration of geology and three-dimensional planning in the different processes of landscape management, in a perspective of sustainable development.
Presently, these geological information, have been used for seismic microzonation mapping and other regional projects (for example : evaluation and mapping of resource for ground source heat pump system) will integrate intensively these data.
The "cadastre géologique" web application can be shared by other cantons (currently three are concerned) and possibility of collaboration with other public administrations is open and welcome, in order to use common tools to collect, manage and publish geological data.

Figure 1. Example of screenshots from the "cadastre géologique" web portal (www.geocad1.vd.ch). This web application is written in PHP using MySQL (Open Source components).

12.11

Borehole Evapometer measurements: Detection of zones with different hydraulic conductivities in the Opalinus Clay

Lukas Glur*, Paul Bossart*, Martin Herfort**, Edi Meier*** & Christophe Nussbaum****

* *Swisstopo, Route de la Gare 65, CH-2882 St-Ursanne.*
** *Swiss Federal Nuclear Safety Inspectorate HSK, CH-5253 Villigen-HSK,*
*** *Edi Meier und Partner AG, Jägerstrasse 2, CH-8406 Winterthur.*
**** *Institut Géotechnique, Route de la Gare 65, CH-2882 St-Ursanne*

The estimation of physical parameters such as hydraulic conductivity or evaporation rate in different structural and lithological units of the Opalinus Clay is very important for assessing safe radioactive waste disposal. This study was carried out in the Mont Terri rock laboratory in the framework of the evaporation logging experiment. New equipment, the borehole evapometer, has been developed by swisstopo in recent years. The borehole evapometer is now ready for in-situ hydraulic testing in very low permeable formations.

The present aim of this evaporation logging experiment is to detect zones with varying hydraulic conductivities in the Opalinus Clay, which were measured by HSK and swisstopo. Of particular interest is the comparison between the excavation damaged zone (EDZ) and undisturbed Opalinus Clay. The measurements were carried out at several depths along three boreholes cutting through the EDZ.

The borehole evapometer is a tool for estimating the evaporation rate and the hydraulic conductivity in a packed-off borehole test interval of 1m length. This method uses a constant air flow through the borehole test interval. By measuring differences in relative humidity and temperature, the evaporation rate and the resulting hydraulic conductivity can be calculated. The integrated evaporation rate over the whole test section can be obtained, as well as local evaporation rates along fractures cutting the borehole wall.

Several experimental set-ups and procedures were applied and compared, including variations in duration, frequency, spatial, temporal and instrumental resolution, air-flow direction, imposed humidity difference, borehole inclination and time of day. The results were compared with drillcore mappings, high-resolution optical televiewer (DOPTV) and seismic measurements of the respective boreholes (Yong 2007) and mineralogical analysis of core samples.

The measurements of temperature, humidity as well as the derived evaporation rates and hydraulic conductivities (k) depend strongly on the experimental procedure and the borehole history. A correlation with the extent of the EDZ and with borehole depth is visible. The calculated k values range from 10-13 to 10-15 m/s and are comparable to undisturbed Opalinus Clay. Temperature decreases and absolute humidity increases with borehole depth in all tested boreholes. The method is suitable for determining small-scale k values in low-permeability formations.

REFERENCES

Yong, Salina. 2007. A three-dimensional analysis of excavation-induced perturbations in the Opalinus Clay at the Mont Terri Rock Laboratory, PhD thesis, ETH Zurich.

12.12

Dynamic Monitoring of Load Tests by Kinematic Terrestrial Laser Scanning

David Grimm* & Hans-Martin Zogg*

**Institute of Geodesy and Photogrammetry ETH Zurich, Wolfgang Pauli-Strasse 15, CH-8093 Zurich ([grimm, zogg]@geod.baug.ethz.ch)*

In relation with maintenance works of the runway at the Hamburg Airport in Germany, a convenient method to reinforce the soil surrounding the concrete runway was subject of investigation. A fixing of the soil is important with regard to aircrafts accidentally passing over the runway. To prove the suitability of the soil fixings, load tests were performed on three different purpose-built test fields (Figure 1).

For these tests, the aircraft was simulated by a crane with a weight of about 200 tons. The crane drove backwards into the test fields. Besides the sinking of the crane into the test fields, the size of the bow wave, which occurs on the first wheel while driving into the mud, was of main interest. The surface of the test fields had to be permanently monitored during the test drives.

For the dynamic monitoring of the occurring bow wave, three different geodetic measurement methods were considered: photogrammetry (videogrammetry), kinematic terrestrial laser scanning (TLS), and range imaging (RIM). Finally, the monitoring was performed by kinematic TLS. Photogrammetry would have required additional illumination of the scenery. Furthermore, the soil surface was homogeneous and colour variances could hardly be detected. The RIM technology, a new measurement technology for geodetic engineering (Kahlmann & Ingensand, 2007), did not fulfil the requirements in terms of measurement accuracy. Nevertheless, this new technology allows the acquisition of full 3D-images and promises big advantages compared to traditional measurement methods for the future. In addition, the soil was expected to be wet and partially inundated. Thus, a requirement of the used laser scanner had to be the feasibility to measure through a layer of water with a thickness of several centimetres (Vogel, 2008).

Consequently, the profile laser scanner SICK LMS200-30106 by Sick AG (Zogg & Grimm, 2008) was mounted underneath the crane in front of the crane wheel for the dynamic monitoring of the occurring bow wave during the load tests (Figure 2). The laser fan was adjusted along the driving direction of the crane (Figure 3). The crane was additionally tracked by three total stations for the localisation in a global coordinate system. For the detection of the bow wave size, the relative position of the profile scanner was sufficient. The surface, which had not been run over yet by the crane, served as horizontal reference for the profiles. This also enabled the elimination of inclination variations of the profile scanner along the driving direction.

To make possible a practicable analysis of the measurements, particular software was developed. The software automatically classified the point cloud into points on the wheel and points on the soil surface. Thus, the height of the bow wave could be detected in each scanning profile (Figure 4 and Figure 5). Finally bow waves with a size of up to 18 cm could be located. Accordingly, the tests pointed out that kinematic TLS was a qualified measurement method for this particular application.

REFERENCES

Kahlmann, T., & Ingensand, H. 2007: Range Imaging Metrologie: Einführung, Untersuchungen und Weiterentwicklungen. In: “Allgemeine Vermessungsnachrichten (AVN)”, Vol. 11-12/2007, pp. 384-388.

Vogel, T 2008: Untersuchungen und Ansätze für die automatisierte Auswertung von 3D-Punktwolken. Master Thesis. Institute of Geodesy and Photogrammetry, ETH Zurich, Switzerland.

Zogg, H.-M., & Grimm, D. 2008: Kinematic Surface Analysis by Terrestrial Laser Scanning. In: Proceedings of "1st International Conference on Machine Control and Guidance", Zurich.

Figure 1. Test field for the load tests.

Figure 2. 2D-laser scanner mounted underneath the crane.

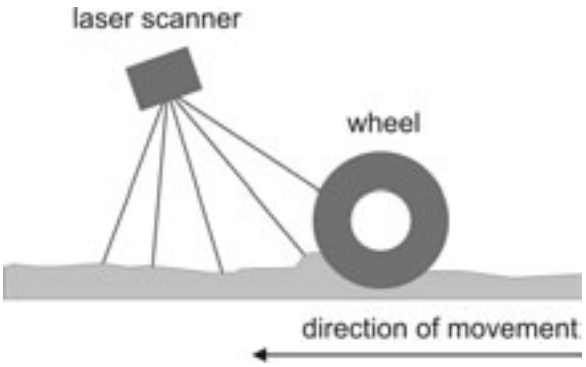

Figure 3. Measurement setup.

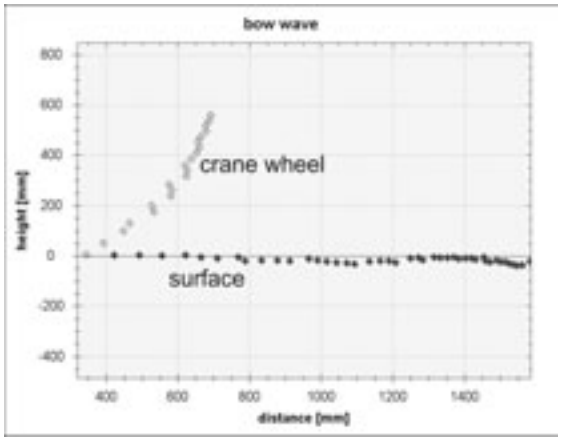

Figure 4. Profile measurements before the crane entered into the test field.

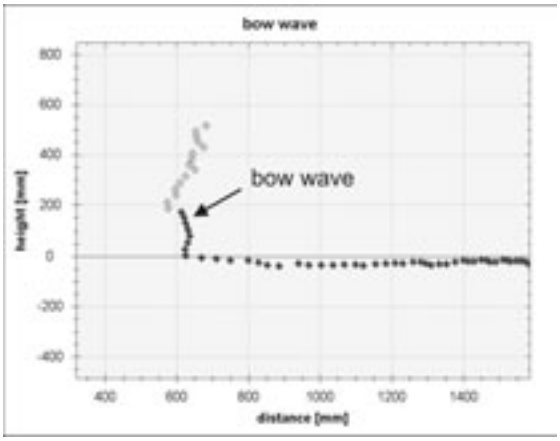

Figure 5. Detection of bow wave while driving into the test field.

12.13

Geomorphologic mapping of Lake Lucerne - the potential of high-resolution bathymetry data

Hilbe Michael*, Anselmetti Flavio S.*, Eilertsen Raymond** & Hansen Louise***

*Eawag, Swiss Federal Institute of Aquatic Science and Technology, CH-8600 Dübendorf; michael.hilbe@eawag.ch
**Geological Survey of Norway (NGU), N-9296 Tromsø
***Geological Survey of Norway (NGU), N-7491 Trondheim

Water bodies are major «blank areas» on the sheets of the Geological Atlas of Switzerland. Geomorphologic and geologic data for the lake floors included in these maps are sparse and only few published geological maps of Swiss lakes exist (e.g. Schindler, 1976). These are mainly based on single beam echosounder data, reflection seismic profiles and surface sediment samples. However, the acquisition and evaluation of large amounts of data covering entire lakes are laborious and may nevertheless fail to yield a sufficiently high resolution required to detect small-scale features on the lake floor. Recently collected high-resolution swath bathymetry data for parts of Lake Lucerne now provide a digital terrain model of the lake bottom with a resolution similar to that of airborne laser scanning on land, allowing an accurate identification of sublacustrine morphologic features.

A raster dataset with a cell size of 1 m was acquired using a Geoacoustics GeoSwath interferometric sonar system at 125 kHz coupled with accurate GPS positioning (swipos-GIS/GEO service). At this scale, it is possible to image not only small structures, but also surface textures of the lake floor. Backscatter intensity recorded along with depth data gives additional information on the properties of the sediment. Comparing the new data with existing limnogeologic studies (e.g. Schnellmann et al., 2005; Strasser et al., 2007) allows the mapping of for instance subaqueous slides, rockfall deposits and moraine ridges.

Using the large Weggis slide (Schnellmann, 2005; Figure 1) as an example, further details can be resolved. The slide covers most of the gently dipping northern slope of the Vitznau basin and was triggered by an earthquake in 1601 A.D. The scar, a 4 to 7 m-high step, can be traced along the slope over a distance of more than 6 km. The intact Holocene sediment drape above the scar is characterised by a smooth surface with diffuse depressions and elevations representing pre-existing glacial features or older slide scars. The sliding surface below the scar has a rough texture and consists of glacial deposits and bedrock (high backscatter amplitude and visible bedding) under a thin post-slide cover (Strasser et al., 2007). Chunks of apparently undisturbed sediment and minor mass flow deposits rest on a slope terrace. Deformation of the basin plain sediments resulting from gravitational loading by the slump deposits at the toe of the slope is expressed by an array of arch-shaped ridges on the flat lakebed.

Merging the new data with existing high-resolution terrain models will provide a seamless view on the geomorphology of lakes and their catchments. The integration of the swath bathymetry and backscatter data with selected reflection seismic profiles and sediment samples can be an efficient approach to complement geologic maps within water bodies.
This study was funded by the Federal Office of Topography (swisstopo), the Federal Office for the Environment (BAFU) and the Federal Department of Defence, Civil Protection and Sport (VBS).

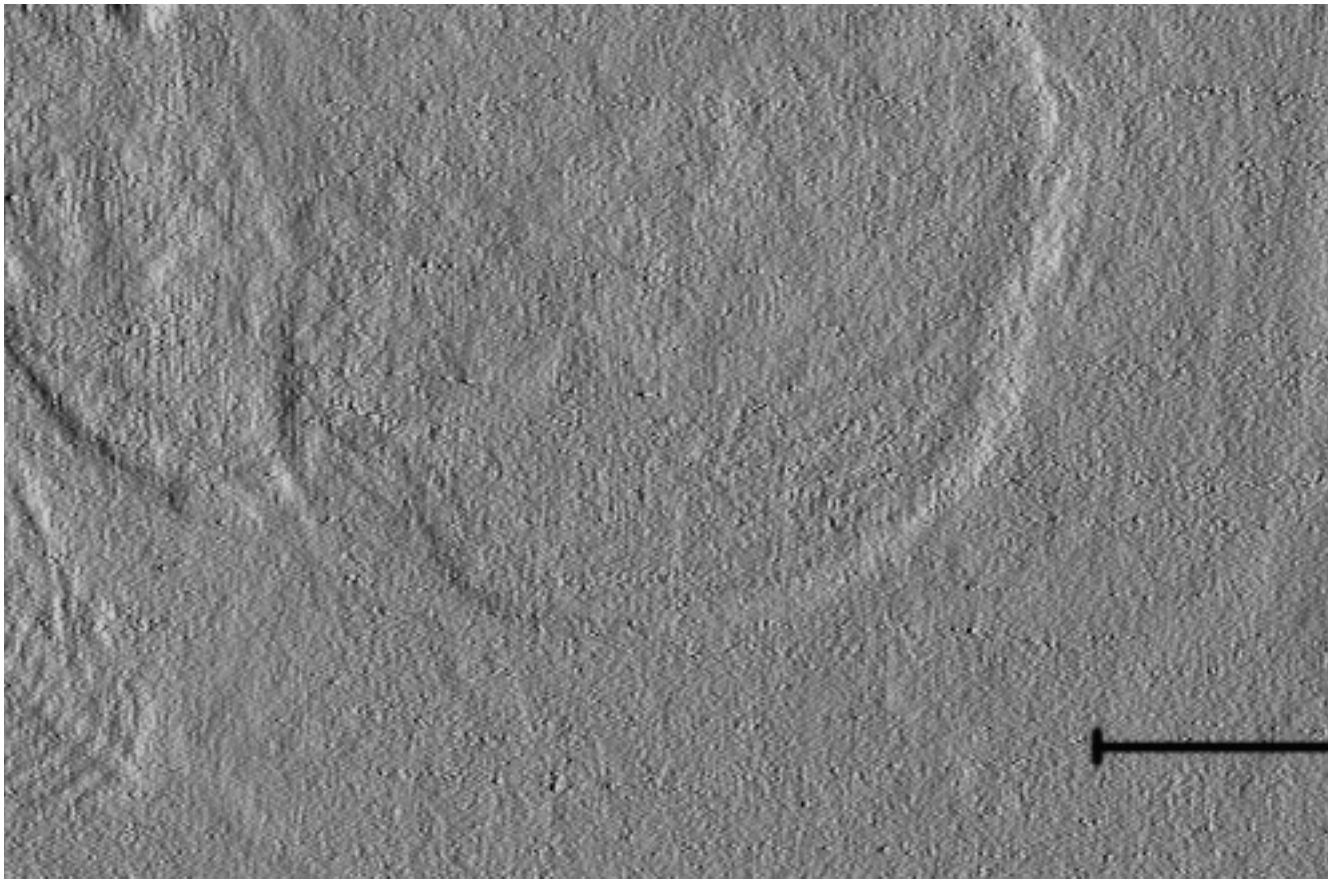

Figure 1: Shaded relief of the Weggis slide showing a prominent slide scar, different surface textures on the sliding plane and deformation features on the basin plain. Illumination from east.

REFERENCES

Schindler, C. 1976: Eine geologische Karte des Zürichsees und ihre Deutung. Eclogae geol. Helv. 69, 125-138.

Schnellmann, M., Anselmetti, F.S., Giardini, D. & McKenzie, J.A. 2005: Mass movement-induced fold-and-thrust belt structures in unconsolidated sediments in Lake Lucerne. Sedimentology 52, 271-289.

Strasser, M., Stegmann, S., Bussmann, F., Anselmetti, F.S., Rick, B. & Kopf, A. 2007: Quantifying subaqueous slope stability during seismic shaking: Lake Lucerne as model for ocean margins. Marine Geology 240, 77-97.

12.14

A 3D geological model of North-East Switzerland, a GIS solution

Jordan Peter*, Schwab Marco*, Schneider Heinz*, Schnellmann Michael**, Weber Hanspeter**, Neaf Henry*** & Alber Wilfried****

* *Böhringer AG, Mühlegasse 10, 4104 Oberwil*
** *Nagra, Hardstrasse 73, 5430 Wettingen*
*** *Büro für angewandte Geologie, Vadianstrasse 41a, 9000 St. Gallen*
**** *Albert Consulting, Altenburgstr. 30, 5430 Wettingen*

This paper presents a geological 3D model of northern Switzerland (from Oensingen to Lake Bodan). It consists in a 25m raster grid corresponding to the DEM25 of the Federal Office of Topography. It is based on an extensive collection of data about the underground: geological maps, historical isolines maps, borehole data, seismic data and geological profiles were used to construct the elevation of 4 important geological horizons. The raw data are the basis for the construction of isolines that were designed from experts in a GIS environment and only them where used as input for interpolation. In order to model the discontinuities and faults, the construction of isolines and the interpolation were performed in separated segments and merged in a further step.
This extensive work of transposition of geological data into Isolines originates in the facts that all classical interpolation methods (IDW, Spline, Kriging) applied on points do not correctly represent the geological pattern expected between hard data (e.g. boreholes). Geological interpretation and accepted geological concepts have also better been integrated into the model.
The resulted model represents finally the stage of knowledge about the extent of a geological horizon and incorporates an "interpolated" summary of numerous source of information about the underground. This opens the door for landuse management in the vertical dimension, underneath the biosphere.

12.15

Analysing landslide features through scale using the wavelet transform – Theory and application to the earth flow type landslide of Travers (Switzerland)

Kalbermatten Michael*, Turberg Pascal**

* *Laboratoire de systèmes d'information géographique, Ecole Polytechnique Fédérale de Lausanne, Ecublens, CH-1015 Lausanne (michael.kalbermatten@epfl.ch)*
** *Laboratoire de géologie de l'ingénieur et de l'environnement, Ecole Polytechnique Fédérale de Lausanne, Ecublens, CH-1015 Lausanne*

The analysis of specific features of a landslide is often conducted through visual terrain assessment. In recent years, LIDAR (LIght Detection And Ranging) data acquisition has made it possible to produce high resolution (0.5-2 meters resolution) digital elevation models (DEM). The visual analysis of high resolution DEMs is a new way used by geologists to characterise landslide features through the abstraction of scale-dependent features. Thus, the geologist carries out a multiscale analysis of the high resolution DEM due to the fact that geological features (composing a landslide e.g.) are not visible at one specific scale, but nested in each other.

The wavelet transform (Mallat, 2000), is a localized frequency analysis (or filter) for image generalization. It is possible to divide the continuous scale into discrete scale intervals. At each discrete scale level (or generalization level), we can analyse high frequency structural features and reconstruct these features at high resolution.

We present a case study where we assess the scale dependence on a landslide located near Travers (Val-de-Travers, Canton of Neuchâtel, Switzerland). A LIDAR survey had been carried out one month after the landslide. Derived from these raw elevation data points, collected through LIDAR, a DEM was interpolated (1 meter resolution).

The study area was visually and geologically analysed by a geologist. Thereafter the results were compared to the images obtained by the wavelet transform details coefficients.

In our presentation we show that there are significant links between geological features and the wavelet-transform results. They can be related to the evaluation of the stability over the observed area but also to the sliding mechanism itself. The features that we have detected can be classified through the intervals of discrete scale defined by the transform and thus could lead to associate a specific scale to the identification of a particular process (slide, flow, etc.) or a particular characteristic of the landslide (thickness, geological heterogeneity, etc.). In that sense, it could greatly help in hazard and risk assessment.

REFERENCES

Mallal, S. 2000: Une exploration des signaux en ondelettes, Les éditions de l'école polytechnique, France.

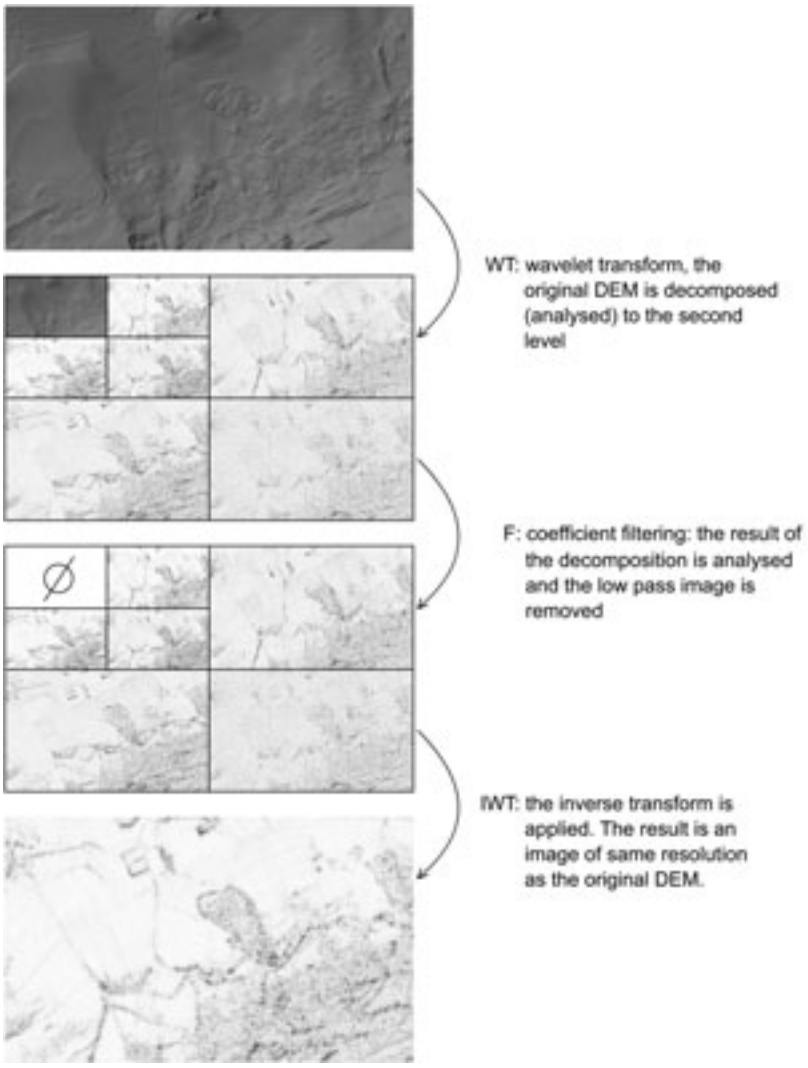

Figure 1. Wavelet transform – analysis, filtering and synthesis.

12.16

"GeoKernels.org": kernel-based methods for spatio-temporal data. Analysis, modelling and geo-visualisation

Kanevski Mikhail*, Pozdnoukhov Alexei*, Timonin Vadim*

*Institute of Geomatics and Analysis of Risk (IGAR), University of Lausanne, CH-1015 (Mikhail.Kanevski@unil.ch)

This poster presents general problems and approaches to spatial data analysis, modelling using machine learning (Artificial Neural Networks and Statistical Learning Theory) and visualisation using GIS tools and web-mapping. A range of examples (available online at the www.geokernels.org website) are presented which illustrate the theory of machine learning algorithms (adaptive data-driven methods) case studies including topo-climatic modelling and software modules. Web server contains also several teaching-oriented interactive tools highlighting the properties of the methods of spatial data acquisition, analysis, modelling and mapping. An example devoted to the operational use of machine learning approaches presented in the poster and available at (see www.geokernels.org) concerns an automatic web-service for online real-time temperature mapping.

The map presented in Figure 1 was generated automatically and is based on the measurements from 70 stations of MeteoSwiss. The profile of the temperature along the route is presented as a one-dimensional graph (bottom-right). The Google Earth satellite image is used as a background image.

Figure 2 presents an example of interactive spatial data input and automatic spatial classification using Support Vector Machines (SVM) which is a workhorse of Statistical Learning Theory. Parameters of the model were chosen automatically with a leave-one-out cross-validation procedure.

Future developments deal with adaptation, testing and validation of machine learning models for automatic spatio-temporal data analysis, modelling and geo-visualisation of raw data and the results, including simulated data and real case studies from environmental pollution, natural hazard risk mapping, and renewable resources assessments.

Acknowledgements. The study was partially supported by the Swiss National Science Foundation projects GeoKernels (project No 200021-113944) and Clusterville (project No 100012-113506).

REFERENCES

Kanevski, M. and Maignan, M. 2004. Analysis and Modelling of Spatial Environmental Data. EPFL Press, 288 pp.
Kanevski, M. (Editor). 2008. Advanced Mapping of Environmental Data. ISTE Ltd., John Wiley & Sons Inc, 313 pp.

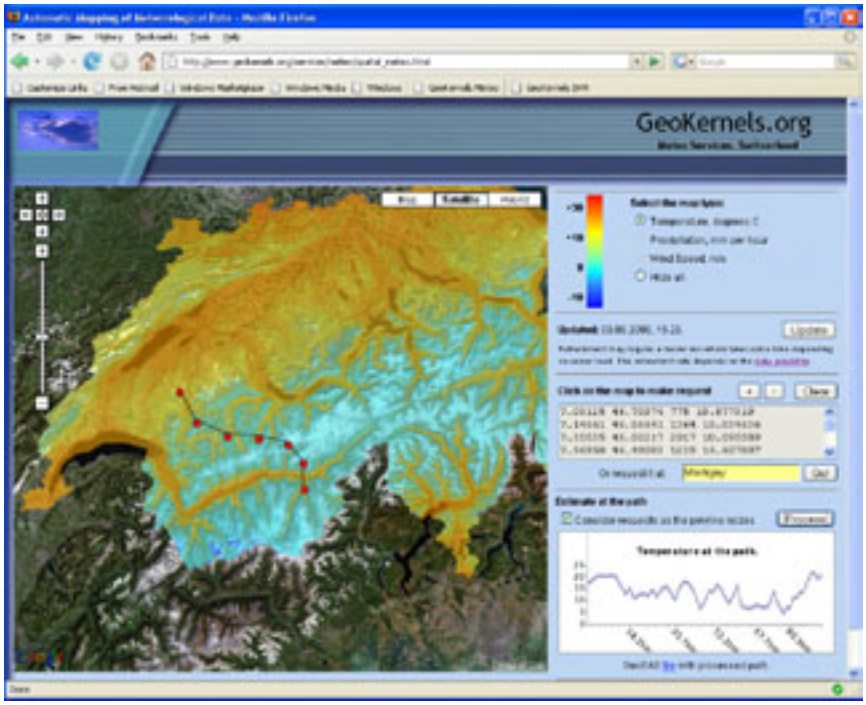

Figure 1. Online mapping of the current air temperature in Switzerland.

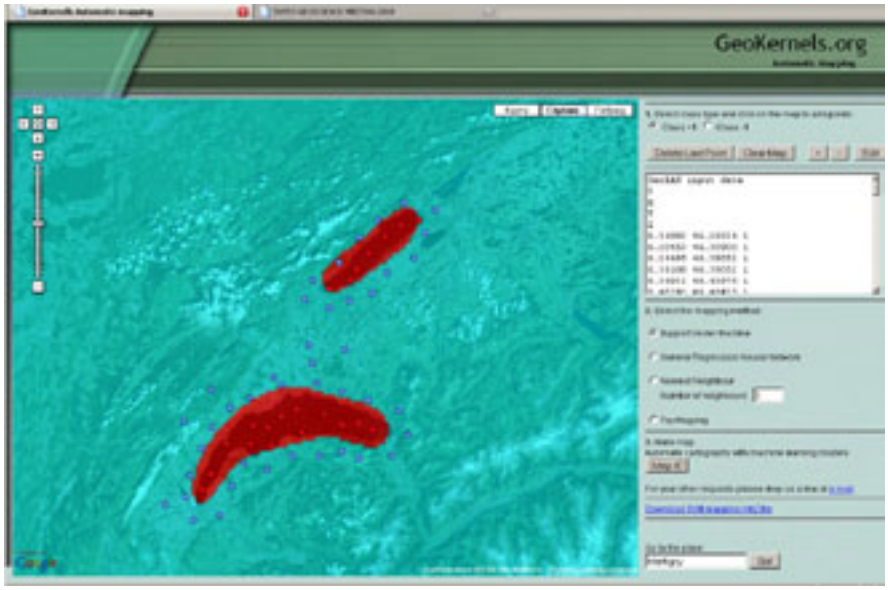

Figure 2. Result of a binary classification task using an interactive SVM model.

12.17

New coordinates for Switzerland: Completion of the Swiss national triangular transformation network for precise transformations between the old reference frame LV03, the new LV95 and global ones like ETRF

Kistler Matthias, Brockmann Elmar, Marti Urs, Métraux Cédric, Papafitsorou Ageliki, Ray Jérôme, Schlatter Andreas, Vogel Bruno, Wiget Adrian and Wild Urs.

swisstopo, Seftigenstrasse 264, 3084 Wabern
matthias.kistler@swisstopo.ch

The year of 2007 saw the completion of a basic geographical data-set of the greatest importance for the establishment of the national spatial data infrastructure SDI, the national triangular transformation network. This new data-set permits the elimination of the systematic deformations resulting from the first Federal survey of Switzerland completed in 1903 which reached a maximum of 2 to 3 m as well as the local distortions from the cadastre survey on the cantonal level.
Switzerland was subdivided into almost 12'000 triangles, each having its own affine transformation parameters matched to local conditions. In addition, to prove the accuracy of the transformation, the cantonal authorities have measured almost 50 000 control points. The results were excellent: on average, geographical data in Switzerland can now be transformed into the new, error-free LV95 reference frame or in a global one like ETRF with an accuracy of 3 cm.
The national triangular transformation network will also be implemented in the Swiss Positioning Service swipos as a new real-time option with GPS correction as well as "old reference frame adaptation": GPS users, who have to work in the old, for many applications still valid LV03 datum, can so position or measure with an accuracy of a few centimetres without establishing a local fit. Furthermore a new software REFRAME including all relevant transformations (position / height) and the geoid undulations for Switzerland was released as client version as well as web service. The accuracy of the transformation can be accessed through a web GIS application for everywhere in Switzerland.
It is foreseen, that the new reference frame LV95 will be introduced for all geobasis data regulated by federal law by 2016 at the latest.

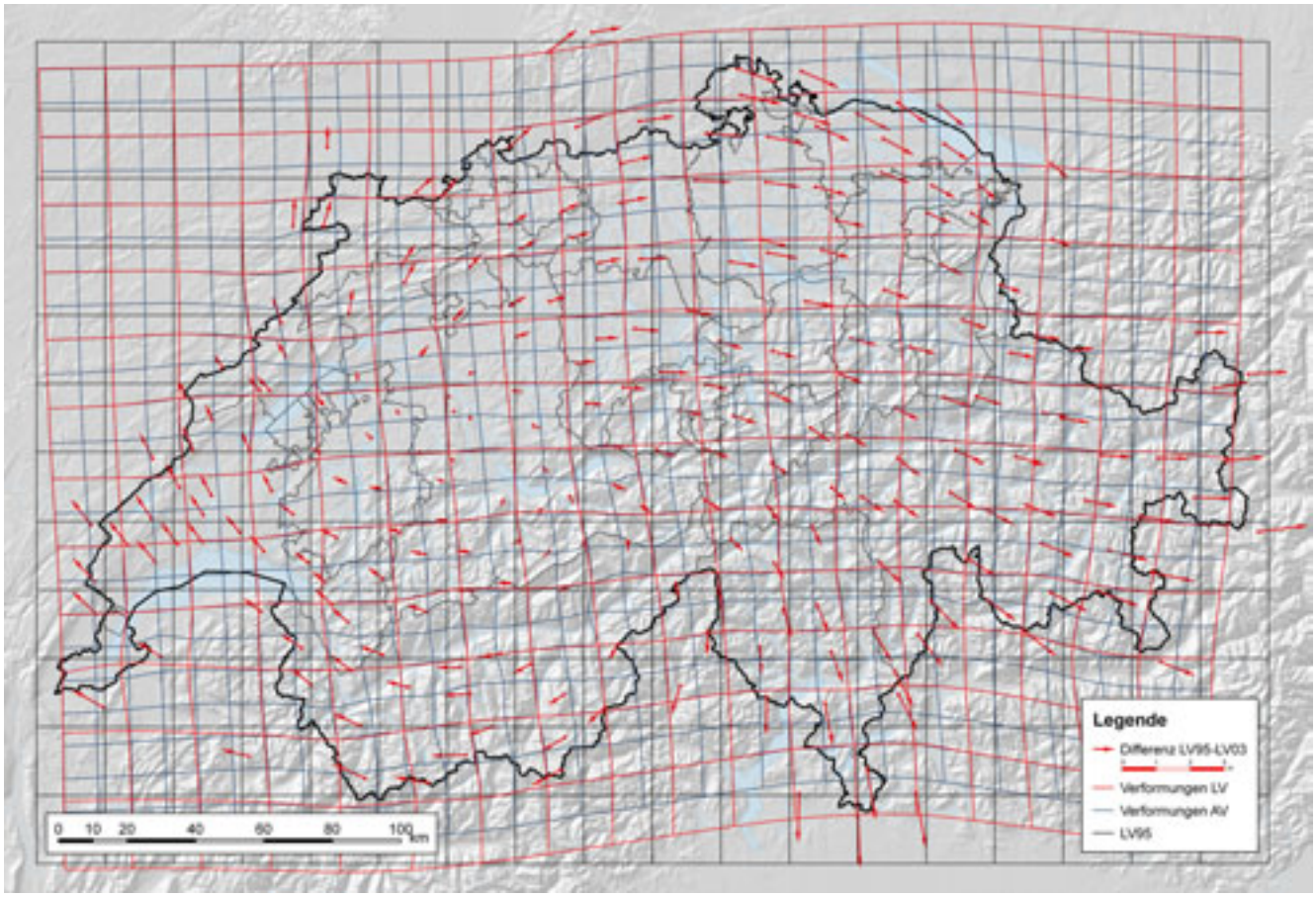

Deformations of the reference frame of 1903 still in use today (LV03 = red grid with the deformations from the national survey and the blue grid including also the local distortions from the cadastre level) compared to the new Swiss reference frame of 1995 (LV95 = black grid). The red arrows point from LV03 (red) to LV95 (black) and thus also the direction and amount of the local deformation.

REFERENCES

Balmer, W., Dräyer Relling S. (2005). Wechsel des Bezugsrahmens LV03 ' LV95: Standortbestimmung für die Geodaten von swisstopo im Hinblick auf ein Konzept für die Verwaltung von Produkten in den Bezugsrahmen LV95 und LV03. Interner Report swisstopo.

Jenny, B., Weber, A. and Hurni, L. (2007). Visualising the planimetric accuracy of historical maps with MapAnalyst. Cartographica, 42-1, p. 89-94.

Kistler, M., Papafitsorou, A., Marti, U., Ray, J., Vogel, B., Wild, U. and Métraux, C. (2007). Completion of the Swiss National triangular transformation network: Precise transformation between the old reference frame LV03, the new LV95 and global frames. Swiss National Report of Geodetic Activities in the years 2003 to 2007, Swiss Geodetic Commission, p. 17-20.

Kistler, M., Ray, J. (2007): Neue Koordinaten für die Schweiz: Fertigstellung der nationalen Dreiecksvermaschung, neue Transformations-Software REFRAME und Eröffnung des Internet-Portals "Bezugsrahmenwechsel". Geomatik Schweiz 9 / 2007, p. 432-437.

Marti, U., Nocera R. (2003). Fineltra: Affine Transformation von Lagekoordinaten und Umrechnung von LV03 in LV95 und umgekehrt. swisstopo Manual 06-d.

Ray, J., Marti U. (2007): Reframe - Bezugsrahmenwechsel in Lage und/oder Höhe. swisstopo Manual 07-d.

Ray, J., Marti U. (2007): Fineltra-Lite: Affine Transformation von Lagekoordinaten und Umrechnung von LV03 in LV95 und umgekehrt. swisstopo Manual 06b-d

swisstopo (2006). Neue Koordinaten für die Schweiz: Der Bezugsrahmen LV95. Informationsbroschüre.

swisstopo - Eidg. Vermessungsdirektion (2007): Überführung der amtlichen Vermessung in den Bezugsrahmen der Landesvermessung 1995 (LV95): Konzept.

12.18

The National Gravity Network of Switzerland

Urs Marti

Federal Office of Topography swisstopo, Geodesy, Seftigenstrasse 264, CH-3084 Wabern (urs.marti@swisstopo.ch)

In 2003, a project LSN2004 (Landesschwerenetz 2004) was started by swisstopo to modernize the national gravity network of Switzerland. This new network is based on the existing gravity network of 1995 and is connected to several stations of the European gravity network UEGN. In this project, 4 new absolute stations were established and some existing ones were re-measured with the FG5 absolute meter of the Federal Office of Metrology (Metas). So today, the Swiss absolute (zero order) gravity network consists of about 15 stations, which are mostly located in stable buildings and far away from traffic and ground water zones.

In order to improve the accuracy and stability of the network, additional high precision relative measurements between the absolute stations are performed with SCINTREX-CG5 gravity meters in collaboration with the University of Lausanne and ETH Zurich. With repeated observations, the accuracy of LSN2004 should also allow the first determination of gravity changes and derived vertical movements in Switzerland.

The densification of the zero order network (1st and 2nd order network) is performed by relative measurements on stable levelling and GPS benchmarks. This network consists of about 120 stations.

Based on this national gravity network (LSN), the detailed observations are performed. One data set of more than 5000 points is located along the national levelling lines and is used for the reduction of levelling observations and the determination of rigorous orthometric heights.

The second important detailed data set of more than 32'000 points was collected and re-processed by the Swiss Geophysical Commission and the University of Lausanne. It covers the whole country and is presented in the form of 1:100'000 gravity anomaly maps. This data set is a very important contribution to the determination of the Swiss geoid model and is used for geophysical and geological interpretation.

The poster shows the concepts of LSN2004, presents the observations performed so far and gives an overview of the available gravity measurements in and around Switzerland.

Figure 1. Absolute gravity stations in and around Switzerland.

12.19

COLTOP 3D: A software dedicated to analyze relief using large DEM and massive 3D-imaging cloud points

Metzger Richard, Jaboyedoff Michel & Oppikofer Thierry

Institute of Geomatics and Risk Analysis , University of Lausanne, 1015 Lausanne (richard.metzger@unil.ch)

The increasing precision of ground-based Lidar technologies makes possible to perform more detailed systematic structural and morphological analyses than ever reached before. Using the orientation of each single collected vertex, a point cloud data set can be represented by a 3D image where each single point has a color defined by the local dip and strike direction, which allows a very simple slope analysis. This can also be applied to any surface reconstructed through the data set, making the detection of planar structures within a cliff, i.e. in the presence of overhangs, possible, which is not with classical 2D digital elevation models. Such simple analyses applied to 3D clouds of points make it possible to quickly identify structural features affecting topography. They open new perspectives in relief analysis. This paper describes the basis (kernel) of a software (Coltop-3D) which is dedicated to perform these tasks.

More specifically, the paper will focus on:

1. data organisation and management, as terrestrial laser scanners allow for capturing dense 3-dimensionnal data set (up to millions of points) on the surface of an object, within a few minuts. Without such organisation , the post-treatment and the standard operating use of such large data set may impair an in-depth analysis for specific applications, such as landslide and rockfall analysis.

2. dip and strike direction estimation from raw data points. Numerous work have pinpointed that eigenanalysis of the covariance matrix of a local neighborhood can be used to estimate local surface properties, and hence the normal. Once the normal is known, it is straightforward to compute the dip and strike direction. Moreover, it will be shown that eigenanalysis may be used to semi-automatically remove folliage from data sets.

A case study (Hegguraksla cliff site, located in the Norway) will also be presented.

12.20

A GIS approach for tsunami risk assessment

Monia Molinari*, Massimiliano Cannata*

**Institute of Earth Sciences – SUPSI, Trevano, C.P 72, CH-6952 Canobbio*

The tragic event of Sumatra brought to the international attention a natural phenomenon that is well known by most inhabitants of coastal areas: the tsunami. During the event of the 26th December 2004, a series of unusual high waves, up to 15 m, hit the coastal regions of Indonesia, Sri-Lanka, India, Thailand, Bangladesh, Maldives, Somalia and Kenya causing over 230˙000 victims.
Although these natural disasters cannot be avoided, their effects, such fatalities or damage to property, can be reduced through preventive and adequate protection measures. With respect to this goal the availability of flood risk maps would certainly help to foster the development of mitigation measures.
For this reason a procedure that enable GIS users to conduct tsunami risk assessment by means of a series of GRASS scripts that implement the approach proposed in Federici et al. (2006) and validated in Cannata et al. (2007) was created.
This procedure allows to assess the maximum vertical height of the tsunami wave at the coast (run-up) and the subsequent inundation on the mainland. The procedure takes into account local morphological characteristics, vegetation and urbanization through the usage of a digital terrain model, landuse, and cadastre map.
This presentation illustrates the procedure through a case study located in Olbia, a Mediterranean city on the Sardinia island's east coast.

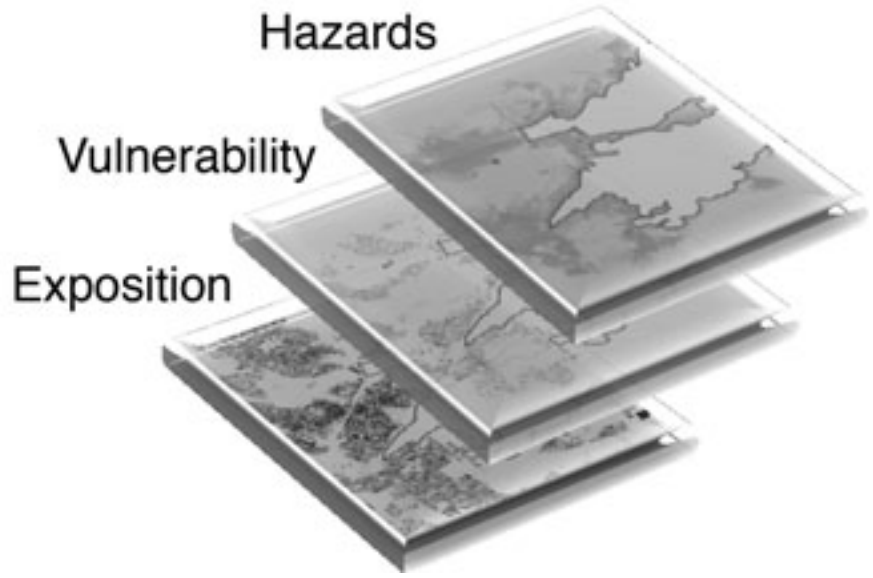

Figure 4. Steps of the tsunami risk assessment and respective maps.

REFERENCES

Cannata, M., Federici, B. & Molinari, M. 2007: Mappe di inondazione dovute a tsunami mediante il gis grass: applicazione all'isola di St. Lucia, Caraibi, proceedings of VIII Italian GRASS user meeting, Palermo, Italy.

Federici, B. & Cosso, T. 2006: Tsunami inundation maps and damage sceneries through the GIS GRASS, proceedings of FOSS4G2006, Lausanne, Switzerland.

12.21

The Geological Information System Switzerland

Oesterling Nils*, Kühni Andreas*, Kündig Rainer**

Swiss Geological Survey, Federal Office of Topography swisstopo, Seftigenstrasse 264, CH-3084 Wabern (nils.oesterling@swisstopo.ch)
***Swiss Geotechnical Commission, ETH-Zürich CAB E77, Universitätstrasse 6, 8092 Zürich*

Geological information is of great importance for society because it is implied in a large number of products of our everyday life. Traffic constructions like roads and railway tunnels and the supply with fossil energy resources are only the most obvious products for which geological know-how is crucial. But even common products like toothpaste and cat litter would not exist without geological information and knowledge.

For a wide range of disciplines in the geo-sciences geological information is an important basis for decision-making processes. For instance, information on the stability of bedrock and superficial deposits is essential for choosing specific building sites for houses, tunnels, etc. Questions concerning the search for radioactive waste disposal sites can only be answered with the help of geological data and information. Furthermore geological data supply basic information for the preparation of natural hazard maps, a topic, which is becoming increasingly import in recent years (e.g. extreme flooding of Swiss rivers in the summer of 2005 and rock fall directly striking a car on the Gotthard Highway (A6) in 2006).

To be able to address the challenges of the modern society described above, it is essential that geological information is easy accessible. Recent developments and advancements of IT-technologies like the Internet, GIS, Web-Services, etc. enables us to distribute and exchange the required information in an interoperable way, so that everyone who need information, can use it easily.

Like some other Geological Surveys, the British Geological Survey (BGS) for instance, gives numerous examples for applica-

tions of their geological data, its respective importance and how data and services can be presented and distributed via the internet (cf. http://www.bgs.ac.uk/britainbeneath/; http://www.bgs.ac.uk/ services/home.html). The accessibility of data is easy and in many cases free of charge and the relevance and importance of such data is easy understandable for professionals and laymen.

Compared to the UK, geological information in Switzerland is only poorly accessible. This is on the one hand, because complete geological coverage of Switzerland on the detail scale is not achieved yet, and on the other hand, because geological investigations and its coordination in Switzerland are carried out by a large number of institutions (e.g. Platform Geosciences of the Swiss Academy of Natural Sciences (scnat), Swiss Geological Survey (SGS), Swiss Geotechnical Commission (SGTK), Swiss Geophysical Commission (SGPK), Geological Institutes of Swiss universities, and different other organisations). As a consequence tasks and responsibilities of the different institutions are often not clearly visible and access to existing geological data and services is difficult. Restricted communication between the players of the "Geo-Scene" and missing coordination of activities enhances this problem.

To overcome the problems mentioned above, the development of an Information System for Geology in Switzerland is intended. Such a centralised, web based information system not just makes the existing geological and geo-scientific datasets and services available, but also gives an overview of the Geo-Scene Switzerland and its national and international organisational integration. Furthermore, geological terms and selected sites of the swiss geology (e.g. Glarner Hauptüberschiebung at Lochseite, Schwanden, Glarus) are described and presented for non-professionals.

As part of the National Spatial Data Infrastructure of Switzerland (NSDI) the Geological Information System is thought to be the gateway to geo-sciences in general and to geological sciences in Switzerland in particular.

The primary objectives of such an information system are:

- Make existing geological data available and web accessible
- Visualise the organisational integration of the players of the swiss Geo-Scene
- Develop a centralised information-platform for professionals, semi-professionals and laymen
- Strengthen the public awareness of geology and geo-sciences in Switzerland

12.22

GIS helps water resources management

Fabio Oliosi*, Stéphane Storelli**

** ESRI Géoinformatique SA, rte du Cordon, 7 1260 Nyon, Switzerland (F.Oliosi@ESRI-Suisse.ch)*
*** Centre de Recherches Energétiques et Municipales (CREM), Rue des Morasses 5, CH-1920 MARTIGNY (stephane.storelli@crem.ch)*

In Alpine regions like in other areas around the world, local administrations (communes) have the duty to manage water resources and distribution. The quality, the available quantity and the cost of water may vary spatially, from valley to valley and from village to village. Very often, when big differences exist, a waste of this precious resource may occur along the distribution channel. Web GIS technology may help to share geographic knowledge and improve water cycle management.
With a financial aid of the Swiss Confederation[1], a group of private firms, public administrations and universities are currently carrying out a project on Integrated Municipal Facilities Management of Water Resources (SyGEMe), in western Switzerland.
SyGEMe's goal is to build up a common IT infrastructure and web services to support small water network managers. GIS is the best platform to carry out specific analysis over a bigger water basin and helps managers to synchronize their actions on the network.
This paper presents some interesting aspects of this project and emphasizes the role of GIS.

REFERENCES

Gianella, S. (2005). Strategisches Informationsmanagement für die Abwasserentsorgung. Dissertation ETH Zürich Nr. 16045: Eidgenössische Technische Hochschule Zürich.

Gianella, S., Gujer, W. (2006a). Improving the information governance of public utilities through an organizational knowledge base. Paper accepted for: WCEAM 2006: First World Congress on Engineering Asset Management, 11-14 July 2006, Gold Coast, Australia.

Gianella, S., Gujer, W. (2006b). Modeling critical knowledge for information governance in public wastewater utilities. Paper accepted for: HIC 06: 7th International Conference on Hydroinformatics, 4-8 September 2006, Nice, France.

Storelli, S. (2005). Exploitation et maintenance des réseaux urbains. GWA Nr. 12/2005 pag.969-974.

[1]KTI/CTI, Office federal de la formation professionnelle et de la technologie, Effingerstrasse 27, 3003 Berne, Switzerland

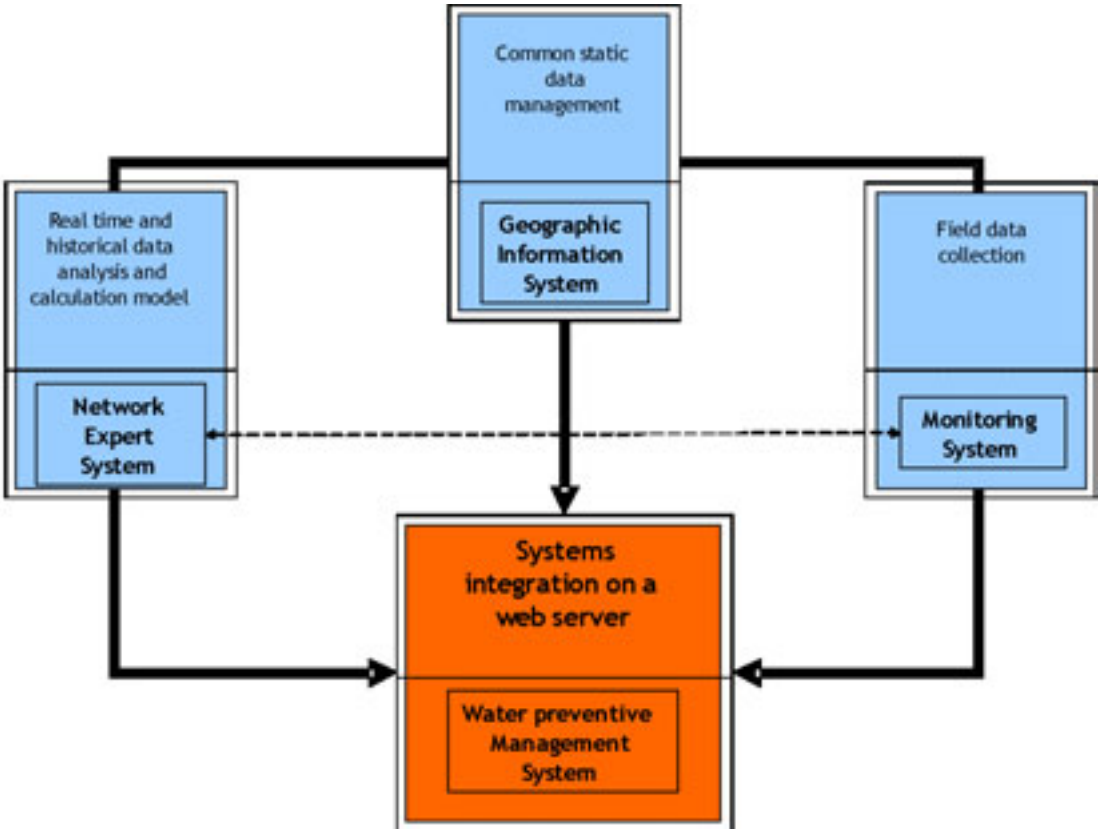

Figure 1. SyGEMe main related components

12.23

The geotype concept to develop GIS oriented analysis in engineering geology applications

Parriaux Aurèle*, Turberg Pascal*, Kalbermatten Michael**, Golay François**, Lance Jean-Marc

* *Laboratoire de géologie de l'ingénieur et de l'environnement, Ecole Polytechnique Fédérale de Lausanne, Ecublens, CH-1015 Lausanne (pascal.turberg@epfl.ch)*
** *Laboratoire de systèmes d'information géographique, Ecole Polytechnique Fédérale de Lausanne, Ecublens, CH-1015 Lausanne*
***Etablissement d'assurance contre l'incendie et les éléments naturels du Canton de Vaud, Avenue Général Guisan 56, CH-1009 Pully*

In territorial projects where geological information and GISs are coupled to perform spatial analysis, an explicit definition of geological descriptors is required. Thus, a conceptual model of the geological diversity has to be set up, according to the goal of the project, to differentiate the relevant units of the underground.
Here, a conceptual model of the geology for the canton of Vaud, Switzerland, is proposed. This model basically adapts the information of the Swiss geological atlas. It is composed of 41 geological units called "geotypes". Twenty of them are used to define hard rocks, principally on petrographical considerations, and the last 21 define quaternary deposits essentially on sedimentological criteria. The principles, requirements, conditions and objectives of this model are discussed.
This geotype model was applied to map the foundation soils all over the canton of Vaud (3200 km^2) in the frame of its seismic microzoning. This large scale cartographic project, where different contractors worked in parallel, was associated to a GIS concept specifically designed for the geotype model. This GIS concept is explained.
We describe why this combined geological-GIS method was necessary during the realization phase of the project, how it significantly enhanced the overall capacity of spatial analysis and in which way data maintenance will be simplified.

Main results from this case study are pointed out and discussed:

- Realization of the first synthetic geotype map of the canton of Vaud (figure 1) and associated map of foundation soils;
- Geological consistency between maps realised by different authors;
- Transparency and traceability of the successive data processing operations, from raw geological information to end products;
- Valorisation of the geological information to be combined in the future to other territorial information through GIS (e.g. digital elevation models (DEMs), comprehensive development area maps, geological cadastre).
- GIS capacity for easy re-actualization of maps.

Adaptations of this method to other geological environments or for other engineering projects (natural hazards, groundwater protection) are ongoing developments.

REFERENCES

Parriaux, A., Turberg, P. 2007: Les géotypes pour une représentation géologique du territoire. Tracés, 15/16, 11-17.

Parriaux, A., Turberg, P., Lance, J.-M., Giorgis, D. 2007: La méthode des geotypes pour le microzonage sismique. Tracés, 15/16, 19-24.

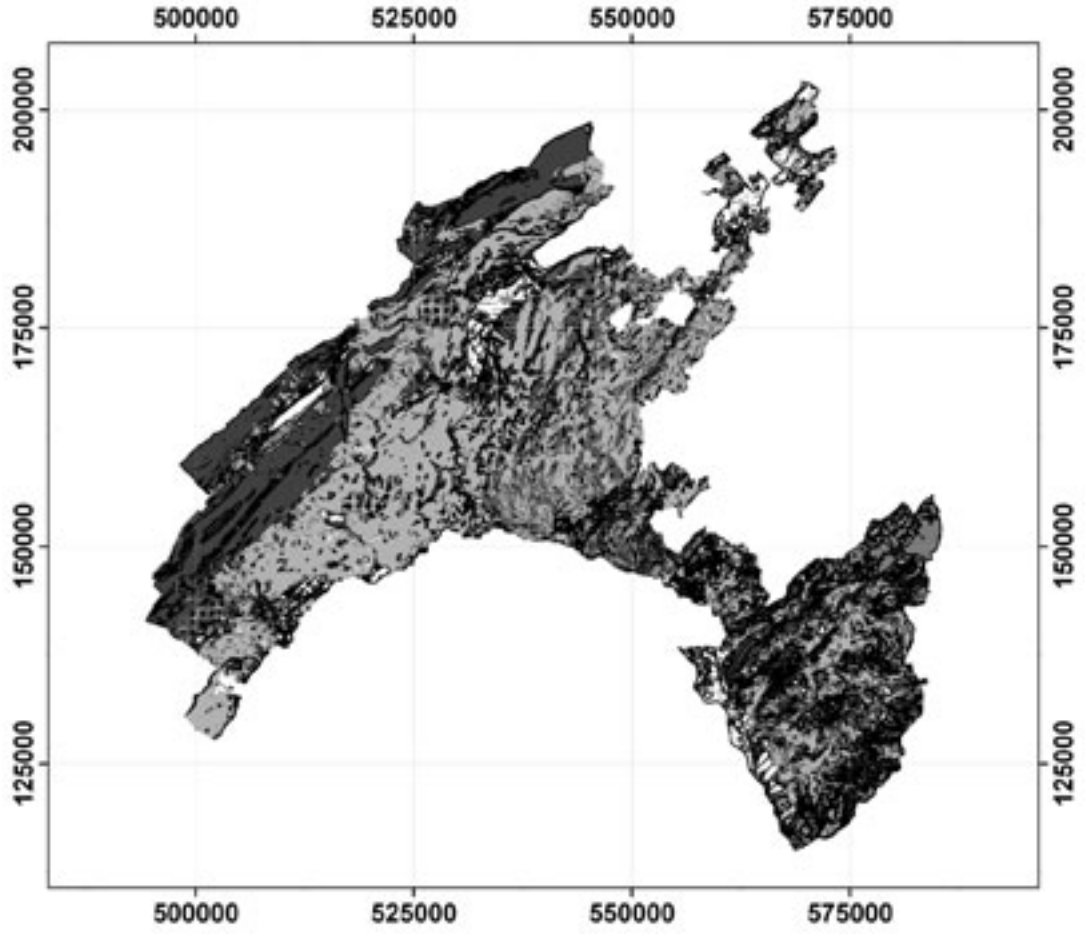

Figure 1: First ever synthetic representation of the geological conditions over the whole surface of the canton of Vaud, Switzerland, according to the geotype method described in this paper.

12.24

Hydrogeology and geochemical characteristics of groundwater in a porous aquifer connected with two karst systems, in Southern Switzerland.

Sebastián Pera*

Istituto Scienze della Terra, Via Trevano, CH-6952 Canobbio

Groundwater origin and hydrogeological processes strongly affects geochemical evolution of water within the aquifers. Because of that several studies uses major ion geochemistry as tracers giving insights on groundwater flow processes. This methodology has been applied successfully in different hydrogeological contexts (Grassiand and Cortecci, 2005; Dafny et al, 2006; Wang et al, 2006;).

The Laveggio aquifer, located in southern Switzerland, is an important source of drinking and industrial water for the Mendrisiotto district. Constituted by glacial and fluvioglacial deposits, it fills a valley developed over an important structural feature: the Lugano Line (IGIC, 1989). The aquifer, discharging to the Lugano lake is laterally limited by two important karst systems: The Monte Generoso and The Monte San Giorgio basins. Due to the structural evolution of the area the two karst systems have distinctive characteristics, the Monte Generoso Basin constituted mainly by limestones outcorps while in the San Giorgio basin dolomites are present (Bernoulli, 1964).

Several monitoring campaigns were carried out by the public authorities in order to acquire information about the quality of groundwater. 17 wells were sampled during several years and samples analyzed for major elements, pH, temperature, conductivity and some organic pollutants.

In this work geochemical data was directly interpreted and spatially represented by using a geographic information system (GIS). We used the results of the chemical analysis to study the hydrodynamic of the aquifer and the relationship with the karst systems.

Figure 1. showing Laveggio aquifer and rsampling stations.

REFERENCES
Bernoulli, D. 1964: Zur Geologie des Monte Generoso (Lombardische Alpen), Kommission bei Kümmerly & Frey AG, Geographischer Verlag, Bern 134 pages.
E. Dafny, A. Burg and H. Gvirtzman, 2006: Deduction of groundwater flow regime in a basaltic aquifer using geochemical and isotopic data: The Golan Heights, Israel case study, Journal of Hydrology Volume 330, Issues 3-4, Pages 506-524.
Grassiand S. Cortecci G, 2005: Hydrogeology and geochemistry of the multilayered confined aquifer of the Pisa plain (Tuscany – central Italy), Applied Geochemistry Volume 20, Issue 1, Pages 41-54
IGIC, 1989: Modello Falda Laveggio. unpublished report, Istituto Geologico ed Idrologico Cantonale – Canton Ticino, Switzerland.
Wang, Y. Guo, Q. Su, C. Ma, T. 2006: Strontium isotope characterization and major ion geochemistry of karst water flow, Shentou, northern China, Journal of Hydrology Volume 328, Issues 3-4.

12.25

GIS modelling: a first step toward 3D geology with the "Sion" map

Sartori Mario *, Ornstein Pascal* , Schreiber Lucien* and Jemelin Laurent**

*CREALP – Research center on alpine environment, Industrie 45, CH-1951 Sion (mario.sartori@terre.unige.ch)
** Swiss Geological Survey, Federal Office of Topography swisstopo, Seftigenstrasse 264, CH-3084 Wabern

Problematic.- How to optimize the geologic field mapping and the data processing to produce a consistent GIS geological model of the territory optimized for spatial analysis? What are the additional data and interpretations needed to make this GIS model useful for subsequent 3D developments? What are the constraints for placing the GIS model at the center of a Swiss geological data storage system?

Aim of the "Sion" project.- This long-term project is based on collaboration between the Crealp and the Swiss Geological Survey for the achievement of the geological cover of the Valais territory, a priority task for natural hazards management. New methods and new tools are tested as part of the geological mapping and GIS modelling of the Sion sheet (Geological Atlas of Switzerland 1:25'000). The aim is also to allow the geologist cartographer to build from its analogical and digital field data a GIS project fully compatible with a global geological information system.

Constraints.- The GIS project has to be fully compatible with the Swiss Geological Survey Data Model and to reach a perfect topological consistency. The GIS model also has to allow the export of data toward the Swisstopo cartographicclassically editing process in order to produce classical analogical maps without loss of quality.

"Sion" Methodology.- In comparison with a classically edited geological map, this method needs more interpretation from the authors in order to build (where possible) separated bedrock and drifts layers in a "2.5D" model, a necessary step toward future 3D analysis abilities. The Data Model of the GIS should be defined before- and refined during- the field acquisition. The editing of the data in the GIS follows a construction technique solving the problems of superposition of lines and polygons edges shared by several layers. Only polyline- and point-type layers are used to edit the topology of the objects. Besides defining the objects and their attributes, it is necessary to attribute all the lines after their semantic significance (often multiple). The whole spatial model, including polygon-type layers, is finally derived from these construction layers.

Specific geological GIS software.- The implementation of the "Sion" method could be problematic without a specifical GIS tool able to manage the complex Data Base, the full attribution of lines and objects, so as to make topological and semantic validations. ToolMap is an open-source, cross-platform (Windows, Linux, Mac) software developed by CREALP and Swisstopo. Data Base management and GIS edition functions are specifically designed to create a GIS project from the geological data according to the "Sion" Method.

Results.- Feasibility of placing GIS modelling at the center of the Geological Atlas production process is presently tested with the "Sion" sheet. New potentials in term of geotechnical and hydrogeological analysis are provided thanks to the integrated tectonic sketch making possible to define in any point the nature of the bedrock, proven or supposed. Later steps toward 3D modelling would be possible if data on drifts thickness are available. The Data Base management of such a GIS model is complex, but it will be highly simplified by the use of ToolMap. This complexity stimulates in the other hand homogenization between adjacent sheets through semantic clarification of objects definition and through stratigraphical and tectonic revisions.

12.26

ToolMap – 'SION' method: development of a new GIS Framework for digital geological mapping

Schreiber Lucien*, Ornstein Pascal*, Sartori Mario*, Kuehni Andreas**

*CREALP – Research center on alpine environment, Industrie 45, CH-1951 Sion (lucien.schreiber@crealp.vs.ch)
** Swiss Geological Survey / Federal Office of Topography (Swisstopo)*

With the constant development and the spreading of use of information systems as well as modelling, analysing and visualisation tools, the need for digital data is increasingly growing. During the last few years, this trend was strongly marked in geosciences especially in fields such as engineering geology and geological mapping.
Classically, a geological map gives a 2-D modelling of a complex 3-D environment. Mapped entities are defined by i) a collection of geologic features which carry a geometry (point, line, polygon) in association with numerous descriptive attributes (e.g. lithological, chronological, structural, morphological ones) and ii) the relationships between these objects. Handling information required to build digital geological maps implies of first analysing and extracting semantic content of the geologic objects and of identifying their spatial relationships.
Since a few years, CREALP has developed, in close collaboration with the Swiss Geological Survey (SGS), the 'SION' method, an innovative approach for implementing geological maps in digital format using GIS technology. This methodology aims at providing a consistent geological GIS fulfilling a number of strong requirements like:

- Storing and modelling geological objects in an exhaustive and accurate way through a robust data model
- distributing the geologic features in relevant layers according to their geological meaning
- developing an efficient method for geometrical construction of the digital map solving issues related to superposition of objects associated with multiple layers.
- implementing a data model offering powerful capabilities of analysis (spatial and non-spatial).

As a natural extension of this technique, CREALP launched in 2006 the development of ToolMap a standalone software program that fully implements the principles that underlie the method. ToolMap provides tools that abstract, organize and transform field data to the relevant digital datasets used to generate the digital geological map and derived geothematic maps. This is achieved through the integration in ToolMap of i) a versatile relational database that allows the handling of geospatial data (geometry and attributes) with various levels of complexity and ii) a GIS engine with the associated tools for editing, geoprocessing and validating data (topological and semantic rules).

This open-source and cross-platform (Windows, Linux, Mac) software is actually developed in coordination with the SGS in the framework of the production of maps of the Geological Atlas of Switzerland at 1:25 000 scale (GA25). The Beta version was recently tested for successfully implementing the new geological data model that underlies the geological information system of Switzerland being developed by the SGS.

Although initially dedicated to digital geological mapping, ToolMap is very suitable for handling other types of data because of its open design and its comprehensive functionalities.

ToolMap and its built-in concept offer a new technical framework for a full integration of GIS technology into the geological map production cycle (fig. 1). The close combination of a step-by-step process and dedicated tools is a pledge for ensuring constant quality and consistency in the production of digital geological maps. This GIS-centred approach offers the ability for the geologist to enhance field data acquisition and map accuracy by combining, at each stage of geological mapping, geological data with other geo-spatial datasets such as DEM, digital orthophotos, multi-scale topographic maps.
This way, geological surveys and geoscientists can increase use and usability of their data by providing more powerful digital cartographic products especially in terms of spatial analysis and geological data management.

REFERENCES

Sartori, M., Ornstein, P., Métraux, C., Schreiber, L. & Kuehni A. 2006: From geological cartography to digital maps : spatial data model and GIS tool. ECONGEO 2006, Barcelona, proceedings, vol. II 189-191.

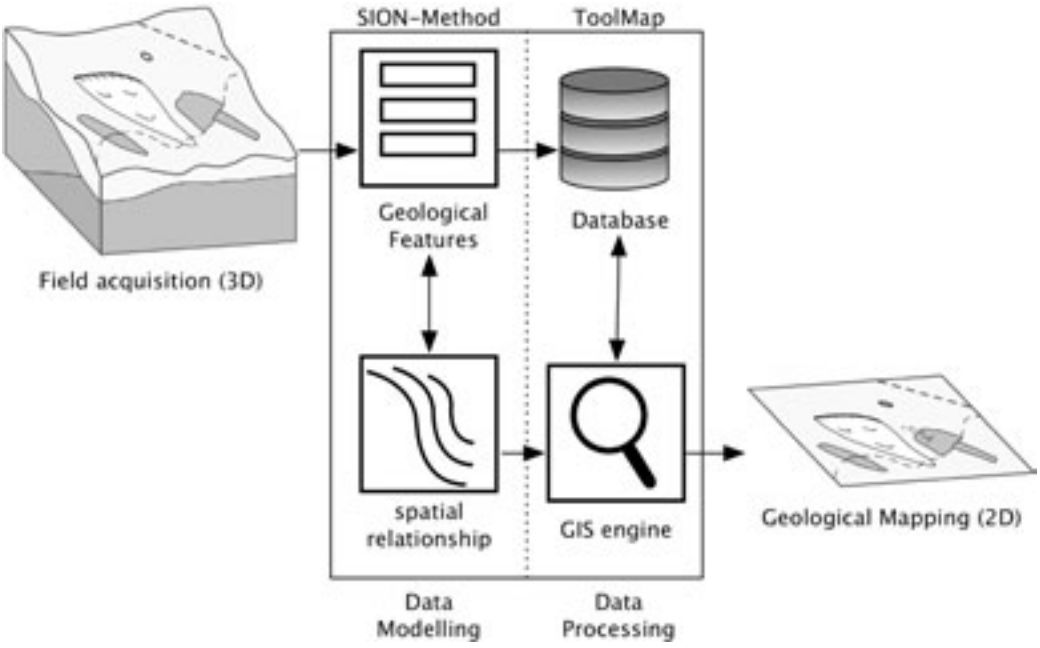

Figure 1. GIS Framework for digital geological mapping consisting of two components: the SION-Method and TOOLMAP software

12.27

Real-Time Mapping and Monitoring Capability of Geological Features by Airborne Laser Scanning

Jan Skaloud*, Philipp Schaer*, Phillip Tomé**, Yannick Stebler*

*EPFL-TOPO, Station 18, CH-1015 Lausanne (jan.skaloud@epfl.ch)
**Nemerix, PO Box 425, CH-6928 Manno (philip.tome@nemerix.ch)

The amount of unstable rock in the Alps is expanding with the retreat of glaciers. The terrestrial 3-D laser scanning has become a standard technique to monitor movement of some of them. For instance, the Northern wall of Eiger has been monitored by means of a commercial device placed on the opposite side of the valley. However, the area of rock movement that can be monitored by this approach is limited in size by a) the characteristics of the neighbouring relief; b) the accessibility of the monitoring side; c) the ranging attributes of the scanner. The nature of Alps is such that these limits are exceeded in many zones of natural hazards related to the slope movement.

We present a rapid way of obtaining the 3D laser point cloud for the purpose of monitoring by means of Airborne Laser Scanning (ALS). The ALS technology is well established in generating Digital Surface Models (DSM) and Digital Terrain Models (DTM) over larger surfaces. However, the traditional ALS is not suitable for mapping steep terrain or cliffs. Also, the monitoring capabilities of this technology are limited by the lapse of time between data acquisition and data processing. Such delay is related to the trajectory evaluation as well as to the amount of data produced by the airborne scanner. Depending on the nature of the work and the system used, it can take from hours to days to generate the 3D laser point cloud after the flight execution. We introduce an ALS system that drops all these inconveniences.

The Scan2map system has been under development at EPFL with various partners over the last decade (Fig.1). It combines GPS, INS, ALS and a medium format digital camera in one solid mount which can be used in nadir or oblique configuration during the same flight; hereby allowing mapping horizontal (valley bottoms) and vertical features (cliffs) while maintaining optimal geometry between the scanner and the mapped object. More recently, the functionality of the Scan2map has been extended 1) to improve the monitoring of the scanning progress (Fig. 2); 2) to generate the 3D laser point cloud in real-time (Fig.3); 3) to analyze the quality of the point cloud within the flight. If the communication between the on-board and reference GPS receivers is established, the accuracy of the real-time generated point cloud is obtained at cm-level and corresponds to that of post-processing. The resulting data are then ready to be fed to movement/deformation analysis tools as in the case of 3D terrestrial laser scanning.

The paper presents the system concept and characteristics, the strategy adopted for data processing and communication as well as results from actual missions.

Figure 1. Handheld mapping system (Scan2map) installed in a helicopter.

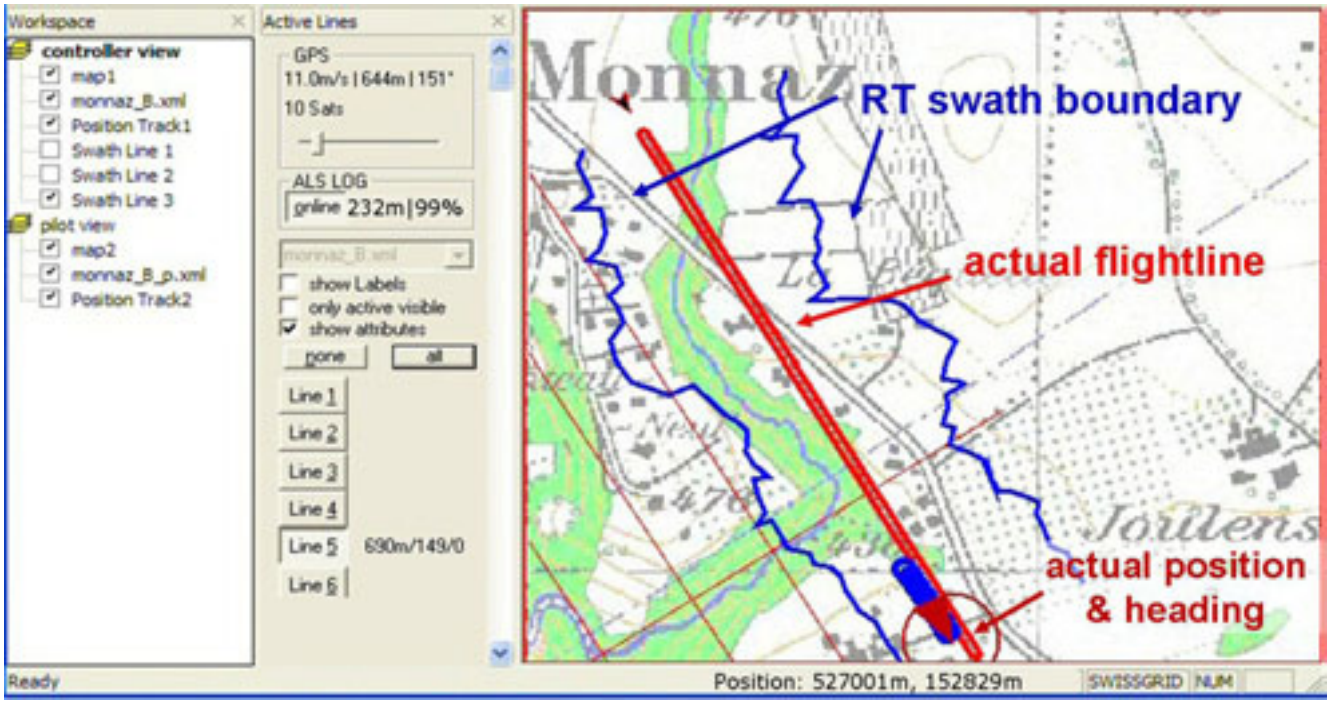

Figure 2. Overview of main functionalities of the flight management interface.

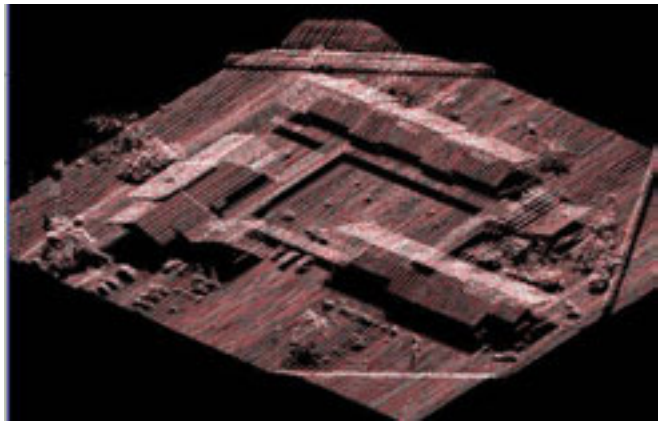

Figure 3. Laser point cloud generated in real-time with cm-level accuracy.

12.28

Estimation of local tectonic movements using continuous GNSS network

Villiger Arturo*, Heller Oliver*, Geiger Alain *, Kahle Hans-Gert*, Brockmann Elmar**

*Geodesy and Geodynamics Lab, Institute of Geodesy and Photogrammetry, ETH Zürich (arturo.villiger@geod.baug.ethz.ch)
**Swisstopo

The objective of project TECVAL is to assess local crustal movements with modern geodetic techniques in an area north of the Rhône valley extending from Martigny to Raron. Although the Valais is a region of relatively high seismic activity within Switzerland, the deformation rates reveal small amounts only. Nevertheless, the main challenge is to detect these movements by GPS at a high level of significance.

The stations for the evaluated network are part of the Automated GPS Network (AGNES), operated by Swisstopo, or built up for this project and run by ETHZ. In order to determine movements relative to the Eurasian plate and to assess a new rotation pole the network includes European stations from IGS and RGN. The relative time series are evaluated in a local topocentric coordinate system. Due to the small tectonic velocities seasonal and other disturbing effects have to be taken into account. To this end the time series have to be available for at least a few years. To determine the velocities from time series a robust estimator has been used. This approach significantly reduces the influence of outliers. After the robust elimination of outliers the final velocity is determined by a least square estimation.

In order to verify the achieved results in this area the uplift can be compared to a model calculated from levelling measurements.

13. Global change – lessons from the geological past

Helmut Weissert, Peter O. Baumgartner

13.1

Impacts, volcanism, sea-level and climate fluctuations: towards a multi-causal scenario for the Phanerozoic extinctions, a lesson from the Past

Adatte Thierry

Institut de Géologie et Paléeontologie, Anthropôle, Université de Lausanne, 1015 Lausanne, Suisse

Mass extinctions in the Phanerozoic are closely related with severe climate changes and sea-level fluctuations. The consistent association of large magmatic provinces (LIPs and CFBPs) with all but one (end-Ordovician) of the five major Phanerozoic mass extinctions suggests that volcanism played a major role. Faunal and geochemical evidence from the end-Permian, end-Devonian, end-Cretaceous and Triassic/Jurassic transition suggests that the biotic stress was due to a lethal combination of tectonically induced hydrothermal and volcanic processes, leading to eutrophication in the oceans, global warming, sea level transgression and ocean anoxia. It must be concluded that major magmatic events and their long-term environmental consequences are major contributors, though not the sole causes of mass extinctions. Sudden mass extinctions, such as at the K/T boundary, may require the coincidence of major volcanism and a very large impact. Mass extinction is therefore the culmination of many factors which contributed to high-stress environmental conditions, including longterm perturbations (volcanism, e.g. Deccan traps for the end-Cretaceous, cooling, sea-level fluctuations) and short terms events (impacts). No single kill mechanism can really be identified. Whether studies into Earths oceans and climate change are conducted in the present or the past, they remain of fundamental importance in predicting the future. A grasp of how climate has behaved and evolved in the past allows us to put into context what we see today and better understand what could lye ahead tomorrow. The mass extinction events that punctuate Earth's history are still enigmatic and therefore understanding their various causal mechanisms can provide us with a powerful tool in accessing future climate scenarios.

13.2

Eutrophication of marginal seas by river input: The Middle Jurassic Western Tethys compared to the Modern Caribbean

Baumgartner Peter O.* & Tschudin Pascal*

* *Institut de Géologie et Paléontologie, University of Lausanne. Anthropole, CH-1015 Lausanne, Switzerland. (Peter.Baumgartner@unil.ch)*

The Caribbean - Gulf of Mexico marginal sea (15-30° N) is discussed here in terms of a potential circulation model for the Middle Jurassic Western Tethys. Both seas share a similar size, latitude, lie W of a large ocean and are characterized by a system of complicated sub-basins, shelves and islands. High nutrient input in the Caribbean results from direct river input (Mississippi, Orinoco) and indirect transfer of nutrient-rich freshwater transported by ocean currents – the subject discussed here in detail.

The Amazon and Orinoco Rivers shed together approximately 8000 $km^3\ yr^{-1}$ freshwater into the tropical Atlantic Ocean and the Caribbean Sea. This corresponds to 20% of the global continental runoff at a rate of ≈0.2 Sv. Undisturbed river systems carry ≈20µg of dissolved P and >40µg of total dissolved N per L of water [3] resulting in a minimal flux of $1.6 * 10^{11}$ g yr^{-1} P and $>3.2 * 10^{11}$ g yr^{-1} N. Particulate transport may be a multiple of the above values. Taking a C/P ratio of 500-1000 in Caribbean marine organisms implies that this water-mass is capable of fixing 80-160 Tg of organic carbon and (assuming a K/Si ratio of 1) >0.32 Tg of Si annually. The Amazon and Orinoco river inputs form large plumes that are carried into the Southern Caribbean by the North Brazil Current (NBC ≈20 Sv). In the Southern Caribbean surface water salinity, temperature and nutrient availability vary seasonally with the variation of freshwater input from the rivers and the position of the Intertropical Convergence Zone (ITCZ) that determines the oceanic current pattern. During summer and fall NBC rings (around 400 km in overall diameter, average ≈9 Sv) separate from the main current, translate northwestward toward the Caribbean Sea, stall around 14-18°N and decay shedding important amounts of nutrient laden, low salinity water into the area of the Windward Antilles.

While the physical oceanography of the system is now well described, its impact on Caribbean ecosystems is poorly documented. There are reports of increasing and rapid demise of coral reefs in the Windward Antilles from areas devoid of local pollution, but no relationship with declining Amazon and Orinoco water quality has been established. We suspect that the

rapidly increasing deforestation of the last 20-30 years in the catchment areas of the two large S-American rivers may have increased the nutrient load of their waters, due to increased erosion of organic top soils. The area most affected by such a change must be the SE-Caribbean, where the freshwater pulses are most evident.

The Middle Jurassic (or more exactly the Toarcian to middle Oxfordian) is a time interval of important fluctuations of $\partial^{13}C$ with long lasting highs in the Aalenian - early Bajocian and the Middle Callovian to Middle Oxfordian intervals. These fluctuations have been interpreted in terms of high C_{org} cycling and low C_{carb} production during positive peak times. While the N-Tethyan margin is swamped by detrital material washed off the Eurasian continent, southern Tethyan sediments of this time are characterized by meso- to eutrophic biogenic facies: green radiolarites in basins and monotonous, grey, microbial, often siliceous limestones on platforms such as the High Karst and the Pelagonian. Both pelagic and shelf areas of S-Tethys were beyond the reach of detrital input, but experienced increased nutrient levels throughout most of the Middle Jurassic.

Radiolarite occurrences in Tethyan basins have been explained by upwelling either in a peri-equatorial ocean basin or in monsoonal circulation system. However, the more elaborate reconstructions of he middle Jurassic Tethys show a complicated system of poorly interconnected oceanic basins with often deeply submerged margins separated by submerged shelves on micro-continents. To produce upwelling in all these relatively narrow basins, especially the Alpine Tethys, seems very difficult. An equatorial current system cannot be made responsible either, because palaeolatitudes of the mid Jurasssic Tethyan basins are between 20° and 40° N. Another fact speaks clearly against an equatorial current system: The Jurassic Central Atlantic is devoid of biosiliceous sediments. The presence of pelagic carbonates (above the CCD) throughout the Jurassic must be interpreted as the consequence of surface waters that are more oligotrophic than those of the adjacent Tethys and Paleo-Pacific. The Jurassic Atlantic was a “mediterranean” ocean basin such as the Modern Red Sea. Important bottlenecks (Paleo-Gibraltar, S-Florida-Bahamas) exist through the middle and late Jurassic and must have prevented a voluminous (10-20 Sv) water exchange between the Atlantic and its neighbouring basins.

While the mid Jurassic global setting is right for meso- to eutrophic (low C_{carb}.) sedimentation, we need a mechanism to continuously supply nutrients to the Western Tethys. In analogy with the Caribbean-Gulf of Mexico we can imagine that the Tethyan N-Equatorial Current struck the Arabian Platform, was deviated to the N and may have entered the Jurassic Eastern Mediterranean. On its way, it interacted with freshwater plumes of large rivers draining tropical N-Africa. While the suspended load sedimented in the deep Eastern Mediterranean, freshwater plumes rich in dissolved nutrients were carried into the entire S-Tethyan realm providing a constant nutrient input. This input allowed for high accumulation rates of biosiliceous sediments, caused deep water anoxia during peak intervals and microbial carbonates on platforms.

Modern anthropogenic changes in the Amazon – Orinoco - Caribbean system may represent a turning point from C_{carb} rich to C_{carb} poor sedimentation. Golbal Change can be a lesson for the interpretation of the Past.

13.3
Glacial geology and paleoclimate: Stable isotope analysis in Holocene tree rings Mont Miné glacier (VS)

Dessauges Aude*, Leuenberger Markus**, Nicolussi Kurt*** & Schlüchter Christian *

* *Institute of geological sciences, University of Bern, Baltzerstrasse 3, CH-3012 Bern (aude@students.unibe.ch)*
** *Physics Institute, University of Bern, Sidlerstrasse 5, CH-3012 Bern*
*** *Tree-ring Group / Institute of Geography, University of Innsbruck, Innrain 52, A-6020 Innsbruck*

The goal of this study is to reconstruct regional-scale climate variability in the Val d’Hérens in Valais. The period we are investigating is the Holocene. It is known that the early Holocene climate was unstable and characterized by a cool event around 8.2 ka BP (Before Present).
This work was motivated by the recent found of *Pinus cembra* and *Larix decidua* trees during the summer 2006 at the front of the tongue of the Mont Miné glacier, found thanks to the present-day melting of the glacier.
We first reconstructed the environment characteristics and properties where the trees were found and where they lived with a glacial geomorphological map and with a georadar investigation. The reconstruction of the Mont Miné glacier movements helped to show the different phases of advances and retreats of the glacier with time. This analysis of tree’s local environment was then completed by a temporal climate analysis made accessible with the oxygen and carbon tracers measured on cellulose extracted from rings of the found trees. Dendrochronology (Nicolussi 2006) shows that they originat from the early Holocene.

During the investigated period our results show significant changes in the value of $\delta^{18}O$, indicating that the climate already was unstable with warmer and colder periods. We suggest that these signatues indicate that between the years 6450 and 6180 BC the Mont Miné glacier was smaller than today. Climatic conditions during the Holocene were warm enough to allow to the vegetation to grow at an altitude that is currently recovered by the glacier.
The hypothetical advance of the Mont Miné glacier that followed seems to be contemporaneous with the « 8.2 event ». We speculate that before this date the glacier was smaller. During the warmer period the glacier could most likely not advance. It is even possible that the ice was melting during this warmer period. The $\delta^{18}O$ values reach a minimum, which indicates that a cool event occurred and implied the death of the trees.

13.4

A geological perspective on calcareous nannoplankton evolution: biotic response to global change and environmental perturbations?

Erba Elisabetta, Bottini Cinzia, Casellato Cristina Emanuela, De Bernardi Bianca & Tiraboschi Daniele

Dipartimento di Scienze della Terra, Via Mangiagalli 34. 20133 Milano (elisabetta.erba@unimi.it)

Recent environmental changes and climate instabilities pose urgent questions regarding biota ability to keep pace with concurrent excess CO_2, global warming and ocean acidification. Major concerns are addressed to the possibility of near future extinctions causing a biodiversity loss and revealing a biota failure in sustaining rapid and progressive environmental changes accelerated by anthropogenic impacts. However, the findings of new organisms in various ecosystems raise the possibility that global change might stimulate biota speciation and/or innovation: novel life forms might represent temporary adaptation to environmental stress or might be real new species evolved in response to global change.

The ocean, the oldest and largest ecosystem on Earth, best recorded global changes in climate and oceanic physical, chemical and trophic parameters. Within the oceanic biosphere, calcareous phytoplankton plays a special role as: (1) is common and widespread and consists of cosmopolitan and endemic taxa; (2) has a 220 My-long evolutionary history; (3) is one the most effective calcite producers of the planet since the Jurassic; (4) is relevant for both the inorganic and organic carbon cycle; (5) is extremely sensitive to environmental variations; (6) may directs climate change by altering albedo and absorption/emission of atm-CO_2 at large scale.

The Phanerozic geological record of global change unambiguously indicates that the Earth system already experienced conditions of (super)greenhouse and (super)icehouse. Diversity pulses of calcareous nannoplankton are grossly coeval with major events such as climate and sea-level changes, large magmatic episodes and variations in ocean structure and composition, suggesting that evolutionary patterns are intimately linked to environmental modifications.

Our study aims at reconstruction of both tempo and mode of nannoplankton evolution and the causal/casual role of environmental pressure. We explored time-intervals of (1) evolutionary acceleration in absence of coeval environmental change, during a period of presumed climatic stability (Tithonian, latest Jurassic), and (2) global change marked by calcareous phytoplankton adaptation/evolution (Early Aptian Oceanic Anoxic Event 1a; PETM). For each case history calcareous nannofossils have been investigated in sections from different oceans in order to discriminate among local, regional or global causes, and to verify possible diachroneity in calcareous phytoplankton evolution and/or in response to global changes. Calcareous nannofossil species richness, first and last occurrences and abundance (relative and absolute) have been achieved. Morphometric analyses of selected taxa have been performed to separate malformation, under-calcification, over-calcification, and real ultrastructure changes.

Three speciation models were proposed: phyletic gradualism, punctuated equilibrium and punctuated gradualism. Phyletic gradualism holds that new species arise from slow and steady transformation of populations providing gradational fossil series linking separate phylogenetic species. Punctuated equilibrium explains the appearance of new species by rapid speciation occurring in small peripheral isolated populations, followed by migration to other areas where the fossil sequence usually shows a series of sharp morphological breaks. Punctuated gradualism implies long-lasting evolutionary stasis interrupted by rapid, gradual phyletic transformation without lineage splitting.

The Jurassic-Paleogene case-histories investigated provide examples of all evolutionary patterns in calcareous nannoplankton. Preliminary results suggest: (1) potentially different speciation styles of coccoliths versus nannoliths; (2) that punctuated gradualism prevails in intra-generic speciation, whereas punctuated equilibrium dominates inter-generic speciation; (3) that most new morphotypes associated with extreme, global change represent ephemeral adaptations rather than true species. Although climate and environmental changes have been instrumental for directing nannoplankton evolution, epi-

sodes of major innovation occurred during times of ecosystem stability suggesting very successful diversification and adaptations to steady conditions. Contrary to general models, extreme events such as OAE1a and PETM did not cause extinctions among calcareous nannoplankton.

13.5

The rise and fall of the Urgonian empire

Föllmi Karl B.*, Godet Alexis**, Bodin Stéphane***, Linder Pascal****, de Kaenel Eric*****, Adatte Thierry*, Stein Melody*

* *Institut de Géologie et Paléontologie, Université de Lausanne, CH-1015 Lausanne*
** *Neftex Petroleum Consultants Ltd., Oxfordshire, GB-OX14 4RY*
*** *School of Earth, Atmospheric and Environmental Sciences, University of Manchester, GB-M13 9PL*
**** *Institut de Géologie, Université de Neuchâtel, CH-2009 Neuchâtel*
***** *DeKaenel Paleo-Research, CH-2000 Neuchâtel,*

Urgonian-type shallow-water carbonates of late early Cretaceous age exhibit a typical facies characterized by the presence of large benthic foraminifera, green calcareous algae, calcareous sponges, chaetetids, stromatoporoids, and the co-occurrence of corals and rudists. Urgonian carbonates occur on a global scale in shallow-waters of tropical and subtropical regions and represent a photozoan, oligotrophic community of carbonate producers, which was unique for the Cretaceous - a time of otherwise frequent eutrophic episodes, which translated into oceanic anoxic events and platform-drowning episodes.
The onset and demise of the Urgonian regime is controversially dated, which is for a large part related to different calibration schemes for large benthic foraminifera used by different research groups. We present new ammonite and nannofossil-based data from the helvetic Alps and the western Swiss Jura, which suggest that the onset of the Urgonian did not occur before the late Barremian, after a long period of erosion, condensation and phosphogenesis related to the drowning of the Hauterivian carbonate platform, for which its onset is related to the Faraoni anoxic episode. The demise of the Urgonian platform appears synchronous on a world-wide scale and is dated as middle early Aptian, just before the unfolding of the Selli anoxic episode.
The exact timing of the Urgonian period allows us to tie the evolution of Urgonian platforms and especially their demise to environmental and paleoceanographic change in a way, which resembles the actual development of so-called "dead zones" in shallow-water areas and the progressive loss of reefs on a world-wide scale.

13.6

Oceanic and climatic Changes during the Albian- Cenomanian: the World at the End of Pangea

Giorgioni Martino*, Weissert Helmut*, Bernasconi Stefano*

**ETH Zürich, Geologisches Institut, Universitätstrasse 16, CH-8090 Zürich (martino.giorgioni@erdw.ethz.ch)*

The mid-Cretaceous is renown for being a period in Earth's history when the global conditions differed drastically from those of today. There were exceptionally high temperatures, an absence of permanent polar ice sheets, very high sea level and strong greenhouse effect. The behavior of Earth's climate system and its ruling factors in such warm conditions are still poorly understood and represent a tantalizing topic in Earth and climate sciences.
New paleotemperature and CO_2 estimates reveal that the period from the Albian to the Turonian was the warmest of the all Cretaceous and that this warming cannot be explained by enhanced greenhouse effect only. Quantitative models show a relationship between the thermal maximum and a major re-arrangement of oceanic circulation due to the opening of the Equatorial Atlantic Gateway (EAG) that brought the definitive break-up of the super-continent Pangea.
During the Albian deep-water sediments in the Western Tethys are characterized by more or less alternating varicolored facies testifying to very unstable conditions at the bottom of the ocean, punctuated by three organic matter rich intervals, identified as minor Oceanic Anoxic Events (OAE 1b, OAE 1c, OAE 1d). In the uppermost Albian, after the end of the OAE 1d, this sedimentation pattern is replaced by more homogeneous facies that span the Cenomanian interval until the last major Cretaceous Oceanic Anoxic Event (OAE 2).
This work provides stratigraphical, sedimentological, and geochemical data of Albian-Cenomanian sections from Lusitanian Basin (Portugal) and Southern Alps (Northern Italy). During the Albian-Cenomanian these areas were part of the North

Atlantic and the Western Tethyan realms respectively and they must have been particularly susceptible to the changes induced by the opening of the EAG. We present correlation between the two regions and possible evidences of the major climate changes that took place at that time. The aim is to test whether these changes can be related to the opening of the EAG, supporting the prediction of the models, or other factors played a significant role on the mid-Cretaceous oceanic-climatic system.

REFERENCES

Bellanca, A. et al. 1996: Orbitally induced limestone/marlstone rhythms in the Albian-Cenomanian Cismon section (Venatian region, northern Italy): sedimentology, calcareous and siliceous plankton distribution, elemental and isotope geochemistry. Palaeogeography Palaeoclimatology Palaeoecology, vol. 126, pp. 227-260,

Bersezio R. 1992: La Successione Apriano-Albiana del Bacino Lombardo (Alpi meridionali). Giornale di Geologia, serie 3a, vol. 54/1, pp. 125-146, Bologna

Bice, K. L. & Norris R. D. 2002: Possible atmospheric CO_2 extremes of the Middle Cretaceous (late Albian-Turonian). Paleoceanography, vol. 17, n. 4

Bice, K. L. et al. 2006: A multiple proxy and model study of Cretaceous upper ocean temperatures and atmospheric CO_2 concentrations. Paleoceanography, vol 21, PA2002, doi: 1029/2005Pa001203, 2006

Petrizzo, M. R. et al. 2008: Late Albian paleoceanography of the western subtropical North Atlantic. Paleoceanography, vol. 23, PA1213, doi: 10.1029/2007PA001517

Poulsen, C. J. et al. 2001: Response of the mid-Cretaceous global oceanic circulation to tectonic and CO_2 forcings. Paleoceanography, vol 16, n. 6, pp. 576-592, December

Poulsen, C. J. et al. 2003: Did the rifting of the Atlantic Ocean cause the Cretaceous thermal maximum? Geology, vol. 31, n. 2, pp. 115-118

Reichelt, K. 2005: Late Aptian-Albian of the Vocontian Basin (SE-France) and Albian of NE-Texas: Biostratigraphic and paleoceanographic implications by planktic foraminifera faunas. Dissertation der Geowissenschaftlichen Fakultät der Eberhard-Karls-Universität Tübingen.

Rey, J. et al. 2003: Les séquences de dépot dans le Crétacé inférieur du Bassin Lusitanien. Comunicacoes do Instituto Geológico e Mineiro, 90, 15-42

Wilson, P. A. & Norris R. D. 2001: Warm tropical ocean surface and global anoxia during the mid-Cretaceous period. Nature, vol. 412, 26 July

13.7

Neogene global cooling and its impact on diatom size evolution

Girault France E.[1], Weller Andrew F. [1,2] & Thierstein Hans R.[3]

[1]*Geological Institute, ETH, CH-8092, Zurich, Switzerland*
(france.girault@erdw.ethz.ch)
[2]*Present address: Geosoft Australia Pty Ltd, 14/100 Railway Road, Subiaco WA 6008, Australia*
[3]*Geological Institute, ETH Zurich and University Zurich, Universitätstrasse 6, CH-8092 Zurich, Switzerland*

A major characteristic among skeletonized phytoplankton in the ocean is that they depend on the availability of bio-limiting nutrients in the photic zone. Competition (inter- and intra-group) for these bio-limiting nutrients together with present and past changes in oceanic conditions are potential dominant drivers of the adaptation and resulting evolution of these microorganisms. Over the Cenozoic and particularly since the Neogene, diatoms have become the most efficient group for nutrient uptake, by far outcompetiting the coccolithophores in nutrient-rich areas and assuming dominance in the oceanic cycling of dissolved silica.

Here we explore the utility of a quantitative measure, mean test sizes of centric diatoms and their variability, to characterize the macro-ecological patterns in today's oceans and the evolutionary response of this group in the past. Size and morphological characteristics of the centric diatom frustules (diameter >20 μm) were collected using recently developed automated light microscopy and image analysis techniques for a statistically representative number of specimens (i.e. 250-700) per sample. We present initial results of these size analyses by comparing our macro-ecological calibration in 46 Holocene core-top samples from tropical to polar environments with the macro-evolutionary patterns observed in DSDP/ODP sites from the Southern Ocean, the Equatorial and the North Pacific over the past 20 million years at a temporal sampling resolution of 0.3-2 m.y.

Although our Holocene sample set shows large variability in environmental conditions, changes in the mean size of centric diatom assemblages are rather small. In contrast, during the Neogene mean sizes of centric diatoms show large variability through time with regional shifts occurring during well-known climatic and oceanic events (i.e. onset of northern hemisphere glaciation). These patterns imply an evolutionary trend possibly related to Neogene global cooling and related reorganizations of water masses and their dissolved silica pools. Since diatoms are the primary competitors of coccolithophores for nutrients among the skeletonized phytoplankton, their evolutionary emergence to dominance would imply coeval consequences for the evolution of the coccolithophores.

13.8

Confirmation of an exceptional sea-level highstand at +20 m during MIS 11 (400'000 ka BP) from Bahamian sedimentary rocks: a credible scenario for future global warming?

Godefroid Fabienne*, Kindler Pascal*, Samankassou Elias*

*Section of Earth Sciences, University of Geneva, Maraîchers 13, CH-1205 Geneva, Switzerland (fabienne.godefroid@terrre.unige.ch)

The discovery of elevated marine and lacustrine deposits near Glass Window (North Eleuthera, Bahamas) validates the controversial sea-level highstand at about +20 m during Marine Isotope Stage (MIS) 11. Considered as the longest interglacial of the past half million years, MIS 11 is an excellent candidate for providing a credible scenario for a future, human-induced, global warming.

Two stratigraphic sections (GW1 and GW2) including five carbonate units were logged near Glass Window in North Eleuthera Island. Sedimentological, petrographic and geochronological (amino-acid racemization dating) analyses were performed.

On both sections, which form high cliffs about 18 and 22 m high, Unit 1 consists of cross-stratified biopeloidal limestone showing a late generation of fibrous rim cement of marine origin. This late cementation entirely affects this first unit. The boundary between Units 1 and 2 is represented by a planar erosional surface. Unit 2 displays well-defined planar bedding at both sites, whereas faint cross-stratifications are also visible at GW 1. It consists of laminated biopeloidal grainstone containing *Halimeda* fragments and rounded lithoclasts derived from Unit 1, and is further characterized by an early generation of isopachous fibrous cement. The upper part of Unit 2 shows one thick laminated crust including numerous spherulites of cyanobacterial origin, and is capped by a reddish paleosol. The top of the GW 2 section is represented by an oolitic/peloidal grainstone (Unit 3), whereas the upper part of GW 1 includes one bioclastic (Unit 4) and one oolitic (Unit 5) unit, separated by a paleosol.

The values of alloisoleucine/isoleucine (A/I) ratios average at 0.740, 0.737, 0.652, 0.467, and 0.371 for Units 1 to 5, respectively.

Based on these analyses, Units 1, 3, 4 and 5 can be identified as eolianites dating from MIS 11 (A/I = 0.740), MIS 9 (A/I = 0.652), MIS 7 (A/I = 0.467) and MIS 5e (A/I = 0.371), respectively. Exposed between +12 and +14.5 m, the basal part of Unit 2 can be interpreted as subtidal and beach deposits, whereas its upper part, at +15 m, likely corresponds to lacustrine (pond) sediments, both dating from MIS 11 (A/I= 0.737). The presence of spherulites of cyanobacterial origin shows that the thick laminated crust at the top of Unit 2 was formed at the surface, and not within a soil profile. Considering the subsidence affecting Eleuthera Island (1 m/100 kyr), the beach and pond deposits of Unit 2 and the marine cements present in Unit 1 indicate that sea level reached an elevation of about +20 m during MIS 11, implying the collapse of both the Greenland and the West-Antarctic ice-sheets, and the partial melting of the East-Antarctic ice-sheet.

The Earth's orbital parameters were about the same during MIS 11 than today (i.e. MIS 1). Climatic conditions and climate evolution during these two interglacials can, therefore, be compared. The prominent melting of polar ice-sheets and the associated sea-level fluctuation at +20 m occurred at the end of MIS 11, and were probably linked to its exceptional duration (20-35'000 yrs). Stage 1 began only 12'000 years ago and, thus, the prospect of a 20 m rise in sea level appears rather remote in time. However, the present-day, human-induced increase in atmospheric greenhouse gases may drastically accelerate the disintegration of polar ice-sheets, triggering a catastrophic elevation of sea level in the next decades or centuries. The MIS 11 stratigraphic record from the Bahamas shows that this is possible.

13.9

Evidence for major climatic change at the Smithian-Spathian boundary from low palaeolatitudinal records

Hermann Elke*, Hochuli Peter A.*,**, Bucher Hugo*,**, Brühwiler Thomas*, Goudemand Nicolas* & Ghazala Roohi***

*Paläontologisches Institut und Museum, Karl Schmid-Strasse 4, CH-8006 Zürich (ehermann@pim.uzh.ch)
**Geologisches Institut, Universitätsstrasse 16,CH-8050 Zürich
***Pakistan Museum of Natural History, Garden Avenue, PK-44000 Islamabad

The delayed recovery of marine and terrestrial ecosystems after the end-Permian extinction event is still up for debate. Focusing on the Smithian-Spathian boundary, palaeoecological changes are reflected by a significant global faunal turnover as indicated by ammonoids (Brayard et al. 2006) and conodonts (Orchard 2007) as well as a change in the palynological associations of the Boreal realm. There, the Smithian-Spathian transition is marked by a conspicuous change from spore dominated assemblages in the Smithian to gymnosperm dominated assemblages in the Spathian (Galfetti et al. 2007a).
Here, we present the composition of the Early Triassic microfloras of Nammal, Salt Range, Pakistan. Ammonoids and conodonts provide the high resolution age control of the studied section (Brühwiler et al. 2007).
The late Smithian palynological assemblages are characterized by a general dominance of hygrophytic elements. Slightly below the Smithian-Spathian boundary, between the *Anasibirites* beds and the *Glyptophiceras* beds, the composition changes dramatically with a drastically increasing proportion of xerophytic elements. This event coincides with the onset of a positive shift in the $\delta^{13}C$ record marking the Smithian-Spathian boundary (Galfetti et al. 2007b). Preliminary results from southern Tibet also indicate a similar trend from hygrophyte-dominated to xerophyte-dominated assemblages across the boundary.
Thus, there is evidence for the Smithian-Spathian boundary climatic event from high as well as from low palaeolatitudes, demonstrating its global significance.

REFERENCES

Brayard, A., Bucher, H., Escarguel, G., Fluteau, F., Bourquin, S., Galfetti, T. 2006: The Early Triassic ammonoid recovery: Paleoclimatic significance of diversity gradients, Palaeogeography, Palaeoclimatology, Palaeoecology, 239, 374-395.

Brühwiler, T., Bucher, H., Goudemand, N., Brayard, A. 2007: Smithian (Early Triassic) Ammonoid successions of the Tethys: New preliminiary results from Tibet, India, Pakistan and Oman, New Mexico Museum of Natural History and Science Bulletin, 41, 25-26.

Galfetti, T., Hochuli, P. A., Brayard, A., Bucher, H., Weissert, H., Virgan, J. O., 2007a: Smithian/Spathian boundary event: Evidence for global climatic change in the wake of the end-Permian biotic crisis, Geology, 35, 291-294.

Galfetti, T., Bucher, H., Ovtcharova, M., Schaltegger, U., Brayard, A., Brühwiler, T., Goudemand, N., Weissert, H., Hochuli, P. A., Cordey, F., Goudun, K. 2007b: Timing of the Early Triassic carbon cycle perturbations inferred from new U-Pb ages and ammonoid biochronozones, Earth and Planetary Science Letters, 258, 593-604.

Orchard, M.J. 2007: Conodont diversity and evolution through the latest Permian and Early Triassic upheavals, Palaeogeography, Palaeoclimatology, Palaeoecology, 252, 93-117.

13.10

Reduced oxygen concentrations in the abyssal North Pacific during the last glacial period – implications for oceanic carbon storage

Jaccard Samuel*, Galbraith Eric**, Haug Gerald*, Sigman Daniel**

*D-ERDW, ETHZ, Universitätstr. 16, CH-8092 Zurich (samuel.jaccard@erdw.ethz.ch).
**Department of Geosciences, Princeton University, Princeton, NJ 08544, USA.

The deep North Pacific represents an end-member of the modern circulation regime. It is far from sites of deep-water renewal, and so is enriched in CO_2 and dissolved nutrients due to the accumulation of the products of remineralised organic matter along the path of global deep-water circulation. For the same reasons, deep North Pacific waters show a depletion in dissolved oxygen.

Reconstructions of $\delta^{13}C$ distribution for the glacial Pacific Ocean show that deep water below 2000 - 2500 m was depleted in $\delta^{13}C$ when compared with mid-depth and upper ocean waters. Below 2000 m, the deep waters were enriched in nutrients and metabolic CO_2, while nutrient concentrations in the intermediate depth Pacific were apparently lower. Partition of CO_2 in favor of the deep ocean would have contributed to decrease atmospheric ρCO_2 during cold periods.

This hypothesis has been tested by studying the sedimentary distribution of redox-sesitive trace metals (Mo & U) in two sediment cores spanning the abyssal subarctic Pacific. The fundamental control on sediment redox state is the balance between the flux of organic matter to the seafloor and the flux of oxidants to the sediment from overlying seawater. Thus, variations in sedimentary redox state are linked to changes in the magnitude of biological export and the role of ocean circulation. Comparison of redox-sensitive trace metals abundance with reconstruction of biogenic flux to the sediment will yield inferences about relative changes of oxygen concentrations at the water-sediment interface.

Sediments deposited during the last ice age are enriched in authigenic U when compared to the Holocene Here, the export production proxies Ba/Al and biogenic opal indicate that the local flux of biogenic detritus to the seafloor was generally reduced during the last glacial period. Given this evidence, the enhanced U accumulation must have been a response to substantially lower bottom water O_2 and, by inference, the glacial North Pacific contained a higher concentration of respired carbon than today. Although the absence of Mo enrichments argues that anoxia did not develop in the vicinity of our core sites, oxygen concentrations may have dropped far below their current concentrations during the last ice age. If this elevated respired carbon burden is representative of the deep glacial Indo-Pacific Ocean, it could represent the primary reservoir of glacial CO_2 sequestration. It results, that a significant fraction of CO_2 has been sequestered into the deep ocean during glacial periods leading to a large reduction of atmospheric ρCO_2, that is widely documented in Antarctic ice cores.

13.11

Cretaceous carbon cycle and climate: The Barremian-Early Aptian C-cycle perturbation

Keller Christina E.*, Giorgioni Martino*, Garcia Therese I.*, Bernasconi Stefano M.*, Hochuli Peter**, Weissert Helmut*

*Geological Institute, ETH Zürich, Universitätsstr. 16, CH-8092 Zürich (Christina.Keller@erdw.ethz.ch)
**Palaeontological Institute, University of Zürich, Karl Schmid-Strasse 4, CH-8006 Zürich

Late Early Cretaceous marine sediments feature a fascinating succession of repeated greenhouse pulses interrupted by episodes of cool climate, which is indicated by the several important positive carbon isotope anomalies documented in the sedimentary record.
The Ontong-Java volcanism is thought to be the trigger of the major positive carbon isotope excursion in the Aptian (Larson & Erba 1999). However, this volcanic activity predates the isotope excursion considerably (Tejada et al. 2002). This led to the hypothesis that the "Aptian greenhouse pulse" already began in the Barremian (Weissert & Erba 2004; Coccioni et al. 2004) with a first CO_2 pulse initiating climate warming and a first perturbation of the global carbon cycle. This is evidenced by deposition of black shales and a positive carbon isotope excursion during the mid-Barremian (mid-Barremian event of Coccioni et al. 2004). Accelerated organic carbon burial caused a decrease of the atmospheric CO_2 levels and induced a cooling event, which is thought to have resulted in a renewed carbonate-dominated sedimentation in the Late Barremian/Early Aptian oceans.

In this study, a composite Late Hauterivian-Early Aptian Tethyan record is presented combining carbonate carbon isotope values with magnetostratigraphic and biostratigraphic data. From the Late Hauterivian to the early Early Aptian, the carbonate carbon isotope values fluctuate essentially between 1.6‰ and 2.4‰. The most positive values are reached during the early Aptian pre-OAE 1a excursion with carbonate carbon isotope values of up to 3‰.

The different sections feature extremely variable thicknesses, which seems to be due to frequent sedimentary hiati, a pattern that is well-known from Barremian-Aptian successions and is interpreted to result from increased current intensities.
The distribution pattern of black shales combined with the carbon isotopes allows to assign the black shales to the known over-regional events such as the Faraoni Event in the Late Hauterivian or the OAE 1a in the Early Aptian.

The studied sections highlight the variability and complexity of sedimentary deposits at various positions in the different basins at the southern margin of the Tethyan Ocean and allow a varied insight into the ocean-atmospheric evolution of the Early Cretaceous.

REFERENCES
Coccioni, R., Galeotti, S., Marsili, A. & Sprovieri, M. 2004: The Mid-Barremian event (MBE): The prelude to the OAE 1a. Geophysical Research Abstracts, 6, 05130.
Larson, R.L. & Erba, E. 1999: Onset of the mid-Cretaceous greenhouse in the Barremian-Aptian: Igneous events and the biological, sedimentary, and geochemical responses. Paleoceanography, 14 (6), 663-678.
Tejada, M.L.G., Mahoney, J.J., Neal, C.R., Duncan, R.A. & Petterson, M.G. 2002: Basement geochemistry and geochronology of central Malaita, Solomon islands, with implications for the origin and evolution of the Ontong Java Plateau. Journal of Petrology, 43, 449-484.
Weissert, H. & Erba, E. 2004: Volcanism, CO_2 and palaeoclimate: a Late Jurassic-Early Cretaceous carbon and oxygen isotope record. Journal of the Geological Society, 161, 695-702.

13.12

The initiation of OAE1a revealed by a high resolution biomarker carbon isotope record

Mehay Sabine*, Keller Christina E.*, Bernasconi Stefano M.*, Weissert Helmut*, Erba Elisabetta**

* *Department of Earth Science, Geological institute, ETH, 8092 Zürich, Switzerland (sabine.mehay@erdw.ethz.ch)*
** *Department of Earth Sciences, University of Milan, Via Mangiagalli 34, Milan, 20133, Italy*

Oceanic anoxic events (OAEs) are time envelopes in the Cretaceous when ocean conditions favoured the episodic deposition of organic-rich sediments on a global scale. The first Cretaceous oceanic anoxic event (OAE1a, Early Aptian, ≈120 million years ago) is marked by an enigmatic negative carbon isotope ($\delta^{13}C$) spike of up to 3‰ in marine carbonates and of 4 to 5‰ in the organic carbon at its base (Schlanger & Jenkyns, 1976; Menegatti et al., 1998). This carbon-cycle perturbation is believed to reflect a massive release of ^{13}C depleted carbon into the ocean and the atmosphere. Because the Early Aptian is known as a period of greenhouse conditions, this light carbon has been proposed to derive from the dissociation of methane hydrates (Dickens, 2003). The aim of our study is to elucidate the initiation of OAE1a in an attempt to anticipate the possible evolutions of both atmospheric and oceanic ecosystems on Earth, under warmer climate than today.

Because exchanges between ocean and atmosphere pools are faster than the resolution of the carbon isotope records available so far for the OAE1a and bulk $\delta^{13}C$ combines effects of a whole ecosystem, a higher resolution carbon isotope study on specific biomarkers is essential. Bulk and biomarkers $\delta^{13}C$ were therefore measured at sampling intervals of 2000 to 6000 years on samples from the Cismon core (Southern Alps, Italy), showing one of the best stratigraphic resolution for the OAE1a interval at low latitudes (Li et al., 2008).

The new carbon isotope record shows a stepwise initiation of OAE1a which was divided into five intervals, covering ≈70 kyr. They successively describe a massive outgassing of mantle CO_2, a temperature rise, an increase in carbon-isotope fractionation and partial methane hydrates dissolution. This evidences that the negative carbon isotope spike recorded at the onset of OAE1a was probably caused by a combination of different processes affecting the carbon-cycle and primarily triggered by an intense volcanic activity, linked to the Ontong-Java Plateau large igneous province.

REFERENCES
Dickens, G. R. 2003: Rethinking the global carbon cycle with a large, dynamic and microbially mediated gas hydrate capacitor, Earth Planet. Sci. Lett., 213, 169-183.
Li, Y.-X. et al. 2008: Toward an orbital chronology for the early Aptian Oceanic Anoxic Event (OAE1a, ≈120Ma), Earth Planet. Sci. Lett., doi: 10.1016/j.epsl.2008.03.055.
Menegatti, A. et al.1998: High-resolution $\delta^{13}C$ stratigraphy through the early Aptian "Livello Selli" of the Alpine Tethys, Paleoceanography, 13, 530-545.
Schlanger, S.O. & Jenkyns, H.C. 1976: Cretaceous anoxic events: Causes and consequences, Geol. Mijnbouw, 55, 179-184.

13.13

Evidence of sulfidic marine environment after the Triassic-Jurassic mass-extinction event

Richoz, Sylvain1,2, Van De Schootbrugge, Bas1, Püttmann Wilhelm3, Heunisch Carmen4, Quan Tracy M.5, Fiebig Jens1 & Pross Joerg1,

(1) Institute of Geosciences, Goethe University Frankfurt, Altenhoeferallee 1, Frankfurt, 60438, Germany, van.de.Schootbrugge@em.uni-frankfurt.de , Jens.Fiebig@em.uni-frankfurt.de, joerg.pross@em.uni-frankfurt.de.
(2) Institute of Paleontology, University Vienna, Athenstrasse 14, 1090 Vienna, Austria, Sylvain.Richoz@univie.ac.at.
(3) Institute for Atmosphere and Environment, Goethe University Frankfurt, Altenhoeferallee 1, Frankfurt, 60438, Germany, puettmann@kristall.uni-frankfurt.de.
(4) State Authority for Mining, Energie and Geology, Geocenter Hannover, Stilleweg 2, Hannover, 30655, Carmen.Heunisch@lbeg.niedersachsen.de
(5) Institute of Marine and Coastal Sciences, Rutgers University, 72 Dudley Road, New Brunswick, NJ 08901, quan@marine.rutgers.edu.

The Triassic-Jurassic boundary (T-J; 201 Ma) marks one of the so called Big Five mass-extinction events that may have led to the extinction of more than 80% of all marine invertebrates. The extinction of marine and terrestrial biota is increasingly linked to the outgassing of large volumes of CO_2 and SO_2 during the emplacement of the Central Atlantic Magmatic Province, however the exact kill mechanisms and the long-term effects of this large igneous province remain to be elucidated. Here, we present multi-disciplinary data, including organic geochemical, isotope (C, N) and microfossil data, from 3 cores in Luxemburg (Rosswinkel), and northern (Mariental) and southern Germany (Mingolsheim) that provide evidence for prolonged environmental instability during the earliest Jurassic. Organic geochemical analyses show elevated quantities of the biomarker isorenieratane in the lowermost Hettangian following a major overturn of terrestrial vegetation (fern spike) as documented by palynological analyses. Isorenieratane derives from the brown strains of photosynthetic green sulphur bacteria (Chlorobiaceae) that require both light and free hydrogen sulfide in the water column. The presence of abundant aryl isoprenoids (isorenieratane and its diagenetic products) in Luxemburg and N Germany suggests that marginal marine basins in NW Europe became salinity stratified and developed intense Photic Zone Euxinia (PZE) after the mass extinction event. This excludes euxinia as kill mechanism. Nitrogen and carbon isotope data from organic matter support the development of shallow marine anoxia in NW Europe. Our observations are consistent with the long-term effects of CO_2 release and greenhouse warming. Repeated and prolonged PZE in the Tethys Ocean may have contributed to the slow recovery of shallow marine ecosystems after the Triassic-Jurassic boundary.

13.14

Paleoredox changes associated with the Early Aptian Oceanic Anoxic Event

Westermann Stéphane*, Matera Virginie**, Fiet Nicolas***, Adatte Thierry* & Föllmi Karl B.*

**Institut de géologie et de paléontologie, Université de Lausanne, Antrople, CH-1015, LAUSANNE,*
***Institut de géologie et d'hydrogéologie, Université de Neuchâtel, Emile-Argand 11, CH-2007 NEUCHATEL,*
**** AREVA, 33 rue La Fayette,F-75442 PARIS, France*
(Email : Stephane.Westermann@unil.ch)

The Cretaceous is characterized by short periods during which widespread oceanic anoxic conditions developed, documented by the extensive deposition of organic carbon–rich sediments (Schlanger and Jenkyns, 1976). The early Aptian OAE, labelled OAE 1a, corresponds to one of the most studied anoxic event within the Cretaceous. This event is characterized by a positive excursion in $\delta^{13}C$, preceded by a pronounced negative spike, which was interpreted as the result of a pulse of methane release from clathrates from the ocean to the atmosphere (Weissert and Erba, 2004). In our study, we aim at improving our understanding of palaeoceanographic change leading to this event and test the proposed models by investigating phosphorus (P) and redox-sensitive trace-metals (TM) contents in sections through lower Aptian sediments along a basin-shelf transect in the western Tethys. We complement our geochemical analysis by the analyses of organic matter contents.
We selected three representative sections: Gorgo a Cerbara (central Italy) in the Umbria Marche basin, Glaise l'Ermitage (SE France) located in the Vocontian trough and Cassis/La Bédoule (SE France) located along the Provencal platform.

The general trend in P accumulation shows an increase at the onset of the early Aptian event followed by a rapid decrease. This suggests an increase in nutrient input, whereas the return to lower values through the first part of the anoxic event may be related to a weakened capacity to retain P in the sedimentary reservoir due to bottom water oxygen depletion. This general pattern is contrasted by the data of Gorgo a Cerbara which also show P-enrichments at the top of the Livello Selli. We compared these enrichments to the total organic carbon (TOC) values. The shales with the maximum TOC values also correspond to those with the highest P content. We also calculated C_{org}:P_{tot} ratios and observed that the highest values corresponds to the top of the Selli level. This is interpreted as a reflection of the decreased capacity of storing and preserving phosphorus in oxygen-depleted sediments.

TM exhibit comparable variations in the basinal settings. In the section of Gorgo a Cerbara, the data for U, V, Mo, Co, As show a low background level, constrasted by different maxima in concentrations near the top of the Selli level. Conversely, in the section of Glaise l'Ermitage and Cassis/La Bédoule , no significant enrichments have been observed in sediments equivalent to the Selli level. The different behaviour of the TM in the studied sections may be related to the palaeogeographic setting of the studied sections. These data seem to indicate anoxic conditions in the basin. In shallower-water environments, conditions may have been less reducing. Moreover, in Gorgo a Cerbara, three distinct enrichments have been observed. This seems to indicate fluctuations in the intensity of water column anoxia during the shift in $\delta^{13}C$.

Our results show that the expression of the OAE 1a is different following the palaeogeographic setting. The evolution of the P trend suggests an increase in nutrient input at the onset of the anoxic event, just after the negative spike in $\delta^{13}C$. TM and high C:P values may indicate anoxia conditions in the deep environment characterized by several anoxic phases with intermittent return to less oxygen-depleted conditions.

REFERENCE

Schlanger, S.O., Jenkyns, H.C., 1976. Cretaceous oceanic anoxic events: causes and consequences. Geologie en Mijnbouw, 55, 179–184.

Weissert, H., Erba, E., 2004. Volcanism, CO_2 and palaeoclimate; a Late Jurassic–Early Cretaceous carbon and oxygen isotope record. Journal of the Geological Society of London 161 (4), 695–702.

14. Deep Earth – From Crust to Core: A Tribute to Peter A. Ziegler

Stefan Schmid, Jon Mosar, Gilles Borel & Pierre Dèzes

International Lithosphere Program (ILP)
Swiss Commission of the International Union of Geological Sciences (IUGS)

14.1

Examples of magmatic processes in the crust and mantle as seen by seismic tomographic imaging: continental rifts and mantle plumes

Achauer Ulrich

EOST-IPG Strasbourg, UMR 7516, Lab de sismologie, 5 rue René Descartes, F-67084 Strasbourg, France (ulrich.achauer@eost.u-strasbg.fr)

Two of the tectonic most active regions on continental plates are rift structures and plumes. Over the last twenty years seismic tomographic imaging projects have been carried out to look in detail at the upper mantle structure of some of these features to shed light on their geodynamic evolution and to figure out their role in the assemblage of continents.
In my presentation I will concentrate on the research of rifting structures and baby plumes related to ECRIS, namely the Limagne Graben/Massif Central and the Rhine Graben/Eifel plume.

The most important result of the seismic investigations in the French Massif Central at the beginning of the 1990' (French-German co-operative project Limagne 91/92) was the proof of an ascending material stream from larger depth (250km), which due to its geochemical and petrological characteristics and its appearance was classified as a plume and which confirmed an already 20 years earlier expressed hypothesis. The really new of the results were that for the first time the exact size and shape of this plume at upper mantle depths was determined, as well as the fact that no plume head ("mushroom") could be found. This led to the expression of "baby plume" for this kind of material up-streaming in order to differentiate this feature to the classical idea of a plume (such as the model by Shilling). The results from the Massif Central triggered similar seismic experiments in other regions of Central Europe with Variscan basement and recent volcanism and led to the proof of another such structure beneath the Eifel volcanic region. It is intruiging that both baby plumes seem to be closely related to parts of the large scale ECRIS system.

An overview will be given of the current state of affairs concerning the seismic research on rifts and baby plumes, as well as possible causes for their presence will be discussed.

14.2

Lithosphere extension : necking instability vs gravity driven spreading

Jean-Pierre Brun and Frederic Gueydan

University Rennes 1

Mechanical modelling substantiates that the modes of lithosphere extension –i.e. narrow rifting vs wide rifting- strongly depend on the existence of two main classes of lithosphere rheological profiles. “Cold and strong” lithospheres have Moho temperatures lower than c.a. 750°C –i.e. the temperature of brittle–ductile transition in mantle rocks- whereas “hot and weak” lithospheres have Moho temperatures higher than this critical value. Necking-type instability occurs preferentially in cold and strong lithospheres that have four-layer-type of strength profiles with the greatest strength located in the sub-Moho mantle. It gives birth to continental rifts that can evolve into passive margins and ultimately lead to continental breakup. Gravity driven spreading occurs preferentially in hot and weak lithospheres whose strength profile exhibits maximum strength at the base of upper brittle crust. It gives birth to wide rifts and core complexes, like in the Basin and Range of the western United States or in the Aegean. The applicability of these end-member-type models to natural systems is discussed from the point of view of Atlantic-type passive margins, in one hand, and backarc-type basins of the Mediterranean, in the other hand.

14.3

Mediterranean Tectonics: IGCP 369 and Transmed Project

William Cavazza*

**Dept. of Earth and Geoenvironmental Sciences, University of Bologna, 40126 Bologna, Italy (william.cavazza@unibo.it)*

The Mediterranean domain provides a present-day geodynamic analog for the final stages of a continent-continent collisional orogeny. Over this area, oceanic lithospheric domains originally present between the Eurasian and African-Arabian plates have been subducted and partially obducted, except for the Ionian basin and the southeastern Mediterranean. A number of interconnected, yet discrete, Mediterranean orogens have been traditionally considered collectively as the result of an “Alpine” orogeny, when instead they are the result of diverse tectonic events spanning some 250 My, from the late Triassic to the Quaternary. To further complicate the picture, throughout the prolonged history of convergence between the two plates, new oceanic domains have been formed as back-arc basins either (i) behind active subduction zones during Permian-Mesozoic time, or (ii) associated with slab roll-back during Neogene time, when during advanced stages of lithospheric coupling the rate of active subduction was reduced. The closure of these heterogenous oceanic domains produced a system of discrete orogenic belts which vary in terms of timing of deformation, tectonic setting and internal architecture, and cannot be interpreted as the end product of a single Alpine orogenic cycle.

Similarly, the traditional paleogeographic notion of a single -albeit complex- Tethyan ocean extending from the Caribbean to the Far East and whose closure produced the Alpine-Himalayan orogenic belt must be discarded altogether. Instead, the present-day geological configuration of the Mediterranean region is the result of the opening and subsequent consumption of two major oceanic basins -the Paleotethys (mostly Paleozoic) and the Neotethys (late Paleozoic-Mesozoic)- and of additional smaller oceanic basins within an overall regime of prolonged interaction between the Eurasian and the African-Arabian plates. Paradoxically, the Alps, long considered as the classic example of Tethys-derived orogen, are instead the product of the consumption of eastward extensions of the central Atlantic ocean, the middle Jurassic Alpine Tethys, and of the North Atlantic ocean, the Cretaceous Valais ocean.

REFERENCES

Cavazza, W., Roure, F., Spakman, Stampfli, G.M. & Ziegler, P.A., eds. 2004: The TRANSMED Atlas: the Mediterranean Region from Crust to Mantle. Heidelberg, Springer-Verlag, 141 pp. + CD-ROM.

Stampfli, G., Borel, G., Cavazza, W., Mosar, J. & Ziegler, P.A., eds. 2001: The Paleotectonic Atlas of the PeriTethyan Domain (CD-ROM). European Geophysical Society.

Ziegler, P.A., Cavazza, W., Robertson, A.H.F. & Crasquin-Soleau, S., eds. 2001: Peritethyan Rift/Wrench Basins and Passive Margins. Mémoires du Muséum National d’Histoire Naturelle, Paris, v. 186, 762 p.

14.4

Thermo-Mechanical Controls on Continental Intraplate Deformation

Sierd Cloetingh

VU University, De Boelelaan 1085, 1081 HV Amsterdam, The Netherlands

Polyphase extensional and compressional reactivation of basins is a common feature in basin evolution. To differentiate between the different modes of basin formation and reactivation of passive margins and extensional basins, the development of innovative combinations of numerical and analogue modeling techniques is key. In this paper we present an overview of our advancement developing and applying analogue and numerical thermo-mechanical models to quantitatively asses the interplay of lithosphere dynamics and basin (de)formation.
Field studies of kinematic indicators and numerical modeling of present-day and paleo-stress fields in selected areas have yielded new constraints on the causes and the expression of intraplate stress fields in the lithosphere, driving basin (de)formation. Temporal and spatial variation in the level and magnitude of intraplate stress have a strong impact on the record of vertical motions in sedimentary basins. Over the last few years increasing attention has been directed to this topic advancing our understanding of the relationship between changes in plate motions, plate-interaction and the evolution of rifted basins.
The actual basin response to intraplate stress is strongly affected by the rheological structure of the underlying lithosphere, the basin geometry, fault dynamics and interplay with surface processes.
Integrated basin studies show that rheological layering and strength of the lithosphere plays an important role in the spatial and temporal distribution of stress-induced vertical motions, varying from subtle faulting to basin reactivation and large wavelength patterns of lithospheric folding, demonstrating that sedimentary basins are sensitive recorders to the intraplate stress field. The long lasting memory of the lithosphere, in terms of lithospheric scale weak zones, appears to play a far more important role in basin formation and reactivation than hitherto assumed. A better understanding of the 3-D linkage between basin formation and basin reactivation is, therefore, an essential step in research that aims at linking lithospheric forcing and upper mantle dynamics to crustal vertical motions, and their effect on sedimentary systems and heat flow.
Vertical motions in basins can become strongly enhanced, through coupled processes of surface erosion/sedimentation and lower crustal flow. Furthermore patterns of active thermal attenuation by mantle plumes can cause a significant spatial and modal redistribution of intraplate deformation, as a result of changing patterns in lithospheric strength and rheological layering.
Novel insights from numerical and analogue modeling aid in quantitative assessment of basin history and shed new light on tectonic interpretation, providing helpful constraints for basin exploration, including understanding and predicting vertical motions (eroded sedimentation record), source fill relationships, and heat flow.

14.5

From the Orogens of Europe to the Origin of the Arctic

David G. Gee*

* *Department of Earth Sciences, Uppsala University, Villavägen 16, Uppsala, SE-752 36, Sweden (david.gee@geo.uu.se)*

The younger orogens of Eurasia such as the Timanides, Caledonides and Uralides, reach northwards across the Arctic continental shelves into an ice-covered basin of ridges and troughs that comprises the least known ocean on Earth. If we are, one day, going to understand these orogens, we have to understand the Arctic Ocean; likewise, the origin of the latter will remain an enigma until we can identify and reconstruct the character of the continental and other fragments that are scattered around the basin. And there is really no way of understanding any of the pre-Vendian orogens until we've got the younger ones right!

EUROPROBE's concern for the major orogens of Europe, from the Uralides along the border of Asia to the Variscides of Iberia and the Atlantic margin (Fig. 1), provided the essential foundation for a new attack on the far north. Peter Ziegler played a key "Godfather's" role in EUROPROBE from birth, and helped deliver it's youngest child, TIMPEBAR. The TIMan-PEchora-BARents (and Kara) seas project sought to track the exposed Vendian and younger orogens northwards to the edge of Eurasian shelf and define their influence on the overlying hydrocarbon-bearing basins. We quickly learned that the

Neoproterozoic lithosphere of the eastern Barents Sea provides a remarkable foundation for the Russian sector of this shelf, with its vast late Paleozoic-Mesozoic troughs and gas reservoirs. But, we are still struggling with the Uralide sutures and the tectonics of Novaya Zemlya, the northern appendage of the Urals and barrier to the Kara shelf and northern part of the West Siberian oil fields (Fig. 2).

EUROPROBE neglected the Caledonides despite Peter's contributions to the Uppsala Caledonide Symposium in 1981. By the mid 1980's and EUROPROBE's birth, we were agreed on the vast lateral displacements of the Caledonian nappes in the Scandes and East Greenland and the remarkable late- to post-orogenic collapse of the orogen that extended far out across the Atlantic continental margins, beneath Mesozoic basins. How these allochthons were emplaced, with outboard oceanic terranes transported eastwards in the Scandes at least 400 km, remained a mystery until we recently began to understand the importance of a hot "extruding" complex (Seve Nappes), sourced from along the outer edge of the underthrusting Baltica margin. The collision of Baltica with Laurentia appears now to provide a singularly well preserved middle to lower crustal analogue for the Himalayas.

TIMPEBAR and subsequent work along the high Arctic margin of western Eurasia, and complementary studies of the Canadian, Alaskan and Russian sectors of the Arctic, are promoting new interpretations of the Phanerozoic orogens. These are stimulating reinterpretations of the Lomonosov, Mendeleev and Alpha ridges in the Arctic Basin, where recent seismic and potential field studies have helped to distinguish continental and ocean crust. As with climate science, there is an acute need to keep science clean of politics in these UNCLOS domains.

REFERENCES

Gee, D. G. and Stephenson, R. A. (eds) 2006: European Lithosphere Dynamics. Geological Society, London, Memoirs, 32.

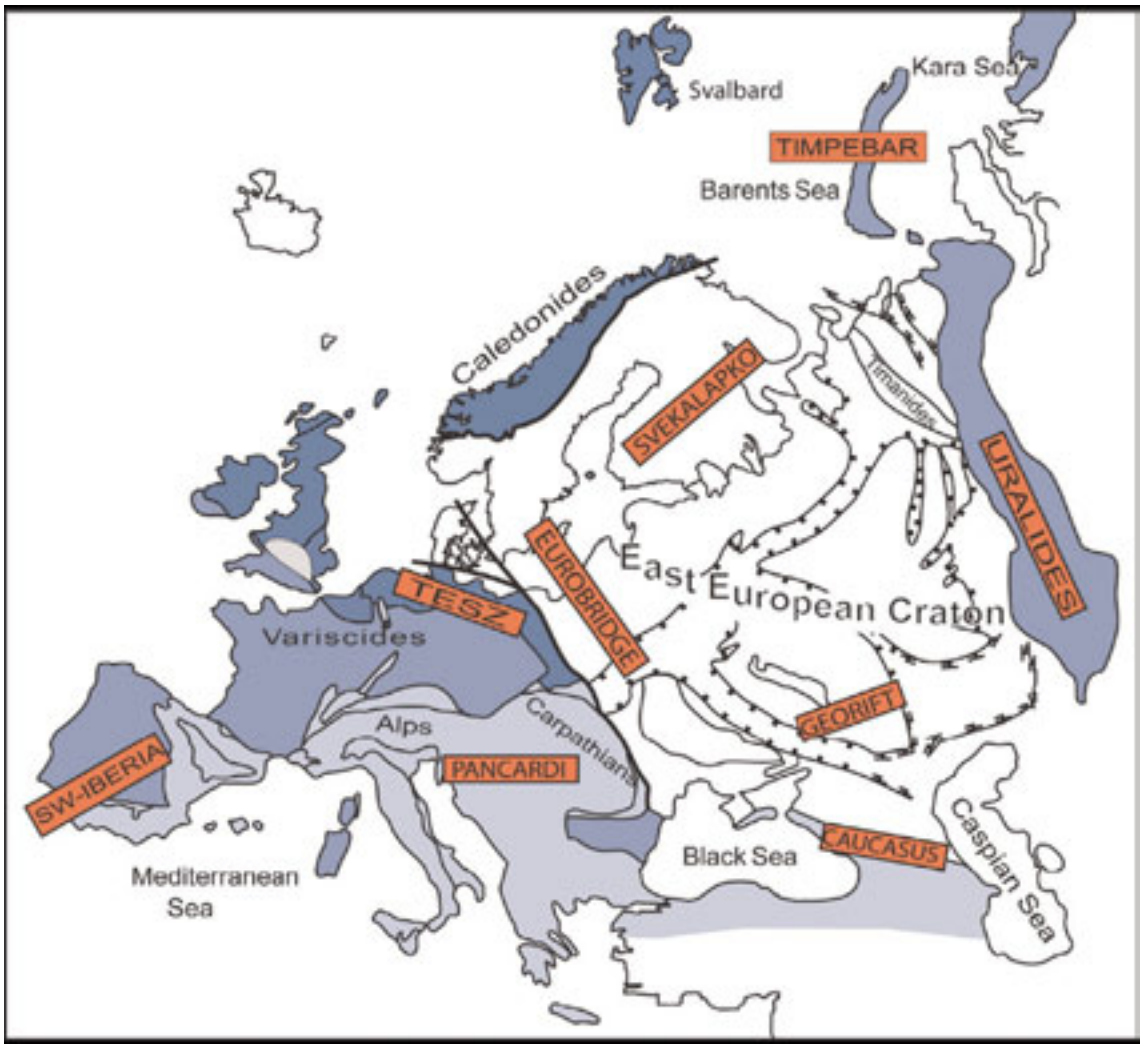

Figure 1. EUROPROBE projects (from Gee, D. G. and Stephenson, R. A. 2006)

Figure 2. Tectonic elements of the western Eurasian Arctic in the Early Cenosoic, during initial opening of the Eurasian Basin and Norwegian-Greenland Sea.

14.6

Evolution of continental structure from the Arching to the present: Views from the Canadian LITHOPROBE program

Alan Green*

*Institute of Geophysics, ETH, HPP O 5.1, Schafmattstrasse 30, CH-8093, Zurich

Integrated multidisciplinary studies of geological targets on the Canadian landmass and adjacent continental margins have been LITHOPROBE's principal objectives since its initiation in 1984. The greatest effort has been directed towards an improved understanding of the structure and evolution of the key tectonic units that comprise the fundamental building blocks

of the North American continent. Many of these tectonic units are exposed, thus allowing correlation between a broad spectrum of geophysical data with the surface geology and with geochronological and geochemical information derived from the surface rocks. At some locations, almost complete cross-sections of the crust have been exposed, whereas at others, it is possible to project the geology from the surface "down-dip" to regions of the crust that have been sampled by the geophysical observations.

Canada's vast geographic expanse and its diverse geology provided the opportunity to evaluate geological structures and processes throughout the history of the Earth. The oldest Arching tectonic units were the focus of studies in three regions of the giant Superior Province and in the Nain and Slave Provinces. Early Proterozoic crustal evolution was explored in the Trans-Hudson, Wopmay, Makkovik and Penokean Orogens, four of the best preserved examples of such orogenic belts. Middle Proterozoic rifting and orogenesis were examined along the Midcontinent (Keweenawan) Rift System and the Grenville Orogen, respectively. Finally, Late Proterozoic to Recent mountain building and tectonic processes were investigated at various locations in the northern Appalachians and southern and northern Canadian Cordillera.

The presentation will be mainly concerned with the results of LITHOPROBE multichannel seismic reflection studies. Seismic sections from many of the investigated Canadian tectonic units and from structures elsewhere will be compared in an attempt to understand crustal evolution through a large portion of Earth's history. Conclusions from this study include:

- crustal structural styles are very similar in the Palaeozoic, Proterozoic and Arching crystalline terrains;
- as a consequence, the rheological properties of the crust must have remained nearly constant from the Arching until today;
- plate tectonic processes very likely extended back to the Arching;
- the origin of deep crustal reflections can be explained by exposures of deep rocks at the surface;
- with a few exceptions, Moho is relatively flat, surprisingly so beneath the topographically rugged Cordillera;
- yet, the character of the Moho is highly variable;
- North American “basement”, supracrustal rocks and lithosphere project 100’s of km west beneath deformed rocks of the Cordillera;
- accreted terrains are typically thin - some are only a few km thick.

14.7

Thrustbelts and foreland basins

Roure François

Institut Français du Pétrole, 1-4 Avenue de Bois-Préau, 92852 Rueil-Malmaison Cedex, France, Francois.Roure@ifp.fr

Thrustbelts are usually characterized by a positive topography above the sea level, which is continuously modified by the conjugate effects of tectonic contraction or post-orogenic collapse, thermo-mechanical processes in the deep lithosphere and asthenosphere, but also by climate and other surface processes influencing erosion rates. Different types of sedimentary basins can develop in close association with orogens, either in the foreland or in the hinterland. Being progressively filled by erosional products of adjacent uplifted domains, these basins provide a continuous sedimentary record of surficial, crustal and lithospheric deformation at and near plate boundaries.
Thrustbelts and foreland basins host also famous petroleum provinces. Basin modeling tools are now more efficient to reconstruct palinspastic structural cross sections and compute the history of temperature, pore fluid pressure, fluid flow circulations and petroleum potential in these complex structural settings.
Selected integrated basin-scale studies in the productive Circum-Mediterranean thrust belts and basins, in Pakistan and the Americas, are used here to document the effects of structures inherited from former orogens, rifts and passive margins, active tectonics and mantle dynamics on the development of petroleum systems and long term evolution of synorogenic basins.

Strong coupling between the thrust belt and its foreland can occur at different times in both subduction-related (i.e. Cordilleran-type) or collision-related (i.e. Alpine-type) orogens, thus accounting for both early and late foreland inversion processes (Ziegler & Roure, 1996; 1999).
Since the mid 80's, deep crustal seismic imaging across many orogens such as the Alps, the Pyrenees and the North American Cordillera has provided direct controls on the deep architecture of the thrust systems (Roure et al., 1990), and a better understanding of the coupling between thin-skinned and thick-skinned tectonics, whereas since the 90's, mantle tomography is progressively documenting the occurrence or absence of lithospheric slabs beneath recent orogens (Cavazza et al., 2004).
In many thrust belts where neither deep seismics nor mantle tomography is yet available, the pending question is to know

whether slab detachment may account for rapid uplift and post-orogenic erosion of former foreland basins, as described in the Central Apennines and North Algeria, or if mantle convection and asthenospheric rise alone can account for post-orogenic uplift, as evidenced in the Alberta and Veracruz basins in Canada and Mexico, respectively (Roure, 2008).
Source to sink studies are also necessary to define the spatial and temporal coupling between erosion, sedimentary transfer and deposition. Until recently, most efforts were devoted to high resolution seismostratigraphic studies coupled with core and outcrop descriptions of the synflexural/synkinematic sedimentary infill of the foreland basins. Today, however, GPS measurements and thermo-chronometers such as Apatite Fission Tracks and U-Th, can provide direct control on the uplift and unroofing history of the hinterland. Ultimately, new techniques must still be developed to provide information on paleo-elevations, which are essential for discriminating between different tectonic models, e.g. orogenic collapse and rollback, and which are also likely to control the boundary conditions (hydraulic heads) required for computing the pore-fluid pressure evolution and hydrocarbon migration in adjacent low lands (Roure et al., 2005).
Further understanding of the coupling between deep (mantle) and surface (climate) processes in orogens and adjacent foreland basins constitutes one of the main current challenges for Earth scientists, which will require access to well documented data bases to feed numerical models, involving a lot of integration and multi-disciplinary team work. International networks such as the Transmed (Cavazza et al., 2004) and ILP task forces and related workshops (Lacombe et al., 2007) may help to initiate these new collaborations. Pioneer work is currently done in Europe (Topo-Europe programme), where continental topography has been indeed widely impacted by the Alpine orogen and recent mantle upwelling in the Western Mediterranean and West European rift system.

REFERENCES

Cavazza, W., Ziegler, P. Spakman, W., Stampfi, G. & Roure, F., eds 2004: The Transmed Atlas: The Mediterranean region from crust to mantle, Heidelberg, Springer-Verlag, 141 p. +CD-ROM.

Lacombe, O., Lavé, O., Roure, F. & Vergés, J., eds. 2007: Thrust belts and foreland basins: From fold kinematics to hydrocarbon systems. Frontiers in Earth Sciences, Springer, 492 pp.

Roure, F. 2008: Foreland and hinterland basins: What controls their evolution? Davos Proceedings, Swiss Journal of Geosciences, in press.

Roure, F., Heitzmann, P. & Polino, R., eds.. 1990: Deep structure of the Alps. Mém. Soc. Géol. France, Paris, 156; Mém. Soc. Géol. Suisse, Zürich, 1; Vol. Sp. Soc. Geol. Italiana,Roma, 1, 350 pp.

Roure, F., Swennen, R., Schneider, F., Faure, J.L., Ferket, H., Guilhaumou, N., Osadetz, K., Robion, Ph. & Vendeginste, V. 2005: Incidence and importance of tectonics and natural fluid migration on reservoir evolution in foreland fold-and-thrust belts. In Brosse, E. et al., eds., Oil and Gas Science and Technology, Oil and Gas Science and Technology, Revue de l'IFP, 60, 67-106.

Ziegler, P. & Roure, F. 1996: Architecture and petroleum systems of the Alpine orogen and associated basins. In Ziegler, P. & Horvath, F., eds., PeriTethys Mem. 2, Mus. Hist. Nat., Paris, 15-46.

Ziegler, P. & Roure, F. 1999: Petroleum systems of Alpine-Mediterranean foldbelts and basins. In Durand, B., Jolivet, L., Horvath, F. & Séranne, M., eds., Geol. Soc. London. Sp. Publ., 156, 517-540.

14.8
Global Plate Reconstructions

Stampfli Gérard M.

Université de Lausanne, Institut de Géologie et Paléontologie,
Anthropole 1015 lausanne
gerard.stampfli@unil.ch

To construct reliable palinspastic models of the Earth major geological elements (basins, mountain belts, continental margins...), plate tectonics constraints must be taken into consideration, besides others elements such as faunal distribution or paleomagnetic data. The work of P. Ziegler over his long carrier has provided in depth investigations of these geological elements in many areas of the world, resulting in state of the art paleogeographic maps of the western world. These geological investigations are the prime material on which plate tectonic models for the past can be built.
Plate tectonic concepts allow to assess the kinematics of displacements of terranes and continents, keeping in mind that these continental entities are part of larger plates. For most continents/terranes, thousand km scale transport can be demonstrated, and used to construct paleogeographic models. These usually consist in simple continental drift models, and therefore, are poorly constrained in term of plate velocities. In such models it is not unusual to find velocities over 50 to 70 cm/y (usually based on paleomagnetic data), which are not acceptable in term of plate tectonics, mainly when they involve large continents like Gondwana. Plate tectonic concepts have been systematically applied to our global palinspastic models

moving away from pure continental drift, not constrained by plate limits, to produce a model that finally is more and more self-constrained. In this approach inter-dependant reconstructions are created from the past to the present. Except during collisions, plates are moved step by step, as single rigid entities. Lithospheric plates are constructed by adding/removing oceanic material (symbolized by synthetic isochrones) to major continents and terranes.
In the last years we changed our tools and moved into GIS softwares and built a geodynamic database to support the reconstructions, and the model was, and still is, extended to the whole globe, spanning the earth history from 600 Ma to 20 Ma, with average steps of 15 Ma.. Our high precision reconstructions allow to measure many geological features in time and space, starting with plate velocities. It is also possible to evaluate the changing space for the world oceanic volume, as oceans are reconstructed in time and their depth can be assessed in function of their age. It is also possible to measure the changing length of mid-ocean ridges and active margins, giving an insight into volcanic activity and thus potential climate changes. The areas of continental masses versus their position in latitude can also be measured. These figures can be confronted to existing paleoclimatic data and eustatic sea level curves, in order the assess the impact of plate tectonic versus short term climatic changes.

14.9

Style, timing, and controls on European intraplate basin inversion in the Late Cretaceous-Paleocene

Randell Stephenson

(VU University Amsterdam, Netherlands; University of Aarhus, Denmark; and University of Aberdeen, United Kingdom)

Peter Ziegler was coincidentally the first geologist I met (except for Sierd) upon my arrival in Europe in mid-June 1989. Peter probably won't remember it but (somehow) I joined up with him and some others at Marseille airport and hitched a ride to a conference we were all attending at Arles. On the way, as we passed outcrops at 120 km/h, I received my first "lecture" on the far-field effects of the Alpine orogeny. Intraplate deformation in Europe was to become one of the main guiding themes of my subsequent career, with Peter as an important mentor in the process. So that more or less covers the "timing" part of this presentation not to mention the "style", which is unique. About "controls", though, it seems that some aspects of the inversion of European basins may not be purely controlled by Alpine (Africa-Europe collision) processes but also by what was happening on other European plate boundaries. Lately, my colleagues at the University of Aarhus and I demonstrated a causal relationship between an abrupt change of European intraplate deformation style and North Atlantic continental rifting at ≈62 Ma. The rifting involved a left-lateral displacement between the North American-Greenland plate and Eurasia, which we think may actually have initiated the observed pause in the relative convergence of Europe and Africa that Peter knows well (as does Pierre). The associated stress change in the European continent was significant and can possibly explain the sudden termination of ≈20 Myr of Late Cretaceous to earliest Paleocene contractional intraplate deformation within Europe to be replaced by low-amplitude intraplate stress-relaxation features. Coincidentally, the pre-rupture tectonic stress may have been large enough to precipitate continental break-up, without the necessity of invoking a thermal mantle plume (viz. Iceland) as a driving mechanism. I'll close with some words about the Dniepr-Donets Basin (and Donbas Foldbelt) – Peter was with me on my very first visit to Ukraine in February 1992 – and how this basin was "inverted" during the same Late Cretaceous-Paleocene time frame as those further west.

Index

Thanks to the sponsors of this event:

Città
di
Lugano

Schweizerische Eidgenossenschaft
Confédération suisse
Confederazione Svizzera
Confederaziun svizra

Bundesamt für Landestopografie swisstopo
Office fédéral de topographie swisstopo
Ufficio federale di topografia swisstopo
Federal Office of Topography swisstopo

Swiss Geological Survey

Museo
cantonale
di storia
naturale

GEOBRUGG®
Protection Systems

BancaStato
BANCA DELLO STATO DEL CANTONE TICINO

ASA | SVV
Schweizerischer Versicherungsverband
Association Suisse d'Assurances
Associazione Svizzera d'Assicurazioni

Basilese
Assicurazioni
Baloise Bank SoBa
AG Mendrisio/Malcantone

SWISS
ENGINEERING
STV UTS ATS
TICINO